NASA Technical Memorandum 102211

Experimental Study of a Three-Dimensional Shear-Driven Turbulent Boundary Layer with Streamwise Adverse Pressure Gradient

David M. Driver and James P. Johnston

May 1990

National Aeronautics and Space Administration

NASA Technical Memorandum 102211

Experimental Study of a Three-Dimensional Shear-Driven Turbulent Boundary Layer with Streamwise Adverse Pressure Gradient

David M. Driver and James P. Johnston, Ames Research Center, Moffett Field, California

May 1990

National Aeronautics and
Space Administration

Ames Research Center
Moffett Field, California 94035-1000

NOMENCLATURE

a_1	structure parameter = $\sqrt{\overline{uv}^2 + \overline{vw}^2}/q^2$
b_{ij}	$\frac{\overline{u_i u_j}}{q^2} - \frac{1}{3}\delta_{ij}$, anisotropy tensor
C_f	skin friction coefficient
C_{f_x}	axial (streamwise) skin-friction coefficient = $\tau_{w_x}/\frac{1}{2}\rho_r U_r^2$
C_{f_z}	circumferential (transverse) skin-friction coefficient = $\tau_{w_z}/\frac{1}{2}\rho_r U_r^2$
C_p	pressure coefficient = $(P\text{-}P_r)/\frac{1}{2}\rho_r U_r^2$
D_{ij}	$-\overline{u_i u_k}\partial U_k/\partial x_j - \overline{u_j u_k}\partial U_k/\partial x_i + (\delta_{i3}\overline{u_j v} + \delta_{j3}\overline{u_i v})\frac{W}{R}$ Model term for $\overline{u_i u_j}$ stress component
k	turbulent kinetic energy = $(\overline{u^2} + \overline{v^2} + \overline{w^2})/2$, assumed $\overline{w^2} = (\overline{u^2} + \overline{v^2})/2$ where $\overline{w^2}$ is not measured
l	mixing length = $\sqrt[4]{\overline{uv}^2 + \overline{vw}^2}/\sqrt{(\partial U/\partial y)^2 + (\partial W/\partial y - W/r)^2}$
p	static pressure
P_{ij}	$-\overline{u_i u_k}\partial U_j/\partial x_k - \overline{u_j u_k}\partial U_i/\partial x_k + (\overline{u_i w}\delta_{j2} + \overline{u_j w}\delta_{i2})\frac{W}{R}$ = Production of $\overline{u_i u_j}$ stress component
Q	resultant velocity vector $\sqrt{U^2 + V^2 + W^2}$
q^2	$\overline{uu} + \overline{vv} + \overline{ww} = 2k$, twice the turbulent kinetic energy
$\overline{qv}$	$-\sqrt{\overline{uv}^2 + \overline{vw}^2}$, total Reynolds stress in x-z plane
Q_{ij}	$\frac{\overline{u_k u_j}\ \overline{u_l u_i}}{k} 2S_{kl} - \frac{\overline{u_l u_k}}{k}[\overline{u_i u_k}(\partial U_j/\partial x_l - \delta_{j2}\delta_{l3}\frac{W}{R}) + \overline{u_j u_k}(\partial U_i/\partial x_l - \delta_{i2}\delta_{l3}\frac{W}{R})]$ modeling term
S_{ij}	$\frac{1}{2}(\partial U_i/\partial x_j + \partial U_j/\partial x_i - (\delta_{i2}\delta_{j3} + \delta_{j2}\delta_{i3})\frac{W}{R})$, Strain rate of i,j component
r	radial distance from centerline of cylinder
R_o	radius of cylindrical model
U, V, W	mean velocity components in x, y, and z directions, respectively
U_i, u_i	component of mean and fluctuating velocity in the i direction where i = 1, 2, or 3 for x, y, or z directions, respectively
U_r	upstream free-stream velocity (used in normalization of data) nominally 30 m/sec
W_s	transverse (circumferential) velocity on surface of rotating cylinder nominally 0, 15, and 30 m/sec
U_s, W_c	mean velocity components parallel and perpendicular to the flow direction at the boundary layer edge (β_e), respectively
$\hat{U}, \hat{W}$	apparent mean velocity components relative to translating wall in x and z directions, respectively, with magnitudes U and $W - W_s$
$\tilde{U}, \tilde{W}$	mean velocity components in directions parallel and perpendicular to γ_τ, principal stress direction
u, v, w	fluctuating velocity components in x, y, and z directions
$\overline{uu}, \overline{vv}, \overline{ww}$	mean-square velocity fluctuations in x, y, and z directions
$\overline{uv}, \overline{vw}, \overline{uw}$	turbulent velocity fluctuation correlations
$\overline{uuu}, \overline{uvv}, \overline{uww}$, $\overline{vuu}, \overline{vvv}, \overline{vww}$, $\overline{wuu}, \overline{wvv}, \overline{www}$, $\overline{uvw}$	turbulent triple-velocity correlation, assumed $\overline{www} = (\overline{uuu + uvv})/2$ and $\overline{vww} = (\overline{vuu + vvv})/2$ where $\overline{uww}$ and $\overline{vww}$ were not measured

$\overline{vk}$	turbulent triple-velocity correlation = $(\overline{vuu + vvv + vww})/2$
u_τ	friction velocity = $\sqrt{\tau_w/\rho_w}$
x, y, z	coordinate system representing axial, normal, and circumferential and distances from the downstream end of spinning cylinder (see fig. 1)
β	skew angle of horizontal velocity vector relative to free stream
δ	local boundary layer thickness based on U=0.99*U_e
δ_w	local boundary layer thickness based on W=0.01*W_s
δ_o	local boundary layer thickness at X=0 for zero $\partial P/\partial x$ case
δ_x^*	x component of displacement thickness, = $\int_o^\delta (1 - U/U_e)(1 + y/R_o)\,dy$
δ_z^*	z component of displacement thickness, = $\int_o^\delta (W/W_s)(1 + y/R_o)\,dy$
δ_c^*	transverse component of displacement thickness, = $\int_o^\delta \frac{W_e}{Q_e}dy$
δ_s^*	streamwise component of displacement thickness, = $\int_o^\delta (1 - \frac{U_s}{Q_e})\,dy$
ε	dissipation rate of kinetic energy
γ_τ	principal stress direction = $tan^{-1}\frac{-\overline{vw}}{-\overline{uv}}$
γ_g	principal strain-rate direction = $tan^{-1}\frac{\partial W/\partial y - W/r}{\partial U/\partial y}$
ϕ_{ij}	Pressure rate-of-strain of $\overline{u_i u_j}$ stress component
ν	molecular kinematic viscosity of air, nominal value of 0.000015 m^2/sec
ν_t	turbulent eddy viscosity
ρ	air density, nominal value of 1.2 kg/m^3
θ_{xx}	x-direction momentum thickness, = $\int_0^\delta (U/U_e)(1 - U/U_e)(1 + y/R_o)\,dy$
θ_{xz}	z-direction angular momentum thickness, = $\int_0^\delta (U/U_e)(W/W_s)(1 + y/R_o)^2\,dy$
τ	total Reynolds shear stress, $\rho\sqrt{\overline{uv}^2 + \overline{vw}^2}$
τ_w	total wall shear stress
τ_{w_x}, τ_{w_z}	axial (streamwise) and circumferential (transverse) wall shear stresses, respectively
ω	specific dissipation rate of turbulence kinetic energy, ε/(0.09*k)
II	$-b_{ij}b_{ji}/2$, second invariant of the b_{ij} tensor
III	$b_{ij}b_{jk}b_{ki}/3$, third invariant of the b_{ij} tensor

Superscript

$\overline{()}$	long time average

Subscripts

$()_e$	edge of boundary layer conditions
$()_r$	reference location, x = –457 mm
$()_x$	x direction
$()_w$	wall conditions
$()_z$	z direction

SUMMARY

The effects of a strong adverse pressure gradient ($\frac{\delta^*}{\tau}\frac{\partial P}{\partial x}$=12) on a three-dimensional turbulent boundary layer are studied in an axisymmetric spinning cylinder geometry. Velocity measurements made with a three-component laser Doppler velocimeter include all three mean flow components, all six Reynolds stress components, and all ten triple-product correlations. Reynolds stress, $\sqrt{\overline{uv}^2 + \overline{vw}^2}$, diminishes as the flow becomes three-dimensional. Lower levels of shear stress were seen to persist under adverse pressure gradient conditions. This low level of stress was seen to roughly correlate with the magnitude of cross-flow (relative to free stream flow) for this experiment as well as most of the other experiments in the literature. Variations in pressure gradient do not appear to alter this correlation. For this reason, it is hypothesized that a three-dimensional boundary layer is more prone to separate than a two-dimensional boundary layer, although it could not be directly shown here. None of the computations performed with either a Prandtl mixing length, $k - \varepsilon$, or a Launder-Reece-Rodi full Reynolds-stress model were able to predict the reduction in Reynolds stress.

1 INTRODUCTION

1.1 Background

Drag on aerodynamic vehicles and the associated consumption of fuel is influenced to a great extent by the turbulence generated at the vehicle surface. The ability to predict and minimize this drag is strongly linked to successful mathematical modeling of the turbulent fluid motion. Deficiencies in turbulence models can lead to significant errors in prediction of drag as well as the lift (at high angle of attack) and stall characteristics of an aircraft. One of the most serious deficiencies a turbulence model can have is an inability to predict flow separation (the lifting of streamlines away from the body). Accurate prediction of separation is important, since separation effectively alters the aerodynamic shape of the vehicle to something other than intended—an effect that generally decreases lift and increases drag.

Mathematical models for turbulence would not be necessary if computers had sufficient memory and speed to compute all of the small scales of turbulent motion from Newton's second law. However, computer memory and speed are still many orders of magnitude too small and too slow to do realistic simulations of engineering flows of interest. While fluid flow can be completely and accurately described by the Navier-Stokes equations (Newton's second law and the Newtonian viscosity law), these equations are difficult to solve when the flow becomes turbulent. Therefore, in order to obtain solutions to all but the simplest flows, it becomes necessary to partially model these equations. One of the favorite methods of simplifying these equations is to time-average them, thus integrating the random motion of the turbulence into a single unknown called the Reynolds stress (tensor variable). The Reynolds stress needs to be mathematically modeled, since a near infinite series of equations would be required to describe it exactly (a counterproductive task). Unfortunately, this integral measure of turbulence (Reynolds stress) can be difficult to model, since it is a very complicated function of strain-rate, history effects, pressure gradient, and flow skewing, and many other flow conditions. Nevertheless, the Reynolds averaging method of simplifying and partially modeling the Navier-Stokes equations is widely (almost exclusively) used in engineering calculations to obtain solutions to practical problems. The following sections will discuss primarily the effects of transverse strain and pressure gradient on the Reynolds stresses.

1.2 Transverse Strain Effects on Turbulence

Useful turbulence models have been developed to describe a wide variety of two-dimensional (2D), that is, unidirectional, flows. Successful models have been developed to describe 2D attached flows with mild pressure gradients. Indeed, some models are capable of qualitatively describing 2D separated flows, although the accuracy of such models leaves room for improvement. By contrast, modeling of 3D (skewed) flows is relatively rare, since there are very few experiments with sufficient data to guide modeling (refs. 1 and 2). Consequently, most turbulence models for 3D flows tend to be simple mathematical generalizations of models developed for 2D flows that include no additional physics. However, the few available experiments indicate a need for inclusion of additional physics in the models.

1.2.1 Reynolds Stress Lag

One flow phenomenon seen in the experiments of Bradshaw and Terrell (ref. 3), Johnston (ref. 4), Elsenaar and Boelsema (ref. 5), and others (refs. 6, 7, 8, 9, 10, and 11), is a lag in the development of the turbulent Reynolds stress field relative to the mean flow field. This phenomenon is not unique to 3D mean flow fields, but it is prominently exhibited by 3D flows. The lag phenomenon is illustrated by the spinning cylinder experiment of Driver and Hebbar (refs. 11 and 12)(fig. 1.1). As the flow proceeds in the streamwise x-direction through the 3D interaction zone, the mean flow strain rate is seen to change direction before the turbulent Reynolds stress vector does—direction changes from –45° upstream to +10° downstream. Another example of lag is given in the "infinite" swept wing experiment of Elsenaar and Boelsma (ref. 5) (fig. 1.2), in which the mean flow strain-rate direction is seen to turn to larger angles (–12°) than the Reynolds stress vector (–5°)—both vectors started at zero, upstream of the 3D interaction zone.

1.2.2 Reynolds Stress Drop

A second 3D phenomenon, seen in the "infinite" swept wing experiment of Bradshaw and Pontikos (ref. 8), is the decay of Reynolds stress, relative to corresponding Reynolds stress in 2D flows. In figure 1.3, the Reynolds stress (indicated by symbols) is lowest at the downstream station where the mean flow is 3D in contrast to the upstream station (indicated by the solid line) where the mean flow is 2D. Similarly in the simulation of Moin, Shih, Driver, and Mansour (ref. 13), the Reynolds stress drops during the time when the mean flow is 3D. Likewise, in the experiment of Driver and Hebbar (ref. 12), Reynolds stresses are lower where the flow is 3D.

One practical way to quantify this departure of the shear stress from a 2D equilibrium boundary layer is to normalize the shear stress by the mean flow gradient, using a mixing length formulation (i.e., $l = \sqrt[4]{\overline{uv}^2 + \overline{vw}^2} / \sqrt{(\partial U/\partial y)^2 + (\partial W/\partial y)^2}$). Two-dimensional boundary layers usually exhibit a linear distribution of l with distance from the wall (i.e., $l = 0.41\,y$) for $y < 0.22\,\delta$ and then a constant distribution of l equal to $0.09\,\delta$ for $y > 0.22\,\delta$. The Pontikos and Bradshaw (ref. 7) flow, shown in figure 1.4, demonstrates a drop in mixing length (Reynolds stress) with distance into the 3D flow. Anderson and Eaton's (ref. 10) wedge flow (fig. 1.5), Muller's (ref. 14) turning flow (fig. 1.6) and DeChow and Felsch's (ref. 9) wing body junction flow (fig. 1.7) all demonstrate a similar drop in length scale with distance along the 3D interaction zone. On the other hand, the spinning cylinder flows of Lohmann (ref. 15) (fig. 1.8) and Bissonnette and Mellor (ref. 16) (fig. 1.9) apparently indicate the opposite trend of mixing length increase

rather than decrease—these flows contain curvature effects which destabilize the boundary layer and consequently increase the mixing length. See appendix A for a discussion of curvature. Even though the spinning cylinder flow of Driver and Hebbar (ref. 12) also contains curvature effects, the mixing length, shown in figure 1.10, appears to decrease below the curvature-corrected model downstream ($X = 15\delta_o$) where the flow experiences 3D effects.

One physical explanation for the observed drop in length scales (Reynolds stress) proposed by Bradshaw and Pontikos (ref. 8) is that shear producing coherent structures of the kind seen in 2D boundary layers are "toppled" over and disrupted by crossflow.

1.2.3 Near Wall Scaling

When the log-law-of-the-wall is modified for 3D flows, it often exhibits a different slope (von Karman constant) than that for 2D flows (refs. 1, 6, 17, 18, and 19). A review of all known 3D log law-of-the-wall assumptions was done by Pierce, McAllister, and Tennant (refs. 17, 18, and 19) in which they found some models gave relatively good agreement, but all of the models exhibited some differences when compared to various data sets. Part of the difficulty with searching for a log law-of-the-wall is the lack of experiments that use independent surface skin-friction measurements which do not rely on a law-of-the-wall assumption.

1.3 Pressure Gradient Effects on Two-Dimensional Boundary Layers

Mean flow measurements have been performed by several researchers in 2D boundary layer flows with adverse pressure gradient (refs. 20, 21, 22, and 23). More recently, experiments which include measurements of the Reynolds stresses have been performed (refs. 24, 25, 26, 27, and 28). Typically, one finds that the adverse pressure gradient reduces the level of stress near the wall, while increasing the stress away from the wall. Prandtl mixing length scales generally drop with increasing adverse pressure gradient. If the flow detaches, the mixing lengths become imaginary (or undefined), making it difficult to adequately devise models based on a Prandtl mixing length. Despite these differences, near wall similarity of the mean velocity (scaled with surface shear) appears to be unaffected by pressure gradient with the exception that similarity is confined to regions closer to the wall. This finding suggests that wall-function-type turbulence models can be used in adverse pressure gradient flows.

1.4 Review of Spinning Cylinder Experiments

This section outlines the previous experiments performed on spinning cylinder geometries. Several such experiments exist in the literature.

1.4.1 Zero Pressure Gradient Cases

In practice, 3D flows usually arise from transverse pressure gradients, such as those that occur on swept wings, rotating turbines, or in curved ducts. Likewise, most experiments (refs. 4, 5, 7, 9, 10, and 14) utilize transverse pressure gradient to generate a crossflow, making it difficult to study viscous effects independent of pressure gradient effects.

An innovative experiment to study a 3D boundary layer without pressure gradient was done by Furuya, Nakamura, and Kawachi (ref. 29). They studied the growth of crossflow produced by a spinning cylinder aligned with a uniform free stream. Bissonette and Mellor (ref. 16) and Lohmann (ref. 15) later reported turbulence measurements on similar configurations, which suggested that turbulent shear stresses may not be simply proportional to the mean flow strain (via scalar eddy viscosity) as is often assumed. Instead, eddy viscosity appeared to be anisotropic (i.e., $-\overline{uv}/(\partial U/\partial y) \neq -\overline{vw}/(\partial W/\partial r - W/r)$). A further experimental and computational study was performed by Higuchi and Rubesin (refs. 30 and 31) in which they studied the decay of crossflow on a stationary section of cylinder immediately downstream of a spinning section. In the computational part of their study, they showed that models which accounted for anisotropy of eddy viscosity predicted crossflow better than those that used scalar eddy viscosity. However, sizable discrepancies remained between the measurements and the calculations, which were thought to be caused by the pressure rate-of-strain model. Higuchi and Rubesin (ref. 30) made direct measurements of skin friction in an unsuccessful effort to find a law of the wall for 3D flow. Later, Driver and Hebbar (ref. 12) measured all six Reynolds stresses as well as the mean flow in the experimental rig of Higuchi and Rubesin, learning that indeed eddy viscosity is anisotropic and needs to be modeled with a full Reynolds-stress-type model. These Reynolds stress measurements along with triple product correlations permitted Reynolds stress equation balances, the results of which showed reasonably good agreement between the various pressure-strain models and pressure-strain deduced from the data. A review of spinning cylinder flows is given by Nakamura and Yamashita (ref. 32).

1.4.2 Combined Pressure Gradient and Transverse Strain Effects

Pressure gradient effects on 3-D boundary layers have been studied in experiments where streamwise pressure gradients are directly linked with crossflow pressure gradients (refs. 4, 5, 7, 9, 10, and 14). In an effort to study the effects of a single component of pressure gradient on 3D flows, Furuya et al. (ref. 33) produced mild streamwise pressure gradients on their rotating cylinder flow by converging and diverging the tunnel walls. They found only minimal effects of streamwise pressure gradient on the developing mean crossflow (no Reynolds stress measurements were performed). Driver and Hebbar (refs. 34 and 35) also looked at a case of adverse axial pressure gradient on a spinning cylinder, in which the pressure gradient was caused by a forward facing step obstruction. Here the transverse component of Reynolds stress was also found to be only minimally affected by the sudden application of streamwise pressure gradient.

1.5 Recent Three-Dimensional Turbulence Modeling Efforts

Reynolds stress behavior appears to be fundamentally different between 3D and 2D flows. The stresses in 3D flows tend to be somewhat lower than in comparable 2D flows. In addition, the transverse component of Reynolds stress (not present in 2D flows) tends to develop significantly more slowly than the mean flow, producing a difference in the direction of the mean flow strain-rate and the Reynolds shear stress direction (sometimes referred to as a lag phenomenon). Turbulence models designed for 2D flows generally fail to predict these two effects. Recognizing these deficiencies in turbulence models, several researchers have proposed modifications of existing models.

Rotta (ref. 36) designed a turbulence model which would produce a lag between the Reynolds stresses and the mean flow strain-rate—an eddy-viscosity model which varies with direction.

$$-\overline{uv} = \nu_{t_{xx}} \partial U/\partial y + \nu_{t_{xz}} \partial W/\partial y$$

$$-\overline{vw} = \nu_{t_{xz}} \partial U/\partial y + \nu_{t_{zz}} \partial W/\partial y$$

where

$$\nu_{t_{xx}} = \nu_t(1 - (T-1)sin^2(\beta))$$
$$\nu_{t_{xz}} = \nu_t(1 - T)sin(\beta)cos(\beta)$$
$$\nu_{t_{zz}} = \nu_t(1 - (T-1)cos^2(\beta))$$

with T = constant (Rotta suggests 0.5), β = local flow angle, and ν_t any scalar eddy-viscosity model. The difficulty with Rotta's model is that it is not Galilean invariant, so it gives different results depending on what reference frame is used to define β. Nevertheless, the model, when applied in a direction parallel to the free stream (viewed from the solid wall), yields improved results over a scalar eddy-viscosity model.

Another attempt at improving modeling of the Reynolds stresses was proposed by Abid (ref. 37), in which he diminishes the streamwise Reynolds stress by the ratio of the displacement thickness components.

$$-\overline{uv} = (1 - |\delta_c^*/\delta_s^*|)\nu_t \partial U/\partial y$$
$$-\overline{vw} = (1 - |\delta_c^*/\delta_s^*|)\nu_t \partial W/\partial y$$

where $\delta_s^* = \int_o^\delta (1 - \frac{Q}{Q_e})dy$ and $\delta_c^* = \int_o^\delta (\frac{W}{Q_e})dy$ with ν_t being any scalar eddy viscosity model. This model produces the desired effect of reducing the Reynolds stress in flows with crossflow. In addition, the model relies on global thickness parameters which may restrict its application to wall bounded flows.

Models which solve a full set of Reynolds stress equations inherently have the ability to develop a lag between the stresses and the mean flow field.

$$\frac{D\overline{u_i u_j}}{Dt} = (-\overline{u_i u_k}\partial U_j/\partial x_k - \overline{u_j u_k}\partial U_i/\partial x_k) + D_{ij} + \phi_{ij} - \varepsilon_{ij}$$

where diffusion (D_{ij}), pressure-strain (ϕ_{ij}), and dissipation (ε_{ij}) all require modeling. This type of model allows the stresses to develop slowly at rates which depend on the mean flow. Furthermore, each stress is allowed to develop somewhat independently of the others, which permits differing growth rates for each stress and thereby enables the stress to develop in a different direction from the mean flow strain-rate. Deficiencies exist with this class of models, but they are difficult to pinpoint because of the inability to directly measure most of the terms in these equations.

1.6 Objectives of Current Study

The experiments described in this report were done in an effort to find correlations linking the degree of three-dimensionality of the mean flow to the drop in Reynolds stress and lag between the stress and the strain-rate. There is a need for parameters which are sensitive indicators of the magnitude of 3D effects on Reynolds stresses—just as $\frac{U}{r}/\frac{\partial U}{\partial y}$ was found to be a parameter useful in indicating the degree of curvature effects.

The intent of this work has been to determine any differences between turbulence in 2D mean flows and turbulence in 3D mean flows. As previously discussed, many modeling assumptions used in 2D flows

do not accurately fit 3D flows. This suggests that there may be fundamental differences between 3D and 2D flows (such as coherent structure differences).

An additional objective is to extend our understanding of 3D boundary layers to include cases of strong adverse pressure gradients. Answers to a few fundamental questions are needed. Is a 3D turbulent boundary layer any more or less prone to separate than a 2D one? How does the apparent drop in Reynolds shear stress (associated with 3D turbulent boundary layers) affect the boundary layer's resistance to separation? Considering that 3D mean flow causes a decrease in Reynolds shear stress, it seems likely that such a boundary layer is more prone to separate in the face of a given longitudinal pressure rise.

This study presents new data on the effects of axial adverse pressure on a shear driven, axially symmetric, 3D turbulent boundary layer along a stationary cylinder. Calculations using a Reynolds-stress equation model are compared with the data. Terms in the transport equations are extracted from the data in order to test various turbulence models.

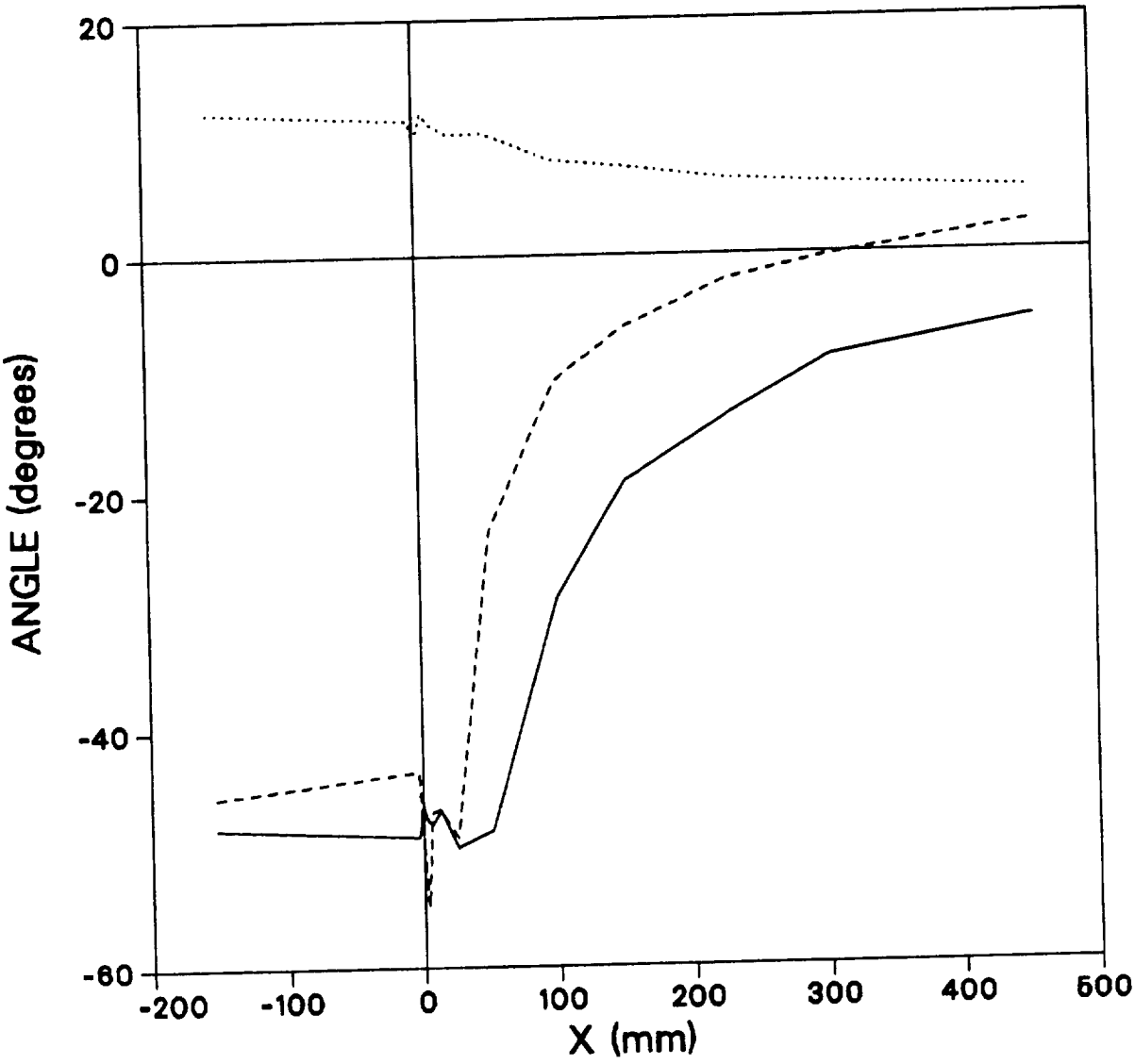

Figure 1.1 Strain Rate and Stress Directions, Relaxing Shear Driven Flow, along a streamline 3 mm up from the wall, ... Flow angle, - - - $Tan^{-1}[(\partial W/\partial r - W/r)/(\partial U/\partial y)]$, —— $Tan^{-1}(\frac{-\overline{vw}}{-\overline{uv}})$.

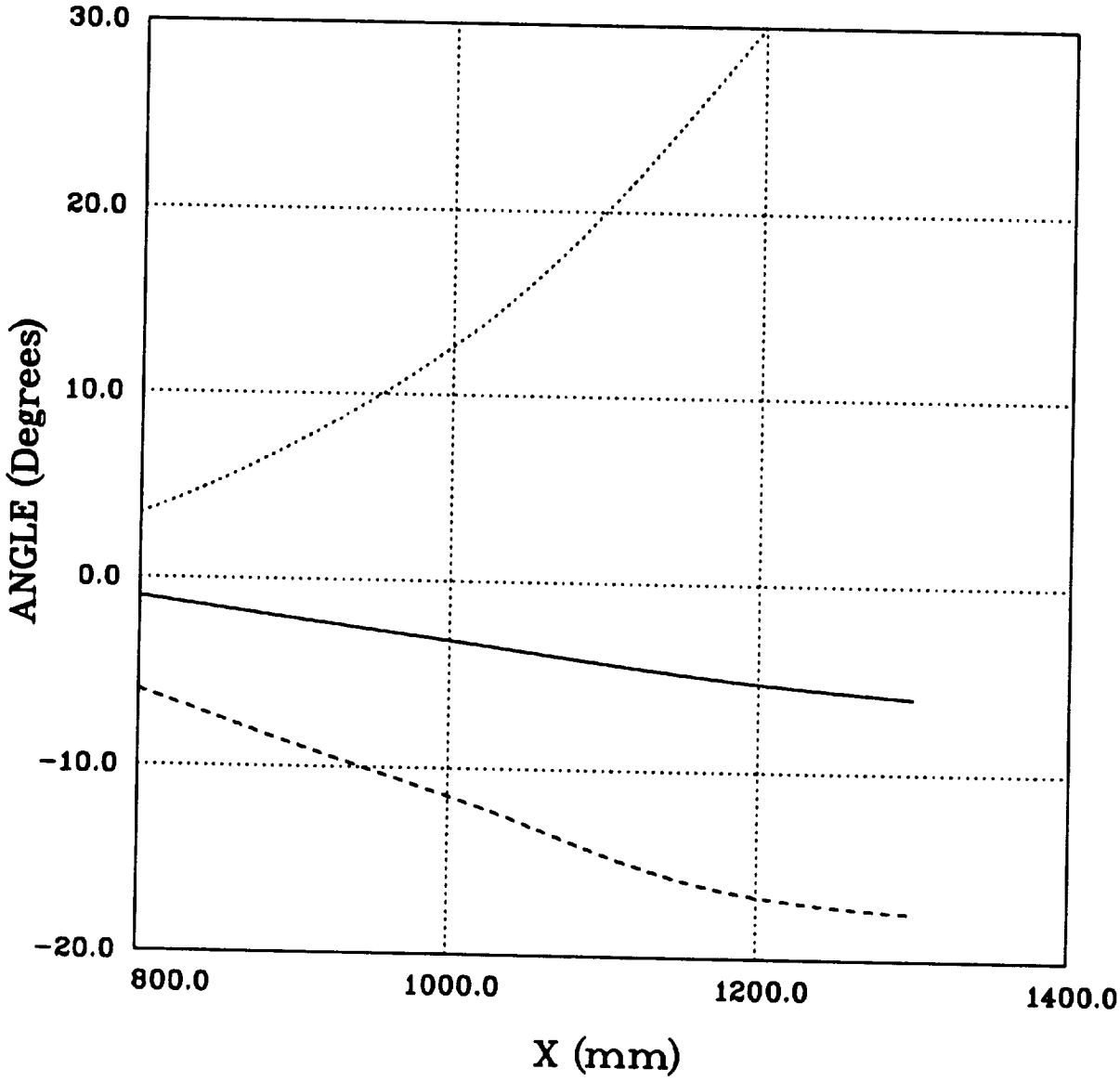

Figure 1.2 Strain Rate and Stress Directions, for NLR "Infinite" Swept Wing Flow along a streamline 14mm up from the wall at the upstream station, - - - $Tan^{-1}[(\partial W/\partial r - W/r)/(\partial U/\partial y)]$, —— $Tan^{-1}(\frac{-\overline{vw}}{-\overline{uv}})$, ... Flow angle.

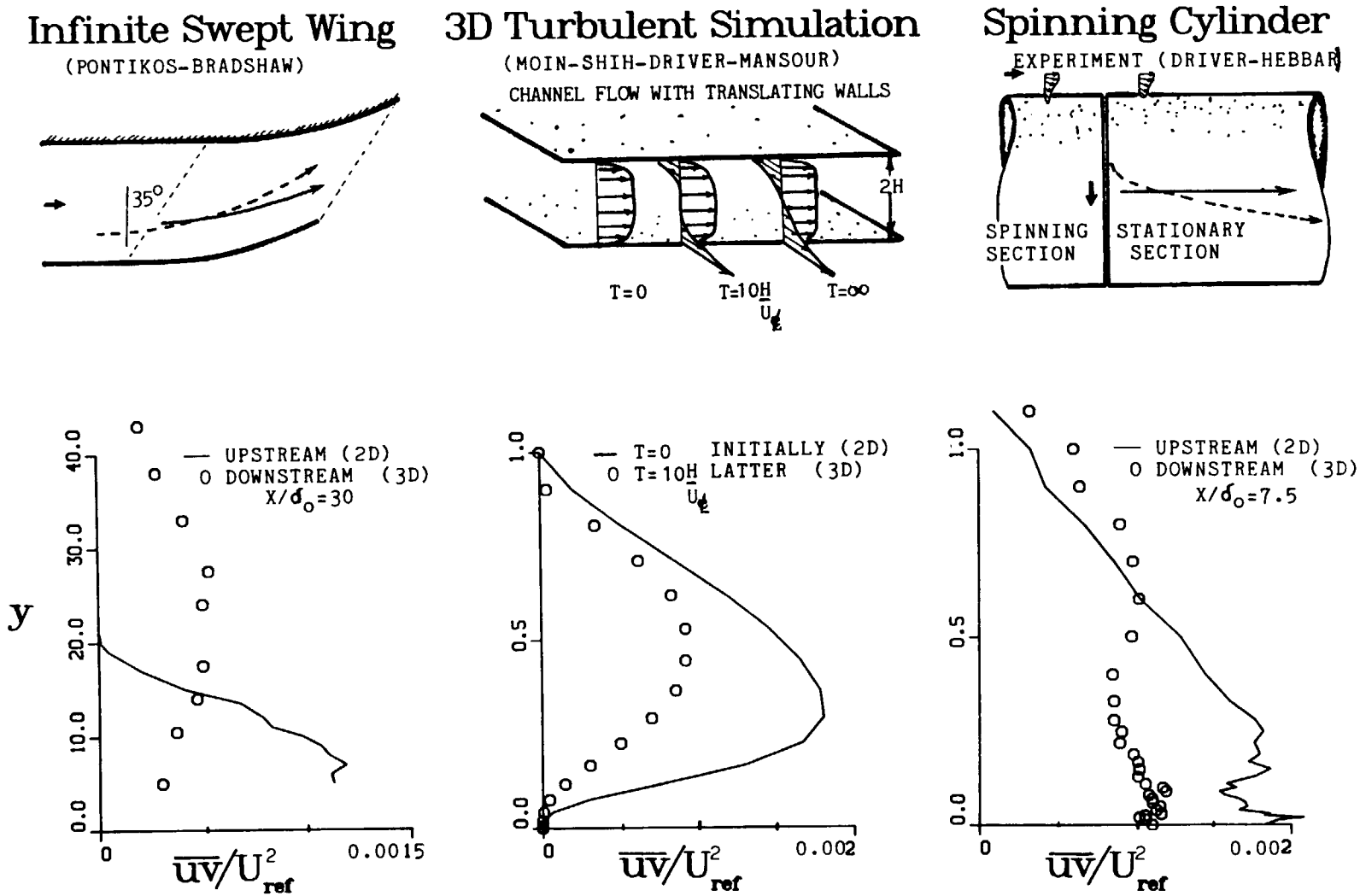

Figure 1.3 Reynolds Shear Stress decay in 3-D Flows, —— Two-dimensional flow, ○ three-dimensional flow.

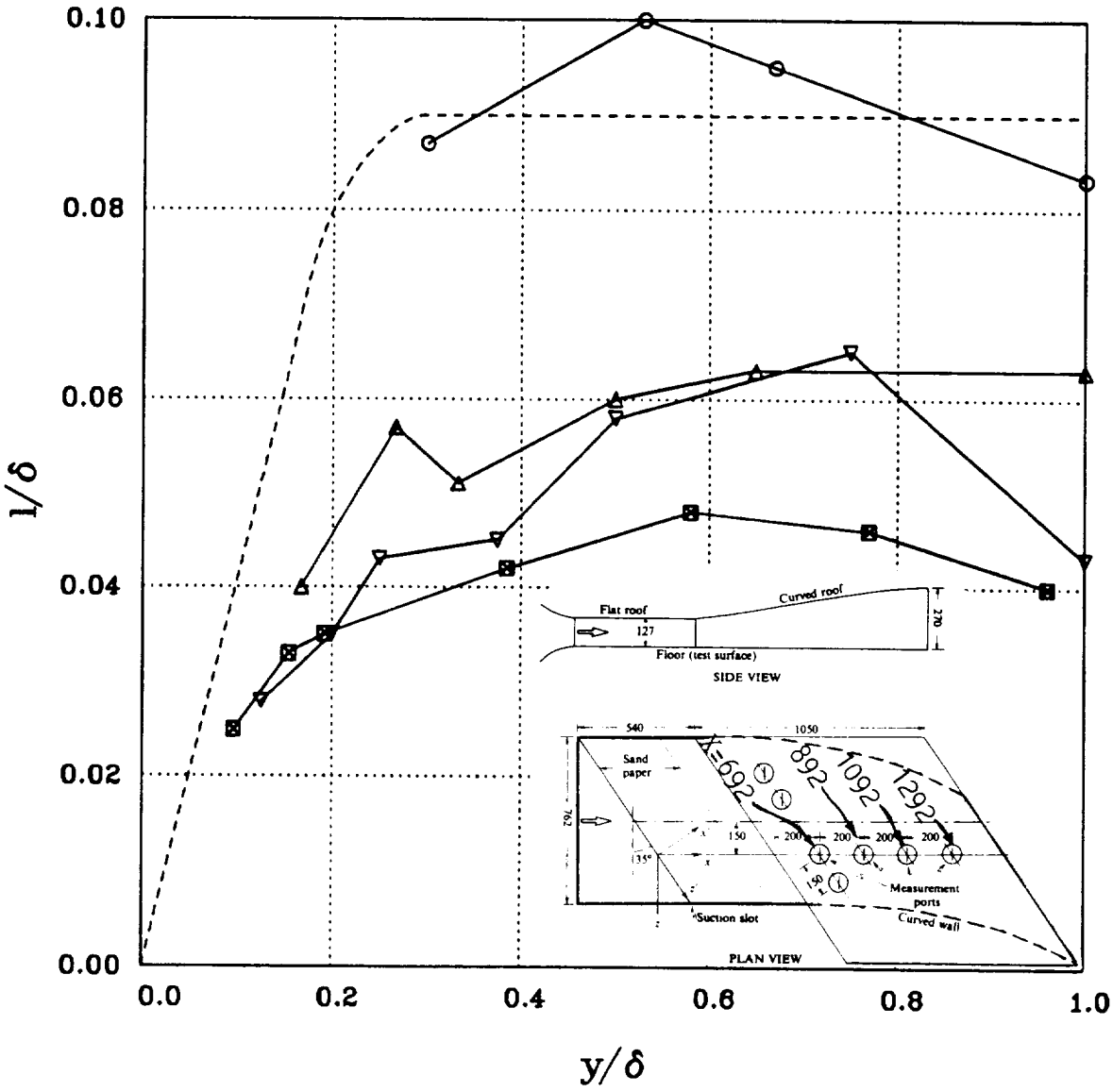

Figure 1.4 Mixing Length Distribution, "Infinite" Swept Wing (Bradshaw-Pontikos), ◯ x=692mm, △ x=892mm, ▽ x=1092mm, ⊠ x=1292mm, - - - Prandtl Mixing Length.

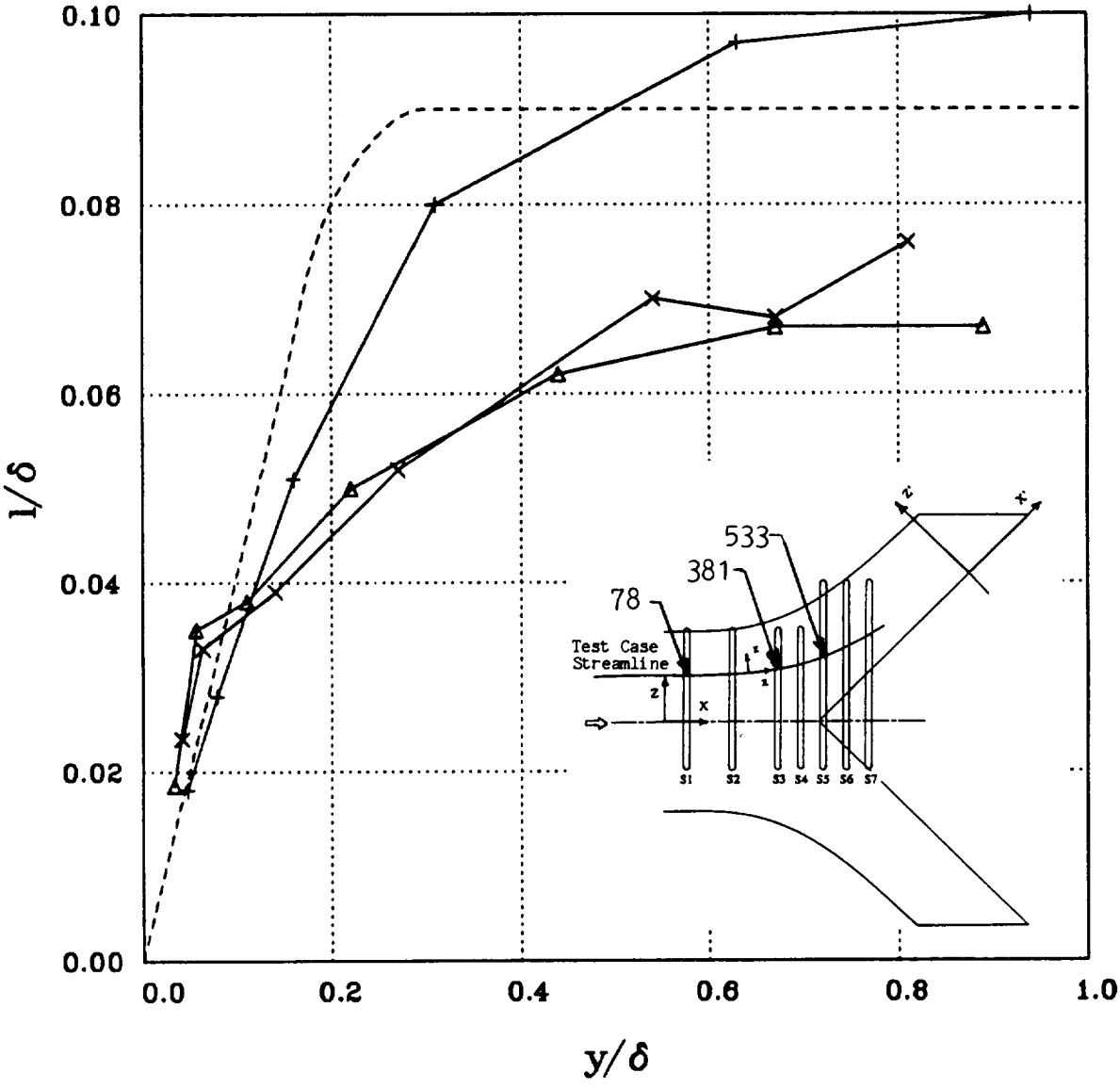

Figure 1.5 Mixing Length Distribution, Wedge Body Junction (Anderson-Eaton), + x=78mm, × x=381mm, △ x=533mm, - - - Prandtl Mixing Length.

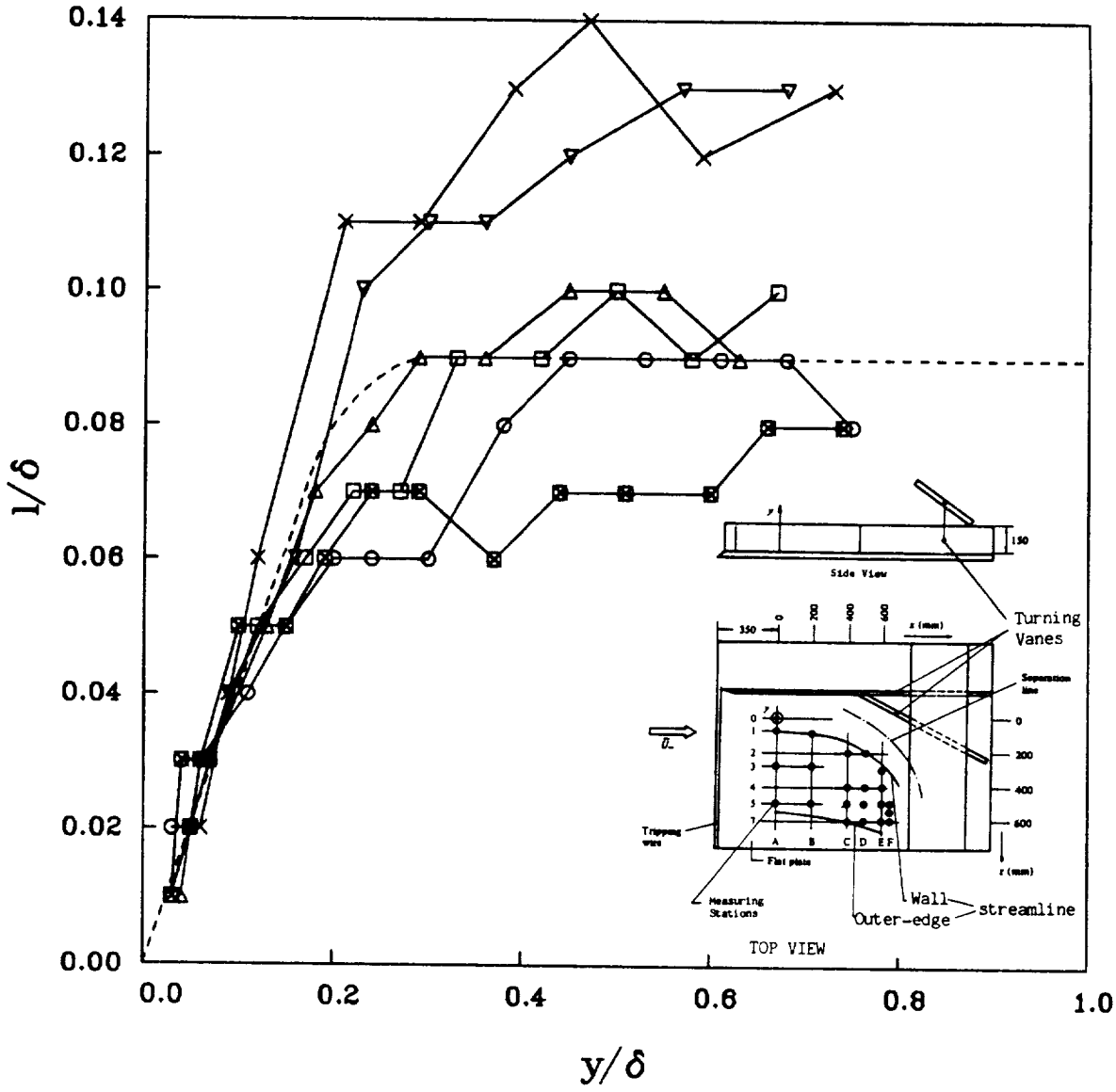

Figure 1.6 Mixing Length Distribution, Turning Flow (Muller), × A5 x=0mm,
▽ B5 x=200mm, △ C5 x=400mm, □ D5 x=450mm,
◯ E5 x=500mm, ⊠ E3 x=500mm z=300mm,
- - - Prandtl Mixing Length.

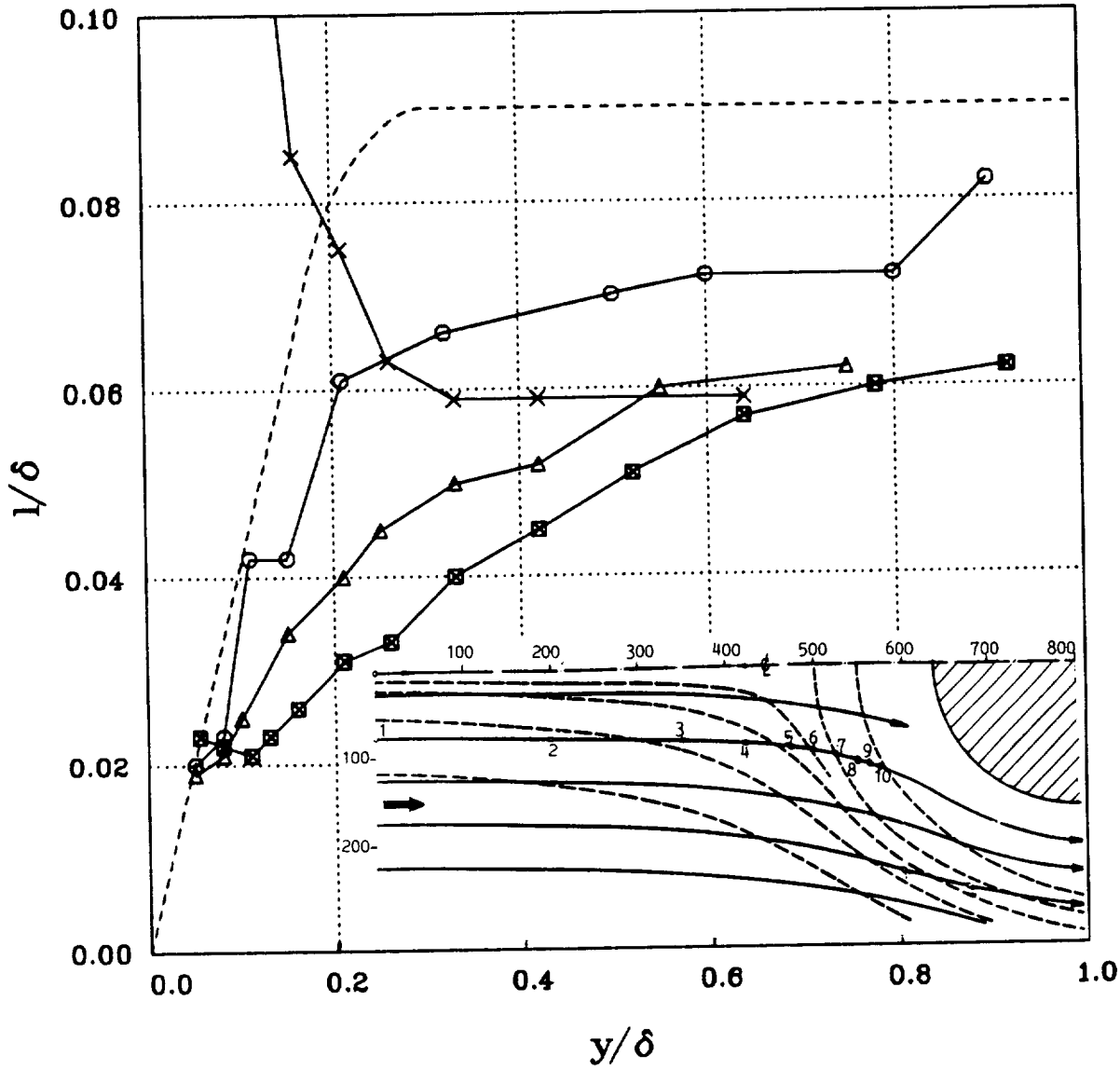

Figure 1.7 Mixing Length Distribution, Wing Body Junction (DeChow-Felsch), ○ S1 x=0mm, △ S6 x=500mm, ⊠ S8 x=550mm, × S10 x=575mm, - - - Prandtl Mixing Length.

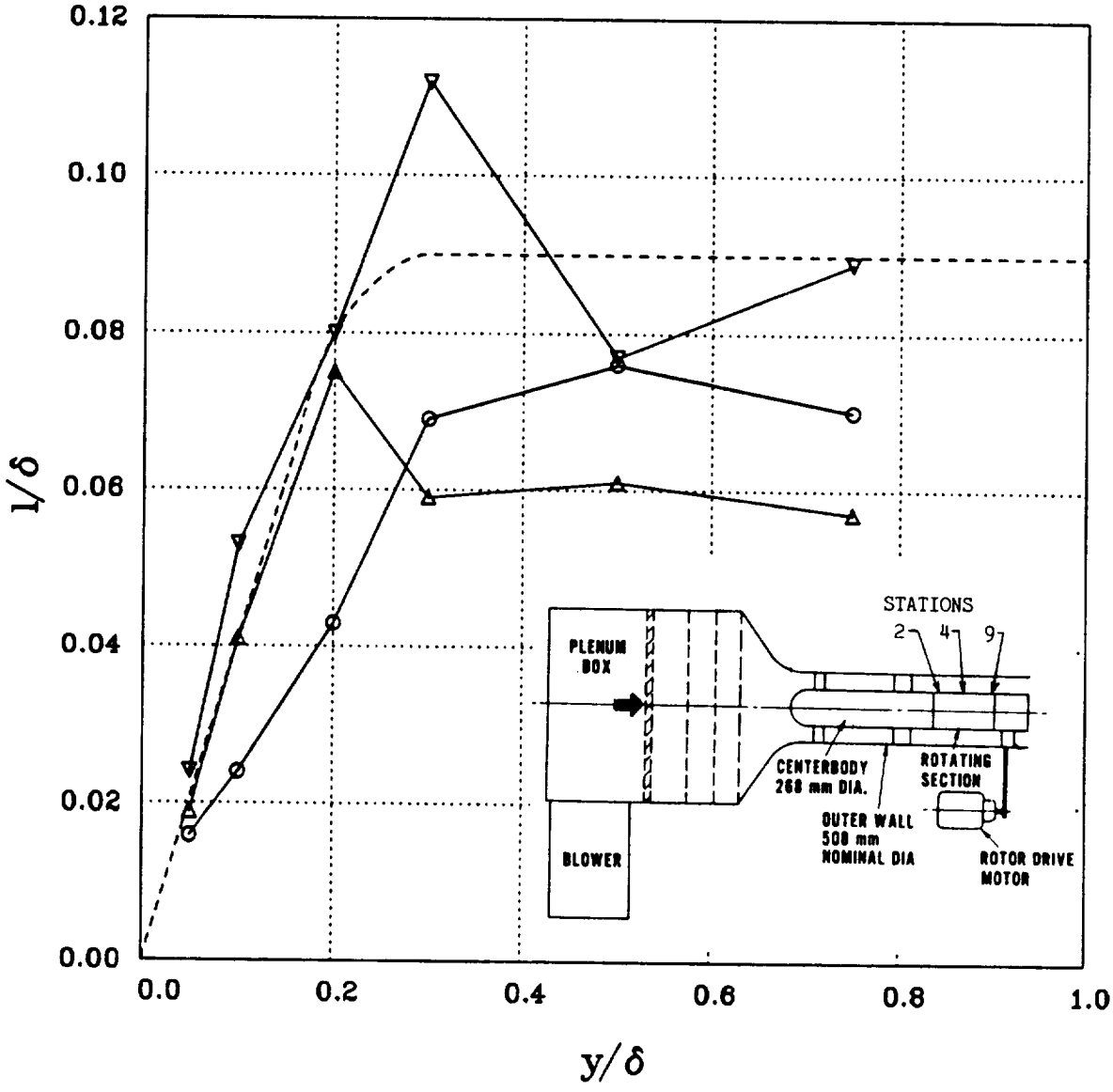

Figure 1.8 Mixing Length Distribution, Spinning Cylinder (Lohmann),
○ Station 2, △ Station 4, ▽ Station 9, - - - Prandtl Mixing Length.

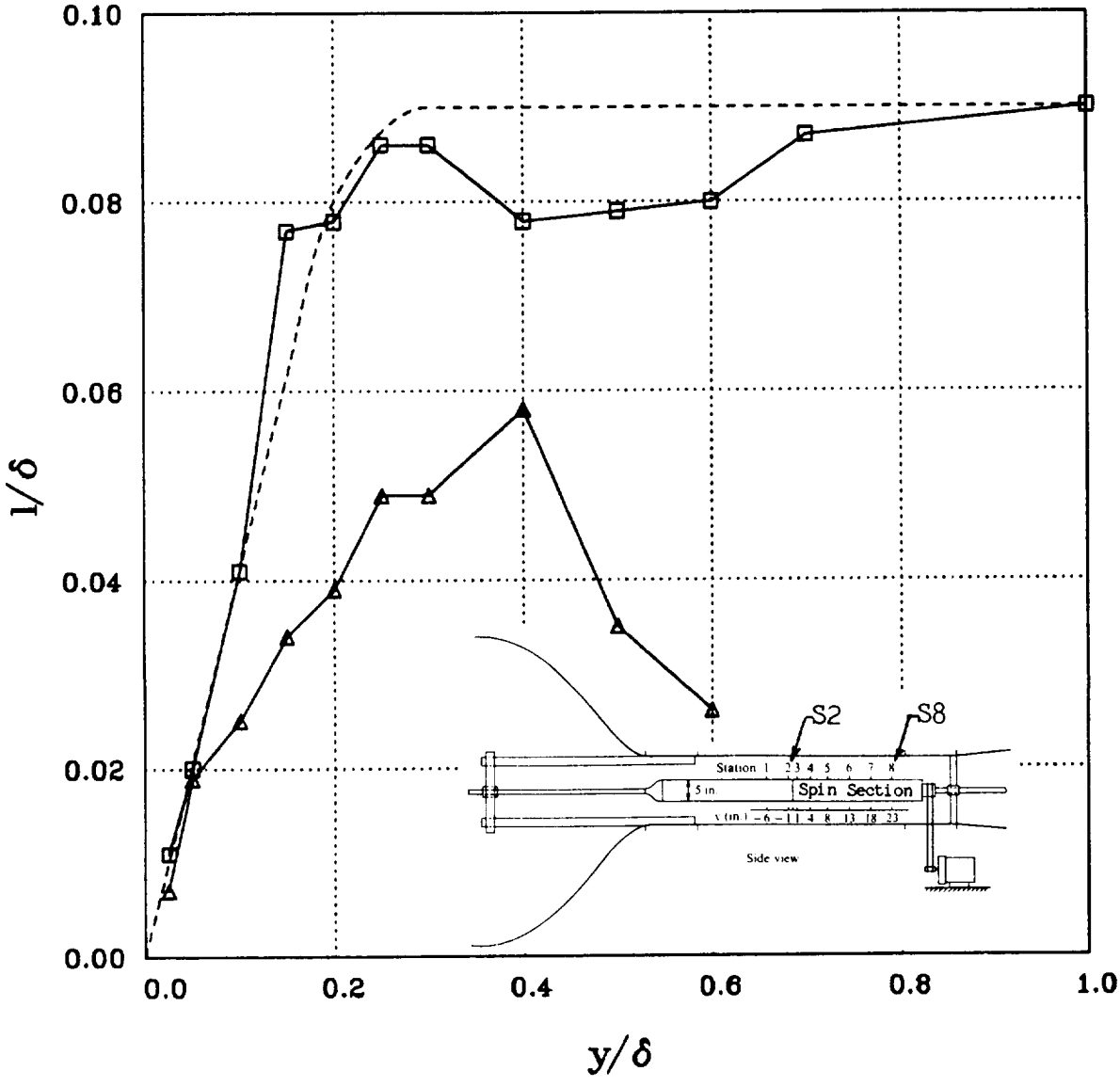

Figure 1.9 Mixing Length Distribution, Spinning Cylinder (Bissonnette-Mellor), △ S2 Beginning of Spin, □ S8 End of spin, - - - Prandtl Mixing Length.

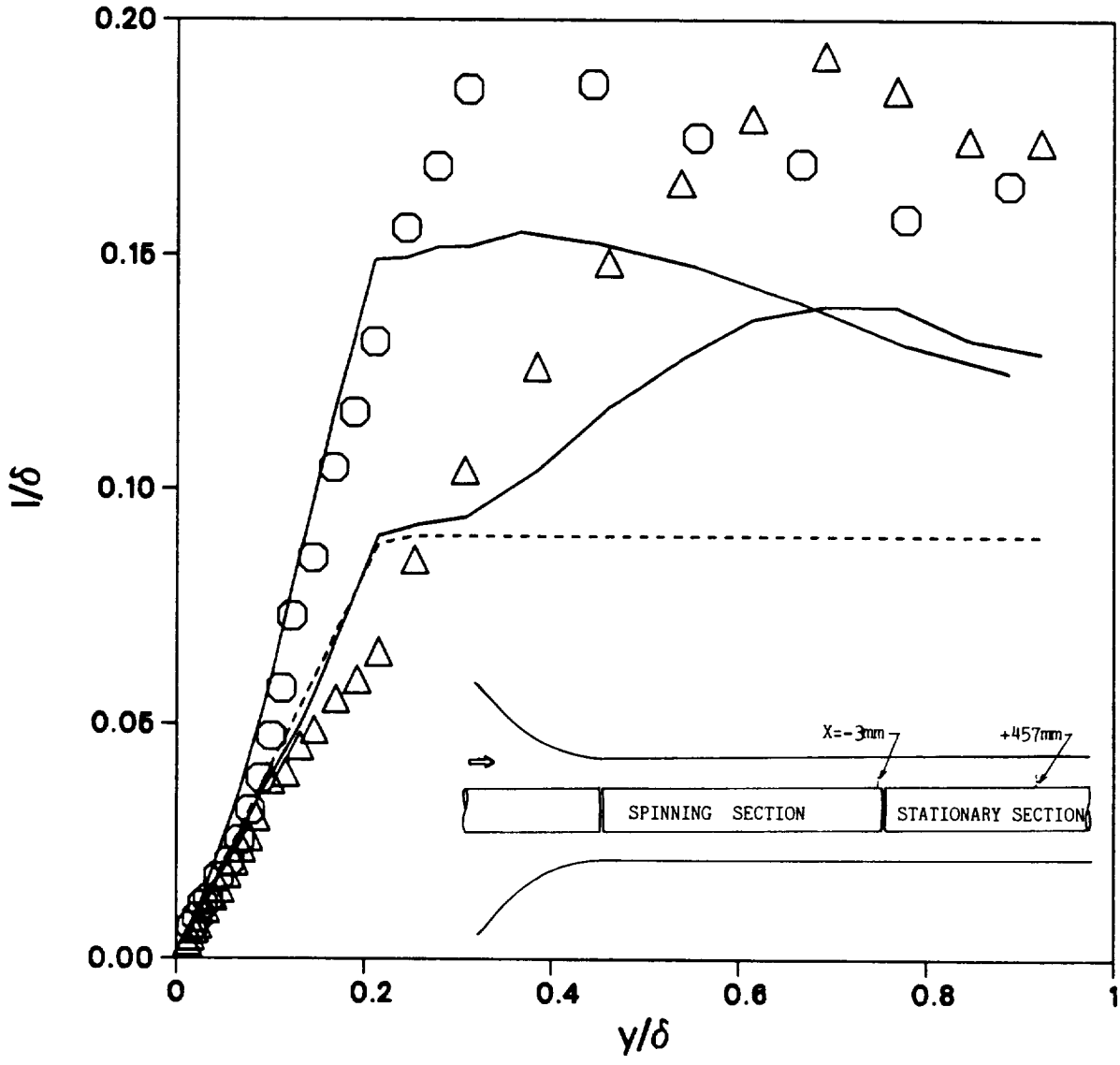

Figure 1.10 Mixing Length Distribution, Relaxation from Spinning Cylinder Flow (Driver-Hebbar), ○ x=-3mm, △ x=457mm, —— $l=l_o(1-7Ri)$, - - - Prandtl Mixing Length.

2 EXPERIMENT FACILITY

The experimental facility, described in this section, provides for the independent study of pressure gradient effects and transverse strain effects, as well as the combined effects of pressure gradient and transverse strain. To understand combined effects, it is necessary to study the individual effects separately in the same facility using the same instruments—this enables the cause and effect relationship to be more easily distinguished. This section also describes the geometry and boundary conditions for these experiments. The instruments used to probe this flow are also described along with the estimated uncertainties for each of these measurements.

Boundary layer flow is often subjected to lateral forces from transverse pressure gradient. One way to simulate these transverse pressure gradient forces is to laterally move the wall beneath the boundary layer. This enables one to easily study various degrees of 3D flow skewing by merely changing the wall speed. Furthermore, flows which contain no lateral flow variations, such as axisymmetric flows or infinite span flows, are far easier to study experimentally, computationally, and analytically. Consequently, an axisymmetric spinning-cylinder geometry was adopted (in which the axis is aligned with external flow) (fig. 2.1). Transverse flow develops on a section of cylinder which is made to rotate at selected speeds with respect to free-stream velocity. Downstream, the transverse flow decays with distance along a stationary section of cylinder.

This flow is characterized by the means of flow zones as shown in figure 2.1. Upstream, on a stationary section, a turbulent 2D boundary layer develops on an axially symmetric cylinder (2D boundary layer zone). The flow then passes over a rotating section of cylinder and the transverse velocity of the cylinder's surface generates a large component of cross flow velocity near the surface (3D interaction zone). Away from the wall, where the effect of this new boundary condition is yet to be felt, the flow remains 2D. Further along the rotating cylinder, the transverse flow reaches the edge of the boundary layer and the flow begins to evolve into a collateral state. As the flow on the spinning cylinder approaches the collateral condition (i.e., unidirectional when viewed from the translating wall) the flow begins to take on the characteristics of a 2D boundary layer again (2D zone). Further downstream, the flow passes on to a stationary, third section of cylinder where the new boundary condition reduces the lateral flow near the surface of the cylinder. The noncollateral condition that develops is a classical 3D boundary layer with a high degree of skewing (3D zone). Far downstream, the boundary layer skewing diminishes to the point that the flow is nearly 2D and flowing parallel with the cylinder's axis (2D zone).

2.1 Wind Tunnel

The experiment was conducted in a low-speed open circuit wind tunnel with the cylinder mounted along its centerline. Sketches of the tunnel are shown in figures 2.2 and 2.3. This facility is a modified version of the rig previously used by Higuchi and Rubesin (ref. 30), and Driver and Hebbar (refs. 12 and 34).

2.1.1 Facility Description

The inlet bell-mouth and settling chamber contained a honeycomb with cells of 4.8 mm diam by 152 mm followed by three fine meshed screens (0.27 mm diam wire woven with 1.9 mm spacing). A

9:1 contraction ratio nozzle delivered flow to the test section. The test section cross section measured 310 mm by 310 mm at the inlet and is 1830 mm long. All four test section walls were contoured from flexible plexiglas to create the diverging portion of the tunnel walls which produced the adverse pressure gradient. A straight (nearly parallel) section 900 mm in length preceded the flexible part of the test section walls. Downstream, at the test section exit, the walls converged again to join the 330 mm by 330 mm exit duct. The exit duct carried the flow a distance of 3100 mm to a vane-and-stator type axial flow fan powered by a variable speed 5 hp DC motor.

The streamwise pressure gradient in the upstream half of the test section was forced to be zero by diverging the tunnel walls slightly to compensate for the blockage effect of boundary layer growth. The streamwise pressure gradient in the second half of the test section could be adjusted by varying the divergence of the tunnel walls (fig. 2.3). The top and bottom walls were adjusted with screw-threaded rods at five jacking stations, while the sidewalls had permanently fixed contours (in an effort to minimize optical obstruction). Three sets of sidewalls were constructed. (1) A straight set produced a zero pressure gradient; (2) the second set began divergence 1060 mm downstream of the test section entrance, a location coinciding with the junction between spinning and stationary cylinders; and (3) a third set diverged 883 mm downstream of the contraction nozzle to produce a pressure gradient which started on the spinning cylinder and grew to a maximum at the end of the spinning cylinder.

Boundary layer suction was applied through slots on all four walls at a location 38 mm upstream of the start of wall divergence to minimize flow separation on the tunnel walls. Suction removed the inner third of the boundary layer, while pulling the more energetic fluid from the outer portion of the boundary layer into contact with the wall. This mass flow removal (about 10% of the incoming tunnel mass flow) produced an additional adverse pressure gradient, associated with the negative displacement effect of suction.

A 140-mm diameter cylinder, divided into three segments, ran the length of the tunnel along its centerline (fig. 2.2). The upstream fixed section was cantilevered from a support web which was attached to the tunnel in the inlet plenum; this section extended through the inlet nozzle and extended 152 mm into the test section where it joined the central rotating section. The 914 mm long rotating section was simply supported by two precision bearings (New Departure Hyatt no. 5604). A drive motor at the upstream end of the fixed section was connected by a central drive shaft to the rotating section. The downstream end of the spinning cylinder was supported by a second cantilevered fixed section. The spinning section and downstream section are improved versions of the cylinder used by Higuchi and Rubesin (ref. 30) and Driver and Hebbar (refs. 12 and 34); the new cylinders had tighter tolerance on the diameters of the two sections. The new spinning and stationary cylinders were made equal in diameter (140 mm) to within ± 0.04 mm ($y^+ < 4$), and an improvement over the previous cylinder the gap between spinning and stationary sections was closed to within 0.2 mm.

The cylinder was fabricated from aluminum tubing with external and internal surfaces machined to eliminate ellipticity and imbalance. Particular care was taken to make the cylinder segments uniform in diameter at the mating ends. The rotating section was machined while spinning on its bearing mounts during the final stages of manufacturing to insure concentricity of the outer surface with the axis of rotation. The downstream stationary section was likewise carefully machined to conform in diameter to the spinning section. All surfaces were uniform in diameter to ± 0.04 mm and polished for a dull mirror finish. The spinning cylinder was carefully balanced at 5000 rev/min thus minimizing the vibration related displacements to less than ± 0.03 mm ($y^+ < 3$).

The boundary layer that grew on the cylinder surface was considered the test region. Measurements were taken primarily on the downstream stationary section where the flow exhibits 3D effects during relaxation back to a 2D boundary layer (fig. 2.4). To trip and thicken the boundary layer, two boundary layer trips consisting of No. 150 sandpaper 51 mm long were placed on the fixed section of cylinder in the inlet 230 mm and 305 mm upstream of the junction with the spinning section. The experiments were performed at nominal free-stream velocities of 15 and 30 m/sec, and the corresponding free-stream turbulence intensities were approximately 1% and 0.6% respectively. The spinning section of the cylinder (914 mm long) was rotated at circumferential speeds of 0, 15 and 30 m/sec depending on the test being conducted. The boundary-layer thickness at the end of the spinning section was 27 mm ($W_s = U_e = 30$ m/sec) and 18 mm (U_e=30 m/sec and $W_s = 0$) giving a Reynolds number based on momentum thicknesses of 6000 and 4000, respectively. The ratio of δ to cylinder radius, R_o, was 0.39 and 0.26 for these cases.

2.1.2 Specific Geometry for Downstream Pressure Gradient Cases

For the first geometry studied the tunnel wall divergence and pressure gradient was imposed, starting near the junction between spinning and non-spinning sections (at X = –4 mm). The tunnel walls were diverged with the wall displacements shown in table 2.1. Here the maximum pressure gradient occurs downstream of the cylinder's junction (X = 0 mm).

2.1.3 Specific Geometry for Upstream Pressure Gradient Cases

A second case was studied in which tunnel wall divergence and pressure gradient was imposed upstream at X = –182 mm. Wall contour locations are shown in table 2.2. In this case, the peak adverse pressure gradient is located at the cylinder's junction, so the maximum pressure gradient occurred at the location of maximum 3D flow skewing (X = 0 mm).

2.2 Instrumentation

Nonintrusive instruments employing optical techniques were used to make most of the flow-field measurements. Probes were avoided since the downstream disturbance created by a probe has been known to alter the upstream flow when strong adverse pressure gradient is present. This section describes the instruments used to measure this flow.

2.2.1 Surface Measurements

Surface pressures were obtained through 0.3 mm diam static tap orifices drilled in the stationary cylinder. Pressures were sensed with a Datametrics Barocel pressure sensor (Type 581D-10T-2B2-V3X, range 10 Torr) and Signal Conditioner (Type 1015), and read by a PDP-11/34 computer with 12-bit A/D converter (5 mV resolution). Accuracies in measuring C_p were better than ± 0.01 based on repeat runs. Other errors were smaller. Additional surface pressure measurements were performed on the rotatable section while it was not spinning by use of static pressure tubes (2.4 mm diam) taped to the cylinder's surface.

Streamwise surface skin friction was measured with a two beam laser-interferometer oil-flow technique, described in reference 38 (fig. 2.5). Silicone oils with viscosities of 10 and 50 centistoke were

applied to the top of the cylinder. Pressure gradient was shown to have an insignificant (less than 0.5%) influence on the oil thinning rate and no correction was applied. The most significant errors were believed to be due to surface roughness. Although the surface was polished to a dull mirror finish, minute polishing marks on the order of one micron depth may have an effect on the oil film which is only about ten microns thick. Uncertainties in the skin-friction coefficient (C_f) were estimated to be $\pm 10\%$ of the measured value.

Additional skin-friction measurements were performed using a surface pitot tube and Preston and Patel's (ref. 39) calibration relating pitot tube pressure to skin-friction. Pitot tube measurements were made where there was no significant crossflow.

Surface flow direction was obtained using oil-flow techniques. Silicone oils with 10, 30, 50, 100, and 200 centistoke viscosities were applied in dot-sized amounts to the top radial generator of the stationary cylinder. After sufficient tunnel run time ($\approx$10 min), the oil traces were lifted from the cylinder's surface using absorbing paper from which the oil flow direction could be read with an uncertainty of $\pm 0.5°$ for an individual run. Repeat runs were performed in order to determine a flow direction to a final accumulated uncertainty of $\pm 1.5°$.

2.2.2 Flow Field Measurements

Three components of velocity were measured using a three-color, coincidence validating, laser Doppler velocimeter (fig. 2.6). Blue (488 nm), green (514.5 nm), and violet (476 nm) beam pairs were used to measure U cos(30.0°) + W sin(30.0°), V and U cos(–30.0°) + W sin(–30.0°) components of velocity, respectively. Each set of beam pairs was intersected at the spanwise midpoint of the tunnel. Angles between beam pairs were nominally 8.00°, thus creating fringe spacings of 3.498 μm, 3.688 μm, and 3.145 μm for the green, blue, and violet beams, respectively. One beam of each of the beam pairs was Bragg shifted 40 Mhz in order to impose a direction bias on the doppler signal, thus allowing direction to be distinguished from the signal. Half-micron-diam polystyrene particles, injected at the inlet of the tunnel, were used to seed the flow which passes through the laser beams (at the beam intersection point). Scattered light from seed particles in the scattering volumes (0.3 mm diam by 3 mm long) was collected by photomultiplier tubes viewing from 30° to the side of direct forward scatter. An aperture on the receiving optics effectively reduced the field of view to a volume $\approx$0.3 mm diam by 1 mm (or $d^+ = 24$ by $l^+ = 80$). This minimal probe volume reduced the probability of multiple (or virtual) seed particle measurements. Counters (TSI Inc. model 1990c), sensing the electrical signal from the photo-multiplier tubes (proportional to scattered light intensity), measured the time for 32 periods with 1 nanosecond resolution. The digital signal created by the counter was read and recorded by a Micro-VAX computer. Occasionally, significant counting errors were encountered where the counter failed to detect a local maximum in the signal, effectively counting the time for 33 periods instead of the desired 32 periods. This was considered noise and the counters discarded most of these measurements through the periodicity test. As a precaution, histogram pruning was carried out in a attempt to eliminate any bad measurements that were counted, however once in a while these spurious signals were indistinguishable from good signals and were erroneously included in the statistical averages (less than 0.1% of the time).

Velocity triplets were decomposed into average and fluctuating components of velocity and averaged together using a 3D velocity bias correction, to obtain U, V, and W mean flow velocities to ± 0.3 m/sec (1% of free stream) and $\overline{uu}$, $\overline{vv}$ and $\overline{ww}$ with accuracy of $\pm 10\%$ of local values. Reynolds shear stresses, $\overline{uv}$,

$\overline{vw}$ and $\overline{uw}$ were determined with accuracies of $\pm 5\%$ of $\sqrt{\overline{u_i^2}}\sqrt{\overline{u_j^2}}$. Velocity triple-product correlations ($\overline{u_i u_j u_k}$), were also calculated; with accuracies of $\pm 4\%$ of $\sqrt{\overline{u_i^2}}\sqrt{\overline{u_j^2}}\sqrt{\overline{u_k^2}}$, high uncertainties are expected in higher order statistics.

The 3D velocity bias correction applied to the data involved multiplying every velocity measurement by a weight function equal to $\overline{Q}$/Q(t) (where $Q = \sqrt{U^2 + V^2 + W^2}$ is the instantaneous resultant velocity). The effect of multiplying this weight function was insignificant in most regions of the flow, however, where the Q/k becomes small the effect on various measured quantities can be significant.

2.3 Flowfield Quality

Good flow axisymmetry was inferred from surface pressures measured circumferentially around the cylinder. Circumferential variations in C_p were less than 0.25% of the upstream dynamic pressure over most of the cylinder. The largest variations (0.5%) were seen at X = 6 mm, where the axial pressure gradient is a maximum (fig. 2.7).

Flow axisymmetry was checked under non-spinning conditions at several stations using a pitot pressure tube (Preston tube method) at the cylinder surface. The skin friction measurements, derived from these pressure measurements, are shown in figure 2.8 for stations X = –762, –305, and –76 mm along the the cylinder. Generally, circumferential distributions of skin friction were uniform to within $\pm 4\%$ (of upstream C_f). The last station is located in the strong adverse pressure gradient portion of the flow; here skin-friction variations are less than 6% of the upstream level, indicating that no significant asymmetries are developing. Nonuniform deposits of seed particles in inlet screens are a major cause of spanwise nonuniformity. Care was taken to clean the laser Doppler velocimeter seed deposits from the inlet screens.

Pressure fluctuations from the downstream fan were detected by use of a high-frequency-response pressure transducer connected through a short length of tubing to various static pressure orifices. Variations in pressure were largest at the downstream end of the test section (nearest the fan); here pressure fluctuations were less than $\pm 1\%$ of the dynamic pressure with frequencies on the order of 25 Hz. Additional test with hot-wire probes also sensed flow variations of 0.5% in magnitude and in the 25 Hz range.

2.4 Computations

Computations were performed using a boundary-layer code developed by Wilcox (ref. 40) for Ames Research Center and is referred to here as the SPIN CODE. The computations solve a finite-differenced set of parabolic boundary-layer equations implicitly in Y and marching in X. The program can incorporate different turbulence models ranging from a simple, mixing-length model to a more complicated Reynolds-stress-equation model (RSE). Earlier calculations by Higuchi and Rubesin (ref. 31) indicated that the RSE model resulted in better agreement with experiments than did the eddy-viscosity models. Therefore, the computations shown in this paper were done with the RSE model.

The RSE model used here was based on the closure equations of Launder, Reece and Rodi (ref. 41), but with length scale established with the specific dissipation rate (ref. 42), ω ($\omega = \varepsilon/0.09k$). The near-wall region is treated with unique damping models which are consistent with those of reference 41.

The computations start upstream on the spinning section at $x/\delta_o = -15$ with experimentally measured values of mean velocities and Reynolds stresses used as starting conditions. Starting the calculations with experimental data ensures that downstream differences between the calculations and experiment are caused by the model assumptions and not the initial conditions.

Table 2.1 Wall displacement settings for adverse pressure gradient case D.

	Wall Displacement		Tunnel dimensions no wall displacement		
X	Top/Bottom	Side	Width	Height	
mm	mm	mm	mm	mm	
0	0	0	305	318	
1010	0	0	305	318	
1019	0	0	305	318	<——— top & bottom wall slot
1032	0	-4	305	318	<——— side wall slots
1061	0	-5	305	319	<——— start wall divergence
1065	0	-5	305	319	<——— Cylinder Jct.
1092	2	-2	305	319	
1118	6	4	305	320	
1143	11	9	305	320	
1168	15	13.5	305	320	
1194	19.8	17.5	305	320	
1219	24.3	21.3	305	321	
1245	25.6	24.1	305	321	
1270	30.0	26.7	305	321	
1321	33.8	30.5	305	322	
1372	37.8	32.5	305	323	
1422	40.6	33.5	305	324	
1473	42.9	34.5	305	324	
1524	39.6	35.6	305	325	
1575	34.0	36.6	305	326	
1600	30.9	36.6	305	326	
1626	26.9	36.6	305	326	
1651	22.2	36.6	305	327	
1676	17.5	36.3	305	327	
1702	12.3	32.5	305	327	
1727	5.6	25.4	305	327	
1753	2.3	17.8	305	327	
1778	-1.1	11.4	305	327	
1803	-2.7	10.2	305	328	
1829	-3.8	10.2	305	329	

Table 2.2 Wall displacement settings for adverse pressure gradient cases B & C.

	Wall Displacement		Tunnel dimensions no wall displacement		
X	Top/Bottom	Side	Width	Height	
mm	mm	mm	mm	mm	
0	0	0	305	306	
832	0	0	305	315	
841	0	0	305	316	<——— top & bottom wall slot
854	0	-4	305	316	<——— side wall slots
883	0	-5	305	317	<——— start wall divergence
914	2	-2	305	317	
940	7	4	305	317	
965	11	9	305	318	
991	15	13.5	305	318	
1016	20.6	17.5	305	318	
1041	24.3	21.3	305	319	
1065	26.9	24.1	305	319	<——— Cylinder junction
1092	30.0	26.7	305	319	
1118	32.5	29.0	305	320	
1143	33.9	30.5	305	320	
1168	36.2	31.8	305	320	
1219	39.6	33.5	305	321	
1270	41.9	35.3	305	321	
1321	43.7	37.1	305	322	
1372	45.1	38.9	305	323	
1422	45.2	40.4	305	324	
1473	44.5	41.9	305	324	
1524	38.7	43.4	305	325	
1575	34.2	45.0	305	326	
1600	30.9	45.7	305	326	
1626	26.9	46.2	305	326	
1651	22.2	46.2	305	327	
1676	17.5	44.5	305	327	
1702	12.3	38.1	305	327	
1727	5.6	28.5	305	327	
1753	2.3	19.1	305	327	
1778	-1.1	12.2	305	328	
1803	-2.7	10.2	305	328	
1829	-3.8	10.2	305	329	

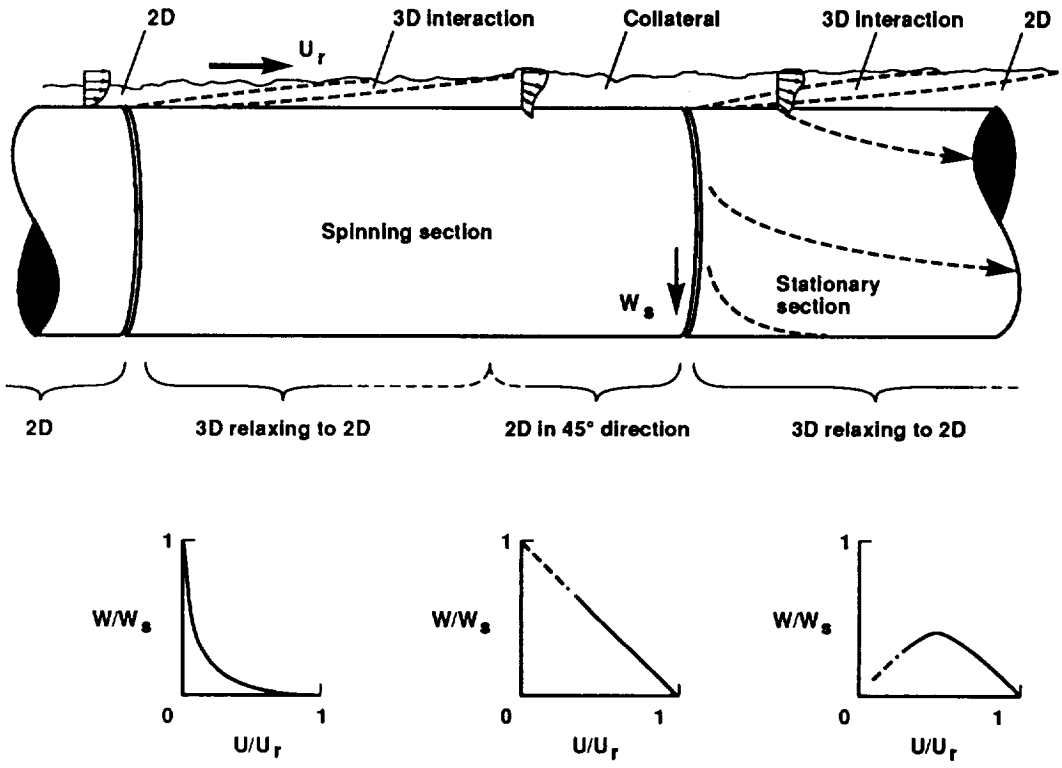

Figure 2.1 Spinning Cylinder Flow Zones.

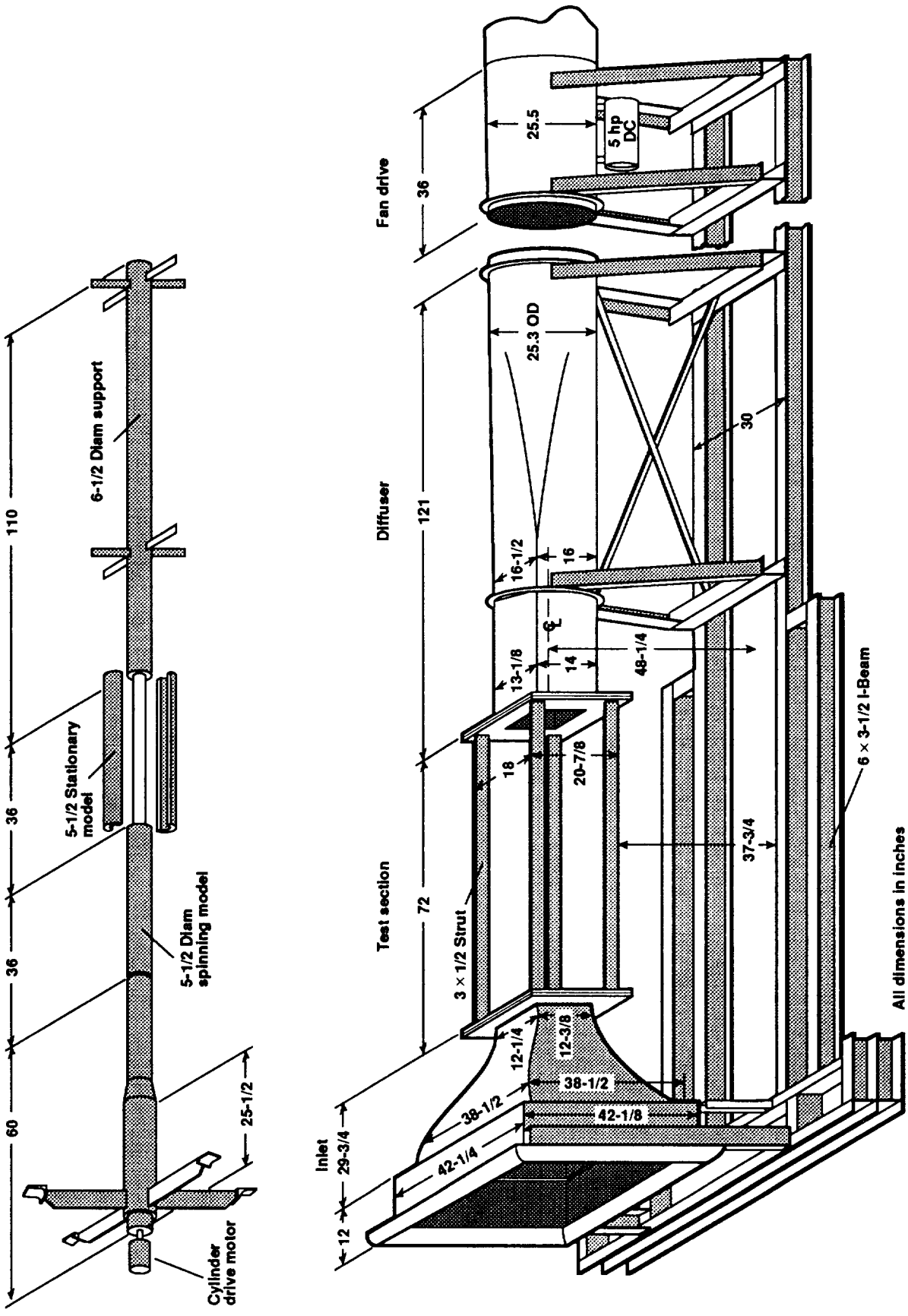

Figure 2.2 Wind tunnel geometry.

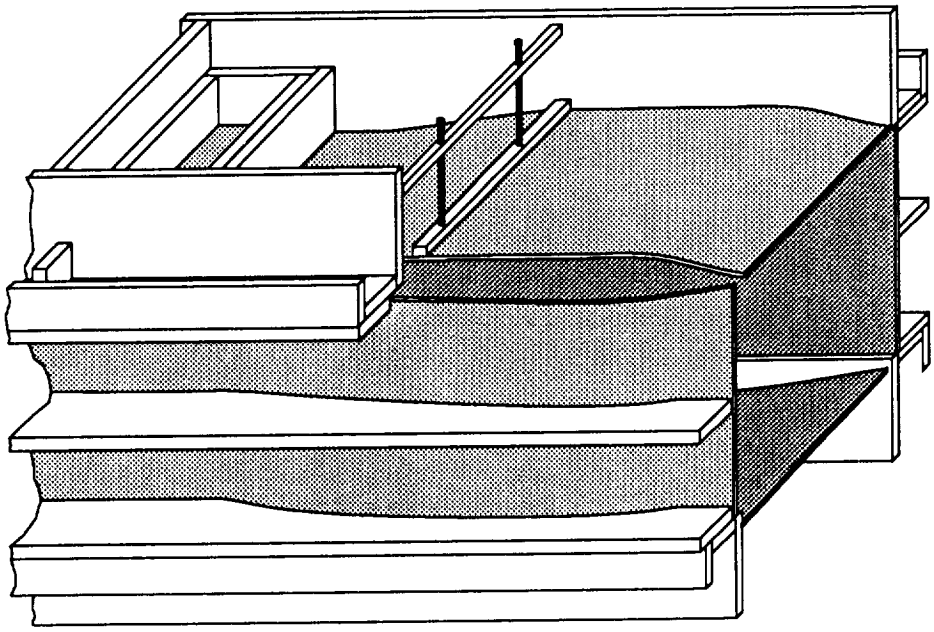

Figure 2.3 Pressure Gradient Test Section Geometry

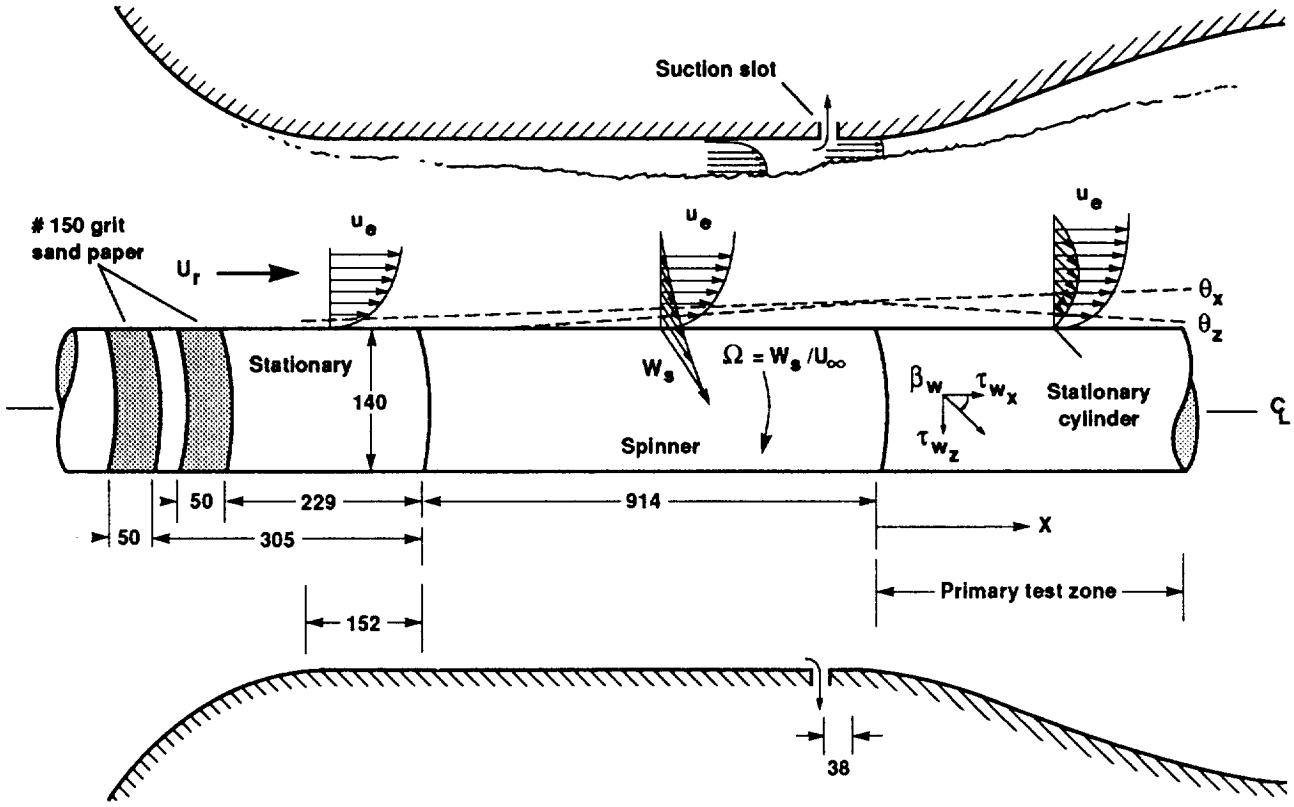

Figure 2.4 Flow Conditions and Test Section Geometry.

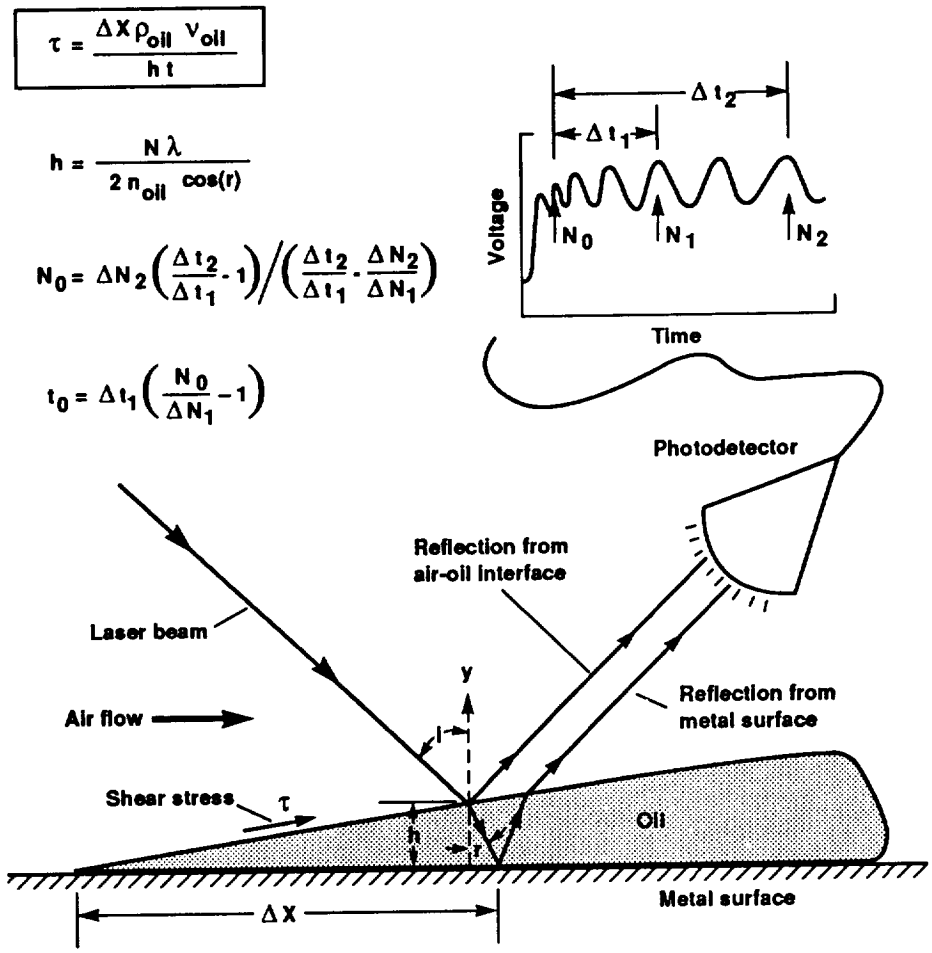

Figure 2.5 Laser oil-flow interferometer technique for measuring Skin-Friction (single beam system).

Figure 2.6 Three-component laser Doppler velocity measuring system.

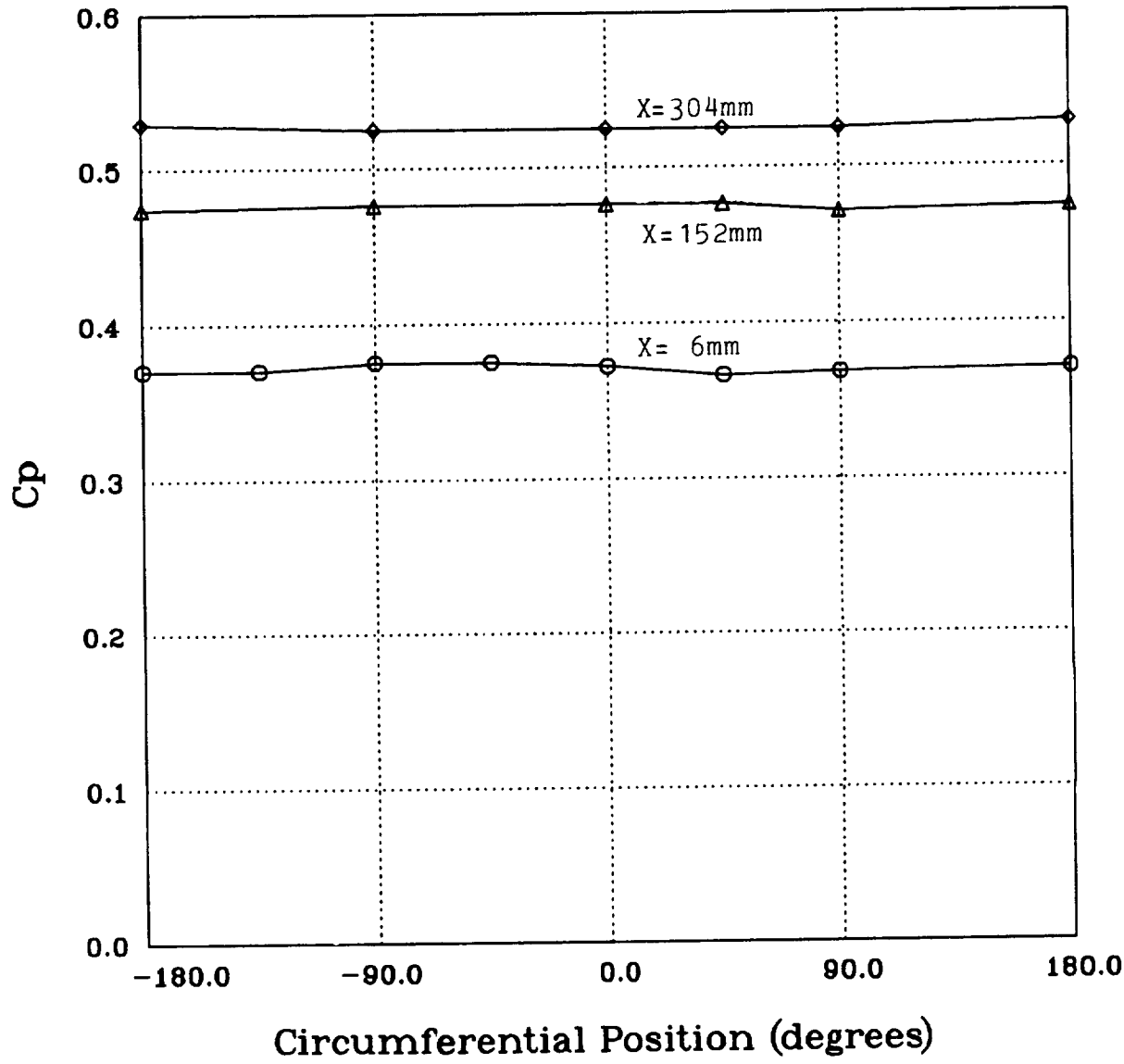

Figure 2.7 Circumferential Distribution of Surface Pressure, case B.S0, ◯ x=6mm, △ x=152mm, ◇ x=304mm.

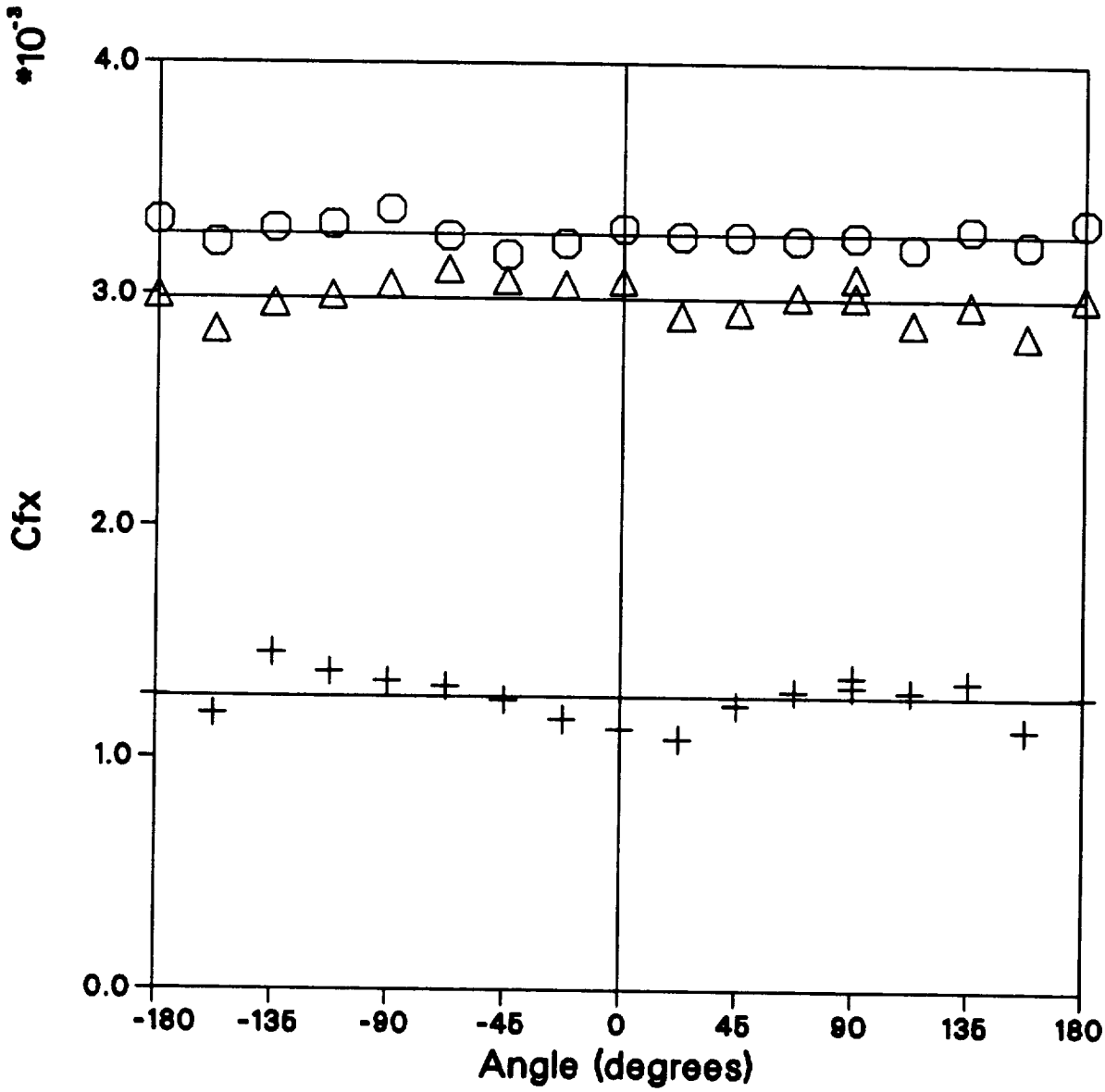

Figure 2.8 Circumferential Distribution of Skin-Friction, case B.S0, ○ x=-761mm, △ x=-304mm, + x=-75mm.

3 PARAMETRIC STUDY

Pressure gradient and spin rate were varied independently in an effort to determine the sensitivity of turbulence in the boundary layer to varying degrees of transverse strain and streamwise deceleration.

3.1 Pressure Gradient Variations

Four cases of pressure gradient were created using different tunnel side wall geometries.

(1) For case A, the walls are parallel (zero $\partial P/\partial x$).

(2) For case B, the wall diverged with mild side wall boundary layer suction, starting at X = –180 mm (mild $\partial P/\partial x > 0$).

(3) For case C, the wall diverged with strong side wall boundary layer suction, starting at X = –180 mm (strong $\partial P/\partial x > 0$).

(4) For case D, the wall diverged with strong side wall boundary layer suction, starting at X = –4 mm (strong $\partial P/\partial x > 0$).

In order to distinguish the different cases, each case will be referred to as case A, B, C, or D. Pressure distributions for these cases with zero cylinder rotation can be seen in figure 3.1. Cases B and C are identical in geometry; the difference in pressure gradient is a result of different tunnel side-wall boundary layer removal rates. In case B, sidewall suction was insufficient to eliminate flow separation in the corners of the diverging test section. For case C, suction was increased in the corners to eliminate flow separation in the outer wall corners, but flow detachment now occurred on the surface of the cylinder at X $\approx$ 50 with reattachment at $\approx$225 mm. Case D has an identical sidewall diffuser shape to that of case C, except the sidewall divergence starts at X = –4 mm instead of –180 mm. Here the cylinder boundary layer is nearly detached by X = 225 mm.

Pressure at the edge of the boundary layer was estimated using Bernouli's equation and laser doppler velocity measurements (see the lines in fig. 3.1). Static pressure outside the boundary layer is nearly equal to the pressure measured on the cylinder's surface; this indicates that boundary layer approximations may be reasonable to use in the regions where the flow is attached. Notice that even though the tunnel wall divergence starts at X = –180 mm for cases B and C and X = –5 mm for case D, the pressure gradient actually starts upstream at –225 mm and –50 mm, respectively.

Stream function, determined from mean velocity measurements, is shown in figure 3.2. The streamlines diverge from the wall for all cases as expected in an adverse pressure gradient boundary layer. Flow separation is evident in case C; here the pressure rise and pressure gradient were increased by 15% over case B. Case D, in which the pressure rise starts farther downstream, shows nearly the same stream function divergence as was seen in case C except that the divergence starts 180 mm downstream.

When the cylinder was spinning, (tangential speed $W_s = U_\tau$), the pressure distributions were nearly the same as for the non-spinning cases (fig. 3.3). Again static pressures at the edge of the boundary layer

were estimated using Bernouli's equation and the laser Doppler velocity measurements (also shown); the difference in pressure across the boundary layer is quite small.

Stream function contours (fig. 3.4) diverge somewhat less than for the corresponding non-spinning cases. Furthermore, case C remains attached, unlike the non-spinning case which separated. The spinning case stays attached not because of transverse strain effects, but instead because of transverse curvature effects, which in this situation tend to destabilize and increase turbulence in the boundary layer (see appendix A for further discussion).

3.2 Spin Rate Variations

In an effort to vary the degree of 3D skewing present in the boundary layer, four cases of spin-rate were considered.

(1) W_s/U_τ = 0(m/s)/30(m/s) = 0.0
(2) W_s/U_τ = 15(m/s)/30(m/s) = 0.5
(3) W_s/U_τ = 30(m/s)/30(m/s) = 1.0
(4) W_s/U_τ = 30(m/s)/15(m/s) = 2.0

To further identify the cases of different spin-rates, each pressure gradient cases A, B, C, and D will include a suffix S0, S$\frac{1}{2}$, S1, or S2 corresponding to the spin rate W_s/U_τ =0, $\frac{1}{2}$, 1, or 2, respectively. For example, the upstream case of weak adverse pressure gradient with the cylinder spinning at a rate W_s/U_τ = 1 is referred to as case B.S1.

Streamwise surface skin-friction measurements for cases B.S0, B.S$\frac{1}{2}$, and B.S1 are shown in figure 3.5. Streamwise friction increases with increased rotation speed because of an increase in turbulent energy associated with rotation. The transverse skin friction was estimated by using the tangent of the measured surface oil flow direction and the measured streamwise skin friction (fig. 3.6). Predictably, transverse skin friction increases with increasing rotational velocity of the cylinder. Figure 3.7 shows the surface oil flow direction from which the transverse skin friction was determined. As expected, surface shear-stress angle increases with cylinder rotational speed. Note that the skin-friction measurements for case B were obtained with the tunnel running under off-design conditions and should be used only qualitatively to visualize trends. Since the cylinder's boundary layer was much thicker than normal for the C_f and β measurements only, these measurements are not compatible with the C_p and LDV measurements which were obtained at the correct conditions.

3.3 Combined Effects of Pressure Gradient and Transverse Strain

Surface skin-friction was also measured for cases C and D (figs. 3.8 through 3.13). Generally, both streamwise and transverse skin friction increase with increased rotational speed.

Conversely, both streamwise and transverse skin friction decrease with adverse pressure gradient. Figure 3.14 shows transverse skin-friction decreasing with increasing streamwise pressure gradient for the cases with W_s/U_τ = 1.0. This is a result of boundary layer thickening due to adverse pressure gradient, which reduces $\partial W/\partial y$ near the wall.

The Clauser parameter, viewed as the ratio of the pressure force to the surface skin-friction force ($\partial C_p/\partial x/(C_{f_x}/\delta^*)$) is often used to characterize the amount of the pressure gradient. The Clauser parameter was evaluated for cases D.S0 and D.S1 (fig. 3.15). In case D.S0 where there is no spin, $\partial C_p/\partial x/(C_{f_x}/\delta^*)$ grows to 80 by $x = 220$ mm (80 implies separation is imminent). For spinning case B.S1, $\partial C_p/\partial x/(C_{f_x}/\delta^*)$ grows to a lower level, 14, as a result of a higher skin-friction level. Slower growth of the Clauser parameter is seen in cases B.S0 and B.S1 where pressure gradient is milder (fig. 3.16). Cases D.S1 (that has spin) and B.S0 (that has no spin) attain comparable asymptotic levels of Clauser parameter.

3.4 Primary Test Case Selection

It was desired to find a case that had the maximum effect of both transverse strain-rate and pressure gradient on the turbulence in the hope that large changes in the turbulence would be easier to analyze than small ones.

The transverse strain-rate is largest for the faster spin rates, making the cases with spin rate of $W_s/U_\tau = 1$ the logical choice of test cases. A spin rate of $W_s/U_\tau = 2$ might have been better, but the reduced free-stream axial velocity needed to achieve this case resulted in a low Reynolds number and a somewhat thicker boundary layer, which results in a narrowing of the inviscid core region outside the boundary layer.

The axial pressure gradient acts primarily on the axial velocity field. However, the transverse strain-rate is also affected by the pressure gradient to some extent; that is, streamline divergence reduces the concentration of transverse momentum near the wall, thus reducing the transverse flow gradients. The reduction in transverse strain-rate (by virtue of streamline divergence) would preferably be small so that the main change in the mean flow strain-rate is felt in the axial component of the strain rate. The only other way that the transverse flow can be affected is through the transverse shear stress. The relationship between the transverse and axial components of Reynolds shear stress is what we hope to study. Transverse wall shear offers one indicator of the degree to which pressure gradient is affecting the transverse flow.

Pressure gradient cases B.S1 and C.S1 provide the largest variation in transverse surface skin friction (fig. 3.14). However, in these cases the pressure gradient is located upstream primarily on the spinning cylinder, where the zero pressure gradient boundary layer is not strictly 3D in nature. The pressure gradient does, however, produce a weak three-dimensionality in the upstream region of the flow—as a result of non-uniform rotation of the strain-rate vector direction through the boundary layer.

Pressure gradient case D.S1, while not producing as much of an effect on the transverse skin friction, does produce most of the pressure gradient on the stationary section where the flow is legitimately 3D in nature. Here, the flow starts off as a 3D boundary layer in a zero pressure gradient and ends up as a 2D boundary layer in a strong adverse pressure gradient.

The effects of adverse pressure gradient on a 3D boundary layer can be observed fairly free of other effects by the use of combinations of cases A.S1, B.S1, C.S1, and D.S1. Useful comparisons can be made between the cases that have adverse pressure gradient and those that do not, since each flow starts with the same upstream boundary layer.

Unfortunately, the effects of transverse strain on an adverse pressure gradient flow are not as easily studied. Comparisons between spinning and non-spinning cases (i.e., D.S1 and D.S0) are desirable but

difficult, since curvature and rotational effects are present in the spinning case while absent in the non-spinning case. In the absence of curvature and rotational effects, the flow on the spinning cylinder should degenerate to a 2D flat plate boundary layer, where the U-velocity component behaves as a standard 2D boundary layer—in other words, U-velocity profiles for cases D.S1 and D.S0 should be identical at X = 0 (see appendix A for an explanation). However, in the spinning case, normal pressure gradient forces destabilize the flow and cause the boundary layer to grow at a faster rate with a nonstandard shape factor and U-velocity distribution. The mismatch in upstream boundary conditions between the spinning and non-spinning cases will quite likely lead to different downstream conditions independent of effects generated by the turbulence. However, cases C.S1 and D.S1, in which the cylinder is spinning, nearly match the boundary layer growth rate of case B.S0 without spin even though the pressure gradients are different, thus providing a means of making meaningful comparisons.

While all cases A.S1, B.S1 ,C.S1, and D.S1 as well as A.S0, B.S0, C.S0, and D.S0 were ultimately surveyed with the 3D LDV, case D.S1 with downstream adverse pressure gradient will probably be the most useful. In this case the two extra rates of strain ($\partial W/\partial y$ and $\partial U/\partial x$) are imposed at the same location in the flow, causing each effect to be at a maximum at the same location. Case D.S1 will be considered the primary test case. Case A.S1 is also of interest, since it serves as a baseline case from which to compare case D.S1 and pressure gradient effects. Likewise, case B.S0 and D.S0 serve as a baseline 2D cases from which to study transverse strain effects on pressure gradient flows. A full set of three-component LDV measurements was acquired including velocity triple-product correlations for each case (the results are tabulated in appendix C).

3.5 Flow Quality of Primary Test Cases

Flow axisymmetry for non-spinning case D.S0 was assessed using circumferential static wall pressure distributions at three axial stations along the cylinder (fig. 3.17). Variations of less than ± 0.01 in C_p indicate good axisymmetry of static pressure. Similar results were shown earlier for case B.S0 in figure 2.7.

A more sensitive measure of flow axisymmetry is surface skin friction (shown in fig. 3.18) is case D.S0. In this case, C_f is uniform to within ± 0.0002 (7%), which is considered satisfactory. Furthermore in regions of the flow with strong streamwise pressure gradient, good circumferential uniformity persists. Similarly good axisymmetry of axial skin-friction is seen in case C.S0 (fig. 3.19) and case B.S0 (fig. 2.8).

Integral momentum balances were computed using the measured velocities, surface skin friction, and static pressure, and applying the following integrated form of the momentum integral equation

$$\theta_{xx} = \frac{1}{1-C_p}\left(\theta_{xx_o} + \frac{1}{2}\int_{C_{p_o}}^{C_{p_x}} \delta^* dC_p + \frac{1}{2}\int_{x_o}^{x} C_{f_x} dx + \left[\int_{R_o}^{R_o+\delta} \frac{r}{R_o}(\overline{u^2}/U_o^2)\,dr\right]_{x_o}^{x}\right)$$

where θ_{xx_o} and C_{p_o} are the momentum thickness and coefficient pressure, respectively, at $x = x_o$. Momentum thickness determined from the balance equation is compared with the measured momentum thickness for each pressure gradient case shown in figures 3.20 (non-spinning case) and 3.21 (spinning case). The measured momentum thickness and the momentum thickness from the balance are in good agreement. For

the most part, the momentum balances to within $\pm 5\%$, with the exception of case B.S1 which is unbalanced by as much as $\pm 25\%$. Such minimal differences in the momentum balance are an indication of the good self-consistency of the data and axisymmetry of the flow.

The poor balance in the case of B.S1 is most likely caused by asymmetries produced by the asymmetric separation in the corners of the tunnel sidewalls. This case has been rejected and will not be analyzed in subsequent sections; it is however a good example of the sensitivity of momentum balance to flow asymmetries.

Remarkably, the best momentum balance is for the non-spinning case (C.S0) with separation (fig. 3.20). Typically, separating flows are unsteady and experience asymmetries, but this separating flow seems to be quite axisymmetric as noted in the circumferential skin-friction distribution, tuft visualizations (not shown), and good momentum balances.

Transverse flow momentum thickness, calculated for the spinning case A.S1, increases up to X = 0, then decays slowly downstream of X = 0 (fig. 3.22). The pressure gradient adds to the growth of the transverse momentum thickness; however, it does not add to the transverse momentum. Normalization by U_e in the definition of θ_{xz} causes the growth in θ_{xz}. Scatter in the data is a result of slight asymmetries in the external flow (which creates unwanted transverse flow gradients). Transverse momentum thickness determined from the momentum balance,

$$\theta_{xz} = \theta_{xz_o} - \frac{1}{2}\frac{U_o U_o}{W_s U_e}\int_{x_o}^{x} C_{f_s} dx$$

compares reasonably well with the measurements for each of the cases.

The displacement thickness computed from the mean flow measurements increases very rapidly for the three cases of adverse pressure gradient without spin (fig. 3.23). The displacement thickness, however, does not increase quite so rapidly in the spinning cases (fig. 3.24). The only difference between cases B and C is a mere 10 to 20% difference in the pressure distribution; however, the displacement thicknesses differ by a factor of three or more in both the spinning and non-spinning cases.

The transverse flow displacement thickness generally increases with distance along the spinning cylinder upstream of X = 0 (fig. 3.25). For case A.S1, the transverse flow displacement thickness slowly diminishes downstream of X = 0. Pressure gradient causes the displacement thickness to grow more rapidly.

The shape factor for the non-spinning flows increases rapidly with distance along the pressure gradient (fig. 3.26). All cases start with $H = 1.35$ in the upstream zero pressure gradient part of the flow. Shape factors of 2.4 to 2.8 or greater usually signify that the boundary layer is about to separate as is the case for C.S0 and D.S0 (detachment at X = 50 and 300 mm, respectively). Case B.S0 grows least rapidly since this case has the smallest pressure gradient. The shape factor for the spinning flows, shown in figure 3.27, grows much less rapidly to maximum values of 1.75—far from the separation criteria of $H = 2.4$.

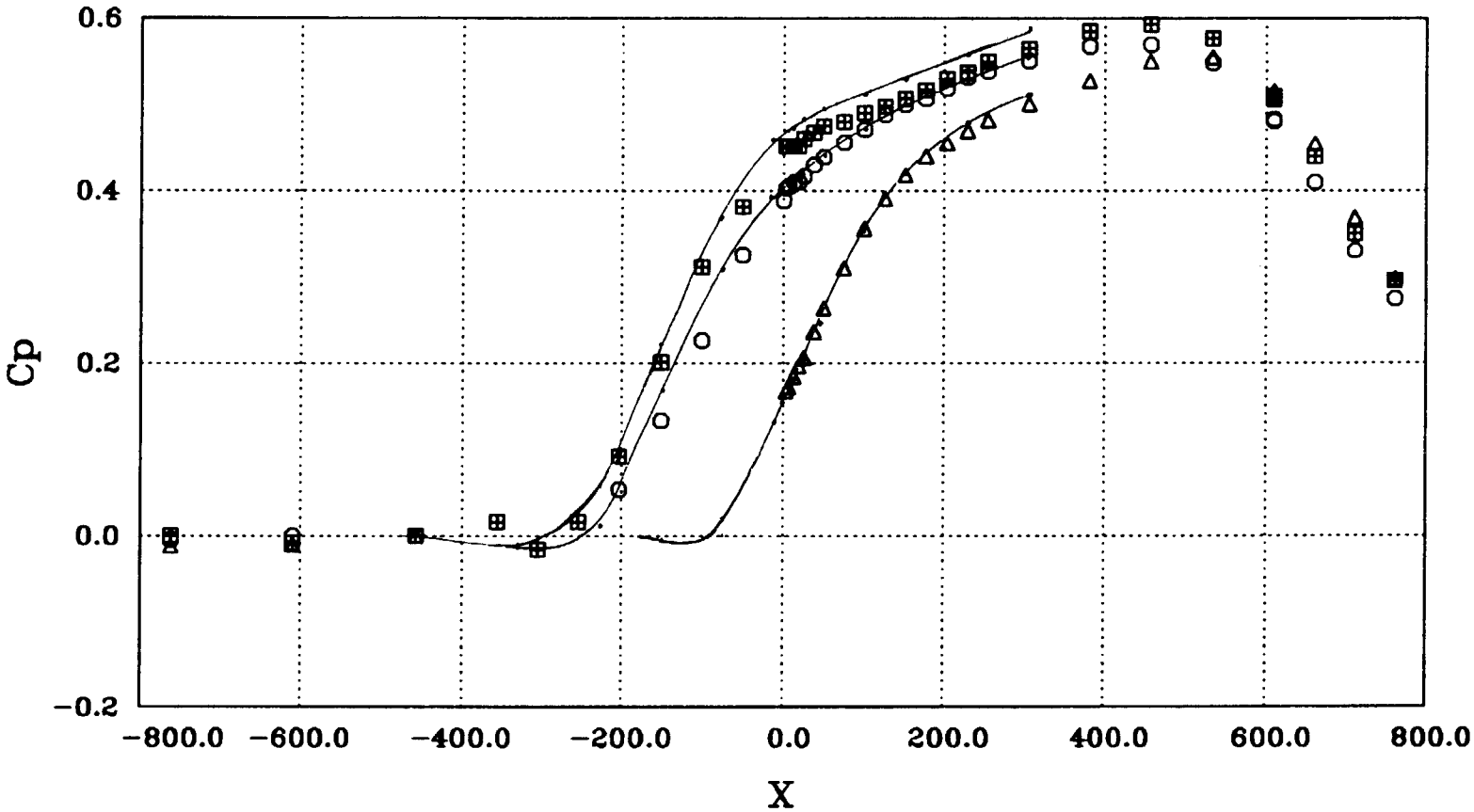

Figure 3.1 Surface Pressure Distributions for Various Diffuser Geometries–No Spin Cases, ◯ Case B.S0, ⊞ Case C.S0, △ Case D.S0, —— pressure deduced from LDV.

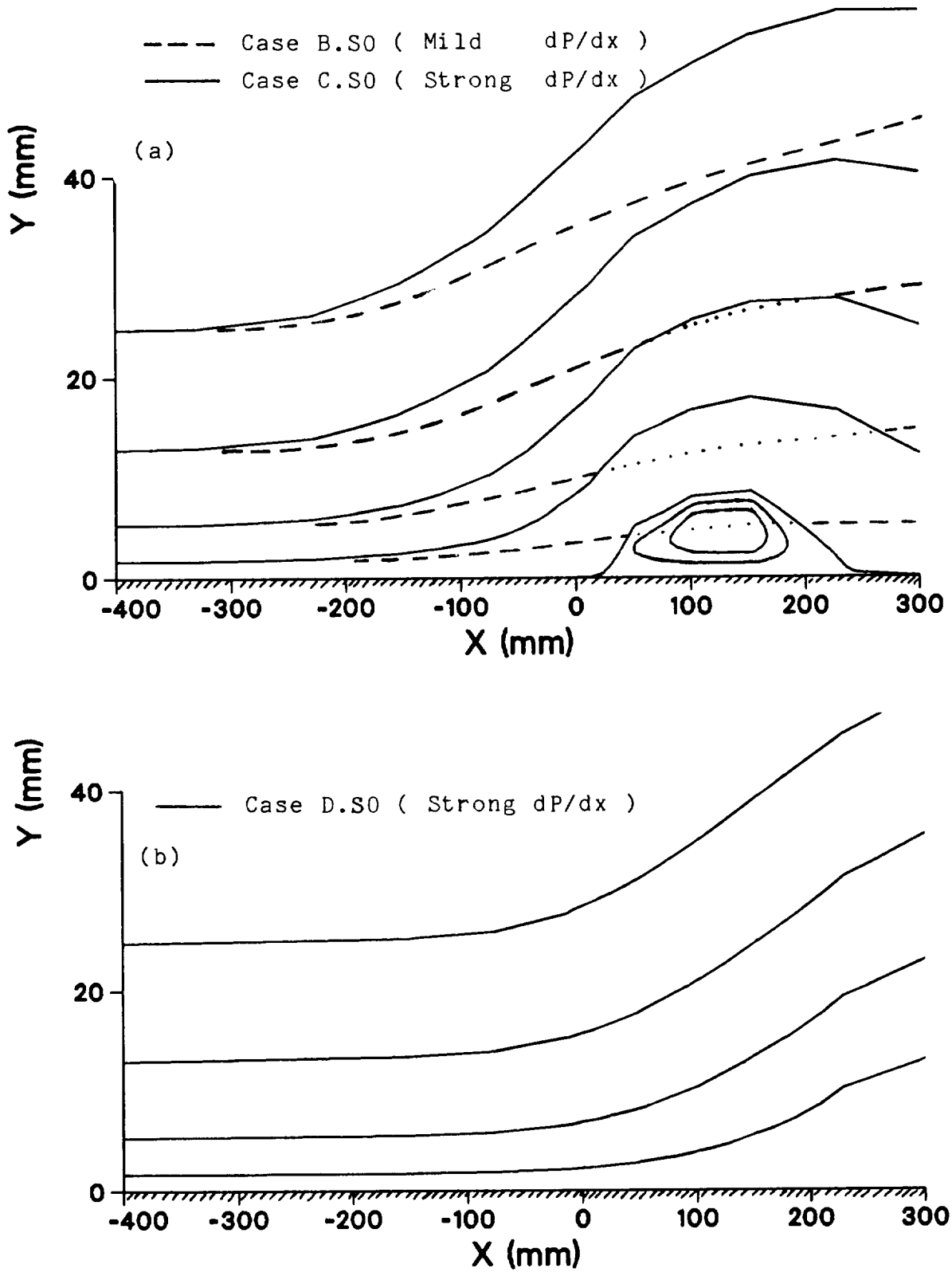

Figure 3.2 Stream function contours for corresponding diffuser geometries–no spin cases, a) - - - Case B.S0, —— Case C.S0; b) —— Case D.S0.

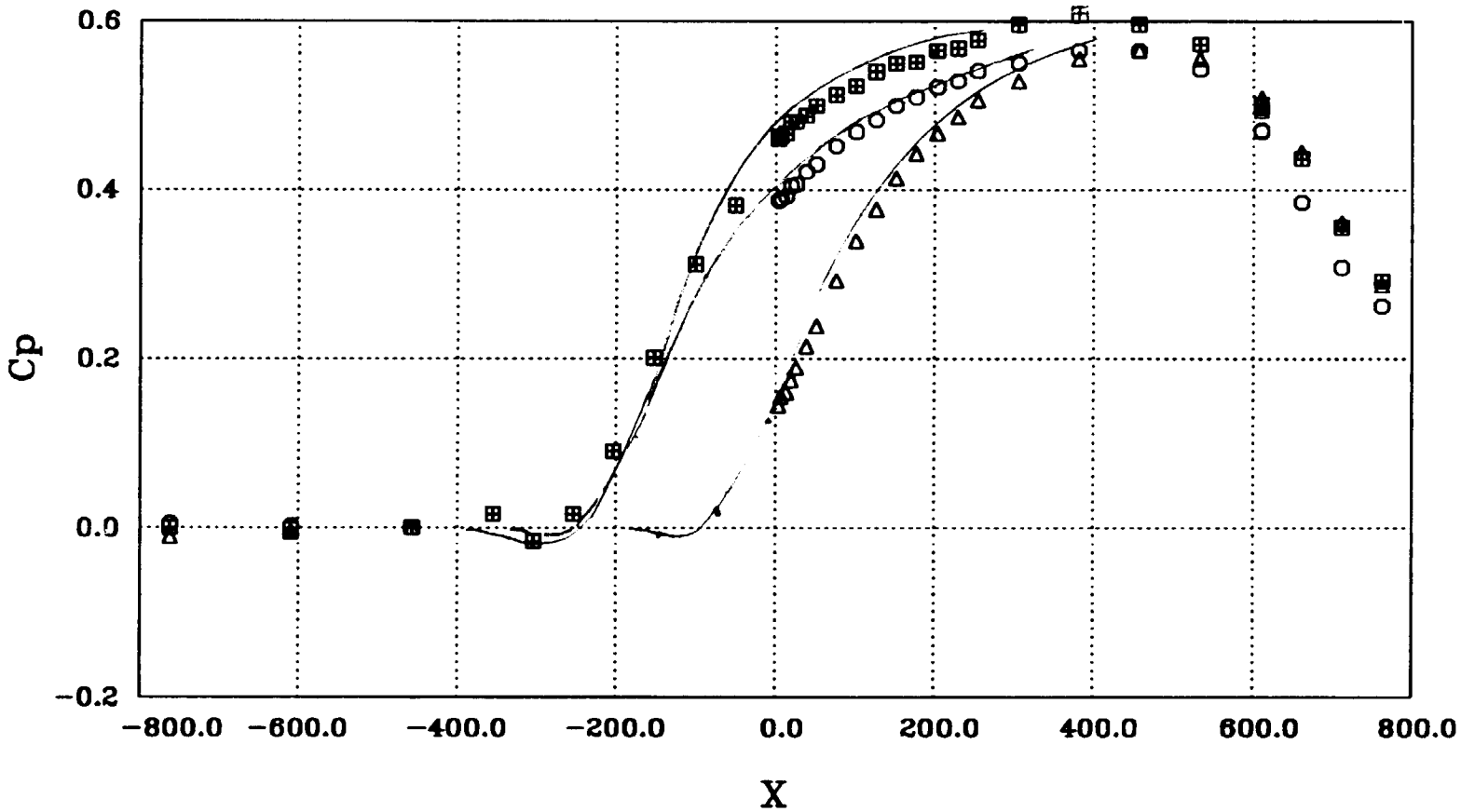

Figure 3.3 Surface Pressure Distributions for Various Diffuser Geometries–Spinning Cases, ○ Case B.S1, ⊞ Case C.S1, △ Case D.S1, —— pressure deduced from LDV.

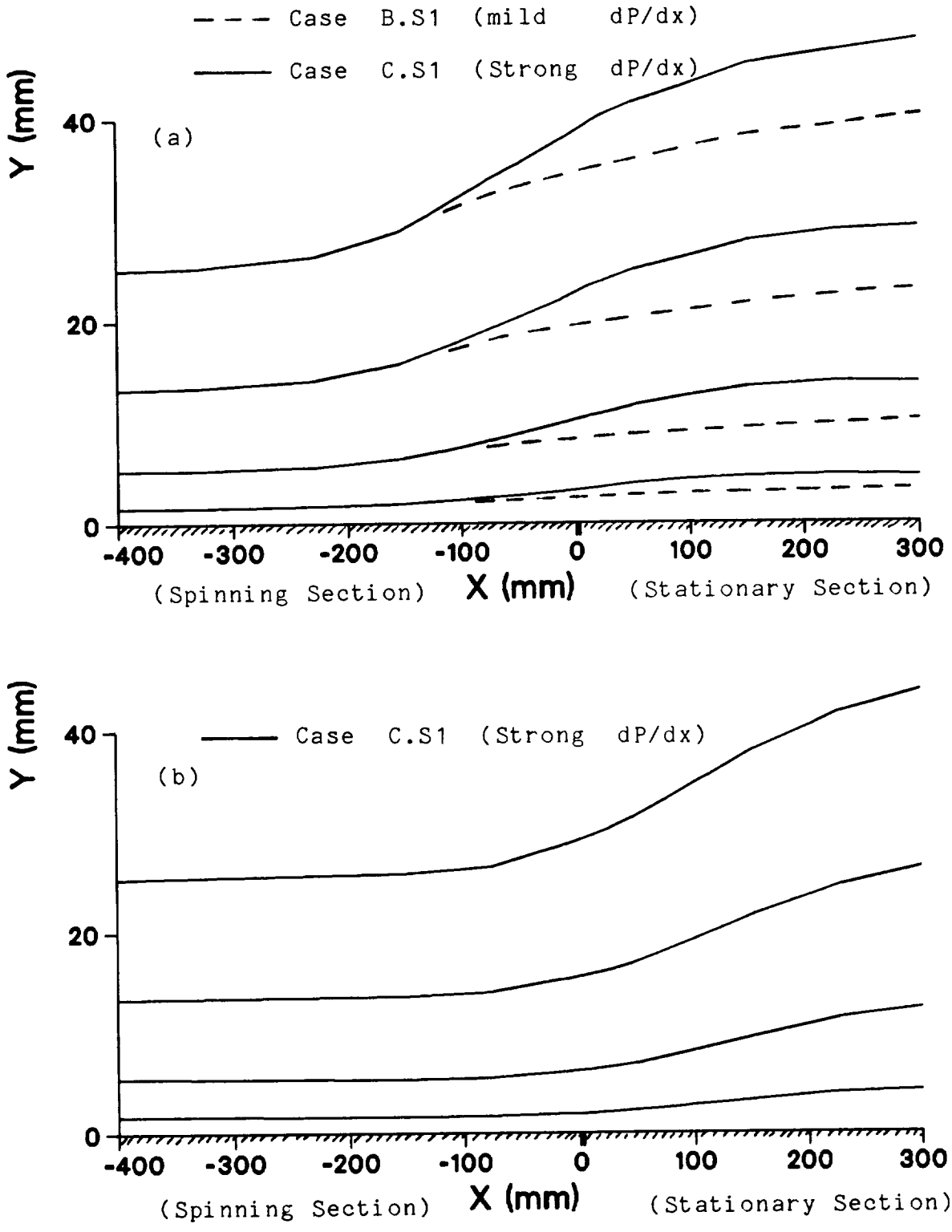

Figure 3.4 Stream function contours for corresponding diffuser geometries–spinning cases, a) - - - Case B.S1, —— Case C.S1; b) —— Case D.S1.

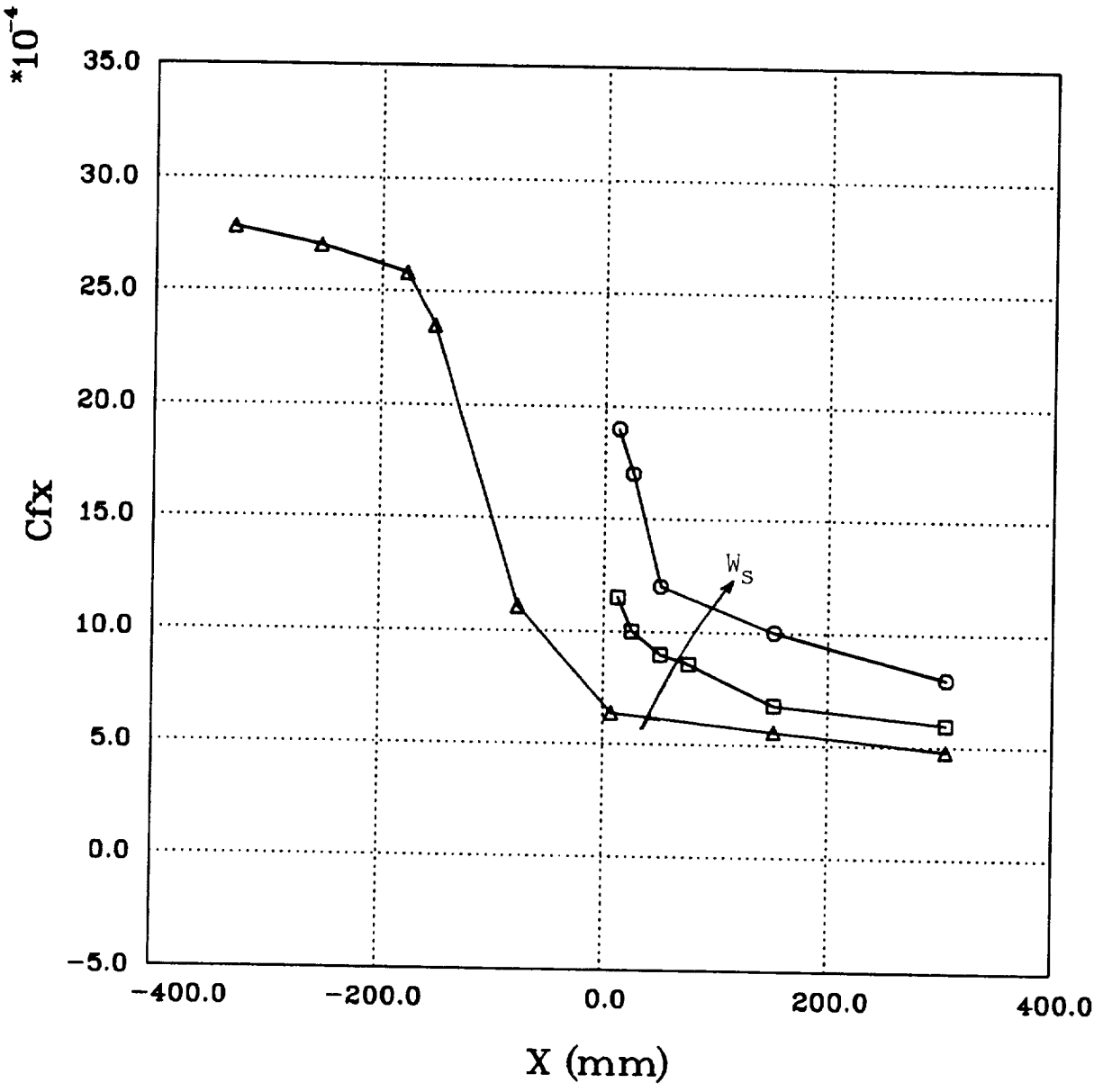

Figure 3.5 Axial skin-friction component, for mild dP/dx case B;* △ W_s/U_r=0, □ W_s/U_r=1/2, ○ W_s/U_r=1.

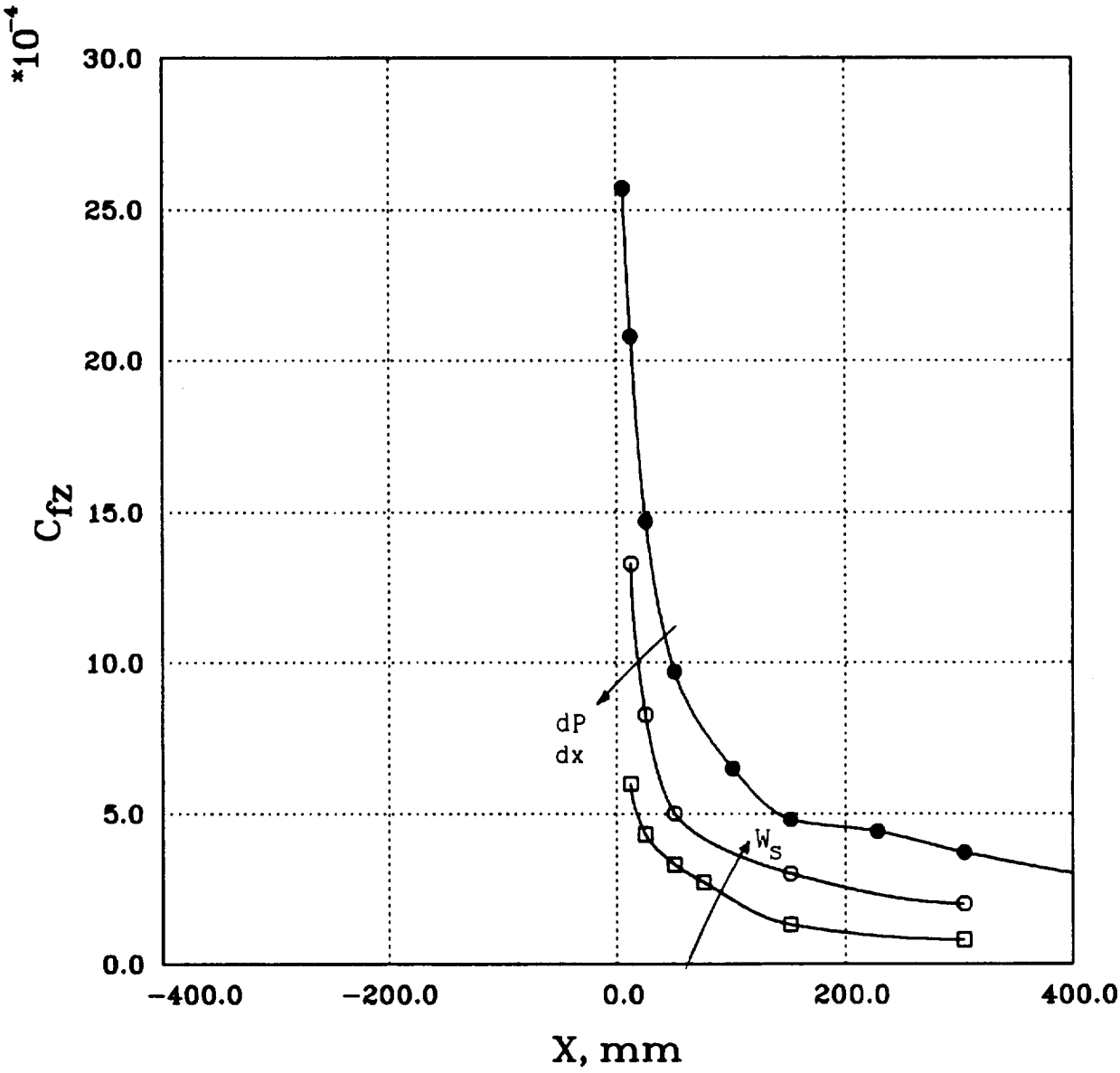

Figure 3.6 Transverse skin-friction component, for mild dP/dx case B,* □ W_s/U_r=1/2, ○ W_s/U_r=1, • zero dP/dx W_s/U_r=1.

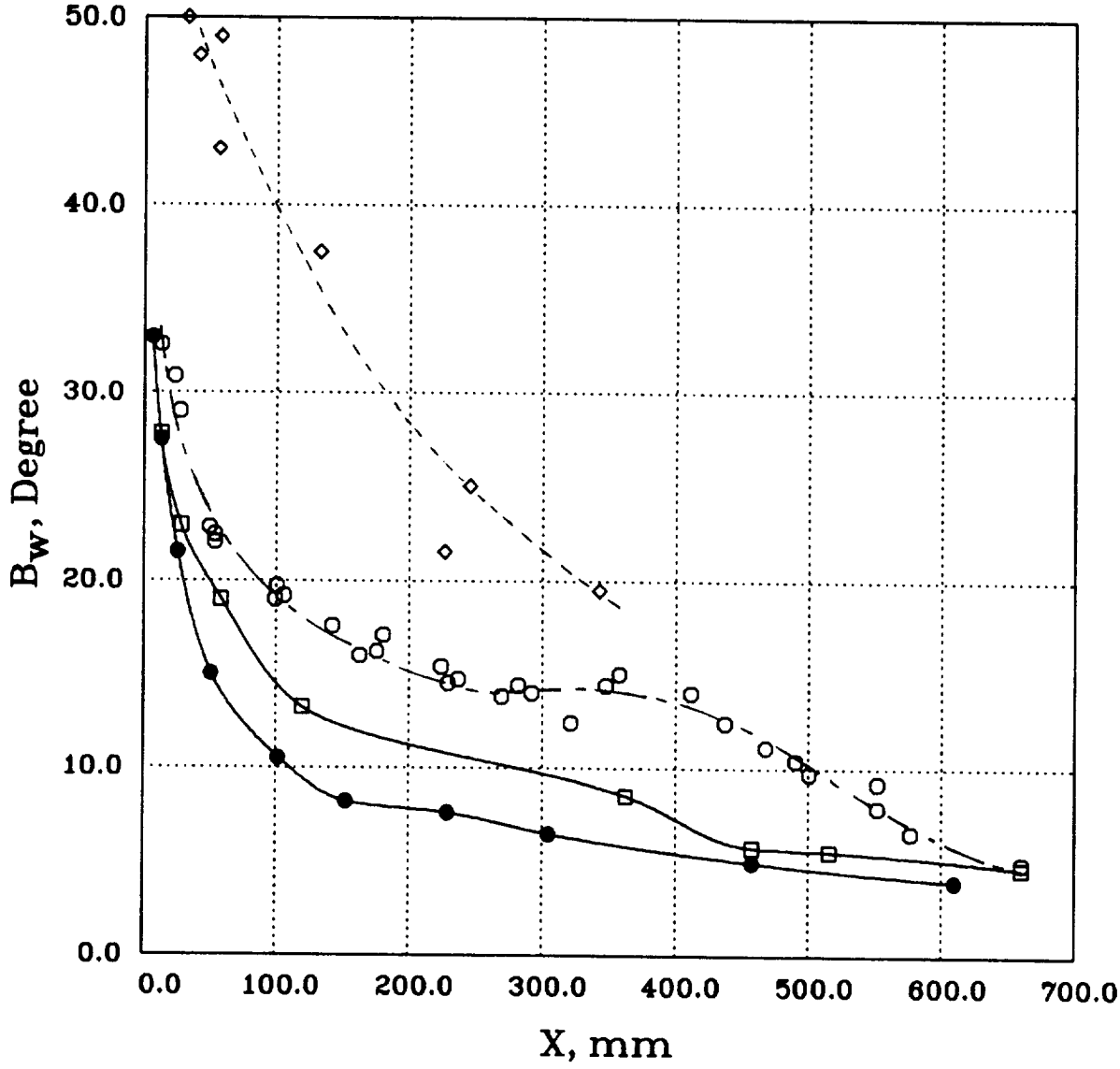

Figure 3.7 Surface oil flow direction distribution, for mild dP/dx case B*,
□ W_s/U_r=1/2, ○ W_s/U_r=1, ◇ W_s/U_r=2, • zero dP/dx W_s/U_r=1.

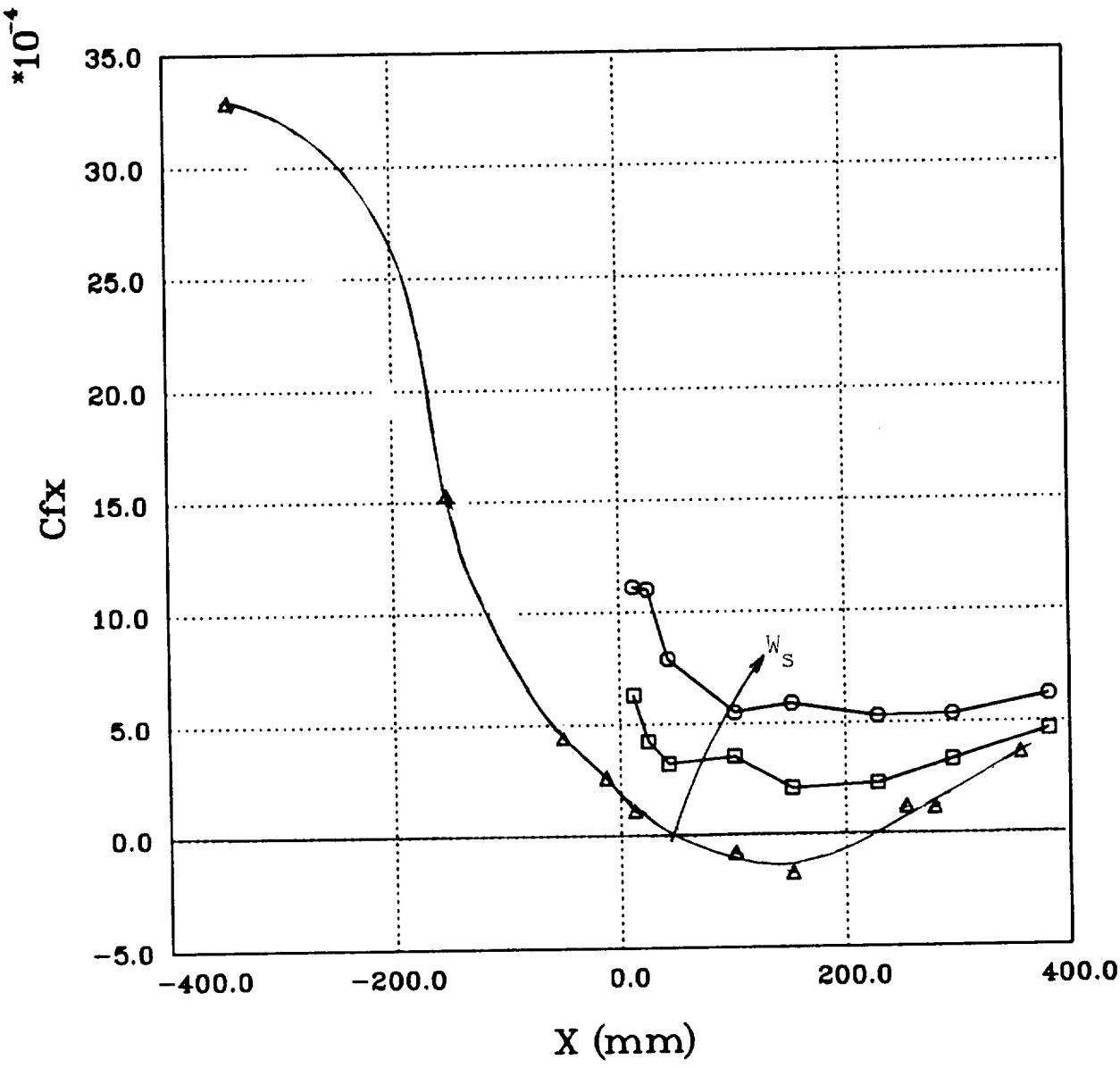

Figure 3.8 Axial skin-friction component, for strong dP/dx case C, △ W_s/U_r=0, □ W_s/U_r=1/2, ○ W_s/U_r=1.

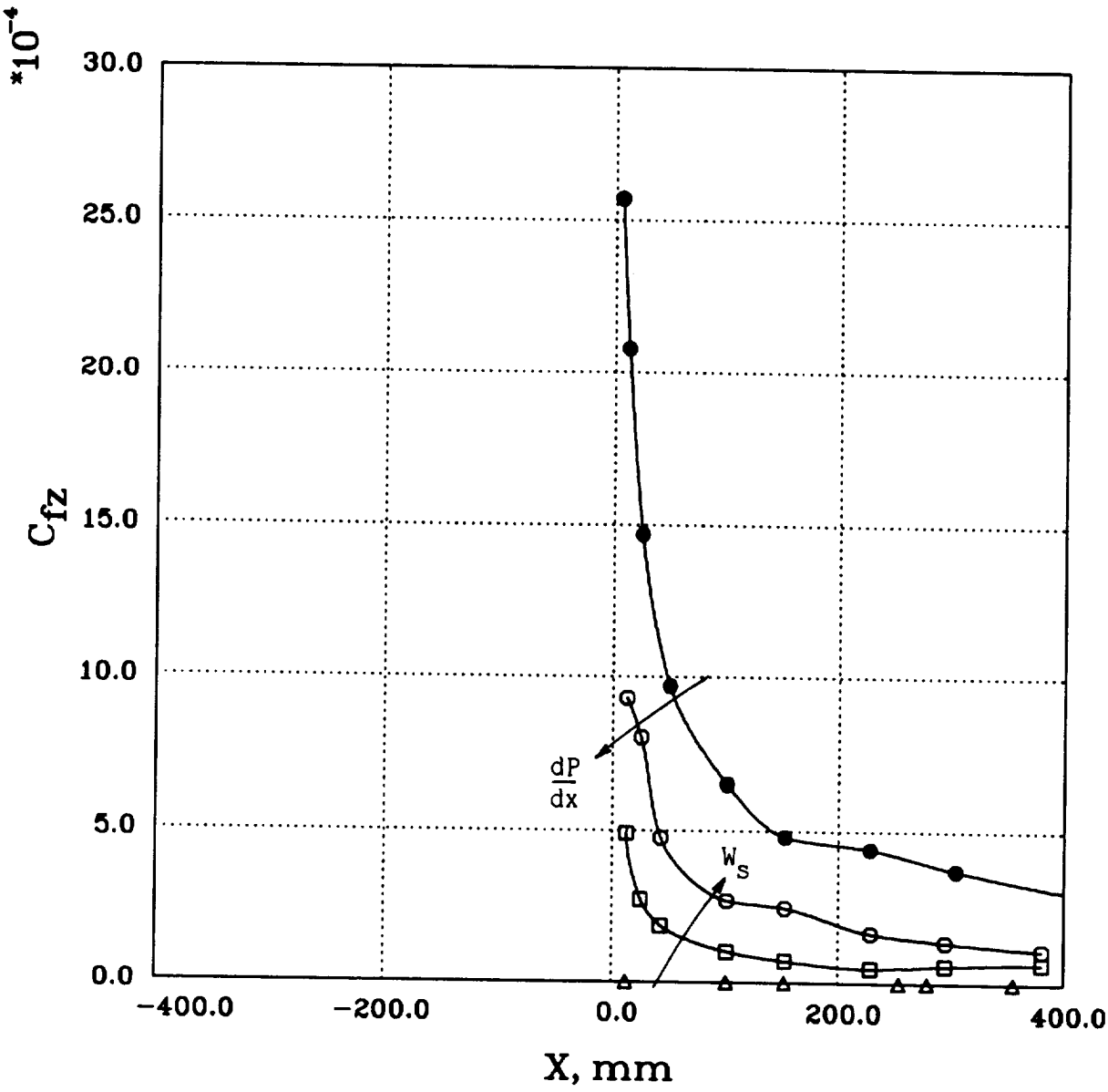

Figure 3.9 Transverse skin-friction component, for strong dP/dx case C,
△ W_s/U_r=0, □ W_s/U_r=1/2, ○ W_s/U_r=1, • zero dP/dx W_s/U_r=1.

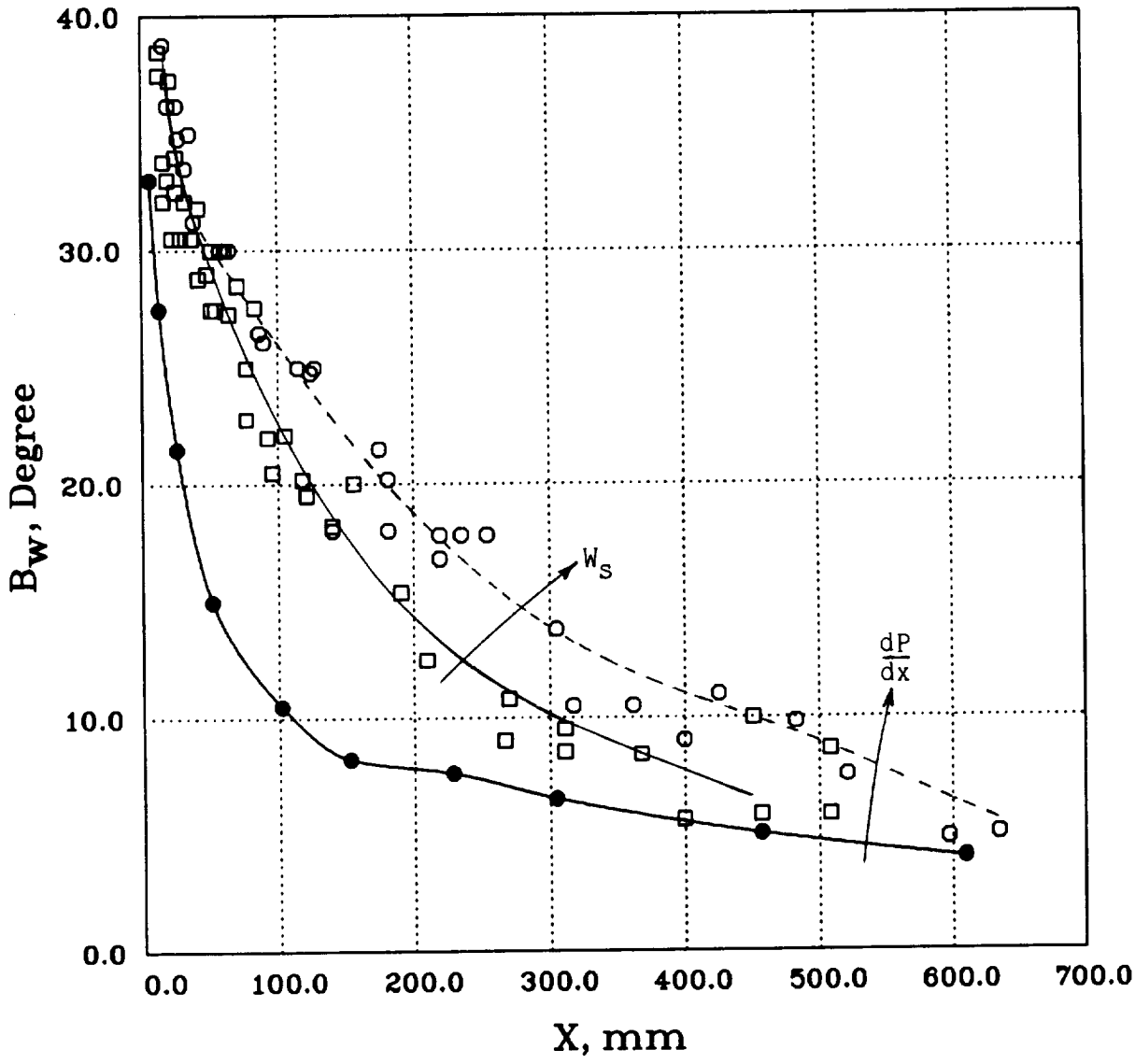

Figure 3.10 Surface oil flow direction distribution, for strong dP/dx case C, □ W_s/U_r=1/2, ○ W_s/U_r=1, • W_s/U_r=1 zero dP/dx.

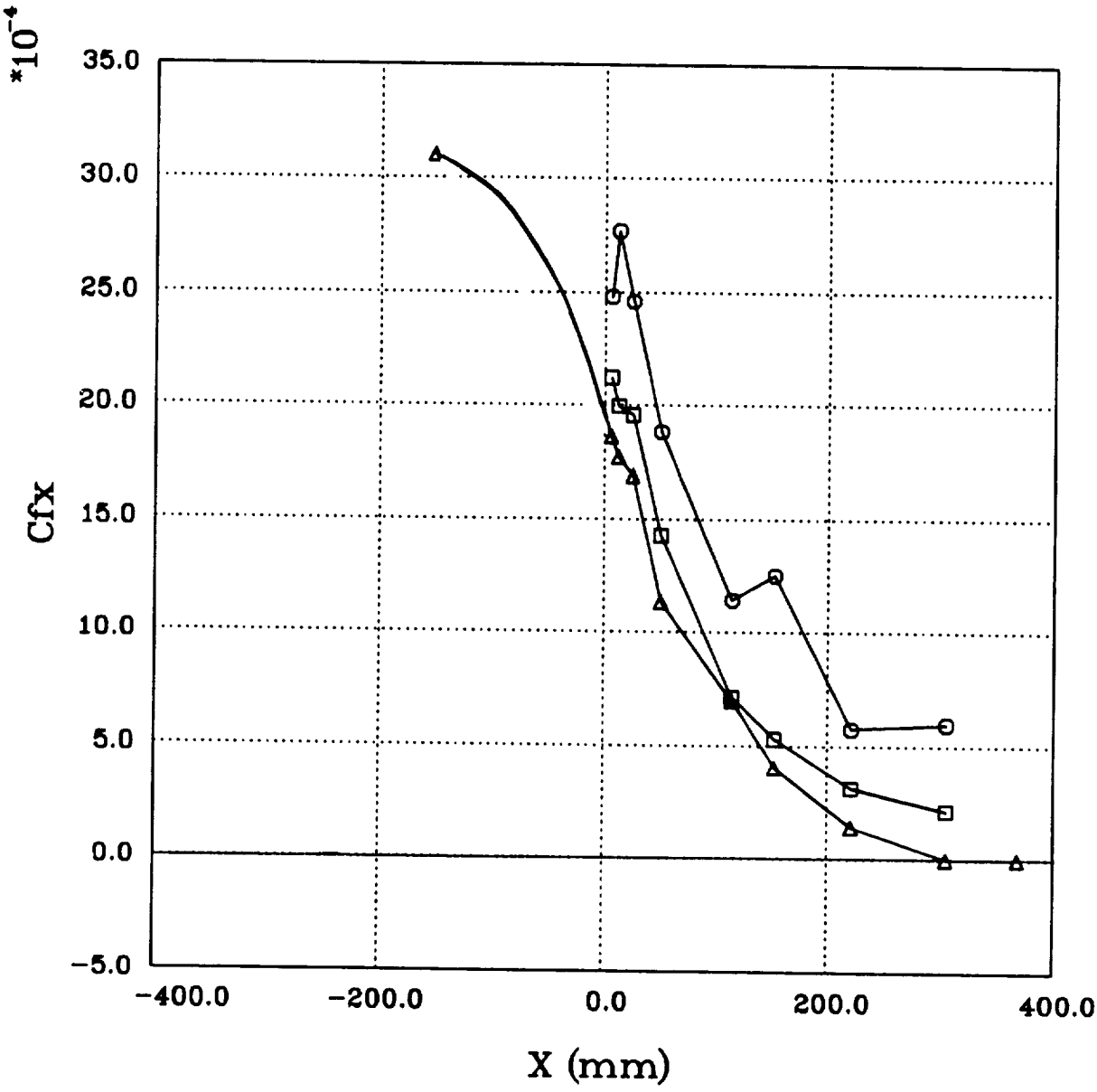

Figure 3.11 Axial skin-friction component, for strong dP/dx case D, △ W_s/U_r=0, □ W_s/U_r=1/2, ○ W_s/U_r=1.

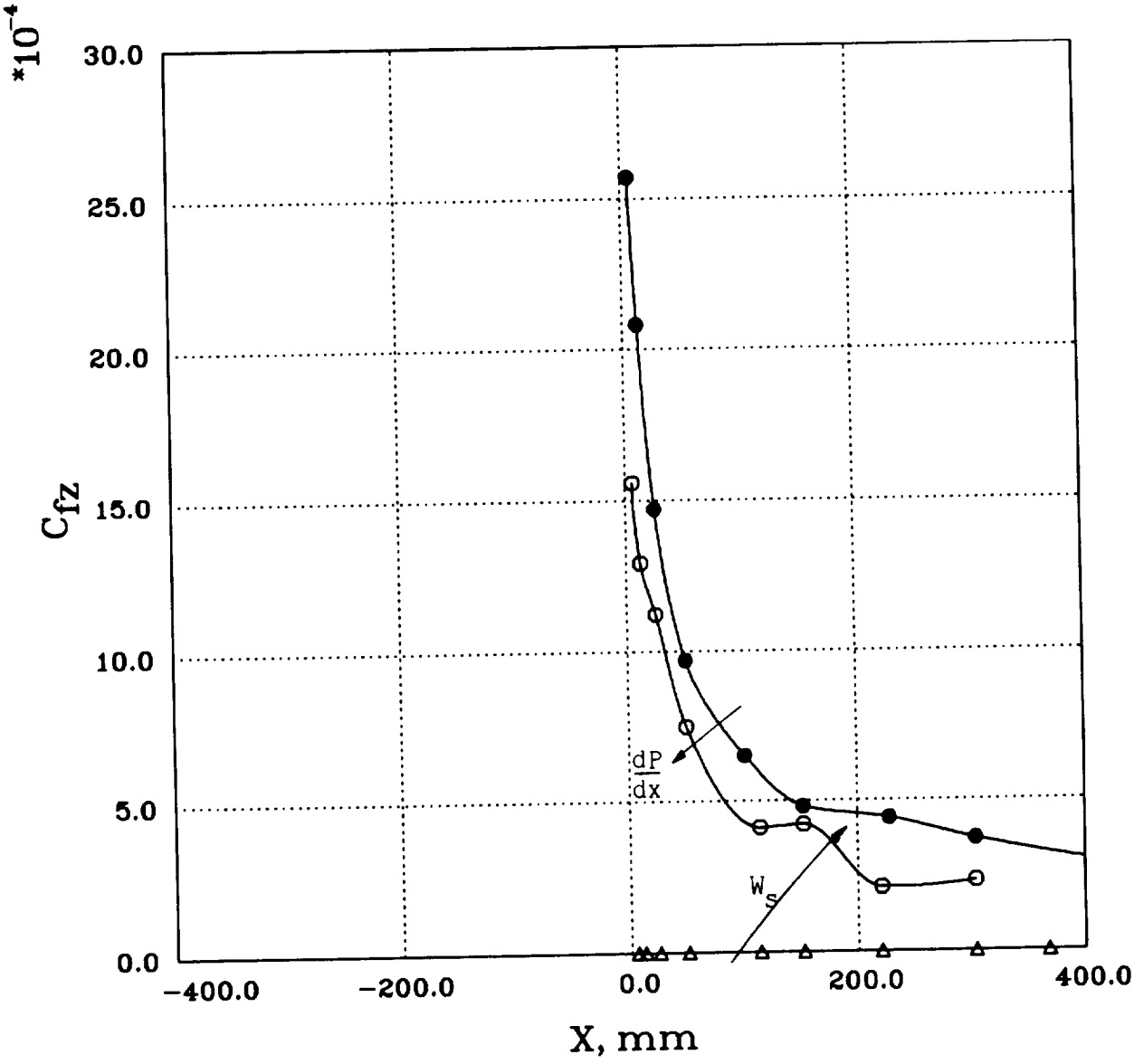

Figure 3.12 Transverse skin-friction component, for strong dP/dx case D, △ W_s/U_r=0, ○ W_s/U_r=1, • zero dP/dx W_s/U_r=1.

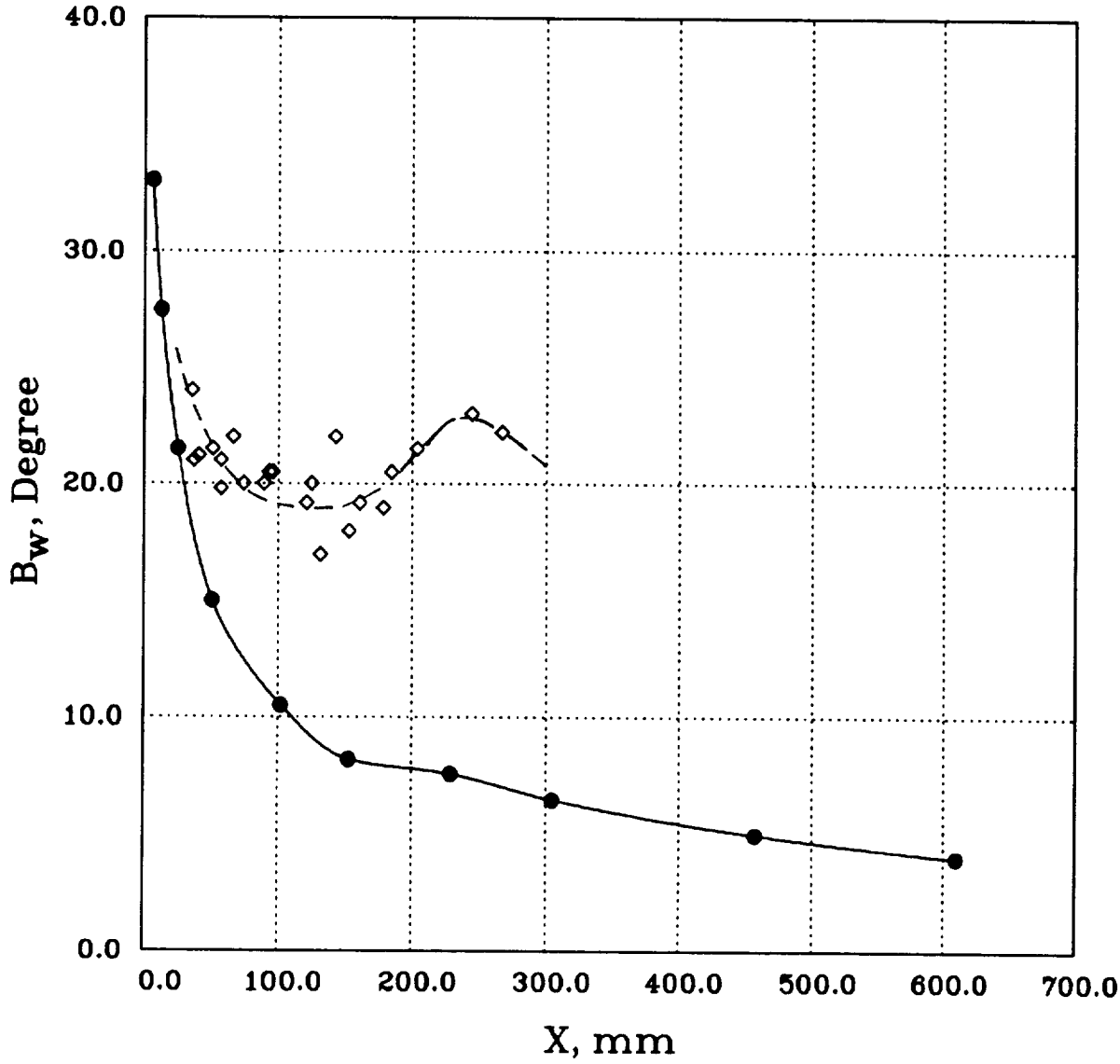

Figure 3.13 Surface oil flow direction distribution, for strong dP/dx case D, ◇ W_s/U_r=1, • Case A.S1 zero dP/dx W_s/U_r=1.

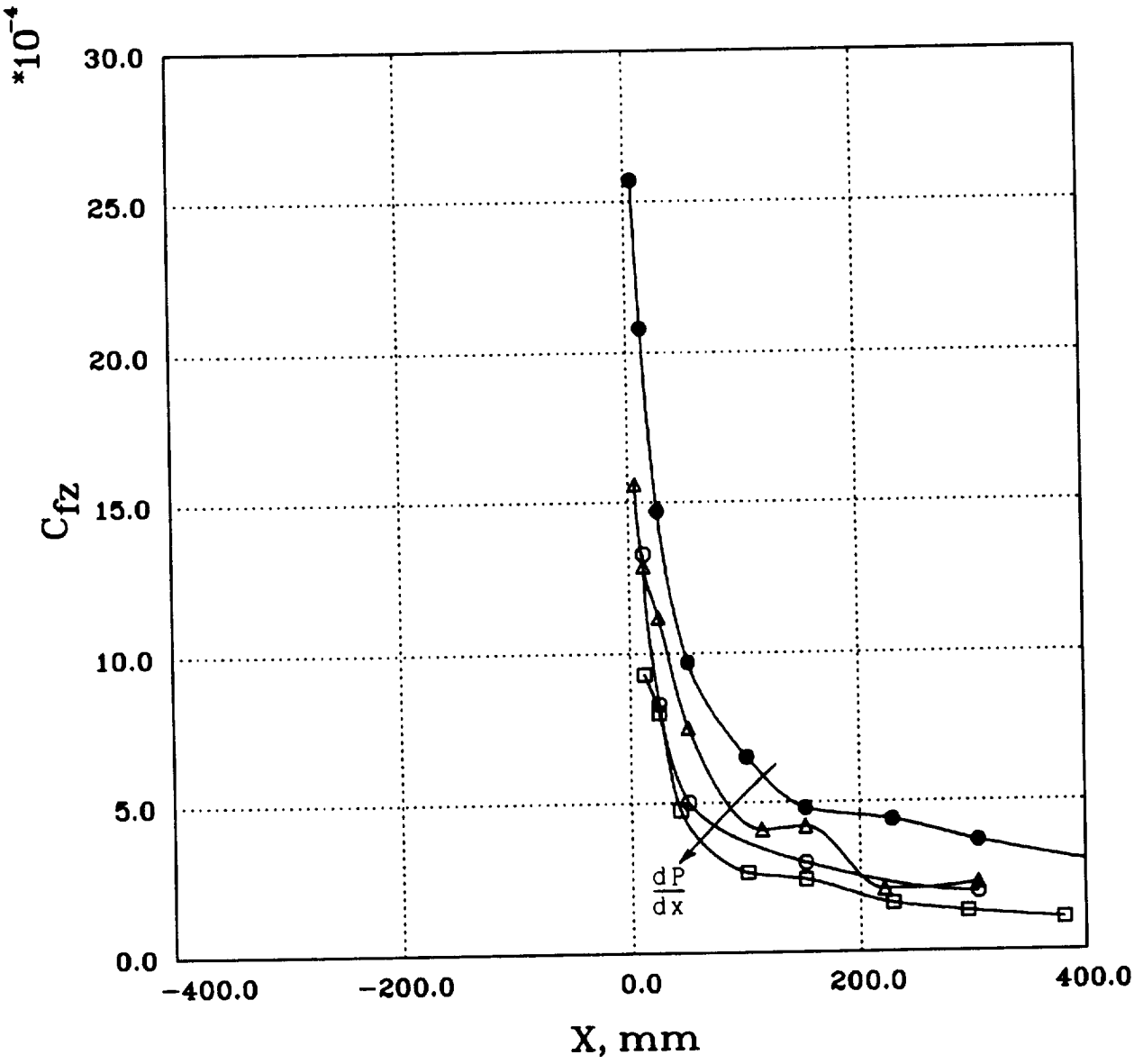

Figure 3.14 Pressure gradient effect on transverse skin-friction component for cases with $W_s/U_r = 1$, • Case A.S1, ○ Case B.S1, □ Case C.S1, △ Case D.S1.

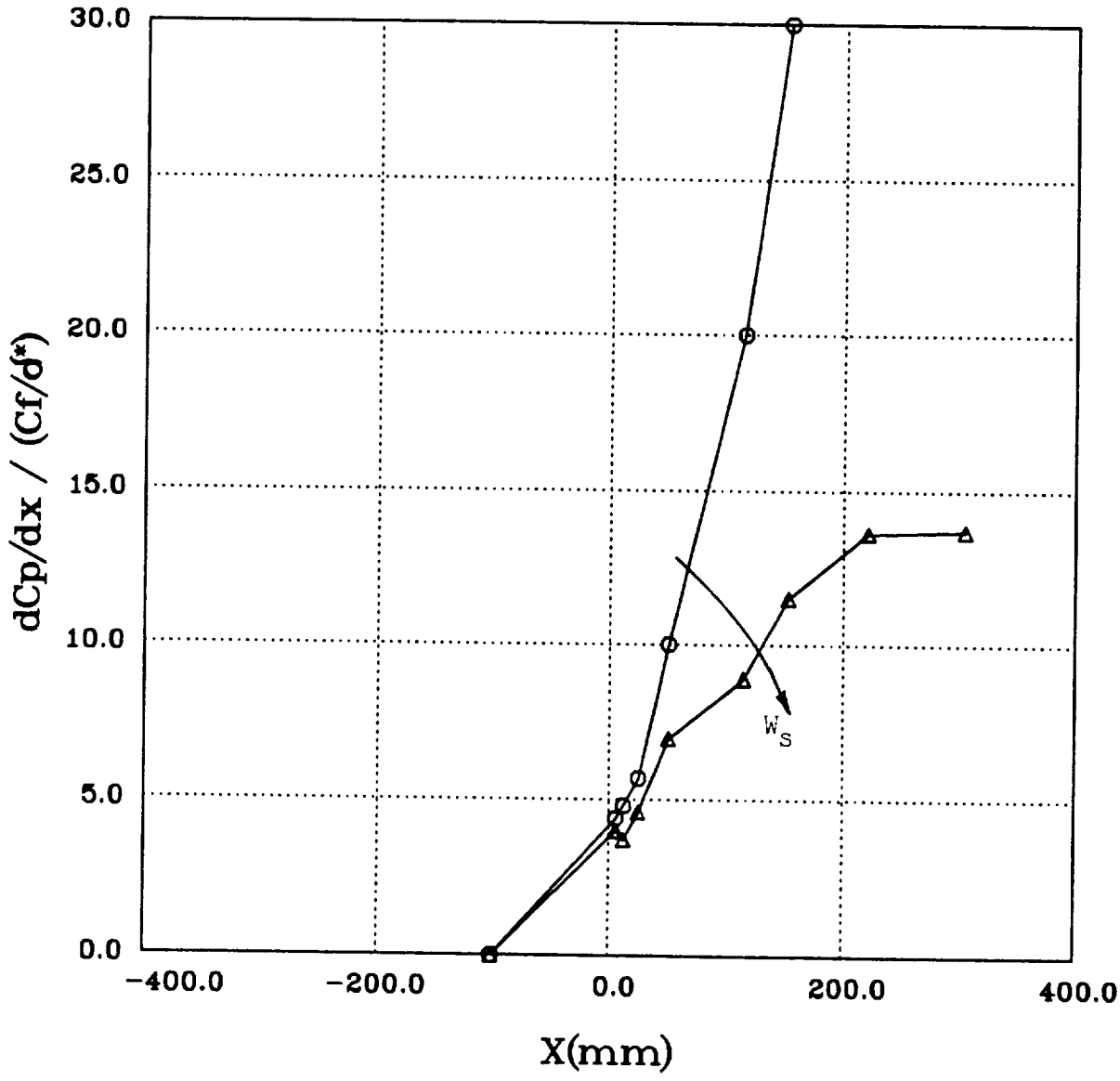

Figure 3.15 Clauser parameter distribution, ○ Case D.S0, △ Case D.S1.

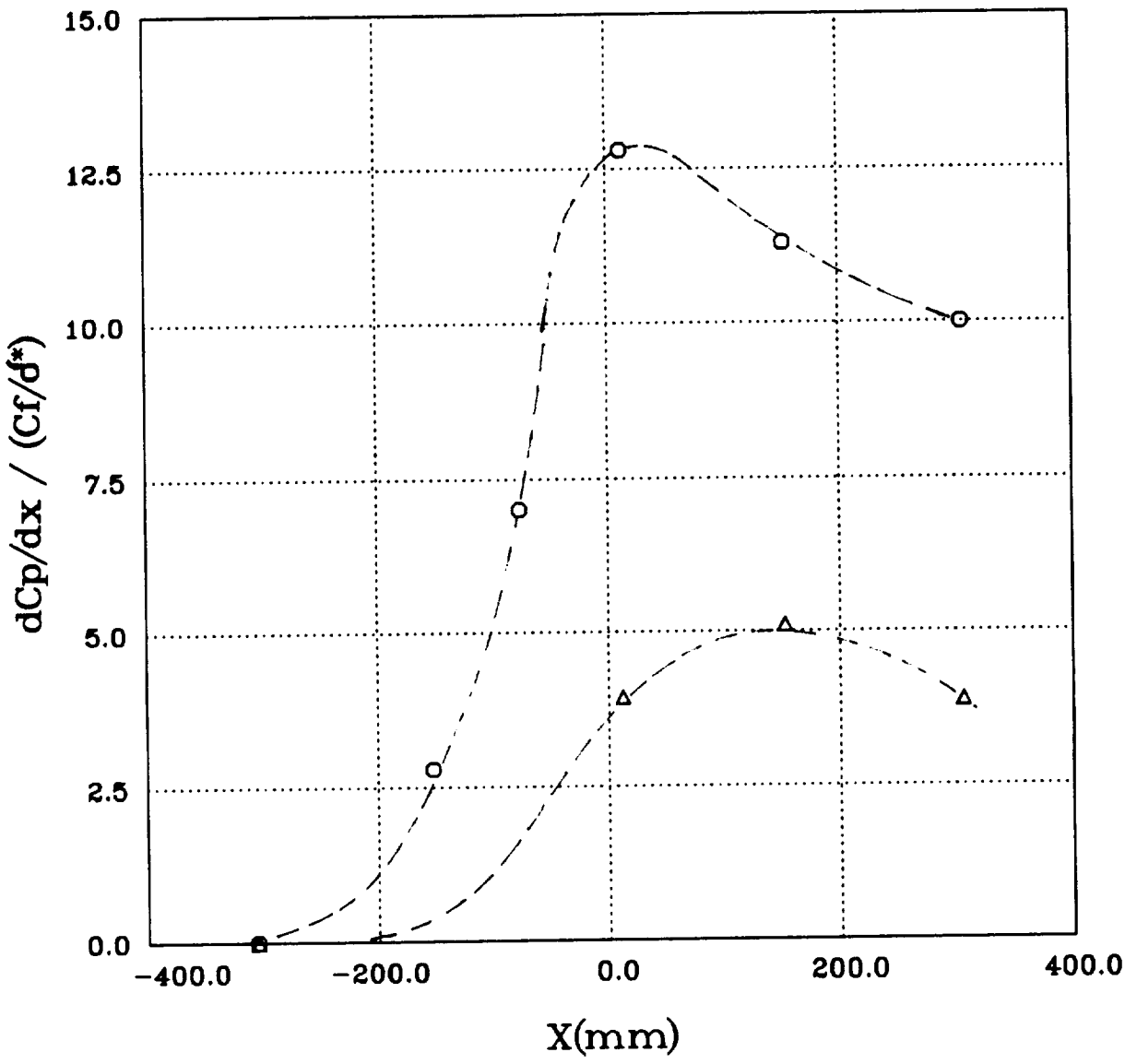

Figure 3.16 Clauser parameter distribution, ○ Case B.S0, △ Case B.S1.

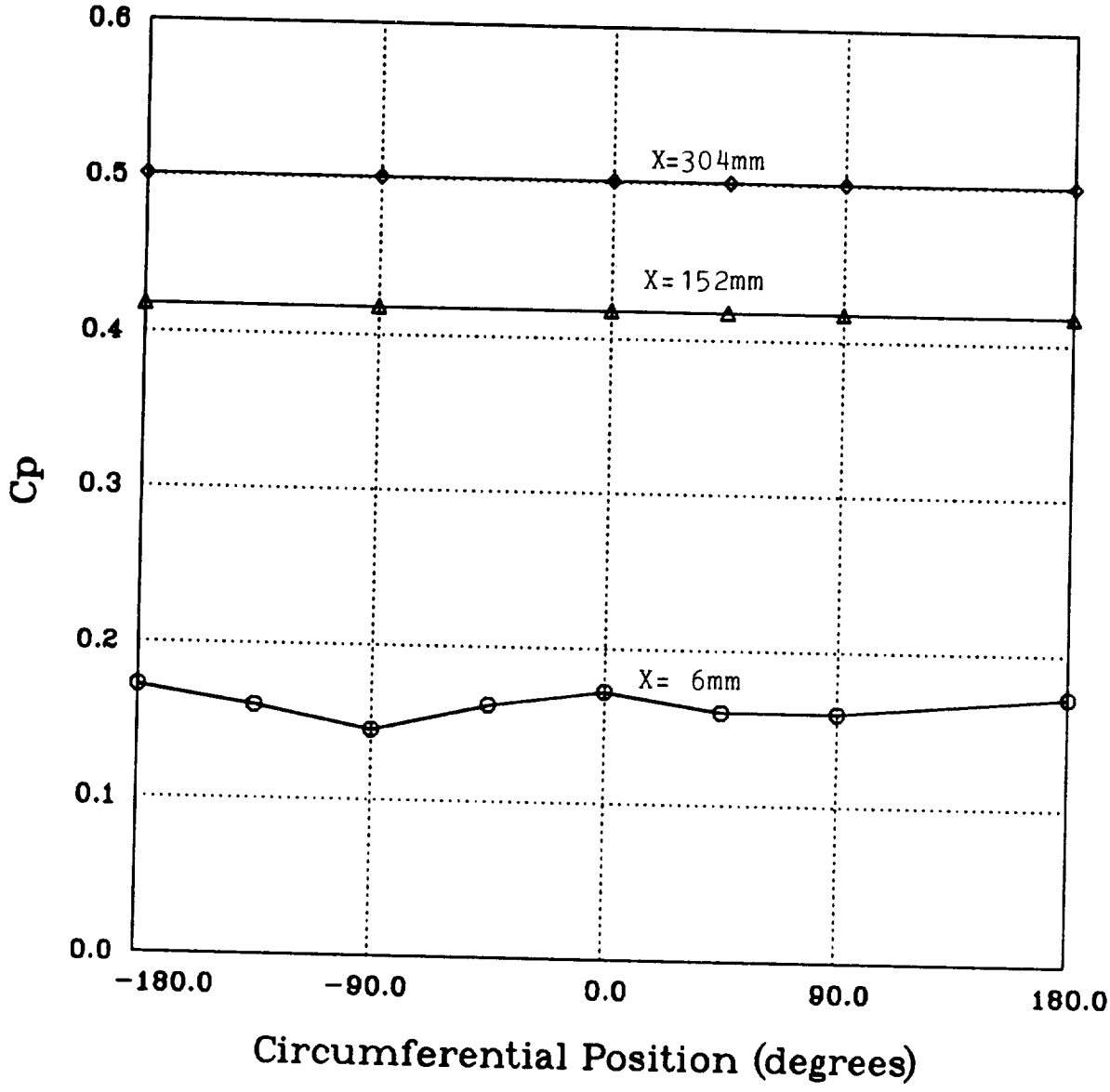

Figure 3.17 Circumferential distribution of static wall pressure for Case D.S0, ○ x=6mm, △ x=152mm, ◇ x=304mm.

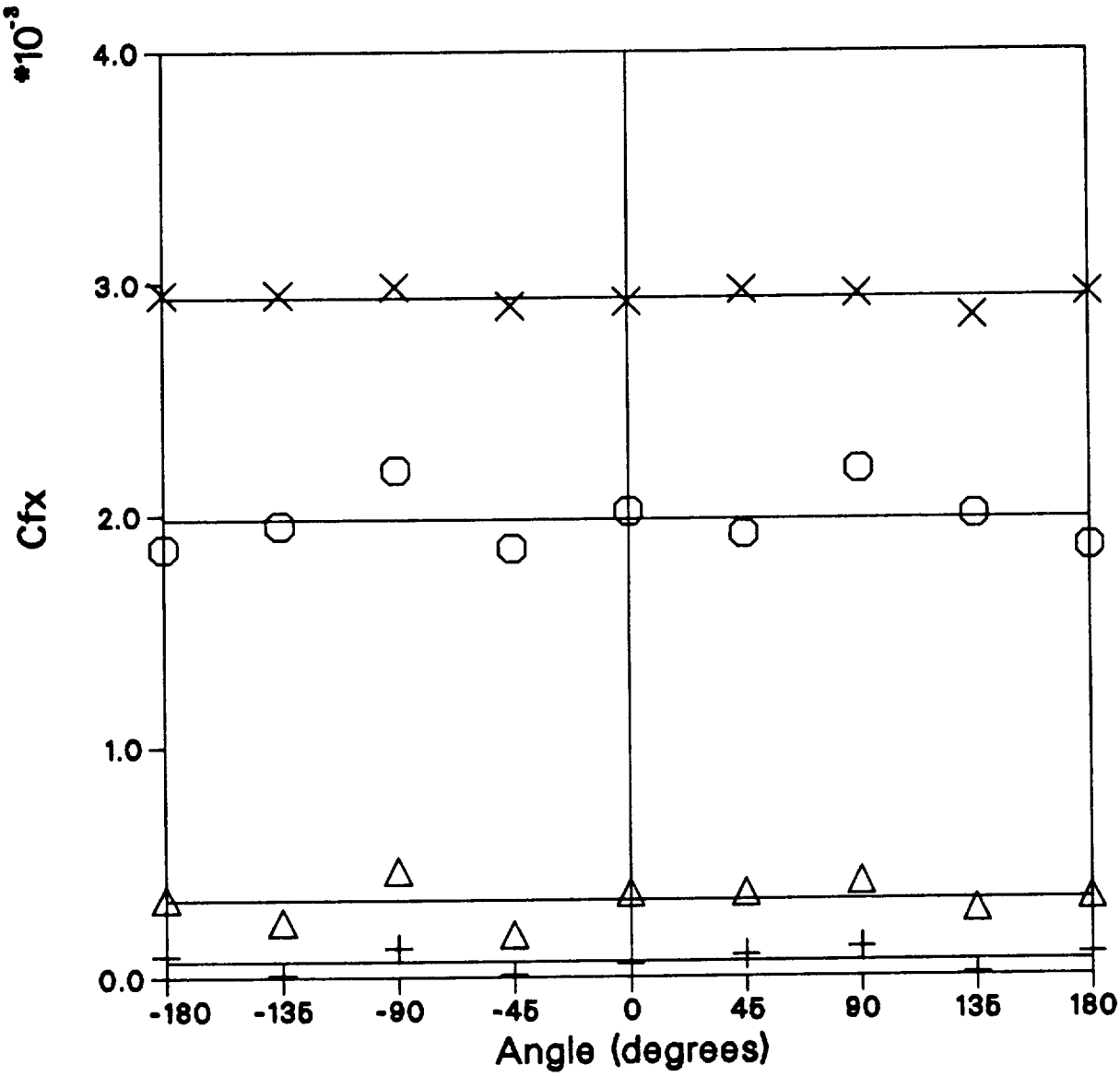

Figure 3.18 Circumferential distribution of axial skin-friction for case D.S0, × x=-457mm, ◯ x=6mm, △ x=152mm, + x=304mm.

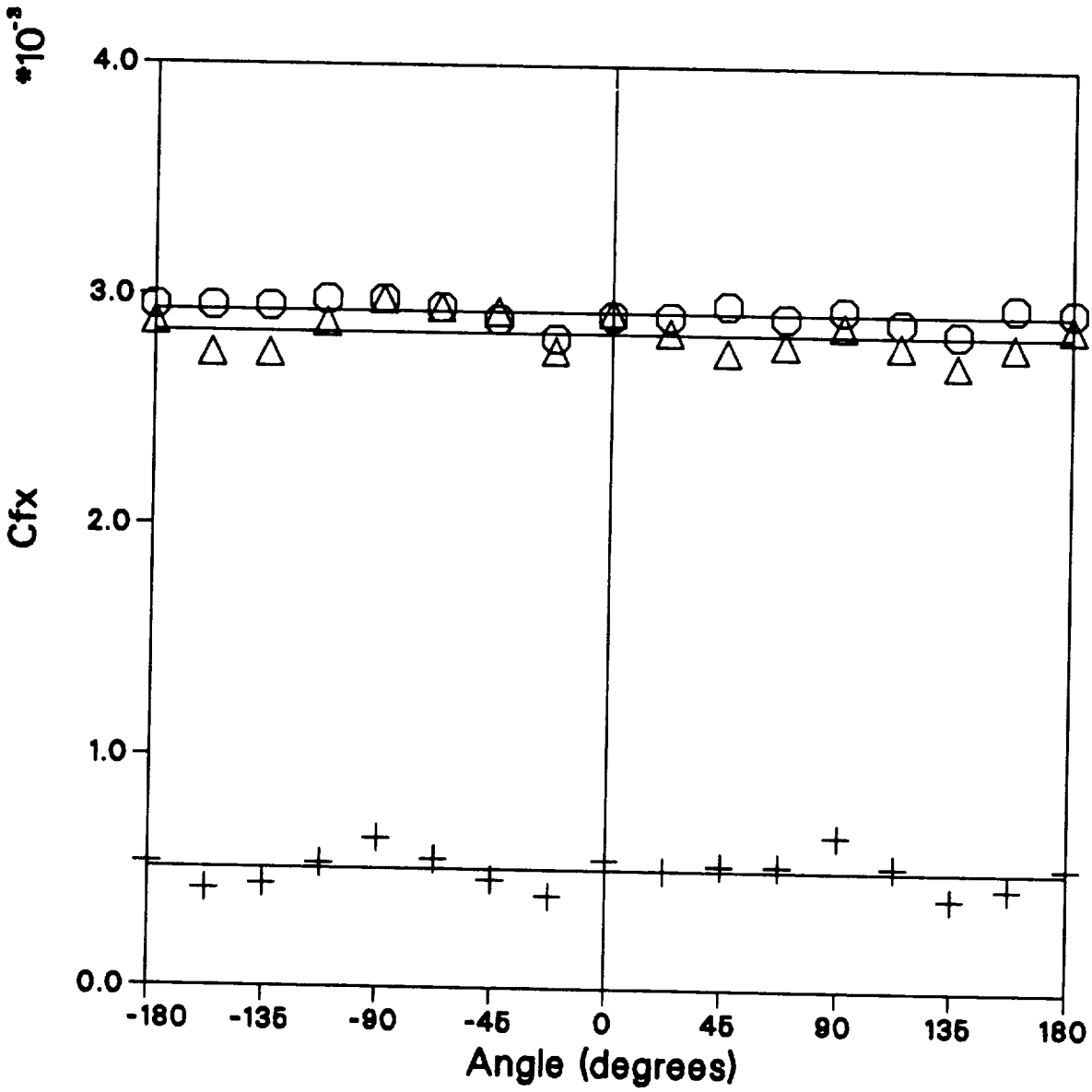

Figure 3.19 Circumferential distribution of axial skin-friction for case C.S0, ○ x=-457mm, △ x=-304mm, + x=-75mm.

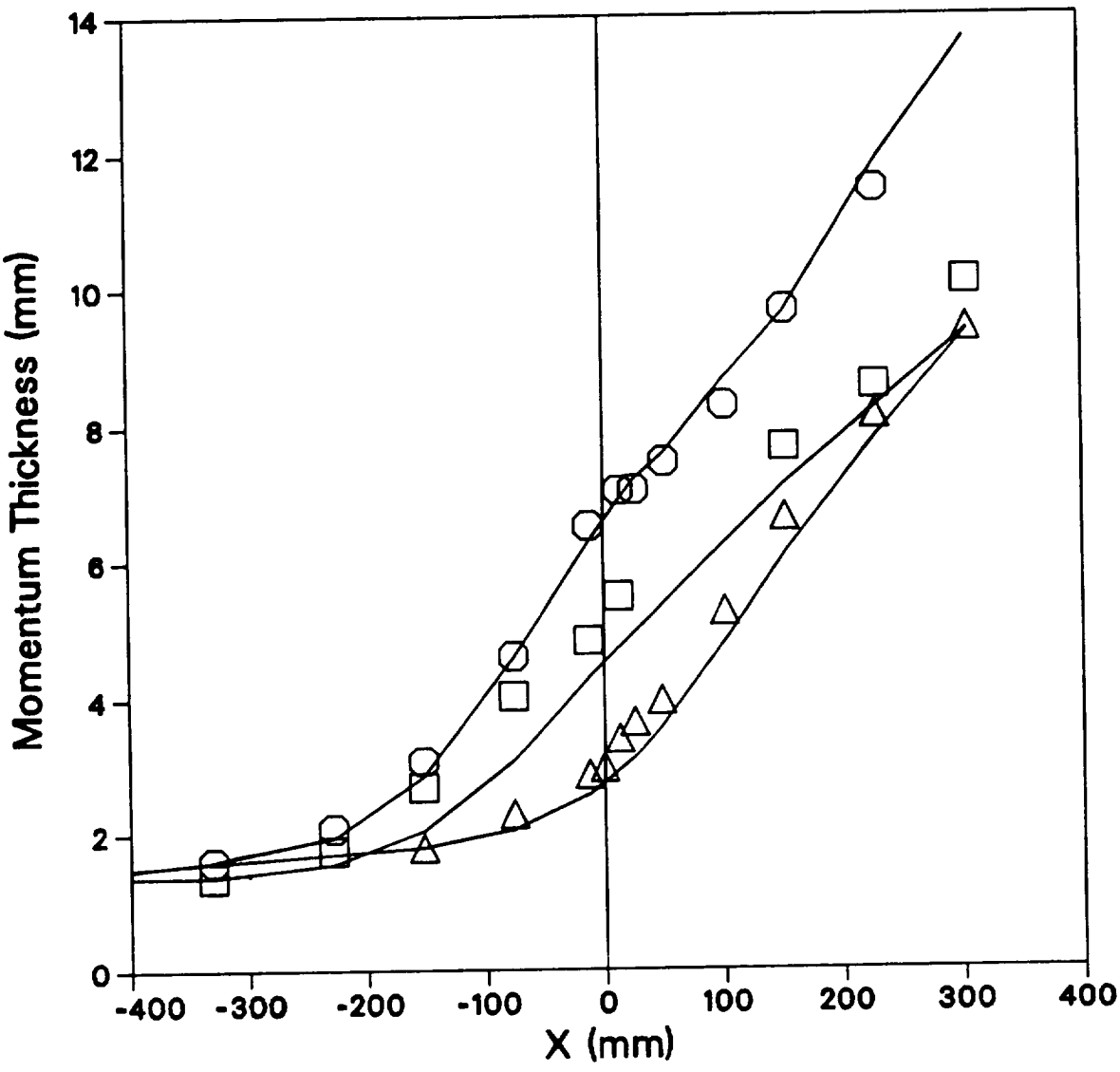

Figure 3.20 X-Momentum thickness distribution measured and balance for momentum equation for $W_s = 0$, □ Case B.S0, ○ Case C.S0, △ Case D.S0, —— momentum balance thickness.

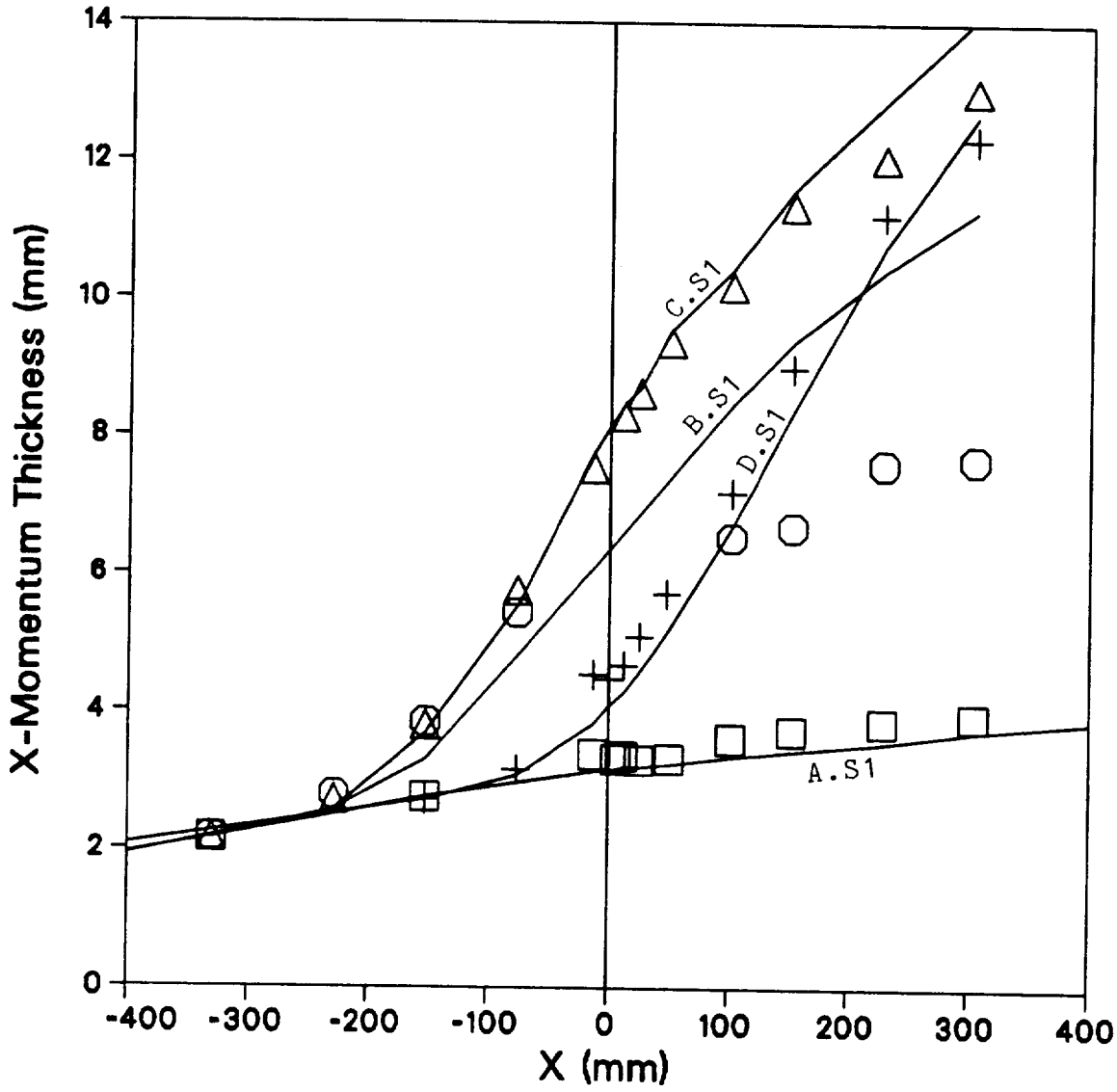

Figure 3.21 X-Momentum thickness distribution measured and balance for momentum equation for $W_s = U_r$, □ Case A.S1, ○ Case B.S1, △ Case C.S1, + Case D.S1, — momentum balance thickness.

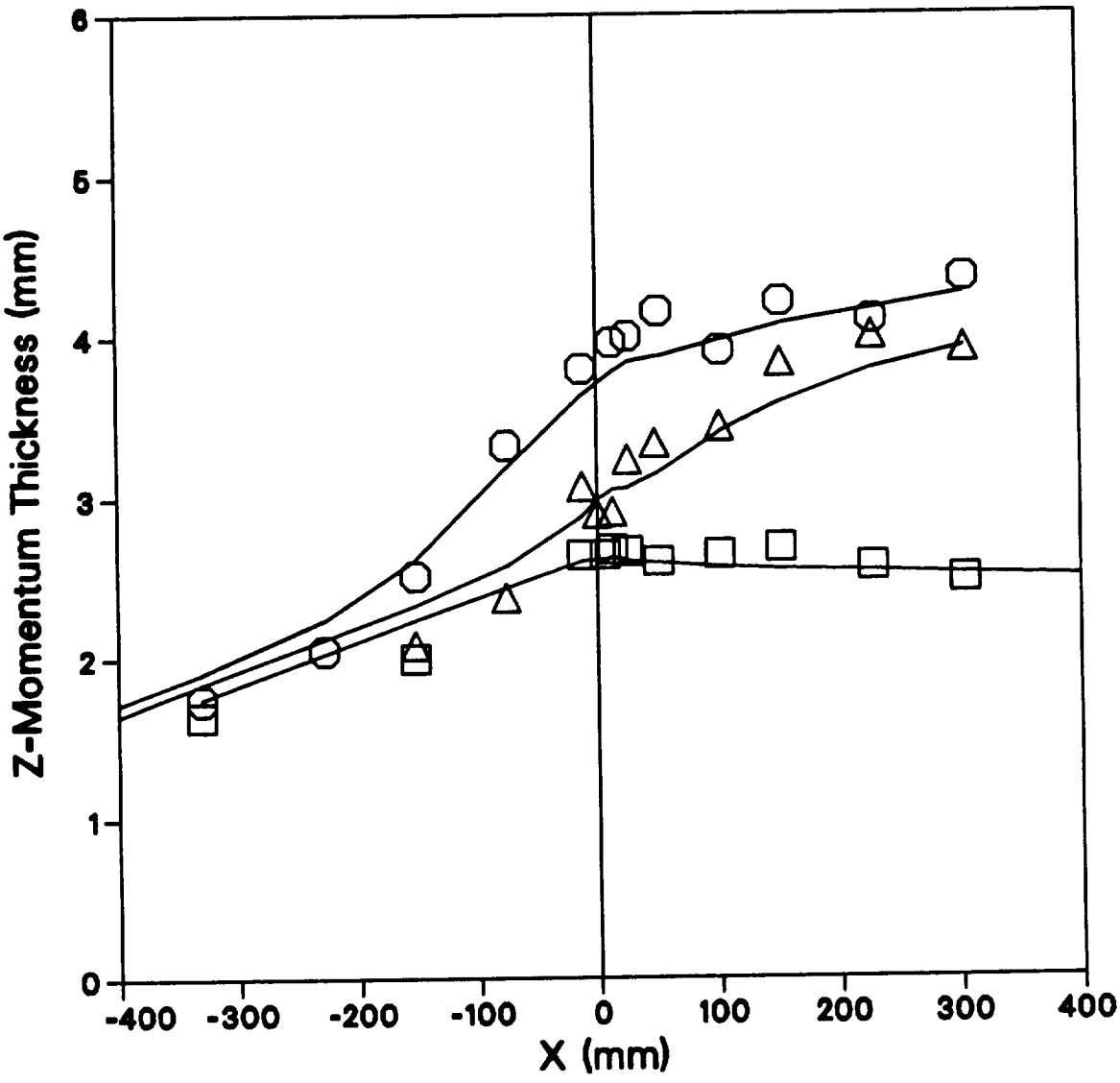

Figure 3.22 Z-Momentum thickness distribution measured and balance for momentum equation for $W_s = U_r$, □ Case A.S1, ○ Case C.S1, △ Case D.S1, —— momentum balance thickness.

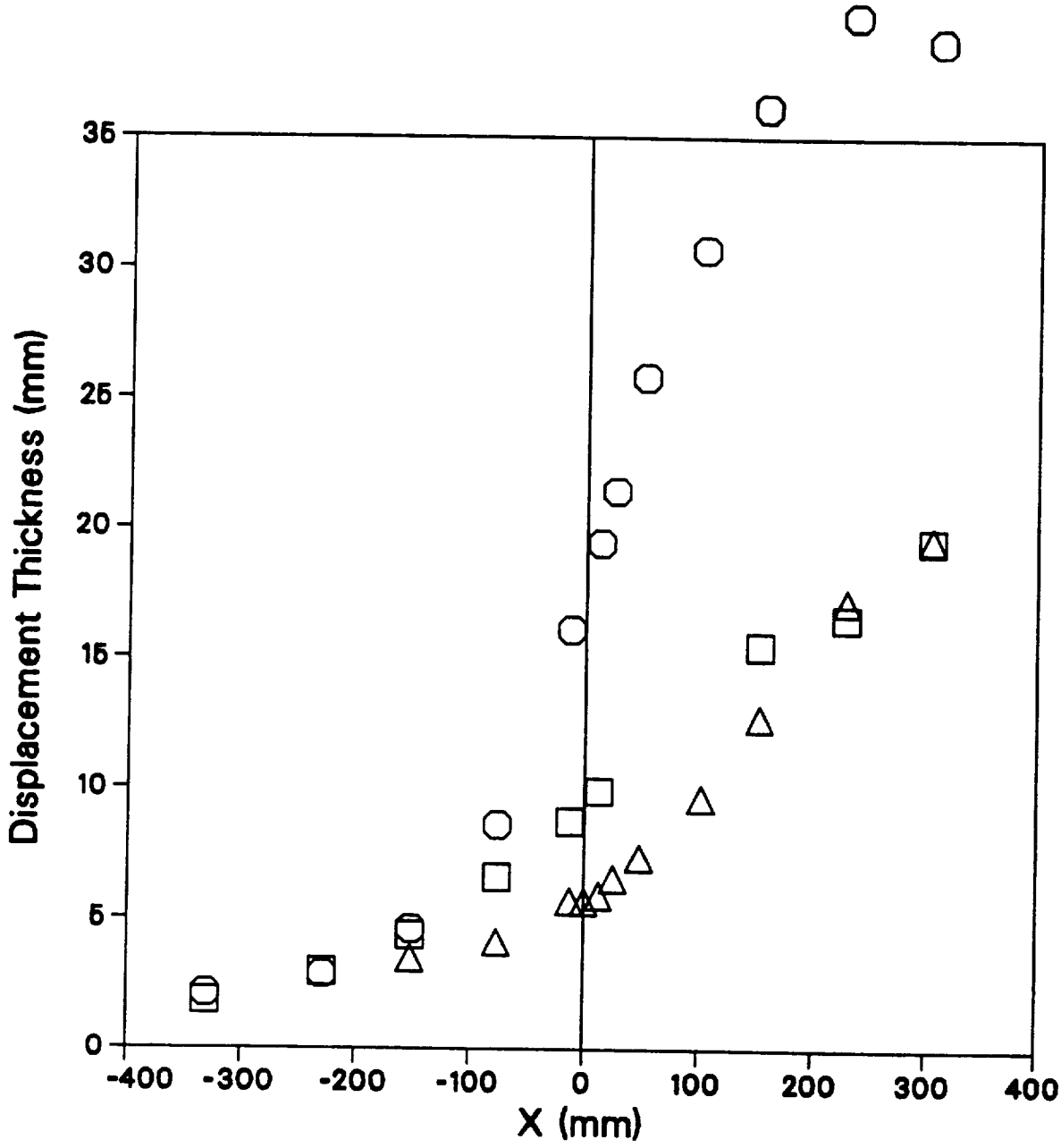

Figure 3.23 X-Displacement thickness distribution for $W_s = 0$, □ Case B.S0, ○ Case C.S0, △ Case D.S0.

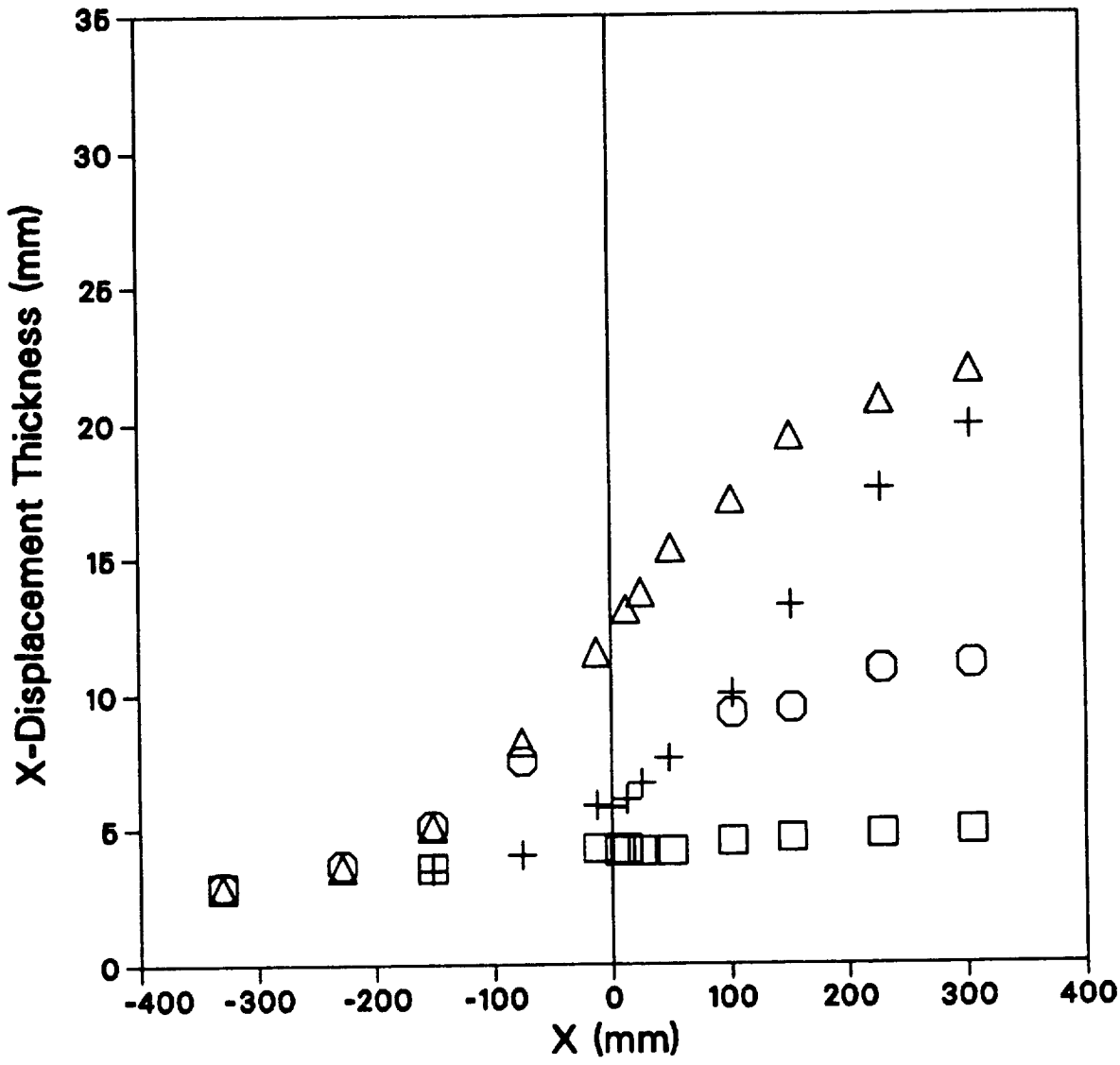

Figure 3.24 X-Displacement thickness distribution for $W_s = U_r$, □ Case A.S1, ○ Case B.S1, △ Case C.S1, + Case D.S1.

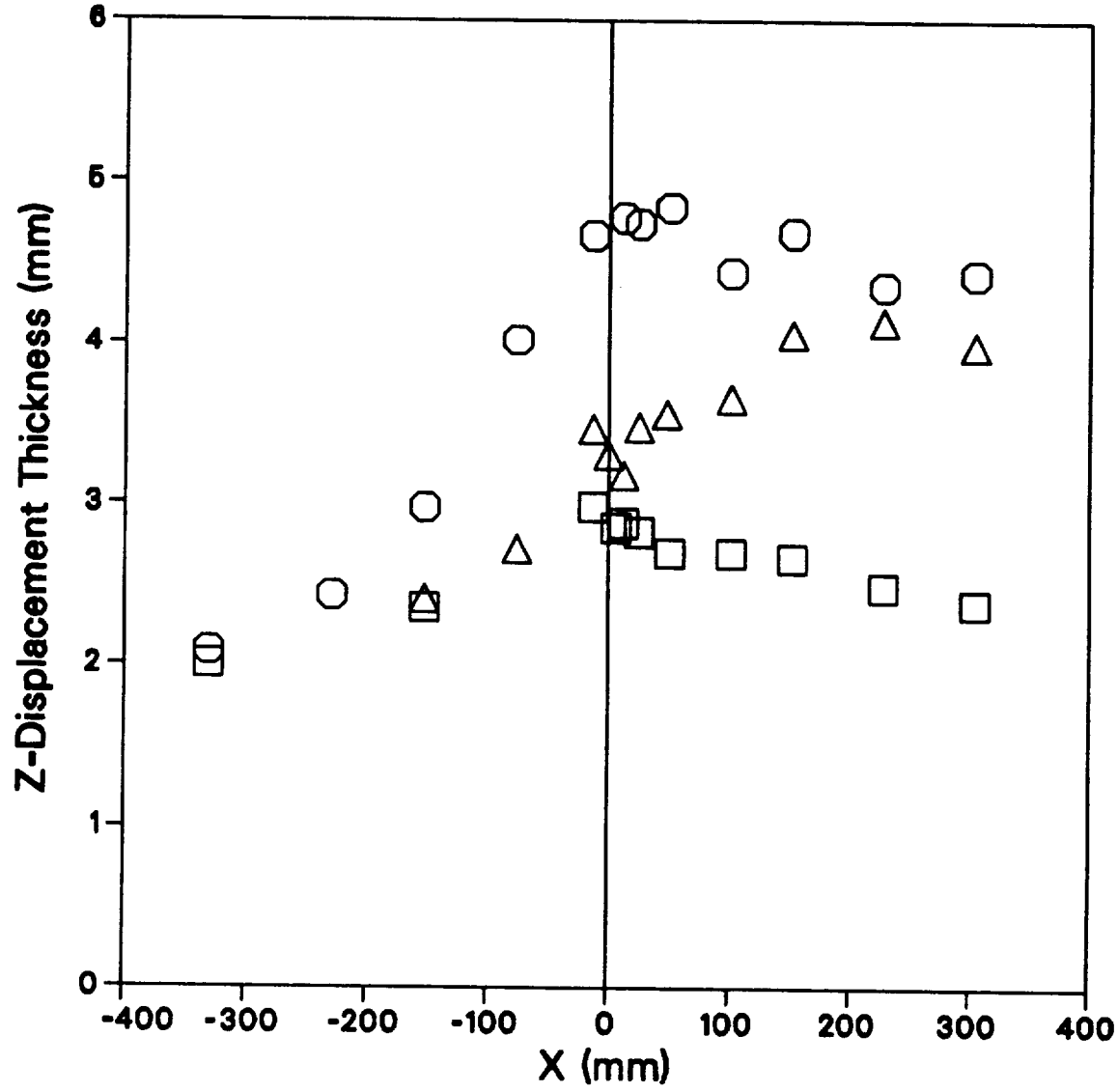

Figure 3.25 Z-Displacement thickness distribution for $W_s = U_r$, □ Case A.S1, ○ Case C.S1, △ Case D.S1.

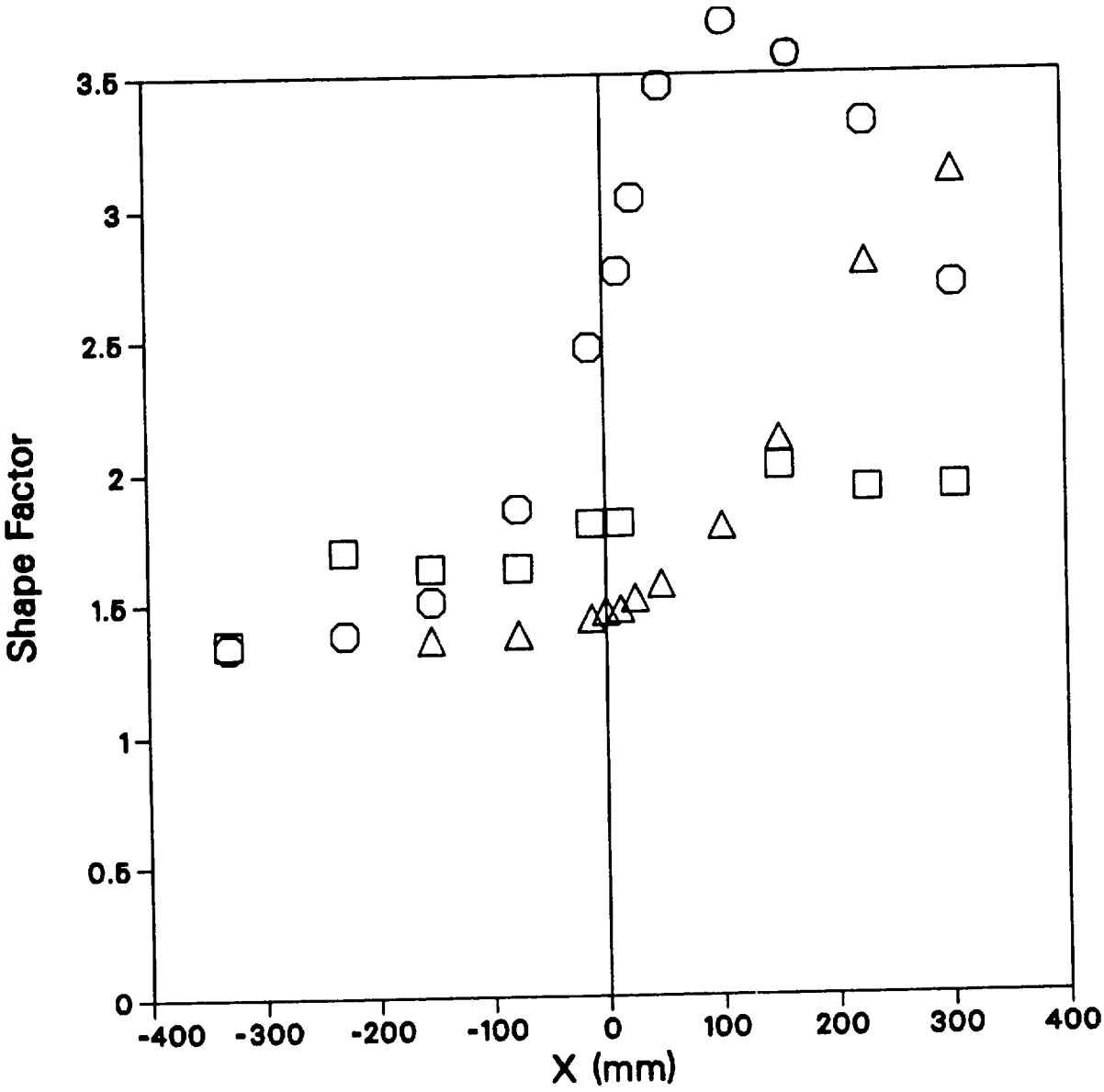

Figure 3.26 X-Shape factor distribution for $W_s = 0$, □ Case B.S0, ○ Case C.S0, △ Case D.S0.

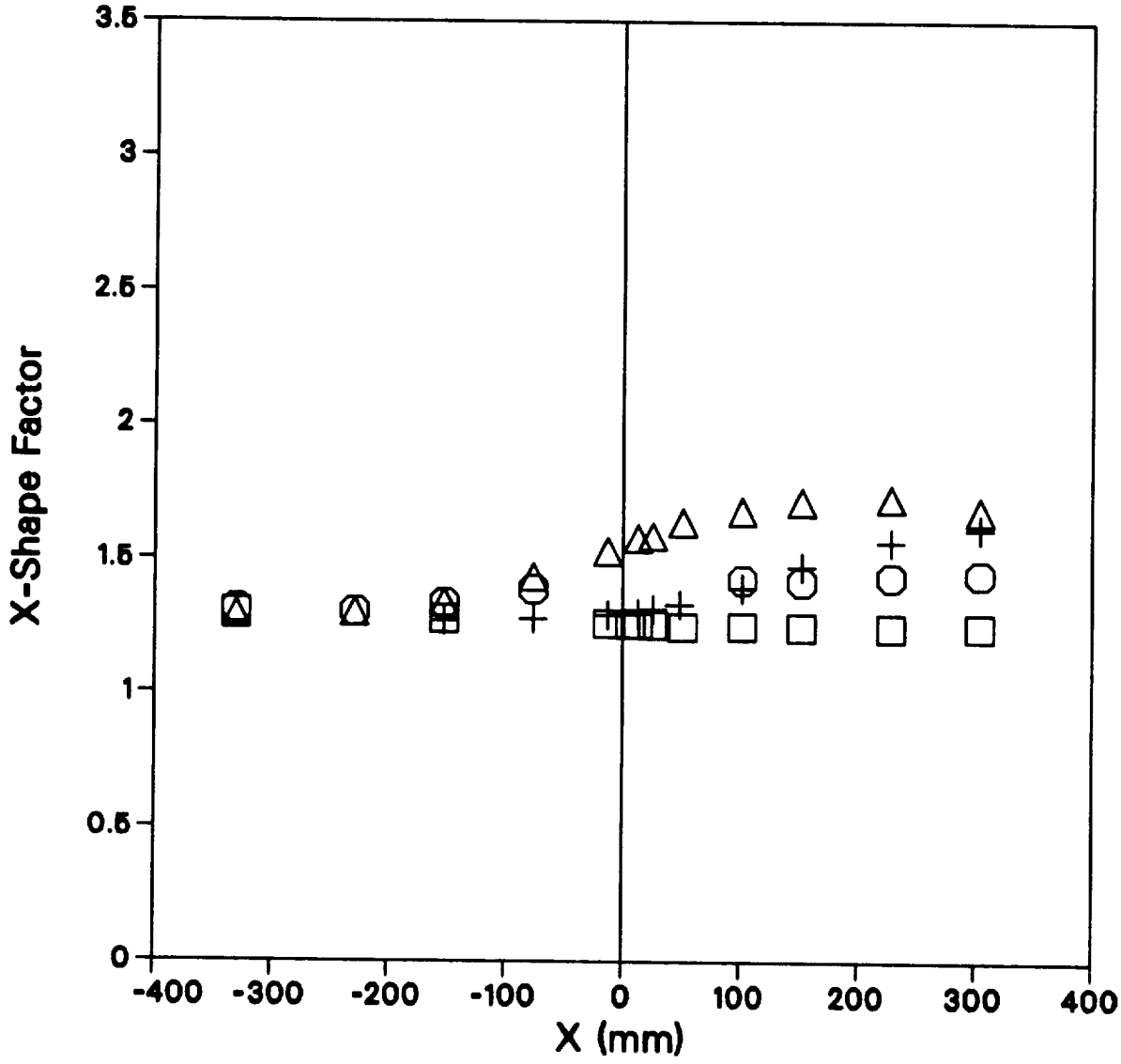

Figure 3.27 X-Shape factor distribution for $W_s = U_r$, □ Case A.S1, ○ Case B.S1, △ Case C.S1, + Case D.S1.

4 RESULTS AND DISCUSSION

Complete profiles of mean velocity, Reynolds stress, and triple product velocity correlations were obtained for each of the four different pressure gradient cases. Since the objective is examination of turbulence modeling, only those data which are applicable for making a particular point in this regard will be discussed. However, all of the data are tabulated in appendix C. The pressure gradient case D.S1 will be the primary source of discussion in this section. In case D.S1, a strong pressure gradient is applied at x = –25 mm and W_s, the cylinder surface spin rate equals U_r, the reference free-stream speed.

4.1 Mean Velocity Field

Mean flow longitudinal velocity measurements for the spinning case with strong adverse pressure gradient (case D.S1) are shown in figure 4.1. Increasing flow retardation is seen with distance X, a result of adverse pressure gradient. When velocity is normalized by the edge velocity (fig. 4.2), the profiles at the last two stations begin to approach self-similarity, probably a result of reaching a sustained Clauser parameter condition ($\beta_c = constant = 14$).

The mild adverse pressure gradient case B.S0 (which has no spin), is shown in figure 4.3. This case is similar to case D.S1 in that it has a nondimensional pressure gradient $\beta = 12$, close to the spinning case; however, case B.S0 does not approach a self-similar state (fig. 4.4). Only sparse data were taken, since this was not a primary test case.

The spinning and non-spinning cases differ most notably in the size of the incoming boundary layer, the spinning case being thicker. Also, the shapes of the two upstream boundary layers are different; the spinning case has higher momentum in the inner region (probably due to curvature effects). These differences persist downstream in the form of a thicker boundary layer with disproportionately high momentum near the wall for the spinning case.

High levels of transverse flow (W) are seen near the surface of the spinning cylinder in case D.S1 (fig. 4.5). These high levels diminish downstream on the stationary section of the cylinder. Conversely, in the outer region of the flow, W is seen to continue increasing with distance downstream as a result of diffusion. Comparing profiles of W versus stream function, it appears that W is fairly constant along streamlines in the outer layer (fig. 4.6). Actually, in the absence of viscous forces, angular momentum is the quantity that should be conserved along streamlines. However, profiles of Wr (fig. 4.7) do not collapse any better than did profiles of W, the reason being that Reynolds stress gradients (i.e., diffusion) are acting at the outer edges of the boundary layer as well as close to the wall. When y is normalized by δ, profiles of W exhibit a better degree of self similarity in the outer region (fig. 4.8)—δ increases with turbulent diffusion as well as streamline divergence (the pressure gradient degrades the self-similarity). The location where $W = 0.01W_s$ (referred to as δ_w) coincides with the edge of the boundary layer ($y = \delta$) as defined by $U = 0.99U_e$. The region near the wall, where self-similarity breaks down, grows outward with distance downstream along the stationary cylinder.

A hodograph plot (W vs. U) illustrates the collateral nature of the flow at the end of the spinning section ($X = -152$ mm) indicated by the nearly linear distribution of velocity $W/W_s = U/U_e - 1$ shown in figure 4.9. Collateral means that the flow is traveling in a single direction relative to an observer

moving with the wall, independent of distance from the wall (see appendix B for a detailed discussion). In a coordinate system traveling with the wall, the apparent velocity components $\hat{W}$ and $\hat{U}$ have magnitudes $W/W_s - 1$ and U/U_e. One can see that the flow measured nearest the wall ($y/\delta = 0.01$) is traveling in a direction equal to $-47.5°$ ($\hat{W}/W_s = W/W_s - 1 = -0.62$ and $U/U_e = 0.56$). Likewise the flow at the edge of the boundary layer is traveling in a direction equal to the $-45°$ ($\hat{W}/W_s = W/W_s - 1 = -1$ and $U/U_e = 1$). This boundary layer appears to behave like a 2D turbulent boundary layer which is traveling in the $-45°$ direction. Collateral flow is the self-similar state which one would expect when the transverse flow on the rotating section is fully developed.

Transverse flow downstream, in the zero pressure gradient case A.S1, exhibits a self-similar region in the outer region of the flow (fig. 4.10). However, the self-similar region diminishes with distance downstream as a result of viscous forces emanating from the surface of the stationary cylinder.

For the case with pressure gradient (D.S1), the self-similar region persists (fig. 4.11). Note that a U_e normalization is used for W instead of W_s because U_e changes with position. Here again, the deviation of the inner region from self-similarity is a result of viscous forces generated by shear with the cylinder surface.

4.2 Reynolds Stress Distribution

Spinning Section

Reynolds stress components are shown in figure 4.12 for spinning case A.S1, at upstream station X = −152 mm where the pressure gradient is zero. The streamwise and transverse components of Reynolds stress exhibit symmetry. That is, the transverse component of Reynolds stress $\overline{vw}$ is nearly equal to the streamwise component of Reynolds stress $-\overline{uv}$, and the normal stresses $\overline{ww}$ nearly equals $\overline{uu}$. This symmetry is expected since the lateral wall speed is equal to that of the free-stream velocity making production of stresses in those two directions equal.

If the stresses are evaluated in a coordinate direction aligned with the principal stress direction ($\approx -45°$), a more typical 2D behavior of the stresses is found. The normal stress components in this new coordinate system ($\overline{\tilde{u}\tilde{u}}$, $\overline{\tilde{v}\tilde{v}}$ and $\overline{\tilde{w}\tilde{w}}$) approach the usual 4:2:3 ratio seen in 2D boundary layers (fig. 4.13). Also the Reynolds shear stress component, $\overline{\tilde{u}\tilde{v}}$, approaches τ_w/ρ near the wall, while $\overline{\tilde{v}\tilde{w}}$ is zero everywhere (by definition). The stresses in this coordinate direction are comparable to the stress components measured for the non-spinning case A.S0. Component $\overline{\tilde{u}\tilde{w}}$, not shown, also is nearly zero in this coordinate system. This boundary layer behaves like a 2D turbulent boundary layer which is traveling in the $-45°$ direction. Indeed the surface streaky structures visualized on the spinning cylinder of Collini, Fulachier, and Dumas (ref. 43) were seen to be aligned in a nearly $-45°$ direction, with streak spacing, z^+, approximately equal to 100—the usual value for a 2D boundary layer.

Zero Pressure Gradient Stresses Evolution

Turbulent kinetic energy for the zero pressure gradient spinning case (A.S1) (fig. 4.14) decreases significantly with distance along the stationary cylinder. High levels of kinetic energy are seen at the upstream stations on the spinning cylinder, here the surface translation acts as a source of production.

Downstream, on the stationary section, the kinetic energy is seen to decay as a result of the removal of transverse strain (the source of $\overline{w^2}$ production).

Figure 4.15 shows the evolution of $\overline{w^2}$ for zero pressure gradient case A.S1. Here, $\overline{w^2}$ drops by a factor of three or more in the inner region, eventually approaching levels comparable with a 2D boundary layer (case A.S0). Figure 4.16 shows that the $\overline{v^2}$ stress component decreases as well, since it feeds on the energy available from the $\overline{w^2}$ and $\overline{u^2}$ components. The $\overline{u^2}$ component also decreases, since it becomes the sole source of turbulent kinetic energy production after production of $\overline{w^2}$ is removed after cessation of spin (downstream) (fig. 4.17). In addition, $\overline{u^2}$ decays because the other two components $\overline{v^2}$ and $\overline{w^2}$ are feeding off of the $\overline{u^2}$ component via pressure-strain.

Turbulent Reynolds shear stress, $-\overline{uv}/U_\tau^2$, for spinning case A.S1 is shown in figure 4.18. The relatively large upstream levels of stress exemplified by the peak values at x = –152 mm ($-\overline{uv}_{max}/U_\tau^2$ = 0.0023) are a result of the method of normalization. It is more appropriate to normalize the upstream Reynolds stresses with velocity $\tilde{Q}_\tau$ ($\tilde{Q}_\tau = \sqrt{U_\tau^2 + W_s^2}$) associated with the apparent velocity near the wall. The peak stress component associated with this coordinate direction (≈–45°), $-\overline{\tilde{u}\tilde{v}}_{max}/\tilde{Q}_\tau^2 = 0.0016$, is comparable to that of a 2D boundary layer of similar momentum thickness. It follows that component $\overline{uv}/\tilde{Q}_\tau^2$ equals $cos(-45°)\overline{\tilde{u}\tilde{v}}/\tilde{Q}_\tau^2$ = 0.0011.

The $\overline{uv}$ stress profiles shown in figure 4.18 decay with downstream distance along the stationary cylinder. Unlike kinetic energy production, $\overline{uv}$ stress production does not directly depend on transverse strain. Indirectly though, $\overline{uv}$ stress production can drop as a result of decreases in $\overline{v^2}$, which follows from decreases in $\overline{w^2}$. Downstream, the stress has dropped to levels lower than those for a comparable 2D boundary layer (indicated by the line in fig. 4.18 from case A.S0). The additional drop in stress, below the levels seen in a 2D boundary layer, is believed to be a result of 3D effects.

The transverse Reynolds stress component, $\overline{vw}$, changes sign in the inner region (below $y/\delta \approx 0.1$) as the flow passes from the spinning to the stationary section (fig. 4.19). The $\overline{vw}$ stress change from positive to negative is caused by a change in sign of the transverse strain-rate as a result of the new wall boundary condition. The region of self-similarity in the outer layer is slowly encroached on by the inner layer as the flow convects downstream.

This experiment offers a clear illustration of cause and effect which can be demonstrated through use of the Reynolds stress transport equations.

Adverse Pressure Gradient Stress Evolution

Figure 4.20 shows the evolution of kinetic energy in an adverse pressure gradient with spin (case D.S1). Near the wall the kinetic energy drops with distance along the stationary cylinder to levels lower than those for the zero pressure gradient case (case A.S1). In the outer region, the kinetic energy levels at the last station (X = 304 mm) approach the energy levels seen in a 2D boundary layer of comparable pressure gradient (case B.S0).

Profiles of the Reynolds stress component $\overline{uv}$ are shown in figure 4.21. They evolve in much the same way as does the kinetic energy for the pressure gradient case D.S1. The stress decays with distance along the stationary cylinder as a result of cessation of spin. The inner region decreases drastically with

decreases in the pressure gradient—this is also seen in the 2D adverse pressure gradient case (case B.S0 in fig. 4.21). The outer region does not decrease as much as it did for the zero pressure gradient case as a result of increased production caused by steeper velocity gradients. The stress level at the downstream station is comparable to the stresses in a comparable 2D adverse-pressure-gradient boundary layer (case B.S0 at X = 152 mm).

The evolution of $\overline{vw}$ stress is shown in figure 4.22 for the adverse pressure gradient case. These profiles demonstrate the change in sign of the stress as the flow moves from the spinning to the stationary section. The $\overline{vw}$ stress at X = 304 mm is generally lower (by as much as 40%) than the stress in the zero pressure gradient case A.S1 (fig. 4.22).

The total stress, $\sqrt{\overline{uv}^2 + \overline{vw}^2}$, behaves similarly to the $-\overline{uv}$ stress although the overall levels are higher (fig. 4.23, case D.S1). Normalizing by the apparent velocity $\tilde{Q}_r^2 = U_r^2 + W_s^2$ instead of U_r^2 brings the $\sqrt{\overline{uv}^2 + \overline{vw}^2}$ stress in line with what one might expect for that of a 2D boundary layer of the equivalent Reynolds number.

Figure 4.24 shows the evolution of the $-\overline{uw}$ stress for the adverse pressure gradient case D.S1. The stress component $-\overline{uw}$ undergoes a change of sign from the spinning to non-spinning sections of cylinder, that follows the change in sign of the strain-rate angle.

4.3 Reynolds Stress Contribution to Momentum Balance

The effect of turbulence on the evolution of the mean flow field needs to be assessed in order to determine the importance of turbulence modeling to the mean flow solution. Where pressure forces are largely responsible for the mean flow accelerations, turbulence models may not be very important to the solution of the mean flow. However, near surfaces the shear forces (laminar and turbulent) tend to be large because of steep velocity gradients caused by the no-slip condition at the wall. One way to assess the importance of the turbulence model is to examine terms in the momentum equation. Ignoring laminar viscous stresses which are small (except very near the wall, where LDV measurements were not possible), the terms in the axial momentum equation are

$$DU/Dt = -\frac{1}{\rho}\partial P/\partial x - \frac{1}{r}\partial(r\overline{uv})/\partial r - \partial\overline{u^2}/\partial x$$

Individual terms are shown in figure 4.25 for the adverse pressure gradient case D.S1. The $\frac{1}{\rho}\partial P/\partial x$ term, inferred locally from the equation balance, compares very well to the measured pressure gradient at the wall. Here the streamwise momentum loss is almost exclusively a result of streamwise pressure gradients. The Reynolds stress terms are relatively small compared to the pressure gradient and convection terms everywhere except near the wall. Near the wall the stress acts to balance the pressure gradient and re-energize the mean flow. At the wall, the laminar component of shear stress is solely responsible for balancing the pressure gradient. However, away from the wall, beyond $y/\delta = 0.5$, small amounts of stress add to the pressure forces, thus contributing to a further loss in flow momentum. The momentum extracted from the outer region of the flow is transferred to the inner region. This redistribution of momentum maintains forward flow near the wall at the expense of decelerating the outer flow. Note that in a zero-pressure-gradient flow, the stress would be acting to retard the flow across the whole layer.

Another way to determine the effect of turbulence on the mean flow is to compare the measured velocities with velocities calculated assuming no shear stresses (figs. 4.26 and 4.27 for cases D.S1 and B.S0, respectively). By looking back along a streamline to a location of origin (say x_i = –76 mm) and applying Bernoulli's equation ($Q = \sqrt{Q_i^2 - \frac{2}{\rho}(P - P_i)}$) we calculated the velocity which the fluid would have obtained if the flow had been solely acted on by pressure forces, not shear forces. The differences between the measured and calculated inviscid velocities are due to the shear forces. The measurements indicate that momentum has been carried from the high-speed outer flow to the low-speed inner flow by turbulent mixing between the two regions. Both spinning and nonspinning cases are similar.

Rate of change of transverse momentum for the spinning case (D.S1) is balanced solely by the transverse shear stress (fig. 4.28). The transverse momentum equation is given by

$$DW/Dt + \frac{VW}{r} = -\frac{1}{r^2}\partial(r^2\overline{vw})/\partial r$$

For the location shown, momentum is being lost in the wall region as a result of Reynolds stress forces generated by the stationary wall. In the outer region, the flow gains momentum as a result of turbulent diffusion of momentum outward into the free stream.

4.4 Reynolds Stress Vector Direction

A common but incorrect assumption often used in turbulence modeling is that the Reynolds stress is proportional to the mean flow strain-rate. As a consequence of this assumption, the stress vector direction is assumed to be the same as the strain-rate vector direction. This section will demonstrate the degree to which the stress and strain-rate vector directions differ from each other in the spinning cases with and without adverse pressure gradient.

Strain-rate direction in the zero pressure gradient case A.S1 is shown in figure 4.29 to vary with distance from the cylinder surface. The strain-rate direction at the station shown (X = 100 mm) differs from that of the upstream X = –12-mm station. Upstream, both the strain-rate and stress vectors point in approximately the same direction throughout the boundary layer; this direction (–45°) corresponds to the flow direction relative to the moving wall. Downstream, on the stationary section, the strain-rate turns more toward the new flow direction of +10° (relative to stationary wall), while the stress continues to point in the –45° direction, throughout most of the boundary layer. Near the wall the stress turns toward the strain-rate direction. The angle of the stress lags the strain-rate.

Imposition of a pressure gradient (case D.S1) does not immediately affect the stress vector direction (fig. 4.30) even though the strain-rate vector is inviscidly rotated from –42° to –35° in the outer part of the flow. The lack of difference between the Reynolds stress direction in the two cases is an indication of the relatively slow rate of response by the stresses to rapid changes in the strain-rate.

4.5 Reynolds Shear Stress Decay in Three-Dimensional Flows

Reynolds stress has been observed to decay in flows with transverse strain. Bradshaw and Pontikos (ref. 8) saw this in an "infinite"-swept-wing flow experiment. Bradshaw (ref. 8) advanced the hypothesis

that generation of streamwise vorticity in the mean flow could lead to toppling of the large scale eddies in the flow and thus reduce the Reynolds stress.

The spinning cylinder flow also experiences a drop in Reynolds shear stress in the relaxation zone, but does so primarily as a result of a step function drop in wall shear (in response to the new boundary condition $W_s = 0$). Consequently, it is difficult to determine how much of the drop in Reynolds stress is a result of 3D effects and how much is a result of the changing boundary condition. However, case C.S1, with the pressure gradient imposed upstream on the spinning cylinder produces a 3D effect while maintaining a constant boundary condition ($W_s = U_r$).

The pressure gradient imposed upstream on the spinning cylinder causes the mean flow (viewed in a moving wall frame) to turn further away from the tunnel axis from $\approx -47°$ (in the upstream direction) toward $\approx -58°$ (fig. 4.31). Conversely, the strain-rate vector rotates in the opposite direction toward –34° from its upstream direction of –42°. The strain rate vector rotates in one direction while the mean flow rotates in the opposite direction—this is accomplished purely by inviscid means ($\partial P/\partial X > 0$). This reorientation of the strain-rate direction in the outer flow is believed by Bradshaw and Pontikos (ref. 8) to be responsible for reduction of Reynolds stress, perhaps via an eddy toppling mechanism.

In fact a drop in Reynolds stress is observed (figs. 4.32 and 4.33). Both $\overline{uv}$ and $\overline{vw}$ stress are reduced by 10% or 20% in the outer region of the flow. A drop in $\overline{vw}$ is expected due to a drop in $\partial W/\partial r$ gradients resulting from flow divergence caused by boundary layer growth. However, an increase in $\overline{uv}$ is expected; $\overline{uv}$ stress typically increases in a 2D boundary layer with adverse pressure gradient (fig. 4.34). Consequently, there does seem to be a drop in Reynolds stress with rotation of the mean flow strain-rate vector direction.

Another measure of how much the Reynolds stress drops is the structure parameter a_1 ($a_1 = \sqrt{\overline{uv}^2 + \overline{vw}^2}/2k$). Profiles of $2a_1$ (fig. 4.35) also exhibit slightly lower than usual levels (the usual level being 0.3) for spinning case C.S1 with upstream pressure gradient. Bradshaw and Pontikos (ref. 8) saw a similar drop in this parameter for their swept wing flow. The drop in structure parameter may be in part due to adverse pressure gradient which tends to reduce it; figure 4.36 shows an adverse pressure gradient with zero spin (case B.S0). However, using the stress component in the streamwise direction rather than the X-direction produces a structure parameter which is less affected by pressure gradient (fig. 4.37).

The relaxation zone of case A.S1 under zero pressure gradient conditions exhibits a reduction in structure parameter in response to the new boundary condition (fig. 4.38). The level of $2a_1$ on the upstream spinning section is a bit higher than usual for a flat plate boundary layer, due to destabilizing rotational effects which tend to make the turbulent mixing a little more efficient (highly correlated). However, downstream, in the relaxation zone, $2a_1$ undershoots the usual value for a flat plate which is probably due to 3D effects.

Pressure gradient case D.S1 produces a larger decay of the structure parameter (fig. 4.39). The reduction in structure parameter seems to be a cumulative effect of transverse strain as well as streamwise pressure gradient. The value of a_1 is frame-of-reference dependent as was shown in the 2D pressure gradient case (B.S0). However, the appropriate choice of coordinate frames is not obvious for 3D flows, since the strain-rate direction is not aligned with the streamline direction.

The lowering of the Reynolds shear stress in case C.S1 is comparable to but not as large as that seen in the Bradshaw and Pontikos (ref. 8) "infinite" swept wing experiment where the reduction is on the order of a factor of two. The Reynolds shear stress decreases on the order of 10 or 20% in the spinning cylinder experiment. The two experiments produce approximately the same disparity between mean flow and strain-rate directions (20° to 30°), so it is not clear why the drop is so much larger in the "infinite" swept wing experiment than it is in the spinning cylinder experiment. Perhaps a more appropriate parameter is the degree of absolute turning of the strain-rate direction. In the Bradshaw-Pontikos flow, the strain-rate direction changes by 10°; while in the spinning cylinder flow it is only 5°.

4.6 Turbulent Transport Equations

In section 4.2, the impact of the turbulence on the mean flow momentum was examined. In this section the impact of the mean flow on the turbulence will be examined. The turbulent stresses often exhibit large variations along streamlines. For example, contours of kinetic energy, $\overline{uv}$-stress, and $\overline{vw}$-stress for case A.S1 show steep gradients in the streamwise direction (figs. 4.40(a),(b),(c)). The steep gradients are directly caused by the step change in boundary condition ($W_s = U_r$ to $W_s = 0$). Similarly, large streamwise gradients of k, $\overline{uv}$, and $\overline{vw}$ are seen in the pressure gradient case D.S1 (which has spin), due in part to the pressure gradient and in part to the change in boundary condition (figs. 4.41(a),(b),(c)). Also, cases D.S0 and C.S0 (the no-spin cases) show large streamwise gradients of k and $\overline{uv}$, which are caused solely by the adverse pressure gradient (figs. 4.42(a),(b) and 4.43(a),(b)). These streamwise flow variations can be traced to changes in the mean flow strain-rate. Equations for the transport of turbulence can be derived from first principles, which show the relationship between the turbulence and the mean flow. This procedure is followed in the next two sections.

4.6.1 Kinetic-Energy Balance

The turbulent kinetic-energy equation is used in some models to provide information needed in the model for the Reynolds stresses. While the equation can be derived from first principles, some of the terms in it involve new variables which require further modeling. Nevertheless, the hope is that the kinetic energy equation (albeit modeled) retains information about the history of the flow, information which is otherwise lost when an equilibrium model is used. Hopefully, modeling the terms in the kinetic-energy equation is easier (more accurate) than modeling the kinetic energy itself.

Terms in the turbulent kinetic-energy equation were calculated from

$$\underbrace{Dk/Dt}_{Convection} = \underbrace{[-\frac{1}{r}\partial(r\overline{vk})/\partial r - \partial\overline{uk}/\partial x]}_{Diffusion} - \underbrace{\varepsilon}_{Dissipation}$$

$$\underbrace{[-\overline{uv}\partial U/\partial r - \overline{vw}(\partial W/\partial r - W/r) - (\overline{u^2} - \overline{v^2})\partial U/\partial x]}_{Production}$$

using the experimental data, except for dissipation rate for which there are no data. The dissipation rate had to be inferred from the balance of the equation. Terms in the equation were evaluated along a path of constant stream function (the streamline in the 2D case) which originates in the log layer at $y = 1.27$ mm ($y^+ \approx 100$) and $X = -457$ mm (figs. 4.44 and 4.45 for cases D.S0 and D.S1, respectively). Upstream, in

the unperturbed boundary layer, the production of kinetic energy is virtually equal to the dissipation rate, while convection and turbulent diffusion are nearly zero. This is expected for an equilibrium boundary layer under zero-pressure-gradient conditions.

Kinetic energy production rate for spinning case D.S1 (fig. 4.45) is significantly higher than for that of the non-spinning case (approximately double)—this is due to the extra rate of strain from transverse flow, which contributes up to half of the total production. Downstream on the stationary section, where transverse strain has diminished, the production rate decreases to a level comparable to that for the non-spinning case.

The turbulence is in a state close to equilibrium, because production is very nearly equal to dissipation. In other words, the evolution of the kinetic energy is apparently slow relative to the rates of creation (production) and destruction (dissipation). It is somewhat surprising to see this state of near-equilibrium, since it was expected that the turbulence would be pushed out of equilibrium in this rapidly evolving mean flow.

4.6.2 Reynolds Stress Equation Balance

The increasingly popular Reynolds stress-equation models involve the solution of partial differential equations for the individual components of the Reynolds stress. These equations, while derivable from first principles, require modeling of many of the terms. Reynolds stress equation modeling is needed in nonequilibrium flows where the evolution of Reynolds stress lags the evolution of the mean flow-strain rate.

All terms in the equation for $\overline{uv}$ Reynolds stress were calculated using the data directly, except for pressure-strain and dissipation of $\overline{uv}$ stress.

$$\underbrace{D\overline{uv}/Dt - \overline{uw}W/r}_{Convection} = \underbrace{-\frac{1}{r}\partial(r\overline{uv^2})/\partial r - \partial\overline{vu^2}/\partial x + \overline{uw^2}/r}_{Diffusion}$$

$$\underbrace{(-\overline{v^2}\partial U/\partial y + \overline{uw}W/r)}_{Production} + \underbrace{\phi_{uv}}_{Pressure-strain} - \underbrace{\varepsilon_{uv}}_{Dissipation}$$

These unmeasurable terms, pressure-strain and dissipation, are grouped together and inferred from the balance of the equation. Dissipation of $\overline{uv}$ stress (ε_{uv}) is believed to be small and this lumped sum will be referred to as the pressure strain for ease of discussion. Terms in the $-\overline{uv}$ stress equations were evaluated along the same path of constant stream function as that for the kinetic-energy equation (originating at $y = 1.27$ mm, $y^+ \approx 100$) (figs. 4.46 and 4.47 for cases D.S0 and D.S1).

In both spinning and non-spinning pressure gradient cases, the pressure strain is virtually equal to the production of $\overline{uv}$ stress. In comparison, convection and diffusion of $\overline{uv}$ stress, are extremely small. The pressure strain (plus dissipation), which requires modeling, is almost exclusively balanced by the production term. Physically, pressure strain is the mechanism by which turbulent energy is exchanged from one component to another.

In the spinning case the convection and diffusion terms are somewhat larger than in the non-spinning case, but relative to production they are still very small. The small relative size of the convective term (for which the model equation is solved) could make it difficult to design a pressure-strain model which will accurately predict the observed drop in $\overline{uv}$ stress associated with transverse strain.

Terms in the $\overline{vw}$ stress equation given by

$$\underbrace{D\overline{vw}/Dt - (\overline{w^2} - \overline{v^2})W/r}_{Convection} = \underbrace{+(-\frac{1}{r}\partial(r\overline{wv^2})/\partial r - \partial\overline{uvw}/\partial x - (\overline{wv^2} - \overline{w^3})/r)}_{Diffusion}$$

$$\underbrace{(-\overline{v^2}\partial W/\partial r + \overline{uw}W/r)}_{Production} + \underbrace{\phi_{vw}}_{Pressure-strain} - \underbrace{\varepsilon_{vw}}_{Dissipation}$$

were calculated for the spinning case (D.S1) along the same streamline as were used for evaluating the $\overline{uv}$ stress equation (fig. 4.48). Production of $\overline{vw}$ stress, the largest term in the equation, is seen to decay with distance downstream of the spinning cylinder. This drop in production corresponds to the absence of spin and, therefore, a decrease in the $\partial W/\partial y$ gradients. Pressure strain likewise drops along with production. Convection is negative, which indicates a net decay of $\overline{vw}$ stress with distance along the streamline. Unlike the $\overline{uv}$ stress equation, convection of $\overline{vw}$ stress is relatively large compared to production, providing more leeway for error in modeling the pressure-strain term. Negative diffusion indicates there is a net outflow of $\overline{vw}$ stress away from this streamline via turbulent mixing.

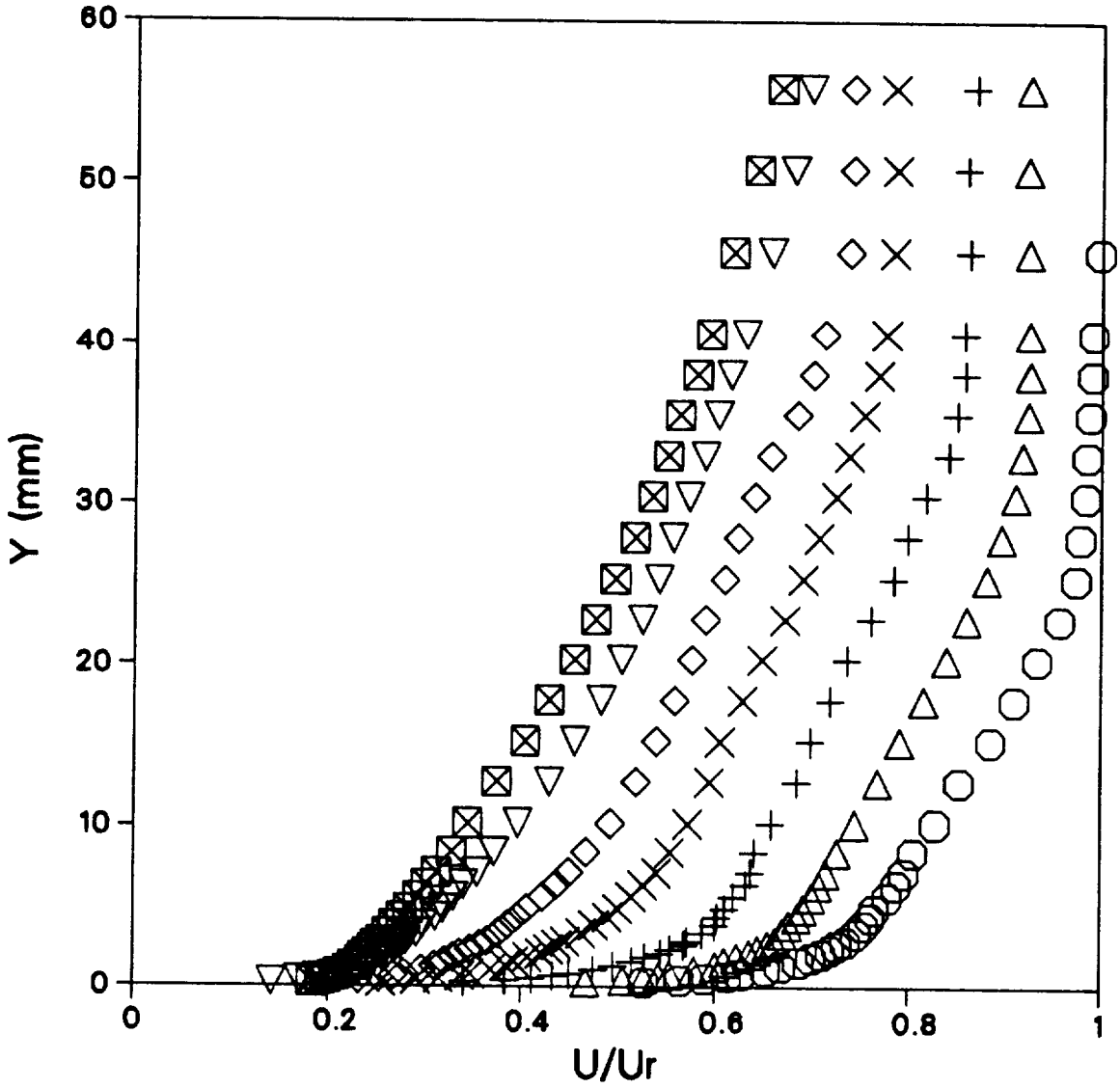

Figure 4.1 Streamwise velocity distribution for spinning Case D.S1, ◯ x=-76mm, △ x=−12mm, + x=48mm, × x=101mm, ◇ x=152mm, ▽ x=228mm, ⊠ x=304mm.

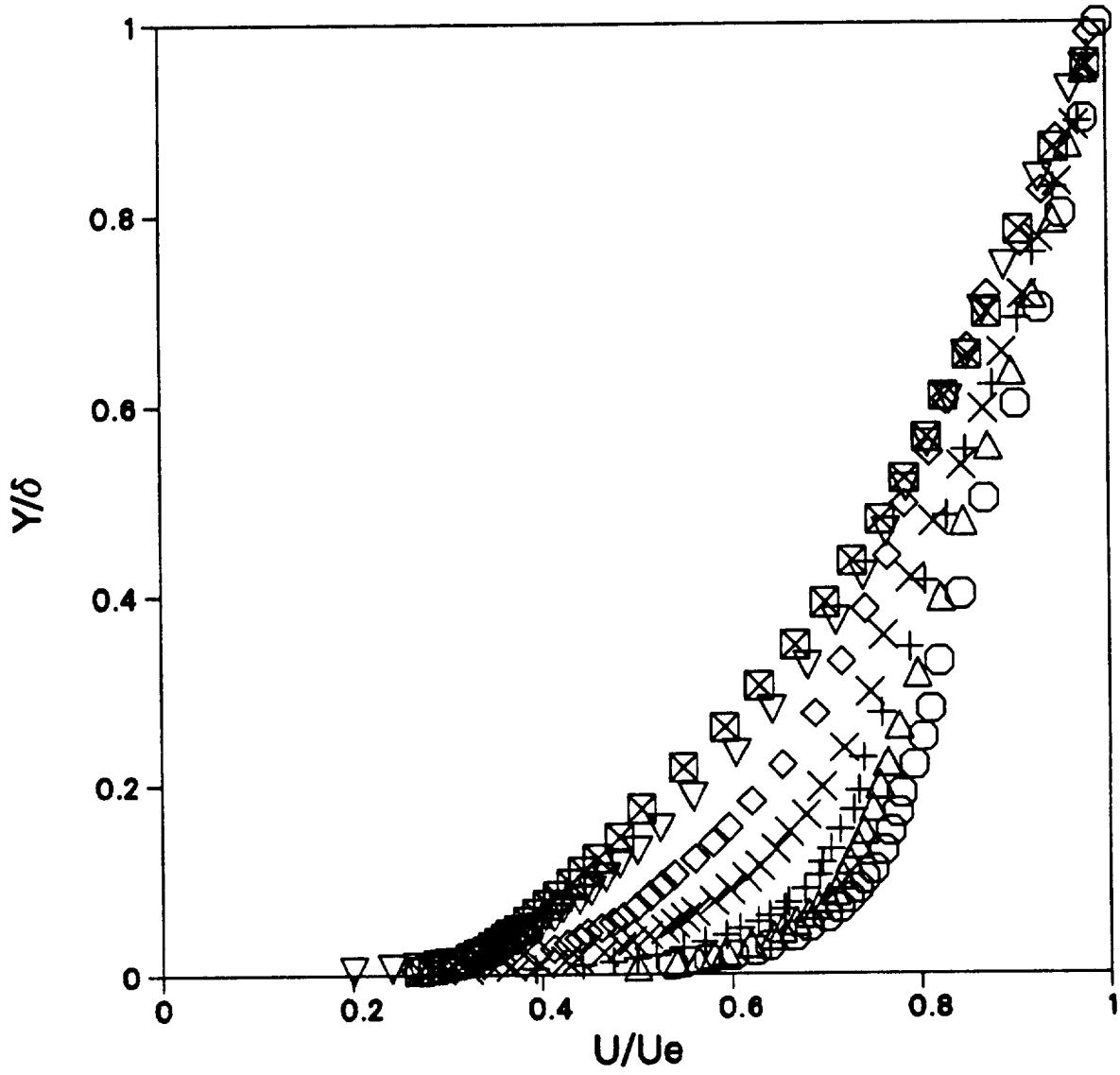

Figure 4.2 Normalized streamwise velocity distribution for spinning Case D.S1, ○ x=-76mm, △ x=−12mm, + x=48mm, × x=101mm, ◇ x=152mm, ▽ x=228mm, ⊠ x=304mm.

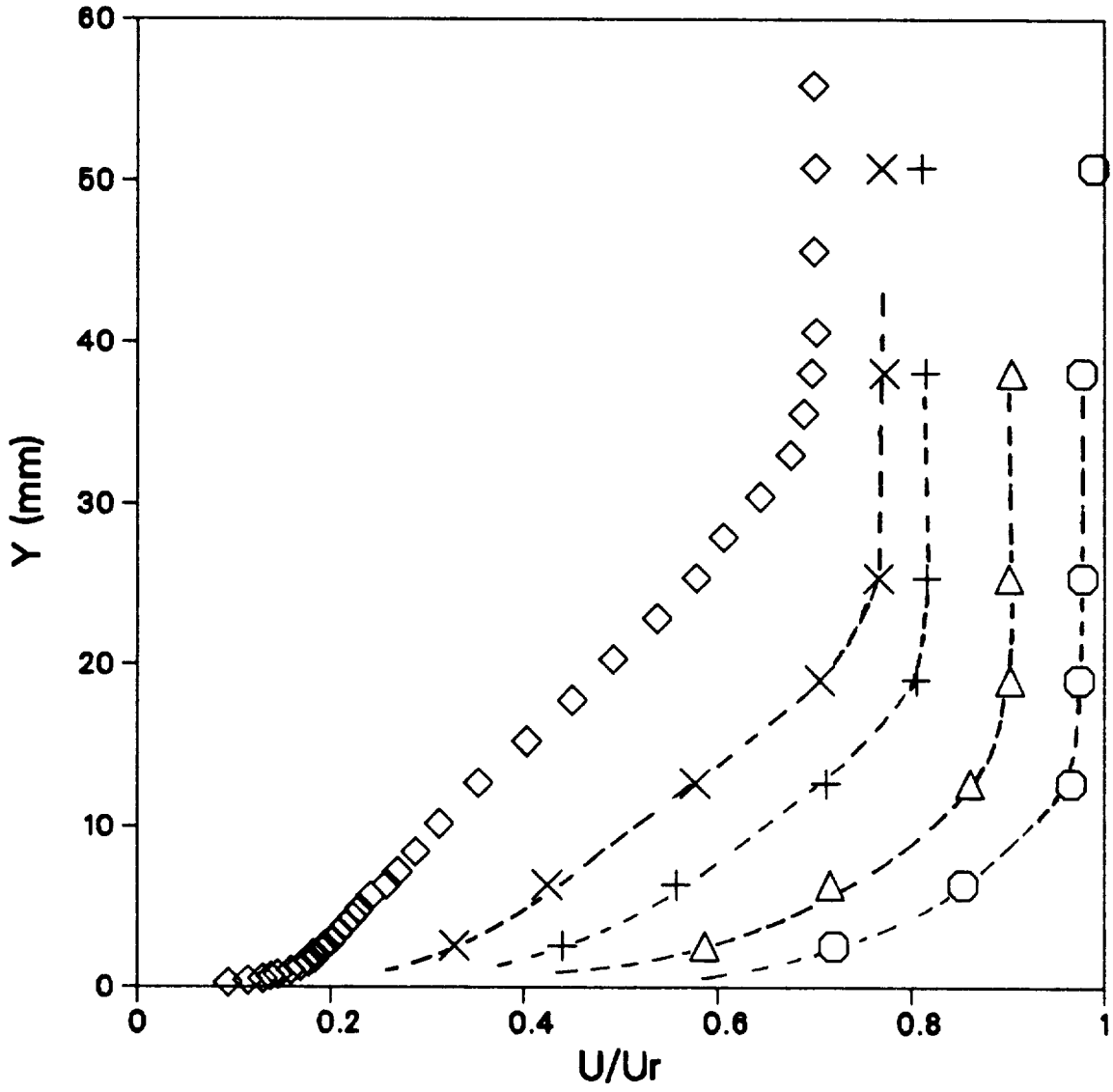

Figure 4.3 Streamwise velocity distribution for non-spinning case B.S0, ◯ x=-228mm, △ x=−152mm, + x=-76mm, × x=−12mm, ◇ x=152mm.

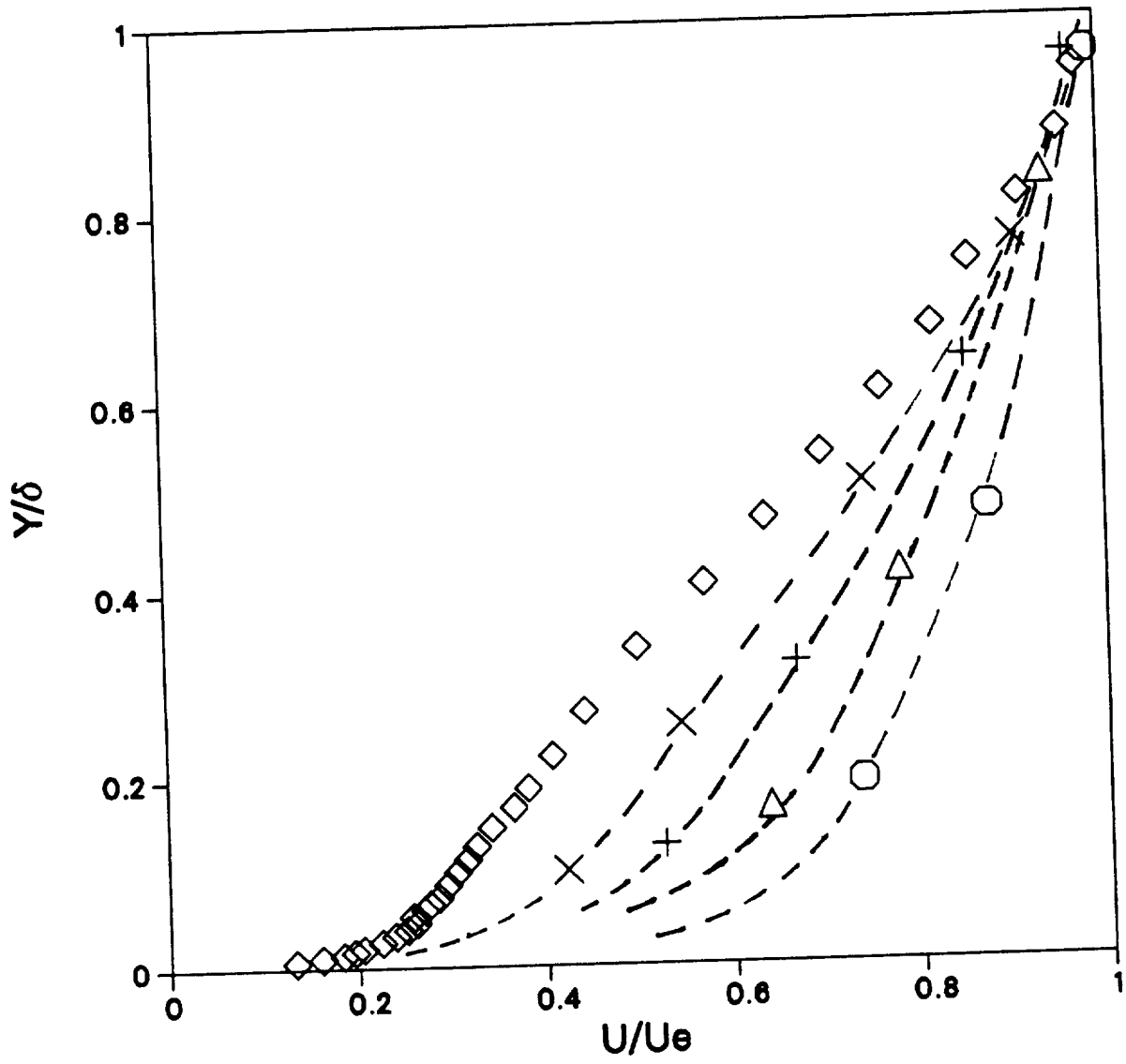

Figure 4.4 Normalized streamwise velocity distribution for non-spinning Case B.S0, ◯ x=-228mm, △ x=−152mm, + x=-76mm, × x=−12mm, ◇ x=152mm.

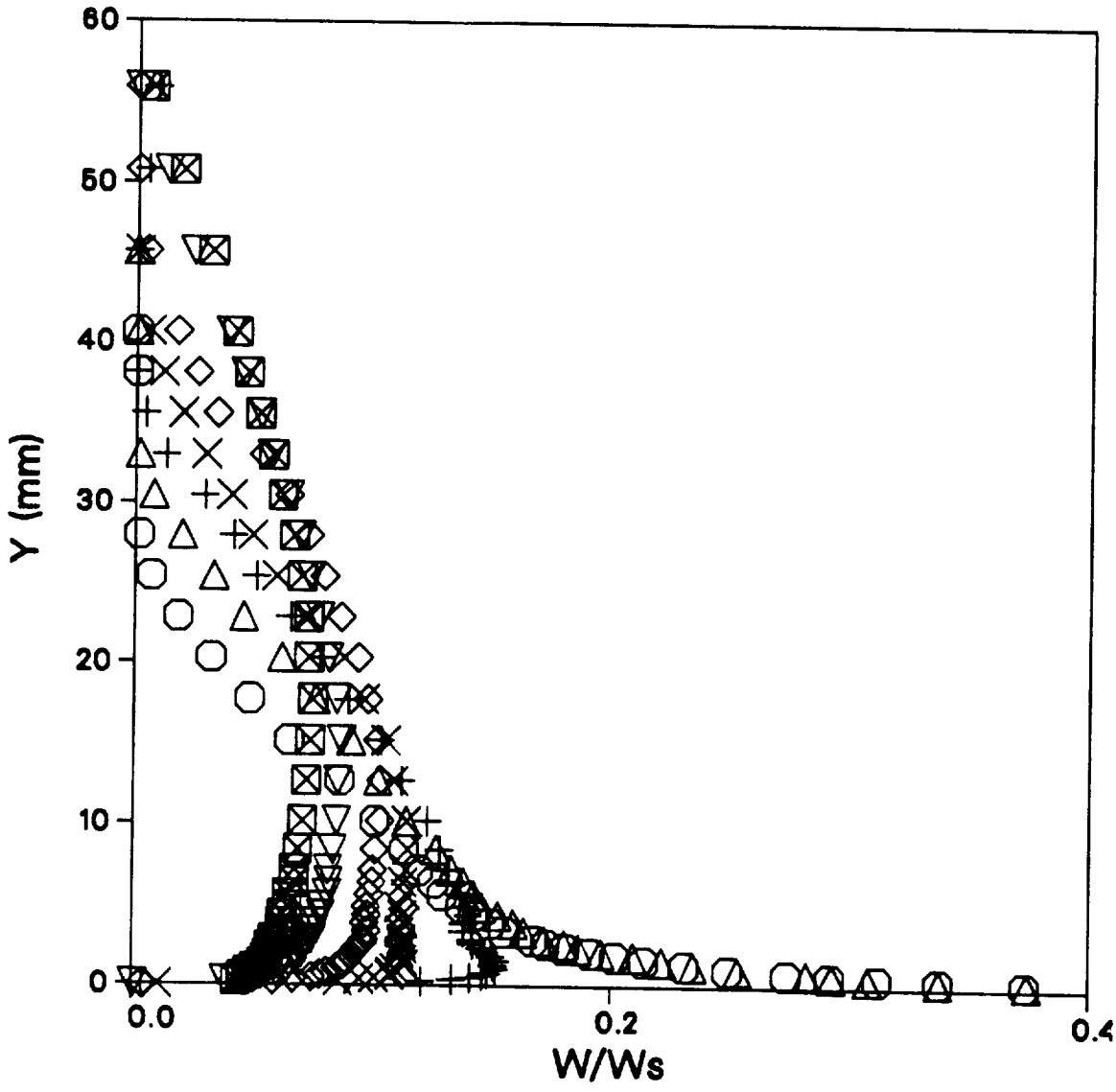

Figure 4.5 Transverse velocity distribution for spinning case D.S1, ◯ x=-76mm, △ x=−12mm, + x=48mm, × x=101mm, ◇ x=152mm, ▽ x=228mm, ⊠ x=304mm.

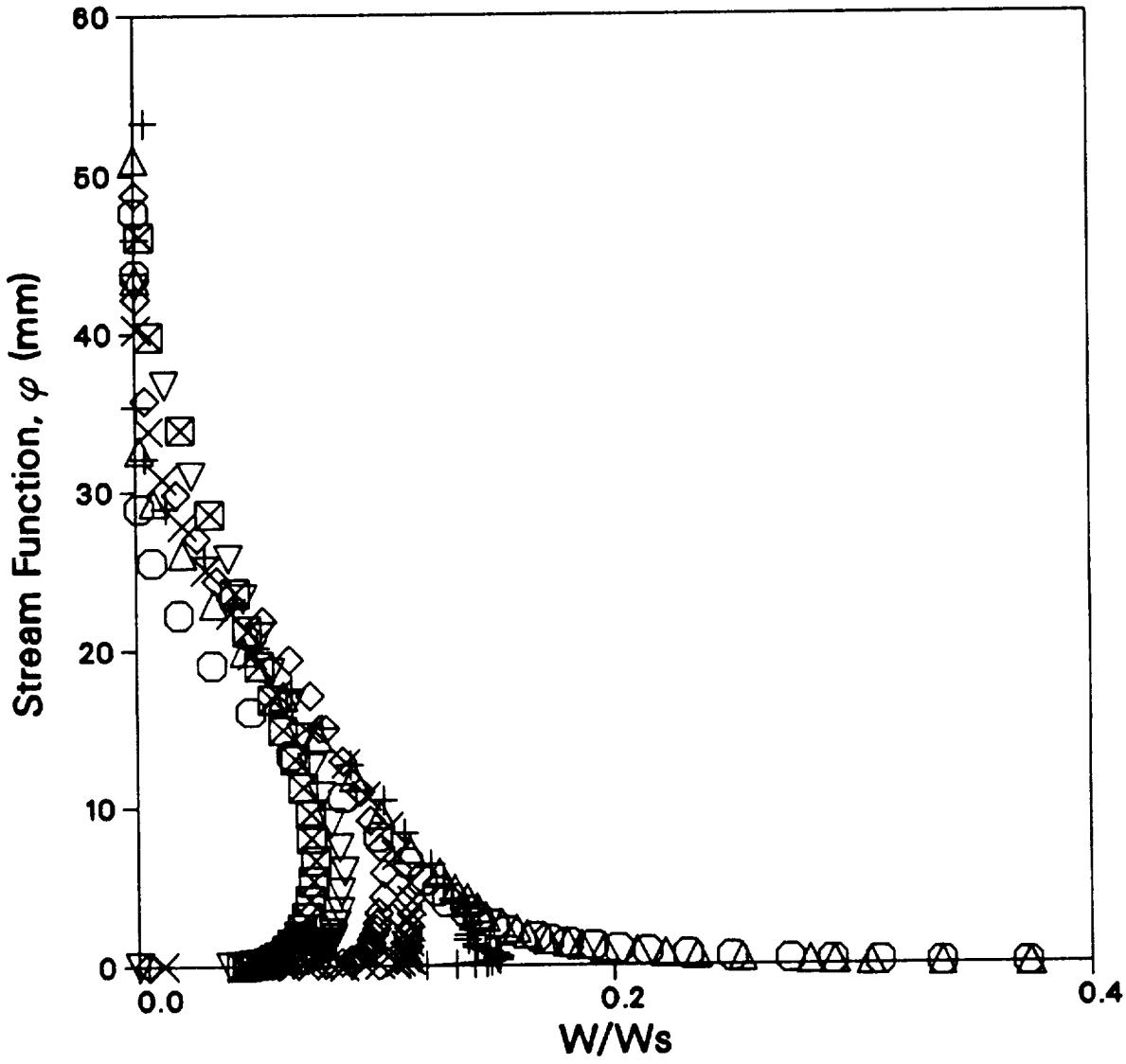

Figure 4.6 Transverse velocity versus stream function for spinning case D.S1,
◯ x=-76mm, △ x=−12mm, + x=48mm, × x=101mm, ◇ x=152mm,
▽ x=228mm, ⊠ x=304mm.

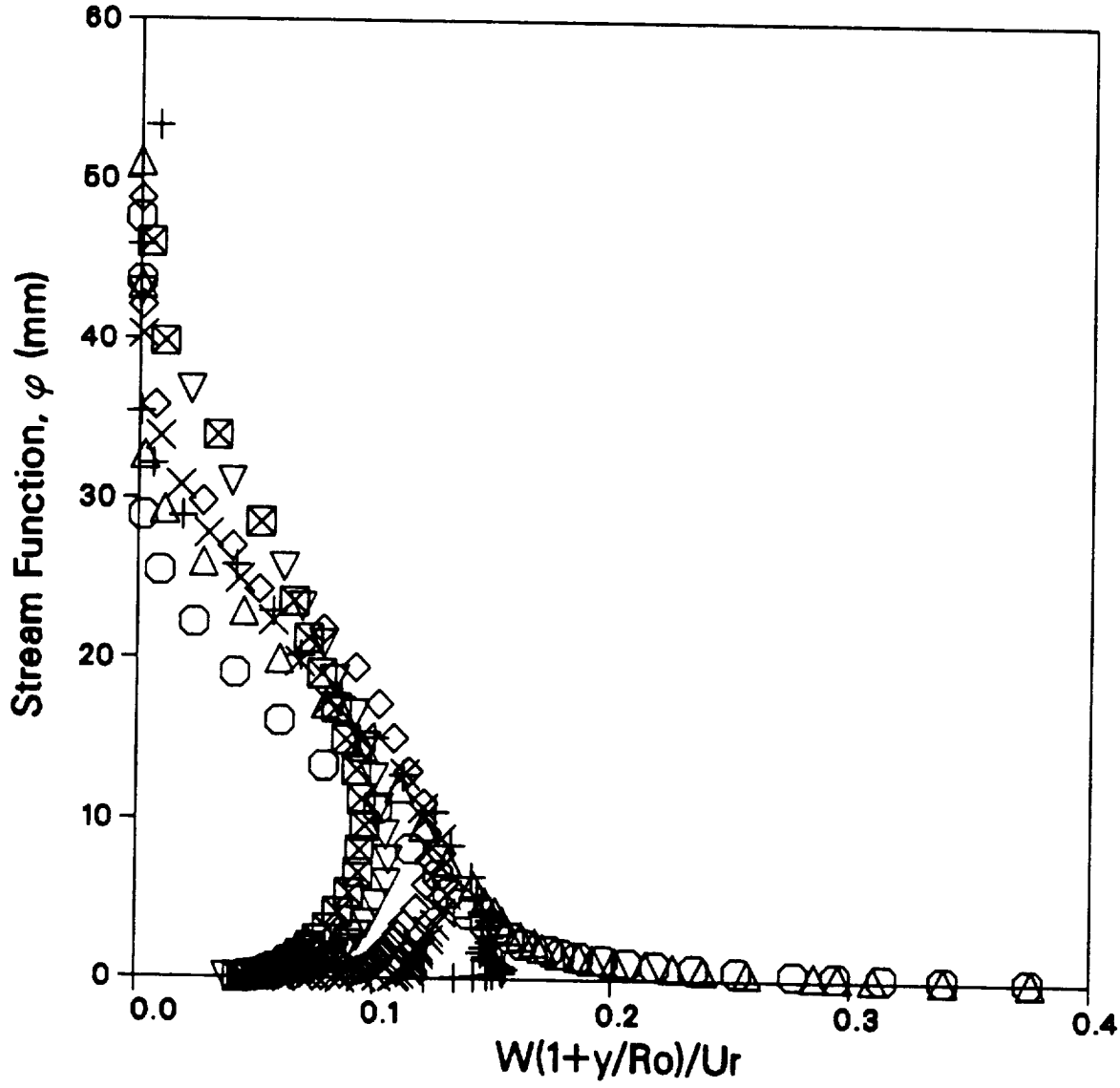

Figure 4.7 Angular momentum versus stream function for spinning case D.S1, ○ x=-76mm, △ x=−12mm, + x=48mm, × x=101mm, ◇ x=152mm, ▽ x=228mm, ⊠ x=304mm.

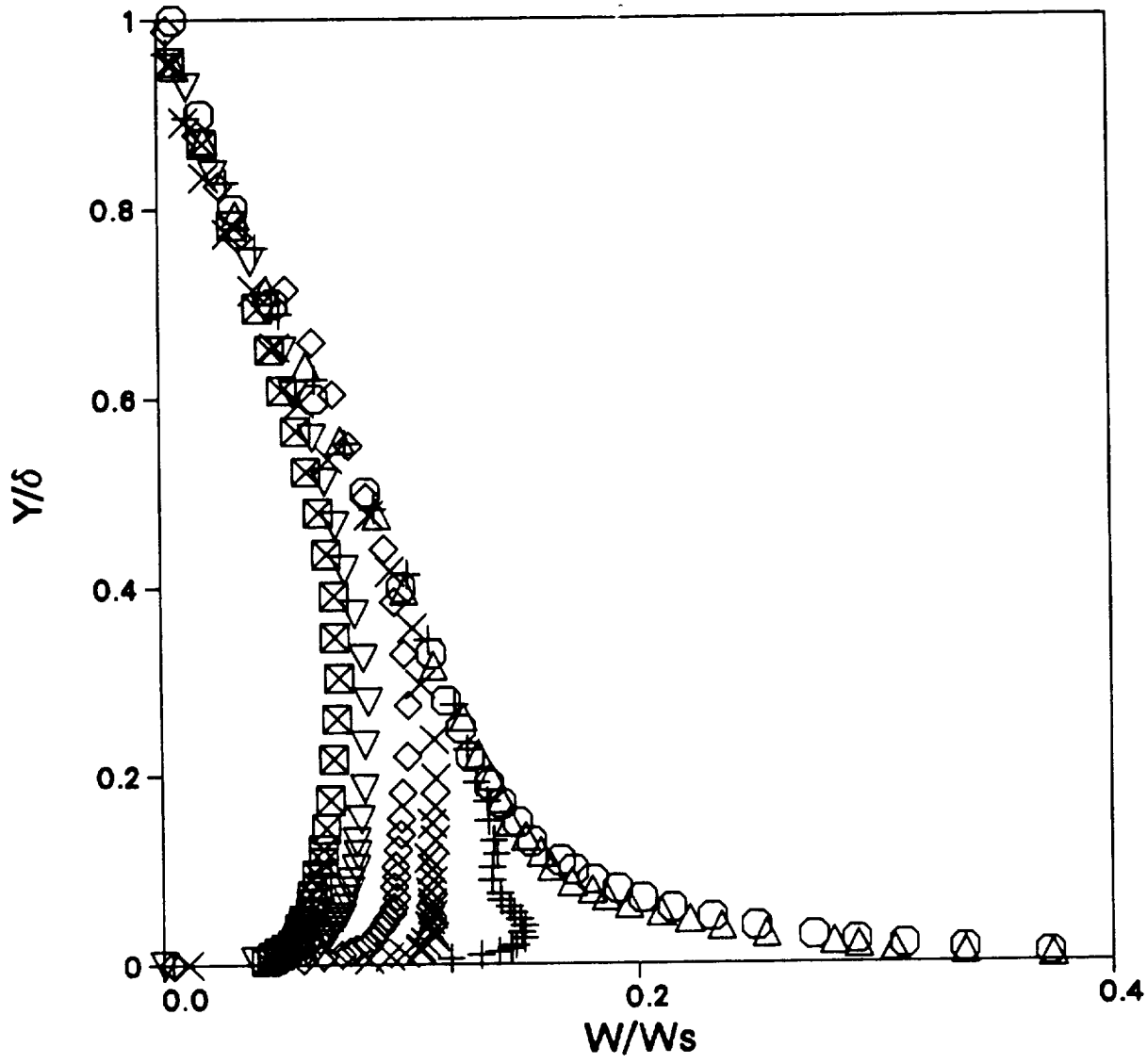

Figure 4.8 Normalized transverse velocity distribution for spinning case D.S1,
◯ x=-76mm, △ x=−12mm, + x=48mm, × x=101mm, ◇ x=152mm,
▽ x=228mm, ⊠ x=304mm.

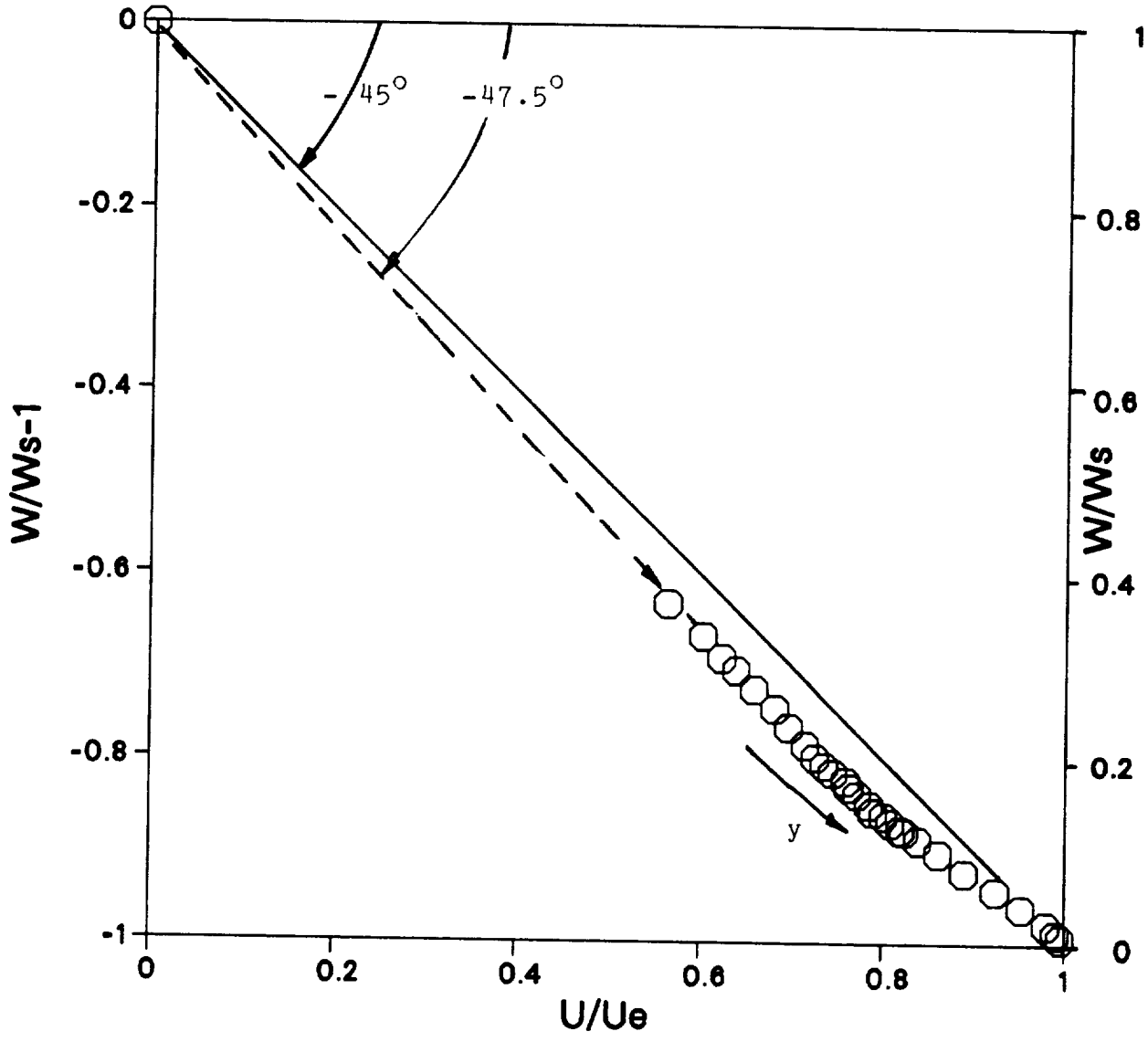

Figure 4.9 U vs W hodograph of upstream flow (@X=−152mm) for spinning case A.S1.

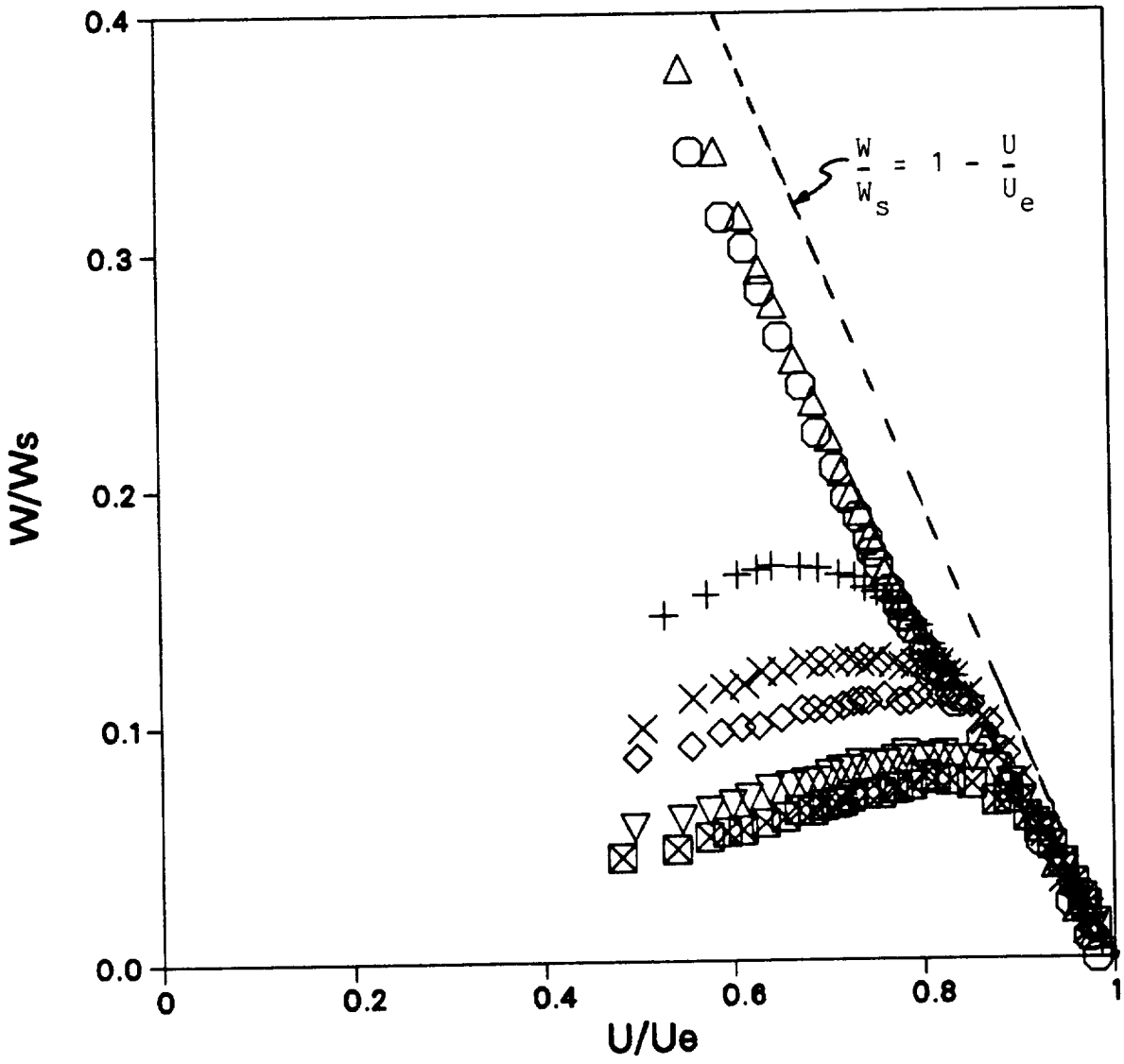

Figure 4.10 U vs W hodograph evolution for zero pressure gradient, spinning case A.S1, ◯ x=−152mm, △ x=−12mm, + x=50mm, × x=101mm, ◇ x=152mm, ▽ x=304mm, ⊠ x=457mm.

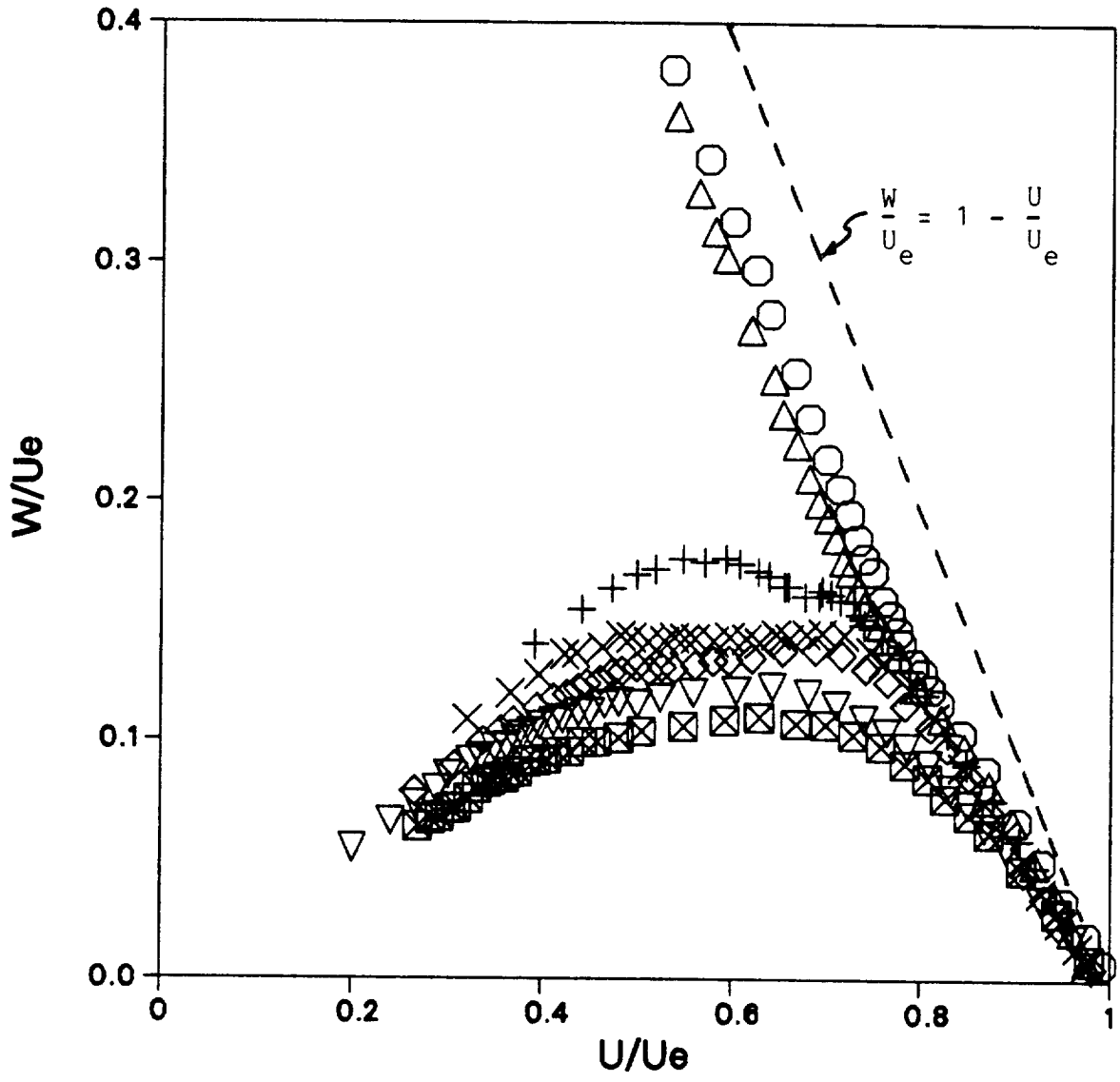

Figure 4.11 U vs W hodograph evolution for adverse pressure gradient, spinning case D.S1, ○ x=−76mm, △ x=−12mm, + x=48mm, × x=101mm, ◇ x=152mm, ▽ x=228mm, ⊠ x=304mm.

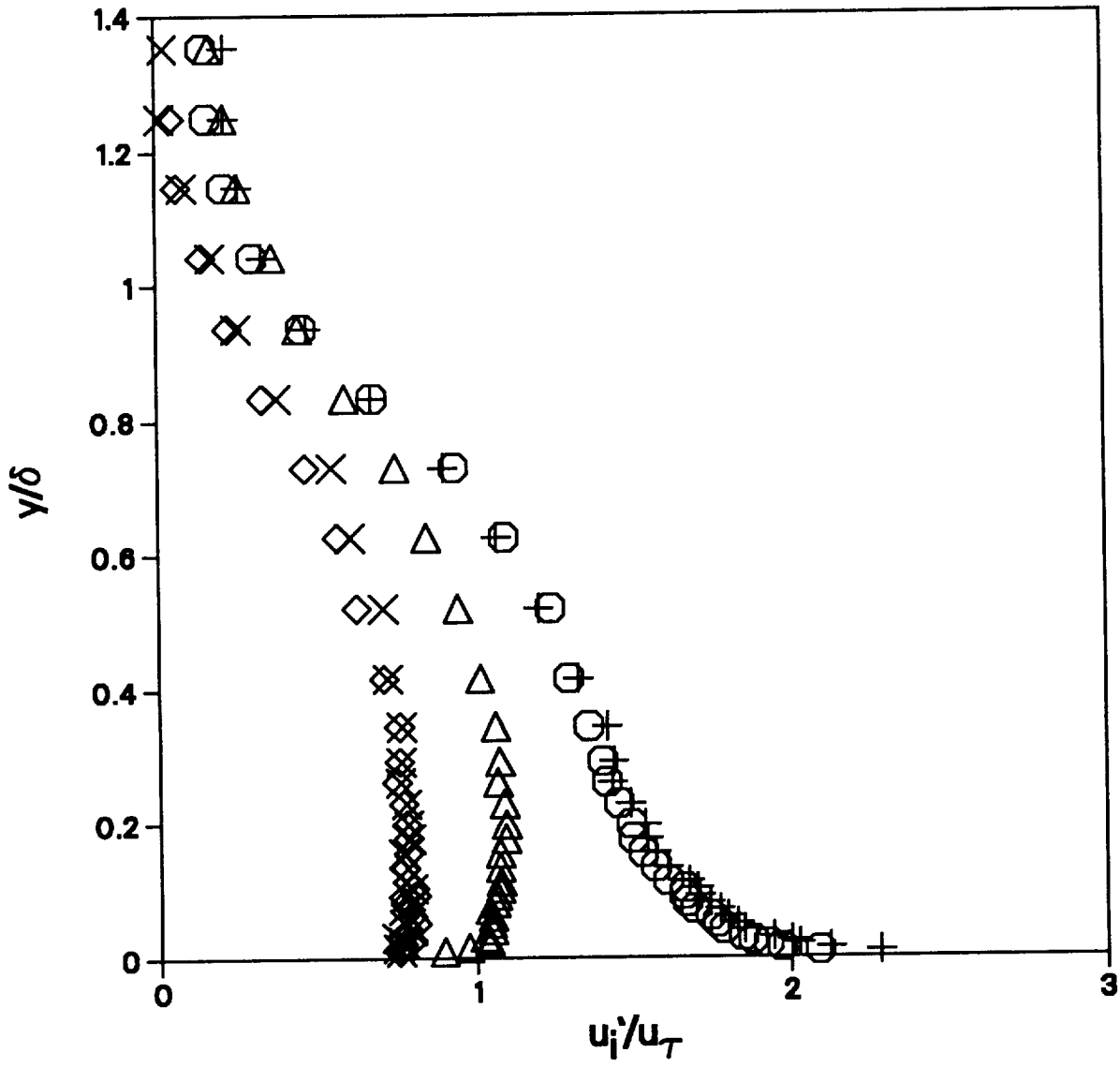

Figure 4.12 Turbulent intensity distribution for upstream profile (X=-150mm) of spinning case D.S1, ◯ u'/u_τ, △ v'/u_τ , + w'/u_τ , × $\sqrt{-\overline{uv}}/u_\tau$, ◇ $\sqrt{\overline{vw}}/u_\tau$.

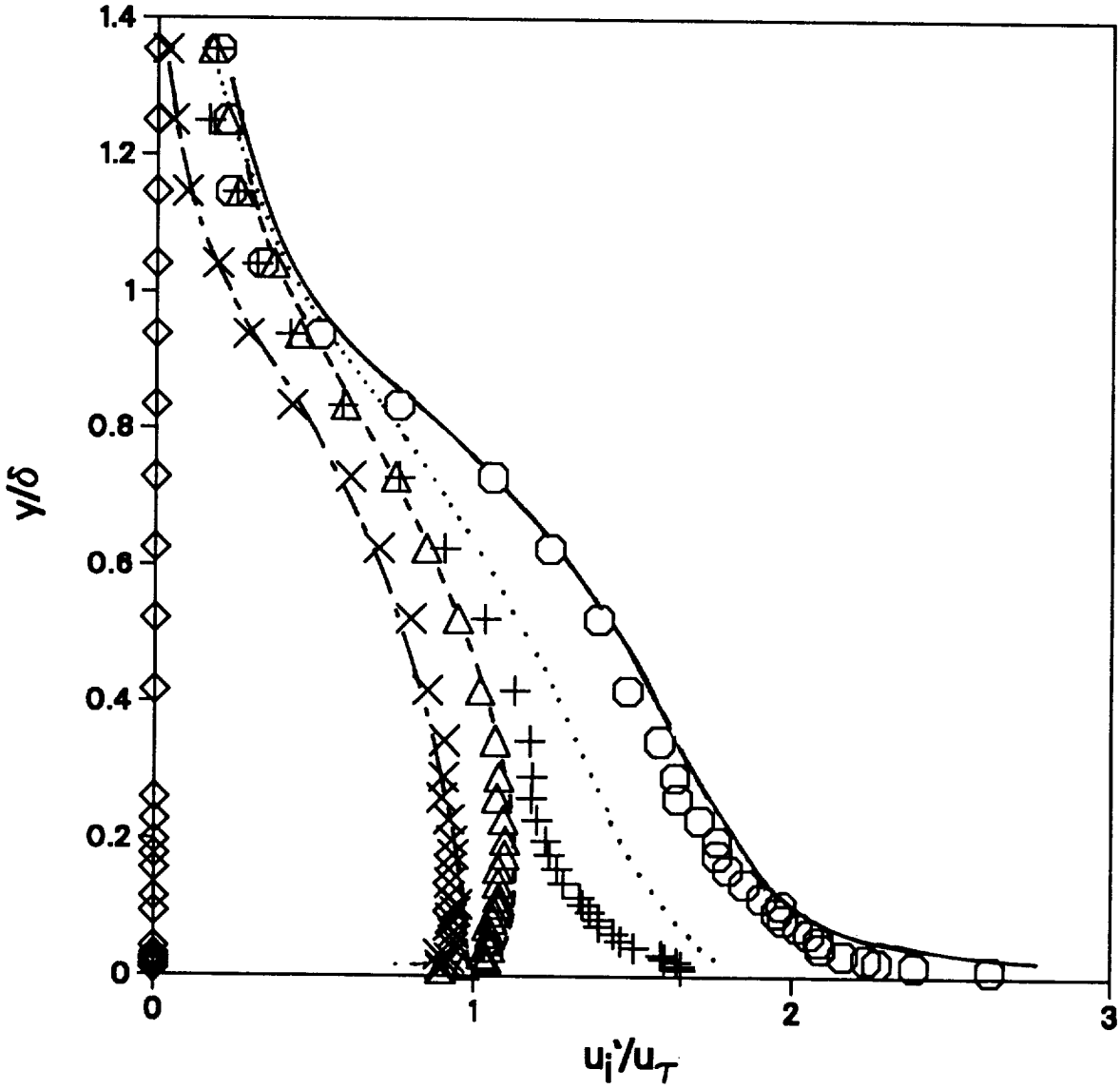

Figure 4.13 Turbulent intensities in principal stress directions for upstream profile (X=–150mm) of spinning case D.S1, ○ $\widetilde{u}'/u_\tau$, △ $\widetilde{v}'/u_\tau$, + $\widetilde{w}'/u_\tau$, × $\sqrt{-\widetilde{\widetilde{uv}}}/u_\tau$ ◇ $\sqrt{\widetilde{\widetilde{vw}}}/u_\tau$; compared to 2D case D.S0 (X=–150mm), —— u'/u_τ, - - - v'/u_τ, ... w'/u_τ, – - – $\sqrt{-\overline{uv}}/u_\tau$.

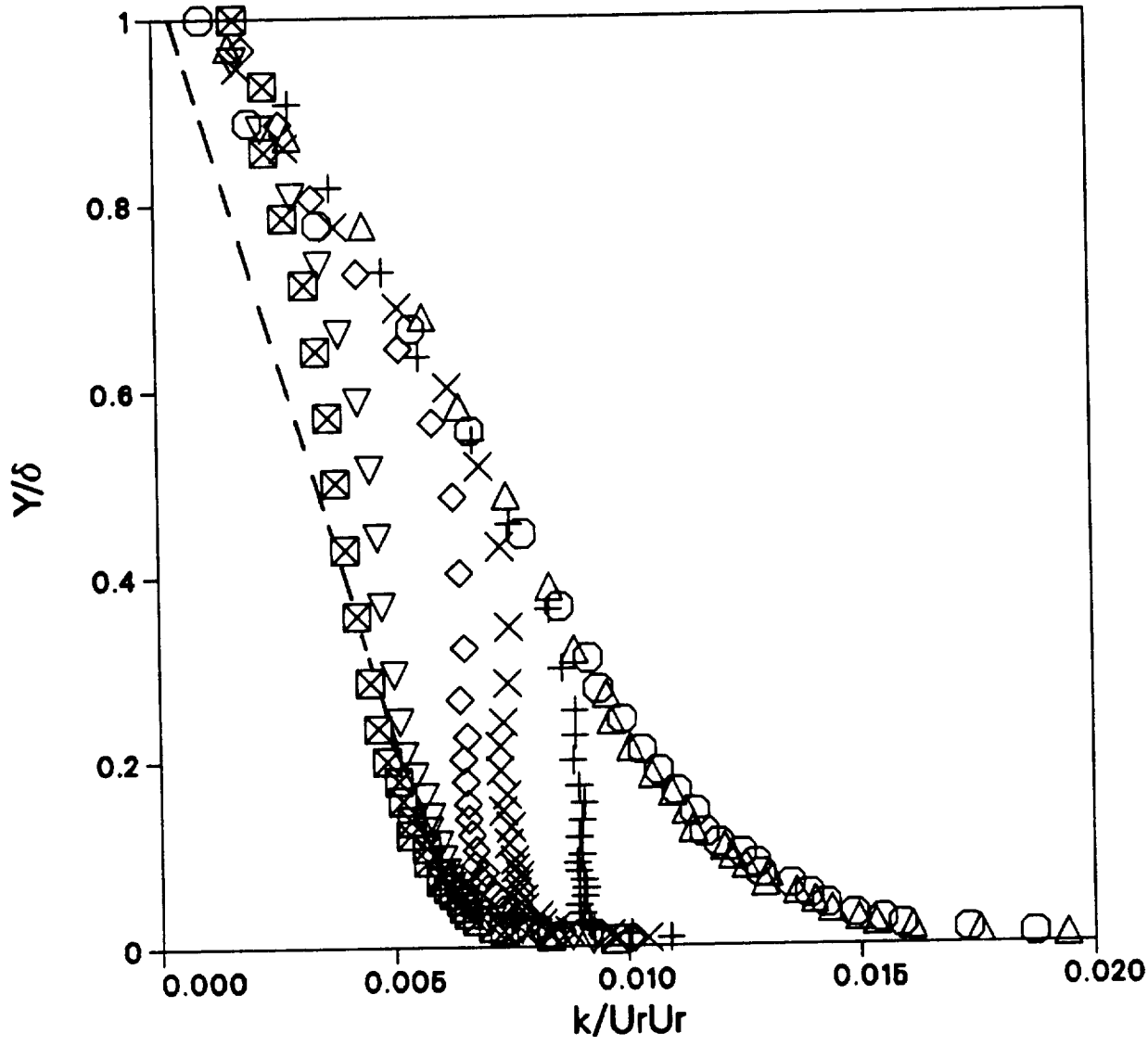

Figure 4.14 Kinetic energy evolution for zero pressure gradient, spinning case A.S1, ◯ x=−152mm, △ x=−12mm, + x=50mm, × x=101mm, ◇ x=152mm, ▽ x=304mm, ⊠ x=457mm, - - - 2D case A.S0 @X=−152mm.

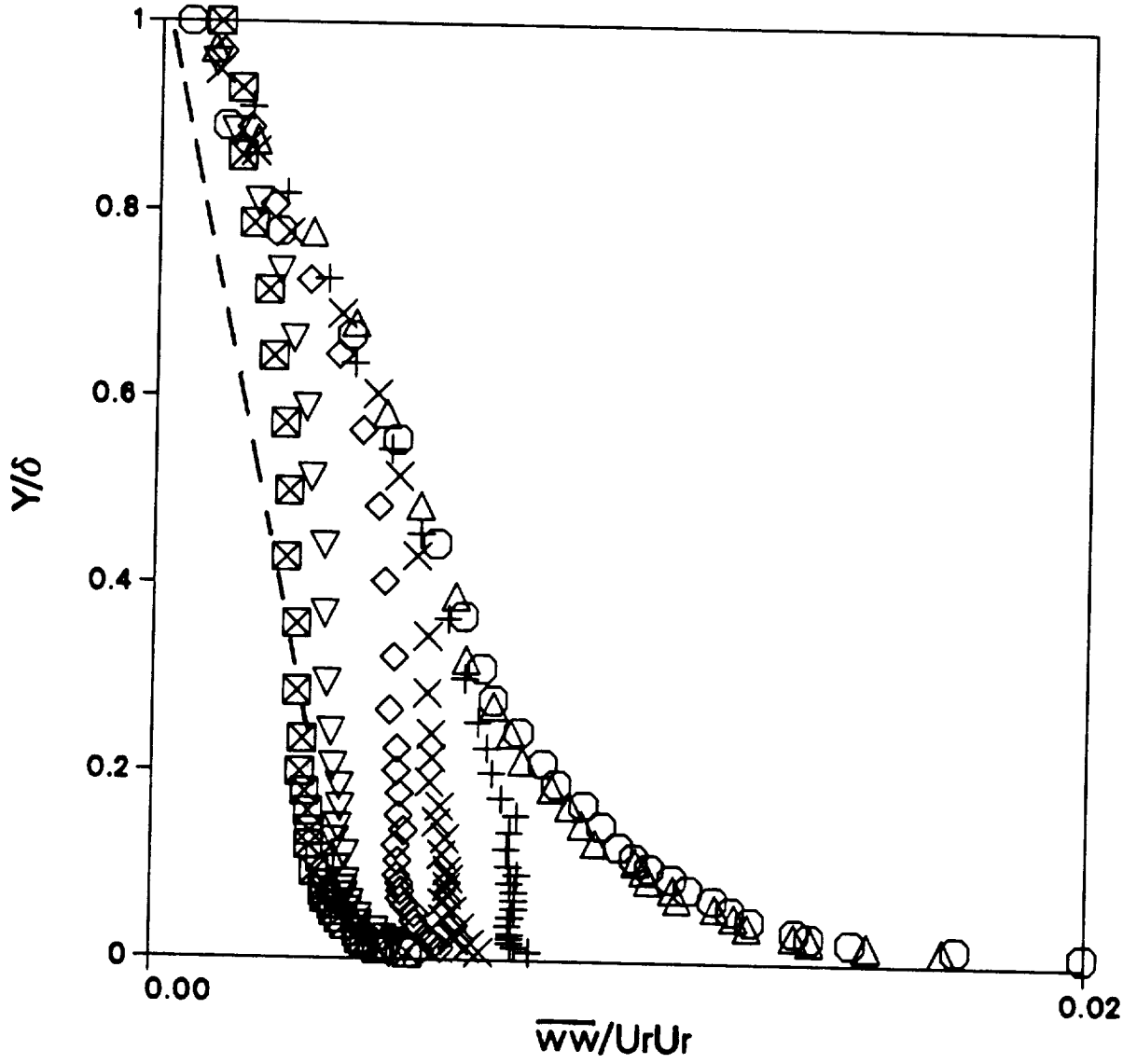

Figure 4.15 $\overline{w^2}$ component evolution for zero pressure gradient, spinning case A.S1, ◯ x=−152mm, △ x=−12mm, + x=50mm, × x=101mm, ◇ x=152mm, ▽ x=304mm, ⊠ x=457mm, - - - 2D case A.S0 @X=−152mm.

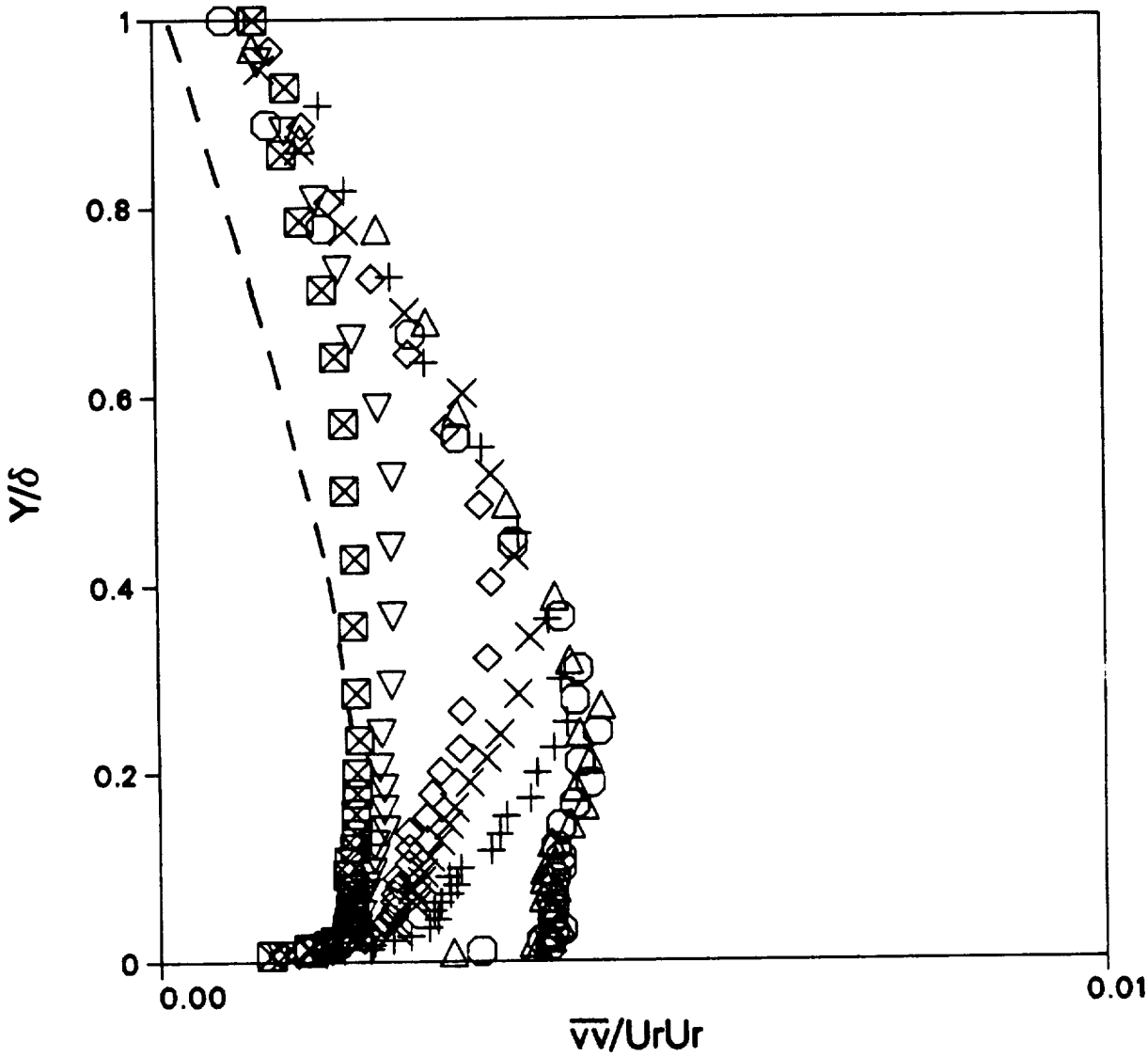

Figure 4.16 $\overline{v^2}$ component evolution for zero pressure gradient, spinning case A.S1, ◯ x=−152mm, △ x=−12mm, + x=50mm, × x=101mm, ◇ x=152mm, ▽ x=304mm, ⊠ x=457mm, - - - 2D case A.S0 @X=−152mm.

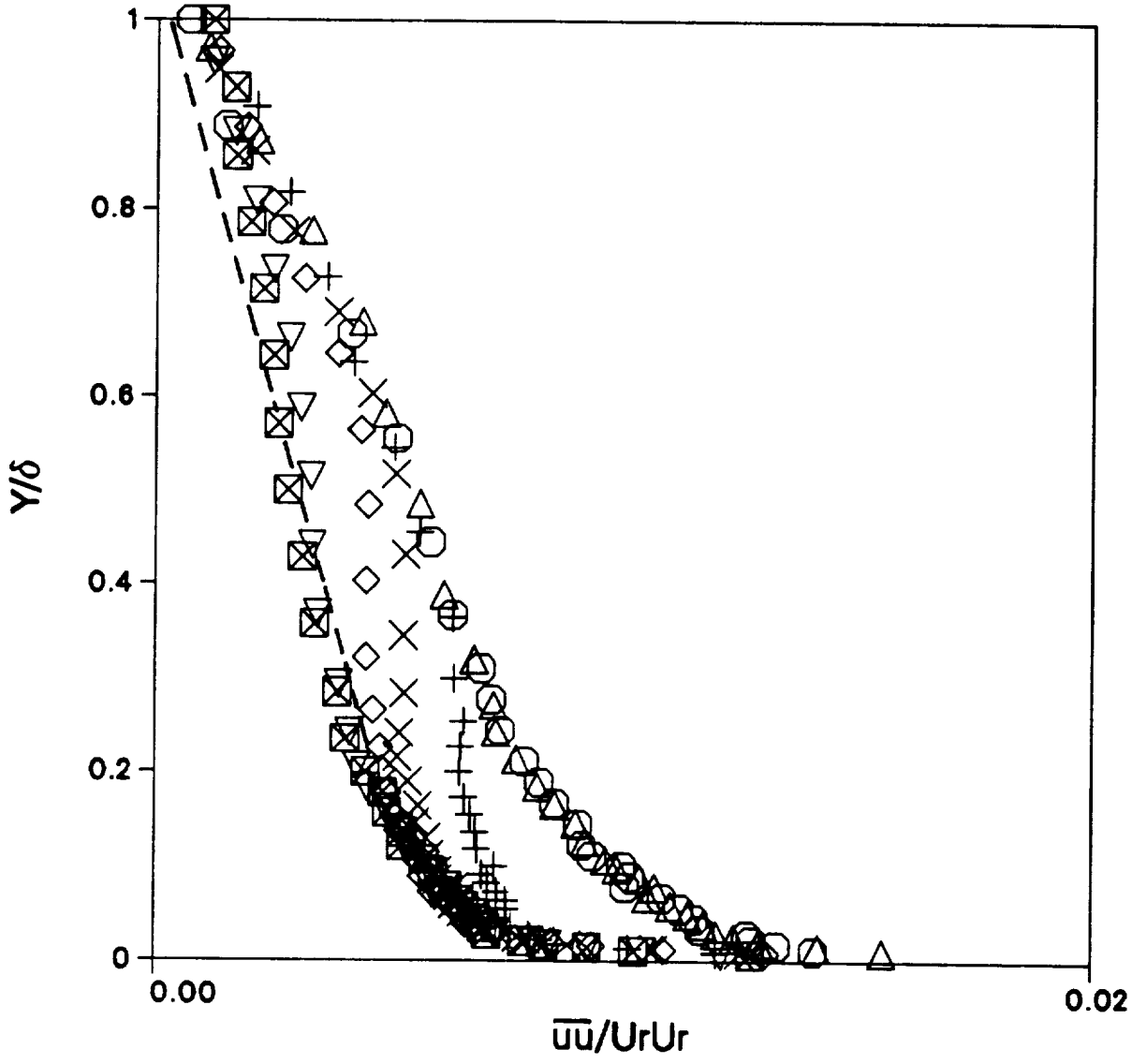

Figure 4.17 $\overline{u^2}$ component evolution for zero pressure gradient, spinning case A.S1, ◯ x=−152mm, △ x=−12mm, + x=50mm, × x=101mm, ◇ x=152mm, ▽ x=304mm, ⊠ x=457mm, - - - 2D case A.S0 @X=−152mm.

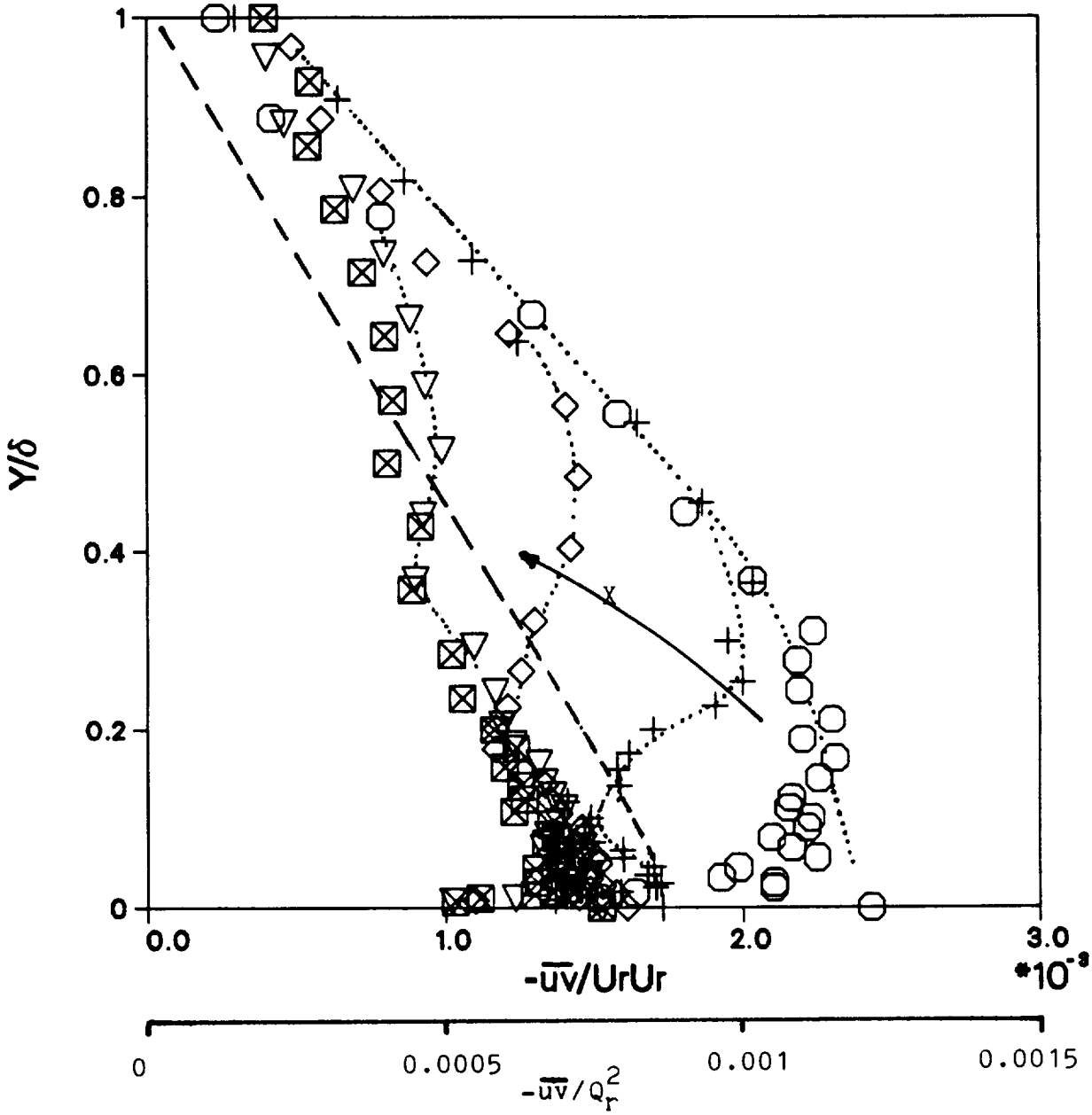

Figure 4.18 $-\overline{uv}$ component evolution for zero pressure gradient, spinning case A.S1, ◯ x=−152mm, + x=50mm, ◇ x=152mm, ▽ x=304mm, ⊠ x=457mm, - - - 2D case A.S0 @X=−152mm.

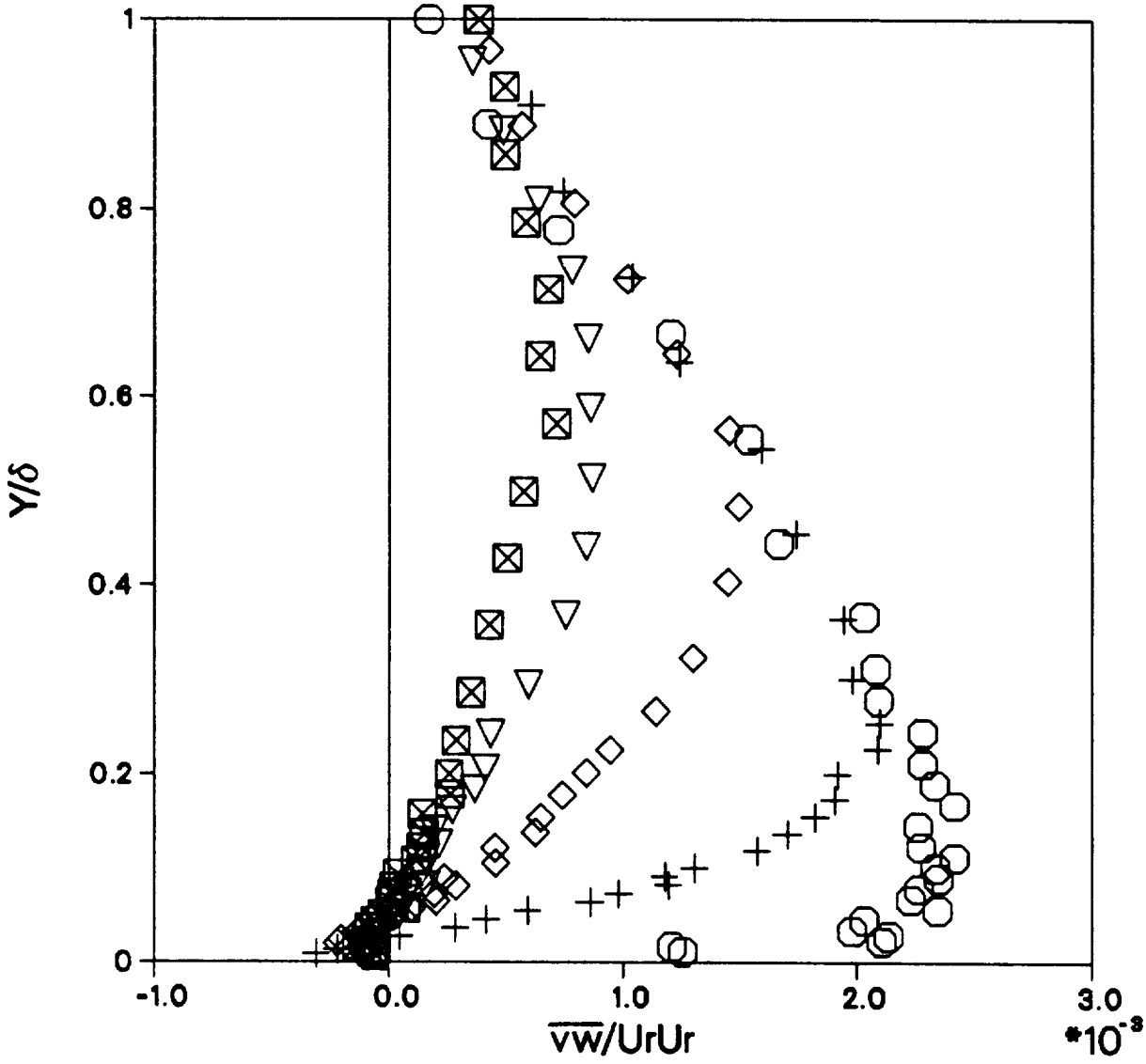

Figure 4.19 $\overline{vw}$ component evolution for zero pressure gradient, spinning case A.S1, ◯ x=−152mm, + x=50mm, ◇ x=152mm, ▽ x=304mm, ⊠ x=457mm.

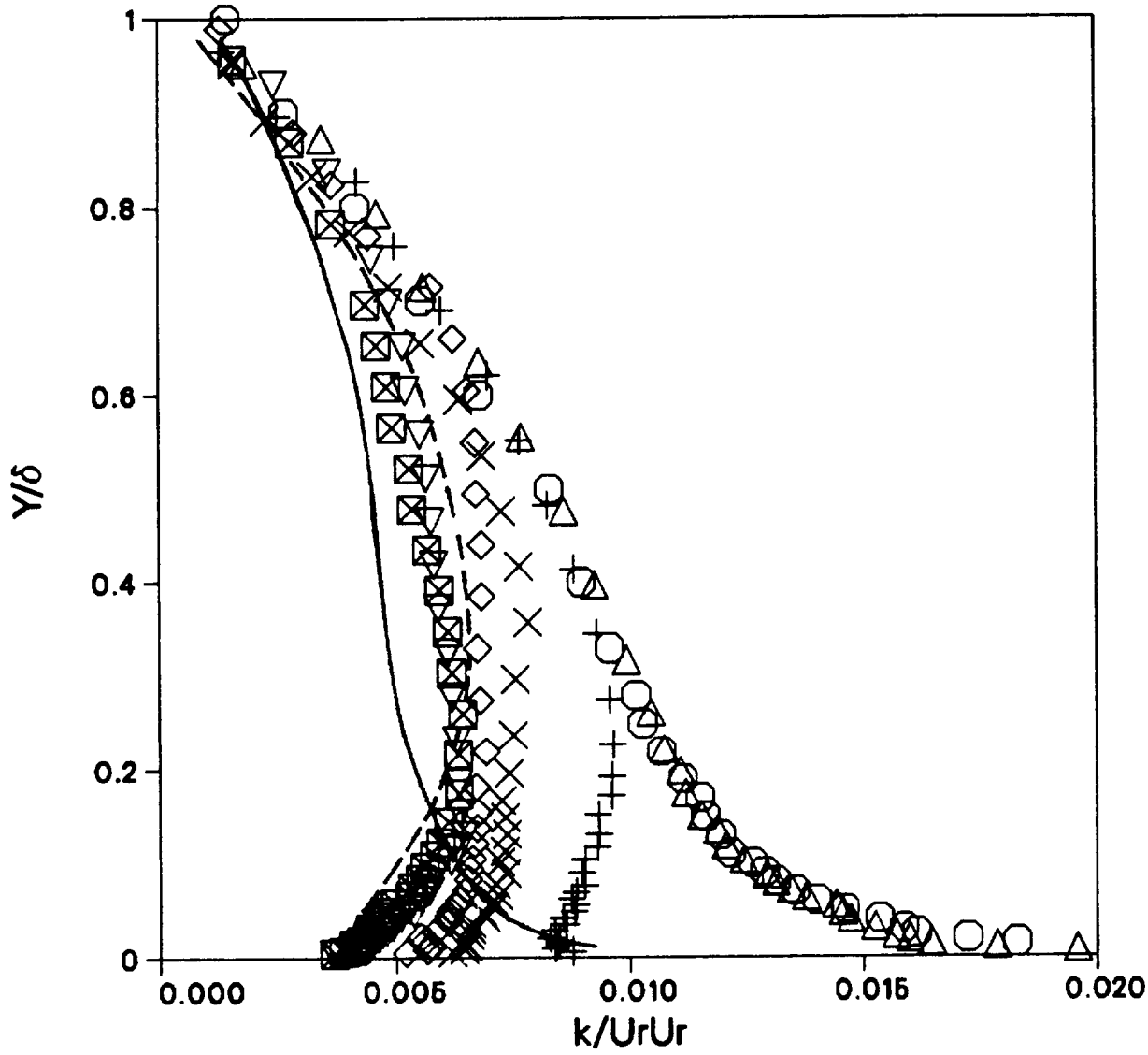

Figure 4.20 Kinetic energy evolution for adverse pressure gradient, spinning case D.S1, ○ x=-76mm, △ x=−12mm, + x=48mm, × x=101mm, ◇ x=152mm, ▽ x=228mm, ⊠ x=304mm, - - - 2D $\partial P/\partial x$ case B.S0 @X=152mm, —— 3D zero-$\partial P/\partial x$ case A.S1 @X=304mm.

C-2

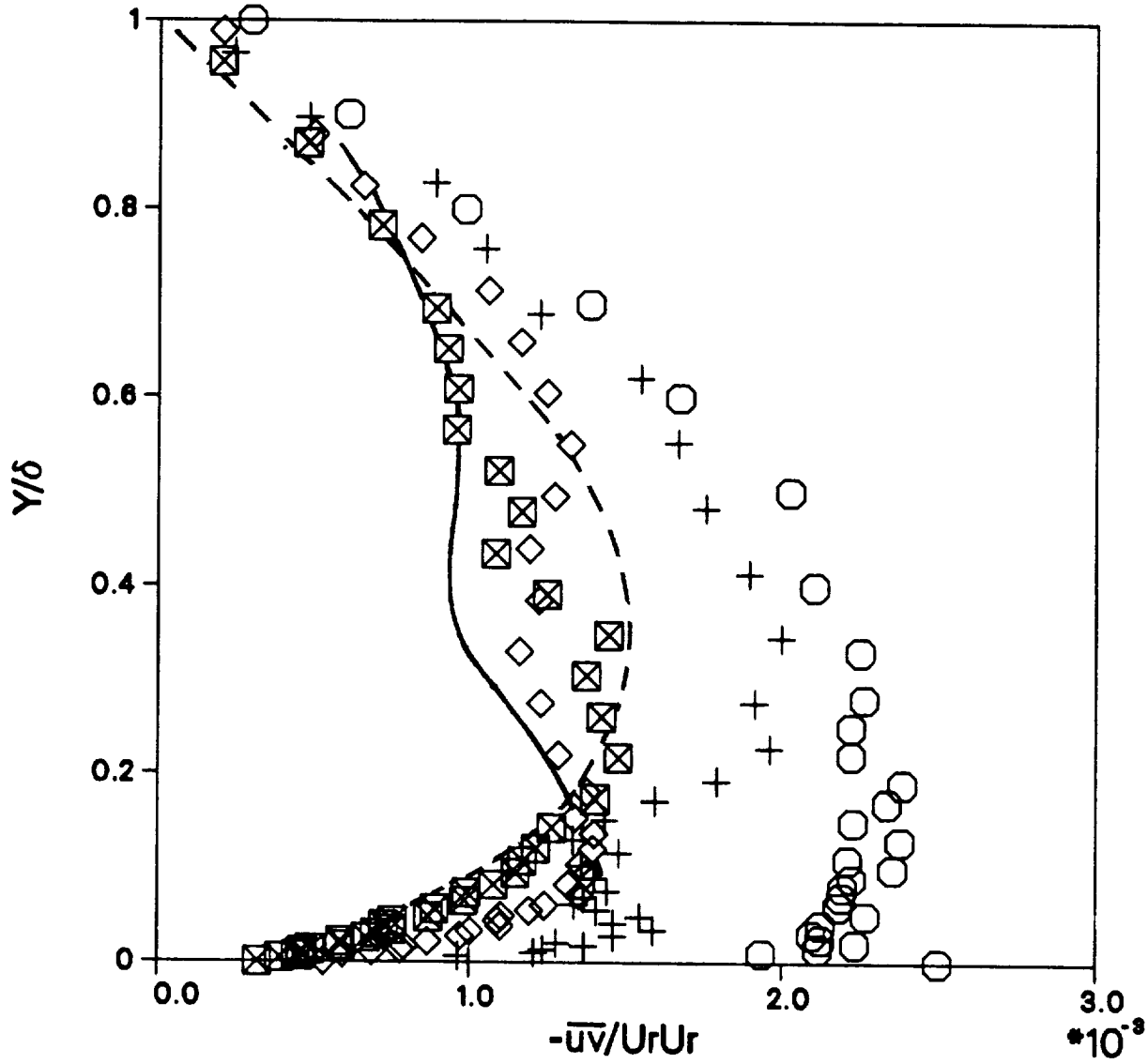

Figure 4.21 $-\overline{uv}$ component evolution for adverse pressure gradient, spinning case D.S1, ◯ x=−76mm, + x=48mm, ◇ x=152mm, ⊠ x=304mm, - - - 2D $\partial P/\partial x$ case B.S0 @x=152mm, —— 3D zero-$\partial P/\partial x$ case A.S1 @x=304mm

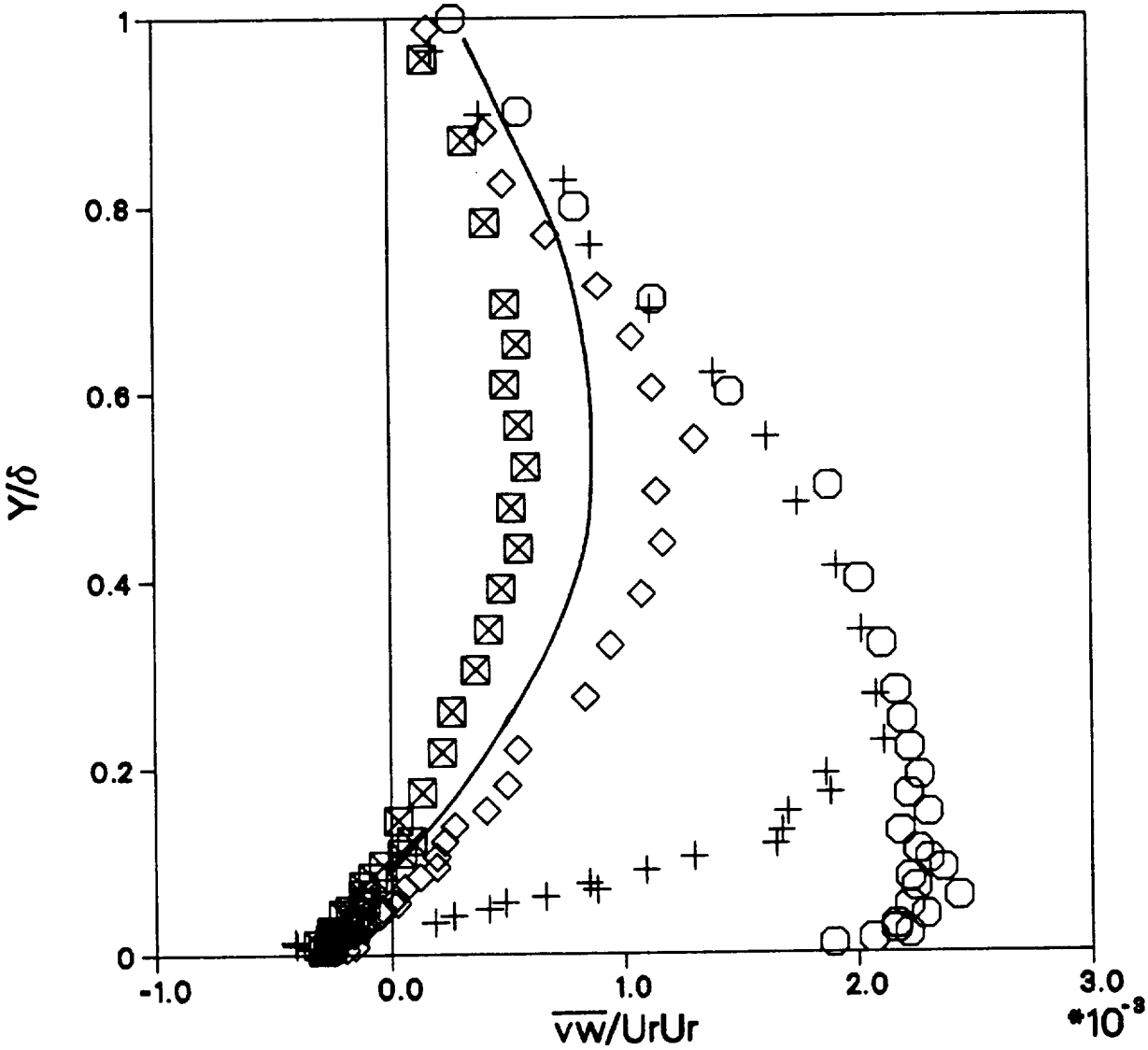

Figure 4.22 $\overline{vw}$ component evolution for adverse pressure gradient, spinning case D.S1, ◯ x=−76mm, + x=48mm, ◇ x=152mm, ⊠ x=304mm, —— 3D zero-$\partial P/\partial x$ case A.S1 @x=304mm

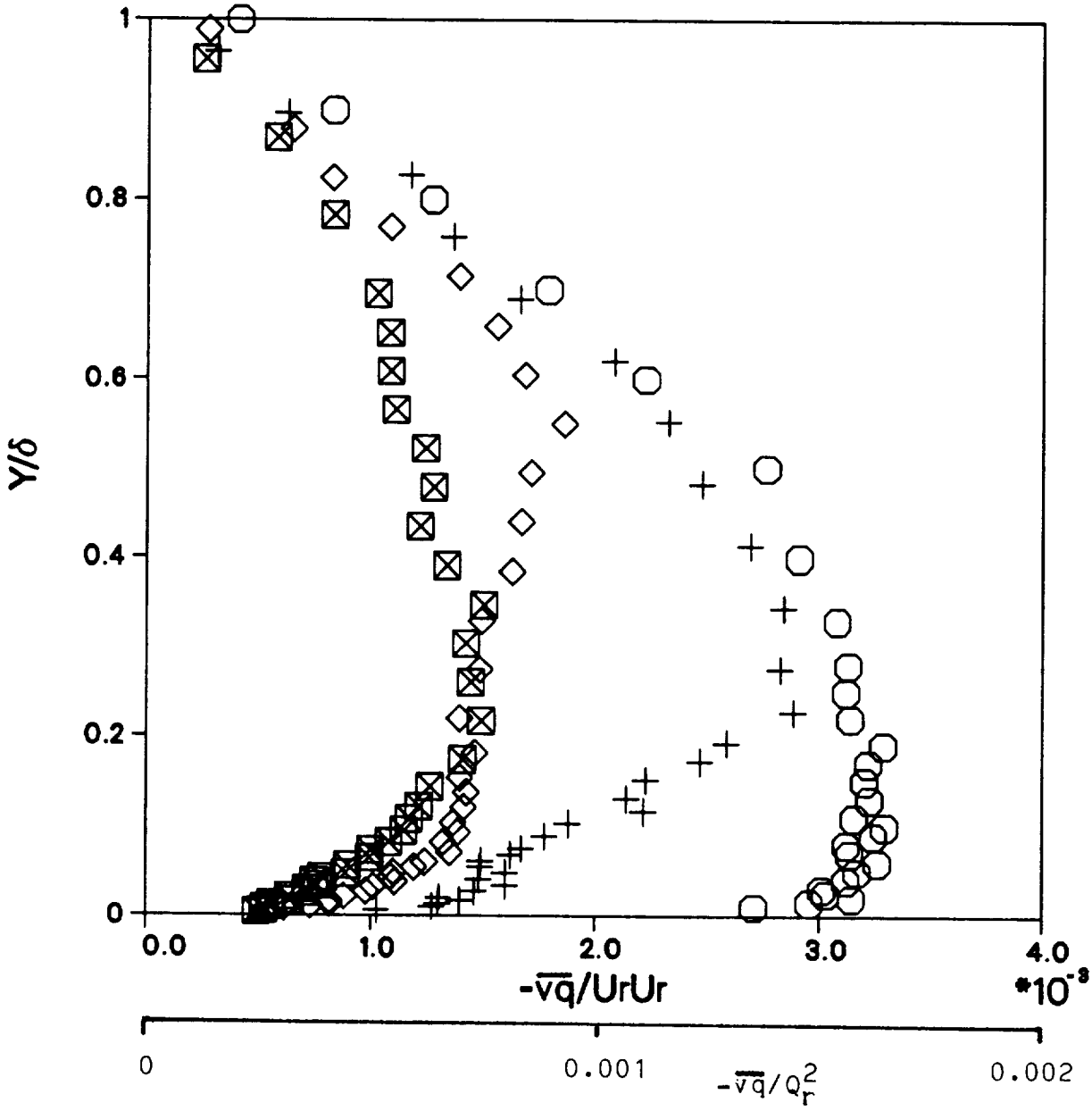

Figure 4.23 $\overline{vq} = -\sqrt{\overline{uv}^2 + \overline{vw}^2}$ component evolution for adverse pressure gradient, Spinning Case D.S1, ◯ x=−76mm, + x=48mm, ◇ x=152mm, ⊠ x=304mm.

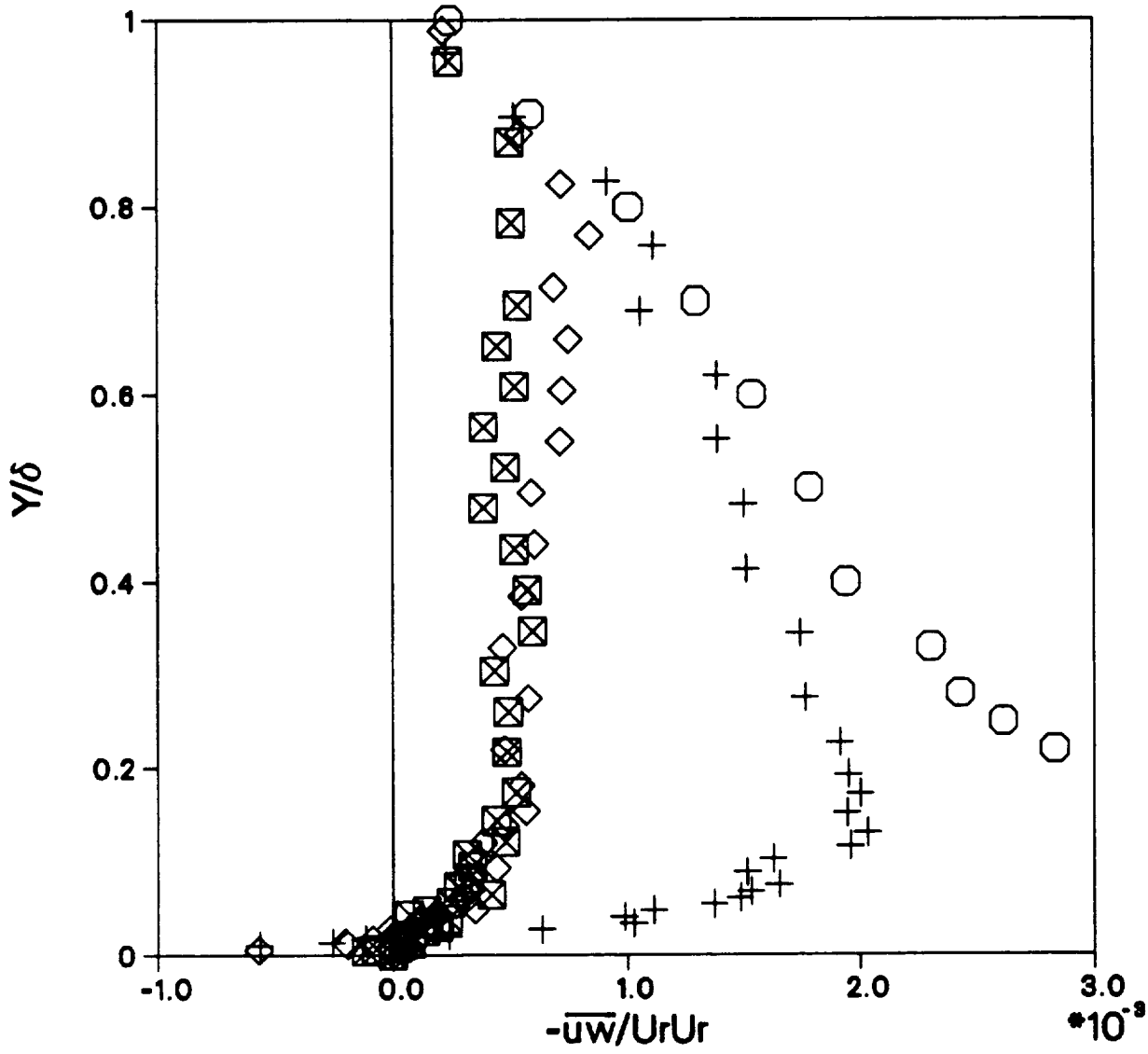

Figure 4.24 $-\overline{uw}$ component evolution for adverse pressure gradient, spinning case D.S1, ◯ x=-76mm, + x=48mm, ◇ x=152mm, ⊠ x=304mm.

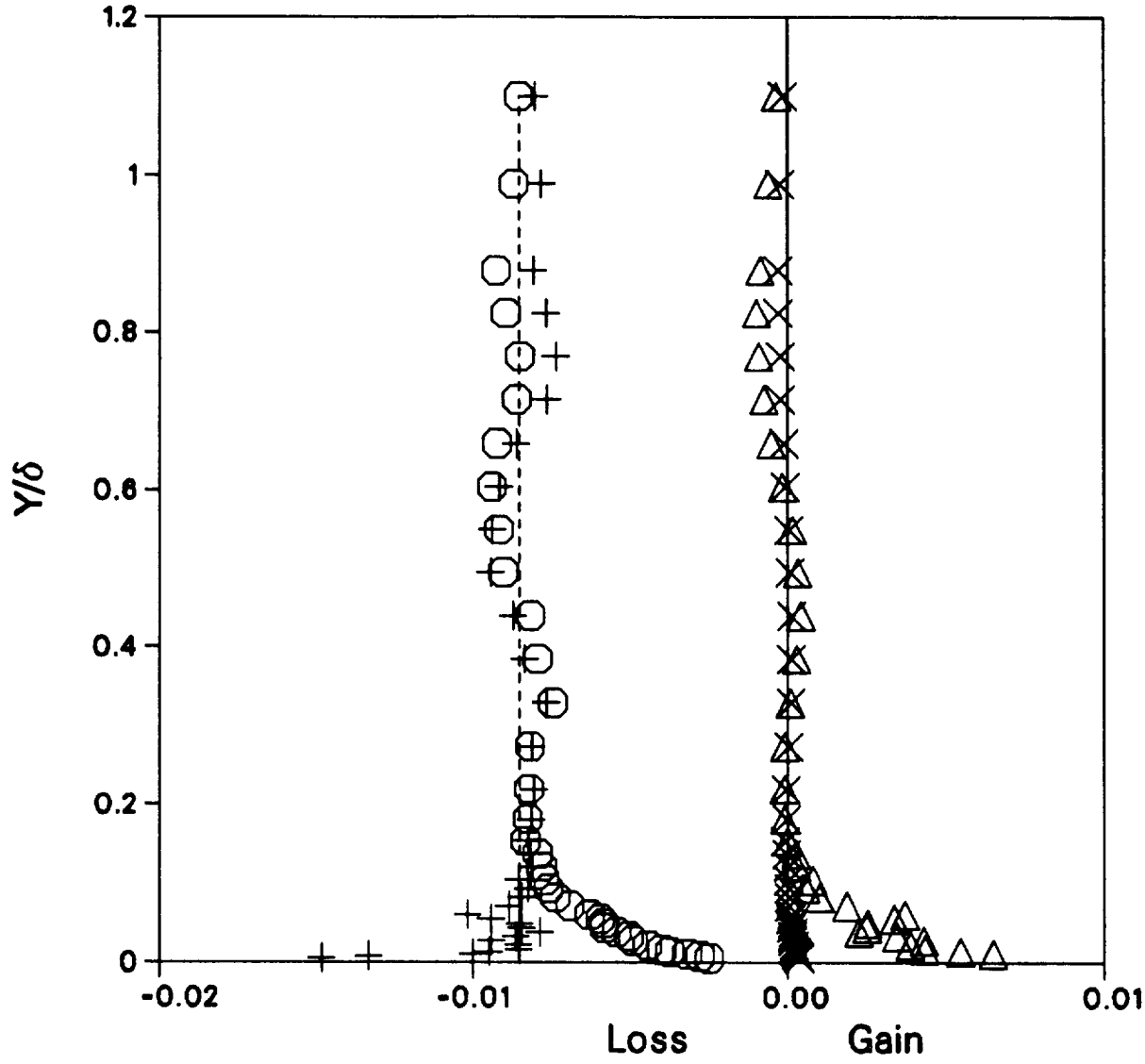

Figure 4.25 U-Momentum equation balance profile @X=150mm for adverse pressure gradient, spinning case D.S1, ○ (DU/Dt) δ/U_r^2, + $(-\partial P/\partial x)\ \delta/U_r^2$, △ $(-\partial(r\overline{uv})/\partial r)\delta/rU_r^2$, - - - $(-\partial P_w/\partial x)\delta/U_r^2$, × $(-\partial\overline{uu}/\partial x)\delta/U_r^2$.

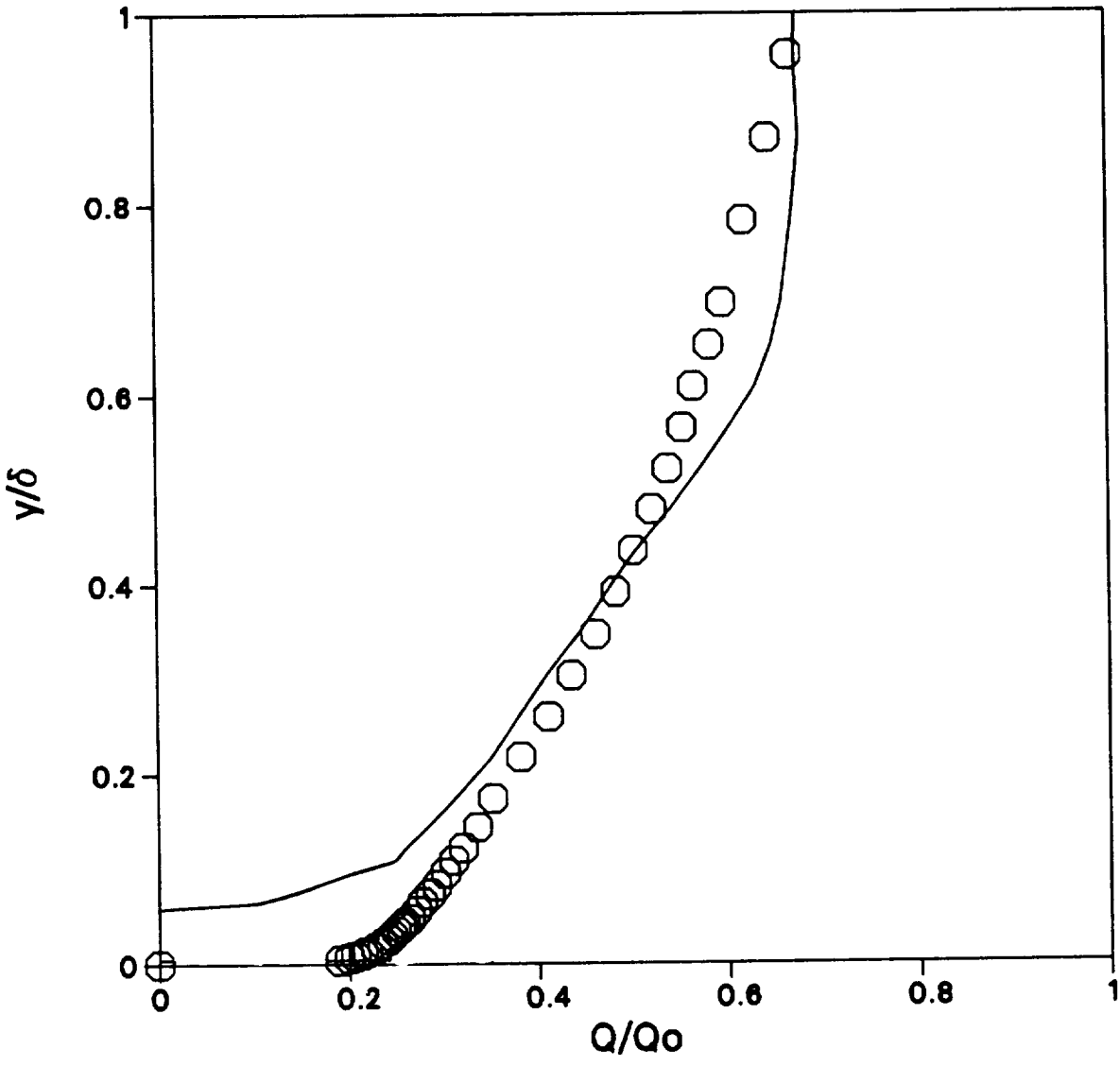

Figure 4.26 Measured compared to inviscid velocity distribution for spinning case D.S1, ○ x=304mm, — inviscid evolution of x=−152mm profile.

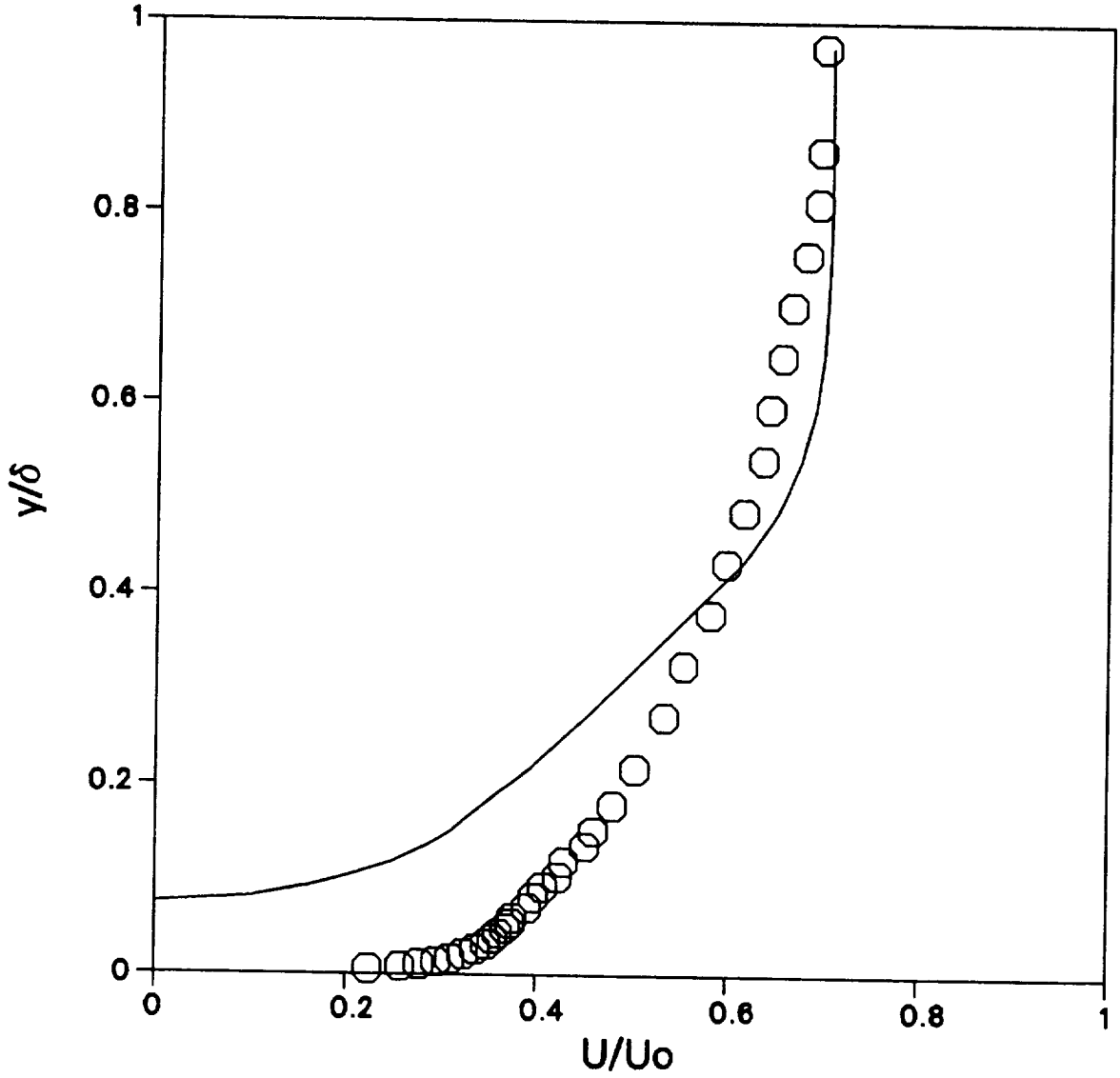

Figure 4.27 Measured compared to inviscid velocity distribution for non-spinning case B.S0, ◯ x=152mm, — Inviscid evolution of x=-228mm profile.

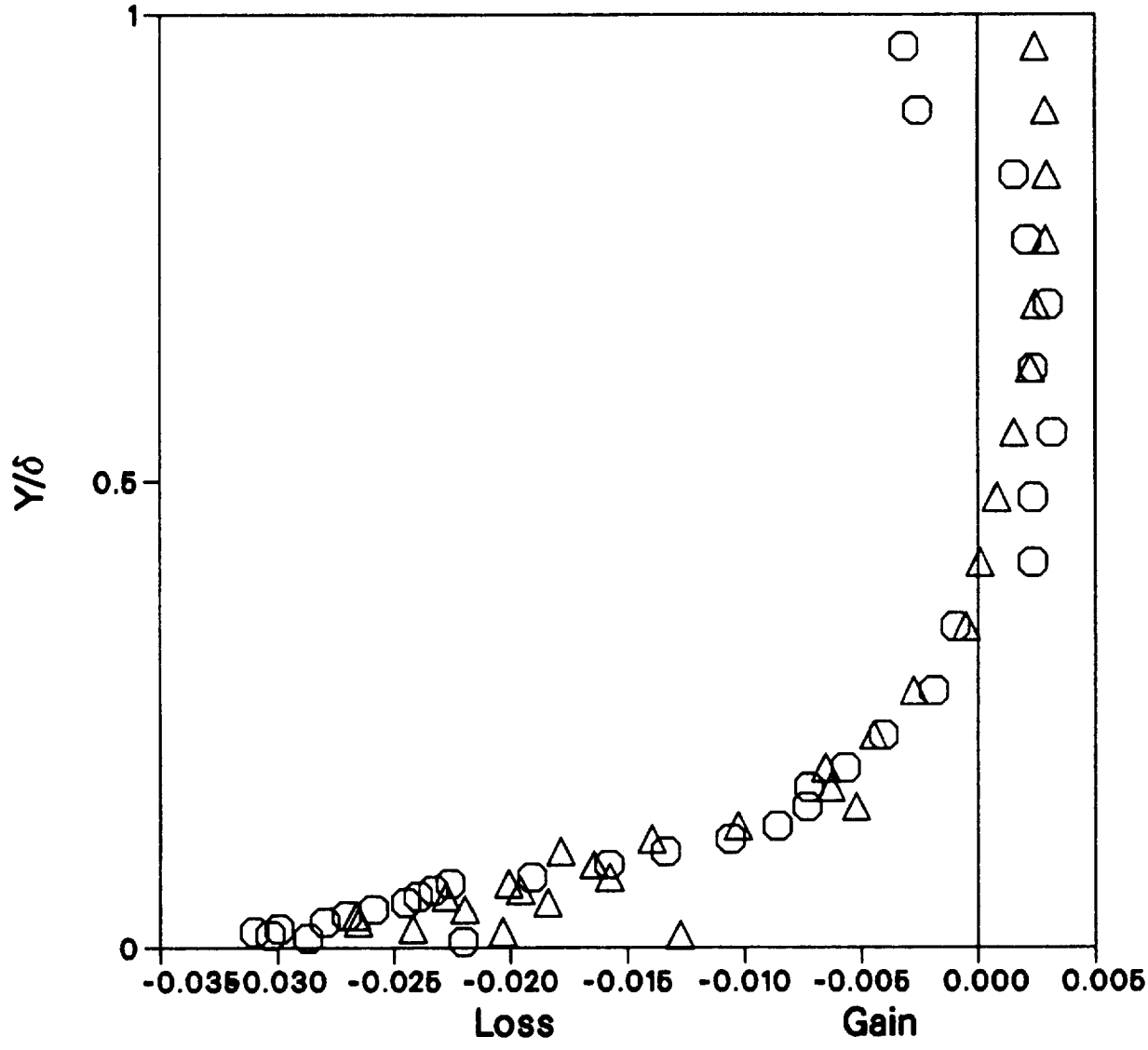

Figure 4.28 W-Momentum Equation Balance Profile @X= 50mm for adverse pressure gradient, spinning case D.S1, ○ (DW/Dt) δ/U_r^2, △ $(-\partial(r\overline{v}\overline{w})/\partial r)\delta/rU_r^2$.

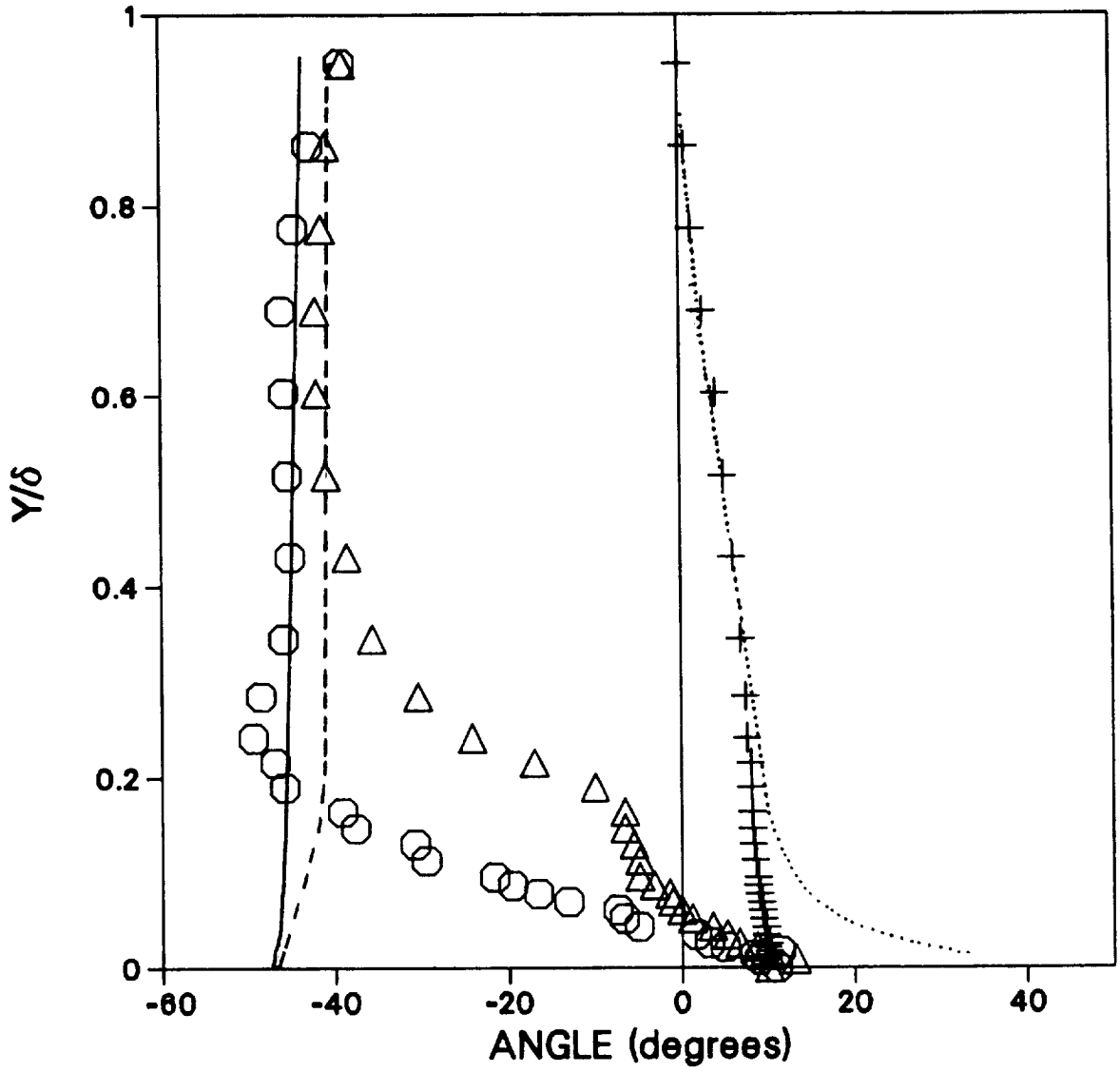

Figure 4.29 Strain-rate and stress direction profile for zero pressure gradient spinning case A.S1 @X=100mm; △ $\mathrm{Tan}^{-1}((\partial W/\partial r - W/r)/\partial U/\partial r)$, ○ $\mathrm{Tan}^{-1}(-\overline{vw}/-\overline{uv})$, + Flow angle $\mathrm{Tan}^{-1}(W/U)$; (compared to X=-12mm), - - - $\mathrm{Tan}^{-1}((\partial W/\partial r - W/r)/\partial U/\partial r)$, —— $\mathrm{Tan}^{-1}(-\overline{vw}/-\overline{uv})$, ... Flow angle $\mathrm{Tan}^{-1}(W/U)$.

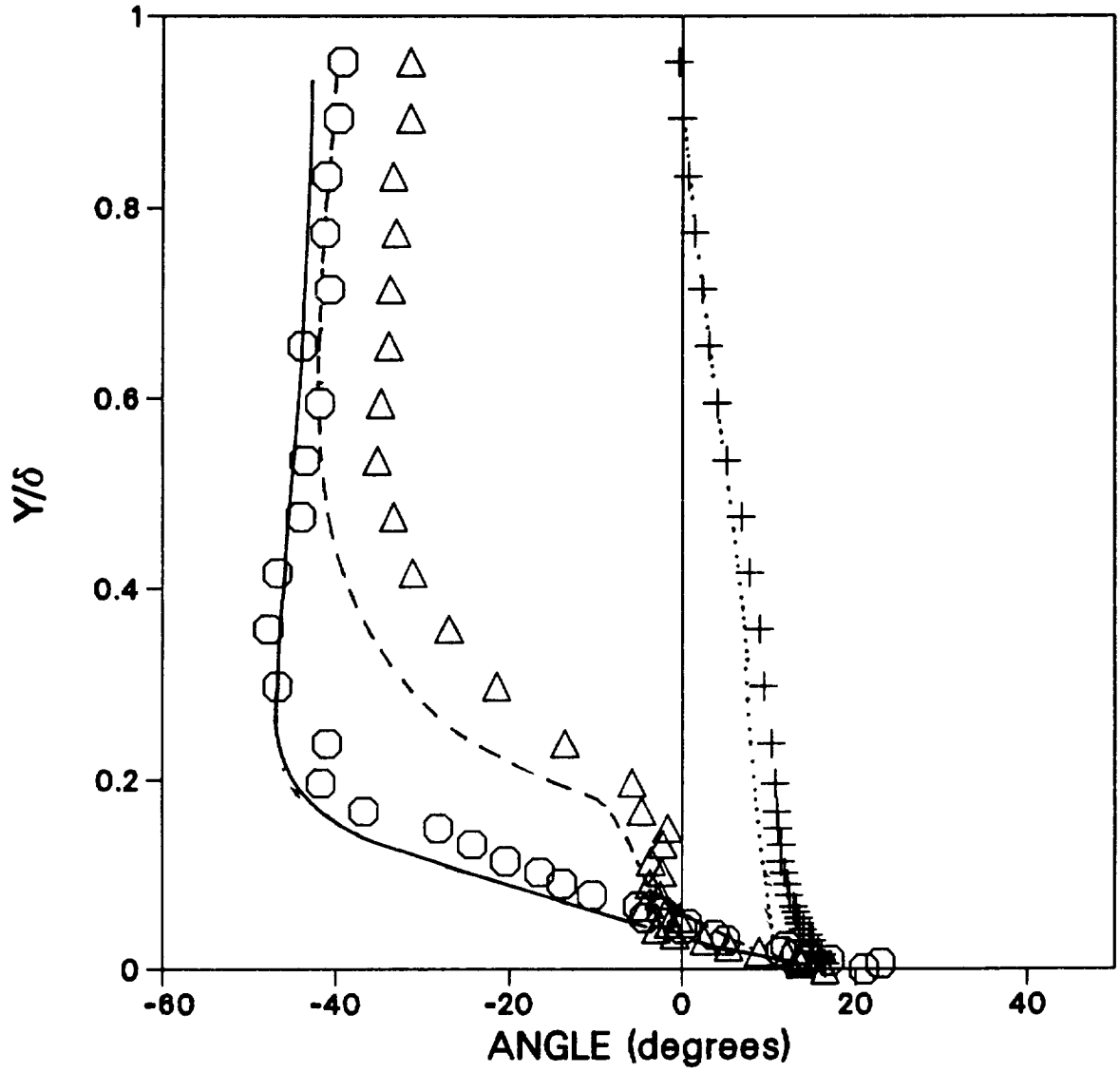

Figure 4.30 Strain-rate and stress direction profile for adverse pressure gradient spinning case D.S1 @X=100mm; △ $\mathrm{Tan}^{-1}((\partial W/\partial r - W/r)/\partial U/\partial r)$, ◯ $\mathrm{Tan}^{-1}(\text{-}\overline{vw}/-\overline{uv})$, + Flow angle Tan^{-1}(W/U); (compared to case A.S1 @X=100mm), - - - $\mathrm{Tan}^{-1}((\partial W/\partial r - W/r)/\partial U/\partial r)$, —— $\mathrm{Tan}^{-1}(\text{-}\overline{vw}/-\overline{uv})$, ... Flow angle Tan^{-1}(W/U).

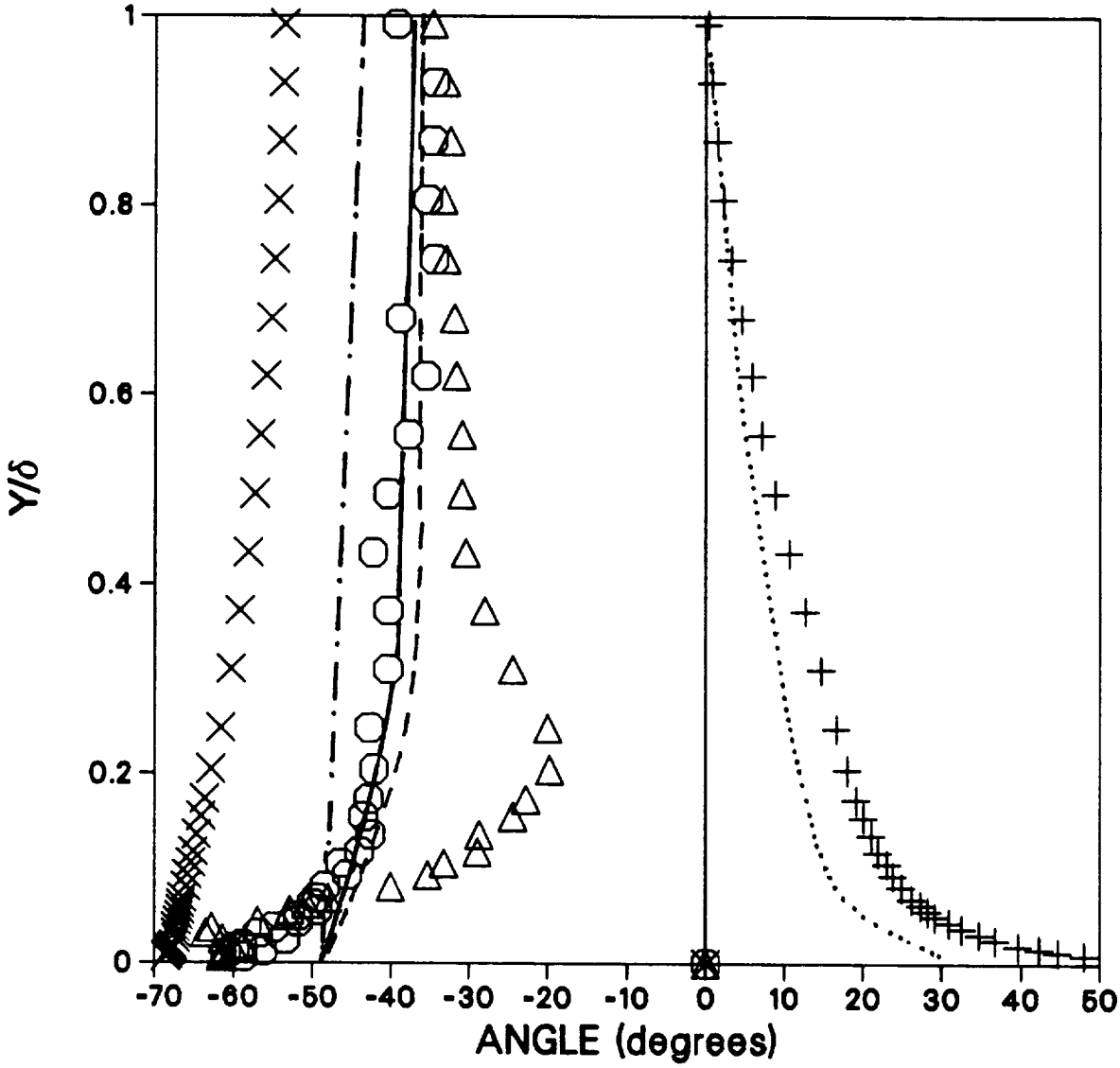

Figure 4.31 Strain-rate and stress direction profile for adverse pressure gradient spinning case C.S1 @X=-12mm; △ $\mathrm{Tan}^{-1}((\partial W/\partial r - W/r)/\partial U/\partial r)$, ○ $\mathrm{Tan}^{-1}\frac{-\overline{vw}}{-\overline{uv}}$, + Flow angle $\mathrm{Tan}^{-1}\frac{W}{U}$, × Relative flow angle $\mathrm{Tan}^{-1}\frac{W-W_s}{U}$; (compared to X=-330mm), - - - $\mathrm{Tan}^{-1}((\partial W/\partial r - W/r)/\partial U/\partial r)$, —— $\mathrm{Tan}^{-1}(-\overline{vw}/-\overline{uv})$, ... Flow angle, - - - relative flow angle.

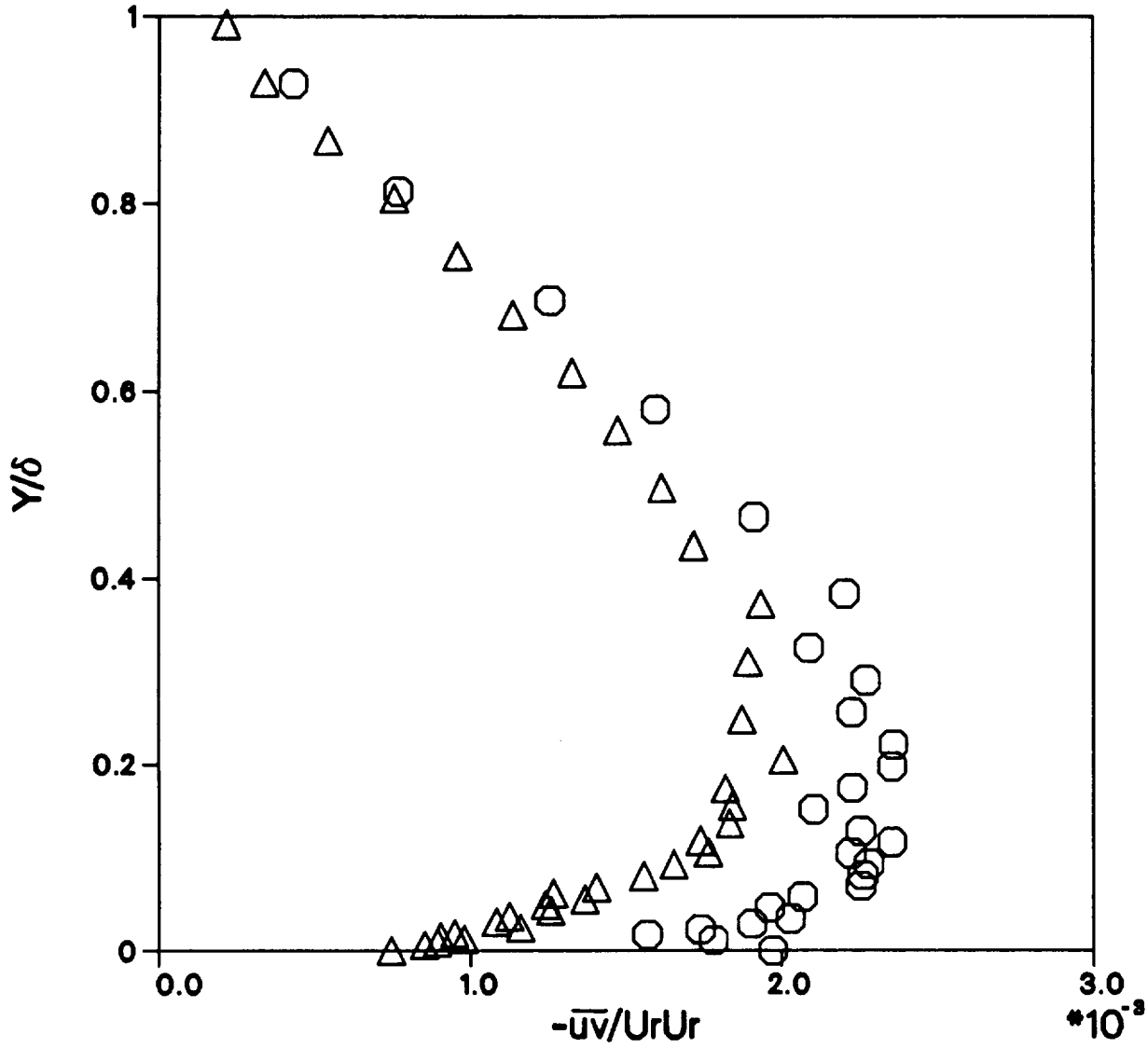

Figure 4.32 $\overline{uv}$ stress distribution for adverse pressure gradient, spinning case C.S1, ○ x=-228mm, △ x=−12mm.

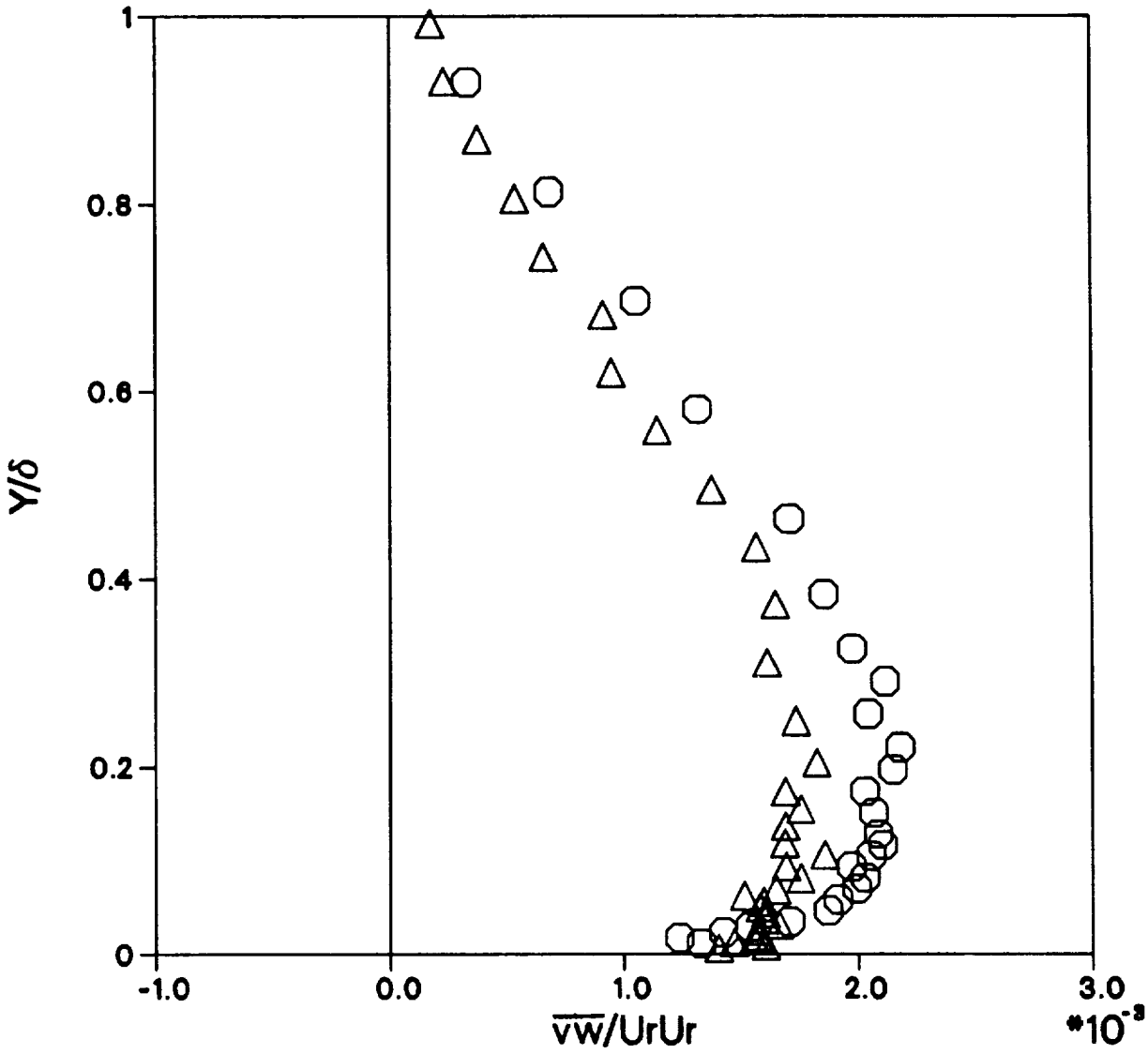

Figure 4.33 $\overline{vw}$ stress distribution for adverse pressure gradient, spinning case C.S1, ○ x=-228mm, △ x=−12mm.

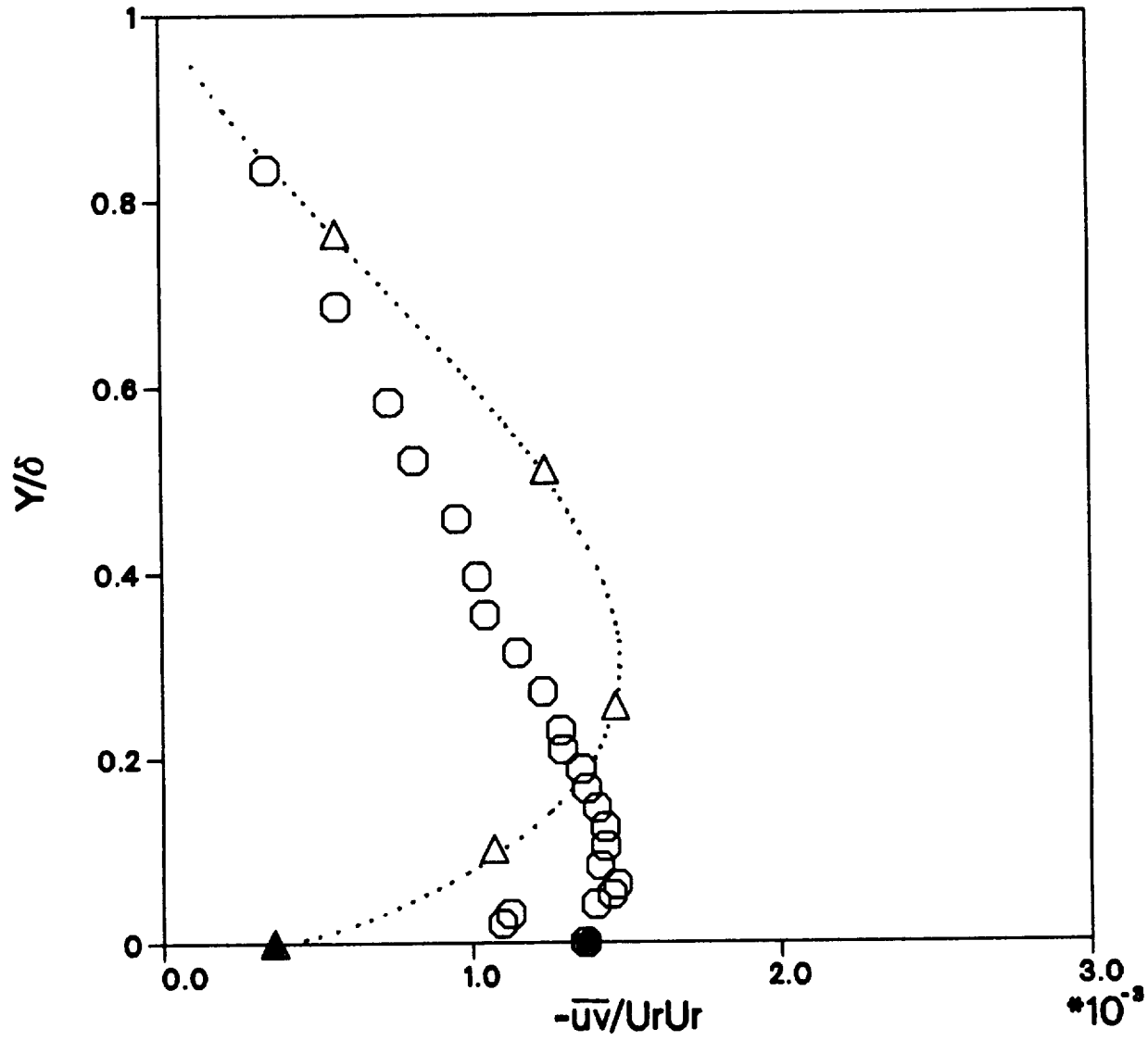

Figure 4.34 $\overline{uv}$ stress distribution for adverse pressure gradient, non-spinning case B.S0, ○ x=-330mm, △ x=−12mm.

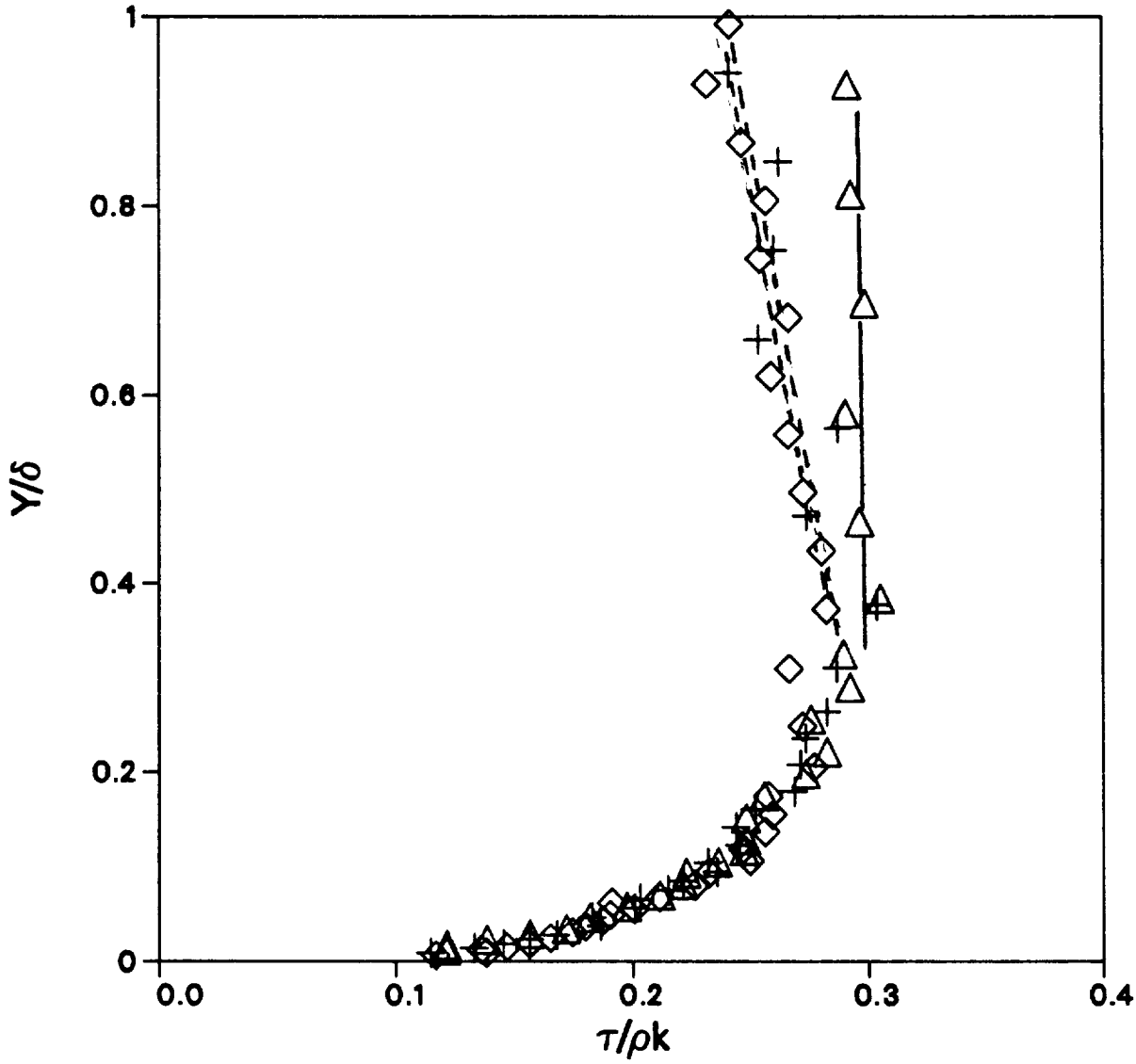

Figure 4.35 $\tau/\rho k$ distribution for adverse pressure gradient, spinning case C.S1, $\triangle$ x=-228mm, + x=−152mm, $\diamond$ x=−12mm, — 2D zero $\partial P/\partial x$ case.

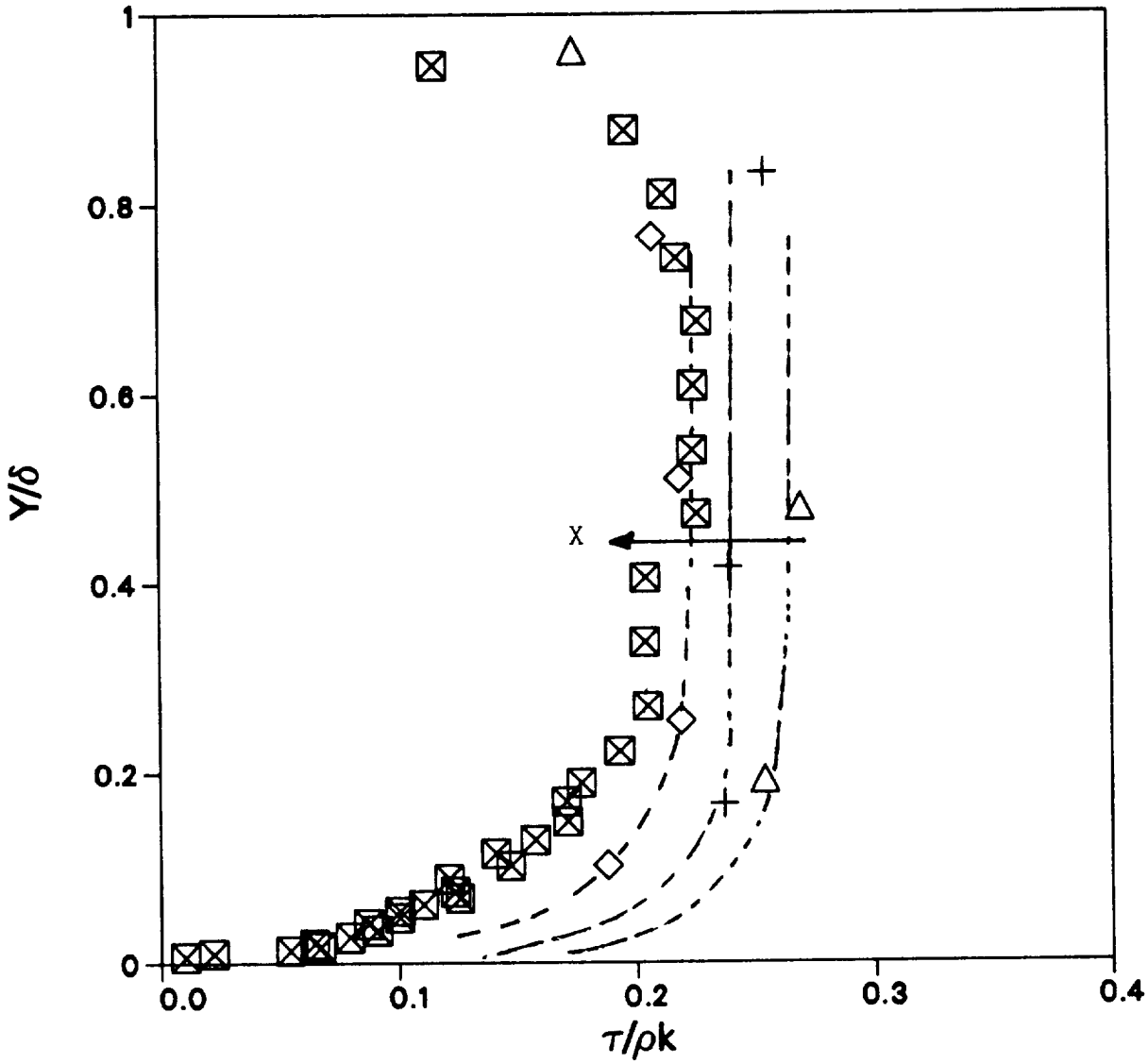

Figure 4.36 $\tau/\rho k$ distribution for mild adverse pressure gradient, non-spinning case B.S0, $\triangle$ x=-228mm, + x=−152mm, $\diamond$ x=−12mm, $\boxtimes$ x=152mm.

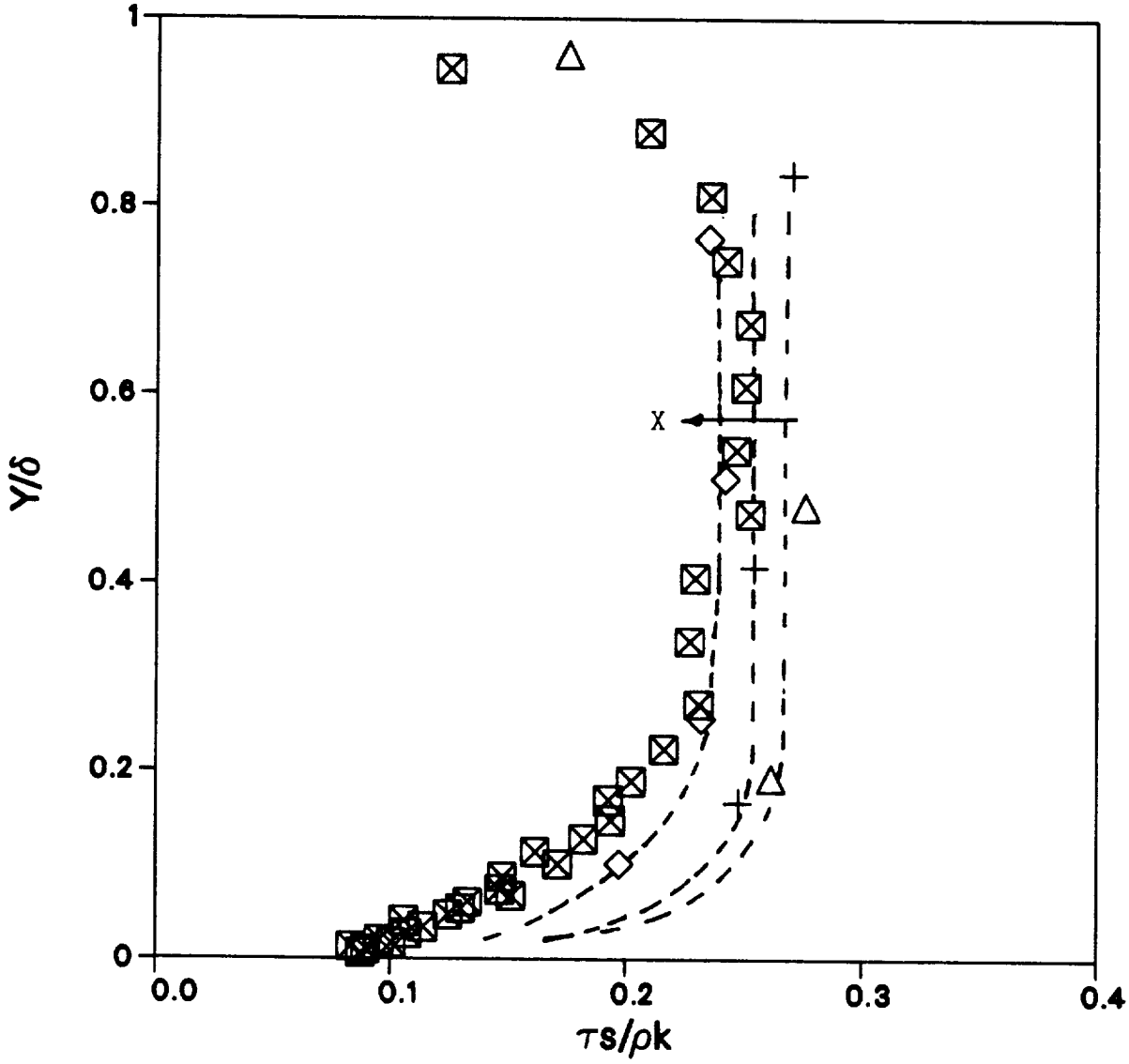

Figure 4.37 Streamwise aligned $\tau/\rho k$ for mild adverse pressure gradient, non-spinning case B.S0, △ x=-228mm, + x=−152mm, ◇ x=−12mm, ⊠ x=152mm.

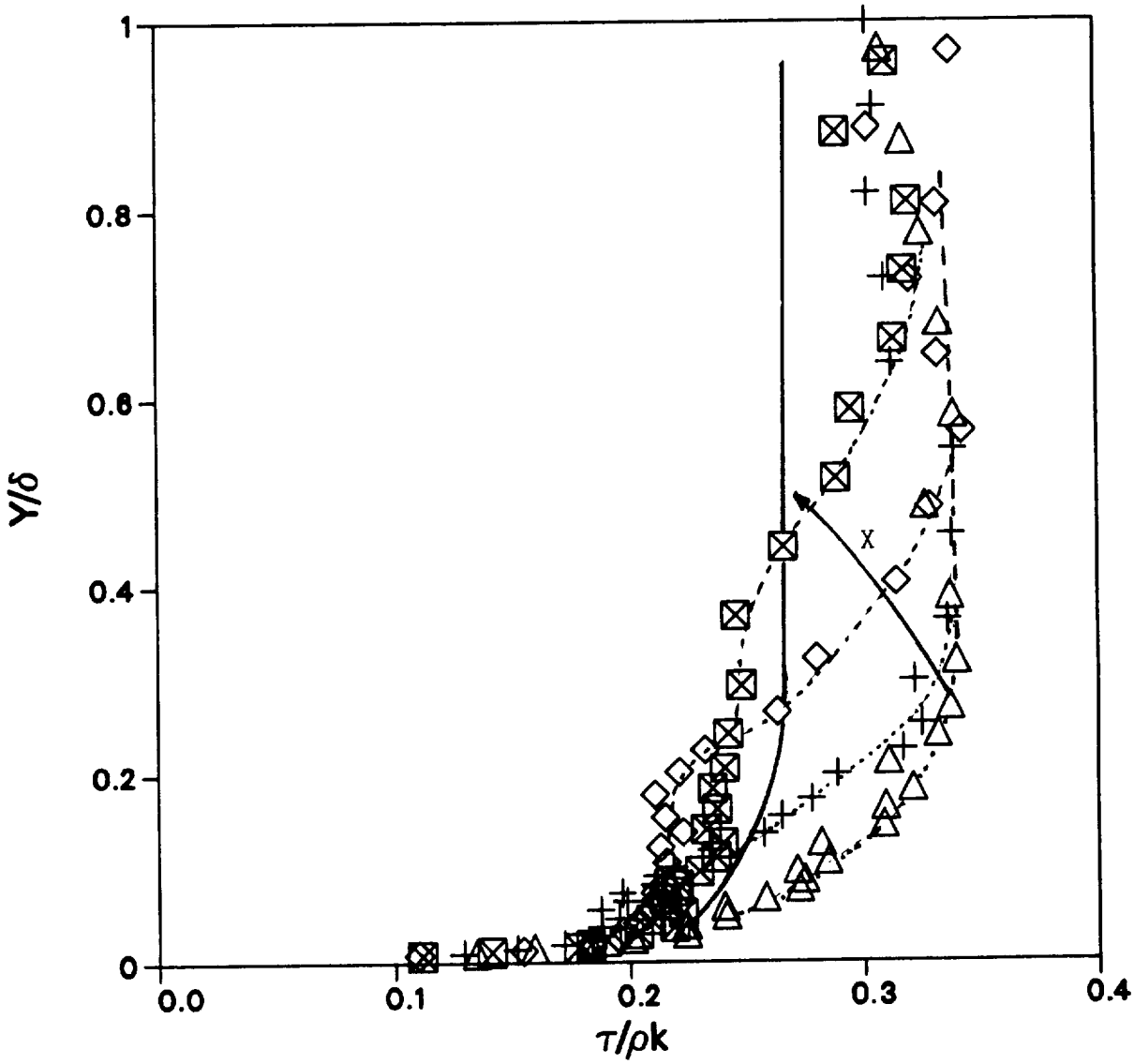

Figure 4.38 $\tau/\rho k$ distribution for zero pressure gradient, spinning case A.S1, $\triangle$ x=−12mm, + x=51mm, $\diamond$ x=152mm, $\boxtimes$ x=304mm, —— 2D zero $\partial P/\partial x$ case.

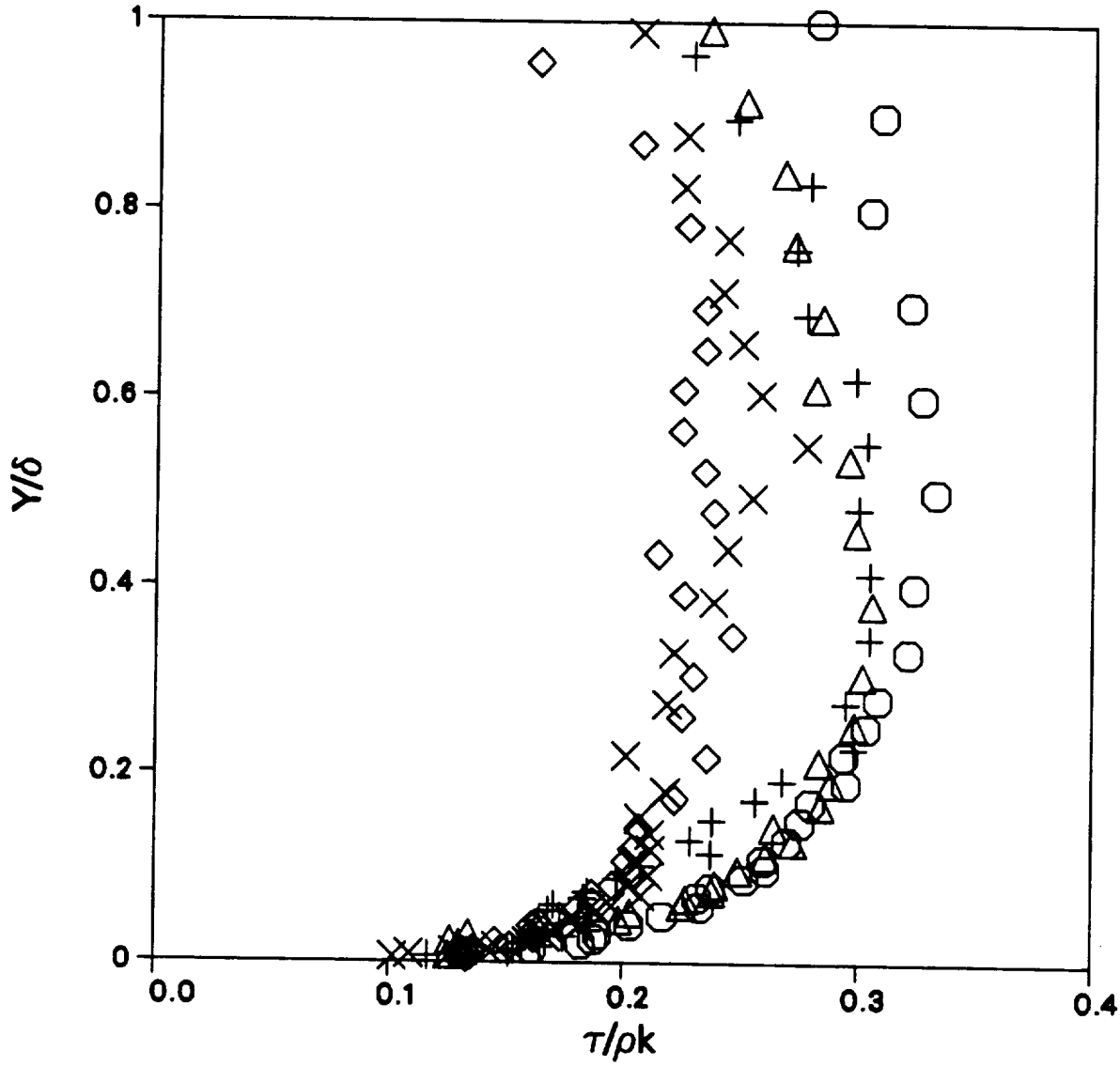

Figure 4.39 $\tau/\rho k$ distribution for adverse pressure gradient, spinning case D.S1, ○ x=-76mm, △ x=12mm, + x=48mm, × x=152mm, ◇ x=304mm.

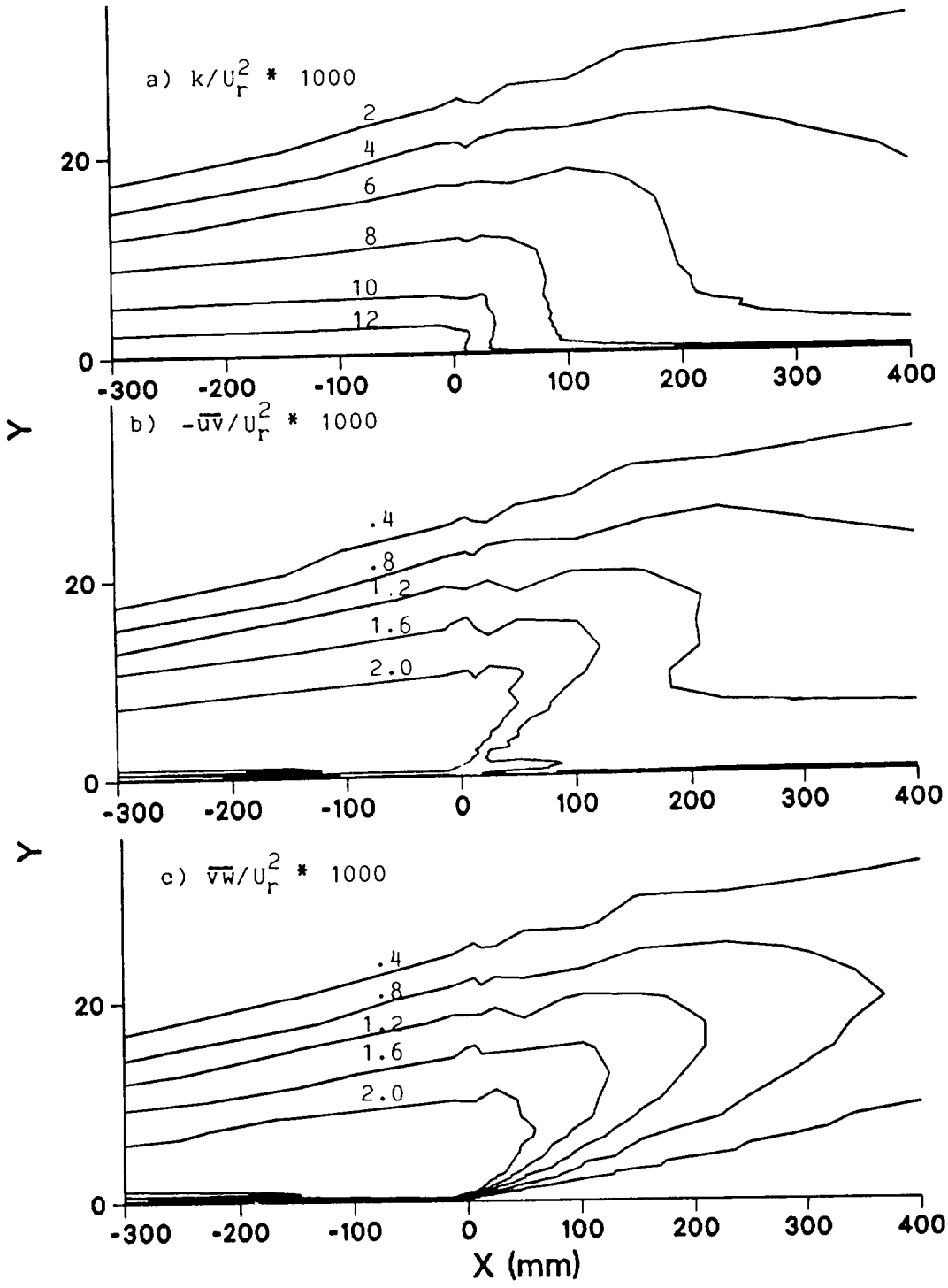

Figure 4.40 Stress contour plots for zero pressure gradient, spinning case A.S1, a) k, b) $\overline{uv}$, c) $\overline{vw}$.

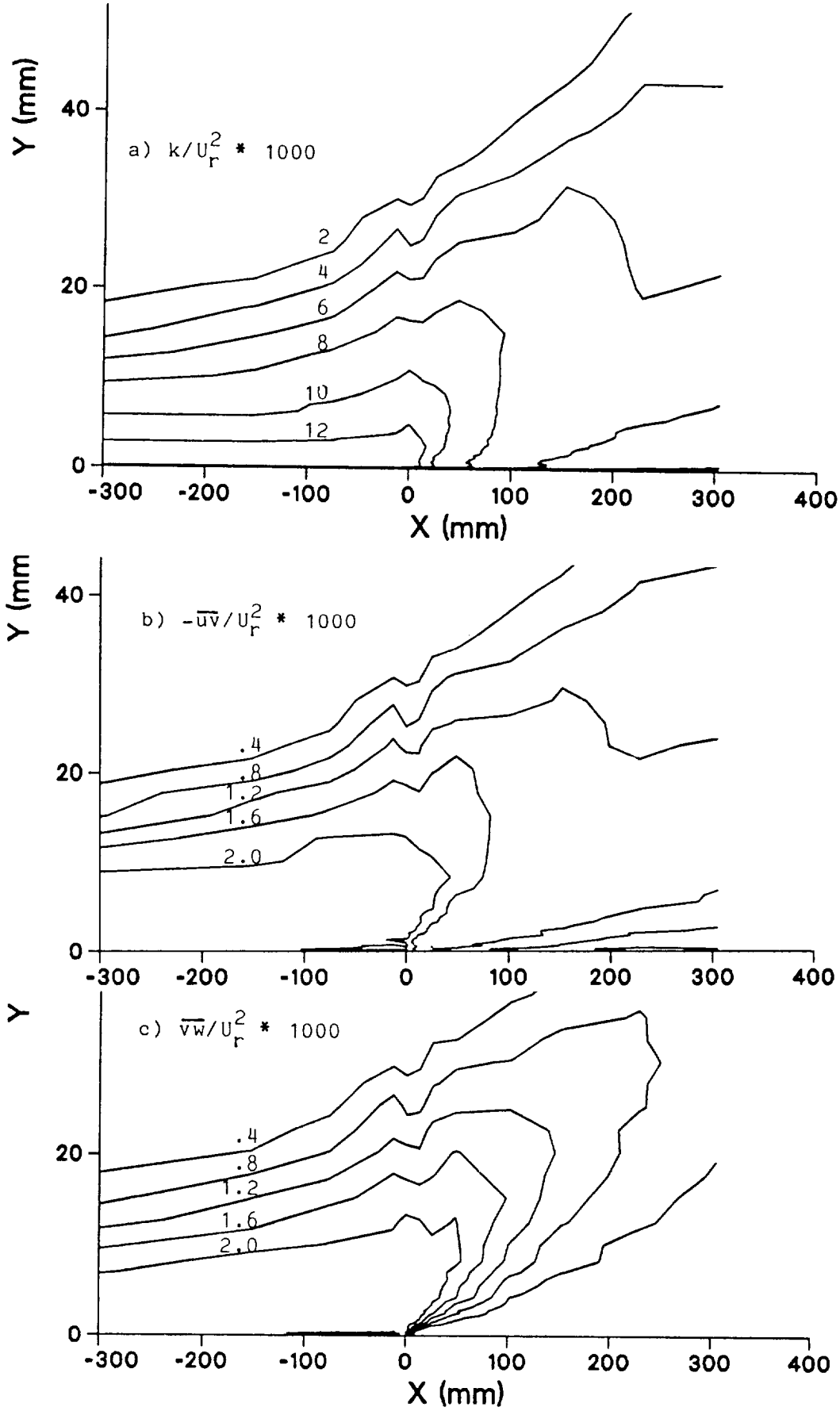

Figure 4.41 Stress contour plots for adverse pressure gradient, spinning case D.S1, a) k, b) $\overline{uv}$, c) $\overline{vw}$.

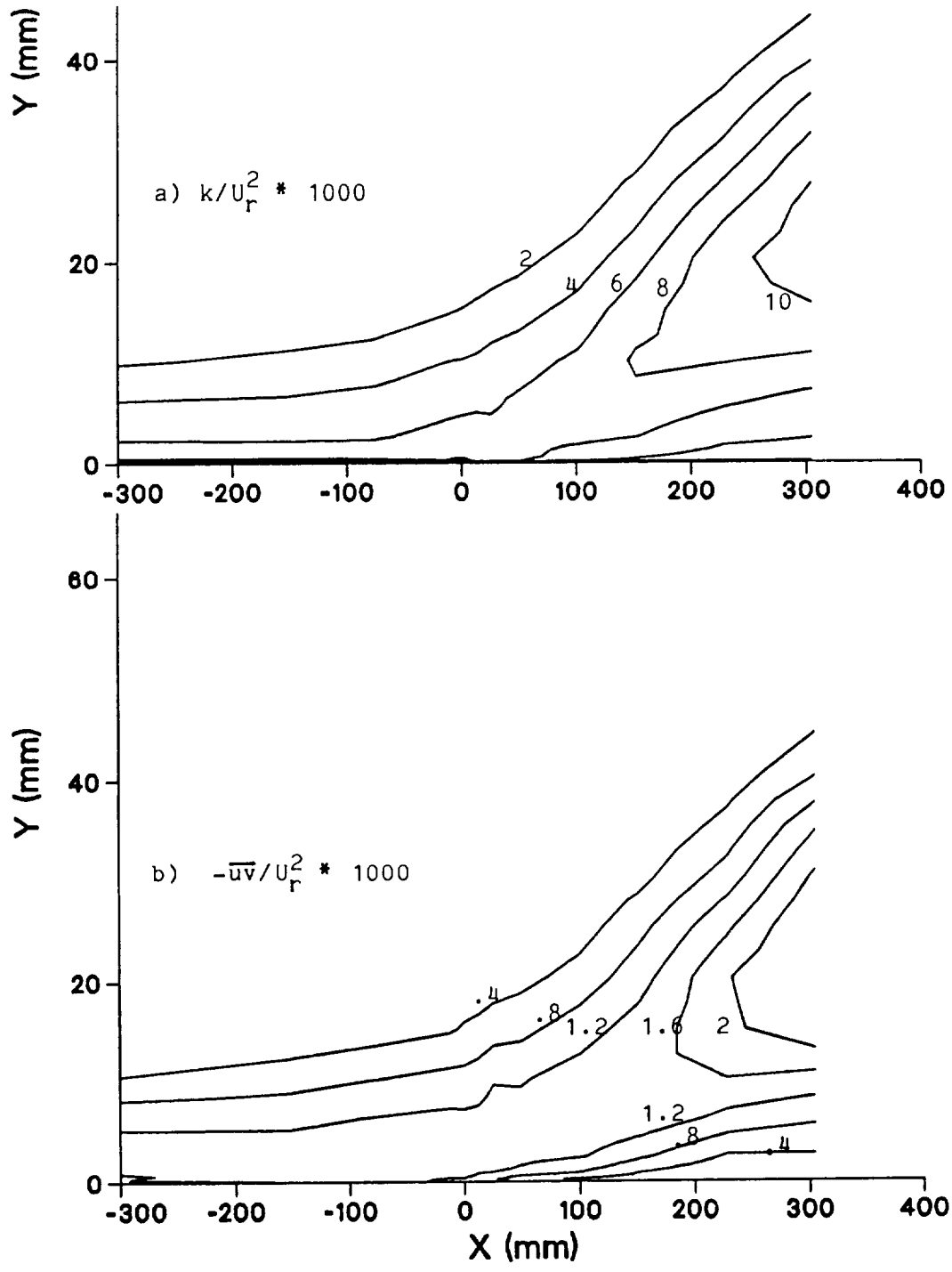

Figure 4.42 Stress contour plots for adverse pressure gradient, non-spinning case D.S0, a) k, b) $\overline{uv}$.

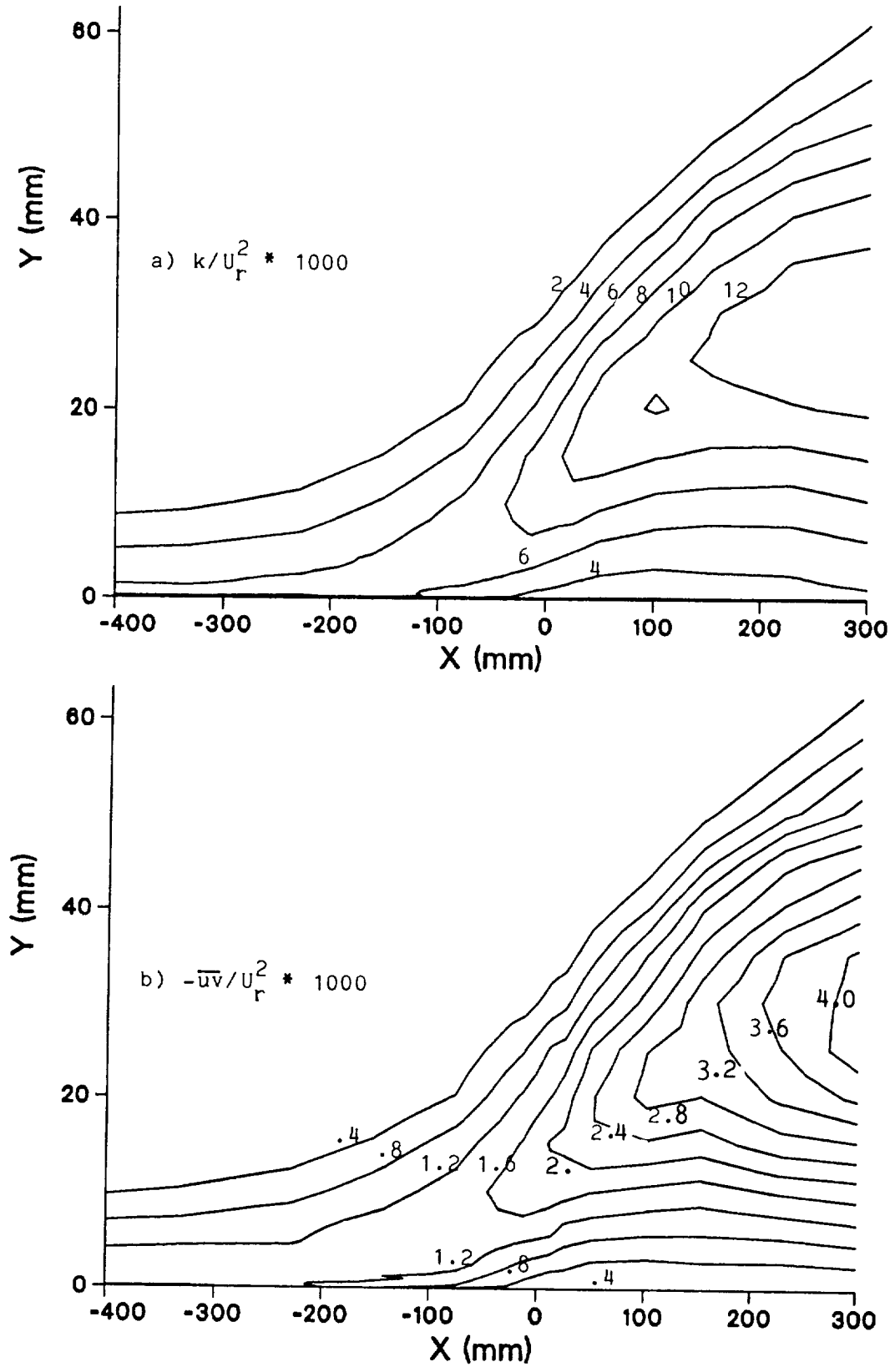

Figure 4.43 Stress contour plots for adverse pressure gradient, non-spinning case C.S0, a) k, b) $\overline{uv}$.

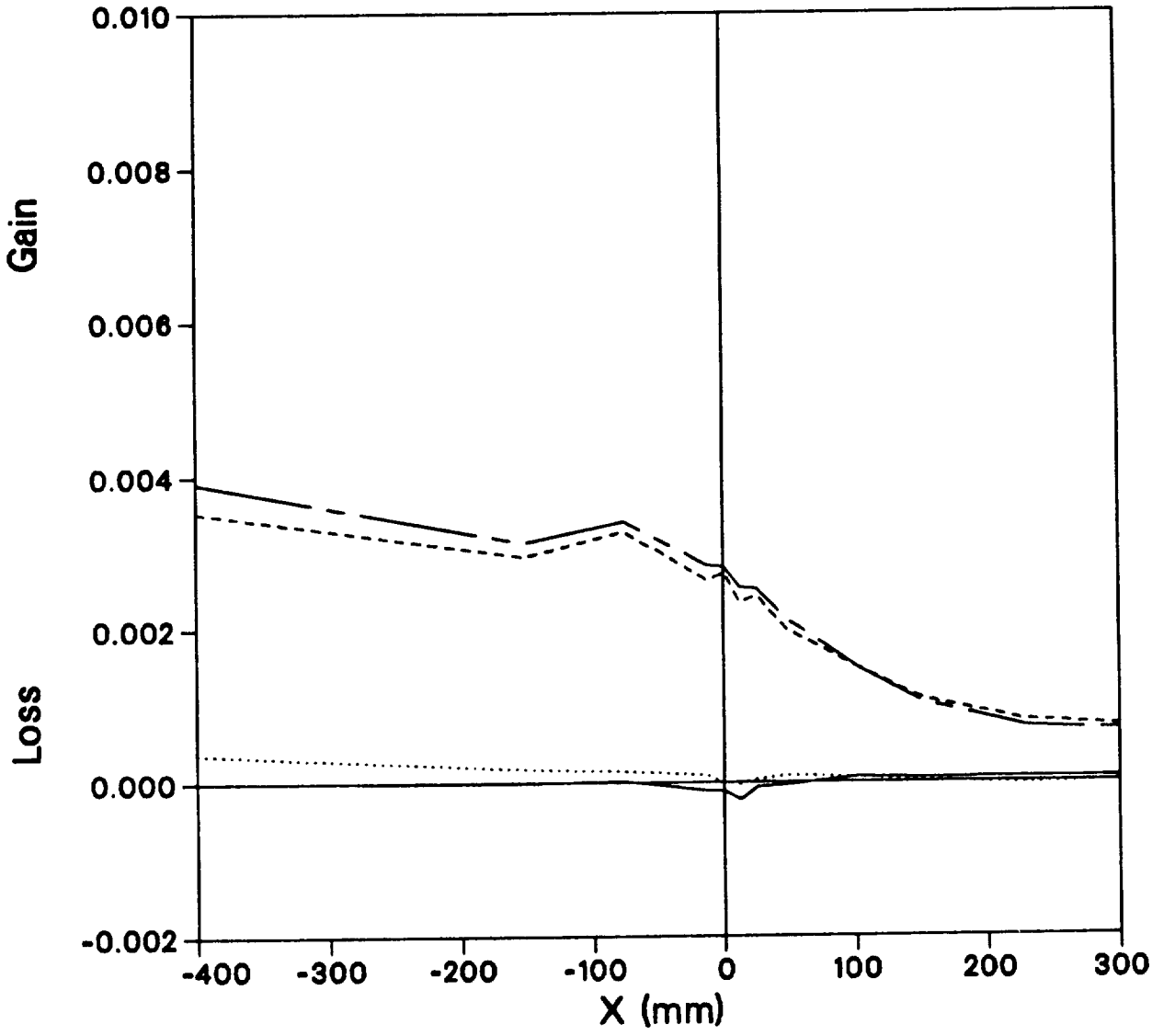

Figure 4.44 Kinetic energy equation balance along streamline @y=1.27mm for adverse pressure gradient, no-Spin case D.S0, —— $(Dk/Dt)\delta_o/U_r^3$, - - - $(Production)\delta_o/U_r^3$, ... $(Diffusion)\delta_o/U_r^3$, – – – $(-Dissipation)\delta_o/U_r^3$.

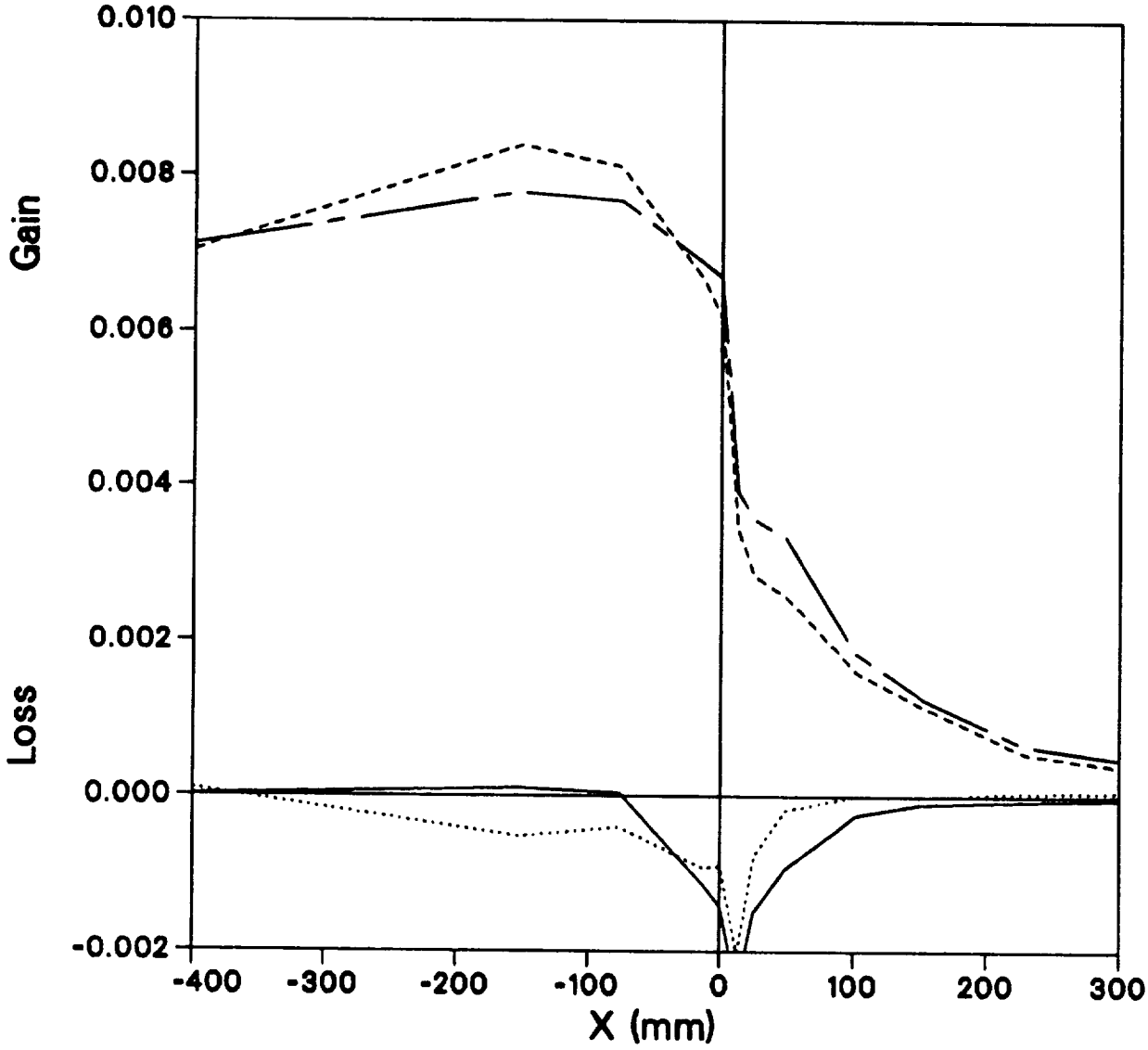

Figure 4.45 Kinetic energy equation balance along streamline @y=1.27mm for adverse pressure gradient, spin case D.S1, — $(Dk/Dt)\delta_o/U_r^3$, - - - $(Production)\delta_o/U_r^3$, ... $(Diffusion)\delta_o/U_r^3$, – – – $(-Dissipation)\delta_o/U_r^3$.

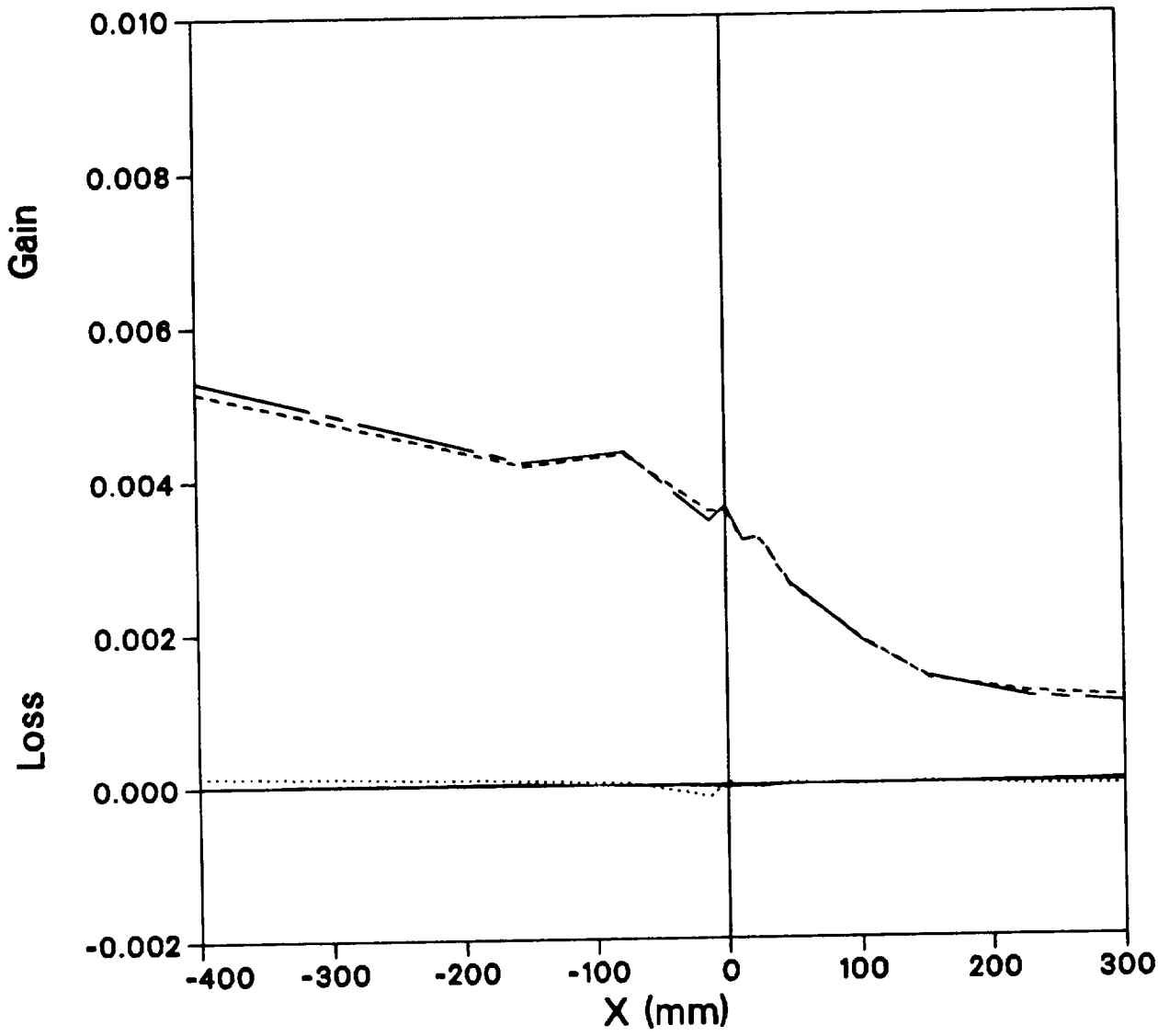

Figure 4.46 $\overline{uv}$ stress equation balance along streamline @y=1.27mm for adverse pressure gradient, no-Spin case D.S0, —— (D-$\overline{uv}$/Dt)δ_o/U_r^3, - - - (Production$_{uv}$)δ_o/U_r^3, ... (Diffusion$_{uv}$)δ_o/U_r^3, – – – (–Pressure-Strain+Dissipation$_{uv}$)δ_o/U_r^3.

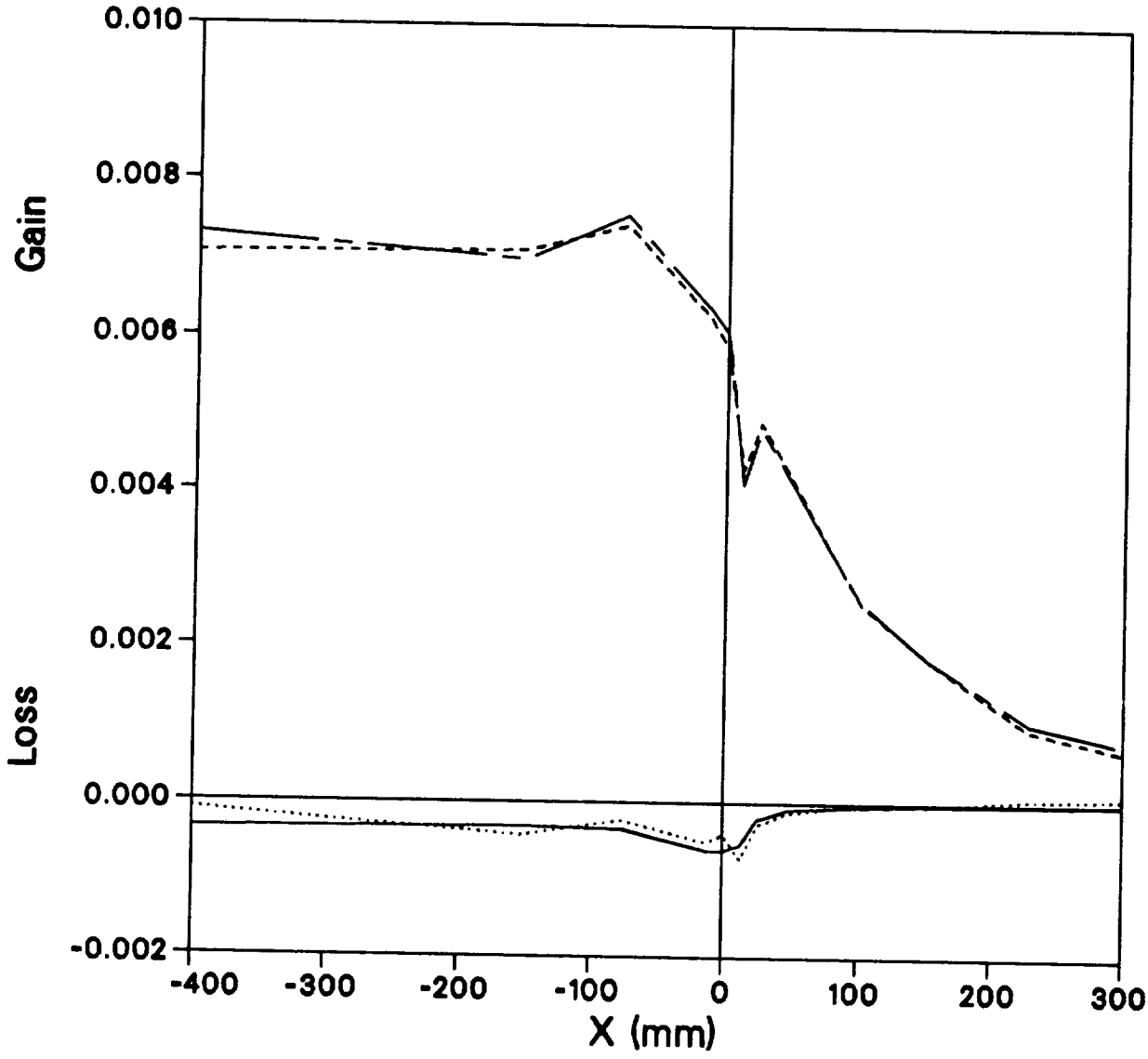

Figure 4.47 $\overline{uv}$ stress equation balance along streamline @y=1.27mm for adverse pressure gradient spin case D.S1, —— (D-$\overline{uv}$/Dt)δ_o/U_r^3, - - - (Production$_{uv}$)δ_o/U_r^3, ... (Diffusion$_{uv}$)δ_o/U_r^3, – – – (-Pressure-Strain+Dissipation$_{uv}$) δ_o/U_r^3.

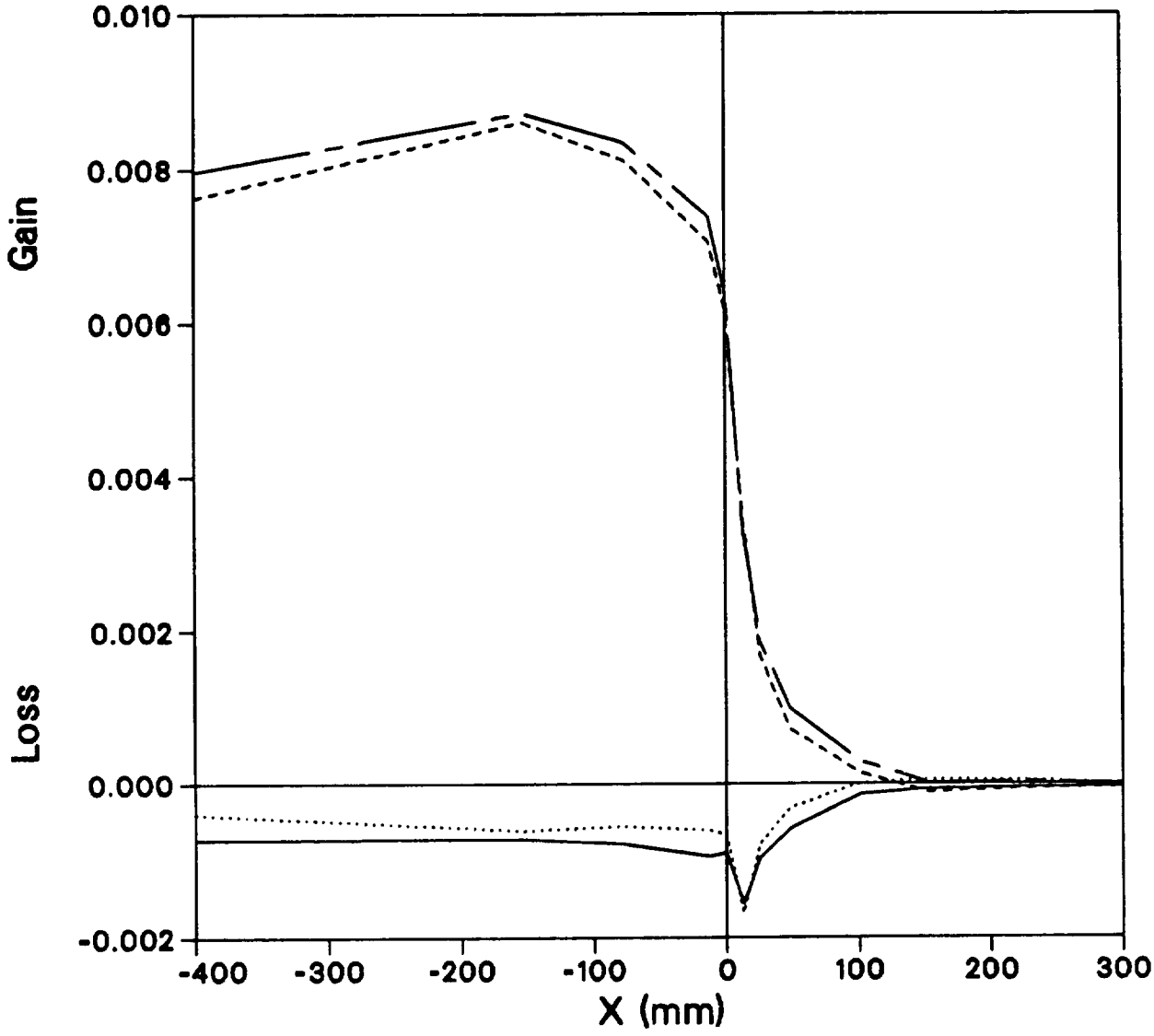

Figure 4.48 $\overline{vw}$ stress equation balance along streamline @y=1.27mm for adverse pressure gradient spin case D.S1, —— $(\mathrm{D}\overline{vw}/\mathrm{Dt})\delta_o/U_r^3$, - - - $(\mathrm{Production}_{vw})\delta_o/U_r^3$, ... $(\mathrm{Diffusion}_{vw})\delta_o/U_r^3$, – – – (–Pressure-Strain + $\mathrm{Dissipation}_{vw})\delta_o/U_r^3$.

5 TURBULENCE MODELING

The key to accurate solutions of the Reynolds averaged Navier-Stokes equations is the turbulence model. Turbulence models are empirical correlations derived from observations in a limited number of flows. The correlations are not perfect, but are hopefully of sufficient accuracy that they produce solutions to the Reynolds averaged Navier-Stokes equations that closely mimic nature. Usually, many assumptions (empirical correlations) are used to model the Reynolds stress. In this section, tests of some of these assumptions will be described and some suggestions for additional empirical correlations will be discussed.

5.1 $\overline{uv}$ Reynolds Stress Model Assumptions

One way to test a model assumption is to insert experimental data directly into the model and compare the result (the modeled quantity) with the experimental measured value.

For example, Reynolds stress is often modeled using the product of an algebraically prescribed length scale and the local velocity gradient (suggested by Prandtl). For our flow the mixing length model takes the form

$$\overline{u_i u_j} = -l^2 \, 4 S_{ij} \sqrt{S_{mn} S_{nm}}$$

where l = the lesser of $0.41y$ or 0.09δ (or $l = 0.09\delta \, Tanh(0.41y/0.09\delta)$). Sometimes l is multiplied by $(1 - 7 * Ri)$ to account for the destabilizing effects of rotation and curvature.

Other models use an eddy-viscosity algebraic expression

$$\overline{u_i u_j} = -\nu_t \, 2 S_{ij}$$

The eddy viscosity, ν_t, is often calculated using $\nu_t = \nu_{t_o}[1 - exp(\nu_{t_i}/\nu_{t_o})]$ where $\nu_{t_i} = (0.41y)^2 \, 2\sqrt{S_{mn}S_{nm}}$ and $\nu_{t_o} = 0.0168\delta^* U_e/[1 - 5.5(y/\delta)^6]$ (suggested by Cebeci and Smith (refs. 44 and 45)). Alternatively, the somewhat more sophisticated models solve differential equations for k and ε which are then used to form an eddy-viscosity equal to $\nu_t = C_\mu k^2/\varepsilon$ with $C_\mu = 0.09$ (suggested by Jones and Launder (ref. 46)).

All of these models can be evaluated using the data without recourse to further assumptions. For example the modeled $\overline{uv}$ and $\overline{vw}$ stresses can be calculated using the measurements of $\partial U/\partial y$, $\partial W/\partial y$, k and ε (experimentally deduced). In zero pressure gradient without spin (case D.S0 at X = −152 mm) all of the models fit reasonably well (fig. 5.1) with the exception of the $k - \varepsilon$ model near the wall, below $y/\delta = 0.2$. No damping function has been applied to the $k - \varepsilon$ model in this analysis, and incorporating one would surely improve the comparison.

The modeling deficiency associated with the $k - \varepsilon$ model arises from the incorrect assumption that C_μ is a constant equal to 0.09 everywhere in the flow. This value for C_μ was derived from the assumption that production equals dissipation and $(\tau/\rho)/k = 0.3$ (i.e., $C_\mu = (\frac{\tau}{\rho k})^2 = 0.09$). However, we saw in section 4.5 that $(\tau/\rho)/k$ is not constant, but is a function of the pressure gradient, proximity to the wall, and three-dimensionality. Consequently the model $\nu_t = C_\mu k^2/\varepsilon$ overpredicts $\overline{uv}$ and $\overline{vw}$ near the wall (fig. 5.1). This analysis is a little unfair, since the $k - \varepsilon$ model solves for different k and ε values than are actually measured in the experiment and consequently errors in the prediction of k and ε compensate for

errors in the assumption that $(\tau/\rho)/k = 0.3$. For example, the $k-\varepsilon$ model underpredicts the level of k near walls, consequently compensating for the erroneous assumption $(\tau/\rho)/k = 0.3$.

In the non-spinning adverse pressure gradient flow (case D.S0,) the various turbulence models start to deteriorate (fig. 5.2). The $k-\varepsilon$ model generally overpredicts the level of stress as a result of the erroneous assumption that $(\tau/\rho)/k = 0.3$. The mixing-length models of Prandtl and Cebeci-Smith overpredict the stress in the outer region of the flow and underpredict the stress near the wall. Accuracy of the turbulence model in the near wall region is critical to obtaining good calculations. The mixing length models produce a y^2 increase in $\overline{uv}$ stress with distance from the wall while measurements indicate that $\overline{uv}$ stress grows more linearly. This observation led Johnson and King (ref. 47) to propose the following model which produces a more linear distribution of $\overline{uv}$ stress.

$$\overline{uv} = -\sqrt{(\tau/\rho)_{max}}\, l\, (\partial U/\partial y)$$

$$\overline{vw} = -\sqrt{(\tau/\rho)_{max}}\, l\, (\partial W/\partial y - W/r)$$

where $l = 0.09\delta\ tanh(0.41y/0.09\delta)$. The term $(\tau/\rho)_{max}$ is solved for by an auxiliary ordinary differential equation. This model greatly improved the prediction of separating flows such as those of Simpson (ref. 26) and Bachalo-Johnson (ref. 28). Indeed this model (using measured $(\frac{\tau}{\rho})_{max}$) fits the data from the current experiment quite well (fig. 5.2). The other models tend to overpredict the $\overline{uv}$ shear stress in the outer region. This overprediction provides one possible reason why those models historically predict a separation zone which is too small; larger $\overline{uv}$ stress tends to reduce the ability of the flow to detach.

Under conditions of adverse pressure gradient with spin (case D.S1 at X = 304 mm), the mixing length models also produce a y^2 growth of $\overline{uv}$ Reynolds stress with distance from the wall rather than the more linear growth seen in the experiment (fig. 5.3). The Johnson-King model exhibits a nearly linear distribution of $\overline{uv}$ stress. The $k-\varepsilon$ model still has the usual difficulties near the wall. The $\overline{vw}$ stress component is underpredicted by all of the models in the inner portion of the flow primarily due to the incorrect assumption that eddy viscosity is isotropic (equal in all directions).

5.2 $\overline{vw}$ Reynolds Stress Turbulence Modeling Assumptions

Lack of isotropy of the eddy-viscosity is a symptom of a lag phenomenon, e.g., where turbulence is slow to respond to changes in the mean flow strain rate as was seen in section 1.2.1. If the response of the stress to the strain were fast (i.e., no lag) the stress would be proportional to the strain-rate (i.e., isotropic). The fact that turbulence is not quick to respond to changes in the mean flow strain-rate is illustrated by the difference in direction of the mean-flow strain-rate vector, $tan^{-1}((\frac{\partial W}{\partial y} - \frac{W}{r})/\frac{\partial U}{\partial y})$, and the Reynolds stress vector, $tan^{-1}(-\overline{vw}/-\overline{uv})$. Typically, the two directions are not the same (fig. 5.4).

Models which assume the stress is directly proportional to the strain rate (Boussinesq approximation) inherently are incapable of reproducing this lag phenomenon. Prandtl mixing-length, Cebeci-Smith and Jones-Launder models fall into this category and are referred to as equilibrium models, since they assume that anything which happens to the mean flow immediately affects the turbulence. These models produce a stress direction which is the same as the strain-rate direction, an assumption which is sometimes useful but not generally accurate.

An attempt to fix the equilibrium models by reducing the transverse stress component was made by Rotta who proposed the T-model, given by

$$\overline{uv} = -\nu_{t_{xx}}\partial U/\partial y - \nu_{t_{xz}}(\partial W/\partial y - W/r)$$
$$\overline{vw} = -\nu_{t_{xz}}\partial U/\partial y - \nu_{t_{zz}}(\partial W/\partial y - W/r)$$

where

$$\nu_{t_{xx}} = \nu_t(1 - (T-1)sin^2(\beta))$$
$$\nu_{t_{xz}} = \nu_t(1 - T)sin(\beta)cos(\beta)$$
$$\nu_{t_{zz}} = \nu_t(1 - (T-1)cos^2(\beta))$$

with T = constant (Rotta suggests 0.5), β = local flow angle, and ν_t = a scalar eddy-viscosity model. The model result varies with choice of coordinate direction from which to reference β. For our flows, a choice of reference direction which is aligned with the cylinders axis produces a stress direction which is less accurate than the scalar eddy-viscosity model (fig. 5.4). Alternatively, if one applies the T-model in a coordinate system which translates with the spinning cylinder surface, a different model result is obtained (also shown). This demonstrates the lack of Galilean invariance in the Rotta T-model.

Rodi proposed another alternative to the Boussinesq approximation which is referred to as an algebraic stress model, given here by

$$\overline{u_i u_j} = q^2\left(\frac{1}{3}\delta_{ij} + \frac{(P_{ij} - \frac{1}{3}P_{kk}\delta_{ij}) + \phi^1_{ij}}{P_{kk} - (1 - C_1)\varepsilon_{kk}}\right)$$

where the Naot, Shavit, and Wolfshtein (ref. 48) model for the fast portion of the pressure strain model was used

$$\phi^1_{ij} = -\hat{\alpha}(P_{ij} - \frac{1}{3}P_{kk}\delta_{ij})$$

and Rotta's model for the slow part of the pressure strain was adopted

$$\phi^2_{ij} = -C_1 b_{ij}\varepsilon_{kk}$$

along with $\varepsilon_{ij} = \frac{2}{3}\delta_{ij}\varepsilon$; in addition $\hat{\alpha} = 0.6$ and $C_1 = 1.5$ were used, as suggested by Rodi. This model produces a stress that is proportional to the rate of stress production. Unfortunately, it is no better at predicting the direction of the stress vector than the Boussinesq approximation (fig. 5.4). In retrospect, this result might have been expected, since production is directly proportional to the strain rate. The failure of the model can be traced to the pressure-strain model used by Rodi in which pressure strain is assumed to be proportional to the production.

Launder, Reece, and Rodi (ref. 41) proposed adding additional terms to the pressure-strain model of Naot-Shavit-Wolfshtein model, giving the following form for the fast term

$$\phi^1_{ij} = -\hat{\alpha}(P_{ij} - \frac{1}{3}P_{kk}\delta_{ij}) - \hat{\beta}(D_{ij} - \frac{1}{3}P_{kk}\delta_{ij}) - \hat{\gamma}q^2 S_{ij}$$

along with Rotta's slow term

$$\phi^2_{ij} = -C_1 b_{ij}\varepsilon_{kk}$$

$\hat{\alpha} = \frac{C_2+8}{11} - 0.015\frac{k^{3/2}}{\varepsilon y}, \hat{\beta} = \frac{8C_2-2}{11} + 0.015\frac{k^{3/2}}{\varepsilon y}, \hat{\gamma} = \frac{30C_2-2}{55}, C_2 = 0.4, C_1 = 1.5 - 0.125\frac{k^{3/2}}{\varepsilon y}$ (suggested by Launder, Reece, and Rodi). Substitution of this model into Rodi's algebraic form produces an equally poor prediction of the stress vector direction compared to the Naot-Shavit-Wolfshtein model (fig. 5.4). While D_{ij} by itself points in a directions somewhat closer to that of the stress vector, this combination of D_{ij} and P_{ij} points in a direction further away from the stress direction than do any of the individual constituents in the relationship.

Shih and Lumley (ref. 49) suggested a model form for the fast and slow parts of the pressure strain involving nonlinear combinations of stress and strain

$$\phi_{ij}^1 = -\hat{\alpha}(P_{ij} - \frac{1}{3}P_{kk}\delta_{ij}) - \hat{\beta}(D_{ij} - \frac{1}{3}P_{kk}\delta_{ij}) - \hat{\gamma}q^2 S_{ij} + \lambda b_{ij}P_{kk} - \zeta Q_{ij}$$

$$\phi_{ij}^2 = -C_1 b_{ij}\varepsilon_{kk}$$

where

$$\hat{\alpha} = \frac{2}{3}(\frac{4}{5} - \alpha_5), \hat{\beta} = -\frac{2}{3}(\frac{4}{5} + 8\alpha_5), \hat{\gamma} = -(\frac{2}{5} + 4\alpha_5), \lambda = \frac{3}{5}, \zeta = \frac{1}{5},$$

$$C_1 = 1 + \frac{1}{2}\hat{C}_f F, \alpha_5 = -[1 + 3.5(1 - \sqrt[4]{1-F})]/10, F = 1 + 9(II + III),$$

$$\hat{C}_f = \frac{1}{9}exp(-7.77/\sqrt{Re})[72/\sqrt{Re} + 80.1ln(1 + 62.4(-II + 2.3III)],$$

$$Re = (q^2)^2/(9\varepsilon\nu)$$

Substituting this model into Rodi's algebraic form yields a stress vector direction which is not much of an improvement over the simple Naot-Shavit-Wolfshtein model, also shown in figure 5.4.

Fu, Launder, and Tselepidakis (ref. 50) proposed a variation on the model of Shih and Lumley, given by

$$\phi_{ij}^1 = -\hat{\alpha}(P_{ij} - \frac{1}{3}P_{kk}\delta_{ij}) + \lambda b_{ij}P_{kk} - \zeta Q_{ij} - r[-8II(P_{ij} - D_{ij}) + 12b_{mi}b_{nj}(P_{mn} - D_{mn})]$$

$$\phi_{ij}^2 = -C_1 b_{ij}\varepsilon_{kk} + 32II\sqrt{F}(4.8)[b_{im}b_{mj} + \frac{2}{3}II\delta_{ij}]\varepsilon$$

where

$$\hat{\alpha} = \frac{3}{5}, F = 1 + 9(II + 3III)$$

$$\lambda = \frac{3}{5}, C_1 = 1 - 32II\sqrt{F}$$

$$\zeta = \frac{1}{5}$$

$$r = 0.7$$

Using this model in the algebraic stress formulation also shows no improvement in modeling the stress vector direction over the simple Naot-Shavit-Wolfshtein model, also shown in figure 5.4.

It is important to note that the pressure-strain deduced from the experiment does not even point in the direction of the stress vector. This implies that the evolution of the stress contains significant history effects that can not be accounted for in an equilibrium model.

Under adverse pressure gradient conditions, the model's predictive capability does not change (see figure 5.5 for case D.S1). All models shown perform similarly in pressure gradient as they do in zero pressure gradient. Also, the Launder-Reece-Rodi model appears to be the least desirable for modeling the pressure-strain term in the algebraic Reynolds stress model.

5.3 Pressure Strain Models

Nonequilibrium models such as the Reynolds-stress transport equation models (RSE) allow for a slow evolution of the modeled stresses in response to sudden changes in the mean flow strain, through the use of rate equations. This enables development of a difference between the stress and strain-rate directions with only minimal imbalances between the production and pressure strain. Indeed, to some extent, this lag effect is modeled successfully by the RSE models as was seen in the calculations of Driver-Hebbar (ref. 12); however, predictions of the lag were not as large as were seen experimentally. The source of the difficulties probably lies with the pressure strain model, since it is the largest of the modeled terms.

Terms in the Reynolds stress transport equation for $-\overline{uv}$ stress were calculated using the data for zero pressure gradient A.S0 (that has no spin) and are shown in figure 5.6. Production, convection (D-$\overline{uv}$/Dt), and diffusion are computed directly from the measurements, while pressure strain (minus dissipation) is deduced from the balance of the equation. For the purpose of the following discussion, the combination of pressure strain and dissipation ($\phi_{ij} - \varepsilon_{ij}$) will be grouped together and referred to as the pressure strain. As was noted in section 4.6.2, the production and pressure-strain terms are much larger than the convective term for which the equation is being solved. This puts a burden on the pressure-strain models to be extremely accurate.

The pressure strain models of Naot, Shavit, and Wolfshtein (ref. 48), Launder, Reece, and Rodi (ref. 41), Fu and Launder (ref. 50), and Shih and Lumley (ref. 49) were compared with the experimentally deduced pressure strain. The models for pressure strain (given in section 5.2) include the model dissipation ($\phi^1_{ij} + \phi^2_{ij} - \frac{2}{3}\delta_{ij}\varepsilon$) to be consistent with the experimentally deduced measure of pressure strain.

For the 2D zero pressure gradient case (fig. 5.6), there is not much difference between each of the models with the exception of the Shih-Lumley model which overpredicts the pressure strain. With the exception of the Shih-Lumley model, each of the models mimic rather closely the experimentally deduced pressure strain. Despite the appearance of a good agreement, the differences are large compared to the minute size of the convective term for which the equation is being solved. While uncertainty in the absolute size of the pressure strain term is large (on the order of 25%), the difference between the modeled and measured pressure strain is known more accurately (better than 10% of pressure strain).

Under adverse pressure gradient conditions (case D.S0), the pressure strain decays in the inner region, reflecting the loss in production (fig. 5.7). The rate of change of $-\overline{uv}$ stress (convective term) remains small with respect to the pressure strain term. The only region where convection is of any significance relative to the pressure strain term is in the outer layer, where entrainment is taking place. Here, the models begin

to deteriorate; each model underpredicts the pressure strain by as much as 20%, with the exception of the Shih-Lumley which continues to overpredict the pressure strain. The Launder-Reece-Rodi and Fu-Launder models do produce a slightly better agreement near the wall. The difference between the Shih-Lumley model and the other models is due primarily to the proposed model for the slow term. If the complicated function for $\hat{C}_f$ is replaced with a constant of 1.5 the Shih-Lumley model compares much better with the other models.

The situation changes little for the case with spin and pressure gradient (D.S1) (fig. 5.8). Each model tends to under-predict the magnitude of the pressure strain term, except the Shih-Lumley model which is closer to the data. An under-prediction of the pressure strain when added to the production rate would result in a net positive generation of $-\overline{uv}$ stress, which would then lead to creating more $-\overline{uv}$ stress (i.e., positive convective term). This is opposite to the trend observed experimentally in which the the $-\overline{uv}$ stress was seen to decay with distance into a 3D interaction zone.

The advantage of using a Reynolds-stress-equation type model is seen when one looks at the $\overline{vw}$ stress equation (fig. 5.9 for case D.S1). Here, the rate of change of $\overline{vw}$ stress (convective term) is large compared to the pressure strain and production term; a fact which gives more leeway to make mistakes in modeling the pressure strain without invalidating the solution. Underprediction of the stress by the models is a concern, but not as much of a concern as it was in the $-\overline{uv}$ equation. The Shih-Lumley model compares best with the data, however, if $\hat{C}_f$=1.5 is adopted, the model gives approximately the same underprediction of the pressure strain as do the other models.

The inaccuracies in the models for pressure strain may be balanced by other inaccuracies. The errors in the pressure strain models ultimately cause the flow solution to converge to a different equilibrium condition, which may be different only in terms of the allocation of energy to the individual normal stresses. The errors may not significantly effect the shear stress which is the term of greatest interest for this model. To evaluate the net effect of erroneous assumptions computations of the entire flow field must be done. These are given in chapter 6.

The Reynolds-stress transport equation models are generally regarded as the best physical model for generating anisotropy between the individual stresses. A measure of the anisotropy is embodied in the second and third invariants (II and III) of the anisotropy tensor. These quantities can be plotted against each other in the Lumley (ref. 51) triangle plot to evaluate the nature of the turbulence. For example the spinning case A.S1 with zero pressure gradient is shown in figure 5.10 for two profiles in the flow, x = −152 mm and x = +152 mm. Here the upstream profile follows the right-hand side of the triangle which represents axisymmetric expansion type flow (two of the principal stress components are nearly equal and the third much larger). Downstream, in the 3D interaction zone the data tend to move more toward the left-hand side of the triangle which represents axisymmetric contraction (i.e., two of the principal stress components are nearly equal to each other and the third is much smaller).

Under adverse pressure gradient conditions, case D.S1 with spin, the shift from the right-hand side of the triangle to the left-hand side is more dramatic (fig. 5.11). Data appearing closer to the left-hand corner of the triangle indicate that turbulent vortex elements in the flow are becoming more aligned in a particular direction. Interestingly, computations which solve the boundary layer equations using the Launder-Reece-Rodi model produce an anisotropy which is virtually identical in character everywhere in this flow; see figure 5.12 for the solution to case D.S1. The Reynolds stress transport equation model develops the same

anisotropy independent of distance from the wall, conditions of pressure gradient, or transverse strain. This paradox implies that this model is no better than the model that assumes that the principal stresses in the flow follow a 4:2:3 relationship. The failure to generate different degrees of anisotropy is disturbing, since the motivation for solving the full Reynolds stress transport equations was used to obtain improved predictions of anisotropy.

5.4 Structure Parameter Sensitivity To Three-Dimensional Flow

The structure parameter ($(\tau/\rho)/q^2$) is assumed to be equal to a constant, 0.15, in the $k-\varepsilon$ model as well as many other turbulence models. However, the various 3D mean flow experiments produce $(\tau/\rho)/q^2$ values which differ from 0.15 in a seemingly random way (fig. 5.13). For example Pontikos and Bradshaw (ref. 8) saw a 50% lower level of $(\tau/\rho)/q^2$ in a flow with only 7° of free-stream flow turning angle, while Muller (ref. 14) saw less than a 20% reduction in a flow which undergoes 17° of flow turning angle. Anderson and Eaton (ref. 10) saw 70% lower levels $(\tau/\rho)/q^2$ than the usual 0.15, in a flow with 22° of free-stream flow turning. The zero pressure gradient spinning cylinder case of this study has an effective free-stream flow turning of 45° and only a 30% lower level of $(\tau/\rho)/q^2$. Determination of the causes of the different magnitudes of decay in the stresses is critical to creating turbulence models for this effect.

To further complicate matters, the level of $(\tau/\rho)/q^2$ appears to vary through the 3D boundary layer (fig. 5.13). Generally speaking, the lowest levels of $(\tau/\rho)/q^2$ are seen near the wall (in the vicinity of $y = 0.1\delta$) while somewhat higher levels are seen away from the wall. It might be argued that the reduction in stress originates locally near the wall, and with time (or distance downstream) diffuses outward in a boundary-layer-type growth. The degree to which the reduced level of stress propagates outward (via diffusion) seems to vary from one experiment to another. For example, Pontikos-Bradshaw and Elsenaar-Boelsma indicate reduced levels of $(\tau/\rho)/q^2$ in the outer portion of the boundary layer while Johnston's forward-facing swept-step experiment (ref. 4) and the spinning cylinder experiment show high levels of $(\tau/\rho)/q^2$ in the outer region. The varying levels might be a result of the relatively long distance traveled by the flow in the Pontikos-Bradshaw and Elsenaar-Boelsma experiments ($X \approx 30\delta$), relative to that of Johnston's and the current experiment (referred to as Driver-Johnston, in which the flow travels $x < 10\delta$). If the flow travels a longer distance through the 3D interaction zone, a greater degree of diffusion is permitted outward from the wall. After reviewing several experiments, it is our belief that the Reynolds stress initially drops near the wall ($y/\delta \approx 0.1$) leaving the outer regions of the boundary layer to be reduced as a result of subsequent outward diffusion.

The extent to which the 3D effects have diffused outward into the flow can be estimated by locating the y-position in the boundary layer below which the $(\tau/\rho)/q^2$ quantity deviates from the upstream 2D levels referred to as δ_{3D}. This location can be plotted as a function of distance downstream into the 3D interaction (fig. 5.14). It appears that the thickness of the 3D interaction δ_{3D} increases with distance downstream in roughly a $1 - exp(-x/10\delta_o)$ type of growth. One should not read too much into this plot, since no attempt was made to sort out the separate effects of pressure gradient, rate of turning, or what ever else might affect structure parameter.

It seems likely that the extent of decrease in $(\tau/\rho)/q^2$ is associated with the degree of three-dimensionality. One parameter that is characteristic of the magnitude of the three-dimensionality is $|W_c/Q_\delta|$, the ratio of cross-stream velocity to free-stream velocity. The lowest level of $(\tau/\rho)/q^2$ in the vicinity of

$y/\delta = 0.1$ was plotted against $|W_c/Q_\delta|$ for each of the available experiments (fig. 5.15). With the exception of the Muller and Terrell-Bradshaw experiments, there appears to be a fairly high degree of correlation between $(\tau/\rho)/q^2$ and $|W_c/Q_\delta|$. Each experiment roughly follows a $(\tau/\rho)/q^2 = 0.15e^{-C_w|W_c/Q_\delta|}$-type behavior, where $C_w = 2.4$. Note that this correlation holds for the flows examined where W_c decreases with distance downstream as well as for flows where it increases in the streamwise direction.

Abid (ref. 37) proposed using the ratio of crossflow to streamwise displacement thickness, δ_c^*/δ_s^*, to characterize the crossflow. This parameter is plotted against $(\tau/\rho)/q^2|_{y/\delta\approx 0.1}$ (fig. 5.16). He proposed diminishing the Reynolds shear stress by $1 - \delta_c^*/\delta_s^*$ so that

$$(\tau/\rho)_{3D} = (\tau/\rho)_{2D} MAX(1 - |\delta_c^*/\delta_s^*|, |\delta_c^*/\delta_s^*|)$$

This relationship, when applied to the structure parameter, correlates reasonably well with the data up to the point where $|\delta_c^*/\delta_s^*| < 0.5$; however, for $|\delta_c^*/\delta_s^*| > 0.5$ the agreement worsens (fig. 5.16). A model of the form $(\tau/\rho)_{3D} = (\tau/\rho)_{2D} e^{-C_{w_2}|\delta_c^*/\delta_s^*|}$ appears to fit better (where $C_{w_2} = 1.2$).

The flow skew angle $|\beta_w - \beta_\delta|$ also correlates reasonably well with $((\tau/\rho)/q^2)_{y\approx 0.1\delta}$ (fig. 5.17). Curve $(\tau/\rho)_{3D} = (\tau/\rho)_{2D} e^{-C_{w_3}|\beta_w - \beta_\delta|}$ is also shown (with $C_{w_3} = 0.017$). All three of these parameters $|W_c/Q_\delta|$, δ_c^*/δ_s^*, and $|\beta_w - \beta_\delta|$ are measures of the magnitude of the transverse flow velocity.

Physically, $|W_c/Q_\delta|$ describes the magnitude of the streamwise vorticity relative to the spanwise vorticity. The good correlation between the drop in $(\tau/\rho)/q^2|_{y\approx 0.1\delta}$ and the magnitude of the transverse flow indicates that streamwise mean vorticity is somehow interfering with the turbulence processes. One might think that streamwise vorticity would be a better parameter to use, however, streamwise vorticity varies with location in the boundary layer (even changes sign) and is zero at the point of maximum crossflow where the effective drop in stress is the largest.

The rate of boundary layer turning (i.e., flow curvature) might also affect the reduction of Reynolds stress, the transverse flow forces could conceivably affect the shear stresses. Nevertheless, the decrease in $(\tau/\rho)/q^2|_{y\approx 0.1\delta}$ with the magnitude of the free-stream turning rate appears not to exhibit any particular correlation (fig. 5.18).

It appears that the magnitude of the crossflow velocity correlates best with the magnitude of $(\tau/\rho)/q^2|_{y\approx 0.1\delta}$. This is unfortunate, since any relationship involving crossflow velocity explicitly is not Galilean invariant. Models of crossflow velocity can be altered by a uniform translation of the axes system because the models lack coordinate system independence. The lack of this independence makes it impossible to create a turbulence model which is truly general and applicable under a variety of different coordinate systems. However, the proposed correlation,

$$(\tau/\rho)/q^2|_{y\approx 0.1\delta} = 0.15e^{-C_w|W_c/Q_\delta|}$$

(with $C_w = 2.4$) does roughly fit a wide variety of 3D flows. Further assumptions about the shape of the distribution of $(\tau/\rho)/q^2$ through the boundary layer are necessary, such as assuming that $(\tau/\rho)/q^2$ equals $(\tau/\rho)/q^2|_{y=0.1\delta}$ everywhere in the boundary layer. This assumption may not hurt the overall calculations, since models of the outer regions of the flow tend to be less critical to the accurate solution of turbulent boundary layer problems.

5.5 Mixing Length Sensitivity To Three-Dimensional Flow

The Reynolds stress when normalized by the mean flow strain-rate yields a quantity referred to as the mixing length. Mixing length distributions for 2D zero pressure gradient flows were found by Prandtl to increase with distance from the wall at a rate of κy ($\kappa = 0.41$). Beyond 0.22δ, the mixing length was seen to be a constant at a value of 0.09δ. Experimental estimates of mixing length for 3D flows, are also seen to grow as κy in a region very near the wall (fig. 5.19); however, beyond y of 0.05δ the mixing lengths are considerably lower than for that of a 2D flow. This is in contrast to the finding that $(\tau/\rho)/q^2$ was primarily affected in the inner region of the flow. The implication is that the near-wall Reynolds stress adjusts rapidly to the new strain field while kinetic energy does not, and away from the wall, both Reynolds stress and kinetic energy adjust slowly to the new strain field. The data from the spinning cylinder study exhibit larger mixing lengths in the outer region due to the destabilizing effect of transverse surface curvature; however, downstream (in the 3D interaction zone) they are lower relative to upstream levels. The fact that the mixing length formulation fits reasonably well in the inner region of the flow helps to explain why historically the mixing length models have found some acceptance for predicting attached 3D flows. One possible reason for the lower mixing length in the outer region is the lag phenomenon—as the mean flow strain rate increases with increasing crossflow the turbulence initially fails to generate additional Reynolds stress, resulting in a lower value for $\sqrt{\tau/\rho/(\frac{\partial U}{\partial y}^2 + \frac{\partial W}{\partial y}^2)}$ (i.e., mixing length).

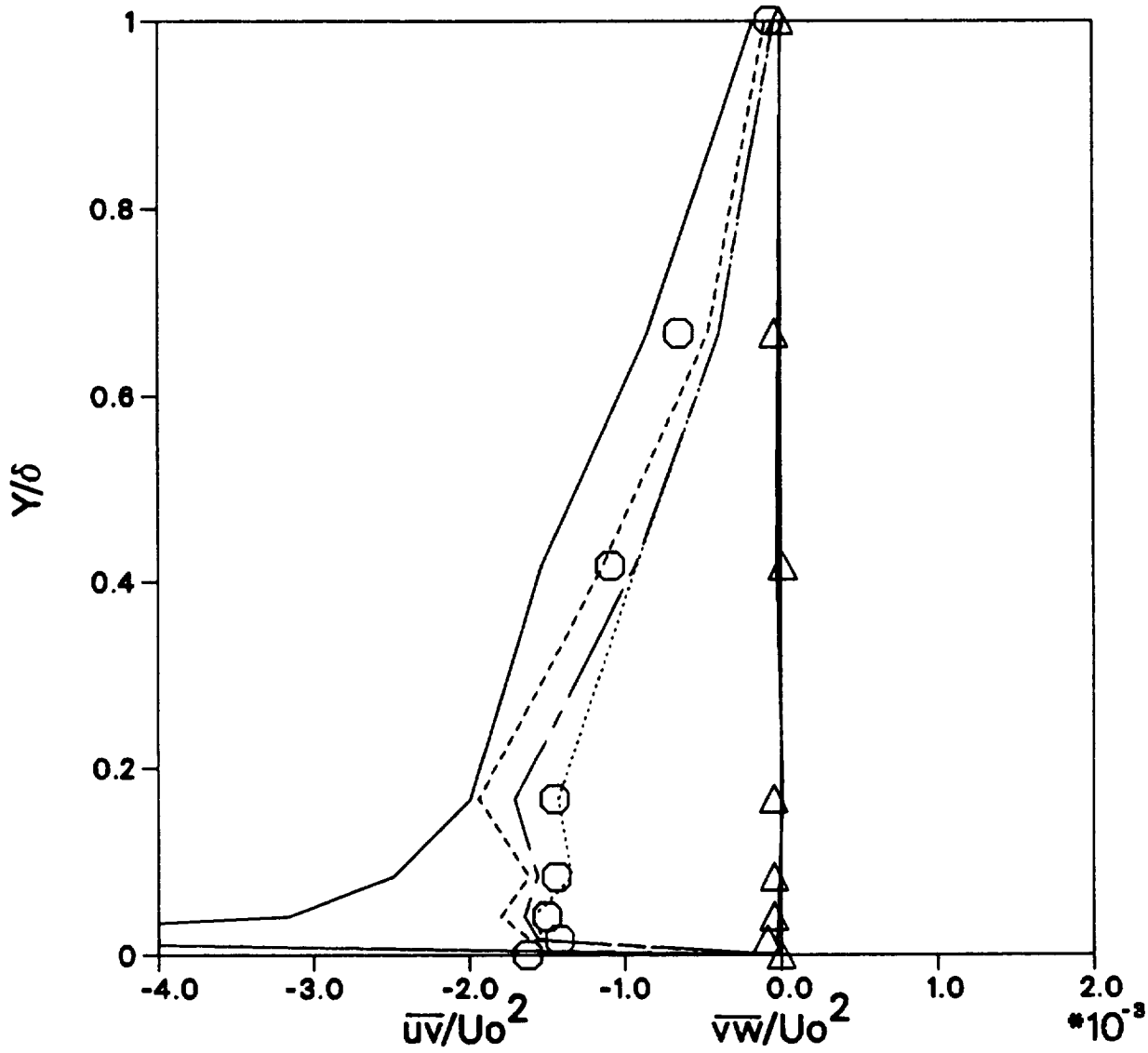

Figure 5.1 $\overline{uv}$ & $\overline{vw}$ stress models compared with data for case D.S0 at X=−152mm. ○ $\overline{uv}$ & △ $\overline{vw}$ measurements, - - - Prandtl w/curvature, – – – Johnson-King Model, —— Jones-Launder $\nu_t = 0.09k^2/\varepsilon$, ... Cebici-Smith model.

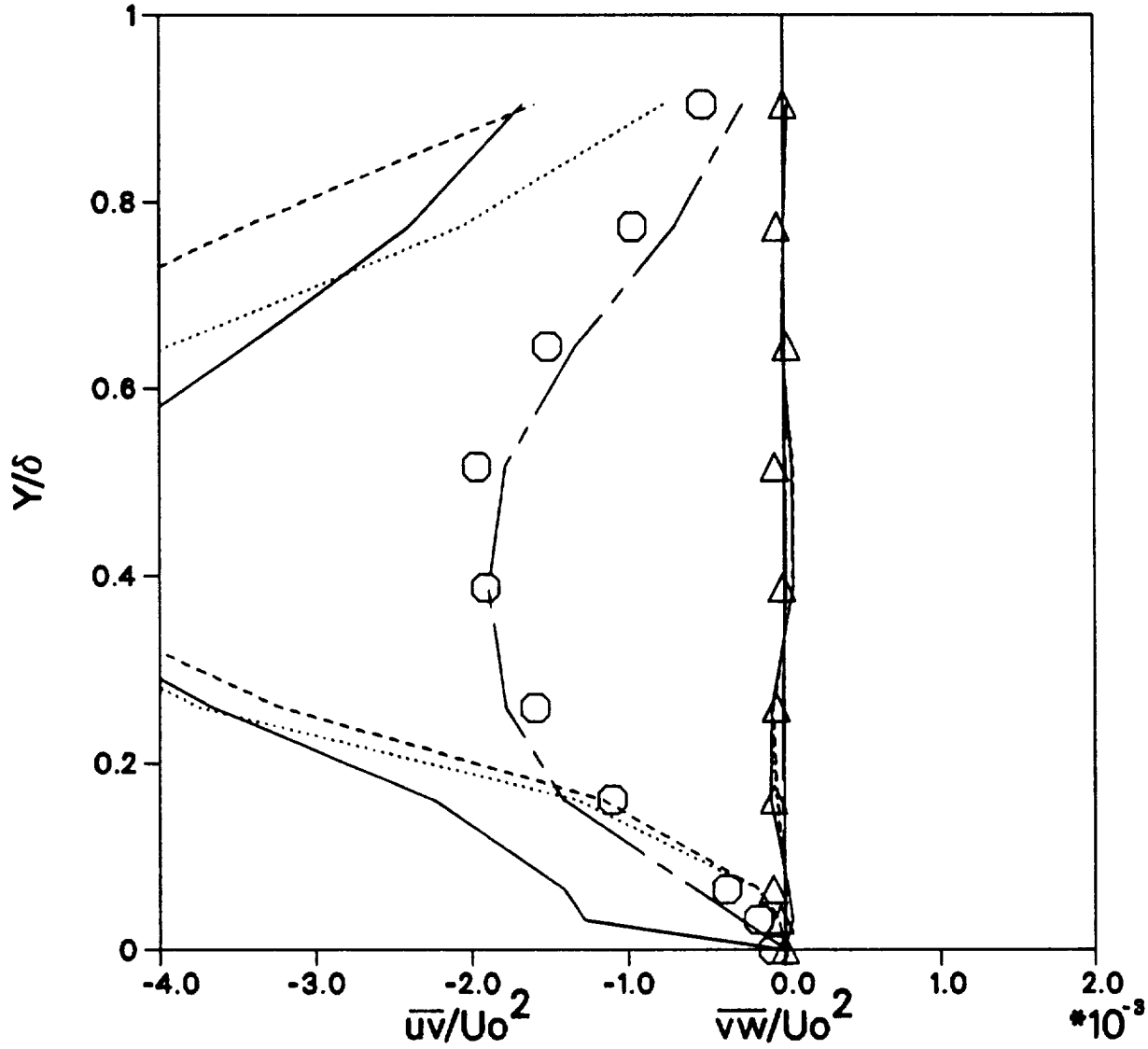

Figure 5.2 $\overline{uv}$ & $\overline{vw}$ stress models compared with data for case D.S0 at X=+225mm. ○ $\overline{uv}$ & △ $\overline{vw}$ measurements, - - - Prandtl w/curvature, – – – Johnson-King Model, —— Jones-Launder $\nu_t = 0.09k^2/\varepsilon$, ... Cebeci-Smith model.

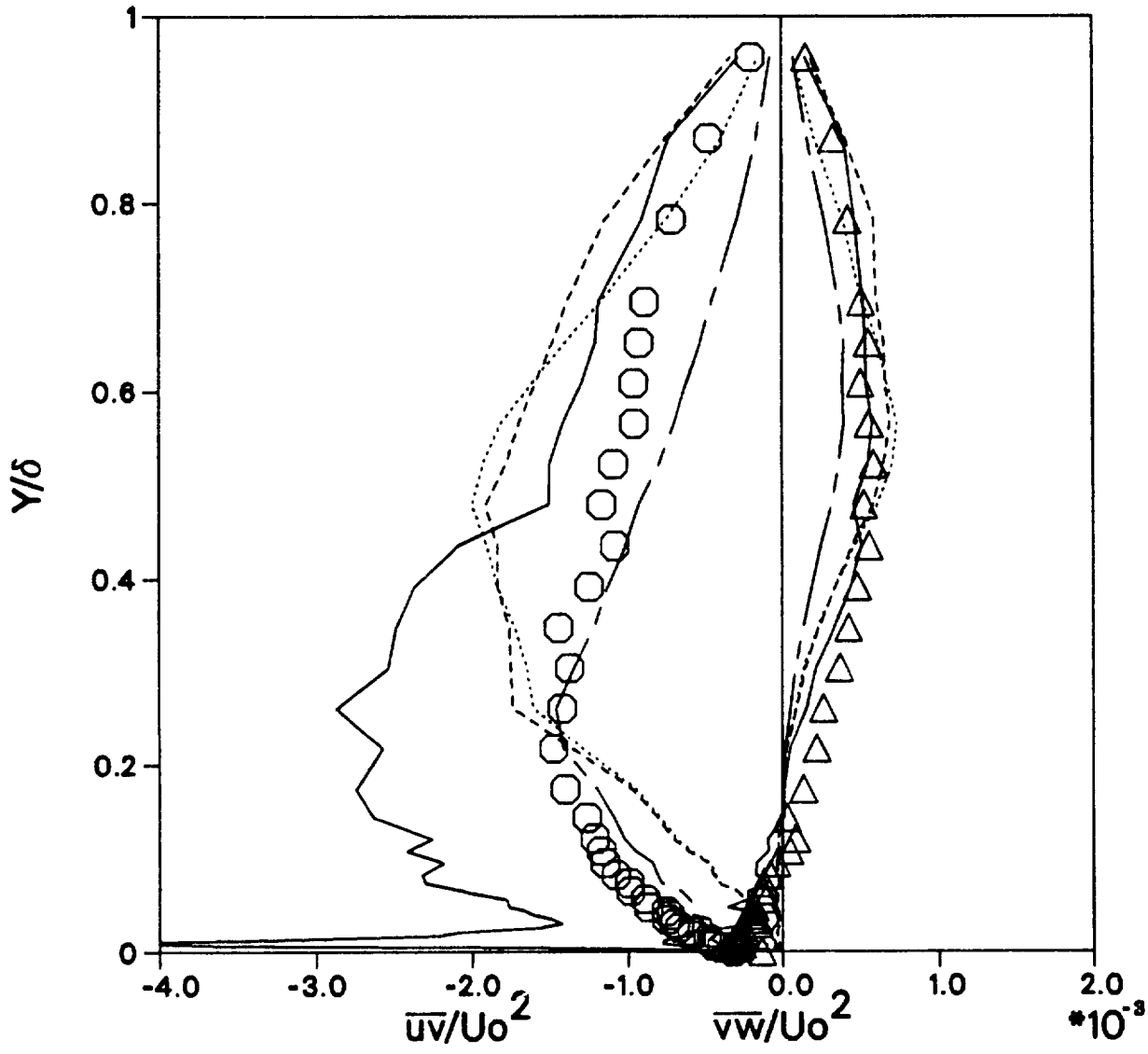

Figure 5.3 $\overline{uv}$ & $\overline{vw}$ stress models compared with data for case D.S1 at X=+304mm. ○ $\overline{uv}$ & △ $\overline{vw}$ measurements, - - - Prandtl w/curvature, – – – Johnson-King Model, —— Jones-Launder $\nu_t = 0.09k^2/\varepsilon$, ... Cebeci-Smith model.

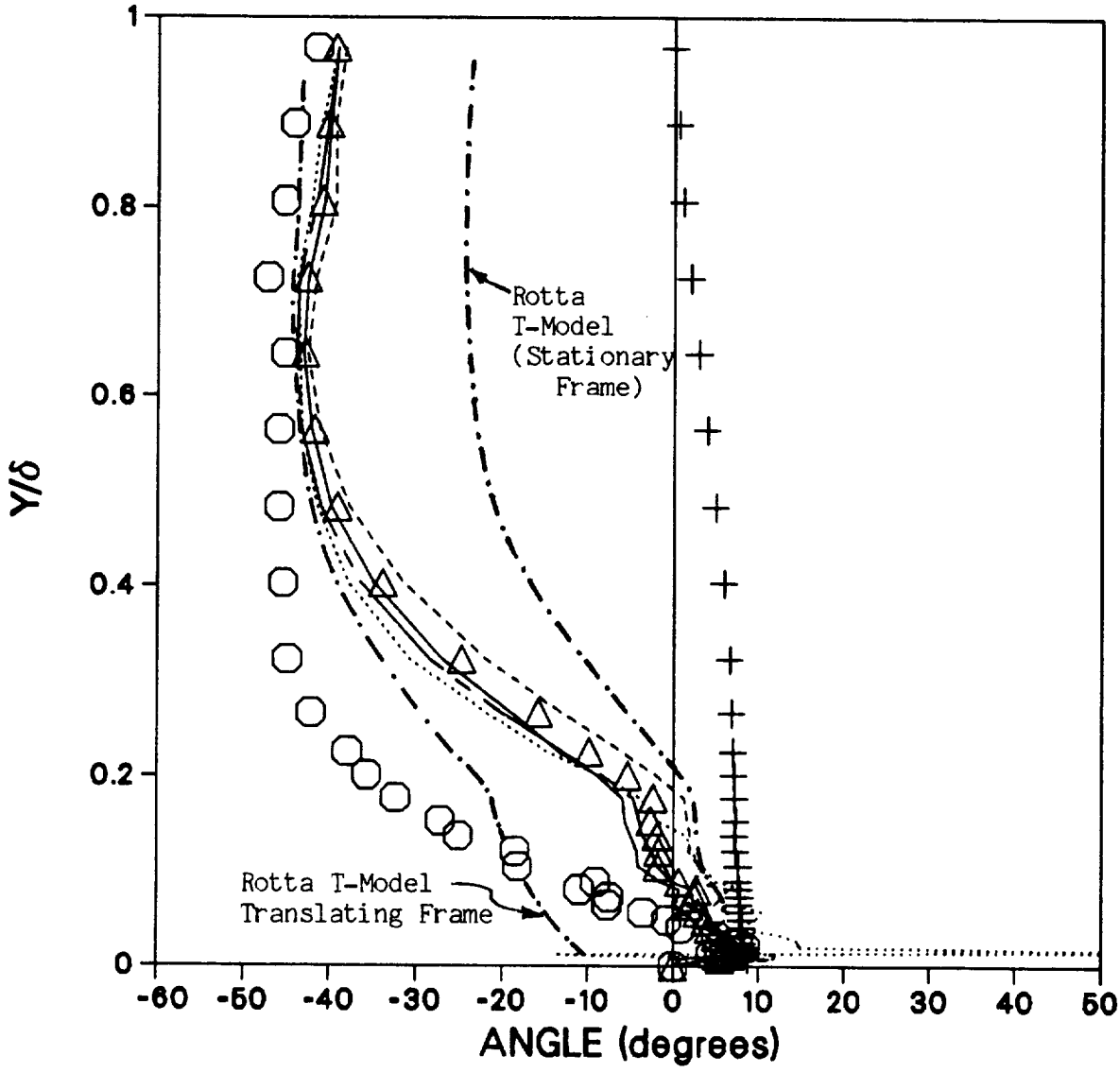

Figure 5.4 Measured stress direction compared to modeled stress direction for case A.S1 at X=152mm. △ $\mathrm{Tan}^{-1}((\partial W/\partial r - W/r)/\partial U/\partial r)$, ○ $\mathrm{Tan}^{-1}\frac{-\overline{vw}}{-\overline{uv}}$, + Flow angle $\mathrm{Tan}^{-1}(W/U)$; ..... Rotta T-model for $\mathrm{Tan}^{-1}(\frac{-\overline{vw}}{-\overline{uv}})$, algebraic stress models for $\mathrm{Tan}^{-1}(\frac{-\overline{vw}}{-\overline{uv}})$ using pressure-strain model of —— Rodi-NWS, - - - LRR, ... Fu-Launder, – – – Shih-Lumley.

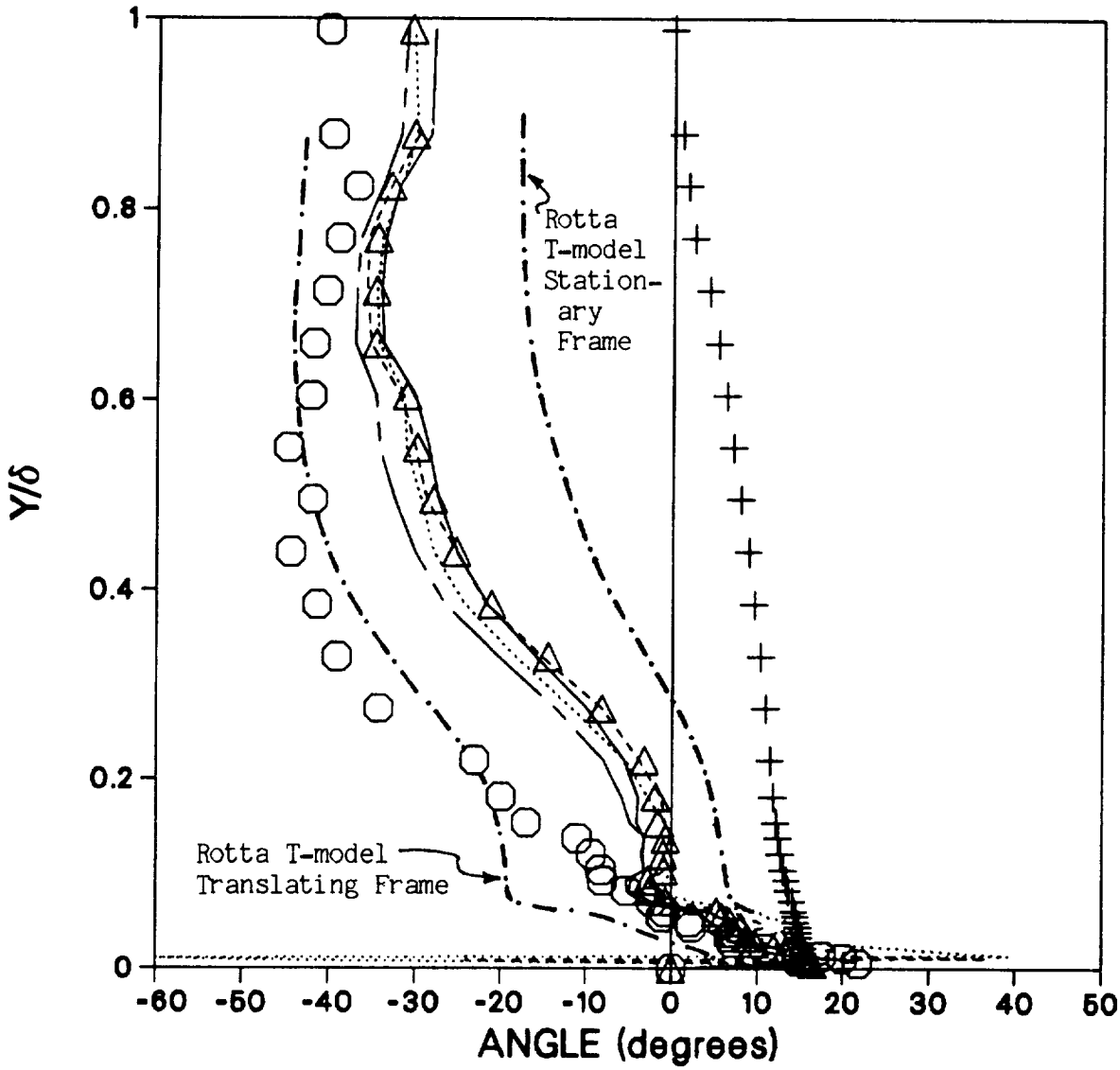

Figure 5.5 Measured stress direction compared to modeled stress direction for case D.S1 at X=152mm. △ $\mathrm{Tan}^{-1}((\partial W/\partial r - W/r)/\partial U/\partial r)$, ○ $\mathrm{Tan}^{-1}\frac{-\overline{vw}}{-\overline{uv}}$, + Flow angle $\mathrm{Tan}^{-1}(W/U)$; ..... Rotta T-model for $\mathrm{Tan}^{-1}(\frac{-\overline{vw}}{-\overline{uv}})$, algebraic stress models for $\mathrm{Tan}^{-1}(\frac{-\overline{vw}}{-\overline{uv}})$ using pressure-strain model of —— Rodi-NWS, - - - LRR, ... Fu-Launder, - - - Shih-Lumley.

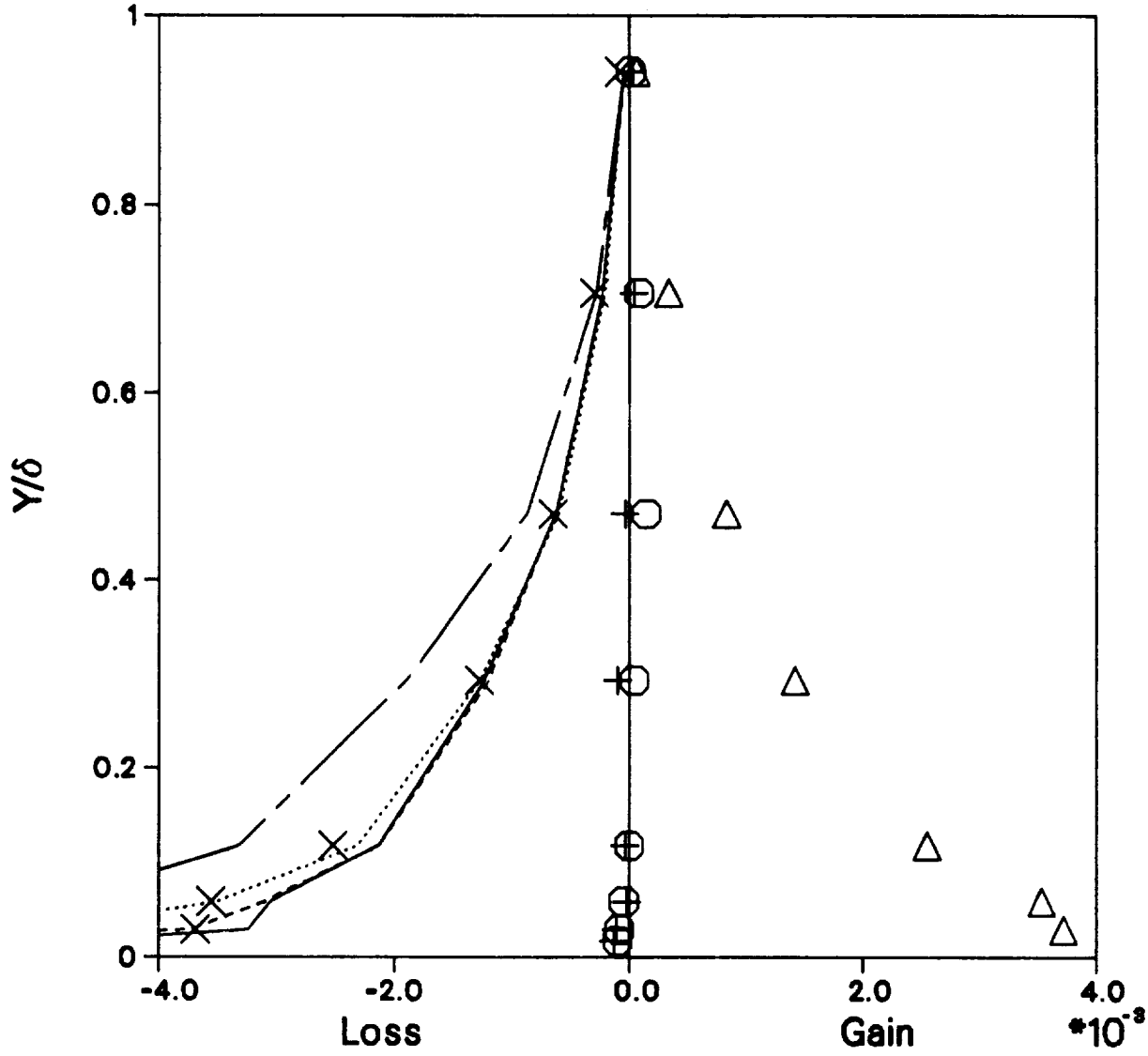

Figure 5.6 $-\overline{uv}$ stress Equation balance compared with models for case D.S0 at X=12mm, ○ (D-$\overline{uv}$/Dt) δ_o/U_r^3, △ (Production$_{-uv}$) δ_o/U_r^3, + (Diffusion$_{-uv}$) δ_o/U_r^3, × (Pressure-Strain - Dissipation$_{-uv}$) δ_o/U_r^3; Pressure strain models, —— NWS, - - -LRR, ...Fu-Launder, – - – Shih-Lumley.

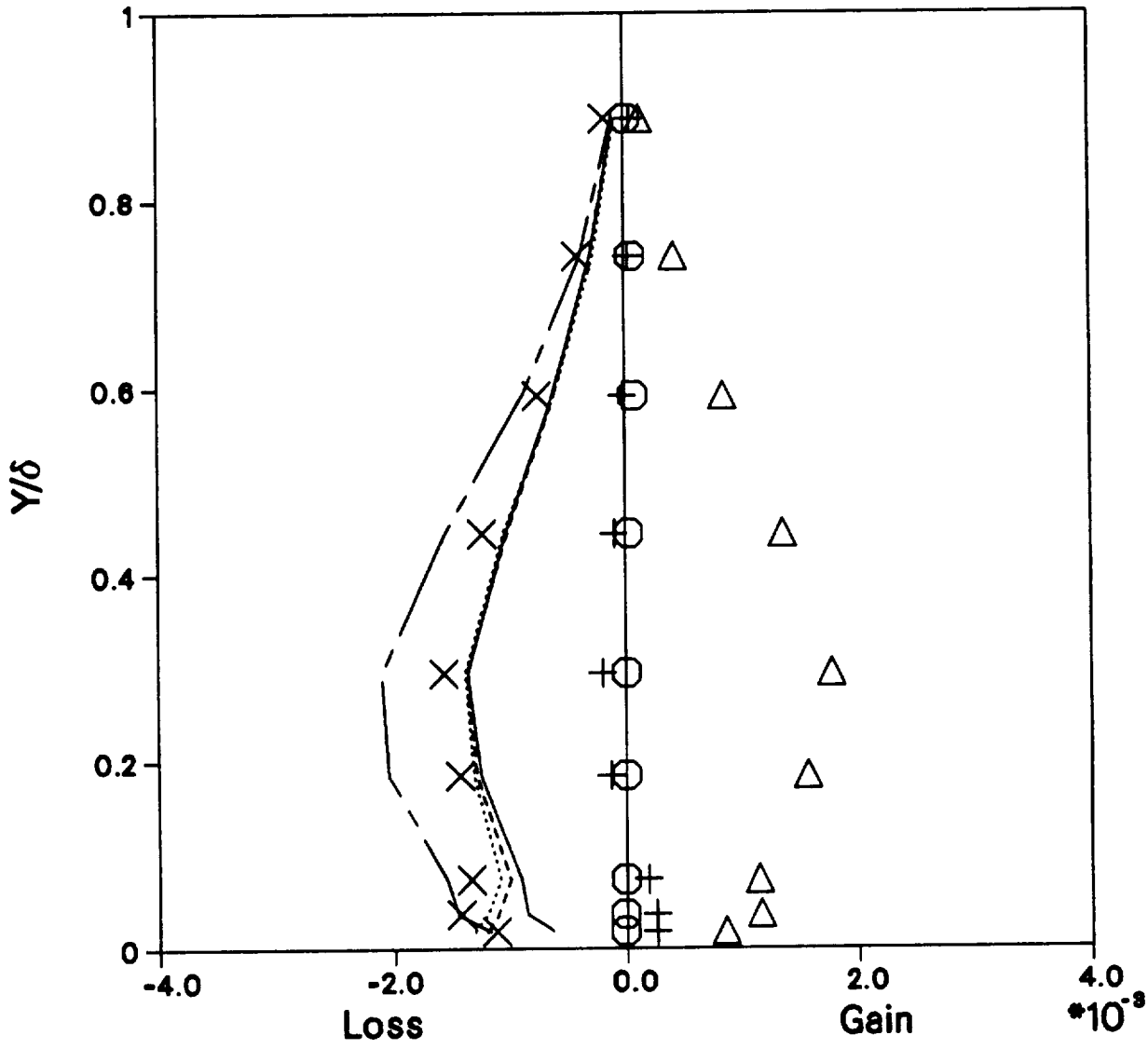

Figure 5.7 $-\overline{uv}$ stress Equation balance compared with models for case D.S0 at X=152mm, ○ (D-$\overline{uv}$/Dt) δ_o/U_r^3, △ (Production$_{-uv}$) δ_o/U_r^3, + (Diffusion$_{-uv}$) δ_o/U_r^3, × (Pressure-Strain - Dissipation$_{-uv}$) δ_o/U_r^3; Pressure strain models, —— NWS, - - -LRR, ...Fu-Launder, – - – Shih-Lumley.

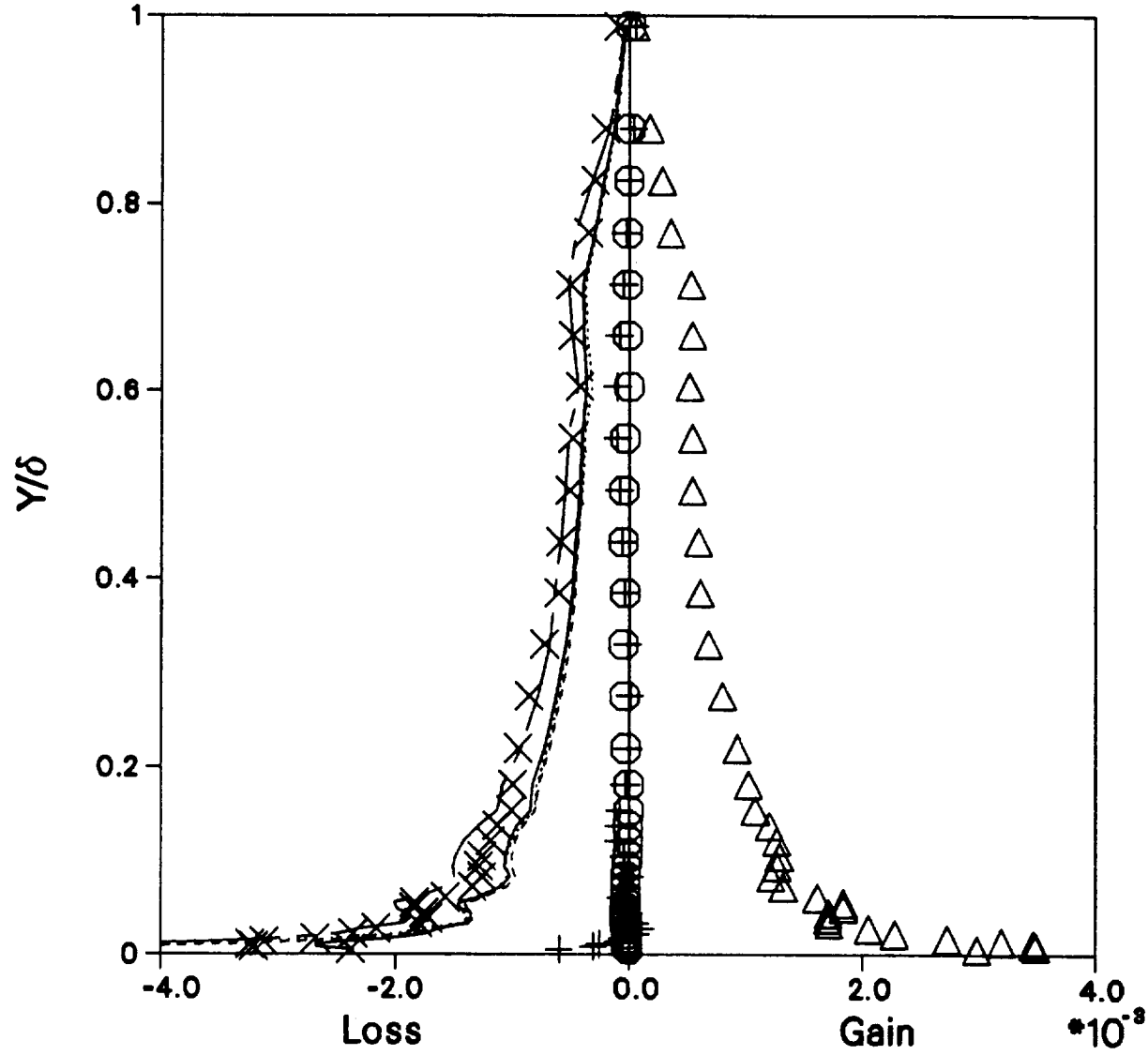

Figure 5.8 $-\overline{uv}$ stress Equation balance compared with models for case D.S1 at X=152mm, ○ (D-$\overline{uv}$/Dt) δ_o/U_r^3, △ (Production$_{-uv}$) δ_o/U_r^3, + (Diffusion$_{-uv}$) δ_o/U_r^3, × (Pressure-Strain - Dissipation$_{-uv}$) δ_o/U_r^3; Pressure strain models, —— NWS, - - -LRR, ...Fu-Launder, – – – Shih-Lumley.

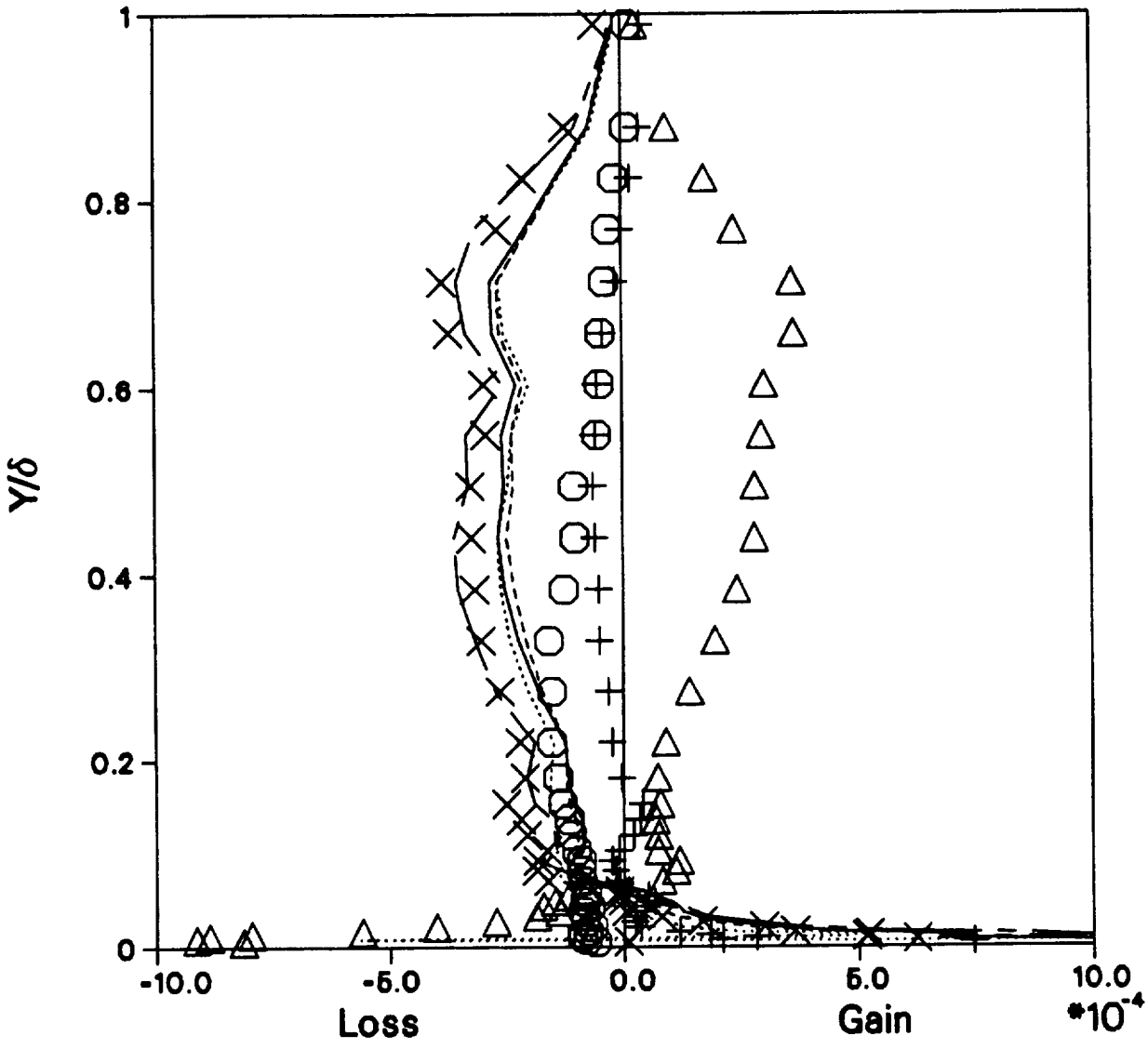

Figure 5.9 $\overline{vw}$ stress Equation balance compared with models for case D.S1 at X=152mm, ○ (D$\overline{vw}$/Dt) δ_o/U_r^3, △ (Production$_{vw}$) δ_o/U_r^3, + (Diffusion$_{vw}$) δ_o/U_r^3, × (Pressure-Strain - Dissipation$_{vw}$) δ_o/U_r^3; Pressure strain models, —— NWS, - - -LRR, ...Fu-Launder, – – – Shih-Lumley.

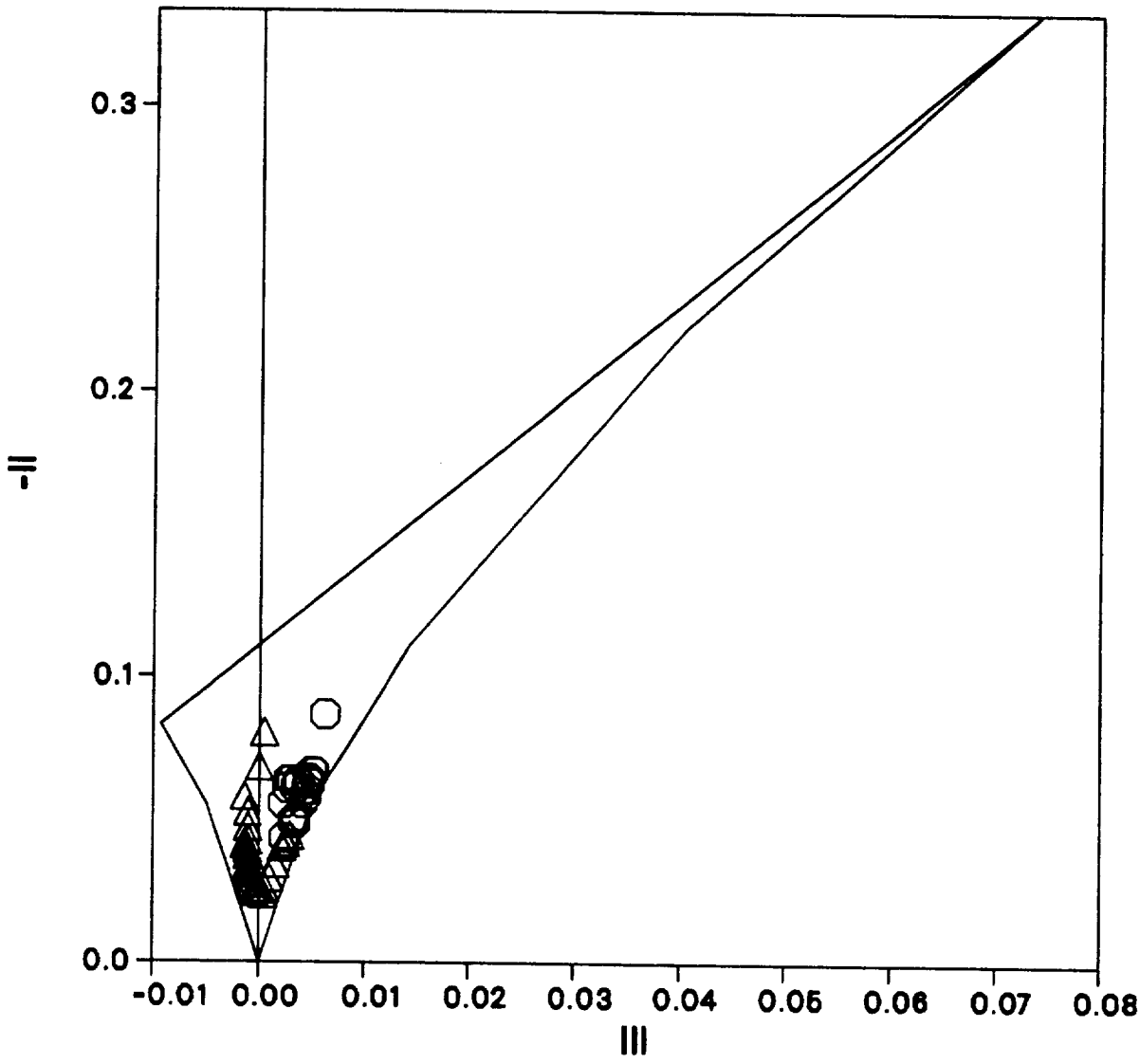

Figure 5.10 Anisotropy map for measurements of case A.S1 at ○ x=−152mm and △ x=+152mm.

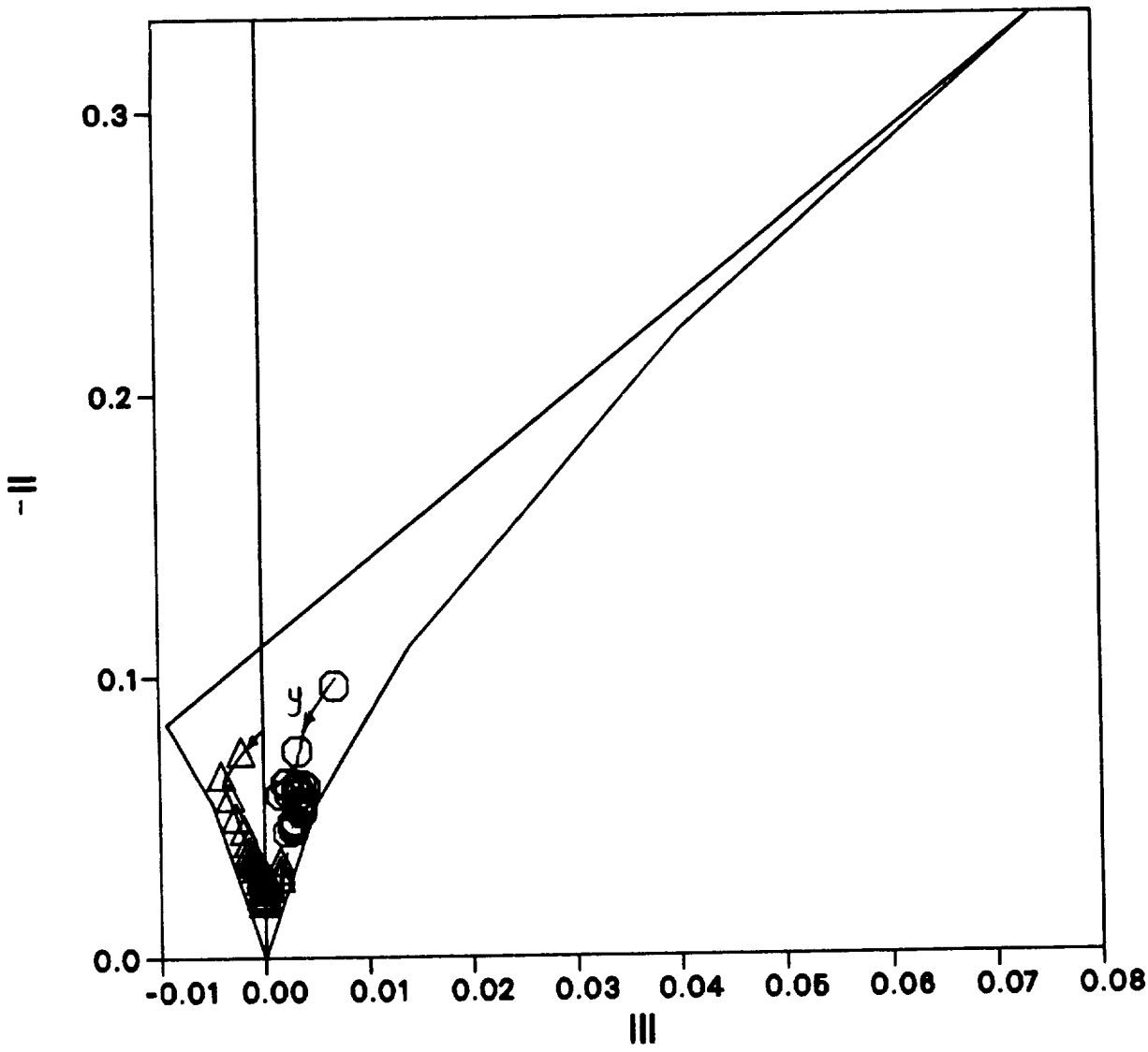

Figure 5.11 Anisotropy map for measurements of case D.S1 at ◯ x=−152mm and △ x=+152mm.

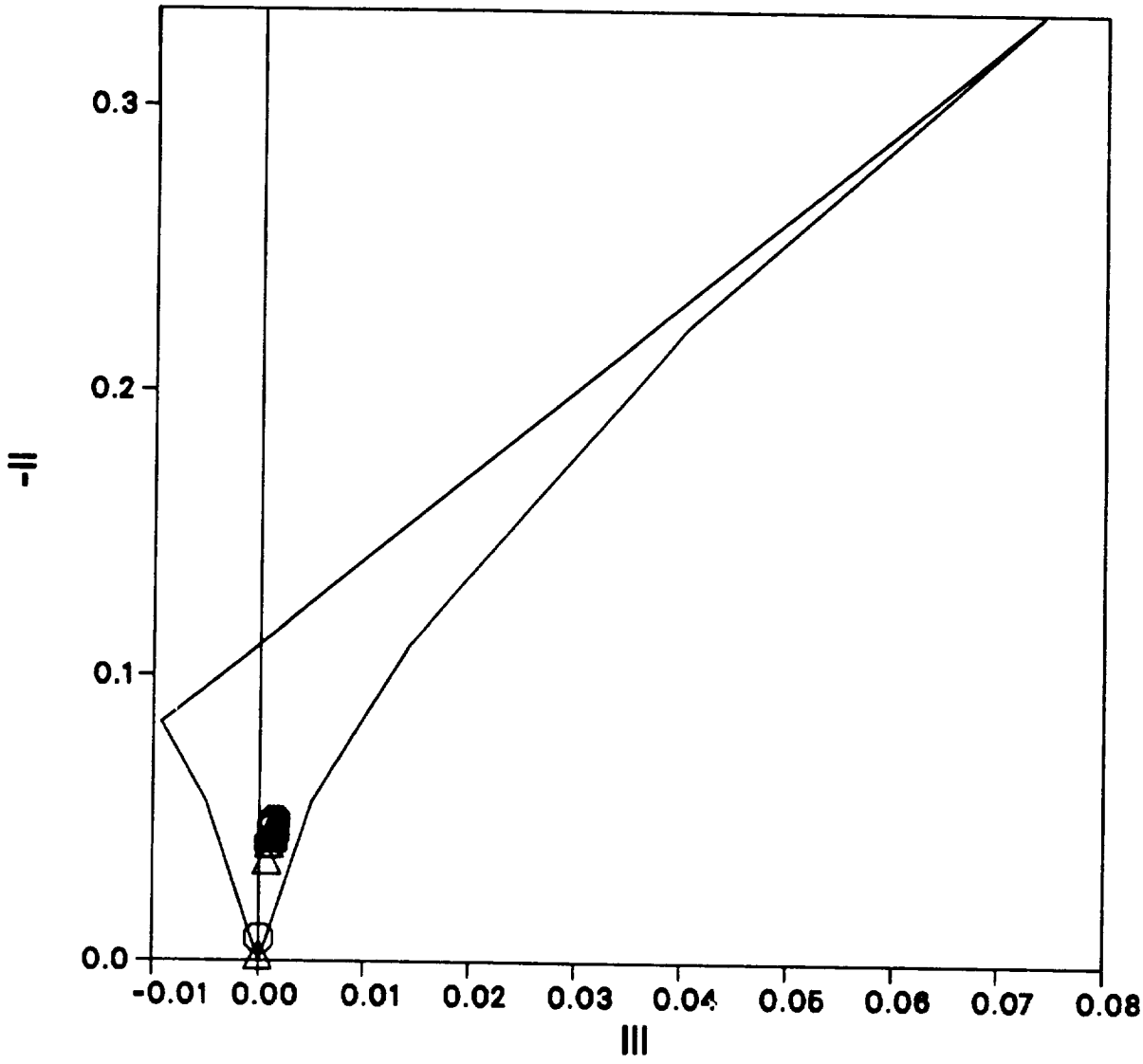

Figure 5.12 Anisotropy map for LRR model computations of case D.S1 at ○ x=−152mm and △ x=+152mm.

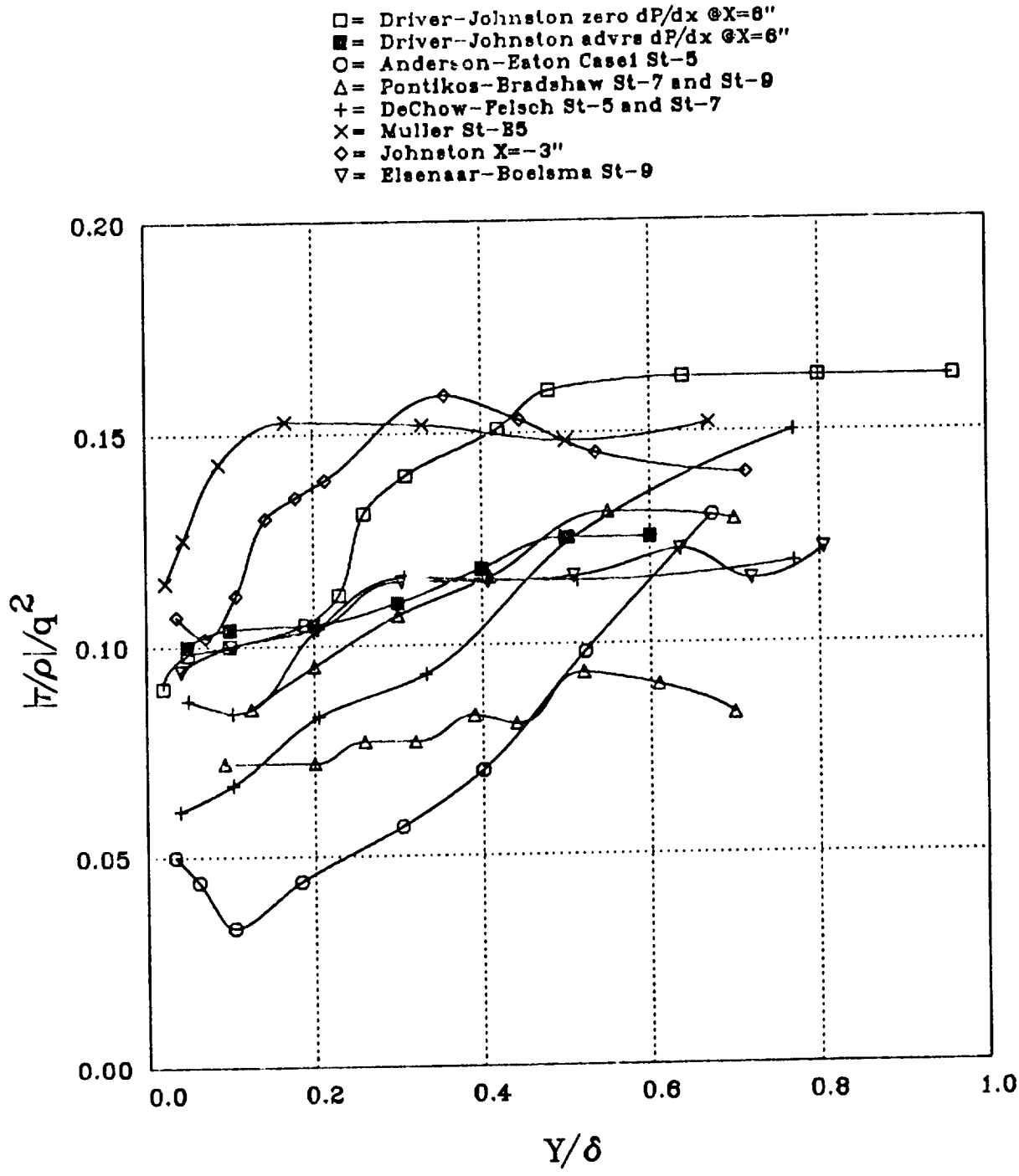

Figure 5.13 Structure parameter profiles for various experiments.

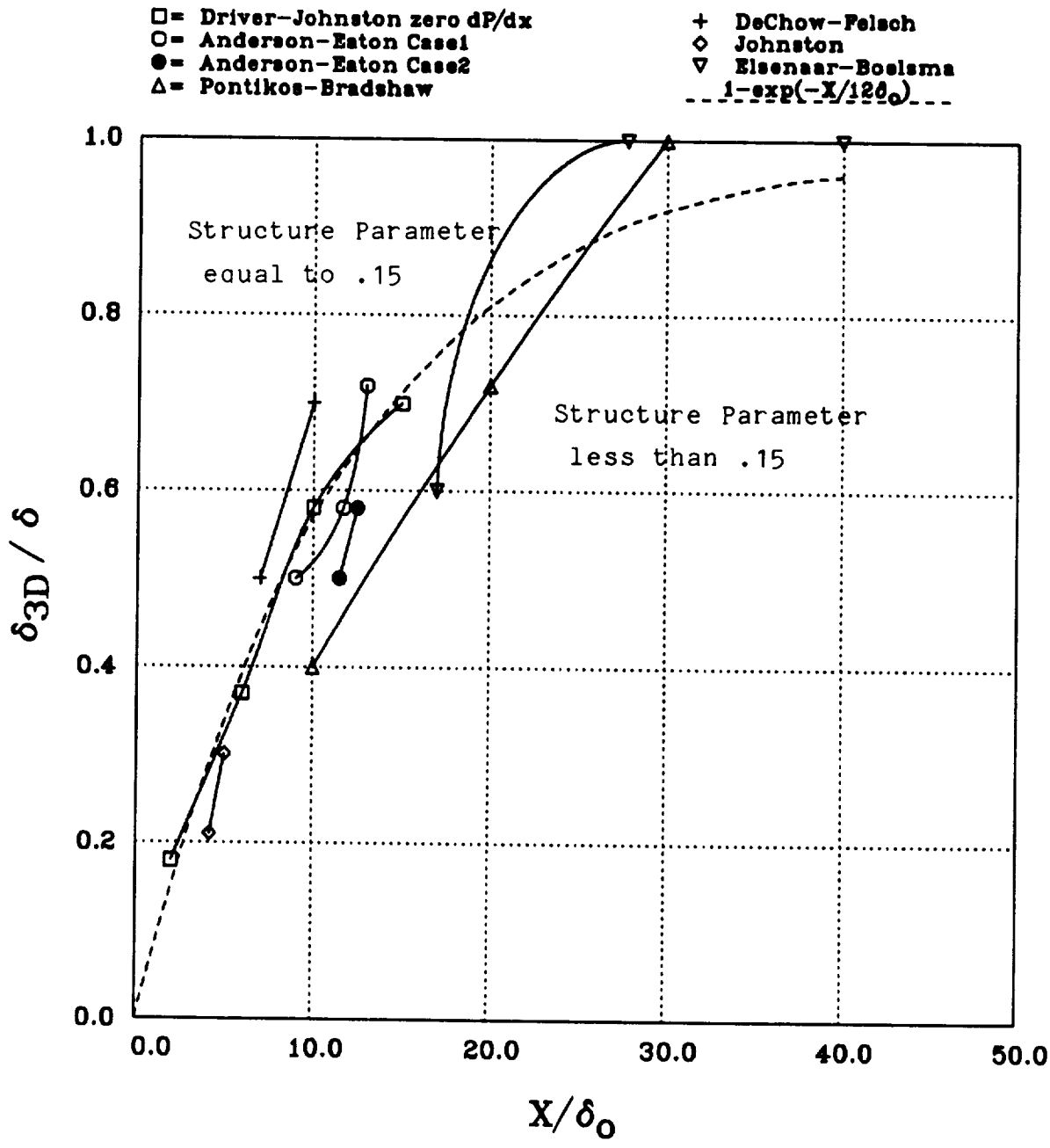

Figure 5.14 Domain of sub-normal structure parameter for various experiments.

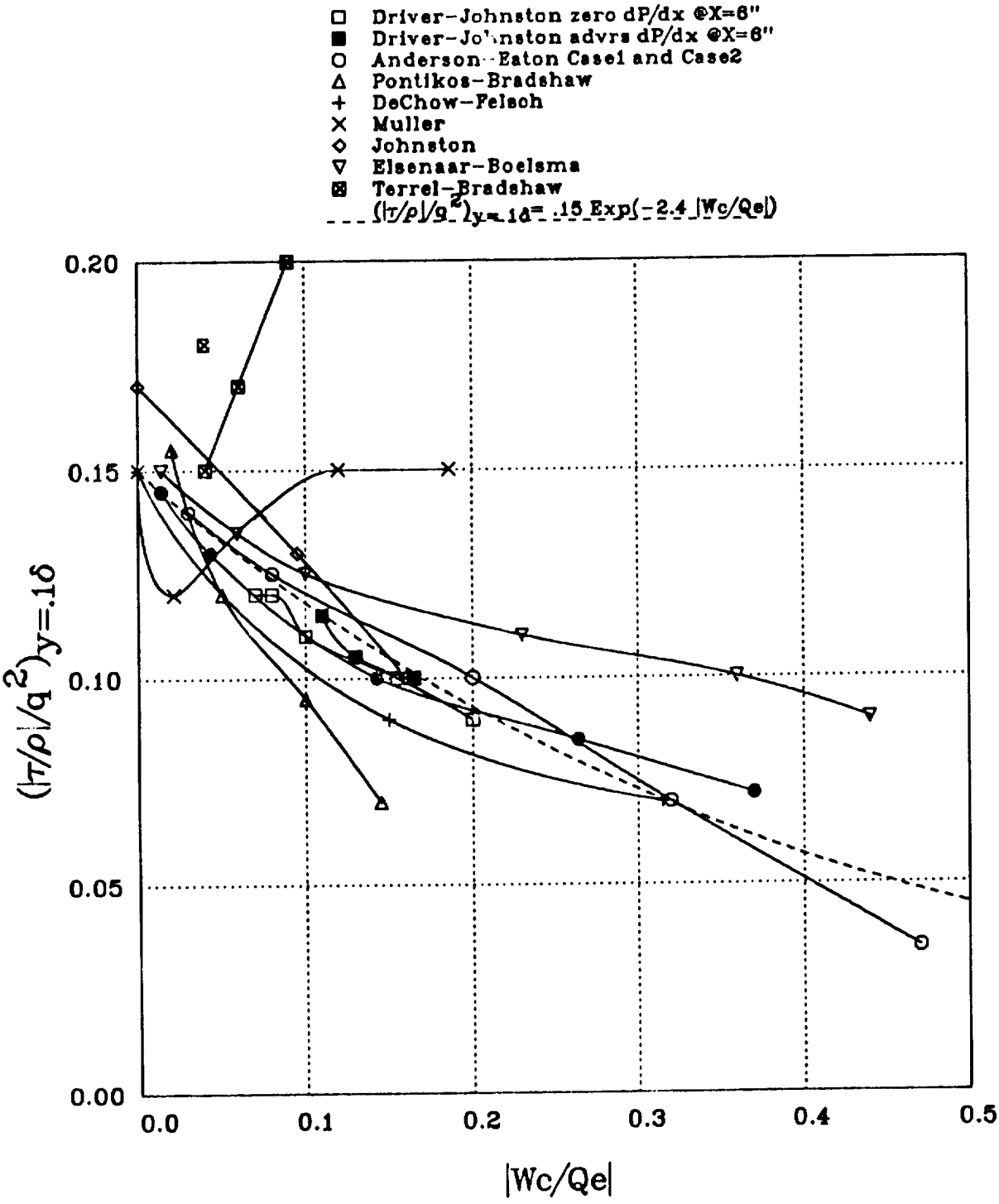

Figure 5.15 Structure parameter verses peak transverse flow velocity.

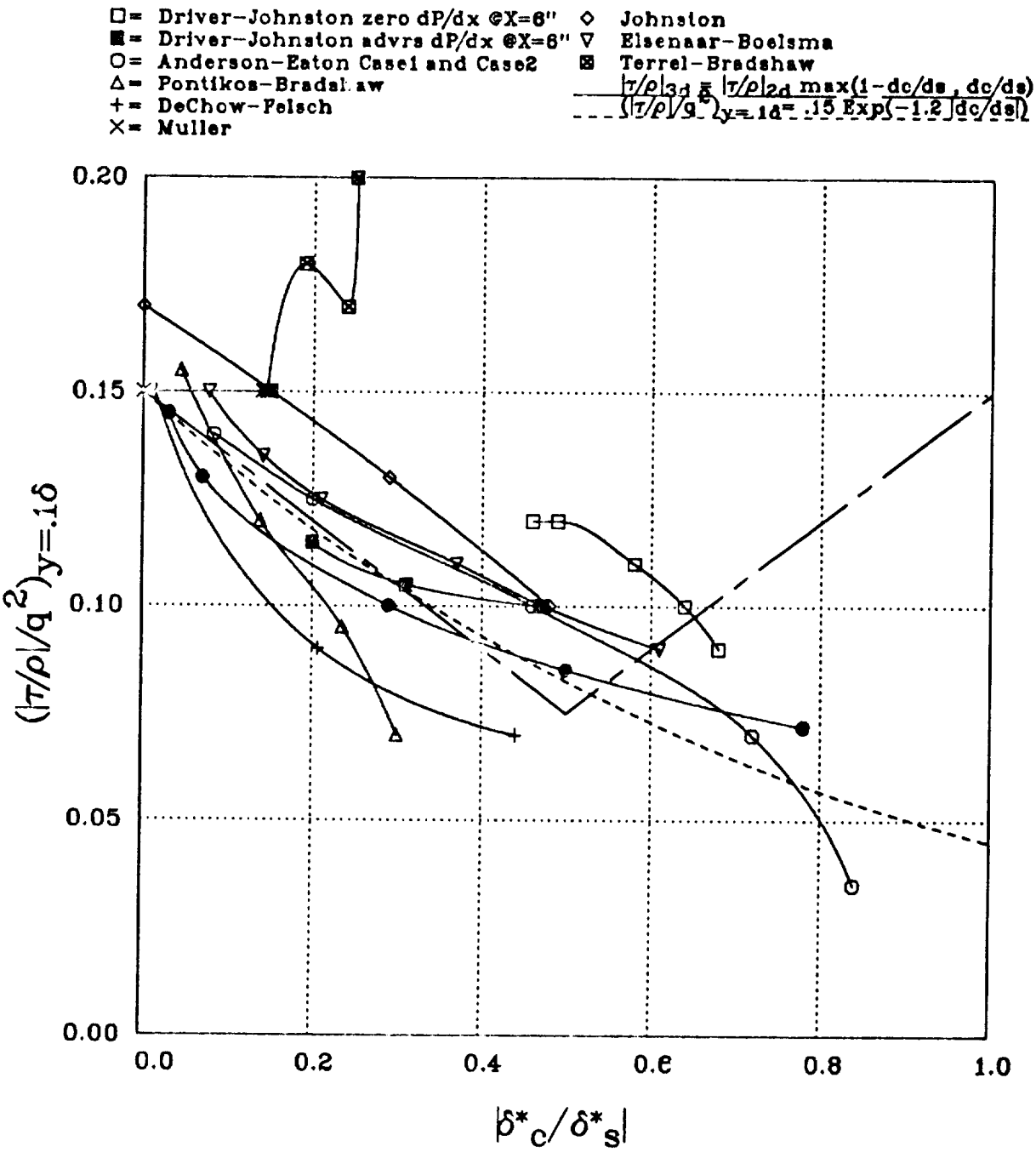

Figure 5.16 Structure parameter verses transverse flow displacement thickness.

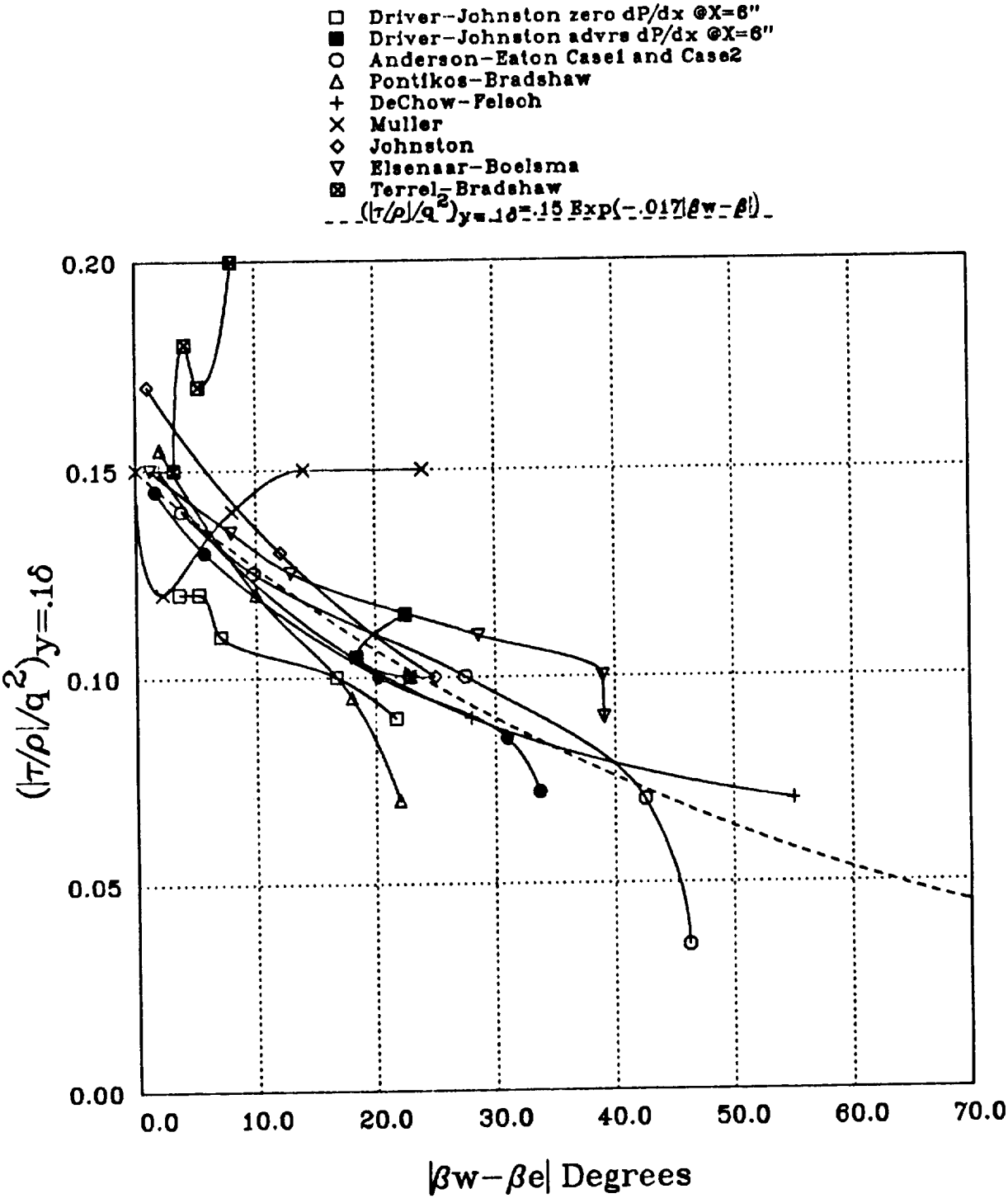

Figure 5.17 Structure parameter verses maximum flow skew angle.

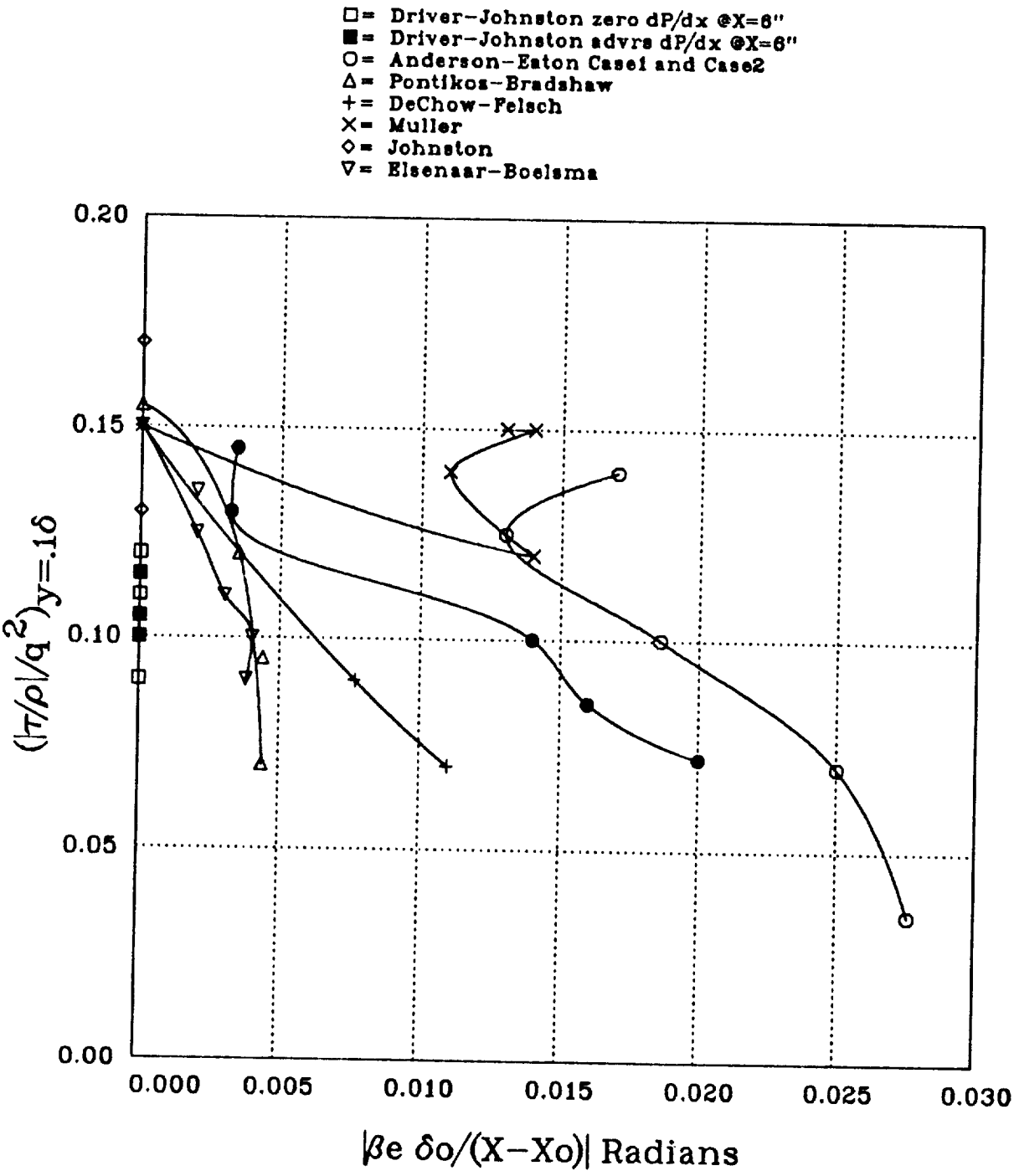

Figure 5.18 Structure parameter verses turning rate.

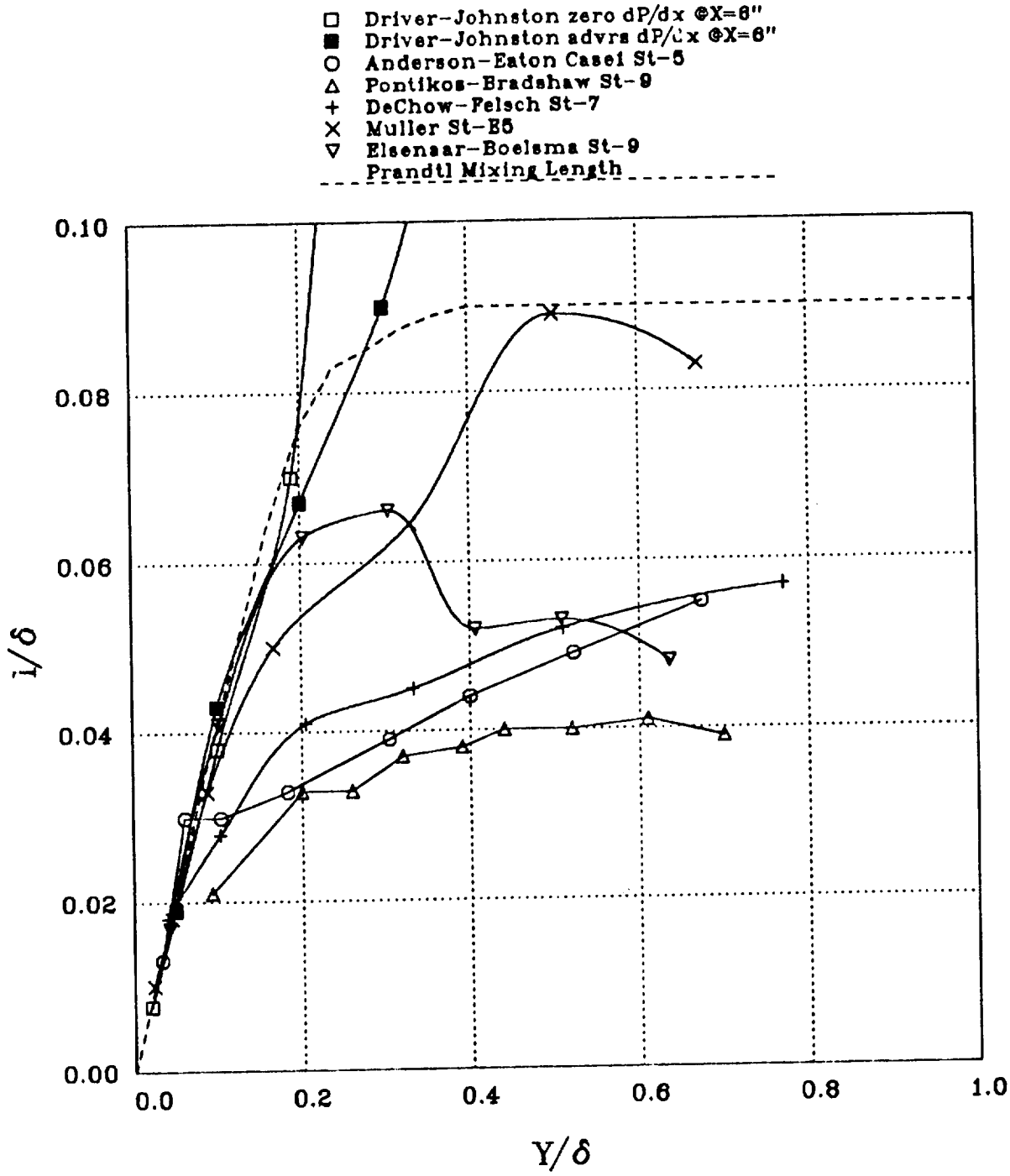

Figure 5.19 Mixing length profiles for various experiments.

6 COMPUTATIONS

Computations were performed on each of the pressure gradient cases with and without spin. Comparisons are made with the measurements in this chapter. The computations were performed with a boundary layer solver (ref. 40) which relies on the usual boundary layer assumptions and a prescription of the streamwise pressure gradient. Experimental upstream flow conditions were used as initial conditions for the computations. The external pressure gradient was prescribed using the experimental measurements of wall static pressure. The computations employed three separate turbulence models: (1) Launder, Reece, and Rodi (ref. 41) full Reynolds stress equation model (with ω^2 equation instead of ε equation), (2) Wilcox and Rubesin (ref. 42) $k - \omega^2$ equation model, and (3) Prandtl mixing length model—without curvature correction.

The comparisons are given in one-page summary sheets (figs. 6.1 through 6.7), showing a series of postage stamp plots of U/U_τ, W/U_τ, $-\overline{uv}/U_\tau^2$, $\overline{vw}/U_\tau^2$, and k/U_τ^2 for streamwise locations X = –430, –152, –12, 25, 50, 101, 152, 228, and 304 mm. The plots are organized so that each row corresponds to a single variable, and each column corresponds to a single streamwise location. These plots facilitate visualization of the whole flow at a glance, making it possible to assess the overall flow solution and any gross inadequacies of the turbulence model. The measurements are represented by dashed lines and the computations are represented by solid lines. The calculations were discontinued when flow detachment was detected; consequently, some of the plots do not include the latter stations in the flow.

6.1 Zero Pressure Gradient

Computations with the Launder-Reece-Rodi turbulence model for the case of zero pressure gradient with spin (case A.S1) are shown in figure 6.1. The top row shows that U/U_τ velocity is accurately calculated throughout the flow. The second row shows that W/U_τ velocity is slightly overpredicted near the wall and underpredicted away from the wall at locations downstream of the spinning section. Calculations fail to predict the reduction of the streamwise Reynolds stress, $-\overline{uv}/U_o^2$, seen in the third row, probably due to the imprecision of the physics in the model. The transverse component of Reynolds stress, $\overline{vw}/U_o^2$ (seen in the fourth row) is generally underpredicted in the outer part of the boundary layer and overpredicted in the inner part of the boundary layer. Kinetic energy, k/U_o^2, seen in the bottom row is generally underpredicted throughout the flow, except at the beginning where measured kinetic energy is used as an initial condition. Underprediction of the kinetic energy has always been a problem with the $k - \varepsilon$ equation type models (in this case $k - \omega^2$); it is probably due to errors in the dissipation rate equation.

Calculations in the nonspinning case of zero pressure gradient are in excellent agreement with the data (not shown here).

6.2 Adverse Pressure Gradient with Transverse Flow

Computations with the Launder-Reece-Rodi turbulence model for the adverse pressure gradient case with spin (case D.S1) are shown in figure 6.2. The calculations are generally satisfactory. While the average transverse momentum thickness is generally comparable between the calculations and the experiment, the distribution of transverse momentum shows differences—too much momentum near the wall in the calculations while not enough away from the wall. This erroneous distribution of momentum resulted

from underprediction of the peak stress levels in the calculations of the $\overline{vw}/U_o^2$ stress shown in the fourth row. The streamwise stress $-\overline{uv}/U_o^2$, shown in the third row, is again overpredicted as it was in the case of zero pressure gradient (the model's missing physics). Kinetic energy is underpredicted as usual.

Calculations using the $k-\omega^2$ model (fig. 6.3) produced much the same results as did the Launder-Reece-Rodi model. There are differences between the two models, although they are small. The $k-\omega^2$ model produces a larger W-velocity near the wall (see second row) than did the Launder-Reece-Rodi model, and this is due to the even smaller peak level of $\overline{vw}/U_o^2$ stress predicted by the $k-\omega^2$ (see fourth row). This is probably a result of the model's assumption that the stress is isotropic.

Calculations using the mixing length model (fig. 6.4) produce much worse results than either of the other two models. The calculations produce generally poor results due to the lack of curvature correction terms in the model. Due to the mismatch in U-velocity profiles from the start, use of the pressure gradient makes the differences even larger, until the predicted flow ultimately separates.

6.3 Adverse Pressure Gradient without Transverse Flow

The calculations based on the Launder-Reece-Rodi model (fig. 6.5) are in quite good agreement with the data for case D.S0 with no spin and adverse pressure gradient. The calculation produces premature separation at the x = 210 mm station (not shown), a station that is close to the experimental separation point, near x = 250 mm.

Calculations based on the $k-\omega^2$ model are not as good (fig. 6.6). The calculated displacement thickness is too small and the calculation fails to separate. Reynolds stress may be responsible for this failure to separate, insomuch as it grows too large—larger Reynolds stress reduces the ability of the flow to separate.

Calculations based on the mixing length model produce results as poor as the $k-\omega^2$ model (fig. 6.7). The calculated displacement thickness is too small, the calculation fails to separate, and the Reynolds stress is too large.

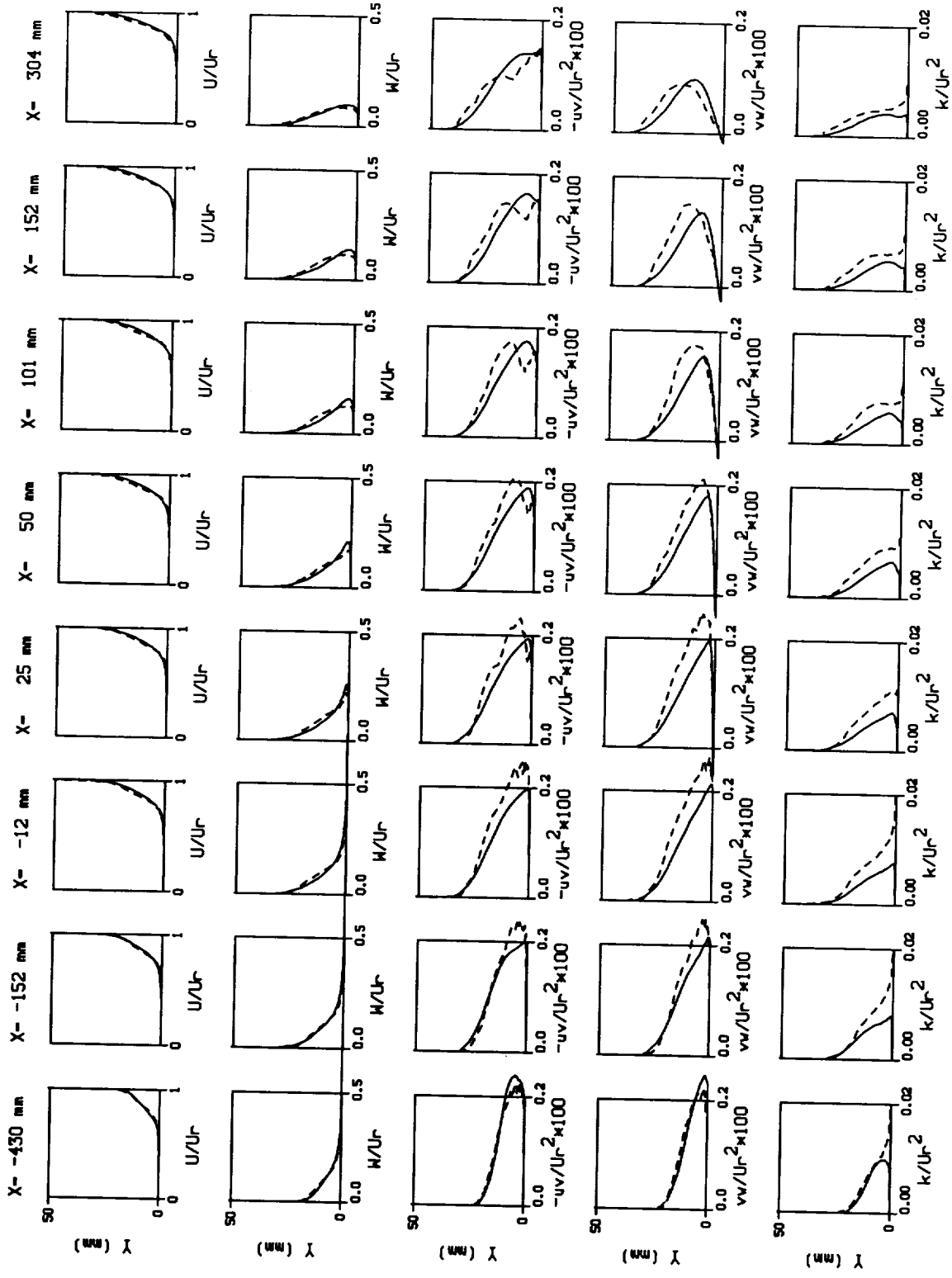

Figure 6.1 Computations of case A.S1 using Launder-Reece-Rodi model compared to experiment, - - - experiment, —— computation.

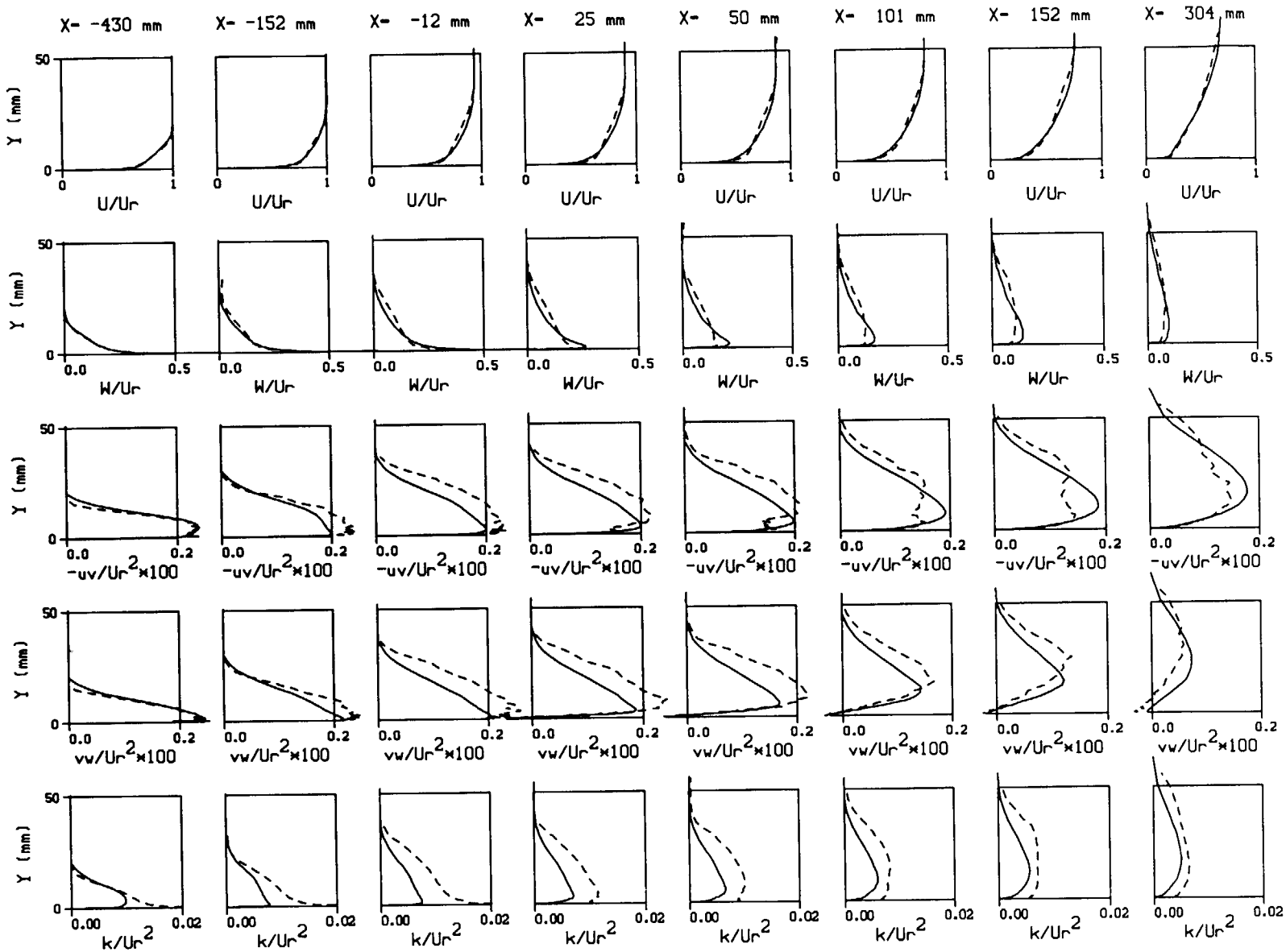

Figure 6.2 Computations of case D.S1 using Launder-Reece-Rodi model compared to experiment, - - - experiment, —— computation.

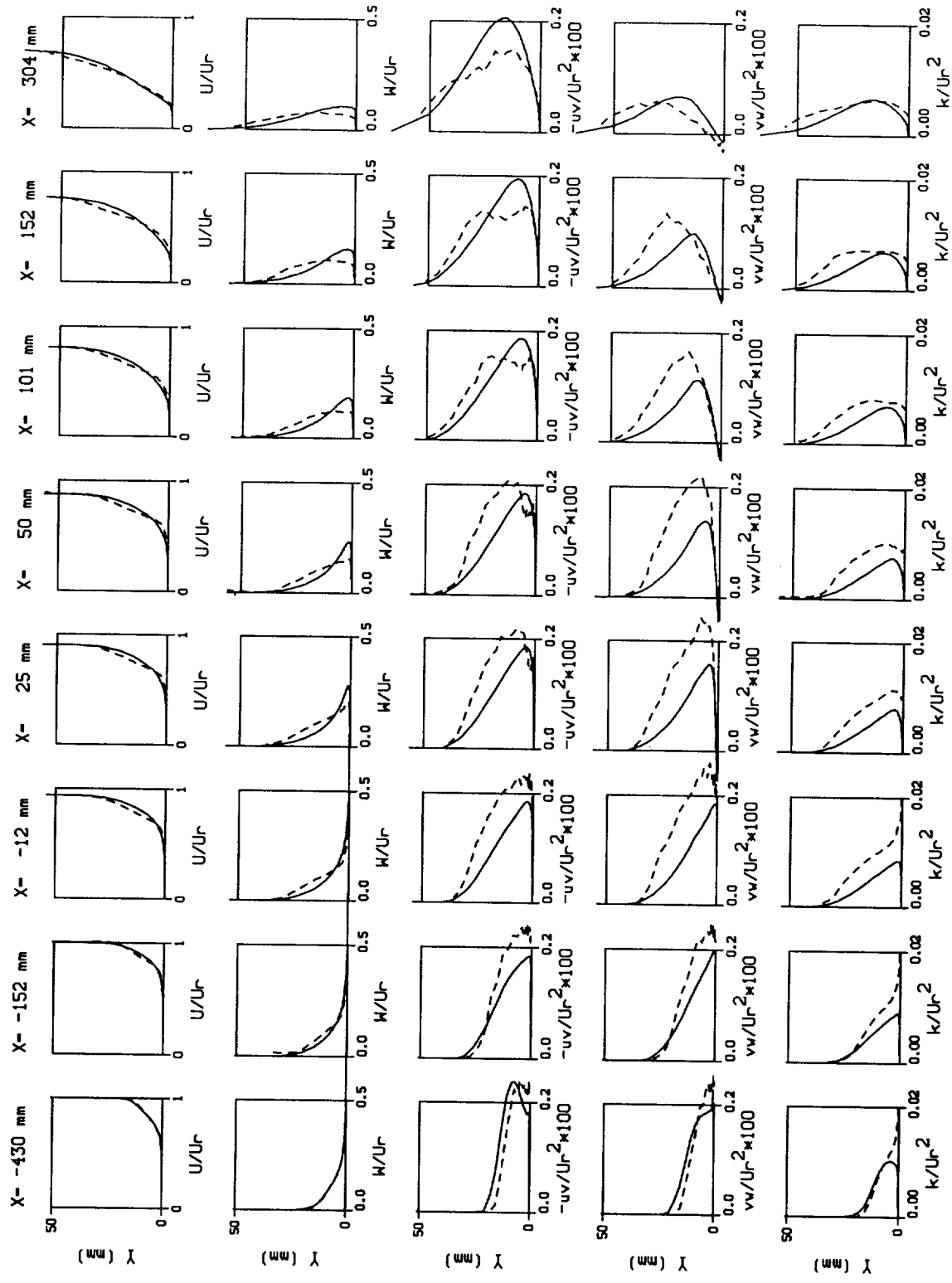

Figure 6.3 Computations of case D.S1 using $k - \omega^2$ model compared to experiment, - - - experiment, —— computation.

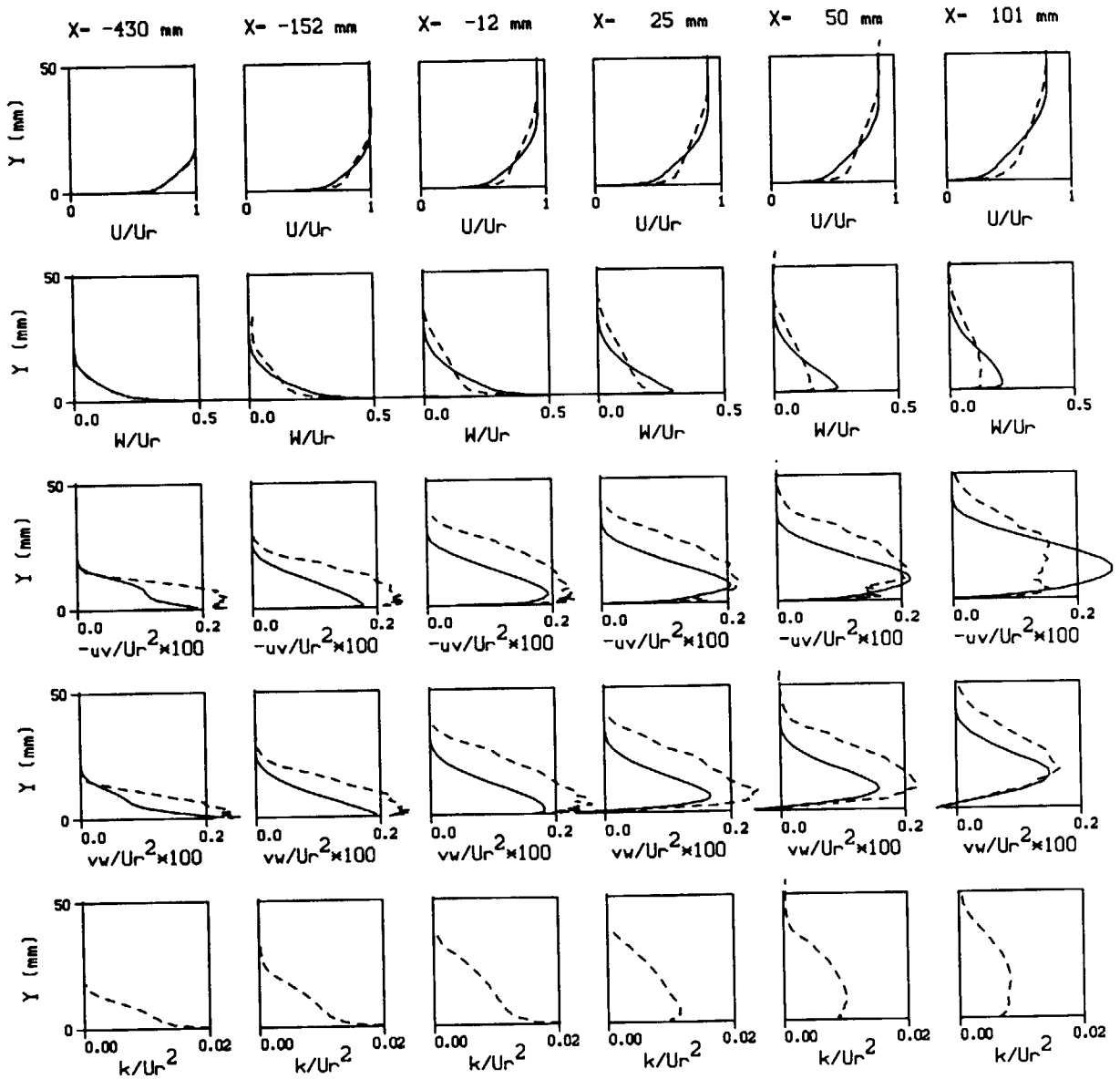

Figure 6.4 Computations of case D.S1 using Prandtl mixing length model compared to experiment, - - - experiment, —— computation.

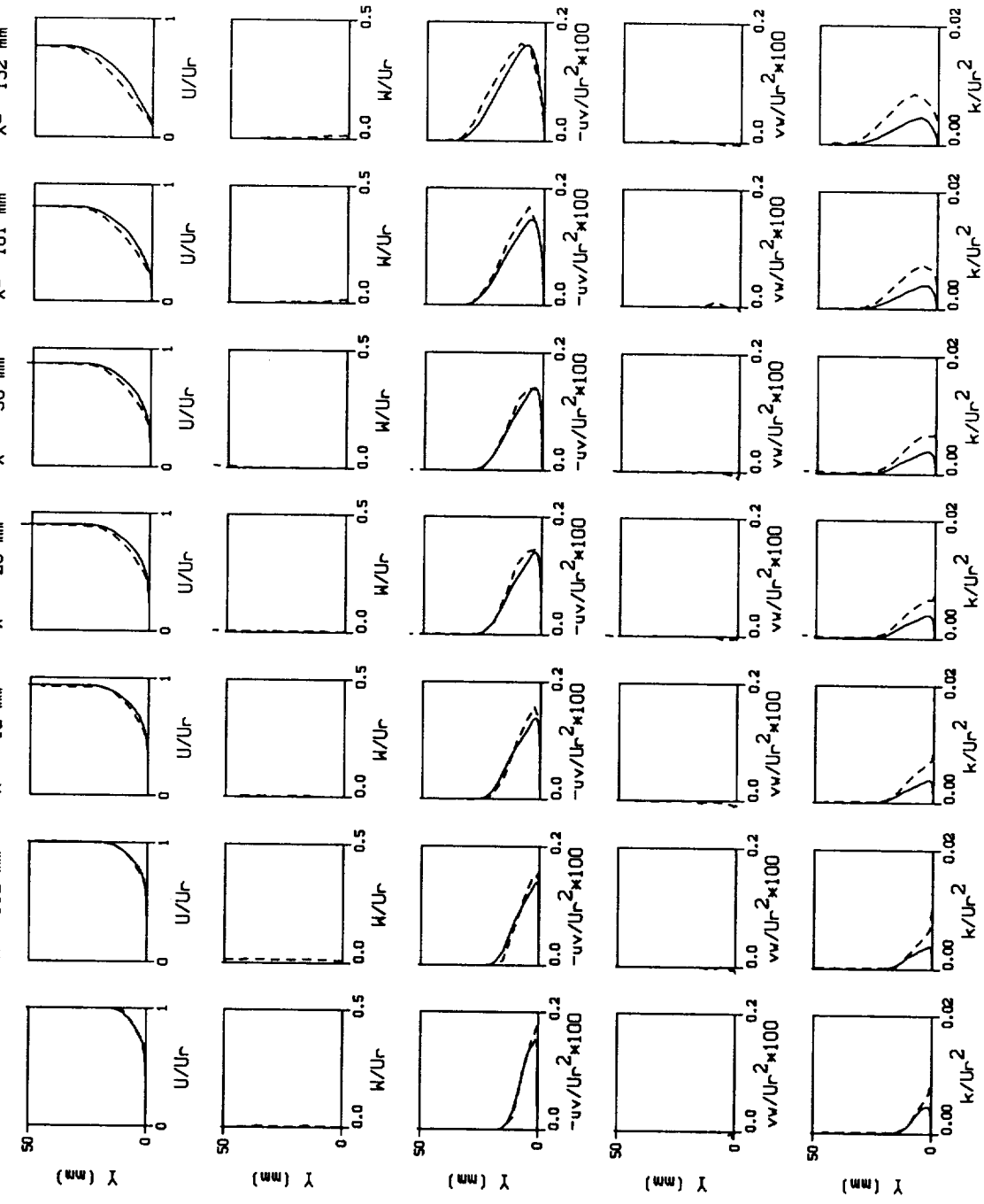

Figure 6.5 Computations of case D.S0 using Launder-Reece-Rodi model compared to experiment, - - - experiment, —— computation.

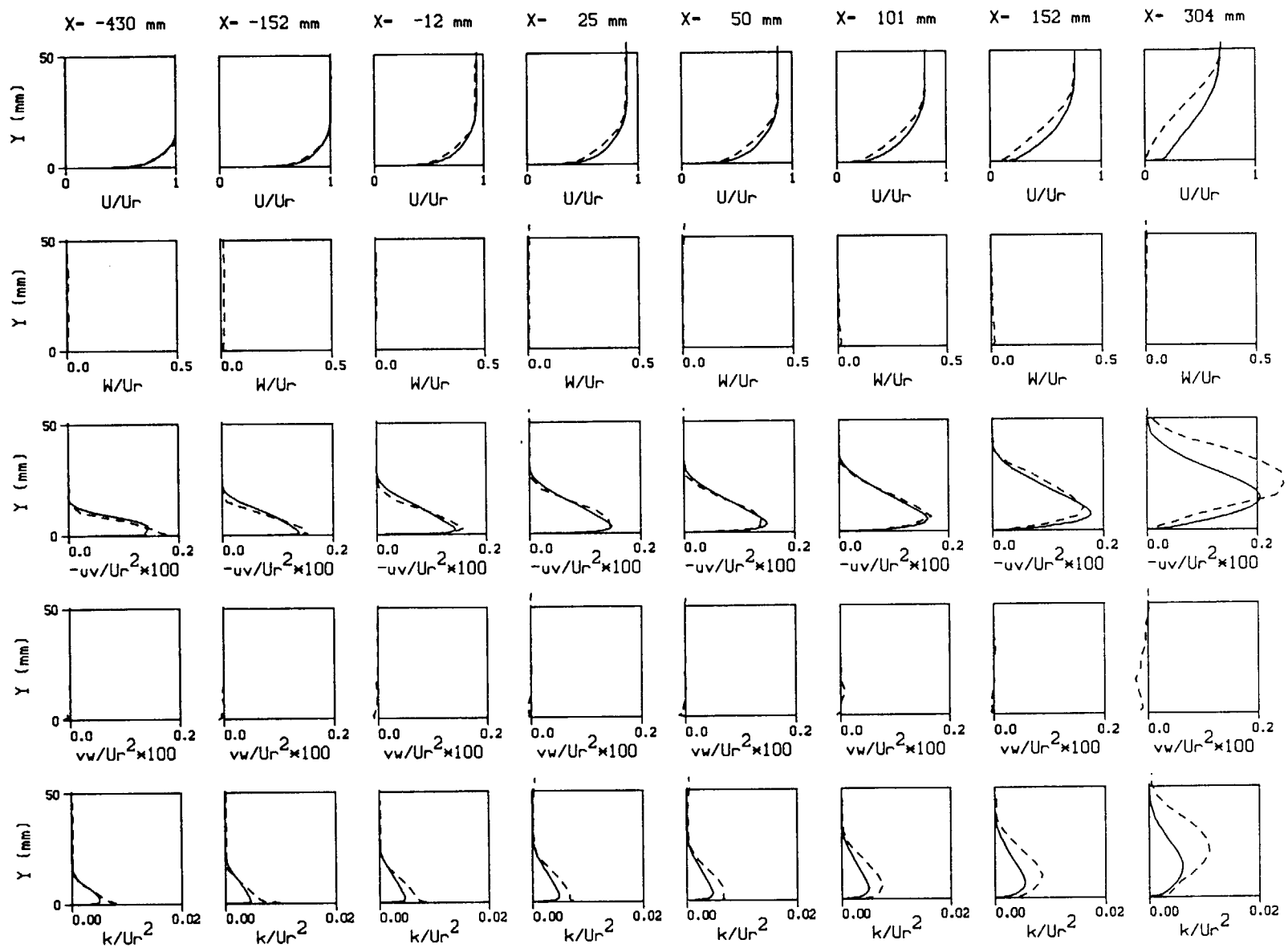

Figure 6.6 Computations of case D.S0 using $k - \omega^2$ model compared to experiment, - - - experiment, —— computation.

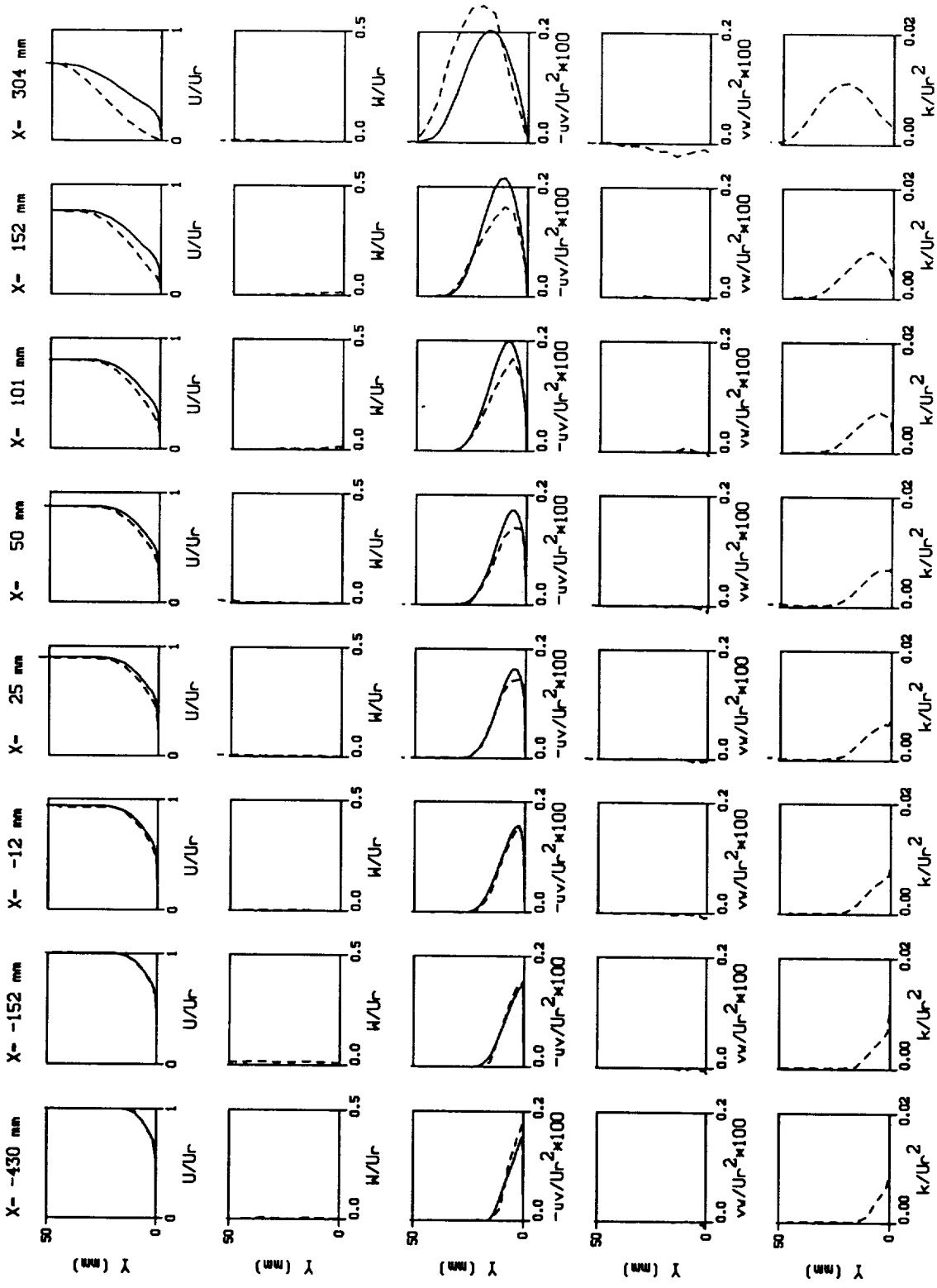

Figure 6.7 Computations of case D.S0 using Prandtl mixing length model compared to experiment, - - - experiment, —— computation.

7 SUMMARY AND CONCLUSIONS

An axisymmetric flow containing both pressure gradient and transverse strain effects was measured in detail, providing the necessary measurements to evaluate a wide variety of single-point turbulence closure models. The boundary layer that developed on the surface of a cylinder (axis aligned with external flow) was perturbed with externally applied pressure gradients and various translating wall boundary conditions (segment of cylinder rotated). Two wall translation speeds $W_s = 0$ and $W_s = U_r$ were studied for four cases of adverse pressure gradient. The experiment offers axisymmetry for ease of analysis and calculation, while retaining the main features of a three-dimensional boundary layer.

The primary accomplishment was the measurement of mean and fluctuating velocities with sufficient detail and accuracy to evaluate not only various models, but also the terms in the transport equations for turbulent Reynolds stresses. Almost all quantities currently used in the single-point closure turbulence model were measured. Quantities not measured were extracted from equation balances.

In addition, calculations were performed on each test case employing a Prandtl mixing length model, a two-equation model, and a full Reynolds stress model. This was done in an effort to resolve the relative ability of each these kind of models to solve three-dimensional flows. The calculations did not involve any modification to models.

Finally, a variety of three-dimensional flow experiments were reviewed in a search for general correlations which might improve models for three-dimensional boundary layers. Two useful correlations relating to effects of cross-stream flow were found.

7.1 Three-Dimensional Effects

The fully developed boundary layer at the downstream end of the spinning cylinder closely resembles that of a two-dimensional boundary layer, which is collateral in the $tan^{-1}(-W_s/U_e)$ direction ($\approx -45°$ for the primary cases studied here).

The effect of the sudden change in wall boundary condition (from $W_s = U_e$ to $W_s = 0$) on the mean flow produces a highly skewed three-dimensional boundary layer, which relaxes back to a two-dimensional boundary layer with distance downstream in an exponential manner.

The effect of the sudden change in wall boundary condition on the turbulence is to diminish (i.e., remove) one of the sources of production (due to transverse strain); this results in a reduced level of turbulence. The high degree of mean flow skewing in the boundary layer also contributes to a further reduction in the Reynolds stress levels, resulting in shear stress levels lower than for those of a comparable two-dimensional boundary layer—a conclusion shared by most previous experiments on three-dimensional boundary layers. The ratio of shear stress to kinetic energy drops (by 30%) below the usual level found in two-dimensional boundary layers. The reductions in stress initially occur near the wall and diffuse outward toward the edge of the boundary layer with distance downstream (reaching the edge by $X = 10\delta_o$).

Reductions in the transverse component of Reynolds stress were seen to severely lag the reductions in the mean flow strain-rate, which suggests that isotropic eddy viscosity models are inappropriate.

7.2 Pressure Gradient Effects

The pressure gradient reduces the level of mean flow strain-rate near the wall, while generating relatively small levels of secondary strain rate $\partial U/\partial x$.

As a result of the pressure gradient, the turbulence Reynolds stress diminishes in the inner region of the flow. The usual increase in stress is seen in the outer region of the flow for the two-dimensional cases, while for the three-dimensional cases, the outer-region stress increase is less dramatic as a result of mean flow skewing.

An inviscid rotation of the mean flow strain-rate vector direction, produced by the pressure gradient, appeared to reduce the Reynolds shear stress—as was the case in the Pontikos-Bradshaw experiment; however, the drop in stress was suspected to be a result of the pressure gradient rather than mean flow skewing.

7.3 Turbulence Models

The Prandtl mixing length modeling assumption, applied to adverse pressure gradient, was shown to produce an undesirable y^2 growth of Reynolds shear stress with distance from the wall as opposed to the linear growth seen in the experiment.

The ratio of Reynolds shear stress to kinetic energy was not a constant equal to 0.3 (as is assumed in the $k-\varepsilon$ model), but instead a strong function of adverse pressure gradients, mean flow skewing, and proximity to walls. In fact, $\frac{\tau/\rho}{k}$ taken at $y = 0.1\delta$ was found to correlate fairly well with the degree of mean flow skewing for a wide range of three-dimensional experiments. The lower levels of $\frac{\tau/\rho}{k}$ found for adverse pressure gradients could be partially accounted for by the use of streamwise aligned components of stress.

The convective transport terms in the Reynolds stress transport equations for $\overline{uv}$ Reynolds stress and kinetic energy were small relative to the production terms despite the presence of extra rates of strain $\partial W/\partial y$ and $\partial U/\partial y$. However, the convective term in the $\overline{vw}$ equation is large relative to the production term, making a model that uses the Reynolds-stress transport equation plausible. The pressure strain models of Launder, Reece, and Rodi and Naot, Shavit, and Wolfshtein produced almost identical levels of modeled pressure strain which compared quite well with the experimentally deduced levels of pressure strain. This was the case for all situations—zero pressure gradient, adverse pressure gradient, and transverse strain.

Computations employing $k-\omega^2$ and full Reynolds stress models (Launder-Reece-Rodi) in general calculated the mean flow quite well with and without pressure gradients; the full Reynolds stress model produced slightly more accurate results in calculating the transverse component of flow. Computations using a Prandtl mixing length model failed to predict the mean flow as accurately as the other two models, primarily due to the model's insensitivity to rotational effects (curvature correction was not used). The $k-\omega^2$ and full Reynolds stress model also lacked sufficient sensitivity to rotational effects to completely match the velocity profiles at the end of the spinning section. No model was able to predict the drop in the $\overline{uv}$ component of Reynolds stress resulting from three-dimensional effects.

Future work would be best done using a large cylinder radius relative to the boundary layer thickness in order to minimize curvature and/or rotational effects. The curvature and/or rotational effects in this experiment are relatively large compared to the curvature effects that one would find on most external aerodynamic shapes, although the curvature is comparable to that seen in compressor blade problems. By eliminating curvature effects, it would be possible to answer the initial question: Is a 3D boundary layer any more or less prone to separation than a 2D boundary layer? Further experiments involving 3D separation are needed to test the notion that a 3D boundary layer is more prone to separate than a 2D boundary layer.

As for an explanation of the Reynolds stress decreases in three-dimensional boundary layers, direct numerical simulations (now in progress) offer the best hope, rather than guessing (also in progress).

REFERENCES

1. Johnston, J. P.: Experimental Studies in Three Dimensional Turbulent Boundary Layers. Report MD-34, Thermosciences Div., Dept. of Mechanical Engineering, Stanford Univ., July 1976.

2. Berg, B., van de: Three-Dimensional Shear Layer Experiments and Their use as Test Cases for Calculation Methods. National Aerospace Laboratory, The Netherlands, NRL MP 86036 U, 1986.

3. Bradshaw, P.; and Terrell, M. C.: The Response of a Turbulent Boundary Layer on an "Infinite" Swept Wing to the Sudden Removal of Pressure Gradient. NPL Aero Report No. 1305. Aeronautical Research Council Fluid Motion Sub-Committee, Oct. 1969, A.R.C.31 514.

4. Johnston, J. P.: Measurements in a Three-Dimensional Turbulent Boundary Layer Induced by a Swept, Forward-Facing Step. J. Fluid Mechanics, vol. 42, 1970, pp. 823-844.

5. Elsenaar, A.; and Boelsma, S.: Measurements of the Reynolds Stress Tensor in a Three-Dimensional Turbulent Boundary Layer under Infinite Swept-Wing Conditions. National Aerospace Laboratory, The Netherlands, NRL TR 74095 U, 1974.

6. van den Berg, B.; Elsenaar, A.; Lindhout, J.; and Wesseling, P.: Measurements in an Incompressible Three-Dimensional Turbulent Boundary Layer, Under Infinite Swept-Wing Conditions, and Comparison with Theory. J. Fluid Mechanics, vol. 70. pt. 1, 1975, pp. 127-148.

7. Pontikos, N.; and Bradshaw, P.: The Structure of Three-Dimensional Turbulent Boundary Layers. Department of Aeronautics, Imperial College, London, England, Ph.D. Thesis, Sept. 1982.

8. Bradshaw, P.; and Pontikos, N.: Measurements in the Turbulent Boundary Layer on an "Infinite" Swept-Wing. J. Fluid Mechanics, vol. 159, 1985, pp. 105-130.

9. DeChow, R.; and Felsch, K. O.: Measurements of the Mean Velocity and of the Reynolds Stress Tensor in a Three-Dimensional Turbulent Boundary Layer Induced by a Cylinder Standing on a Flat Wall. Proceedings of Symposium on Turbulent Shear Flows, Apr. 1977, University Park, PA, vol I.

10. Anderson, S.; and Eaton, J.: An Experimental Investigation of Pressure Driven Three-Dimensional Turbulent Boundary Layers. Report MD-49, Thermosciences Div., Dept. Mechanical Engineering, Stanford Univ., Stanford, CA, June 1987.

11. Driver, D. M.; and Hebbar, S. K.: Experimental Study of a Three-Dimensional, Shear-Driven, Turbulent Boundary Layer Using a Three-Dimensional Laser Doppler Velocimeter. AIAA Paper 85-1610, July 1985.

12. Driver, D. M.; and Hebbar, S. K.: Experimental Study of a Three-Dimensional, Shear-Driven, Turbulent Boundary Layer. AIAA J., vol. 25, no. 1, Jan. 1987., pp. 35-42.

13. Moin, P.; Shih, T.; Driver, D.; and Mansour, N.: Numerical Simulation of a Three-Dimensional Turbulent Boundary Layer. AIAA Paper 89-0373, Jan. 1989.

14. Muller, U.: Measurements of the Reynolds Stresses and the Mean Flow Field in a Three-Dimensional Pressure Driven Boundary Layer. J. Fluid Mechanics, vol. 119, pp. 121-153.

15. Lohmann, R.: The Response of a Developed Turbulent Boundary Layer to Local Transverse Surface Motion. Transactions of ASME, J. Fluids Engineering, vol. 98, Sept. 1976, pp. 354-363.

16. Bissonnette, L. R.; and Mellor, G. L.: Experiments on the Behavior of an Axisymmetric Turbulent Boundary Layer with a Sudden Circumferential Strain. J. Fluid Mechanics, vol. 63, pt. 2, Apr. 1974, pp. 369-413.

17. Pierce, F.; McAllister, J.; and Tennant, M.: A Review of Near-Wall Similarity Models in Three-Dimensional Turbulent Boundary Layers. J. Fluids Engineering, vol. 105, Sept. 1983, pp. 251-256.

18. Pierce, F.; McAllister, J.; and Tennant, M.: Near-Wall Similarity in a Pressure-Driven Three-Dimensional Turbulent Boundary Layer. J. Fluids Engineering, vol. 105, Sept. 1983, pp. 257-262.

19. Pierce, F.; McAllister, J.; and Tennant, M.: Near-Wall Similarity in a Shear-Driven Three-Dimensional Turbulent Boundary Layer. J. Fluids Engineering, vol. 105, Sept. 1983, pp. 263-269.

20. Clauser, F.: Turbulent Boundary Layers in Adverse Pressure Gradients. J. Aeronautical Science, vol. 21, 1954, pp. 91-108.

21. Schubauer, G. B.; and. Spangenberg, W. G.: Forced Mixing in Boundary Layers. J. Fluid Mechanics, vol. 8, 1960, pp. 10-32.

22. Perry, A.: Turbulent Boundary Layers in Decreasing Adverse Pressure Gradients. J. Fluid Mechanics, vol. 26, 1966, pp. 481-506.

23. Samuel, A. E.; and Joubert, P. N.: A Boundary Layer Developing in an Increasingly Adverse Pressure Gradient. J. Fluid Mechanics, vol. 66, 1974, pp. 481-505.

24. Perry, A. E.; and Schofield, W. H.: Mean Velocity and Shear Stress Distribution in Turbulent Boundary Layers. Physics of Fluids, vol. 16, no. 12, Dec. 1973, pp. 2068-2081.

25. Simpson, R. L.; Chew, Y. T.; and Shivaprasad, B. G.: The Structure of a Separating Turbulent Boundary Layer. Part 1. Mean Flow and Reynolds Stresses. J. Fluid Mechanics, vol. 113, 1981, pp. 23-51.

26. Simpson, R. L.; Chew, Y. T.; and Shivaprasad, B. G.: The Structure of a Separating Turbulent Boundary Layer. Part 2. Higher-order Turbulence Results. J. Fluid Mechanics, vol. 113, 1981, pp. 53-73.

27. Schofield, W. H.: Equilibrium Boundary Layers in Moderate to Strong Adverse Pressure Gradients. J. Fluid Mechanics, vol. 113, 1981, pp. 91-122.

28. Bachalo, W. D.; and Johnson, D. A.: Transonic Turbulent Boundary-Layer Separation Generated on an Axisymmetric Flow Model. AIAA J., vol. 23, Nov. 1985, pp. 1684-1692.

29. Furuya, Y.; Nakamura, I.; and Kawachi, H.: The Experiment on the Skewed Boundary Layer on a Rotating Body. Bulletin of Japan Society of Mechanical Engineers, vol. 9, 1966, p. 702.

30. Higuchi, H.; and Rubesin, M. W.: An Experimental and Computational Investigation of the Transport of Reynolds Stress in an Axisymmetric Swirling Boundary Layer. AIAA Paper 81-0416, Jan. 1981.

31. Higuchi, H.; and Rubesin, M. W.: Behavior of a Turbulent Boundary Layer Subjected to Sudden Transverse Strain. AIAA J., vol. 17, Sept. 1979, pp. 931-941.

32. Nakamura, I.; and Yamashita, S.: Boundary Layers on Bodies of Revolution Spinning in Axial Flows. IUTAM Symposium on Three-Dimensional Turbulent Boundary Layers, Berlin, West Germany, Mar. 29-Apr. 1, 1982.

33. Furuya, Y.; Nakamura, I.; Yamashita, S.; and Ishii, T.: Experiments on the Relatively Thick, Turbulent Boundary Layers on a Rotating Cylinder in Axial Flows (2nd Report, Flows under Pressure Gradients). Bulletin of the Japan Society of Mech Eng., vol. 20, no. 140, Feb. 1977, pp. 191-200.

34. Driver, D.; and Hebbar, S.: Three-Dimensional Shear Driven Boundary Layer Flow with Streamwise Adverse Pressure Gradient. AIAA J., Dec. 1989, vol. 27, no. 12., pp. 1689-1697.

35. Hebbar, S.; and Driver, D.: Experimental Investigation of a Swirling, Axisymmetric, Turbulent Boundary Layer with Pressure Gradient. AIAA J., Apr. 1987, vol. 25, no. 4., pp. 521-522.

36. Rotta, J. C.: Further Investigation on Turbulence Models for Three-Dimensional Boundary Layers and Comparisons of Calculations with Infinite Swept Wing Flow Measurements. Viscous and Interacting Flow Field Effects, U.S., West German Data Exchange Agreement, U.S. Naval Postgraduate School, Monterey, CA, 25-26 Apr. 1978.

37. Abid, R.: An Eddy Viscosity For Three Dimensional Boundary Layer Flows. Paper 88-375, presented at First National Fluid Dynamics Congress, 24-28 July 1988, Cincinnati, Ohio.

38. Monson, D. J.: A Nonintrusive Laser Interferometer Method for Measurement of Skin-Friction. Experiments in Fluids, 1983, pp. 15-22.

39. Patel, V. C.: Calibration of the Preston Tube and Limitations on its use in Pressure Gradients. J. Fluid Mechanics, vol. 23, pt. 1, 1965, pp. 185-208.

40. Wilcox, D. C.: Recent Improvements to the Spinning Body Version of the EDDYBL Computer Program. Report DCW-R-24-01, DCW Industries Inc., Studio City, CA, Nov. 1979.

41. Launder, B. E.; Reece, G. J.; and Rodi, W.: Progress in the Development of a Reynolds-Stress Turbulence Closure. J. Fluid Mechanics, vol. 68, pt. 3, 1975, pp. 537-566.

42. Wilcox, D. C.; and Rubesin, M. W.: Progress in Turbulence Modeling for Complex Flow Fields Including Effects of Compressibility. NASA TP-1517, 1980.

43. Collini, P.; Fulachier, L.; and Dumas, R.: Visualization of Streaky Pattern within a Turbulent Boundary Layer on a Moving Wall. Euromech Conference Presentation, Oct. 1985.

44. Cebeci, T.; and Smith, A. M. O.: Analysis of Turbulent Boundary Layers. Academic Press, NY, 1974.

45. Cebeci, T.: Calculation of Three-Dimensional Boundary Layers I. Swept Infinite Cylinders and Small Cross Flow. AIAA J., vol. 12, no. 6, June 1974, pp. 779-786.

46. Jones, W. P.; and Launder, B. E.: The Prediction of Laminarization with a 2-Equation Model of Turbulence. International Journal of Heat and Mass Transfer, vol. 15, Feb. 1972, pp. 301-304.

47. Johnson, D. A.; and King, L. S.: A New Turbulence Closure Model for Boundary Layer Flows with Strong Adverse Pressure Gradients and Separation. AIAA Paper 84-0175, Jan. 1984.

48. Naot, D.; Shavit, A.; and Wolfshtein, M.: Two-Point Correlation Model and the Redistribution of Reynolds Stresses. Physics of Fluids, vol. 16, no. 6, June 1973, pp. 738-743.

49. Shih, T-H.; and Lumley, J. L.: Modeling of Pressure Correlation Terms in Reynolds Stress and Scalar Flux Equations. Report FDA-85-3, Sibley School of Mechanical and Aerospace Engineering, Cornell Univ., 1985.

50. Fu, S.; Launder, B. E.; and Tselepidakis, D. P.: Accommodating the Effects of High-Strain Rates in Modeling the Pressure-Strain Correlation. Univ. Manchester, Mechanical Engineering Department, Report TFD/87/5, 1987.

51. Lumley, J. L.: Computational Modeling of Turbulent Flows. Advances in Applied Mechanics, vol. 18, Academic Press, NY, pp. 123-176.

52. Bradshaw, P.: Effects of Streamline Curvature on Turbulent FLow. NATO, AGARDograph No. 169, Aug. 1973.

APPENDIX A

EFFECTS OF CURVATURE AND ROTATION ON THE BOUNDARY LAYER

Evidence of the destabilizing effects of rotation on the turbulence can be seen in the experimentally deduced mixing length

$$l = \sqrt[4]{\overline{uv}^2 + \overline{vw}^2} / \sqrt{(\partial U/\partial r)^2 + (\partial W/\partial r - W/r)^2}$$

In a 2D flat-plate type boundary layer, the mixing length appears to obey the usual $l_o = 0.41y$ scaling near the wall and $l_o = 0.09\delta$ away from the wall (fig. A.1). In the case with cylinder spinning the l/δ distribution is larger and seems to obey the simple scaling reported by Bradshaw (ref. 52) in which $l = l_o$ (1 – 7Ri), where

$$Ri = 2(W/r)(\partial W/\partial r + W/r)/[(\partial U/\partial r)^2 + (\partial W/\partial r - W/r)^2]$$

Physically, the way to understand the destabilizing effect of rotation is to consider a fluid element (with transverse momentum ρW) (fig. A.2). The orbital path of the fluid around the cylinder is maintained by an inward pressure force. The fluid is perturbed (bumped) away from its original orbit to a new orbit of larger R where there is less inward pressure force. Here the pressure force is unable to hold the fluid in orbit, and the fluid will now travel on a path which diverges outward from the cylinder. This essentially contributes to a thickening of the boundary layer. Conversely, fluid which is bumped inward towards the center of rotation would be further drawn inward by the pressure gradient (which increases with proximity to the wall).

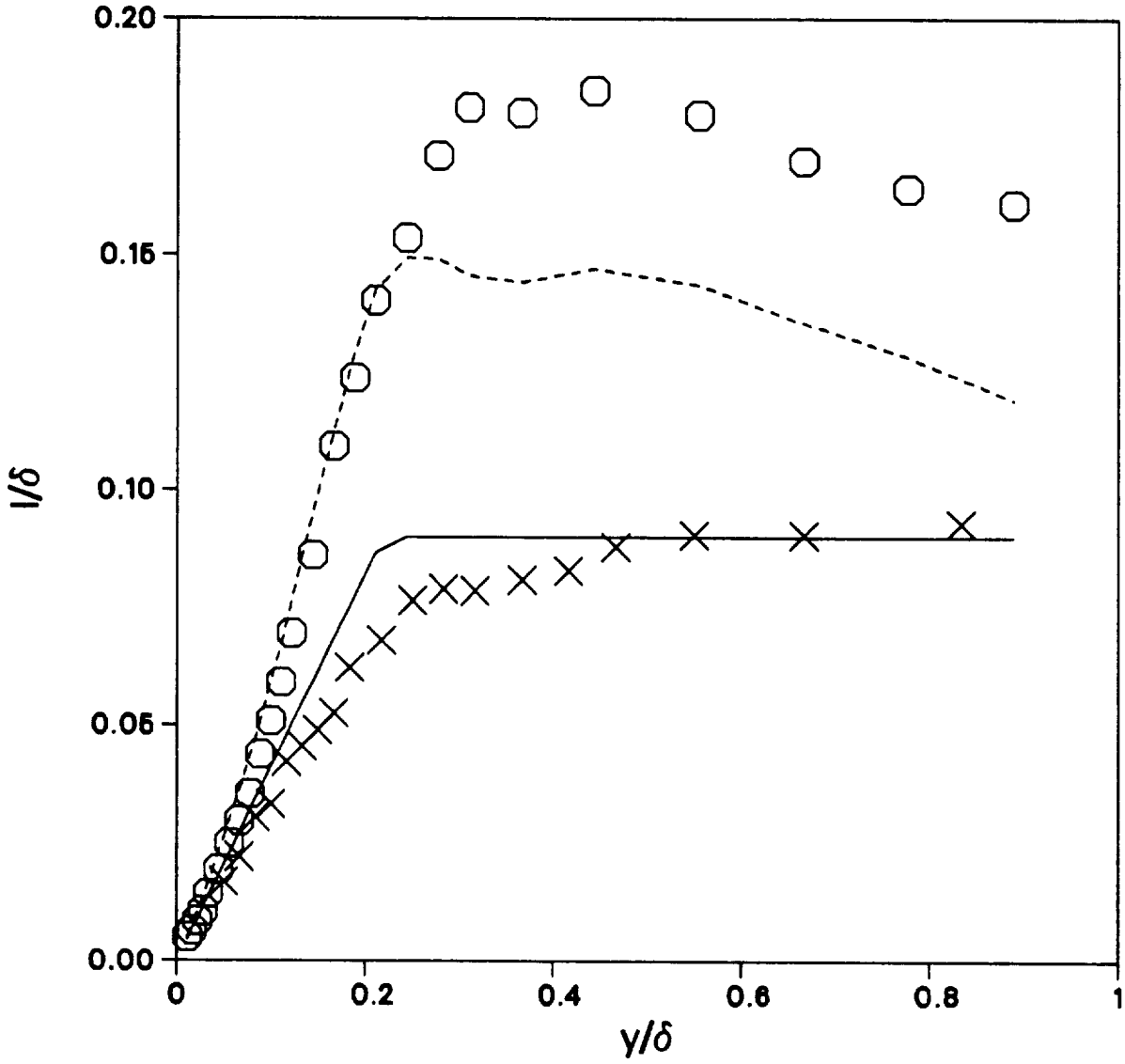

Figure A.1 Mixing length distribution for; ○ spinning case A.S1 @x=−12mm, △ no-spin case A.S0 @x=−12mm, —— Prandtl Mixing Length, and - - - (1-7Ri)*Prandtl.

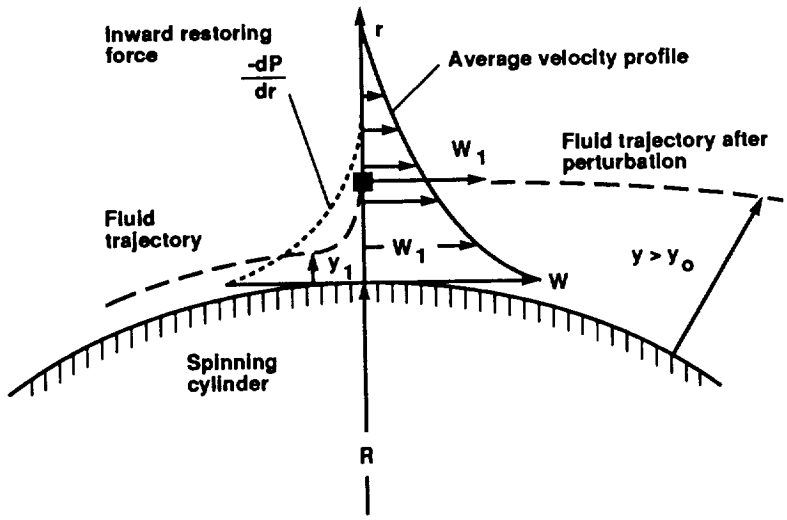

Figure A.2 Curvature/Rotational Effects.

APPENDIX B

COLLATERAL FLOW

While the flow on the spinning cylinder does contain transverse strain, it is not strictly speaking a three-dimensional or three-component boundary layer, instead it is a two-dimensional, two component boundary layer when viewed from a frame of reference translating with the cylinder's surface.

Consider the velocity components at the end of the spinning cylinder viewed from a stationary frame of reference (fig. B.1(a)). The two components of velocity appear dissimilar. When one plots the W velocity component verses the U velocity component, the resulting curve is a straight line (collateral condition).

Now if one considers the two velocity components in a frame of reference translating with the cylinder's surface (fig. B.1(b)), the two components appear similar. Indeed, if one plots the new velocity component $\hat{W}_s$ versus U, the resulting curve is a straight line which intersects zero. One can think of each of these points on the line as the end of a vector whose origin as at zero. Each vector has the same direction $\hat{\beta}$. In other words, in this translating coordinate frame, the flow everywhere in the boundary layer is traveling in the same direction. Such a flow is called collateral or unidirectional, which is why it is said to be a 2D boundary layer traveling in a 45° direction (for $W_s = U_e$) relative to the tunnel centerline.

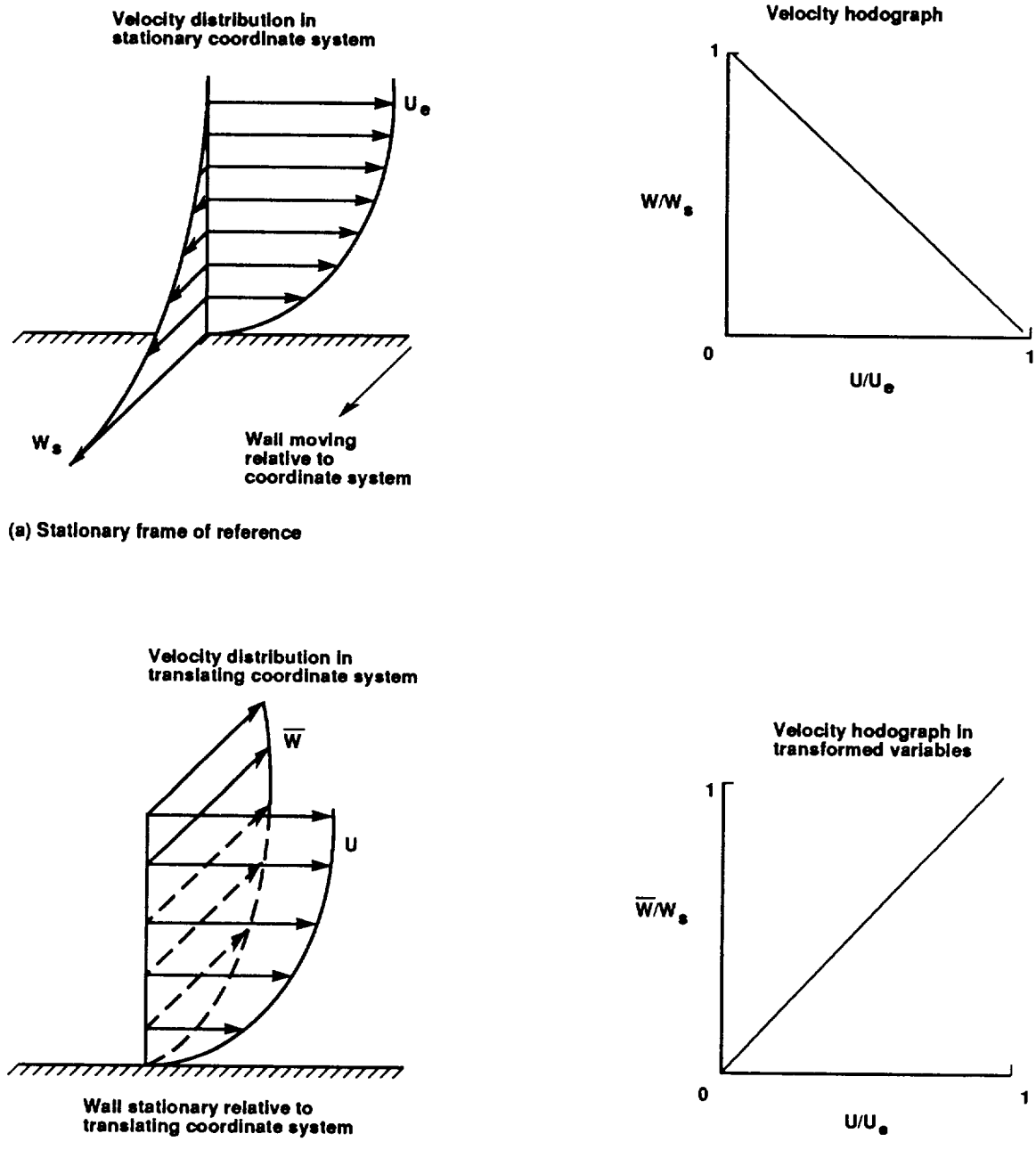

Figure B.1 Frame of Reference Transformation to Translating Coordinates System.

APPENDIX C

PRESSURE GRADIENT CASES A, B, C, AND D

This section contains tabulated values (tables C.1 through C.5) of the surface pressure, flow angles, skin-friction, and velocity field data, acquired for cases pressure gradient cases A, B, C, and D.

The measurements are described in section 3. Laser measurements of the mean and fluctuating quantities were calculated using a 3D velocity bias correction. The bias correction is described in section 2.2.2.

SURFACE PRESSURE DISTRIBUTIONS

	CASE B.S0	CASE B.S1	CASE C.S0	CASE C.S1	CASE D.S0	CASE D.S1
X(mm)	Cp	Cp	Cp	Cp	Cp	Cp
-914.400	0.007	0.017	0.002	0.002	-0.017	-0.012
-762.000	-0.005	0.005	0.000	0.000	-0.012	-0.010
-609.600	0.000	0.002	-0.008	-0.002	-0.010	-0.005
-457.200	0.000	0.000	0.000	0.000	0.000	0.000
3.175	0.403	0.387	0.452	0.460	0.167	0.145
6.350	0.405	0.389	0.452	0.463	0.172	0.155
12.700	0.410	0.392	0.452	0.467	0.184	0.160
19.050	0.410	0.404	0.452	0.481	0.197	0.174
25.400	0.417	0.406	0.460	0.481	0.206	0.189
38.100	0.430	0.421	0.467	0.488	0.236	0.214
50.800	0.439	0.430	0.475	0.500	0.263	0.238
76.200	0.456	0.452	0.480	0.512	0.310	0.292
101.600	0.471	0.469	0.490	0.523	0.356	0.339
127.000	0.488	0.483	0.498	0.540	0.391	0.376
152.400	0.500	0.500	0.507	0.549	0.418	0.413
177.800	0.507	0.510	0.517	0.551	0.440	0.442
203.200	0.519	0.522	0.530	0.565	0.455	0.467
228.600	0.532	0.529	0.538	0.568	0.469	0.486
254.000	0.539	0.541	0.550	0.577	0.482	0.506
304.800	0.551	0.550	0.565	0.596	0.501	0.528
381.000	0.568	0.565	0.585	0.605	0.528	0.555
457.200	0.570	0.565	0.593	0.596	0.550	0.565
533.400	0.549	0.543	0.577	0.572	0.555	0.555
609.600	0.481	0.469	0.510	0.502	0.516	0.509
609.854	0.483	0.471	0.507	0.498	0.506	0.494
660.400	0.410	0.385	0.440	0.437	0.455	0.445
711.200	0.330	0.308	0.350	0.355	0.369	0.361
762.000	0.274	0.262	0.295	0.292	0.297	0.287
812.800	0.267	0.248	0.282	0.285	0.273	0.268
-355.600	--		0.016			
-304.800	--		-0.016			
-254.000	--		0.016			
-203.200	0.053		0.091			
-152.400	0.133		0.201			
-101.600	0.226		0.311			
-50.800	0.325		0.381			
0.000	0.388		--			

Table C.1 Surface pressure distribution for cases B,C & D.

CASE A.S1/2

X(mm)	X(in)	B(deg)
13.5	0.53	15.0
36.8	1.45	11.0
129.5	5.1	6.5
247.7	9.75	4.7
355.6	14.0	4.5
457.2	18.0	4.8
508.0	20.0	3.8
11.4	0.45	17.0
31.7	1.25	11.0
76.2	3.0	10.0
139.7	5.5	7.0
285.8	11.25	4.9
482.6	19.0	3.3
565.2	22.25	3.6

CASE A.S1

X(mm)	X(in)	B(deg)
15.9	0.625	25.3
25.4	1.0	20.5
38.1	1.5	18.7
54.0	2.125	13.5
82.6	3.25	11.8
104.8	4.125	10.0
117.5	4.625	9.0
28.6	1.125	21.0
44.5	1.75	16.8
57.15	2.25	14.0
79.4	3.125	13.0
95.3	3.75	11.0
117.5	4.625	9.8
139.7	5.5	8.8
8.6	0.34	30.5
12.7	0.5	27.8
38.1	1.5	17.8
63.5	2.5	13.0
83.8	3.3	11.0
101.6	4.0	9.8
127.0	5.0	9.3
152.4	6.0	8.0
185.4	7.3	8.8
223.5	8.8	7.7
269.2	10.6	7.5
292.1	11.5	6.8
360.7	14.2	6.2
406.4	16.0	6.3
469.9	18.5	4.8
514.4	20.25	4.9
577.9	22.75	3.8
641.4	25.25	4.0
6.4	0.25	33.5
12.7	0.5	27.2
6.4	0.25	33.0
9.1	0.36	30.2
9.5	0.375	30.5

CASE B'.S1/2 (*)

X(mm)	X(in)	B(deg)
12.7	0.5	27.8
27.9	1.1	22.9
58.4	2.3	19.0
119.4	4.7	13.2
363.2	14.3	8.5
457.2	18.0	5.8
515.6	20.3	5.6
660.4	26	4.7

CASE B'.S1 (*)

X(mm)	X(in)	B(deg)
53.3	2.1	22
99.1	3.9	19
162.6	6.4	16
223.5	8.8	15.4
292.1	11.5	14.0
358.1	14.1	15.0
436.9	17.2	12.4
500.4	19.7	9.7
551.2	21.7	9.2
12.7	0.5	32.6
22.9	0.9	30.9
53.3	2.1	22.4
100.3	3.95	19.7
142.2	5.6	17.6
180.3	7.1	17.1
228.6	9.0	14.5
269.2	10.6	13.8
321.3	12.65	12.4
467.4	18.4	11.1
551.2	21.7	7.9
26.7	1.05	29.0
49.5	1.95	22.8
105.4	4.15	19.2
175.3	6.9	16.2
236.2	9.3	14.7
281.9	11.1	14.4
348.0	13.7	14.4
411.5	16.2	14.0
490.2	19.3	10.4
576.6	22.7	6.6
660.4	26	5.0

CASE B'.S2 (*)

X(mm)	X(in)	B(deg)
8.9	0.35	66
31.8	1.25	50
55.9	2.2	43
6.3	0.25	67
40.6	1.6	48
245.1	9.65	25
342.9	13.5	19.5
14.0	0.55	65
57.1	2.25	49
132.1	5.2	37.50
226.1	8.9	21.50

CASE C.S1/2

X(mm)	X(in)	B(deg)
15.9	0.625	33.8
19.0	0.75	33.0
25.4	1.00	32.5
41.3	1.625	31.8
50.8	2.00	30.0
69.9	2.75	28.5
95.3	3.75	20.5
12.7	0.5	37.5
20.6	0.81	37.3
31.75	1.25	32.1
47.6	1.875	29.0
63.5	2.5	27.3
82.6	3.25	27.6
104.8	4.125	22.1
155.6	6.125	20.0
190.5	7.50	15.4
266.7	10.50	9.0
311.2	12.25	9.5
457.2	18.00	5.8
508.0	20.00	5.8
15.9	0.625	32.1
22.2	0.875	30.5
28.6	1.125	30.5
41.3	1.625	28.8
54.0	2.125	27.5
76.2	3.00	25.0
117.5	4.625	20.2
269.9	10.625	10.8
311.2	12.25	8.5
368.3	14.5	8.4
400.0	15.75	5.6
508.0	20.0	8.6
12.7	0.5	38.5
25.4	1.0	34.0
36.5	1.44	30.5
50.8	2.00	27.5
76.2	3.00	22.8
92.1	3.625	22.0
120.7	4.75	19.5
139.7	5.50	18.2
209.6	8.25	12.5
450.9	17.75	10.0

CASE C.S1

X(mm)	X(in)	B(deg)
15.9	0.625	38.8
27.0	1.063	34.8
38.1	1.5	31.2
63.5	2.5	30.0
114.3	4.5	25.0
139.7	5.5	18.0
181.0	7.125	18.0
219.0	8.625	16.8
6.4	0.25	49.0
25.4	1.00	36.2
34.9	1.375	35.0
60.3	2.375	30.0
88.9	3.5	26.1
123.8	4.875	24.8
174.6	6.875	21.5
219.1	8.625	17.8
254.0	10.00	17.8
304.8	12.00	13.8
362.0	14.25	10.5
425.5	16.75	11.0
482.6	19.0	9.8
596.9	23.5	4.8
19.1	0.75	36.2
31.7	1.25	33.5
57.2	2.25	30.0
85.7	3.375	26.5
127.0	5.00	25.0
181.0	7.125	20.2
235.0	9.25	17.8
317.5	12.5	10.5
400.0	15.75	9.0
520.7	20.5	7.5
635.0	25.0	5.0

CASE D.S1

X(mm)	X(in)	B(deg)
40.6	1.6	21.2
57.1	2.25	19.8
95.3	3.75	20.5
130.8	5.15	17.0
152.4	6.0	18.0
177.8	7.0	19.0
36.8	1.45	21.0
50.8	2.00	21.5
66.0	2.60	22.0
88.9	3.50	20.0
120.6	4.75	19.2
35.6	1.40	24.0
57.1	2.25	21.0
73.7	2.90	20.0
92.7	3.65	20.5
124.5	4.9	20.0
142.2	5.6	22.0
160.0	6.3	19.2
184.1	7.25	20.5
203.2	8.0	21.5
243.8	9.6	23.0
266.7	10.5	22.2

* Note: The surface oil flow direction for case B' was obtained while the tunnel was running in an off design condition (i.e., the boundary layer was 50% thicker due to dirty inlet screens). This data should be used qualitatively only, and "should not" be used in conjunction with the Cp data or the LDV data which was obtained using design conditions.

Table C.2 Surface oil-flow direction for cases A, B, C & D.

CASE A.S1

X(mm)	X(in)	Cfx	Cfz
6.4	0.25	0.00396	0.00257
12.7	0.50	0.00399	0.00208
25.4	1.00	0.00373	0.00147
50.8	2.00	0.00361	0.00097
101.6	4.00	0.00351	0.00065
152.4	6.00	0.00331	0.00048
228.6	9.00	0.00327	0.00044
304.8	12.00	0.00324	0.00037
457.2	18.00	0.00302	0.00027
609.6	24.00	0.00316	0.00022

CASE B.S0 (LDV & Clauser Method)

X(mm)	X(in)	Cfx	Cfz
-457.2	-18	0.0032	0
-330.2	-13	0.0032	0
-228.6	-9.0	0.0030	0
-152.4	-6.0	0.0020	0
-76.2	-3.0	0.00125	0
-12.7	-0.5	0.00077	0
12.7	0.5	0.00063	0
152.4	6.0	0.00033	0
228.6	9.0	0.00033	0
304.8	12.0	0.00032	0

CASE B'.S0 (off design conditions)*

X(mm)	X(in)	Cfx	Cfz
-330.2	-13	0.00278	0
-254.0	-10	0.00270	0
-177.8	-7.0	0.00258	0
-152.4	-6.0	0.00235	0
-76.2	-3.0	0.001105	0
7.6	0.3	0.00064	0
152.4	6.0	0.00056	0
304.8	12.0	0.00048	0

CASE B'.S1/2 (off design conditions)*

X(mm)	X(in)	Cfx	Cfz
12.7	0.5	0.00115	0.0006
25.4	1.0	0.0010	0.00043
50.8	2.0	0.0009	0.00033
76.2	3.0	0.00086	0.00027
152.4	6.0	0.00068	0.00013
304.8	12.0	0.00060	0.00008

CASE B'.S1 (off design conditions)*

X(mm)	X(in)	Cfx	Cfz
12.7	0.5	0.0019	0.00133
25.4	1.0	0.0017	0.00083
50.8	2.0	0.0012	0.00050
152.4	6.0	0.0010	0.00030
304.8	12.0	0.0008	0.00020

* Note: The wall shear stress for case B' was obtained while the tunnel was running in an off design condition (i.e., the boundary layer was 50% thicker due to dirty inlet screens). This data should be used qualitatively only, and "should not" be used in conjunction with the Cp data or the LDV data which was obtained using design conditions.

CASE C.S0

X(mm)	X(in)	Cfx	Cfz
-343.2	-13.5	0.00329	0
-152.4	-6.0	0.00153	0
-50.8	-2.0	0.00044	0
-12.5	-0.5	0.00026	0
12.5	0.5	0.00011	0
101.6	4.0	-.00008	0
152.4	6.0	-.00017	0
254.0	10.0	0.00012	0
279.4	11.0	0.000114	0
355.6	14.0	0.00036	0

CASE C.S1/2

X(mm)	X(in)	Cfx	Cfz
12.7	0.5	0.00063	0.00049
25.4	1.0	0.00042	0.00027
43.2	1.7	0.00032	0.000185
101.6	4.0	0.00035	0.000101
152.4	6.0	0.000206	0.000071
228.6	9.0	0.000227	0.000048
295.3	11.6	0.00033	0.000058
381.0	15.0	0.000467	0.000066

CASE C.S1

X(mm)	X(in)	Cfx	Cfz
12.7	0.5	0.00111	0.00093
25.4	1.0	0.00110	0.00080
43.2	1.7	0.00079	0.000475
101.6	4.0	0.00055	0.000268
152.4	6.0	0.00059	0.000244
228.6	9.0	0.00053	0.000162
295.3	11.6	0.000536	0.000134
381.0	15.0	0.000622	0.000109

CASE D.S0

X(mm)	X(in)	Cfx	Cfz
-152.4	-6.0	0.00310	0
6.4	0.25	0.00186	0
12.5	0.5	0.00177	0
25.4	1.0	0.00169	0
50.8	2.0	0.00113	0
114.3	4.5	0.000695	0
152.4	6.0	0.000405	0
221.0	8.7	0.000142	0
304.8	12.0	0.000000	0
368.3	14.5	0.000000	0

CASE D.S1/2

X(mm)	X(in)	Cfx	Cfz
6.4	0.25	0.00212	-
12.5	0.5	0.001995	-
25.4	1.0	0.001955	-
50.8	2.0	0.001425	-
114.3	4.5	0.000710	-
152.4	6.0	0.000530	-
221.0	8.7	0.000315	-
304.8	12.0	0.000215	-

CASE D.S1

Y(mm)	X(in)	Cfx	Cfz
6.4	0.25	0.00248	0.00156
12.5	0.5	0.00277	0.00129
25.4	1.0	0.00246	0.00112
50.8	2.0	0.00188	0.00075
114.3	4.5	0.00114	0.00041
152.4	6.0	0.00125	0.00042
221.0	8.7	0.000575	0.00021
304.8	12.0	0.000595	0.00023

Table C.3 Surface shear stress measurements with laser oil-flow interferometer.

Cf circumfrential distribution

	Cfx Case B.S0		
Theta(deg)	-761mm	-304mm	-76mm
180.0	0.00332	0.00300	0.00127
157.5	0.00322	0.00283	0.00113
135.0	0.00329	0.00296	0.00133
112.5	0.00321	0.00288	0.00129
90.0	0.00325	0.00300	0.00135
90.0	0.00325	0.00308	0.00131
67.5	0.00324	0.00300	0.00129
45.0	0.00325	0.00293	0.00123
22.5	0.00325	0.00291	0.00108
0.0	0.00329	0.00306	0.00113
-22.5	0.00322	0.00304	0.00117
-45.0	0.00317	0.00306	0.00125
-67.5	0.00325	0.00311	0.00131
-90.0	0.00337	0.00304	0.00133
-112.5	0.00330	0.00300	0.00137
-135.0	0.00329	0.00296	0.00146
-157.5	0.00322	0.00285	0.00119
-180.0	0.00332	0.00300	0.00127

	Cfx Case C.S0		
Theta(deg)	-457mm	-304mm	-76mm
180.0	0.00295	0.00289	0.00054
157.5	0.00297	0.00280	0.00045
135.0	0.00285	0.00272	0.00040
112.5	0.00290	0.00280	0.00054
90.0	0.00295	0.00289	0.00067
67.5	0.00292	0.00280	0.00054
45.0	0.00297	0.00277	0.00054
22.5	0.00292	0.00285	0.00052
0.0	0.00292	0.00294	0.00056
-22.5	0.00282	0.00277	0.00040
-45.0	0.00290	0.00294	0.00047
-67.5	0.00295	0.00295	0.00056
-90.0	0.00299	0.00299	0.00065
-112.5	0.00299	0.00289	0.00054
-135.0	0.00295	0.00275	0.00045
-157.5	0.00295	0.00275	0.00043
-180.0	0.00295	0.00289	0.00054

	Cfx Case D.S0			
Theta(deg)	6mm	152mm	304mm	-457mm
180.0	0.00186	0.00034	0.00009	0.00295
135.0	0.00200	0.00029	0.00001	0.00285
90.0	0.00220	0.00041	0.00013	0.00295
45.0	0.00192	0.00036	0.00009	0.00297
0.0	0.00202	0.00036	0.00006	0.00292
-45.0	0.00186	0.00018	0.00001	0.00290
-90.0	0.00220	0.00046	0.00013	0.00299
-135.0	0.00196	0.00024	0.00001	0.00295
-180.0	0.00186	0.00034	0.00009	0.00295

Table C.4 Surface shear stress measurements with preston tube.

Case A.S1 Station= 1
X=-330.2mm Tunnel Run#= 632 Ue/Uref= 1.000 Date= 426.88 Time=15.21
Bias Corrected data using 1/sqrt(U*U + V*V + W*W + (.01Ur)^2)

					<-- normalized by 0.001 Ue^2 -->						<---------- normalized by 0.0001 Ue^3 ---------->									
LR	Y(mm)	U/Ue	V/Ue	W/Ue	uu	vv	ww	uv	vw	uw	uuu	uvv	uww	vuu	vvv	vww	wuu	wvv	www	uvw
1	0.00	0.000	0.000	1.000	0.00	0.00	0.00	-2.44	2.66	0.00	0.00	0.00	0.00	0.00	0.00	0.00	0.00	0.00	0.00	0.00
2	0.25	0.568	0.013	0.356	15.26	3.34	19.13	-1.80	1.79	-7.60	-2.29	-0.10	-6.94	1.15	0.38	1.96	5.37	0.19	5.24	-1.13
3	0.38	0.608	0.012	0.315	13.16	4.07	16.04	-1.83	1.92	-5.19	-1.43	-0.55	-2.90	0.99	0.43	1.51	2.59	0.36	2.73	-0.73
4	0.51	0.634	0.000	0.293	12.20	3.94	14.66	-1.99	1.94	-4.27	-1.49	-0.62	-2.82	1.09	0.74	2.01	2.18	0.76	3.32	-1.01
5	0.63	0.650	0.002	0.280	11.74	4.13	14.14	-1.99	2.01	-4.12	-1.38	-0.60	-2.32	0.99	0.76	1.40	1.58	0.40	2.60	-0.75
6	0.76	0.663	0.002	0.263	11.20	4.15	13.84	-1.98	1.97	-3.85	-0.56	-0.43	-1.92	0.96	0.65	1.43	1.00	0.38	2.53	-0.50
7	1.02	0.683	0.002	0.240	11.01	4.04	13.02	-1.99	1.75	-4.10	-1.30	-0.60	-1.90	0.94	0.72	1.53	1.44	0.53	2.40	-0.63
8	1.27	0.702	0.003	0.224	10.96	4.16	12.32	-2.17	2.07	-4.20	-1.49	-0.62	-1.44	1.06	0.80	1.47	1.28	0.55	2.01	-0.59
9	1.52	0.712	0.001	0.211	10.07	4.27	11.77	-2.11	2.18	-4.16	-1.70	-0.54	-1.66	1.04	0.91	1.34	1.36	0.61	2.61	-0.52
10	1.78	0.728	0.002	0.199	9.99	4.20	11.06	-2.13	2.13	-3.99	-1.64	-0.63	-1.63	0.99	0.70	1.30	1.56	0.61	2.12	-0.67
11	2.03	0.738	0.003	0.190	9.67	4.29	10.89	-2.09	2.21	-3.98	-1.45	-0.70	-1.56	1.00	0.96	1.57	1.25	0.88	2.40	-0.64
12	2.29	0.743	0.003	0.183	9.41	4.35	10.02	-2.24	2.11	-3.64	-1.16	-0.61	-1.56	0.89	0.76	1.46	1.17	0.82	2.28	-0.62
13	2.54	0.750	0.002	0.176	9.51	4.17	10.35	-2.25	2.20	-3.79	-1.77	-0.73	-1.58	1.06	0.72	1.48	1.45	0.86	2.53	-0.85
14	2.79	0.758	0.005	0.170	8.85	4.37	9.87	-2.27	2.19	-3.44	-1.70	-0.65	-1.12	0.93	0.89	1.39	1.13	0.79	2.80	-0.61
15	3.30	0.774	0.003	0.157	8.38	4.27	9.43	-2.21	2.00	-3.39	-1.57	-0.51	-1.18	0.68	0.63	1.09	1.04	0.62	1.77	-0.51
16	3.81	0.785	0.002	0.150	7.77	4.19	8.72	-2.06	1.99	-3.04	-1.22	-0.62	-1.26	0.75	0.65	1.03	1.13	0.69	2.23	-0.61
17	4.32	0.795	0.005	0.144	7.88	4.38	8.56	-2.19	2.12	-2.84	-1.26	-0.52	-0.94	0.70	0.73	1.10	0.82	0.70	2.03	-0.53
18	4.83	0.807	0.005	0.137	7.46	4.30	8.41	-2.17	2.13	-2.86	-1.54	-0.56	-1.17	0.71	0.84	1.40	1.12	0.87	2.27	-0.65
19	5.59	0.820	0.004	0.126	7.33	4.22	7.83	-1.98	2.01	-2.44	-1.74	-0.57	-0.94	0.58	0.80	1.24	0.67	0.84	2.42	-0.42
20	6.35	0.831	0.004	0.117	6.97	4.23	7.43	-2.09	1.94	-2.25	-1.32	-0.76	-0.92	0.59	1.02	1.06	0.81	0.71	1.67	-0.47
21	7.11	0.843	0.005	0.110	6.56	3.99	7.22	-1.95	1.90	-2.20	-1.81	-0.64	-1.13	0.69	0.92	1.16	0.77	0.88	1.99	-0.62
22	8.38	0.866	0.008	0.095	6.31	3.61	6.27	-1.83	1.66	-1.95	-2.06	-0.68	-0.96	0.70	0.97	0.84	0.85	0.74	2.09	-0.40
23	10.16	0.895	0.007	0.075	5.34	3.10	5.42	-1.62	1.51	-1.73	-2.22	-0.75	-0.97	0.85	1.02	0.97	0.91	0.82	2.15	-0.46
24	12.70	0.938	0.008	0.044	3.87	2.34	3.74	-1.13	0.95	-1.30	-2.20	-0.81	-1.03	0.85	0.97	0.75	0.93	0.63	1.96	-0.45
25	15.24	0.973	0.008	0.019	2.15	1.59	2.07	-0.66	0.51	-0.67	-1.51	-0.52	-0.70	0.64	0.75	0.53	0.62	0.42	1.24	-0.24
26	17.78	0.991	0.006	0.005	0.82	0.84	0.87	-0.24	0.20	-0.21	-0.60	-0.23	-0.28	0.27	0.41	0.24	0.23	0.16	0.51	-0.08
27	20.32	0.997	0.006	0.000	0.24	0.39	0.28	-0.06	0.06	-0.06	-0.11	-0.06	-0.04	0.08	0.17	0.06	0.05	0.06	0.06	-0.02
28	22.86	1.000	0.005	0.000	0.09	0.16	0.15	0.00	0.00	-0.02	0.00	0.00	0.00	0.00	0.02	0.01	0.00	0.00	0.00	0.00
29	25.40	1.001	0.006	0.000	0.07	0.13	0.13	0.00	0.01	-0.01	0.00	0.00	0.00	0.00	0.03	0.00	0.00	0.00	0.01	0.00
30	38.10	1.001	0.008	-0.001	0.05	0.09	0.12	0.00	0.00	-0.01	0.00	0.00	0.00	0.00	0.00	0.00	0.00	0.00	0.00	0.00
31	50.80	1.002	0.008	-0.001	0.05	0.09	0.12	0.00	0.00	-0.01	0.00	0.00	0.00	0.00	0.00	0.00	0.00	0.00	0.01	0.00

Table C.5 LDV measurements for cases A, B, C, and D.

Case A.S1 Station= 2
X=-152.4mm Tunnel Run#= 633 Ue/Uref= 0.996 Date= 427.88 Time=12.09
Bias Corrected data using 1/sqrt(U*U + V*V + W*W + (.01Ur)^2)

					<-- normalized by 0.001 Ue^2 -->						<---------- normalized by 0.0001 Ue^3 ---------->								
LR	Y(mm)	U/Ue	V/Ue	W/Ue	uu	vv	ww	uv	vw	uw	uuu	uvv	uww	vuu	vvv	vww	wuu	wvv	www	uvw
1	0.00	0.000	0.000	1.000	0.00	0.00	0.00	-2.51	2.73	0.00	0.00	0.00	0.00	0.00	0.00	0.00	0.00	0.00	0.00	0.00
2	0.25	0.565	0.020	0.344	14.50	3.49	20.60	-1.56	1.29	-7.07	-1.59	-0.20	-5.54	0.78	0.05	1.82	3.96	0.20	5.09	-0.81
3	0.38	0.599	0.019	0.316	13.67	4.23	17.78	-1.69	1.24	-5.29	-0.53	-0.31	-3.64	0.81	0.32	1.58	1.97	0.03	2.42	-0.56
4	0.51	0.622	0.004	0.303	13.15	4.14	15.46	-2.17	2.17	-4.80	-1.21	-0.77	-2.88	1.33	0.82	1.70	2.39	0.66	2.63	-0.79
5	0.63	0.639	0.005	0.284	13.04	4.27	14.56	-2.17	2.20	-4.61	-1.70	-0.67	-2.31	1.01	0.84	1.49	1.72	0.74	2.66	-0.77
6	0.76	0.658	0.005	0.265	12.03	4.36	14.24	-1.99	2.04	-4.12	-0.98	-0.70	-2.15	0.73	1.21	1.89	1.41	0.65	3.13	-0.41
7	1.02	0.681	0.005	0.243	11.89	4.26	13.25	-2.05	2.10	-4.52	-1.63	-0.60	-2.06	0.96	0.83	1.62	1.71	0.71	2.47	-0.66
8	1.27	0.697	0.004	0.223	11.55	4.27	12.82	-2.32	2.42	-4.36	-1.95	-0.76	-1.80	1.18	0.83	1.79	1.53	0.89	2.73	-0.71
9	1.52	0.715	0.005	0.208	11.17	4.24	12.42	-2.23	2.30	-4.32	-1.30	-0.73	-2.45	1.10	1.03	1.79	1.72	0.86	3.76	-0.82
10	1.78	0.727	0.006	0.195	10.35	4.27	11.87	-2.16	2.33	-4.33	-1.49	-0.64	-2.07	0.93	0.97	1.93	1.63	0.94	3.88	-0.70
11	2.03	0.739	0.006	0.187	10.47	4.29	11.51	-2.28	2.42	-4.43	-2.30	-0.86	-2.41	1.48	0.89	1.77	2.08	0.99	3.52	-0.92
12	2.29	0.751	0.007	0.177	10.29	4.36	11.01	-2.30	2.41	-4.39	-2.01	-0.86	-2.08	1.35	1.01	1.88	2.00	1.14	3.41	-1.01
13	2.54	0.754	0.007	0.172	9.63	4.35	10.66	-2.22	2.49	-3.95	-1.81	-0.88	-1.92	1.29	1.02	1.84	1.64	1.12	2.89	-0.89
14	2.79	0.761	0.006	0.166	9.40	4.30	10.32	-2.23	2.34	-3.92	-1.62	-0.80	-1.80	1.21	0.82	1.55	1.55	0.84	2.77	-0.93
15	3.30	0.772	0.006	0.156	9.31	4.36	9.94	-2.32	2.33	-3.81	-2.22	-1.07	-1.73	1.26	1.07	1.78	1.34	1.10	3.11	-1.00
16	3.81	0.781	0.007	0.149	8.79	4.51	9.54	-2.38	2.49	-3.47	-2.06	-0.92	-1.63	1.30	1.23	1.71	1.45	1.21	3.09	-0.86
17	4.32	0.786	0.007	0.144	8.45	4.68	8.93	-2.27	2.40	-3.26	-1.69	-0.91	-1.43	1.03	1.02	1.52	1.32	0.96	2.86	-0.85
18	4.83	0.796	0.007	0.139	8.12	4.57	8.64	-2.37	2.35	-3.20	-1.63	-0.79	-1.27	0.75	1.03	1.35	1.23	1.00	2.60	-0.66
19	5.59	0.808	0.008	0.130	7.59	4.77	8.10	-2.25	2.35	-2.60	-1.29	-0.83	-0.84	0.83	1.13	1.38	0.78	1.06	2.45	-0.65
20	6.35	0.816	0.009	0.122	7.39	4.52	7.52	-2.25	2.16	-2.53	-1.49	-0.63	-0.85	0.76	0.95	0.99	0.86	0.76	1.83	-0.45
21	7.11	0.828	0.010	0.118	7.16	4.56	7.26	-2.30	2.14	-2.40	-1.78	-0.85	-0.89	0.83	1.13	1.09	0.87	0.92	1.94	-0.63
22	8.38	0.841	0.009	0.107	6.53	4.37	6.84	-2.09	2.09	-2.16	-1.49	-0.72	-0.82	0.72	1.15	0.85	0.93	0.78	1.48	-0.50
23	10.16	0.869	0.011	0.091	6.03	3.86	6.22	-1.86	1.72	-1.74	-1.50	-0.66	-0.74	0.65	1.01	0.80	0.69	0.69	1.57	-0.36
24	12.70	0.897	0.013	0.070	5.29	3.25	5.32	-1.63	1.59	-1.70	-2.05	-0.74	-0.92	0.87	0.93	0.91	1.06	0.72	1.87	-0.53
25	15.24	0.931	0.014	0.047	4.26	2.76	4.27	-1.33	1.24	-1.45	-2.08	-0.78	-1.03	0.82	1.01	0.83	0.88	0.72	2.15	-0.44
26	17.78	0.961	0.011	0.021	2.74	1.80	2.65	-0.81	0.75	-0.96	-1.81	-0.64	-0.85	0.67	0.81	0.71	0.73	0.54	1.72	-0.36
27	20.32	0.981	0.010	0.006	1.52	1.22	1.45	-0.43	0.43	-0.50	-1.15	-0.41	-0.44	0.42	0.55	0.44	0.49	0.39	1.00	-0.22
28	22.86	0.990	0.011	-0.003	0.71	0.75	0.64	-0.24	0.17	-0.20	-0.48	-0.21	-0.20	0.26	0.40	0.20	0.23	0.16	0.31	-0.10
29	25.40	0.999	0.009	0.001	0.32	0.40	0.32	-0.07	0.05	-0.05	-0.18	-0.08	-0.03	0.11	0.17	0.06	0.06	0.05	0.09	-0.03
30	27.94	1.000	0.011	-0.007	0.11	0.21	0.17	-0.01	0.02	-0.03	0.00	-0.01	0.00	0.01	0.06	0.02	0.00	0.01	0.01	0.00
31	38.10	0.998	0.013	-0.006	0.06	0.08	0.11	0.00	0.00	-0.01	0.00	0.00	0.01	0.00	0.00	0.00	0.00	0.00	0.01	0.00
32	50.80	1.003	0.014	-0.005	0.05	0.07	0.10	0.00	0.00	-0.01	0.00	0.00	0.00	0.00	0.00	0.00	0.00	0.00	0.01	0.00

Table C.5 Continued.

Case A.S1 Station= 3
X= -12.7mm Tunnel Run#= 634 Ue/Uref= 0.996 Date= 427.88 Time=12.57
Bias Corrected data using 1/sqrt(U*U + V*V + W*W + (.01Ur)^2)

					<-- normalized by 0.001 Ue^2 -->						<---------- normalized by 0.0001 Ue^3 ---------->								
LR	Y(mm)	U/Ue	V/Ue	W/Ue	uu	vv	ww	uv	vw	uw	uuu	uvv	uww	vuu	vvv	vww	wuu	wvv	www	uvw
1	0.00	0.000	0.000	1.000	0.00	0.00	0.00	-2.50	2.72	0.00	0.00	0.00	0.00	0.00	0.00	0.00	0.00	0.00	0.00	0.00
2	0.25	0.556	0.015	0.369	15.99	3.17	20.78	-1.83	1.95	-8.39	-2.83	-0.37	-7.15	1.11	-0.09	2.13	5.32	0.36	6.08	-1.15
3	0.38	0.593	0.015	0.334	14.55	4.10	17.45	-1.95	2.10	-6.23	-1.21	-0.58	-4.67	1.25	1.05	1.63	3.50	0.58	5.43	-0.92
4	0.51	0.620	0.005	0.306	13.29	4.05	15.79	-2.01	2.26	-5.02	-1.34	-0.66	-2.97	0.96	0.59	1.59	2.48	0.66	4.14	-0.82
5	0.63	0.639	0.007	0.283	12.73	4.24	14.56	-2.19	2.29	-4.43	-1.23	-0.70	-2.07	0.97	0.83	1.17	1.35	0.60	3.27	-0.58
6	0.76	0.653	0.007	0.269	12.34	4.23	14.19	-2.33	2.54	-4.57	-1.02	-0.49	-2.65	0.98	0.75	1.54	1.82	0.92	3.32	-0.71
7	1.02	0.675	0.006	0.245	12.06	4.33	13.18	-2.38	2.31	-4.39	-1.25	-0.69	-1.80	0.94	1.02	1.34	1.43	0.63	2.62	-0.47
8	1.27	0.695	0.008	0.226	11.72	4.24	12.87	-2.43	2.48	-4.47	-1.71	-0.71	-2.21	1.11	1.08	1.66	1.87	0.84	2.93	-0.72
9	1.52	0.712	0.008	0.211	11.32	4.24	12.45	-2.31	2.45	-4.40	-1.23	-0.79	-2.09	1.04	1.08	1.77	1.59	0.93	3.21	-0.69
10	1.78	0.725	0.007	0.196	10.82	4.15	11.62	-2.38	2.47	-4.19	-1.54	-0.68	-2.15	1.08	0.80	1.54	1.70	0.86	3.70	-0.70
11	2.03	0.734	0.009	0.186	10.98	4.30	11.51	-2.46	2.69	-4.50	-2.23	-1.00	-2.14	1.41	1.24	1.84	2.04	1.18	2.87	-0.97
12	2.29	0.745	0.008	0.179	10.64	4.16	10.97	-2.49	2.52	-4.25	-2.46	-0.89	-1.88	1.45	0.95	1.61	1.97	0.99	2.80	-0.92
13	2.54	0.755	0.008	0.169	10.15	4.17	10.87	-2.33	2.50	-4.19	-2.42	-0.89	-2.00	1.32	0.82	1.77	1.70	0.98	3.48	-0.88
14	2.79	0.760	0.009	0.165	9.91	4.28	10.68	-2.48	2.53	-4.24	-2.51	-0.93	-2.53	1.41	0.94	1.79	2.04	1.04	3.48	-0.99
15	3.30	0.770	0.007	0.153	9.45	4.25	9.79	-2.28	2.40	-3.74	-2.15	-0.75	-1.54	1.21	0.71	1.42	1.63	0.94	2.52	-0.83
18	3.81	0.779	0.010	0.147	9.24	4.45	9.48	-2.49	2.57	-3.86	-1.94	-0.87	-1.67	1.13	1.02	1.51	1.57	1.05	2.75	-0.80
17	4.32	0.788	0.011	0.141	8.77	4.61	9.20	-2.44	2.50	-3.47	-2.20	-0.88	-1.37	1.29	0.97	1.66	1.41	1.08	2.84	-0.83
19	4.83	0.797	0.010	0.134	8.39	4.51	8.82	-2.39	2.54	-3.45	-1.93	-0.89	-1.01	1.14	1.04	1.37	1.16	1.11	2.55	-0.76
20	5.59	0.803	0.011	0.129	7.92	4.67	8.17	-2.23	2.33	-2.79	-1.66	-0.70	-1.00	0.91	1.16	1.33	1.00	0.97	2.67	-0.57
21	6.35	0.810	0.010	0.124	7.47	4.56	7.90	-2.33	2.34	-2.67	-1.72	-0.80	-1.07	0.94	1.06	1.19	1.28	1.02	2.29	-0.71
22	7.11	0.824	0.010	0.118	7.41	4.80	7.52	-2.41	2.29	-2.50	-1.87	-0.88	-0.81	1.10	1.25	1.03	1.00	0.90	1.67	-0.62
23	8.38	0.835	0.011	0.110	6.99	4.45	6.90	-2.19	2.21	-2.31	-1.56	-0.58	-0.52	0.64	0.99	0.72	0.90	0.62	1.45	-0.36
24	10.16	0.854	0.014	0.099	6.32	4.29	6.65	-2.05	2.06	-2.02	-1.64	-0.57	-0.72	0.73	1.06	0.85	0.80	0.79	1.29	-0.45
25	12.70	0.876	0.014	0.081	5.79	3.79	5.84	-1.79	1.77	-1.71	-1.49	-0.61	-0.74	0.67	1.01	0.72	0.61	0.67	1.64	-0.36
26	15.24	0.897	0.014	0.064	5.03	3.25	5.05	-1.61	1.59	-1.42	-1.70	-0.69	-0.67	0.75	1.06	0.79	0.67	0.72	1.55	-0.38
27	17.78	0.923	0.018	0.048	4.50	2.92	4.35	-1.43	1.34	-1.31	-1.77	-0.68	-0.78	0.78	0.98	0.79	0.71	0.66	1.59	-0.36
28	20.32	0.949	0.015	0.028	3.39	2.40	3.38	-1.06	1.04	-1.09	-1.87	-0.67	-0.84	0.71	1.05	0.78	0.70	0.71	1.70	-0.38
29	22.86	0.971	0.010	0.008	2.23	1.59	2.11	-0.72	0.60	-0.75	-1.71	-0.60	-0.77	0.71	0.74	0.65	0.65	0.47	1.41	-0.34
30	25.40	0.988	0.011	-0.003	1.11	1.07	1.16	-0.38	0.35	-0.36	-0.80	-0.33	-0.36	0.36	0.58	0.36	0.36	0.32	0.74	-0.17
31	27.94	0.992	0.010	-0.009	0.62	0.74	0.65	-0.24	0.21	-0.20	-0.40	-0.23	-0.20	0.24	0.44	0.24	0.20	0.22	0.36	-0.12
32	30.48	0.996	0.009	-0.012	0.25	0.38	0.30	-0.06	0.06	-0.06	-0.09	-0.04	-0.04	0.06	0.16	0.06	0.04	0.05	0.10	-0.02
33	38.10	1.000	0.010	-0.013	0.07	0.10	0.12	0.00	0.00	-0.02	0.00	0.00	0.00	0.00	0.01	0.00	0.00	0.00	0.00	0.00
34	50.80	1.004	0.010	-0.012	0.06	0.08	0.12	0.00	0.00	-0.01	0.00	0.00	0.00	0.00	0.00	0.00	0.00	0.00	0.01	0.00

Table C.5 Continued.

Case A.S1 Station= 4
X= 6.3mm Tunnel Run#= 635 Ue/Uref= 0.997 Date= 427.88 Time=13.46
Bias Corrected data using 1/sqrt(U*U + V*V + W*W + (.01Ur)^2)

					<-- normalized by 0.001 Ue^2 -->						<---------- normalized by 0.0001 Ue^3 ---------->									
LR	Y(mm)	U/Ue	V/Ue	W/Ue	uu	vv	ww	uv	vw	uw	uuu	uvv	uww	vuu	vvv	vww	wuu	wvv	www	uvw
1	0.00	0.000	0.000	0.000	0.00	0.00	0.00	-1.96	-1.21	0.00	0.00	0.00	0.00	0.00	0.00	0.00	0.00	0.00	0.00	0.00
2	0.25	0.529	0.019	0.296	12.00	2.77	13.23	-1.87	-0.10	-1.40	0.87	-0.04	0.18	0.29	-0.06	0.56	-2.53	-0.58	-1.48	0.94
3	0.38	0.594	0.021	0.288	10.80	3.24	13.27	-1.49	0.41	-2.55	1.16	-0.15	-0.46	0.56	0.16	0.60	-0.18	-0.37	-1.45	0.54
4	0.51	0.629	0.011	0.281	10.54	3.32	13.01	-1.48	1.19	-3.01	1.01	-0.13	-0.78	0.45	0.26	0.33	0.31	-0.32	0.34	0.35
5	0.63	0.651	0.010	0.269	10.20	3.42	12.55	-1.34	1.54	-3.21	0.90	-0.08	-0.76	0.43	0.05	0.37	0.50	-0.06	0.94	0.12
6	0.76	0.666	0.011	0.258	10.67	3.72	12.37	-1.50	1.75	-3.39	0.86	-0.09	-1.16	0.42	0.41	0.54	0.80	0.16	1.48	0.07
7	1.02	0.682	0.009	0.240	11.20	4.00	12.51	-1.91	2.15	-3.53	0.01	-0.43	-1.20	0.54	0.58	0.83	0.84	0.55	1.59	-0.28
8	1.27	0.699	0.008	0.219	10.75	4.02	11.90	-2.00	2.33	-3.83	-0.33	-0.58	-1.14	0.59	0.69	1.28	0.52	0.70	1.88	-0.23
9	1.52	0.715	0.011	0.205	10.76	4.11	11.71	-2.14	2.40	-4.01	-0.88	-0.63	-1.72	0.91	1.00	1.34	1.36	0.78	2.61	-0.49
10	1.78	0.728	0.009	0.194	10.60	4.11	11.34	-2.17	2.49	-3.96	-1.86	-0.82	-1.97	1.15	1.03	1.75	1.67	1.05	2.89	-0.66
11	2.03	0.735	0.010	0.183	10.21	4.04	11.10	-2.19	2.48	-4.04	-2.15	-0.82	-1.67	1.11	0.83	1.42	1.69	0.86	3.18	-0.64
12	2.29	0.748	0.009	0.172	10.13	4.16	10.84	-2.33	2.37	-3.82	-2.31	-0.82	-1.91	1.30	0.82	1.67	1.71	1.01	2.88	-0.76
13	2.54	0.755	0.009	0.165	9.60	4.17	10.52	-2.22	2.45	-3.87	-2.00	-0.79	-2.03	1.20	1.01	1.65	1.61	1.06	3.09	-0.87
14	2.79	0.760	0.011	0.161	9.47	4.21	10.21	-2.27	2.36	-3.77	-1.41	-0.86	-1.55	1.23	0.87	1.54	1.40	0.90	2.94	-0.83
15	3.30	0.773	0.011	0.154	9.36	4.35	10.17	-2.38	2.72	-3.93	-1.95	-0.94	-1.83	1.25	1.05	1.96	1.73	1.36	3.53	-1.02
16	3.81	0.782	0.010	0.147	9.15	4.47	9.36	-2.39	2.47	-3.59	-2.37	-0.90	-1.55	1.26	1.03	1.70	1.67	1.15	2.83	-0.82
17	4.32	0.791	0.011	0.139	8.61	4.59	8.95	-2.44	2.42	-3.30	-1.92	-0.79	-1.19	0.97	1.18	1.40	1.27	1.08	2.53	-0.63
18	4.83	0.795	0.010	0.133	8.37	4.51	8.79	-2.39	2.46	-3.21	-2.11	-0.87	-1.29	1.08	1.11	1.69	1.26	1.15	2.88	-0.80
19	5.59	0.805	0.010	0.127	7.95	4.51	7.77	-2.31	2.21	-2.78	-1.75	-0.76	-1.03	0.97	1.17	1.09	1.10	0.98	1.91	-0.60
20	6.35	0.814	0.012	0.123	7.73	4.63	7.89	-2.37	2.36	-2.71	-1.75	-0.74	-0.91	0.91	1.08	1.20	1.01	0.97	1.85	-0.63
21	7.11	0.821	0.011	0.117	7.14	4.46	7.43	-2.13	2.11	-2.26	-1.43	-0.63	-0.57	0.63	1.05	0.83	0.75	0.85	1.54	-0.37
22	8.38	0.834	0.010	0.109	6.88	4.43	7.11	-2.14	2.23	-2.26	-1.63	-0.77	-0.88	0.81	1.13	1.01	0.92	0.92	1.68	-0.57
23	10.16	0.854	0.012	0.100	6.45	4.37	6.69	-2.10	2.04	-1.98	-1.66	-0.72	-0.49	0.72	1.12	0.70	0.64	0.70	1.47	-0.36
24	12.70	0.880	0.014	0.083	5.77	3.78	5.81	-1.82	1.80	-1.65	-1.59	-0.67	-0.61	0.67	1.11	0.72	0.62	0.71	1.58	-0.33
25	15.24	0.904	0.015	0.063	5.16	3.51	5.16	-1.76	1.69	-1.62	-2.13	-0.82	-0.82	0.88	1.31	0.89	0.83	0.87	1.64	-0.48
26	17.78	0.930	0.014	0.045	4.26	2.81	4.38	-1.32	1.34	-1.37	-1.86	-0.75	-0.91	0.77	1.09	0.99	0.83	0.76	1.95	-0.48
27	20.32	0.950	0.014	0.028	3.37	2.30	3.36	-1.11	1.03	-1.12	-1.95	-0.70	-0.82	0.79	1.07	0.79	0.81	0.71	1.81	-0.41
28	22.86	0.969	0.014	0.013	2.36	1.85	2.33	-0.78	0.78	-0.79	-1.60	-0.60	-0.73	0.66	0.95	0.68	0.67	0.61	1.46	-0.38
29	25.40	0.984	0.014	0.002	1.46	1.29	1.52	-0.45	0.47	-0.52	-0.95	-0.37	-0.48	0.41	0.61	0.45	0.46	0.38	1.00	-0.21
30	27.94	0.994	0.013	-0.007	0.82	0.85	0.78	-0.27	0.23	-0.22	-0.57	-0.26	-0.21	0.29	0.46	0.25	0.25	0.23	0.43	-0.11
31	30.48	0.997	0.013	-0.011	0.39	0.52	0.40	-0.14	0.10	-0.08	-0.21	-0.14	-0.07	0.16	0.29	0.12	0.07	0.09	0.15	-0.04
32	33.02	1.000	0.013	-0.013	0.20	0.31	0.23	-0.04	0.04	-0.03	-0.06	-0.03	-0.02	0.06	0.14	0.06	0.02	0.04	0.05	-0.01
33	38.10	1.000	0.012	-0.013	0.07	0.11	0.12	0.00	0.00	-0.01	0.00	0.00	0.00	0.00	0.01	0.00	0.00	0.00	0.01	0.00
34	50.80	1.002	0.013	-0.013	0.05	0.08	0.11	0.00	0.00	-0.02	0.00	0.00	0.00	0.00	0.00	0.00	0.00	0.00	0.00	0.00

Table C.5 Continued.

Case A.S1 Station= 5
X= 12.7mm Tunnel Run#= 636 Ue/Uref= 0.998 Date= 428.88 Time= 9.06
Bias Corrected data using 1/sqrt(U*U + V*V + W*W + (.01Ur)^2)

					<-- normalized by 0.001 Ue^2 -->						<---------- normalized by 0.0001 Ue^3 ---------->							
LR	Y(mm)	U/Ue	V/Ue	W/Ue	uu	vv	ww	uv	vw	uw	uuu	uvv	uww	vuu	vvv	vww	wuu	wvv	www	uvw
1	0.00	0.000	0.000	0.000	0.00	0.00	0.00	-1.82	-0.85	0.00	0.00	0.00	0.00	0.00	0.00	0.00	0.00	0.00	0.00	0.00
2	0.25	0.519	0.015	0.245	11.57	2.40	10.01	-1.68	-0.28	1.07	-0.74	0.09	-0.09	0.51	0.27	0.42	-1.58	-0.21	-0.76	0.64
3	0.38	0.580	0.017	0.253	10.26	2.95	10.66	-1.78	0.16	-0.80	-0.29	0.03	0.13	0.47	0.08	0.50	-0.88	-0.41	-1.55	0.66
4	0.51	0.616	0.006	0.252	9.97	2.85	10.91	-1.70	0.35	-1.66	0.22	-0.20	0.17	0.41	0.25	0.36	-0.18	-0.44	-1.88	0.43
5	0.63	0.641	0.005	0.247	9.48	3.06	10.81	-1.62	0.79	-2.06	0.45	-0.26	-0.28	0.47	0.15	0.09	0.11	-0.32	-0.79	0.31
6	0.76	0.663	0.006	0.243	9.65	3.10	10.86	-1.47	1.25	-2.43	0.79	-0.11	-0.27	0.33	0.22	0.37	0.17	-0.23	-0.52	0.21
7	1.02	0.686	0.007	0.231	9.08	3.35	10.80	-1.43	1.64	-2.74	0.85	-0.18	-0.33	0.33	0.27	0.39	0.31	0.11	0.29	0.03
8	1.27	0.704	0.008	0.217	9.52	3.74	11.37	-1.65	2.03	-3.12	0.04	-0.29	-0.65	0.46	0.41	0.46	0.56	0.22	0.88	-0.06
9	1.52	0.717	0.009	0.210	9.89	3.73	11.21	-1.85	2.20	-3.44	-0.24	-0.28	-1.21	0.40	0.45	0.60	0.86	0.35	1.72	-0.18
10	1.78	0.727	0.009	0.198	10.08	3.91	11.37	-1.94	2.30	-3.83	-0.81	-0.51	-1.13	0.75	0.63	1.11	1.22	0.64	1.71	-0.44
11	2.03	0.737	0.009	0.186	10.07	4.06	10.90	-2.07	2.32	-3.95	-0.98	-0.61	-1.54	1.03	0.64	1.16	1.53	0.73	2.47	-0.55
12	2.29	0.743	0.009	0.179	9.90	4.22	10.75	-2.17	2.43	-3.93	-1.43	-0.81	-1.51	0.98	0.94	1.34	1.56	0.93	2.25	-0.66
13	2.54	0.750	0.009	0.170	9.55	4.06	10.60	-2.06	2.39	-3.88	-1.47	-0.57	-1.51	0.94	0.66	1.20	1.22	0.82	2.67	-0.56
14	2.79	0.760	0.008	0.163	9.59	4.17	10.43	-2.14	2.36	-3.99	-1.56	-0.69	-1.57	1.01	0.82	1.49	1.61	0.96	2.81	-0.67
15	3.30	0.769	0.011	0.154	9.26	4.24	10.06	-2.25	2.49	-3.84	-1.88	-0.70	-1.37	1.08	0.91	1.51	1.55	1.08	2.92	-0.78
16	3.81	0.778	0.010	0.147	8.83	4.35	9.37	-2.28	2.41	-3.44	-2.35	-0.96	-1.47	1.27	0.99	1.53	1.57	1.02	2.78	-0.84
17	4.32	0.787	0.012	0.142	8.71	4.61	9.26	-2.42	2.63	-3.53	-1.59	-0.81	-1.58	1.19	1.05	1.56	1.36	1.16	2.82	-0.86
18	4.83	0.795	0.011	0.136	8.44	4.58	8.89	-2.36	2.52	-3.37	-1.99	-0.83	-1.28	1.03	0.92	1.52	1.39	1.10	2.44	-0.89
19	5.59	0.804	0.012	0.129	7.90	4.68	7.91	-2.39	2.41	-2.86	-1.97	-0.85	-0.98	0.99	1.13	1.25	0.96	1.01	2.32	-0.61
20	6.35	0.810	0.013	0.124	7.71	4.63	7.99	-2.32	2.22	-2.79	-1.74	-0.77	-0.99	0.78	1.04	1.12	0.95	0.87	2.15	-0.56
21	7.11	0.820	0.014	0.118	7.49	4.61	7.47	-2.28	2.30	-2.56	-1.76	-0.53	-0.61	0.73	0.94	0.86	0.84	0.74	1.51	-0.41
22	8.38	0.836	0.013	0.110	6.77	4.58	6.95	-2.17	2.13	-2.15	-1.46	-0.63	-0.62	0.80	0.82	0.89	0.71	0.76	1.50	-0.46
23	10.16	0.853	0.014	0.102	6.35	4.32	6.54	-2.05	2.11	-1.85	-1.48	-0.61	-0.51	0.73	0.92	0.71	0.71	0.66	1.29	-0.38
24	12.70	0.878	0.016	0.086	5.90	3.87	5.90	-1.89	1.83	-1.73	-1.56	-0.65	-0.59	0.72	0.90	0.70	0.72	0.66	1.50	-0.43
25	15.24	0.899	0.017	0.070	5.17	3.52	5.09	-1.63	1.62	-1.47	-1.70	-0.68	-0.70	0.68	1.05	0.72	0.64	0.65	1.50	-0.32
26	17.78	0.928	0.015	0.048	4.56	2.91	4.47	-1.48	1.40	-1.39	-2.17	-0.78	-0.80	0.90	0.98	0.78	0.79	0.73	1.80	-0.43
27	20.32	0.953	0.011	0.026	3.20	2.24	3.17	-1.04	0.98	-1.06	-1.81	-0.68	-0.87	0.77	0.97	0.78	0.78	0.71	1.74	-0.40
28	22.86	0.969	0.013	0.012	2.34	1.76	2.37	-0.75	0.71	-0.77	-1.50	-0.59	-0.66	0.62	0.96	0.64	0.64	0.58	1.48	-0.30
29	25.40	0.984	0.012	0.000	1.42	1.25	1.38	-0.43	0.43	-0.43	-0.95	-0.38	-0.43	0.40	0.65	0.40	0.39	0.38	0.89	-0.21
30	27.94	0.993	0.011	-0.007	0.73	0.84	0.77	-0.23	0.24	-0.21	-0.44	-0.23	-0.19	0.22	0.44	0.24	0.20	0.23	0.45	-0.10
31	30.48	0.999	0.011	-0.012	0.34	0.52	0.35	-0.10	0.07	-0.08	-0.14	-0.09	-0.06	0.10	0.34	0.08	0.06	0.07	0.11	-0.03
32	33.02	1.000	0.010	-0.013	0.16	0.28	0.21	-0.03	0.03	-0.03	-0.02	-0.02	-0.01	0.04	0.09	0.03	0.01	0.02	0.04	0.00
33	35.56	1.000	0.011	-0.014	0.09	0.18	0.15	-0.01	0.01	-0.03	0.00	-0.01	0.00	0.01	0.05	0.01	0.01	0.01	0.02	0.00
34	38.10	1.000	0.011	-0.014	0.07	0.12	0.13	0.00	0.00	-0.02	0.00	0.00	0.01	0.00	0.01	0.00	0.00	0.00	0.01	0.00
35	50.80	1.001	0.013	-0.013	0.05	0.08	0.11	0.00	0.00	-0.01	0.00	0.00	0.01	0.00	0.00	0.00	0.00	0.00	0.01	0.00

Table C.5 Continued.

Case A.S1 Station= 6
X= 25.4mm Tunnel Run#= 637 Ue/Uref= 0.999 Date= 428.88 Time=10.45
Bias Corrected data using 1/sqrt(U*U + V*V + W*W + (.01Ur)^2)

					<-- normalized by 0.001 Ue^2 -->						<---------- normalized by 0.0001 Ue^3 ---------->								
LR	Y(mm)	U/Ue	V/Ue	W/Ue	uu	vv	ww	uv	vw	uw	uuu	uvv	uww	vuu	vvv	vww	wuu	wvv	www	uvw
1	0.00	0.000	0.000	0.000	0.00	0.00	0.00	-1.74	-0.69	0.00	0.00	0.00	0.00	0.00	0.00	0.00	0.00	0.00	0.00	0.00
2	0.25	0.528	0.016	0.184	11.60	2.01	9.20	-1.62	-0.37	1.31	-1.57	-0.04	0.41	0.59	-0.07	0.41	-1.53	-0.12	-0.92	0.55
3	0.38	0.576	0.016	0.196	10.02	2.55	9.54	-1.64	-0.08	0.15	-0.59	-0.09	0.64	0.51	0.04	0.44	-0.83	-0.12	-1.45	0.51
4	0.51	0.611	0.005	0.203	9.29	2.63	9.24	-1.75	-0.11	-0.64	-0.03	-0.27	0.40	0.56	0.15	0.29	-0.37	-0.25	-0.60	0.38
5	0.63	0.631	0.006	0.201	8.84	2.84	9.35	-1.79	0.33	-1.53	0.63	-0.17	0.16	0.22	0.21	0.21	0.11	-0.02	-0.45	0.19
6	0.76	0.651	0.005	0.203	8.82	2.90	9.55	-1.77	0.49	-1.71	0.67	-0.07	0.16	0.25	0.14	0.16	0.19	-0.19	-0.43	0.22
7	1.02	0.680	0.008	0.197	8.69	3.13	9.35	-1.69	0.76	-2.06	0.50	-0.16	-0.55	0.30	0.28	0.26	0.37	-0.09	0.60	0.19
8	1.27	0.703	0.008	0.194	8.79	3.23	9.27	-1.69	1.12	-2.34	0.24	-0.34	-0.32	0.50	0.39	0.33	0.34	0.02	0.40	0.12
9	1.52	0.724	0.009	0.188	8.64	3.30	9.58	-1.60	1.34	-2.51	0.44	-0.21	-0.72	0.40	0.33	0.47	0.67	0.10	0.82	0.06
10	1.78	0.737	0.008	0.182	8.64	3.39	9.63	-1.50	1.67	-2.69	-0.14	-0.28	-0.74	0.66	0.38	0.41	0.61	0.24	0.83	-0.12
11	2.03	0.749	0.008	0.172	8.57	3.55	9.45	-1.59	1.86	-2.82	-0.36	-0.38	-0.92	0.65	0.41	0.72	0.73	0.47	1.31	-0.23
12	2.29	0.755	0.010	0.168	8.59	3.67	9.69	-1.53	2.04	-3.11	-0.47	-0.39	-0.83	0.61	0.50	0.74	1.00	0.50	1.49	-0.34
13	2.54	0.760	0.009	0.164	8.59	3.69	9.65	-1.65	2.05	-3.14	-0.28	-0.34	-1.01	0.47	0.53	0.93	0.91	0.60	1.70	-0.32
14	2.79	0.769	0.011	0.159	8.42	4.03	9.74	-1.88	2.32	-3.27	-0.65	-0.53	-1.06	0.73	0.65	1.08	1.00	0.79	1.57	-0.33
15	3.30	0.777	0.009	0.152	8.60	4.04	9.40	-1.89	2.35	-3.43	-1.32	-0.57	-1.21	0.86	0.69	1.08	1.24	0.82	1.92	-0.58
16	3.81	0.782	0.011	0.145	8.37	4.32	9.12	-2.06	2.39	-3.41	-0.99	-0.59	-1.13	0.70	0.88	1.12	1.04	0.94	2.27	-0.52
17	4.32	0.791	0.010	0.138	7.87	4.22	9.03	-2.06	2.35	-3.19	-1.35	-0.55	-1.10	0.83	0.83	1.51	0.99	1.07	2.53	-0.60
18	4.83	0.797	0.011	0.135	7.92	4.49	8.51	-2.22	2.38	-3.17	-1.55	-0.66	-1.16	0.90	1.05	1.17	1.21	0.97	2.15	-0.70
19	5.59	0.808	0.013	0.128	7.90	4.60	8.44	-2.33	2.47	-3.08	-1.76	-0.67	-1.08	1.01	1.12	1.25	1.28	1.00	2.44	-0.67
20	6.35	0.813	0.011	0.123	7.57	4.51	7.78	-2.30	2.38	-2.85	-1.58	-0.82	-0.99	0.90	1.10	1.17	0.94	0.92	2.08	-0.67
21	7.11	0.822	0.012	0.121	7.21	4.65	7.45	-2.28	2.44	-2.54	-1.64	-0.63	-0.89	0.79	1.04	1.01	0.93	0.97	1.95	-0.58
22	8.38	0.836	0.011	0.111	6.69	4.56	7.03	-2.16	2.16	-2.17	-1.71	-0.60	-0.70	0.72	0.94	0.73	0.81	0.77	1.64	-0.42
23	10.16	0.854	0.014	0.102	6.54	4.39	6.64	-2.14	2.20	-1.98	-1.61	-0.62	-0.64	0.76	0.95	0.75	0.74	0.64	1.54	-0.41
24	12.70	0.881	0.011	0.083	5.79	3.88	5.93	-1.87	1.87	-1.67	-1.63	-0.61	-0.62	0.56	1.05	0.75	0.68	0.72	1.54	-0.38
25	15.24	0.903	0.014	0.065	4.91	3.39	5.13	-1.47	1.61	-1.38	-1.43	-0.60	-0.64	0.59	1.11	0.70	0.54	0.77	1.63	-0.35
26	17.78	0.927	0.014	0.049	4.41	2.97	4.58	-1.41	1.43	-1.37	-1.89	-0.73	-0.80	0.82	1.03	0.73	0.77	0.73	1.83	-0.42
27	20.32	0.945	0.014	0.031	3.56	2.41	3.46	-1.17	1.11	-1.26	-1.87	-0.70	-0.89	0.85	0.93	0.82	0.92	0.70	1.78	-0.45
28	22.86	0.965	0.014	0.014	2.57	1.92	2.47	-0.88	0.77	-0.85	-1.67	-0.65	-0.74	0.75	0.97	0.71	0.68	0.62	1.50	-0.33
29	25.40	0.986	0.009	-0.002	1.28	1.12	1.32	-0.41	0.44	-0.44	-0.88	-0.36	-0.47	0.40	0.58	0.47	0.45	0.42	0.92	-0.25
30	27.94	0.992	0.009	-0.009	0.62	0.71	0.70	-0.18	0.20	-0.21	-0.36	-0.16	-0.19	0.19	0.31	0.21	0.20	0.16	0.38	-0.09
31	30.48	0.997	0.010	-0.013	0.29	0.42	0.32	-0.10	0.06	-0.07	-0.11	-0.08	-0.04	0.08	0.17	0.06	0.04	0.06	0.11	-0.02
32	33.02	1.000	0.011	-0.013	0.15	0.27	0.21	-0.04	0.03	-0.04	-0.03	-0.04	-0.01	0.03	0.08	0.03	0.02	0.03	0.04	-0.01
33	35.56	1.002	0.011	-0.015	0.09	0.18	0.14	-0.01	0.02	-0.02	0.00	-0.01	0.00	0.01	0.05	0.01	0.00	0.01	0.00	0.00
34	38.10	1.002	0.012	-0.015	0.07	0.12	0.13	0.00	0.00	-0.02	0.00	0.00	0.00	0.00	0.01	0.00	0.00	0.00	0.00	0.00
35	50.80	1.000	0.014	-0.014	0.05	0.08	0.10	0.00	0.00	-0.01	0.00	0.00	0.00	0.00	0.00	0.00	0.00	0.00	0.00	0.00

Table C.5 Continued.

Case A.S1 Station= 7
X= 50.8mm Tunnel Run#= 638 Ue/Uref= 0.996 Date= 428.88 Time=11.18
Bias Corrected data using 1/sqrt(U*U + V*V + W*W + (.01Ur)^2)

					<-- normalized by 0.001 Ue^2 -->						<---------- normalized by 0.0001 Ue^3 ---------->								
LR	Y(mm)	U/Ue	V/Ue	W/Ue	uu	vv	ww	uv	vw	uw	uuu	uvv	uww	vuu	vvv	vww	wuu	wvv	www	uvw
1	0.00	0.000	0.000	0.000	0.00	0.00	0.00	-1.77	-0.56	0.00	0.00	0.00	0.00	0.00	0.00	0.00	0.00	0.00	0.00	0.00
2	0.25	0.530	0.015	0.136	12.25	1.77	8.31	-1.40	-0.32	1.17	-3.01	-0.01	0.59	0.72	0.50	0.30	-1.33	0.09	-0.19	0.28
3	0.38	0.576	0.016	0.145	10.34	2.25	8.00	-1.54	-0.23	0.69	-2.27	-0.16	0.26	0.86	-0.03	0.50	-0.56	-0.05	-0.04	0.34
4	0.51	0.609	0.005	0.153	8.80	2.27	7.90	-1.62	-0.12	-0.02	-0.87	-0.32	0.22	0.66	0.23	0.32	-0.59	-0.09	-0.12	0.31
5	0.63	0.630	0.005	0.155	8.42	2.49	7.89	-1.74	-0.06	-0.18	-0.56	-0.24	0.56	0.55	0.17	0.29	-0.44	-0.13	0.12	0.34
6	0.76	0.645	0.006	0.157	8.17	2.69	7.91	-1.76	0.05	-0.69	-0.27	-0.31	0.33	0.51	0.28	0.23	-0.08	-0.18	-0.69	0.27
7	1.02	0.674	0.005	0.156	7.77	2.89	7.85	-1.71	0.29	-1.04	0.25	-0.24	0.40	0.31	0.35	0.32	0.24	-0.07	-0.57	0.08
8	1.27	0.694	0.007	0.156	7.46	2.98	7.90	-1.74	0.43	-1.10	0.28	-0.20	0.11	0.38	0.29	0.14	0.07	-0.05	-0.48	0.10
9	1.52	0.716	0.008	0.153	7.66	2.94	7.99	-1.63	0.61	-1.61	0.55	-0.21	0.12	0.29	0.30	0.16	0.05	-0.12	-0.12	0.20
10	1.78	0.733	0.007	0.152	7.65	3.02	7.99	-1.63	0.88	-1.75	0.03	-0.27	0.20	0.58	0.28	0.22	0.10	0.01	-0.02	0.15
11	2.03	0.743	0.009	0.147	7.46	3.12	7.99	-1.53	1.00	-1.97	0.36	-0.24	-0.15	0.41	0.29	0.46	0.27	0.16	0.51	-0.06
12	2.29	0.756	0.007	0.145	7.26	3.20	7.88	-1.50	1.22	-2.03	0.01	-0.29	-0.39	0.48	0.27	0.37	0.29	0.17	0.58	-0.05
13	2.54	0.764	0.010	0.143	7.13	3.11	8.04	-1.51	1.20	-2.26	0.04	-0.19	-0.30	0.38	0.19	0.27	0.43	0.14	0.61	0.02
14	2.79	0.773	0.009	0.142	7.40	3.24	7.85	-1.52	1.34	-2.28	-0.28	-0.26	-0.38	0.45	0.36	0.42	0.51	0.27	0.71	-0.11
15	3.30	0.779	0.010	0.137	7.02	3.57	7.80	-1.44	1.61	-2.23	-0.14	-0.33	-0.42	0.43	0.36	0.62	0.53	0.38	0.60	-0.16
16	3.81	0.795	0.008	0.132	6.98	3.66	7.86	-1.62	1.74	-2.56	-0.32	-0.28	-0.65	0.52	0.43	0.66	0.53	0.52	1.23	-0.21
17	4.32	0.801	0.008	0.130	6.87	3.74	8.00	-1.61	1.86	-2.49	-0.40	-0.32	-0.80	0.50	0.64	0.70	0.56	0.45	1.51	-0.31
18	4.83	0.807	0.007	0.123	6.73	4.00	7.66	-1.65	1.95	-2.36	-0.56	-0.36	-0.74	0.56	0.67	0.89	0.76	0.78	1.45	-0.38
19	5.59	0.814	0.009	0.122	6.63	4.07	7.45	-1.74	1.96	-2.37	-0.90	-0.48	-0.61	0.57	0.68	0.78	0.65	0.77	1.39	-0.39
20	6.35	0.820	0.009	0.117	6.66	4.25	7.34	-1.95	2.13	-2.32	-1.03	-0.47	-0.75	0.56	0.79	0.82	0.73	0.70	1.48	-0.41
21	7.11	0.826	0.008	0.114	6.72	4.39	7.14	-2.04	2.14	-2.31	-1.16	-0.51	-0.61	0.57	0.83	0.91	0.69	0.74	1.73	-0.49
22	8.38	0.838	0.008	0.109	6.50	4.33	6.84	-1.99	2.03	-2.10	-1.41	-0.55	-0.68	0.71	0.89	1.00	0.76	0.83	1.66	-0.51
23	10.16	0.855	0.009	0.099	6.48	4.20	6.45	-2.08	1.99	-1.86	-1.55	-0.58	-0.60	0.71	0.94	0.76	0.69	0.71	1.47	-0.37
24	12.70	0.877	0.011	0.082	5.76	3.89	5.81	-1.90	1.78	-1.64	-1.65	-0.61	-0.58	0.74	1.06	0.73	0.62	0.72	1.38	-0.38
25	15.24	0.896	0.014	0.069	5.19	3.50	5.15	-1.68	1.63	-1.44	-1.44	-0.65	-0.67	0.71	0.96	0.75	0.61	0.67	1.45	-0.33
26	17.78	0.925	0.013	0.048	4.28	2.89	4.32	-1.27	1.27	-1.30	-1.78	-0.66	-0.80	0.72	0.96	0.82	0.69	0.76	1.65	-0.36
27	20.32	0.939	0.015	0.036	3.70	2.53	3.71	-1.12	1.06	-1.15	-1.78	-0.66	-0.74	0.68	0.91	0.75	0.62	0.67	1.70	-0.32
28	22.86	0.959	0.015	0.020	2.89	2.04	2.77	-0.88	0.76	-0.91	-1.64	-0.62	-0.71	0.69	0.75	0.63	0.63	0.57	1.46	-0.31
29	25.40	0.971	0.017	0.009	2.14	1.77	2.00	-0.65	0.62	-0.67	-1.36	-0.49	-0.60	0.57	0.88	0.51	0.58	0.48	1.12	-0.26
30	27.94	0.991	0.011	-0.005	0.98	0.98	0.96	-0.30	0.33	-0.32	-0.67	-0.28	-0.31	0.31	0.53	0.34	0.32	0.33	0.60	-0.17
31	30.48	0.991	0.011	-0.010	0.48	0.55	0.49	-0.10	0.11	-0.13	-0.24	-0.09	-0.12	0.11	0.27	0.12	0.12	0.10	0.23	-0.04
32	33.02	1.001	0.011	-0.013	0.21	0.33	0.26	-0.05	0.06	-0.06	-0.08	-0.06	-0.04	0.06	0.13	0.05	0.05	0.05	0.09	-0.02
33	35.56	0.998	0.012	-0.013	0.11	0.20	0.16	0.00	0.01	-0.03	-0.01	0.00	0.00	0.01	0.04	0.01	0.00	0.01	0.02	0.00
34	38.10	1.000	0.012	-0.013	0.08	0.15	0.14	0.00	0.01	-0.02	0.00	0.00	0.00	0.01	0.05	0.01	0.00	0.00	0.00	0.00
35	50.80	1.000	0.013	-0.012	0.05	0.08	0.10	0.00	0.00	-0.02	0.00	0.00	0.00	0.00	0.00	0.00	0.00	0.00	0.00	0.00

Table C.5 Continued.

Case A.S1 Station= 8
X= 101.6mm Tunnel Run#= 639 Ue/Uref= 0.996 Date= 428.88 Time=12.26
Bias Corrected data using 1/sqrt(U*U + V*V + W*W + (.01Ur)^2)

						<-- normalized by 0.001 Ue^2 -->						<---------- normalized by 0.0001 Ue^3 ----------->					
LR	Y(mm)	U/Ue	V/Ue	W/Ue	uu	vv	ww	uv	vw	uw	uuu	uvv	uww	vuu	vvv	vww	wuu	wvv	www	uvw
1	0.00	0.000	0.000	0.000	0.00	0.00	0.00	-1.78	-0.34	0.00	0.00	0.00	0.00	0.00	0.00	0.00	0.00	0.00	0.00	0.00
2	0.25	0.509	0.012	0.090	12.86	1.33	7.27	-1.13	-0.18	1.34	-2.98	-0.04	0.22	0.50	-0.03	0.26	-0.85	0.01	-0.22	0.14
3	0.38	0.562	0.014	0.103	10.98	1.83	6.98	-1.39	-0.21	0.64	-2.86	-0.15	0.40	0.89	0.01	0.23	-0.56	0.02	-0.33	0.14
4	0.51	0.597	0.004	0.107	9.07	1.82	7.08	-1.47	-0.30	0.46	-1.56	-0.22	0.24	0.76	0.06	0.41	-0.30	-0.09	-0.22	0.23
5	0.63	0.618	0.004	0.109	8.50	2.16	6.72	-1.54	-0.13	0.12	-1.30	-0.22	0.24	0.73	0.11	0.24	-0.43	-0.14	-0.58	0.29
6	0.76	0.636	0.004	0.114	7.96	2.17	6.69	-1.52	-0.08	-0.28	-0.70	-0.27	0.36	0.64	0.19	0.15	-0.31	-0.05	-0.04	0.17
7	1.02	0.658	0.006	0.114	7.27	2.53	6.86	-1.62	-0.05	-0.29	-0.67	-0.28	0.19	0.56	0.37	0.33	-0.17	-0.16	-0.44	0.21
8	1.27	0.681	0.007	0.118	7.05	2.54	6.45	-1.57	0.14	-0.60	0.08	-0.15	0.35	0.41	0.25	0.29	0.06	0.01	-0.48	0.08
9	1.52	0.698	0.008	0.117	6.75	2.59	6.67	-1.54	0.18	-0.66	0.19	-0.20	0.25	0.29	0.17	0.11	0.11	-0.10	-0.41	0.13
10	1.78	0.714	0.008	0.118	6.56	2.75	6.44	-1.58	0.20	-0.85	-0.06	-0.25	0.32	0.34	0.23	0.12	-0.15	-0.10	-0.50	0.21
11	2.03	0.730	0.008	0.119	6.45	2.77	6.57	-1.56	0.36	-1.01	0.10	-0.13	0.18	0.24	0.29	0.29	-0.04	-0.07	-0.24	0.17
12	2.29	0.741	0.007	0.118	6.58	2.72	6.54	-1.55	0.46	-1.05	-0.08	-0.18	0.07	0.33	0.33	0.15	0.07	-0.01	-0.29	0.01
13	2.54	0.751	0.008	0.117	6.22	2.83	6.59	-1.55	0.55	-1.15	-0.02	-0.24	0.06	0.39	0.31	0.31	0.09	0.01	-0.01	0.11
14	2.79	0.759	0.008	0.120	6.22	2.85	6.54	-1.54	0.61	-1.20	0.17	-0.22	0.04	0.38	0.16	0.20	0.10	-0.01	0.03	0.10
15	3.30	0.777	0.009	0.117	6.03	2.92	6.41	-1.38	0.78	-1.45	0.20	-0.19	0.03	0.33	0.10	0.24	0.10	0.09	0.02	-0.02
16	3.81	0.787	0.009	0.116	5.95	3.03	6.48	-1.40	0.83	-1.47	0.09	-0.18	-0.04	0.32	0.12	0.15	0.15	0.10	-0.03	0.02
17	4.32	0.799	0.010	0.116	5.72	3.13	6.28	-1.33	1.03	-1.44	-0.25	-0.17	-0.11	0.35	0.16	0.16	0.25	0.13	0.30	0.01
18	4.83	0.810	0.011	0.117	5.77	3.20	6.35	-1.35	1.10	-1.49	-0.14	-0.19	-0.04	0.35	0.11	0.20	0.30	0.18	0.36	-0.03
19	5.59	0.818	0.011	0.117	5.54	3.36	6.11	-1.23	1.26	-1.38	0.08	-0.08	-0.16	0.23	0.14	0.20	0.11	0.20	0.53	-0.04
20	6.35	0.826	0.011	0.117	5.31	3.55	6.16	-1.35	1.45	-1.55	-0.12	-0.12	-0.04	0.33	0.23	0.30	0.24	0.23	0.50	-0.14
21	7.11	0.833	0.012	0.112	5.35	3.69	6.14	-1.31	1.53	-1.42	-0.08	-0.06	-0.04	0.21	0.17	0.21	0.20	0.24	0.49	-0.06
22	8.38	0.841	0.014	0.111	5.45	3.90	6.05	-1.53	1.73	-1.53	-0.31	-0.09	-0.09	0.16	0.24	0.24	0.14	0.27	0.38	-0.09
23	10.16	0.854	0.015	0.104	5.43	4.03	6.03	-1.70	1.75	-1.58	-0.36	-0.27	-0.24	0.26	0.61	0.36	0.22	0.48	0.51	-0.16
24	12.70	0.874	0.016	0.092	5.47	3.87	5.78	-1.77	1.78	-1.45	-1.04	-0.43	-0.47	0.47	0.75	0.57	0.43	0.54	1.03	-0.33
25	15.24	0.890	0.017	0.078	5.25	3.62	5.35	-1.65	1.67	-1.43	-1.17	-0.48	-0.36	0.54	0.77	0.56	0.41	0.54	1.14	-0.26
26	17.78	0.907	0.019	0.066	4.71	3.32	4.84	-1.51	1.55	-1.36	-1.33	-0.60	-0.48	0.62	0.93	0.70	0.57	0.72	1.28	-0.35
27	20.32	0.936	0.015	0.044	3.97	2.70	4.03	-1.26	1.30	-1.29	-1.62	-0.67	-0.82	0.71	1.06	0.85	0.73	0.73	1.77	-0.42
28	22.86	0.955	0.012	0.024	2.98	2.05	2.85	-0.88	0.87	-0.98	-1.76	-0.60	-0.77	0.67	0.94	0.74	0.68	0.63	1.57	-0.33
29	25.40	0.970	0.012	0.012	2.11	1.57	2.07	-0.67	0.62	-0.75	-1.37	-0.51	-0.64	0.57	0.72	0.56	0.64	0.52	1.25	-0.30
30	27.94	0.981	0.013	0.002	1.32	1.14	1.27	-0.44	0.36	-0.42	-0.87	-0.39	-0.39	0.41	0.59	0.35	0.38	0.31	0.76	-0.19
31	30.48	0.992	0.012	-0.005	0.72	0.73	0.71	-0.21	0.19	-0.20	-0.45	-0.18	-0.21	0.21	0.32	0.20	0.21	0.17	0.41	-0.10
32	33.02	0.997	0.012	-0.008	0.34	0.43	0.38	-0.08	0.07	-0.07	-0.14	-0.06	-0.06	0.08	0.15	0.09	0.05	0.05	0.13	-0.02
33	35.56	1.002	0.012	-0.010	0.18	0.30	0.22	-0.04	0.04	-0.03	-0.04	-0.04	-0.02	0.04	0.12	0.04	0.02	0.02	0.04	-0.01
34	38.10	1.000	0.012	-0.010	0.10	0.17	0.15	0.00	0.01	-0.02	0.00	0.00	0.00	0.01	0.03	0.01	0.00	0.00	0.01	0.00
35	40.64	0.998	0.012	-0.010	0.08	0.13	0.13	0.00	0.01	-0.02	0.00	0.00	0.00	0.00	0.02	0.02	0.00	0.01	0.02	0.00
36	50.80	1.002	0.013	-0.010	0.05	0.08	0.11	0.00	0.00	-0.02	0.00	0.00	0.00	0.00	0.00	0.00	0.00	0.00	0.00	0.00

Table C.5 Continued.

Case A.S1 Station= 9
X= 152.4mm Tunnel Run#= 640 Ue/Uref= 0.993 Date= 428.88 Time=12.51
Bias Corrected data using 1/sqrt(U*U + V*V + W*W + (.01Ur)^2)

					<-- normalized by 0.001 Ue^2 -->						<---------- normalized by 0.0001 Ue^3 ---------->									
LR	Y(mm)	U/Ue	V/Ue	W/Ue	uu	vv	ww	uv	vw	uw	uuu	uvv	uww	vuu	vvv	vww	wuu	wvv	www	uvw
1	0.00	0.000	0.000	0.000	0.00	0.00	0.00	-1.65	-0.27	0.00	0.00	0.00	0.00	0.00	0.00	0.00	0.00	0.00	0.00	0.00
2	0.25	0.503	0.011	0.077	13.41	1.31	5.96	-1.13	-0.11	1.04	-2.31	0.02	0.42	0.47	-0.05	0.15	-0.95	-0.01	1.29	0.13
3	0.38	0.561	0.015	0.082	11.15	1.84	6.40	-1.49	-0.11	0.34	-2.88	-0.15	0.24	0.78	0.03	0.25	-0.47	0.00	0.32	0.20
4	0.51	0.593	0.005	0.087	9.59	1.80	6.28	-1.62	-0.17	0.17	-2.22	-0.28	0.18	0.91	0.09	0.23	-0.50	0.00	0.20	0.19
5	0.63	0.615	0.006	0.090	8.69	1.98	6.14	-1.53	-0.23	0.15	-1.56	-0.25	0.22	0.76	0.08	0.29	-0.10	-0.09	-0.12	0.14
6	0.76	0.633	0.006	0.090	7.92	2.19	6.09	-1.57	-0.21	-0.08	-0.66	-0.25	-0.12	0.55	0.20	0.39	-0.24	-0.09	-0.13	0.22
7	1.02	0.657	0.007	0.093	7.44	2.24	5.87	-1.53	-0.13	-0.18	-0.37	-0.21	0.26	0.48	0.23	0.19	-0.08	-0.13	-0.22	0.16
8	1.27	0.679	0.007	0.097	6.81	2.41	5.81	-1.52	-0.02	-0.15	-0.37	-0.19	0.12	0.41	0.33	0.27	-0.15	-0.09	-0.16	0.13
9	1.52	0.691	0.009	0.097	6.72	2.48	5.82	-1.56	0.02	-0.37	0.00	-0.19	0.15	0.31	0.26	0.29	0.01	-0.02	-0.24	0.08
10	1.78	0.708	0.008	0.097	6.66	2.53	5.60	-1.54	0.10	-0.55	-0.16	-0.14	0.29	0.34	0.23	0.18	-0.04	-0.05	0.09	0.11
11	2.03	0.722	0.007	0.099	6.37	2.52	5.50	-1.50	0.21	-0.53	0.11	-0.14	0.39	0.24	0.15	0.20	0.02	0.03	-0.05	0.05
12	2.29	0.733	0.008	0.100	6.08	2.53	5.50	-1.47	0.20	-0.59	0.09	-0.04	0.17	0.18	0.12	0.14	0.01	-0.04	-0.11	0.11
13	2.54	0.741	0.008	0.101	6.20	2.58	5.48	-1.51	0.29	-0.68	-0.02	-0.12	0.20	0.30	0.18	0.12	-0.04	-0.03	-0.21	0.13
14	2.79	0.749	0.008	0.101	5.86	2.54	5.41	-1.50	0.24	-0.54	0.06	-0.12	0.29	0.25	0.09	0.15	-0.15	-0.09	-0.42	0.13
15	3.30	0.766	0.008	0.103	5.77	2.68	5.43	-1.42	0.47	-0.94	-0.11	-0.07	0.28	0.23	0.09	0.15	0.00	-0.06	-0.37	0.10
16	3.81	0.783	0.008	0.100	5.62	2.69	5.39	-1.39	0.46	-0.84	-0.18	-0.10	0.09	0.26	0.07	0.17	0.14	-0.04	-0.22	0.03
17	4.32	0.793	0.009	0.100	5.34	2.69	5.55	-1.37	0.64	-0.94	-0.07	-0.08	0.02	0.22	0.05	0.20	0.08	0.01	0.00	0.01
18	4.83	0.802	0.010	0.103	5.23	2.88	5.44	-1.30	0.67	-1.06	-0.07	-0.09	0.11	0.26	0.07	0.15	0.02	0.02	-0.11	0.05
19	5.59	0.816	0.010	0.103	5.07	2.95	5.45	-1.20	0.76	-1.06	-0.12	-0.08	0.01	0.24	0.08	0.18	0.24	0.03	-0.04	-0.01
20	6.35	0.827	0.012	0.103	4.95	3.04	5.37	-1.20	0.86	-1.03	0.01	-0.04	-0.08	0.15	0.09	0.13	0.30	0.04	0.13	0.03
21	7.11	0.835	0.012	0.103	4.91	3.26	5.39	-1.24	0.97	-1.16	-0.03	-0.04	0.08	0.22	0.05	0.11	0.04	0.09	-0.10	0.01
22	8.38	0.846	0.013	0.101	4.75	3.28	5.20	-1.29	1.17	-1.06	-0.11	-0.13	0.00	0.21	0.18	0.18	0.12	0.10	0.20	-0.01
23	10.16	0.858	0.015	0.099	4.60	3.56	5.29	-1.33	1.33	-1.06	-0.13	-0.07	0.01	0.13	0.28	0.12	0.03	0.18	0.21	0.00
24	12.70	0.879	0.015	0.091	4.60	3.61	5.06	-1.46	1.49	-1.19	-0.47	-0.10	-0.14	0.16	0.46	0.18	0.12	0.23	0.52	-0.03
25	15.24	0.896	0.014	0.077	4.63	3.49	4.91	-1.49	1.54	-1.22	-0.79	-0.35	-0.30	0.38	0.75	0.40	0.36	0.49	0.83	-0.18
26	17.78	0.913	0.014	0.063	4.47	3.13	4.53	-1.44	1.49	-1.35	-1.22	-0.54	-0.47	0.51	0.87	0.56	0.54	0.62	1.32	-0.28
27	20.32	0.930	0.014	0.048	3.98	2.72	3.99	-1.25	1.26	-1.27	-1.53	-0.62	-0.58	0.65	0.92	0.67	0.65	0.62	1.41	-0.31
28	22.86	0.947	0.014	0.034	3.23	2.34	3.32	-0.96	1.04	-0.96	-1.52	-0.57	-0.57	0.63	0.90	0.72	0.59	0.67	1.51	-0.28
29	25.40	0.965	0.014	0.018	2.52	1.88	2.51	-0.81	0.81	-0.85	-1.53	-0.57	-0.74	0.62	0.80	0.68	0.66	0.58	1.46	-0.32
30	27.94	0.975	0.016	0.010	1.95	1.59	1.96	-0.60	0.58	-0.63	-1.21	-0.45	-0.54	0.49	0.76	0.54	0.52	0.44	1.09	-0.24
31	30.48	0.985	0.016	0.001	1.33	1.25	1.35	-0.50	0.44	-0.44	-0.89	-0.43	-0.45	0.46	0.64	0.42	0.39	0.39	0.82	-0.22
32	33.02	0.998	0.012	-0.007	0.46	0.58	0.49	-0.14	0.13	-0.11	-0.23	-0.15	-0.11	0.15	0.27	0.14	0.09	0.13	0.19	-0.06
33	35.56	0.998	0.012	-0.009	0.29	0.38	0.31	-0.08	0.05	-0.07	-0.12	-0.06	-0.06	0.08	0.14	0.06	0.05	0.04	0.09	-0.03
34	38.10	1.000	0.013	-0.010	0.16	0.27	0.22	-0.03	0.03	-0.03	-0.03	-0.03	-0.01	0.05	0.11	0.03	0.02	0.02	0.05	-0.01
37	40.64	1.001	0.012	-0.010	0.09	0.16	0.14	-0.01	0.00	-0.02	0.00	-0.01	0.00	0.01	0.03	0.01	0.00	0.00	0.00	0.00
36	50.80	1.002	0.012	-0.011	0.05	0.08	0.10	0.00	0.00	-0.01	0.00	0.00	0.00	0.00	0.00	0.00	0.00	0.00	0.00	0.00

Table C.5 Continued.

Case A.S1 Station= 10
X= 228.6mm Tunnel Run#= 641 Ue/Uref= 0.992 Date= 428.88 Time=13.57
Bias Corrected data using 1/sqrt(U*U + V*V + W*W + (.01Ur)^2)

					<-- normalized by 0.001 Ue^2 -->						<---------- normalized by 0.0001 Ue^3 ---------->									
LR	Y(mm)	U/Ue	V/Ue	W/Ue	uu	vv	ww	uv	vw	uw	uuu	uvv	uww	vuu	vvv	vww	wuu	wvv	www	uvw
1	0.00	0.000	0.000	0.000	0.00	0.00	0.00	-1.59	-0.26	0.00	0.00	0.00	0.00	0.00	0.00	0.00	0.00	0.00	0.00	0.00
2	0.25	0.484	0.010	0.065	12.83	1.22	6.92	-1.11	-0.20	0.61	-1.54	0.03	0.32	0.37	-0.07	0.14	-0.58	0.01	1.55	0.11
3	0.38	0.548	0.011	0.072	11.40	1.59	6.56	-1.31	-0.13	0.53	-2.35	-0.12	0.36	0.58	0.02	0.20	-0.35	0.02	0.63	0.07
4	0.51	0.586	0.004	0.074	9.25	1.64	6.08	-1.41	-0.13	0.13	-1.38	-0.21	0.12	0.61	0.04	0.34	-0.41	0.04	0.25	0.06
5	0.63	0.605	0.004	0.076	8.42	1.81	5.59	-1.44	-0.11	0.04	-1.07	-0.29	0.18	0.63	0.15	0.23	-0.14	0.00	0.38	0.02
6	0.76	0.622	0.005	0.079	8.09	1.97	5.55	-1.41	-0.14	-0.04	-0.62	-0.22	0.33	0.47	0.17	0.25	-0.26	-0.04	-0.12	0.09
7	1.02	0.648	0.005	0.082	7.25	2.10	5.18	-1.48	-0.13	0.06	-0.02	-0.26	0.22	0.40	0.23	0.25	-0.11	-0.01	0.05	0.06
8	1.27	0.669	0.006	0.083	7.09	2.09	5.35	-1.49	-0.12	0.03	-0.30	-0.16	0.09	0.35	0.15	0.27	-0.11	-0.02	0.03	0.10
9	1.52	0.686	0.007	0.085	6.92	2.23	5.16	-1.56	-0.06	-0.12	-0.28	-0.11	0.27	0.26	0.20	0.21	0.04	-0.04	-0.15	0.06
10	1.78	0.703	0.006	0.086	6.70	2.26	5.12	-1.51	0.00	-0.18	-0.19	-0.18	0.20	0.30	0.21	0.20	-0.32	0.00	-0.10	0.11
11	2.03	0.717	0.005	0.088	6.55	2.27	4.93	-1.53	0.06	-0.18	-0.46	-0.12	0.20	0.35	0.15	0.22	0.08	-0.03	0.01	0.03
12	2.29	0.726	0.008	0.088	6.32	2.36	5.07	-1.51	0.10	-0.34	-0.31	-0.15	0.22	0.29	0.22	0.24	-0.06	-0.02	-0.12	0.08
13	2.54	0.733	0.007	0.089	6.05	2.31	4.89	-1.40	0.14	-0.33	-0.29	-0.14	0.18	0.28	0.19	0.13	0.01	-0.02	-0.28	0.06
14	2.79	0.745	0.006	0.090	5.92	2.36	4.70	-1.38	0.15	-0.33	-0.44	-0.13	0.19	0.31	0.11	0.18	0.07	0.00	-0.21	0.04
15	3.30	0.756	0.008	0.091	5.80	2.46	4.84	-1.48	0.21	-0.28	-0.34	-0.15	0.23	0.39	0.22	0.15	-0.04	-0.04	-0.45	0.04
16	3.81	0.771	0.008	0.092	5.38	2.43	4.67	-1.38	0.27	-0.43	-0.22	-0.08	0.03	0.26	0.18	0.20	0.12	-0.04	-0.11	0.08
17	4.32	0.786	0.007	0.091	5.22	2.54	4.80	-1.39	0.30	-0.47	-0.34	-0.12	0.01	0.26	0.15	0.20	-0.01	-0.06	-0.21	0.11
18	4.83	0.793	0.008	0.092	5.09	2.55	4.92	-1.33	0.43	-0.56	-0.41	-0.13	0.09	0.31	0.18	0.17	-0.09	0.01	-0.09	0.06
19	5.59	0.809	0.009	0.092	4.88	2.56	4.61	-1.24	0.46	-0.57	-0.09	-0.14	0.01	0.23	0.12	0.18	0.10	-0.03	-0.15	0.06
20	6.35	0.822	0.009	0.094	4.79	2.60	4.60	-1.23	0.50	-0.52	-0.32	-0.13	0.02	0.28	0.11	0.09	0.08	-0.05	-0.30	0.11
21	7.11	0.833	0.009	0.095	4.65	2.66	4.59	-1.24	0.60	-0.65	-0.27	-0.06	0.00	0.25	0.06	0.17	0.07	0.04	-0.13	0.05
22	8.38	0.847	0.011	0.093	4.38	2.74	4.60	-1.16	0.80	-0.69	-0.29	-0.06	0.12	0.19	0.07	0.07	0.09	-0.04	-0.22	0.06
23	10.16	0.865	0.009	0.090	4.00	2.89	4.44	-1.08	0.88	-0.67	-0.14	-0.06	-0.05	0.14	0.18	0.09	0.10	0.07	0.06	0.00
24	12.70	0.883	0.011	0.087	3.95	2.98	4.23	-1.16	0.97	-0.68	-0.27	-0.06	-0.09	0.11	0.22	0.13	0.05	0.09	0.19	0.02
25	15.24	0.897	0.013	0.079	3.86	2.94	4.14	-1.13	1.13	-0.75	-0.34	-0.14	-0.06	0.13	0.41	0.22	0.09	0.20	0.40	-0.03
26	17.78	0.911	0.014	0.069	3.77	2.83	4.00	-1.18	1.14	-0.88	-0.58	-0.22	-0.15	0.24	0.54	0.31	0.18	0.27	0.66	-0.07
27	20.32	0.928	0.011	0.058	3.57	2.62	3.78	-1.15	1.17	-0.96	-0.89	-0.42	-0.40	0.43	0.73	0.53	0.33	0.47	1.06	-0.19
28	22.86	0.943	0.013	0.046	3.21	2.29	3.36	-1.01	1.00	-0.95	-1.24	-0.46	-0.47	0.52	0.71	0.57	0.44	0.47	1.21	-0.23
29	25.40	0.956	0.014	0.034	2.93	2.05	2.71	-0.96	0.86	-0.85	-1.42	-0.57	-0.58	0.65	0.84	0.59	0.59	0.51	1.31	-0.30
30	27.94	0.970	0.013	0.022	2.20	1.68	2.08	-0.68	0.65	-0.61	-1.25	-0.51	-0.49	0.53	0.75	0.52	0.44	0.47	1.06	-0.23
31	30.48	0.980	0.013	0.014	1.56	1.34	1.55	-0.52	0.45	-0.47	-1.01	-0.39	-0.43	0.46	0.63	0.42	0.39	0.35	0.90	-0.19
32	33.02	0.988	0.011	0.006	0.90	0.90	0.95	-0.28	0.28	-0.28	-0.54	-0.24	-0.26	0.24	0.45	0.28	0.24	0.25	0.55	-0.11
33	35.56	0.996	0.011	0.001	0.46	0.57	0.50	-0.15	0.14	-0.12	-0.22	-0.15	-0.10	0.14	0.31	0.14	0.10	0.15	0.22	-0.07
34	38.10	0.998	0.011	-0.001	0.24	0.36	0.30	-0.05	0.05	-0.05	-0.08	-0.04	-0.03	0.04	0.14	0.08	0.03	0.05	0.08	-0.01
35	40.64	1.000	0.011	-0.002	0.14	0.23	0.18	-0.02	0.01	-0.03	-0.01	-0.01	0.00	0.02	0.05	0.02	0.01	0.01	0.01	-0.01
36	50.80	1.002	0.012	-0.001	0.06	0.09	0.11	0.00	0.00	-0.02	0.00	0.00	0.00	0.00	0.00	0.00	0.00	0.00	0.01	0.00

Table C.5 Continued.

Case A.S1 Station= 11
X= 304.8mm Tunnel Run#= 642 Ue/Uref= 0.989 Date= 428.88 Time=15.00
Bias Corrected data using 1/sqrt(U*U + V*V + W*W + (.01Ur)^2)

					<-- normalized by 0.001 Ue^2 -->						<---------- normalized by 0.0001 Ue^3 ---------->									
LR	Y(mm)	U/Ue	V/Ue	W/Ue	uu	vv	ww	uv	vw	uw	uuu	uvv	uww	vuu	vvv	vww	wuu	wvv	www	uvw
1	0.00	0.000	0.000	0.000	0.00	0.00	0.00	-1.58	-0.21	0.00	0.00	0.00	0.00	0.00	0.00	0.00	0.00	0.00	0.00	0.00
2	0.25	0.501	0.013	0.054	12.56	1.30	5.33	-1.06	-0.09	0.84	-2.04	0.04	0.75	0.37	-0.11	0.16	-0.47	0.01	0.72	0.17
3	0.38	0.552	0.015	0.057	10.81	1.78	5.70	-1.28	-0.09	0.44	-2.15	-0.12	0.24	0.76	0.00	0.31	-0.07	0.02	0.12	0.05
4	0.51	0.582	0.005	0.060	9.59	1.67	5.47	-1.48	-0.14	0.07	-1.83	-0.12	0.33	0.59	0.03	0.17	-0.43	-0.01	0.17	0.11
5	0.63	0.606	0.006	0.063	8.72	1.83	5.46	-1.46	-0.14	0.23	-0.90	-0.25	0.03	0.53	0.15	0.19	-0.28	-0.02	0.25	0.14
6	0.76	0.623	0.006	0.066	8.32	1.96	5.19	-1.47	-0.08	0.05	-0.49	-0.19	0.11	0.41	0.18	0.23	-0.17	0.04	0.30	0.04
7	1.02	0.645	0.008	0.069	7.53	2.14	5.01	-1.49	-0.07	0.02	-0.13	-0.18	0.19	0.28	0.21	0.13	-0.02	0.02	0.03	0.07
8	1.27	0.667	0.007	0.071	7.30	2.16	4.63	-1.54	-0.04	-0.02	-0.36	-0.21	0.13	0.41	0.19	0.20	-0.15	0.01	0.01	0.11
9	1.52	0.684	0.007	0.072	6.98	2.08	4.63	-1.43	-0.01	-0.07	0.05	-0.18	0.27	0.25	0.18	0.17	-0.15	0.01	0.03	0.06
10	1.78	0.697	0.007	0.072	6.91	2.20	4.42	-1.50	0.05	-0.10	-0.13	-0.11	-0.04	0.25	0.14	0.22	0.09	0.00	0.05	0.00
11	2.03	0.708	0.008	0.075	6.66	2.14	4.44	-1.43	0.05	-0.10	-0.37	-0.13	0.01	0.28	0.18	0.19	-0.16	-0.01	0.04	0.12
13	2.29	0.720	0.008	0.077	6.42	2.17	4.31	-1.38	0.07	-0.10	-0.34	-0.11	0.07	0.26	0.08	0.15	-0.24	-0.07	-0.22	0.10
14	2.54	0.731	0.009	0.077	6.29	2.24	4.29	-1.41	0.08	-0.18	-0.52	-0.09	0.10	0.32	0.12	0.15	0.06	-0.03	-0.08	0.03
15	2.79	0.740	0.008	0.080	6.10	2.25	4.34	-1.39	0.16	-0.20	-0.52	-0.18	0.20	0.34	0.19	0.15	-0.03	0.00	0.01	0.08
16	3.30	0.757	0.009	0.079	6.09	2.32	4.12	-1.43	0.14	-0.22	-0.59	-0.19	0.11	0.39	0.22	0.12	0.11	-0.04	0.03	0.08
17	3.81	0.770	0.010	0.080	5.69	2.34	4.31	-1.45	0.16	-0.20	-0.33	-0.10	0.09	0.19	0.09	0.14	0.05	-0.07	-0.23	0.06
18	4.32	0.780	0.010	0.082	5.51	2.34	4.08	-1.42	0.22	-0.33	-0.52	-0.15	0.11	0.29	0.17	0.20	-0.08	0.00	-0.18	0.04
19	4.83	0.790	0.010	0.084	5.41	2.47	4.14	-1.38	0.20	-0.22	-0.38	-0.11	0.00	0.25	0.15	0.13	-0.08	-0.05	-0.21	0.08
20	5.59	0.808	0.009	0.081	5.09	2.45	4.19	-1.36	0.28	-0.23	-0.51	-0.14	-0.03	0.29	0.17	0.13	-0.03	-0.02	0.02	0.07
21	6.35	0.820	0.010	0.083	4.68	2.45	4.17	-1.27	0.38	-0.28	-0.46	-0.13	0.05	0.34	0.10	0.14	-0.05	-0.05	-0.12	0.08
22	7.11	0.831	0.010	0.084	4.44	2.41	4.02	-1.24	0.43	-0.40	-0.35	-0.04	0.03	0.23	0.08	0.17	0.05	0.00	-0.10	0.06
23	8.38	0.846	0.011	0.081	4.28	2.43	3.96	-1.21	0.45	-0.39	-0.32	-0.06	0.00	0.22	0.05	0.14	0.00	-0.03	-0.18	0.06
24	10.16	0.861	0.012	0.081	4.04	2.54	3.86	-1.14	0.62	-0.52	-0.23	-0.06	-0.02	0.19	0.08	0.10	0.03	0.06	-0.09	0.01
25	12.70	0.886	0.012	0.077	3.57	2.56	3.79	-0.93	0.78	-0.52	-0.27	-0.08	-0.09	0.14	0.15	0.09	0.02	0.06	0.01	0.00
26	15.24	0.902	0.013	0.071	3.44	2.55	3.76	-0.96	0.87	-0.55	-0.32	-0.09	-0.12	0.17	0.18	0.22	0.08	0.06	0.29	0.00
27	17.78	0.914	0.013	0.063	3.41	2.57	3.46	-1.03	0.90	-0.63	-0.47	-0.23	-0.08	0.24	0.38	0.24	0.13	0.22	0.36	-0.06
28	20.32	0.928	0.013	0.054	3.19	2.42	3.32	-0.97	0.89	-0.59	-0.63	-0.23	-0.21	0.26	0.50	0.30	0.16	0.29	0.64	-0.08
29	22.86	0.943	0.012	0.044	2.95	2.14	3.02	-0.92	0.88	-0.78	-0.87	-0.36	-0.33	0.38	0.58	0.37	0.27	0.37	0.90	-0.13
30	25.40	0.958	0.013	0.034	2.59	1.99	2.69	-0.82	0.81	-0.73	-0.99	-0.40	-0.41	0.45	0.61	0.46	0.39	0.44	1.12	-0.19
31	27.94	0.971	0.014	0.023	2.18	1.75	2.19	-0.72	0.66	-0.69	-1.02	-0.45	-0.50	0.43	0.68	0.48	0.45	0.43	1.03	-0.22
32	30.48	0.983	0.014	0.014	1.72	1.43	1.65	-0.48	0.51	-0.46	-0.94	-0.37	-0.39	0.39	0.57	0.42	0.37	0.38	0.83	-0.18
33	33.02	0.988	0.014	0.008	1.22	1.14	1.20	-0.41	0.37	-0.36	-0.69	-0.31	-0.29	0.36	0.47	0.32	0.29	0.30	0.63	-0.15
34	35.56	0.994	0.015	0.004	0.92	0.93	0.95	-0.29	0.27	-0.28	-0.52	-0.23	-0.25	0.26	0.43	0.26	0.24	0.22	0.54	-0.11
35	38.10	1.000	0.013	-0.002	0.40	0.51	0.42	-0.11	0.12	-0.10	-0.19	-0.10	-0.07	0.10	0.21	0.10	0.08	0.10	0.16	-0.04
36	40.64	1.002	0.013	-0.004	0.21	0.32	0.25	-0.04	0.04	-0.04	-0.03	-0.03	-0.01	0.05	0.12	0.04	0.02	0.03	0.04	-0.01
37	45.72	1.001	0.013	-0.004	0.09	0.15	0.14	-0.01	0.01	-0.02	-0.01	-0.01	0.00	0.01	0.03	0.01	0.00	0.00	0.00	0.00
38	50.80	0.997	0.013	-0.004	0.06	0.10	0.12	0.00	0.00	-0.02	0.00	0.00	0.00	0.00	0.00	0.00	0.00	0.00	0.00	0.00

Table C.5 Continued.

Case A.S1 Station= 12
X= 457.2mm Tunnel Run#= 643 Ue/Uref= 0.990 Date= 428.88 Time=16.31
Bias Corrected data using 1/sqrt(U*U + V*V + W*W + (.01Ur)^2)

					<-- normalized by 0.001 Ue^2 -->						<---------- normalized by 0.0001 Ue^3 ---------->									
LR	Y(mm)	U/Ue	V/Ue	W/Ue	uu	vv	ww	uv	vw	uw	uuu	uvv	uww	vuu	vvv	vww	wuu	wvv	www	uvw
1	0.00	0.000	0.000	0.000	0.00	0.00	0.00	-1.55	-0.12	0.00	0.00	0.00	0.00	0.00	0.00	0.00	0.00	0.00	0.00	0.00
2	0.25	0.485	0.013	0.044	12.98	1.18	5.63	-1.05	-0.06	0.65	-2.14	0.07	0.62	0.46	-0.10	0.20	-0.21	0.03	-0.69	0.02
3	0.38	0.543	0.014	0.048	10.44	1.59	4.99	-1.14	-0.08	0.38	-2.44	-0.07	0.26	0.61	0.49	0.17	-0.06	-0.05	-0.42	0.12
4	0.51	0.577	0.005	0.053	9.42	1.58	4.90	-1.32	-0.05	0.16	-1.54	-0.17	0.33	0.60	0.05	0.14	0.03	0.02	0.04	0.06
5	0.63	0.596	0.006	0.055	8.47	1.79	4.70	-1.39	-0.14	0.23	-0.98	-0.25	0.14	0.61	0.12	0.14	0.02	-0.01	0.10	0.03
6	0.76	0.613	0.004	0.055	7.99	1.86	4.59	-1.44	-0.10	0.18	-0.51	-0.23	0.16	0.48	0.18	0.16	-0.31	-0.02	0.07	0.12
7	1.02	0.637	0.005	0.058	7.23	1.99	4.53	-1.34	-0.06	0.13	-0.08	-0.19	0.12	0.29	0.17	0.17	-0.07	-0.01	-0.02	0.04
8	1.27	0.658	0.006	0.061	7.13	1.99	4.27	-1.39	-0.09	0.03	-0.22	-0.15	0.15	0.32	0.17	0.18	-0.16	0.01	0.09	0.07
9	1.52	0.673	0.007	0.063	7.03	2.01	4.14	-1.33	-0.06	0.21	-0.02	-0.13	0.13	0.29	0.18	0.21	-0.07	0.00	-0.14	0.06
10	1.78	0.687	0.007	0.063	6.97	2.06	4.02	-1.44	-0.03	-0.03	-0.23	-0.22	0.09	0.29	0.18	0.14	-0.03	-0.01	0.08	0.02
11	2.03	0.698	0.007	0.065	6.75	2.03	3.97	-1.42	0.07	-0.02	-0.19	-0.15	0.09	0.21	0.20	0.19	-0.13	0.02	0.02	0.04
12	2.29	0.711	0.006	0.066	6.65	2.06	3.81	-1.41	0.01	-0.03	-0.31	-0.13	0.07	0.29	0.14	0.17	-0.05	-0.01	-0.15	0.06
13	2.54	0.719	0.007	0.067	6.32	2.07	3.78	-1.36	0.01	0.04	-0.47	-0.18	0.03	0.28	0.24	0.17	-0.01	0.00	0.10	0.02
14	2.79	0.727	0.008	0.069	6.36	2.04	3.79	-1.40	0.02	-0.02	-0.50	-0.11	0.08	0.29	0.10	0.16	-0.11	-0.03	-0.12	0.06
15	3.30	0.743	0.007	0.070	6.06	2.00	3.57	-1.38	0.04	0.01	-0.64	-0.14	-0.04	0.30	0.16	0.17	-0.04	-0.02	0.17	0.05
16	3.81	0.759	0.007	0.070	5.86	2.01	3.71	-1.26	0.12	-0.04	-0.84	-0.14	0.08	0.41	0.13	0.11	-0.06	-0.03	-0.26	0.07
17	4.32	0.772	0.006	0.072	5.36	2.09	3.44	-1.29	0.14	-0.01	-0.47	-0.12	-0.04	0.28	0.13	0.15	-0.08	-0.03	0.06	0.05
18	4.83	0.778	0.008	0.072	5.38	2.11	3.46	-1.28	0.15	-0.08	-0.58	-0.12	0.02	0.26	0.12	0.13	-0.01	-0.03	-0.08	0.06
19	5.59	0.793	0.008	0.073	5.03	2.10	3.42	-1.22	0.14	-0.09	-0.64	-0.14	-0.01	0.29	0.06	0.12	-0.06	0.00	-0.08	0.00
20	6.35	0.807	0.011	0.077	4.94	2.12	3.33	-1.26	0.26	-0.12	-0.61	-0.08	0.02	0.26	0.08	0.10	-0.05	-0.07	-0.08	0.09
21	7.11	0.818	0.009	0.076	4.55	2.12	3.22	-1.19	0.26	-0.13	-0.51	-0.17	0.04	0.29	0.18	0.10	-0.05	-0.02	-0.01	0.06
22	8.38	0.833	0.011	0.075	4.11	2.14	3.26	-1.08	0.29	-0.16	-0.36	-0.10	-0.02	0.20	0.14	0.11	-0.03	-0.01	-0.08	0.03
23	10.16	0.856	0.009	0.074	3.94	2.12	3.13	-1.04	0.36	-0.15	-0.36	-0.09	-0.10	0.18	0.11	0.12	-0.05	0.01	-0.15	0.04
24	12.70	0.881	0.010	0.067	3.44	2.09	3.10	-0.90	0.44	-0.32	-0.37	-0.08	-0.03	0.17	0.16	0.10	0.00	-0.04	-0.02	0.06
25	15.24	0.894	0.013	0.068	3.17	2.11	2.86	-0.93	0.52	-0.32	-0.27	-0.05	-0.06	0.13	0.13	0.07	0.03	0.07	-0.01	0.01
26	17.78	0.915	0.009	0.060	2.85	2.01	2.90	-0.82	0.59	-0.38	-0.29	-0.12	-0.14	0.13	0.22	0.15	0.04	0.09	0.24	0.00
27	20.32	0.927	0.011	0.055	2.64	2.01	2.79	-0.84	0.73	-0.46	-0.45	-0.23	-0.11	0.21	0.35	0.19	0.09	0.17	0.35	-0.06
28	22.86	0.941	0.011	0.048	2.53	1.91	2.52	-0.81	0.66	-0.48	-0.52	-0.21	-0.18	0.22	0.34	0.21	0.10	0.20	0.44	-0.06
29	25.40	0.952	0.011	0.040	2.31	1.79	2.39	-0.74	0.69	-0.58	-0.63	-0.29	-0.23	0.28	0.45	0.28	0.24	0.27	0.60	-0.12
30	27.94	0.963	0.010	0.032	2.02	1.55	2.05	-0.64	0.60	-0.52	-0.68	-0.29	-0.26	0.30	0.46	0.31	0.26	0.29	0.64	-0.14
31	30.48	0.972	0.010	0.025	1.71	1.37	1.77	-0.55	0.51	-0.49	-0.68	-0.29	-0.29	0.28	0.44	0.31	0.27	0.28	0.76	-0.12
32	33.02	0.976	0.013	0.022	1.68	1.41	1.74	-0.56	0.50	-0.47	-0.69	-0.28	-0.29	0.30	0.48	0.30	0.28	0.28	0.74	-0.12
33	35.56	0.986	0.012	0.014	1.20	1.07	1.28	-0.40	0.39	-0.37	-0.59	-0.26	-0.26	0.30	0.43	0.29	0.28	0.25	0.66	-0.11
34	38.10	0.993	0.011	0.007	0.83	0.87	0.88	-0.27	0.24	-0.19	-0.38	-0.19	-0.16	0.19	0.33	0.20	0.16	0.19	0.40	-0.08
35	40.64	0.997	0.011	0.005	0.57	0.67	0.63	-0.19	0.18	-0.15	-0.23	-0.12	-0.11	0.14	0.25	0.15	0.11	0.13	0.28	-0.05
36	45.72	1.000	0.011	0.000	0.24	0.37	0.29	-0.07	0.07	-0.05	-0.06	-0.05	-0.03	0.06	0.16	0.07	0.03	0.06	0.07	-0.02
37	50.80	1.003	0.009	-0.001	0.09	0.14	0.13	-0.01	0.00	-0.02	0.00	0.00	0.00	0.01	0.02	0.01	0.00	0.01	0.01	0.00

Table C.5 Continued.

Case B.S1 Station= 1
X=-457.2mm Tunnel Run#= 687 Ue/Uref= 0.832 Date= 510.88 Time=11.21
Bias Corrected data using 1/sqrt(U*U + V*V + W*W + (.01Ur)^2)

					<-- normalized by 0.001 Ur^2 -->						<---------- normalized by 0.0001 Ur^3 ---------->								
LR	Y(mm)	U/Ur	V/Ur	W/Ur	uu	vv	ww	uv	vw	uw	uuu	uvv	uww	vuu	vvv	vww	wuu	wvv	www	uvw
1	0.00	0.000	0.000	1.000	0.00	0.00	0.00	-2.28	2.45	0.00	0.00	0.00	0.00	0.00	0.00	0.00	0.00	0.00	0.00	0.00
1	0.25	0.603	-0.029	0.309	12.86	3.42	15.08	-1.81	1.40	-5.18	-1.65	-0.43	-3.20	1.00	0.32	1.52	2.18	0.37	3.65	-0.65
2	0.38	0.623	-0.026	0.292	12.54	3.72	14.28	-1.91	1.47	-4.68	-1.64	-0.49	-2.17	0.87	0.63	1.13	1.30	0.37	2.94	-0.27
3	0.51	0.637	-0.025	0.278	11.68	3.80	13.54	-1.97	1.56	-4.49	-0.76	-0.52	-2.09	0.85	0.53	1.13	1.36	0.37	2.75	-0.38
4	0.63	0.650	-0.023	0.262	11.72	3.70	13.71	-2.01	1.60	-4.54	-1.58	-0.43	-2.18	1.06	0.55	1.28	1.65	0.37	2.84	-0.42
5	0.76	0.661	-0.023	0.251	10.86	3.85	12.70	-1.93	1.67	-4.12	-1.09	-0.54	-1.81	0.98	0.65	1.32	1.33	0.49	2.33	-0.56
6	1.02	0.680	-0.023	0.234	10.43	3.94	11.96	-1.89	1.67	-3.87	-1.68	-0.49	-1.56	0.82	0.49	1.19	1.35	0.54	2.48	-0.50
7	1.27	0.694	-0.021	0.218	10.02	3.92	11.33	-1.93	1.66	-3.95	-1.15	-0.56	-1.44	0.91	0.60	1.08	0.90	0.59	2.22	-0.42
8	1.52	0.706	-0.019	0.207	9.79	3.95	11.39	-1.85	1.71	-4.09	-1.23	-0.50	-1.21	0.85	0.52	1.18	0.98	0.66	2.19	-0.57
9	1.78	0.720	-0.019	0.195	9.71	4.10	10.70	-2.14	1.89	-3.70	-1.25	-0.66	-1.33	1.00	0.75	1.28	1.09	0.55	2.00	-0.59
10	2.03	0.726	-0.017	0.188	9.19	4.07	10.31	-1.92	1.77	-3.75	-1.00	-0.36	-1.13	0.62	0.60	0.94	1.03	0.48	2.37	-0.47
11	2.29	0.732	-0.018	0.180	9.13	4.13	9.99	-2.03	1.81	-3.56	-1.12	-0.46	-1.33	0.61	0.52	1.11	1.06	0.62	1.81	-0.65
12	2.54	0.745	-0.017	0.172	8.85	4.07	9.86	-1.99	1.83	-3.45	-1.34	-0.40	-1.22	0.64	0.46	0.97	1.03	0.54	2.34	-0.50
13	2.79	0.752	-0.015	0.169	8.66	4.19	9.65	-2.10	2.01	-3.39	-0.70	-0.37	-1.12	0.65	0.68	1.02	0.68	0.55	2.52	-0.43
14	3.30	0.765	-0.015	0.156	8.59	4.22	9.33	-2.17	1.97	-3.42	-1.47	-0.39	-0.87	0.62	0.47	0.87	0.90	0.47	1.81	-0.49
15	3.81	0.780	-0.014	0.147	8.34	4.14	8.88	-2.11	1.80	-3.26	-1.50	-0.59	-0.97	0.69	0.77	0.72	0.96	0.67	2.00	-0.44
16	4.32	0.794	-0.012	0.137	7.76	4.09	8.47	-2.02	1.85	-2.88	-1.33	-0.48	-0.97	0.60	0.68	0.92	0.83	0.61	2.11	-0.34
17	4.83	0.804	-0.012	0.126	7.45	3.96	7.94	-2.05	1.68	-2.61	-1.61	-0.64	-0.86	0.69	0.68	0.66	0.85	0.57	1.74	-0.46
18	5.59	0.823	-0.010	0.115	7.28	3.81	7.47	-2.07	1.71	-2.52	-1.90	-0.62	-1.05	0.72	0.79	0.71	0.98	0.56	2.15	-0.51
19	6.35	0.843	-0.010	0.102	6.83	3.53	7.05	-1.90	1.50	-2.29	-2.38	-0.72	-1.20	0.80	0.85	0.73	1.05	0.58	1.93	-0.48
20	7.11	0.861	-0.009	0.089	6.35	3.22	6.53	-1.79	1.42	-2.16	-2.25	-0.65	-1.11	0.81	0.78	0.84	0.99	0.60	2.46	-0.48
21	8.38	0.891	-0.008	0.071	5.38	2.78	5.37	-1.52	1.23	-1.84	-2.49	-0.74	-1.31	0.87	0.79	0.88	1.07	0.65	2.34	-0.54
22	10.16	0.932	-0.007	0.044	3.88	2.03	3.66	-1.11	0.77	-1.32	-2.47	-0.68	-1.17	0.85	0.70	0.68	1.04	0.53	2.03	-0.40
23	12.70	0.970	-0.004	0.018	1.71	1.18	1.63	-0.52	0.40	-0.62	-1.36	-0.41	-0.65	0.52	0.45	0.44	0.67	0.30	1.11	-0.26
24	15.24	0.989	-0.003	0.005	0.38	0.50	0.44	-0.10	0.09	-0.09	-0.17	-0.09	-0.08	0.10	0.20	0.10	0.08	0.08	0.15	-0.05
25	17.78	0.992	-0.004	0.003	0.11	0.18	0.17	-0.01	0.01	-0.02	-0.01	-0.01	0.00	0.01	0.03	0.01	0.00	0.01	0.01	0.00
26	20.32	0.994	-0.004	0.003	0.06	0.11	0.14	0.00	0.00	-0.01	0.00	0.00	0.00	0.00	0.00	0.00	0.00	0.00	0.01	0.00
27	22.86	0.993	-0.004	0.002	0.05	0.09	0.13	0.00	0.00	0.00	0.00	0.00	0.01	0.00	0.00	0.00	0.00	0.00	0.01	0.00
28	25.40	0.993	-0.004	0.001	0.05	0.09	0.12	0.00	0.00	-0.01	0.00	0.00	0.00	0.00	0.01	0.00	0.00	0.00	0.00	0.00
29	27.94	0.992	-0.004	0.000	0.05	0.08	0.12	0.00	0.00	-0.01	0.00	0.00	0.00	0.00	0.00	0.00	0.00	0.00	0.01	0.00
30	30.48	0.994	-0.006	-0.001	0.05	0.08	0.12	0.00	0.00	0.00	0.00	0.00	0.01	0.00	0.00	0.00	0.00	0.00	0.01	0.00
31	33.02	0.994	-0.004	0.002	0.06	0.09	0.17	0.00	0.00	0.01	0.01	0.00	0.01	0.00	0.00	0.00	0.01	0.00	0.03	0.00
32	35.56	0.994	-0.004	0.000	0.05	0.08	0.12	0.00	0.00	-0.01	0.00	0.00	0.00	0.00	0.00	0.00	0.00	0.00	0.00	0.00
33	38.10	0.995	-0.004	-0.001	0.05	0.08	0.13	0.00	0.00	-0.01	0.00	0.00	0.00	0.00	0.00	0.00	0.00	0.00	0.00	0.00
34	40.64	0.994	-0.004	0.001	0.05	0.11	0.12	0.00	0.00	-0.01	0.00	0.00	0.00	0.00	0.09	0.00	0.00	0.00	0.00	0.00
35	45.72	0.996	-0.004	0.002	0.04	0.09	0.12	0.00	0.00	-0.01	0.00	0.00	0.00	0.00	0.00	0.00	0.00	0.00	0.00	0.00
36	50.80	0.996	0.003	0.003	0.05	0.49	0.15	0.00	0.00	-0.01	0.00	0.00	0.01	0.00	0.04	0.00	0.00	0.00	0.01	0.00
37	55.88	0.997	0.002	0.002	0.05	0.55	0.12	0.00	0.00	-0.01	0.00	0.00	0.00	0.00	0.72	0.00	0.00	-0.01	0.00	0.00
38	60.96	0.993	0.000	-0.001	0.05	0.00	0.12	0.00	0.00	-0.01	0.00	0.00	0.00	0.00	0.00	0.00	0.00	0.00	0.00	0.00
39	66.04	0.996	0.000	-0.003	0.05	0.00	0.13	0.00	0.00	0.00	0.00	0.00	0.00	0.00	0.00	0.00	0.00	0.00	0.01	0.00

Table C.5 Continued.

Case B.S1 Station= 2
X=-330.2mm Tunnel Run#= 601 Ue/Uref= 0.772 Date= 314.88 Time=15.24
Bias Corrected data using 1/sqrt(U*U + V*V + W*W + (.01Ur)^2)

					<-- normalized by 0.001 Ur^2 -->						<---------- normalized by 0.0001 Ur^3 ---------->									
LR	Y(mm)	U/Ur	V/Ur	W/Ur	uu	vv	ww	uv	vw	uw	uuu	uvv	uww	vuu	vvv	vww	wuu	wvv	www	uvw
1	0.00	0.000	0.000	1.000	0.00	0.00	0.00	-2.21	2.32	0.00	0.00	0.00	0.00	0.00	0.00	0.00	0.00	0.00	0.00	0.00
41	0.25	0.577	0.016	0.346	14.53	5.22	19.83	-1.22	0.96	-7.62	-0.38	-0.44	0.64	0.89	0.02	1.60	0.06	0.07	0.24	-0.76
42	0.38	0.605	0.018	0.319	13.75	5.55	18.47	-1.46	1.34	-6.47	-0.16	0.06	1.16	0.82	0.04	1.09	-0.46	-0.16	-2.77	-0.43
43	0.51	0.622	0.003	0.301	13.31	4.35	16.37	-1.75	1.48	-5.59	-1.11	-0.36	1.10	0.94	0.45	1.31	-0.12	0.13	0.22	-0.47
44	0.63	0.635	0.005	0.285	12.35	4.29	15.05	-1.91	1.56	-5.09	-0.47	-0.73	0.84	1.01	0.61	1.01	-0.31	0.38	0.56	-0.31
45	0.76	0.648	0.004	0.274	11.94	4.29	14.41	-1.86	1.71	-4.81	-0.18	-0.58	0.32	1.03	0.51	0.97	0.33	0.47	0.63	-0.28
46	1.02	0.666	0.006	0.255	11.75	4.46	13.92	-1.94	1.98	-5.20	-0.53	-0.51	0.90	0.75	0.66	1.09	-0.25	0.66	0.11	-0.53
47	1.27	0.685	0.005	0.232	11.26	4.54	13.48	-2.04	1.95	-4.67	-0.74	-0.65	0.36	0.83	0.73	1.35	0.33	0.64	1.21	-0.55
48	1.52	0.695	0.005	0.219	10.51	4.38	12.00	-2.04	1.94	-4.72	-1.40	-0.64	0.25	1.11	0.62	1.26	0.55	0.48	1.04	-0.61
49	1.78	0.708	0.006	0.204	9.90	4.30	11.24	-1.97	1.82	-4.10	-1.26	-0.48	0.53	1.03	0.60	1.08	0.23	0.47	1.94	-0.59
50	2.03	0.717	0.008	0.198	9.71	4.37	11.55	-1.93	1.89	-4.26	-0.51	-0.56	0.18	0.77	0.64	1.23	0.26	0.50	1.33	-0.50
51	2.29	0.726	0.009	0.192	9.78	4.48	10.94	-2.00	1.85	-3.94	-0.12	-0.45	-0.16	0.70	0.40	0.97	0.41	0.22	1.27	-0.37
52	2.54	0.733	0.009	0.188	9.54	4.55	10.99	-2.09	2.09	-3.94	-1.14	-0.44	0.13	0.80	0.44	0.93	0.29	0.58	1.93	-0.36
53	2.79	0.745	0.008	0.179	9.36	4.46	10.81	-2.01	1.91	-3.71	-0.76	-0.20	-0.21	0.88	0.59	1.43	0.49	0.62	1.71	-0.53
54	3.30	0.759	0.007	0.163	8.79	4.61	10.60	-2.09	2.11	-3.70	-1.25	-0.37	-0.79	0.73	0.58	1.21	0.78	0.66	2.90	-0.49
55	3.81	0.770	0.009	0.157	8.51	4.80	10.21	-2.14	2.26	-3.48	-1.01	-0.65	-0.31	0.77	0.76	1.07	0.83	0.77	2.01	-0.63
56	4.32	0.781	0.008	0.147	8.43	4.81	9.65	-2.24	2.04	-3.37	-1.28	-0.55	-0.23	0.89	0.61	0.88	0.54	0.69	1.80	-0.44
57	4.83	0.788	0.010	0.141	8.45	4.74	9.32	-2.26	2.18	-3.13	-1.50	-0.54	-0.55	0.75	0.78	1.02	0.92	0.79	1.62	-0.61
58	5.59	0.804	0.011	0.131	7.89	4.64	8.98	-2.13	2.04	-2.76	-1.22	-0.41	-0.48	0.57	0.55	0.96	0.60	0.64	2.02	-0.40
59	6.35	0.818	0.010	0.119	7.68	4.50	8.55	-2.19	1.96	-2.73	-1.51	-0.64	-0.60	0.71	0.76	0.94	0.76	0.58	1.81	-0.46
60	7.11	0.830	0.012	0.111	7.73	4.43	8.25	-2.21	2.11	-2.77	-2.00	-0.70	-0.99	0.81	0.92	1.03	1.01	0.62	2.27	-0.47
61	8.38	0.855	0.011	0.097	6.72	4.04	7.51	-1.99	1.83	-2.24	-1.59	-0.70	-0.91	0.65	0.72	0.90	0.61	0.75	2.29	-0.38
62	10.16	0.885	0.011	0.074	6.09	3.65	6.31	-1.88	1.65	-2.19	-2.57	-0.93	-1.33	1.13	1.13	0.98	1.18	0.95	2.56	-0.67
63	12.70	0.935	0.011	0.043	4.13	2.64	4.14	-1.34	1.11	-1.74	-2.46	-0.88	-1.25	1.20	1.02	0.92	1.26	0.77	2.00	-0.60
64	15.24	0.971	0.010	0.019	2.10	1.76	2.46	-0.66	0.63	-0.81	-1.51	-0.56	-0.86	0.69	0.74	0.68	0.69	0.52	1.49	-0.35
65	17.78	0.988	0.008	0.004	0.77	1.00	1.16	-0.25	0.25	-0.30	-0.33	-0.25	-0.26	0.28	0.34	0.28	0.22	0.25	0.43	-0.14
66	20.32	0.994	0.005	-0.002	0.30	0.52	0.63	-0.04	0.03	-0.11	0.00	-0.05	-0.03	0.05	0.04	0.05	0.01	0.02	0.00	-0.02
67	22.86	0.997	0.004	-0.004	0.23	0.43	0.55	0.00	0.02	-0.10	0.00	-0.02	-0.01	0.01	0.02	0.02	0.01	0.03	0.00	-0.01
68	25.40	0.998	0.003	-0.004	0.19	0.37	0.53	0.00	-0.01	-0.08	0.00	0.02	0.00	0.00	-0.01	0.00	0.00	-0.01	-0.01	0.00
69	35.56	0.997	0.007	-0.001	0.18	0.33	0.51	0.00	0.01	-0.06	0.00	0.01	0.00	0.00	0.00	0.00	0.00	0.03	-0.01	0.00
70	45.72	1.006	0.005	-0.005	0.18	0.34	0.50	0.00	0.01	-0.05	0.00	-0.02	-0.01	0.00	-0.01	0.00	0.00	0.04	0.00	0.00

Table C.5 Continued.

Case B.S1 Station= 3
X=-228.6mm Tunnel Run#= 622 Ue/Uref= 0.776 Date= 329.88 Time=12.52
Bias Corrected data using 1/sqrt(U*U + V*V + W*W + (.01Ur)^2)

					<-- normalized by 0.001 Ur^2 -->						<---------- normalized by 0.0001 Ur^3 ---------->								
LR	Y(mm)	U/Ur	V/Ur	W/Ur	uu	vv	ww	uv	vw	uw	uuu	uvv	uww	vuu	vvv	vww	wuu	wvv	www	uvw
1	0.00	0.000	0.000	1.000	0.00	0.00	0.00	-2.01	2.23	0.00	0.00	0.00	0.00	0.00	0.00	0.00	0.00	0.00	0.00	0.00
1	0.19	0.515	0.000	0.385	14.73	0.00	23.12	0.00	0.00	-9.75	-0.85	0.00	-3.69	0.00	0.00	0.00	1.79	0.00	8.73	0.00
2	0.25	0.536	0.002	0.370	14.75	3.31	20.87	-1.24	0.87	-8.53	-1.66	-0.27	-4.53	0.95	-0.03	0.69	3.68	0.21	5.51	-0.53
3	0.38	0.565	0.004	0.338	13.28	3.96	18.25	-1.35	1.04	-6.29	-0.24	-0.10	-2.58	1.11	0.28	1.10	2.19	0.30	4.60	-0.61
38	0.51	0.591	-0.007	0.312	12.68	3.82	16.22	-1.56	1.43	-5.16	-0.55	-0.49	-2.74	0.83	0.58	1.38	2.12	0.56	2.93	-0.68
5	0.63	0.601	-0.004	0.294	12.19	3.99	16.33	-1.49	1.06	-4.85	-0.01	-0.36	-2.09	0.82	0.67	0.75	1.10	0.26	3.80	-0.26
6	0.76	0.617	-0.003	0.281	12.40	4.06	15.88	-1.62	1.21	-4.90	-0.57	-0.37	-1.69	0.99	0.81	0.71	1.17	0.48	2.01	-0.22
7	1.02	0.639	0.000	0.260	12.08	4.19	14.86	-1.71	1.37	-5.12	-1.01	-0.51	-2.20	1.17	0.79	1.01	1.74	0.48	4.18	-0.28
8	1.27	0.657	-0.001	0.243	11.17	4.15	13.91	-1.81	1.65	-4.70	-0.57	-0.48	-1.96	0.97	0.76	1.06	1.49	0.45	4.15	-0.30
9	1.52	0.670	0.000	0.224	10.94	4.20	13.82	-1.87	1.62	-4.68	-0.67	-0.54	-1.36	0.86	0.79	1.26	0.89	0.36	3.51	-0.13
10	1.78	0.683	0.004	0.212	10.99	4.13	12.72	-2.04	1.67	-4.86	-0.67	-0.62	-2.03	0.91	0.58	1.05	1.24	0.51	3.78	-0.45
11	2.03	0.692	0.002	0.201	10.46	4.15	12.18	-1.93	1.81	-4.39	-1.17	-0.62	-1.99	1.15	0.59	0.90	1.36	0.62	3.67	-0.36
12	2.29	0.699	0.005	0.189	10.34	4.33	12.23	-2.11	2.03	-4.47	-1.07	-0.59	-1.41	0.97	0.84	1.02	1.34	0.65	2.81	-0.55
13	2.54	0.706	0.003	0.186	9.91	4.14	11.61	-1.94	1.99	-4.49	-1.62	-0.58	-1.73	0.98	0.54	1.20	1.33	0.59	3.44	-0.61
14	2.79	0.721	0.001	0.177	9.64	4.04	11.11	-2.11	2.05	-4.32	-1.23	-0.64	-1.79	1.20	0.43	1.53	1.31	0.82	3.41	-0.83
15	3.30	0.732	0.002	0.165	9.33	4.42	10.61	-2.12	1.94	-3.89	-1.64	-0.72	-1.64	1.05	0.48	1.33	1.39	0.75	3.39	-0.73
16	3.81	0.739	0.001	0.159	8.85	4.42	10.57	-2.13	2.08	-3.96	-0.89	-0.72	-1.38	0.78	0.66	1.41	0.94	0.79	3.16	-0.63
17	4.32	0.753	0.004	0.151	8.81	4.35	9.65	-2.04	2.06	-3.54	-0.91	-0.53	-1.39	0.61	0.54	1.33	0.95	0.66	2.77	-0.59
18	4.83	0.760	0.005	0.145	8.59	4.50	9.36	-2.20	2.11	-3.56	-1.81	-0.71	-1.20	0.82	0.75	1.19	1.17	0.80	2.52	-0.68
19	5.59	0.767	0.007	0.139	8.19	4.52	9.29	-2.11	2.19	-3.30	-1.66	-0.65	-1.05	0.59	0.84	0.99	0.84	0.69	2.18	-0.55
20	6.35	0.781	0.008	0.132	7.99	4.51	8.91	-2.28	2.26	-3.29	-1.18	-0.63	-0.95	0.71	0.78	1.16	0.82	0.77	2.72	-0.53
21	7.11	0.793	0.009	0.124	8.11	4.38	8.71	-2.18	2.15	-3.15	-1.50	-0.74	-1.01	0.84	0.99	1.08	1.06	0.87	2.09	-0.57
22	8.38	0.814	0.012	0.113	7.45	4.23	8.22	-2.07	2.04	-2.78	-1.43	-0.81	-1.01	0.88	0.86	1.07	0.96	0.79	2.34	-0.56
23	10.16	0.838	0.016	0.097	6.86	3.79	7.30	-1.99	1.86	-2.46	-2.16	-0.82	-0.98	0.80	0.96	1.12	0.81	0.90	2.28	-0.54
24	12.70	0.873	0.026	0.074	5.90	3.37	6.31	-1.76	1.67	-2.27	-2.28	-0.93	-1.34	0.92	1.01	1.09	1.21	0.89	2.75	-0.63
25	15.24	0.915	0.030	0.050	4.64	2.63	4.56	-1.37	1.17	-1.72	-2.59	-0.88	-1.40	0.98	0.93	0.97	1.25	0.75	2.33	-0.55
26	17.78	0.945	0.031	0.028	2.99	1.84	2.87	-0.94	0.77	-1.19	-2.10	-0.76	-1.20	0.85	0.75	0.80	1.13	0.60	1.91	-0.46
27	20.32	0.967	0.032	0.014	1.45	1.19	1.56	-0.54	0.41	-0.56	-1.00	-0.51	-0.69	0.61	0.56	0.50	0.59	0.41	1.10	-0.28
28	22.86	0.983	0.032	0.006	0.42	0.62	0.53	-0.17	0.17	-0.15	-0.11	-0.18	-0.17	0.19	0.29	0.22	0.14	0.19	0.17	-0.08
29	25.40	0.984	0.034	0.006	0.18	0.34	0.25	-0.07	0.05	-0.04	-0.02	-0.07	-0.02	0.09	0.13	0.06	0.02	0.04	0.02	-0.02
30	27.94	0.983	0.036	0.008	0.11	0.16	0.17	-0.01	0.01	-0.02	0.00	-0.01	0.01	0.01	0.02	0.01	0.01	0.01	0.00	0.00
31	30.48	0.985	0.037	0.008	0.08	0.11	0.14	0.00	0.00	-0.02	0.00	0.00	0.01	0.00	0.00	0.00	0.00	0.00	0.00	0.00
32	35.56	0.987	0.042	0.008	0.09	0.08	0.12	0.00	0.00	-0.01	0.00	0.00	0.01	0.00	0.00	0.00	0.00	0.00	0.00	0.00
33	40.64	0.990	0.046	0.008	0.07	0.08	0.11	0.00	0.00	0.00	0.00	0.00	0.01	0.00	0.00	0.00	0.00	0.00	0.00	0.00
34	45.72	0.991	0.051	0.007	0.06	0.09	0.13	0.00	0.00	-0.01	0.00	0.00	0.01	0.00	0.00	0.00	0.01	0.00	0.00	0.00
35	50.80	1.001	0.076	0.005	0.06	0.41	0.13	0.00	0.00	-0.01	0.00	0.00	0.01	0.00	-0.01	0.00	0.01	0.00	0.00	0.00
36	55.88	1.000	0.089	0.004	0.06	0.41	0.14	0.00	0.00	-0.01	0.00	0.00	0.01	0.00	0.01	0.00	0.00	0.00	0.00	0.00
37	60.96	1.009	0.100	0.002	0.08	0.45	0.17	0.00	0.00	-0.02	0.00	0.02	0.01	0.00	0.01	0.00	0.01	-0.02	0.00	0.00

Table C.5 Continued.

Case B.S1 Station= 4
X=-152.4mm Tunnel Run#= 621 Ue/Uref= 0.674 Date= 329.88 Time=11.35
Bias Corrected data using 1/sqrt(U*U + V*V + W*W + (.01Ur)^2)

					<-- normalized by 0.001 Ur^2 -->						<---------- normalized by 0.0001 Ur^3 ---------->								
LR	Y(mm)	U/Ur	V/Ur	W/Ur	uu	vv	ww	uv	vw	uw	uuu	uvv	uww	vuu	vvv	vww	wuu	wvv	www	uvw
1	0.00	0.000	0.000	1.000	0.00	0.00	0.00	-1.79	2.18	0.00	0.00	0.00	0.00	0.00	0.00	0.00	0.00	0.00	0.00	0.00
1	0.19	0.436	0.000	0.373	14.38	0.00	23.92	0.00	0.00	-11.35	-1.43	0.00	1.63	0.00	0.00	0.00	-0.16	0.00	5.56	0.00
2	0.25	0.456	-0.004	0.354	13.15	3.09	19.70	-1.04	1.65	-7.82	-0.93	-0.28	-4.56	0.74	-0.18	1.70	3.00	0.26	6.57	-0.75
3	0.38	0.483	-0.001	0.314	11.77	3.37	16.81	-1.08	1.44	-5.42	0.33	-0.16	-1.92	0.56	0.17	1.43	1.16	0.30	2.75	-0.47
4	0.51	0.502	-0.009	0.297	11.64	3.65	15.52	-1.46	1.82	-4.60	0.76	-0.46	-1.25	0.97	0.52	1.58	1.33	0.58	1.55	-0.63
5	0.63	0.520	-0.009	0.279	11.71	3.75	15.11	-1.38	1.82	-4.32	-0.27	-0.33	-1.42	0.91	0.59	1.45	0.91	0.58	2.50	-0.58
6	0.76	0.531	-0.007	0.265	11.61	3.71	14.00	-1.79	1.96	-4.14	0.31	-0.48	-0.65	0.95	0.31	1.37	0.61	0.55	1.84	-0.29
7	1.02	0.552	-0.005	0.239	10.65	3.89	13.61	-1.64	1.98	-4.10	-0.77	-0.46	-1.10	0.77	0.78	1.42	1.03	0.60	1.57	-0.51
8	1.27	0.572	-0.003	0.224	10.57	3.82	12.50	-1.78	2.11	-4.22	-0.76	-0.45	-1.54	0.78	0.67	1.56	1.17	0.66	2.15	-0.41
9	1.52	0.582	-0.003	0.205	10.55	3.95	12.37	-1.96	2.08	-4.33	-1.29	-0.63	-1.35	1.05	0.71	1.46	1.67	0.74	2.41	-0.72
10	1.78	0.594	-0.001	0.196	10.53	4.00	12.49	-1.93	2.15	-4.20	-1.35	-0.56	-1.38	1.04	0.64	1.37	1.79	0.69	2.50	-0.46
11	2.03	0.602	-0.001	0.182	10.34	4.02	11.66	-1.85	2.04	-3.94	-1.45	-0.57	-1.42	1.18	0.68	1.65	1.46	0.74	2.37	-0.51
12	2.29	0.612	-0.001	0.175	10.03	4.05	11.27	-1.97	2.11	-3.95	-1.25	-0.73	-1.40	1.14	0.58	1.36	1.35	0.83	2.52	-0.70
13	2.54	0.620	0.000	0.166	9.56	4.19	11.08	-1.97	2.12	-3.73	-1.07	-0.63	-1.30	0.99	0.64	1.58	1.40	0.90	3.02	-0.59
14	2.79	0.627	0.002	0.160	9.10	4.09	10.53	-1.83	2.09	-3.70	-1.31	-0.56	-1.42	0.90	0.53	1.43	1.43	0.83	2.35	-0.61
15	3.30	0.634	0.003	0.145	9.06	4.16	10.10	-1.98	2.11	-3.67	-0.80	-0.56	-0.73	0.85	0.70	1.30	0.82	0.87	2.07	-0.59
16	3.81	0.640	0.006	0.138	8.77	4.25	9.55	-2.00	2.07	-3.39	-1.43	-0.55	-0.73	0.83	0.55	1.22	0.97	0.75	1.58	-0.69
17	4.32	0.654	0.005	0.129	8.27	4.15	9.30	-1.90	2.03	-3.31	-0.82	-0.62	-0.65	0.68	0.72	1.17	0.86	0.90	1.69	-0.64
18	4.83	0.660	0.007	0.126	7.99	4.22	9.35	-1.90	1.88	-2.99	-0.45	-0.54	-0.56	0.68	0.61	0.92	0.46	0.66	1.78	-0.38
19	5.59	0.671	0.009	0.119	7.86	4.36	8.81	-1.95	2.12	-2.91	-0.80	-0.57	-0.34	0.62	0.77	1.00	0.56	0.73	1.48	-0.41
20	6.35	0.678	0.011	0.111	7.65	4.33	8.55	-2.00	2.13	-2.70	-0.91	-0.47	-0.35	0.53	0.51	0.92	0.60	0.73	1.44	-0.44
21	7.11	0.691	0.012	0.108	7.61	4.48	8.58	-2.11	2.17	-2.71	-0.45	-0.45	-0.57	0.44	0.77	0.87	0.65	0.77	1.69	-0.37
22	8.38	0.708	0.016	0.101	7.39	4.43	8.07	-2.05	2.12	-2.35	-0.87	-0.39	-0.34	0.49	0.64	0.78	0.41	0.65	1.45	-0.26
23	10.16	0.729	0.018	0.087	7.39	4.10	7.56	-1.97	1.92	-2.47	-1.21	-0.62	-0.49	0.53	0.87	0.73	0.67	0.74	1.39	-0.32
24	12.70	0.763	0.024	0.067	6.55	3.71	6.60	-1.80	1.68	-2.07	-1.45	-0.64	-0.58	0.65	0.85	0.81	0.66	0.75	1.75	-0.38
25	15.24	0.798	0.029	0.050	5.88	3.29	5.79	-1.74	1.54	-1.93	-2.06	-0.68	-0.90	0.93	0.92	0.89	1.03	0.73	1.74	-0.46
26	17.78	0.827	0.031	0.032	4.95	2.58	4.56	-1.38	1.09	-1.68	-2.73	-0.83	-1.20	1.06	0.88	0.84	1.15	0.74	2.15	-0.45
27	20.32	0.857	0.035	0.014	3.55	2.00	3.24	-1.00	0.77	-1.22	-2.34	-0.69	-1.01	0.87	0.71	0.62	1.11	0.55	1.81	-0.42
28	22.86	0.885	0.036	0.001	2.11	1.42	2.01	-0.64	0.50	-0.72	-1.47	-0.57	-0.76	0.63	0.56	0.47	0.71	0.44	1.23	-0.26
29	25.40	0.899	0.037	-0.009	1.07	0.95	1.04	-0.39	0.28	-0.39	-0.77	-0.35	-0.47	0.43	0.40	0.31	0.47	0.26	0.62	-0.19
30	27.94	0.906	0.037	-0.013	0.38	0.52	0.46	-0.15	0.12	-0.12	-0.12	-0.14	-0.10	0.16	0.23	0.15	0.11	0.12	0.15	-0.08
31	30.48	0.909	0.038	-0.013	0.17	0.29	0.26	-0.07	0.06	-0.05	0.00	-0.07	-0.02	0.08	0.10	0.05	0.04	0.05	0.02	-0.02
32	33.02	0.911	0.040	-0.015	0.11	0.17	0.20	-0.01	0.02	-0.01	0.00	-0.02	0.00	0.02	0.02	0.02	0.01	0.01	0.00	0.00
33	35.56	0.913	0.042	-0.016	0.09	0.13	0.20	0.00	0.01	-0.01	0.00	0.00	0.01	0.00	0.01	0.00	0.00	0.00	0.00	0.00
34	40.64	0.914	0.048	-0.013	0.08	0.12	0.19	0.00	0.01	0.01	0.00	0.00	0.02	0.00	0.00	0.00	0.01	0.00	0.00	0.00
35	45.72	0.916	0.054	-0.014	0.08	0.11	0.20	0.00	0.00	0.00	0.00	0.00	0.03	0.00	0.00	0.00	0.01	0.00	0.00	0.00

Table C.5 Continued.

Case B.S1 Station= 5
X= -76.2mm Tunnel Run#= 620 Ue/Uref= 0.601 Date= 328.88 Time=18.00
Bias Corrected data using 1/sqrt(U*U + V*V + W*W + (.01Ur)^2)

					<-- normalized by 0.001 Ur^2 -->						<---------- normalized by 0.0001 Ur^3 ---------->									
LR	Y(mm)	U/Ur	V/Ur	W/Ur	uu	vv	ww	uv	vw	uw	uuu	uvv	uww	vuu	vvv	vww	wuu	wvv	www	uvw
1	0.00	0.000	0.000	0.000	0.00	0.00	0.00	-1.49	2.17	0.00	0.00	0.00	0.00	0.00	0.00	0.00	0.00	0.00	0.00	0.00
1	0.19	0.342	0.000	0.389	13.20	0.00	22.04	0.00	0.00	-8.96	1.32	0.00	-5.23	0.00	0.00	0.00	2.13	0.00	5.88	0.00
2	0.25	0.363	-0.001	0.363	12.37	2.64	19.70	-1.18	2.00	-7.02	0.31	-0.27	-6.71	0.71	-0.09	2.08	3.41	0.51	10.15	-1.13
3	0.38	0.391	0.000	0.316	11.46	3.35	15.85	-1.32	1.92	-4.94	-0.16	-0.30	-4.17	0.72	0.16	1.83	2.34	0.70	5.99	-0.86
4	0.51	0.412	-0.009	0.288	10.85	3.18	14.59	-1.32	1.98	-4.02	0.55	-0.43	-2.97	0.68	0.31	1.53	1.68	0.67	4.62	-0.63
5	0.63	0.421	-0.008	0.268	10.56	3.35	13.48	-1.25	1.80	-3.62	-0.06	-0.34	-2.20	0.72	0.42	1.24	1.09	0.63	3.21	-0.31
6	0.76	0.434	-0.008	0.253	10.57	3.35	13.17	-1.30	1.89	-3.41	0.19	-0.26	-1.76	0.54	0.49	1.18	0.74	0.50	2.38	-0.36
7	1.02	0.451	-0.007	0.226	10.14	3.54	12.22	-1.62	1.89	-3.28	0.49	-0.46	-1.49	0.73	0.61	1.59	0.73	0.79	3.19	-0.38
8	1.27	0.465	-0.003	0.211	9.98	3.67	12.11	-1.63	2.07	-3.48	-0.03	-0.40	-1.12	0.97	0.61	1.19	1.03	0.65	2.58	-0.49
9	1.52	0.478	-0.002	0.191	10.16	3.68	11.09	-1.64	1.97	-3.56	-0.25	-0.50	-1.24	0.82	0.56	1.25	1.06	0.85	2.68	-0.49
10	1.78	0.491	-0.003	0.179	9.56	3.57	11.15	-1.60	1.93	-3.49	-0.46	-0.22	-1.22	0.65	0.36	1.24	1.08	0.70	2.60	-0.29
11	2.03	0.499	-0.002	0.171	9.48	3.70	11.04	-1.76	2.06	-3.65	-0.02	-0.41	-1.39	0.67	0.59	1.44	1.28	0.74	2.91	-0.54
12	2.29	0.505	0.000	0.161	9.24	3.61	10.64	-1.55	1.86	-3.43	-0.27	-0.30	-1.07	0.75	0.43	1.09	1.11	0.67	2.64	-0.39
13	2.54	0.512	-0.001	0.153	8.99	3.76	10.49	-1.87	2.18	-3.69	-0.82	-0.51	-1.43	0.89	0.54	1.50	1.50	0.91	2.23	-0.71
14	2.79	0.516	0.002	0.149	9.04	3.85	10.28	-1.90	2.04	-3.39	-0.55	-0.49	-1.19	0.71	0.48	1.47	1.13	0.85	2.44	-0.52
15	3.30	0.527	0.003	0.142	8.66	4.04	9.89	-1.98	2.10	-3.42	-0.50	-0.49	-1.02	0.77	0.61	1.41	0.99	0.92	2.25	-0.64
16	3.81	0.536	0.005	0.137	8.65	4.05	9.87	-1.85	2.13	-3.12	-0.72	-0.44	-0.80	0.87	0.43	1.34	1.11	0.88	1.78	-0.58
17	4.32	0.542	0.008	0.131	7.94	4.19	9.46	-1.92	2.11	-3.12	-0.36	-0.47	-0.70	0.56	0.64	1.31	0.89	0.96	2.00	-0.53
18	4.83	0.550	0.010	0.126	8.01	4.27	9.27	-1.92	2.13	-2.91	-0.34	-0.56	-0.38	0.72	0.60	1.16	0.84	0.78	1.93	-0.54
19	5.59	0.561	0.011	0.119	7.79	4.25	8.61	-1.87	1.96	-2.52	-0.31	-0.34	-0.27	0.67	0.73	0.91	0.67	0.79	1.28	-0.45
20	6.35	0.572	0.009	0.109	7.43	4.34	8.61	-1.73	1.99	-2.45	-0.45	-0.25	-0.48	0.43	0.47	0.98	0.52	0.69	1.72	-0.33
21	7.11	0.577	0.014	0.107	7.46	4.38	8.18	-1.92	1.99	-2.39	-0.41	-0.35	-0.41	0.61	0.61	0.85	0.78	0.67	1.14	-0.35
22	8.38	0.591	0.016	0.096	6.95	4.34	7.94	-1.85	1.85	-1.94	-0.49	-0.33	-0.13	0.35	0.72	0.50	0.54	0.53	0.65	-0.27
23	10.16	0.610	0.019	0.085	6.83	4.14	7.55	-1.83	1.80	-1.74	-0.39	-0.30	-0.16	0.17	0.48	0.62	0.25	0.58	0.71	-0.25
24	12.70	0.640	0.026	0.074	6.87	4.06	7.14	-1.67	1.68	-1.72	-0.53	-0.22	-0.14	0.17	0.79	0.34	0.34	0.43	0.97	-0.09
25	15.24	0.668	0.030	0.055	6.41	3.62	6.20	-1.79	1.52	-1.69	-0.69	-0.43	-0.34	0.42	0.61	0.52	0.35	0.50	1.05	-0.18
26	17.78	0.693	0.034	0.043	6.01	3.33	5.90	-1.65	1.44	-1.74	-1.20	-0.49	-0.51	0.51	0.66	0.58	0.46	0.51	1.25	-0.26
27	20.32	0.724	0.039	0.028	5.44	2.91	5.01	-1.42	1.22	-1.55	-1.75	-0.59	-0.66	0.69	0.70	0.69	0.57	0.57	1.50	-0.32
28	22.86	0.752	0.042	0.014	4.86	2.53	4.27	-1.28	1.01	-1.57	-2.26	-0.70	-0.94	0.80	0.72	0.70	0.99	0.62	1.77	-0.37
29	25.40	0.777	0.046	0.003	3.95	2.09	3.62	-1.01	0.79	-1.41	-2.41	-0.70	-1.05	0.81	0.73	0.62	1.02	0.55	2.01	-0.35
30	27.94	0.801	0.046	-0.011	2.37	1.54	2.22	-0.65	0.55	-0.83	-1.53	-0.56	-0.79	0.64	0.55	0.51	0.87	0.50	1.27	-0.30
31	30.48	0.814	0.049	-0.021	1.52	1.19	1.47	-0.44	0.38	-0.52	-1.04	-0.41	-0.46	0.47	0.54	0.40	0.60	0.32	0.92	-0.21
32	33.02	0.825	0.050	-0.025	0.75	0.82	0.80	-0.24	0.24	-0.26	-0.37	-0.25	-0.22	0.26	0.36	0.22	0.28	0.22	0.40	-0.13
33	35.56	0.830	0.052	-0.027	0.40	0.52	0.50	-0.13	0.14	-0.11	-0.11	-0.11	-0.09	0.15	0.26	0.14	0.13	0.13	0.16	-0.07
34	38.10	0.832	0.053	-0.030	0.16	0.27	0.28	-0.04	0.06	-0.01	0.00	-0.03	0.01	0.04	0.06	0.05	0.04	0.05	0.02	-0.01
35	40.64	0.830	0.056	-0.032	0.13	0.19	0.23	-0.01	0.03	-0.01	0.00	0.00	0.01	0.02	0.03	0.02	0.02	0.02	0.00	-0.01
36	45.72	0.828	0.060	-0.031	0.08	0.12	0.20	0.00	0.01	0.00	0.00	0.00	0.04	0.00	0.00	0.00	0.00	0.00	0.00	0.00
37	50.80	0.828	0.065	-0.030	0.08	0.10	0.20	0.00	0.01	0.00	0.00	0.00	0.03	0.00	0.00	0.00	0.00	0.00	0.00	0.00
38	55.88	0.827	0.088	-0.033	0.08	0.41	0.22	0.00	0.00	0.03	0.00	0.00	0.04	0.00	0.01	0.00	0.02	0.00	0.00	0.00
39	60.96	0.824	0.095	-0.039	0.08	0.43	0.22	0.00	0.00	0.04	0.00	0.00	0.04	0.00	0.00	0.00	0.02	0.00	0.00	0.00
40	66.04	0.821	0.000	-0.042	0.08	0.00	0.23	0.00	0.00	0.06	0.00	0.00	0.09	0.00	0.00	0.00	0.04	0.00	0.00	0.00

Table C.5 Continued.

Case B.S1 Station= 6
X= 101.6mm Tunnel Run#= 612 Ue/Uref= 0.494 Date= 324.88 Time=11.04
Bias Corrected data using 1/sqrt(U*U + V*V + W*W + (.01Ur)^2)

					<-- normalized by 0.001 Ur^2 -->						<---------- normalized by 0.0001 Ur^3 ---------->									
LR	Y(mm)	U/Ur	V/Ur	W/Ur	uu	vv	ww	uv	vw	uw	uuu	uvv	uww	vuu	vvv	vww	wuu	wvv	www	uvw
1	0.00	0.000	0.000	0.000	0.00	0.00	0.00	-0.57	-0.16	0.00	0.00	0.00	0.00	0.00	0.00	0.00	0.00	0.00	0.00	0.00
1	0.19	0.193	0.000	0.048	5.52	0.00	4.16	0.00	0.00	1.00	1.58	0.00	1.25	0.00	0.00	0.00	0.50	0.00	0.23	0.00
2	0.25	0.231	0.011	0.057	6.47	0.73	4.53	-0.36	-0.23	0.59	1.80	0.06	2.02	-0.07	-0.06	0.02	-0.47	-0.01	-0.81	-0.04
3	0.38	0.264	0.011	0.069	6.55	0.95	5.07	-0.44	-0.25	0.42	1.12	0.07	1.90	0.02	-0.04	0.15	-0.71	0.02	-0.53	-0.04
4	0.51	0.288	0.002	0.076	6.61	0.82	5.23	-0.64	-0.31	0.26	1.37	0.04	1.80	0.06	-0.04	0.10	-0.80	0.01	-0.71	0.03
5	0.63	0.305	0.001	0.082	6.30	0.98	5.04	-0.67	-0.28	0.38	1.01	0.04	1.28	0.09	-0.06	0.04	-0.26	0.00	-0.30	0.01
6	0.76	0.315	0.001	0.086	6.54	1.15	5.25	-0.81	-0.37	0.12	1.00	0.05	1.46	0.08	-0.04	0.04	-0.39	0.01	-0.51	-0.01
7	1.02	0.331	0.001	0.090	6.19	1.41	5.15	-0.78	-0.30	-0.03	1.23	0.07	1.55	-0.02	-0.04	0.11	-0.29	-0.02	-0.27	0.03
8	1.27	0.344	0.002	0.091	6.38	1.62	5.27	-0.85	-0.21	-0.06	1.20	0.06	1.34	-0.06	-0.05	0.09	-0.34	0.02	0.01	0.02
9	1.52	0.359	0.002	0.095	6.26	1.84	5.59	-0.92	-0.15	-0.03	1.10	0.06	1.18	-0.09	-0.05	0.08	-0.08	-0.04	-0.20	0.06
10	1.78	0.363	0.001	0.094	6.22	1.84	5.25	-1.01	-0.14	-0.14	1.00	0.13	1.25	-0.09	-0.08	0.13	-0.27	-0.03	-0.14	0.06
11	2.03	0.372	0.002	0.097	6.44	1.99	5.50	-1.05	-0.13	-0.09	0.82	0.07	1.08	0.01	-0.09	0.09	-0.08	-0.05	-0.19	0.05
12	2.29	0.378	0.002	0.097	6.53	2.12	5.44	-1.16	-0.09	-0.08	0.92	0.10	1.10	-0.05	-0.11	0.13	-0.03	0.00	-0.41	-0.01
13	2.54	0.393	0.001	0.100	6.90	2.27	5.77	-1.19	-0.05	-0.01	0.81	0.13	1.10	-0.04	-0.13	0.05	0.03	-0.06	-0.27	0.13
14	2.79	0.396	0.002	0.102	6.80	2.35	5.41	-1.26	-0.02	0.02	1.09	0.18	0.78	-0.12	-0.11	0.19	0.18	-0.03	-0.12	0.04
15	3.30	0.407	0.004	0.102	6.55	2.46	5.65	-1.19	0.11	-0.08	0.89	0.11	0.92	-0.09	-0.14	0.14	0.07	-0.07	-0.07	0.03
16	3.81	0.411	0.002	0.104	7.20	2.69	5.60	-1.38	0.03	-0.05	0.73	0.11	1.09	-0.05	-0.15	0.09	0.07	-0.07	0.08	0.06
17	4.32	0.427	0.003	0.104	7.10	2.67	5.66	-1.33	0.20	-0.09	0.62	0.12	0.78	0.04	-0.13	0.20	0.17	-0.06	-0.21	0.10
18	4.83	0.435	0.003	0.107	7.24	2.96	5.71	-1.48	0.18	-0.06	0.55	0.03	0.82	0.03	-0.07	0.15	0.08	-0.06	-0.05	0.05
19	5.59	0.452	0.000	0.110	7.44	2.99	5.70	-1.61	0.31	-0.18	0.48	0.12	0.73	0.09	-0.23	0.17	0.26	-0.05	-0.27	0.12
20	6.35	0.463	0.001	0.112	7.46	3.14	5.64	-1.66	0.49	-0.26	0.31	0.07	0.62	0.03	-0.09	0.12	0.10	-0.02	-0.19	0.15
21	7.11	0.477	0.003	0.113	7.35	3.30	5.78	-1.59	0.57	-0.30	0.12	0.09	0.54	0.13	-0.03	0.14	0.13	0.06	-0.06	0.03
22	8.38	0.496	0.002	0.117	7.51	3.49	5.79	-1.53	0.71	-0.28	0.17	-0.12	0.45	0.34	0.02	0.16	0.38	0.03	-0.16	0.00
23	10.16	0.524	0.002	0.117	7.17	3.61	5.71	-1.77	0.84	-0.31	-0.32	-0.22	0.12	0.30	0.18	0.22	0.21	0.13	0.06	0.00
24	12.70	0.549	0.004	0.116	6.81	3.72	5.50	-1.70	1.02	-0.42	-0.64	-0.30	0.17	0.42	0.46	0.26	0.13	0.20	0.07	-0.06
25	15.24	0.576	0.005	0.107	6.58	3.69	5.38	-1.67	1.27	-0.57	-1.13	-0.43	-0.24	0.64	0.75	0.49	0.31	0.44	0.54	-0.23
26	17.78	0.600	0.007	0.100	5.85	3.35	4.85	-1.47	1.25	-0.69	-1.17	-0.54	-0.36	0.63	0.74	0.55	0.36	0.54	0.62	-0.21
27	20.32	0.618	0.006	0.089	5.02	3.07	4.32	-1.31	1.19	-0.73	-1.01	-0.67	-0.32	0.61	0.90	0.49	0.33	0.52	0.74	-0.25
28	22.86	0.631	0.010	0.077	4.84	2.85	4.06	-1.22	1.03	-0.71	-1.23	-0.62	-0.39	0.62	0.84	0.62	0.27	0.53	0.83	-0.29
29	25.40	0.647	0.010	0.065	4.06	2.32	3.41	-0.97	0.86	-0.69	-1.24	-0.49	-0.32	0.56	0.65	0.54	0.25	0.51	0.92	-0.23
30	27.94	0.669	0.011	0.055	3.70	2.09	2.75	-0.87	0.65	-0.72	-1.54	-0.61	-0.40	0.61	0.70	0.54	0.38	0.45	0.91	-0.28
31	30.48	0.678	0.012	0.043	3.06	1.83	2.24	-0.70	0.49	-0.51	-1.43	-0.51	-0.44	0.54	0.72	0.49	0.31	0.43	0.76	-0.25
32	33.02	0.692	0.013	0.035	2.44	1.50	1.79	-0.55	0.33	-0.41	-1.29	-0.42	-0.26	0.43	0.54	0.34	0.26	0.32	0.63	-0.16
33	35.56	0.703	0.014	0.028	1.80	1.19	1.42	-0.44	0.21	-0.29	-0.96	-0.40	-0.13	0.46	0.50	0.27	0.16	0.32	0.45	-0.14
34	38.10	0.712	0.016	0.023	1.35	0.97	1.18	-0.32	0.08	-0.27	-0.71	-0.32	-0.16	0.35	0.33	0.24	0.19	0.22	0.38	-0.13
35	40.64	0.719	0.016	0.018	0.83	0.68	0.83	-0.15	-0.06	-0.14	-0.31	-0.15	0.04	0.17	0.19	0.08	0.04	0.07	0.21	-0.04
36	45.72	0.726	0.019	0.014	0.40	0.37	0.55	-0.02	-0.14	-0.04	0.00	-0.06	0.08	0.06	0.03	0.02	0.00	0.03	0.07	-0.02
37	50.80	0.726	0.021	0.013	0.31	0.23	0.47	0.04	-0.13	-0.03	0.02	0.00	0.08	0.01	0.00	-0.01	-0.02	0.01	0.05	0.00
38	55.88	0.724	0.018	0.013	0.31	0.10	0.48	0.03	-0.06	-0.03	0.03	0.01	0.11	0.00	0.00	0.00	-0.02	0.00	0.08	0.00
39	60.96	0.724	0.019	0.013	0.33	0.10	0.49	0.02	-0.05	-0.03	0.03	0.00	0.10	0.00	0.00	-0.01	-0.03	0.00	0.10	0.00
40	66.04	0.723	0.000	0.011	0.35	0.00	0.53	0.00	0.00	-0.05	0.05	0.00	0.14	0.00	0.00	0.00	-0.03	0.00	0.11	0.00
41	69.85	0.724	0.000	0.012	0.35	0.00	0.52	0.00	0.00	-0.05	0.04	0.00	0.14	0.00	0.00	0.00	-0.04	0.00	0.09	0.00

Table C.5 Continued.

Case B.S1 Station= 7
X= 152.4mm Tunnel Run#= 607 Ue/Uref= 0.489 Date= 323.88 Time=13.13
Bias Corrected data using 1/sqrt(U*U + V*V + W*W + (.01Ur)^2)

					<-- normalized by 0.001 Ur^2 -->						<---------- normalized by 0.0001 Ur^3 ---------->									
LR	Y(mm)	U/Ur	V/Ur	W/Ur	uu	vv	ww	uv	vw	uw	uuu	uvv	uww	vuu	vvv	vww	wuu	wvv	www	uvw
1	0.00	0.000	0.000	0.000	0.00	0.00	0.00	-0.51	-0.14	0.00	0.00	0.00	0.00	0.00	0.00	0.00	0.00	0.00	0.00	0.00
2	0.25	0.225	0.010	0.047	6.80	0.62	3.98	-0.33	-0.17	0.51	2.28	0.08	1.90	-0.11	-0.02	0.00	-0.55	-0.01	-0.47	-0.04
3	0.38	0.260	0.009	0.059	6.74	0.85	4.23	-0.48	-0.19	0.79	1.41	0.11	1.22	-0.02	-0.06	0.03	-0.11	0.02	0.46	-0.01
4	0.51	0.280	0.002	0.061	6.81	0.76	4.43	-0.59	-0.27	0.66	1.62	0.07	1.09	-0.02	-0.04	0.01	0.04	-0.01	0.33	-0.01
5	0.63	0.298	0.003	0.065	6.89	0.99	4.74	-0.69	-0.28	0.49	1.29	0.04	1.08	0.01	0.00	0.02	-0.05	-0.01	0.31	0.00
6	0.76	0.313	0.002	0.066	6.78	1.12	5.14	-0.72	-0.28	0.40	1.10	0.11	1.45	0.01	-0.06	-0.01	0.03	0.05	0.37	-0.03
7	1.02	0.326	0.002	0.072	6.79	1.32	5.17	-0.72	-0.25	0.24	1.36	0.12	1.39	-0.02	-0.06	0.06	0.10	0.03	0.31	-0.01
8	1.27	0.339	0.003	0.074	6.79	1.48	5.36	-0.80	-0.23	0.29	1.31	0.08	1.43	-0.03	0.00	0.10	-0.01	0.02	-0.17	-0.03
9	1.52	0.350	0.003	0.074	7.15	1.70	5.32	-0.85	-0.17	0.23	1.30	0.12	1.24	-0.18	-0.07	0.15	0.24	0.03	0.16	-0.07
10	1.78	0.357	0.001	0.077	6.74	1.72	5.31	-0.85	-0.25	0.09	1.30	0.13	1.42	-0.09	-0.03	0.22	0.09	-0.04	0.20	-0.06
11	2.03	0.363	0.002	0.078	6.79	1.85	5.41	-0.99	-0.22	0.26	1.27	0.08	1.13	-0.07	-0.12	0.13	0.09	-0.03	-0.03	0.03
12	2.29	0.371	0.003	0.077	7.19	2.07	5.49	-1.06	-0.11	0.24	1.31	0.13	1.14	0.00	-0.13	0.18	0.21	-0.01	0.10	0.00
13	2.54	0.376	0.003	0.080	7.21	1.99	5.34	-1.05	-0.14	0.16	1.11	0.14	1.19	-0.11	-0.12	0.08	0.14	-0.01	0.05	0.06
14	2.79	0.378	0.003	0.079	7.22	2.15	5.25	-1.11	-0.15	0.19	1.24	0.19	1.05	-0.10	-0.09	0.15	0.07	-0.01	0.29	0.02
15	3.30	0.393	0.003	0.082	7.57	2.29	5.60	-1.15	-0.09	0.19	1.55	0.13	1.11	-0.17	-0.12	0.14	0.27	0.01	-0.11	0.09
16	3.81	0.400	0.004	0.084	7.64	2.49	5.53	-1.26	-0.08	0.09	1.44	0.18	1.09	-0.07	-0.08	0.06	0.18	-0.06	-0.11	-0.02
17	4.32	0.410	0.003	0.085	7.73	2.51	5.58	-1.31	-0.02	0.30	1.03	0.15	1.06	-0.01	-0.20	0.10	0.25	-0.01	-0.06	0.04
18	4.83	0.425	0.002	0.089	7.88	2.74	5.64	-1.37	0.01	0.31	0.87	0.14	0.94	-0.05	-0.17	0.21	0.35	-0.05	0.07	0.10
19	5.59	0.432	0.003	0.089	8.10	2.81	5.70	-1.38	0.13	0.31	0.85	0.11	0.94	0.07	-0.06	0.06	0.42	-0.07	-0.20	0.07
20	6.35	0.454	0.002	0.094	8.23	2.88	5.73	-1.55	0.15	0.15	0.36	0.09	0.76	0.01	-0.08	0.18	0.39	0.00	-0.05	0.03
21	7.11	0.463	0.003	0.095	8.08	3.00	5.63	-1.50	0.25	0.24	0.72	0.02	0.64	-0.07	0.06	0.20	0.05	0.02	-0.36	0.06
22	8.38	0.483	0.002	0.096	8.22	3.10	5.64	-1.63	0.32	0.04	0.00	-0.07	0.48	0.32	0.03	0.10	0.30	0.02	-0.40	0.00
23	10.16	0.506	0.002	0.100	7.90	3.38	5.45	-1.69	0.43	-0.11	-0.02	-0.09	0.33	0.34	0.12	0.19	0.29	0.04	-0.01	0.07
24	12.70	0.537	0.002	0.099	7.05	3.32	5.44	-1.48	0.68	-0.17	-0.74	-0.22	0.04	0.47	0.24	0.33	0.35	0.18	-0.10	-0.05
25	15.24	0.558	0.004	0.098	7.00	3.26	5.13	-1.45	0.75	-0.23	-0.85	-0.40	-0.26	0.52	0.35	0.30	0.09	0.18	0.49	-0.03
26	17.78	0.586	0.006	0.093	6.08	3.19	4.78	-1.35	0.92	-0.47	-1.18	-0.52	-0.17	0.64	0.57	0.41	0.18	0.33	0.65	-0.10
27	20.32	0.602	0.007	0.085	5.87	2.89	4.36	-1.32	0.99	-0.71	-1.66	-0.51	-0.20	0.71	0.61	0.35	0.30	0.36	0.81	-0.19
28	22.86	0.621	0.009	0.074	4.88	2.63	3.78	-1.09	0.80	-0.66	-1.14	-0.60	-0.28	0.67	0.70	0.53	0.24	0.37	0.85	-0.22
29	25.40	0.640	0.008	0.064	4.35	2.36	3.35	-0.99	0.77	-0.70	-1.49	-0.56	-0.26	0.69	0.68	0.32	0.22	0.43	0.93	-0.21
30	27.94	0.647	0.010	0.053	3.81	2.07	3.01	-0.89	0.67	-0.63	-1.49	-0.56	-0.35	0.66	0.68	0.51	0.36	0.48	0.94	-0.28
31	30.48	0.659	0.013	0.045	3.24	1.87	2.53	-0.69	0.47	-0.53	-1.19	-0.50	-0.37	0.56	0.65	0.39	0.31	0.39	0.78	-0.20
32	33.02	0.670	0.012	0.035	2.71	1.62	2.05	-0.59	0.42	-0.45	-1.25	-0.50	-0.26	0.51	0.53	0.39	0.26	0.40	0.79	-0.25
33	35.56	0.685	0.014	0.026	2.05	1.27	1.56	-0.37	0.19	-0.28	-0.97	-0.34	-0.10	0.38	0.47	0.26	0.18	0.25	0.45	-0.13
34	38.10	0.696	0.015	0.019	1.38	1.03	1.18	-0.27	0.03	-0.24	-0.63	-0.29	0.02	0.31	0.37	0.15	0.16	0.20	0.40	-0.10
35	40.64	0.699	0.016	0.016	1.13	0.81	1.01	-0.20	0.00	-0.22	-0.55	-0.22	0.06	0.26	0.25	0.13	0.04	0.14	0.33	-0.08
36	45.72	0.703	0.018	0.011	0.49	0.47	0.68	-0.01	-0.12	-0.12	-0.04	-0.07	0.24	0.07	0.08	0.02	-0.07	0.05	0.15	-0.01
37	50.80	0.702	0.020	0.005	0.37	0.30	0.54	0.05	-0.14	-0.07	0.02	-0.01	0.19	0.02	0.02	0.00	-0.04	0.01	0.09	0.00
38	55.88	0.708	0.033	0.005	0.40	0.51	0.66	0.08	-0.15	-0.08	0.07	-0.01	0.31	0.01	-0.01	-0.03	-0.07	0.01	0.20	0.00
39	60.96	0.709	0.035	0.003	0.41	0.46	0.61	0.07	-0.12	-0.11	0.06	0.00	0.29	0.00	-0.01	0.00	-0.11	0.00	0.14	0.00
40	66.04	0.711	0.000	0.003	0.41	0.00	0.62	0.00	0.00	-0.09	0.06	0.00	0.20	0.00	0.00	0.00	-0.06	0.00	0.13	0.00
41	71.12	0.706	0.000	0.004	0.44	0.00	0.63	0.00	0.00	-0.06	0.06	0.00	0.17	0.00	0.00	0.00	-0.04	0.00	0.12	0.00

Table C.5 Continued.

Case B.S1 Station= 8
X= 228.6mm Tunnel Run#= 626 Ue/Uref= 0.453 Date= 418.88 Time= 8.38
Bias Corrected data using 1/sqrt(U*U + V*V + W*W + (.01Ur)^2)

					<-- normalized by 0.001 Ur^2 -->						<---------- normalized by 0.0001 Ur^3 ---------->									
LR	Y(mm)	U/Ur	V/Ur	W/Ur	uu	vv	ww	uv	vw	uw	uuu	uvv	uww	vuu	vvv	vww	wuu	wvv	www	uvw
1	0.00	0.000	0.000	0.000	0.00	0.00	0.00	-0.43	-0.13	0.00	0.00	0.00	0.00	0.00	0.00	0.00	0.00	0.00	0.00	0.00
1	0.19	0.187	0.000	0.032	6.54	0.00	3.39	0.00	0.00	0.86	2.45	0.00	1.47	0.00	0.00	0.00	0.14	0.00	0.64	0.00
2	0.25	0.220	0.008	0.040	6.99	0.66	3.86	-0.28	-0.08	0.79	2.42	0.10	1.40	-0.09	-0.02	0.02	0.02	0.03	0.71	-0.04
3	0.38	0.247	0.009	0.042	7.29	0.87	4.39	-0.39	-0.13	0.79	2.02	0.11	1.41	-0.03	-0.04	0.04	0.17	0.00	0.67	-0.05
4	0.51	0.269	0.002	0.045	7.17	0.68	4.85	-0.53	-0.16	0.50	1.74	0.06	1.40	-0.04	-0.01	0.01	0.12	0.00	0.76	-0.02
5	0.63	0.277	0.002	0.047	6.77	0.85	5.01	-0.58	-0.18	0.48	1.90	0.06	1.33	-0.07	-0.04	0.05	0.10	0.02	0.69	-0.04
6	0.76	0.289	0.002	0.049	6.94	0.98	4.99	-0.60	-0.20	0.54	1.31	0.08	1.15	-0.05	-0.01	0.08	0.13	0.00	0.69	-0.03
7	1.02	0.303	0.002	0.051	6.58	1.20	4.94	-0.68	-0.16	0.50	1.07	0.11	1.05	-0.11	-0.06	0.06	0.29	0.01	0.63	-0.04
8	1.27	0.316	0.002	0.053	7.10	1.34	5.22	-0.70	-0.24	0.56	1.36	0.10	1.18	-0.05	-0.04	0.11	0.28	0.00	0.94	0.00
9	1.52	0.325	0.002	0.055	7.09	1.56	5.42	-0.78	-0.20	0.42	1.71	0.07	1.24	-0.15	-0.03	0.20	0.43	0.00	0.65	-0.03
10	1.78	0.336	0.002	0.054	7.07	1.62	5.24	-0.80	-0.11	0.25	1.40	0.07	1.00	-0.01	-0.05	0.07	0.34	0.04	0.67	-0.03
11	2.03	0.340	0.002	0.058	7.31	1.75	5.40	-0.93	-0.10	0.34	1.36	0.05	1.24	-0.05	-0.06	0.06	0.34	0.04	0.60	-0.01
12	2.29	0.344	0.002	0.061	7.60	1.85	5.44	-0.98	-0.17	0.23	1.74	0.11	1.08	-0.06	-0.11	0.15	0.60	-0.01	0.56	-0.10
13	2.54	0.350	0.001	0.059	7.38	1.95	5.36	-0.96	-0.12	0.34	1.39	0.14	0.95	-0.11	-0.14	0.09	0.39	0.03	0.21	-0.06
14	2.79	0.356	0.002	0.059	7.83	2.03	5.47	-0.95	-0.10	0.25	1.11	0.12	1.18	0.03	-0.15	0.08	0.45	-0.07	0.39	-0.02
15	3.30	0.364	0.003	0.058	8.13	2.21	5.52	-1.10	-0.15	0.51	1.14	0.12	1.17	-0.06	-0.15	0.15	0.51	-0.05	0.56	0.02
16	3.81	0.368	0.003	0.059	8.23	2.29	5.31	-1.10	-0.10	0.48	1.95	0.10	0.93	-0.08	-0.12	0.03	0.73	-0.03	0.45	0.01
17	4.32	0.378	0.002	0.061	7.88	2.50	5.55	-1.15	-0.03	0.29	0.70	0.14	0.94	0.05	-0.18	0.08	0.62	-0.02	0.23	0.04
18	4.83	0.387	0.002	0.064	7.94	2.58	5.49	-1.26	-0.01	0.33	0.87	0.18	0.87	-0.09	-0.25	0.03	0.50	-0.01	0.13	0.00
1	5.59	0.409	-0.002	0.068	8.71	2.76	5.49	-1.39	-0.02	0.33	1.15	0.10	0.65	0.15	-0.12	0.16	0.78	0.02	0.28	0.04
2	6.35	0.420	-0.002	0.067	8.58	2.87	5.71	-1.42	0.01	0.34	0.87	0.03	0.75	0.09	-0.06	0.11	0.68	-0.01	-0.24	0.04
3	7.11	0.428	-0.002	0.074	8.74	3.07	5.69	-1.66	0.03	0.46	0.59	-0.04	0.45	0.20	-0.08	0.29	0.62	-0.06	0.08	0.11
4	8.38	0.447	-0.001	0.072	9.26	3.09	5.60	-1.68	0.09	0.37	0.39	-0.08	0.41	0.19	-0.07	0.16	0.57	-0.09	0.09	0.12
5	10.16	0.466	-0.001	0.073	9.16	3.24	5.47	-1.75	0.31	0.11	-0.44	-0.12	0.18	0.54	-0.05	0.15	0.65	0.00	-0.01	-0.02
6	12.70	0.491	-0.001	0.078	8.06	3.31	5.25	-1.74	0.36	0.08	-0.49	-0.27	-0.16	0.63	0.29	0.27	0.31	0.11	0.08	0.06
7	15.24	0.520	-0.001	0.080	7.78	3.28	4.88	-1.47	0.56	-0.23	-1.50	-0.41	-0.27	0.74	0.24	0.20	0.36	0.05	0.28	-0.05
8	17.78	0.542	-0.001	0.077	7.12	3.20	4.61	-1.39	0.67	-0.53	-1.98	-0.56	-0.50	0.90	0.39	0.25	0.50	0.19	0.44	-0.02
9	20.32	0.564	0.004	0.075	6.46	3.07	4.30	-1.30	0.78	-0.47	-2.20	-0.42	-0.55	0.88	0.52	0.31	0.42	0.21	0.62	-0.10
10	22.86	0.582	0.004	0.068	5.41	2.69	4.08	-1.04	0.71	-0.63	-1.31	-0.45	-0.58	0.69	0.48	0.35	0.52	0.31	0.70	-0.15
11	25.40	0.595	0.008	0.061	4.97	2.60	3.62	-0.92	0.75	-0.62	-1.73	-0.45	-0.58	0.61	0.49	0.34	0.44	0.32	0.87	-0.13
12	27.94	0.607	0.010	0.056	4.16	2.37	3.57	-0.76	0.73	-0.58	-1.13	-0.31	-0.52	0.57	0.50	0.41	0.40	0.34	0.98	-0.13
13	30.48	0.620	0.012	0.049	3.74	2.32	3.06	-0.67	0.64	-0.56	-1.14	-0.35	-0.41	0.49	0.54	0.33	0.31	0.36	0.95	-0.12
14	33.02	0.636	0.010	0.037	3.23	1.87	2.45	-0.58	0.49	-0.58	-1.24	-0.38	-0.44	0.55	0.38	0.39	0.38	0.33	0.75	-0.19
15	35.56	0.649	0.008	0.027	2.40	1.50	1.92	-0.40	0.32	-0.41	-1.04	-0.30	-0.34	0.42	0.35	0.30	0.35	0.28	0.69	-0.17
16	38.10	0.656	0.010	0.022	1.86	1.31	1.57	-0.30	0.19	-0.32	-0.68	-0.28	-0.29	0.35	0.35	0.24	0.24	0.23	0.56	-0.10
17	40.64	0.662	0.010	0.015	1.67	1.10	1.28	-0.26	0.19	-0.30	-0.90	-0.26	-0.26	0.30	0.25	0.24	0.24	0.24	0.46	-0.12
18	45.72	0.678	0.014	0.007	0.84	0.75	0.84	-0.07	0.02	-0.15	-0.33	-0.13	-0.11	0.16	0.17	0.11	0.13	0.12	0.24	-0.05
19	50.80	0.680	0.016	0.001	0.49	0.55	0.64	0.01	-0.09	-0.09	-0.05	-0.06	0.01	0.07	0.10	0.04	0.04	0.05	0.17	-0.01
20	55.88	0.682	0.025	-0.001	0.33	0.67	0.51	0.08	-0.14	-0.06	0.03	-0.01	0.09	0.02	0.02	0.00	-0.01	0.01	0.07	-0.01
21	60.96	0.684	0.025	-0.001	0.34	0.58	0.59	0.09	-0.15	-0.08	0.04	-0.01	0.17	0.00	-0.02	-0.01	-0.03	0.02	0.16	0.00
22	66.04	0.683	0.000	-0.002	0.38	0.00	0.63	0.00	0.00	-0.05	0.06	0.00	0.09	0.00	0.00	0.00	0.02	0.00	0.16	0.00
23	71.12	0.682	0.000	-0.003	0.41	0.00	0.69	0.00	0.00	-0.08	0.07	0.00	0.27	0.00	0.00	0.00	0.01	0.00	0.17	0.00

Table C.5 Continued.

Case B.S1 Station= 9
X= 304.8mm Tunnel Run#= 604 Ue/Uref= 0.443 Date= 322.88 Time=18.07
Bias Corrected data using 1/sqrt(U*U + V*V + W*W + (.01Ur)^2)

					<-- normalized by 0.001 Ur^2 -->						<---------- normalized by 0.0001 Ur^3 ---------->									
LR	Y(mm)	U/Ur	V/Ur	W/Ur	uu	vv	ww	uv	vw	uw	uuu	uvv	uww	vuu	vvv	vww	wuu	wvv	www	uvw
1	0.00	0.000	0.000	0.000	0.00	0.00	0.00	-0.41	-0.11	0.00	0.00	0.00	0.00	0.00	0.00	0.00	0.00	0.00	0.00	0.00
1	0.25	0.201	0.011	0.024	6.89	0.56	4.41	-0.16	-0.12	0.22	3.14	0.08	2.81	-0.11	-0.03	-0.03	-0.54	0.02	-0.61	-0.06
2	0.38	0.238	0.011	0.030	7.00	0.72	5.03	-0.30	-0.14	0.14	2.65	0.09	2.79	-0.07	-0.03	-0.03	-0.75	0.02	-0.71	-0.02
3	0.51	0.251	0.004	0.031	7.12	0.59	5.40	-0.46	-0.22	0.16	2.17	0.07	2.63	-0.12	-0.03	0.00	-0.37	-0.01	-0.78	-0.03
4	0.63	0.265	0.003	0.031	7.00	0.72	5.53	-0.44	-0.20	0.15	2.07	0.07	2.28	-0.05	-0.02	0.06	-0.35	0.00	-0.35	-0.07
5	0.76	0.279	0.004	0.036	7.05	0.83	5.74	-0.55	-0.20	0.20	2.15	0.11	2.38	-0.03	-0.05	-0.02	-0.22	-0.01	-0.18	-0.07
6	1.02	0.295	0.003	0.039	7.18	1.04	5.95	-0.58	-0.21	0.13	1.69	0.06	2.29	-0.09	-0.05	-0.06	-0.21	-0.01	0.54	0.00
7	1.27	0.305	0.003	0.036	7.31	1.26	6.18	-0.62	-0.22	0.21	1.40	0.08	2.49	-0.02	0.00	0.07	-0.16	-0.01	0.08	-0.04
8	1.52	0.318	0.003	0.037	7.42	1.39	6.24	-0.65	-0.23	0.03	2.01	0.10	2.26	-0.09	-0.05	0.09	-0.05	-0.04	-0.57	-0.05
9	1.78	0.323	0.004	0.039	7.60	1.50	6.10	-0.73	-0.22	0.30	1.57	0.10	2.05	-0.08	-0.04	0.10	-0.02	-0.03	0.07	-0.04
10	2.03	0.328	0.003	0.042	7.54	1.63	6.30	-0.82	-0.22	0.07	1.85	0.11	2.39	-0.06	-0.09	0.09	0.08	-0.03	-0.60	-0.02
11	2.29	0.333	0.003	0.042	7.60	1.75	6.03	-0.83	-0.16	0.20	1.72	0.10	2.08	0.00	-0.13	0.13	-0.06	0.00	0.19	-0.05
12	2.54	0.341	0.002	0.042	7.91	1.85	6.29	-0.91	-0.16	-0.06	1.73	0.10	2.31	0.00	-0.09	0.09	0.07	-0.01	-0.25	-0.09
13	2.79	0.342	0.002	0.041	7.98	1.90	6.05	-0.93	-0.25	-0.11	1.27	0.14	2.13	-0.13	-0.11	0.10	-0.06	-0.09	-0.16	0.02
14	3.30	0.353	0.002	0.042	7.92	2.11	6.37	-0.91	-0.16	-0.04	1.53	0.11	2.29	-0.11	-0.13	0.21	-0.13	-0.02	-0.33	-0.01
15	3.81	0.362	0.002	0.045	7.95	2.21	6.56	-1.03	-0.22	0.14	1.81	0.21	2.43	0.01	-0.24	0.28	0.33	-0.05	-0.30	-0.03
16	4.32	0.369	0.002	0.045	8.67	2.36	6.55	-1.10	-0.20	-0.11	1.98	0.07	2.63	-0.06	-0.15	0.26	0.02	0.00	-1.10	-0.04
17	4.83	0.379	0.002	0.045	8.73	2.47	6.94	-1.16	-0.18	-0.06	1.93	0.12	2.43	-0.05	-0.15	0.19	0.13	-0.06	-1.33	-0.01
18	5.59	0.386	0.000	0.047	9.00	2.60	6.56	-1.22	-0.15	-0.06	1.20	0.06	2.62	0.21	-0.13	0.20	-0.26	0.01	-1.01	0.07
19	6.35	0.398	-0.002	0.049	9.08	2.69	6.45	-1.26	-0.13	-0.09	1.04	0.04	2.69	0.08	-0.09	0.06	-0.04	-0.03	-0.51	0.14
20	7.11	0.412	0.000	0.051	9.13	2.87	6.73	-1.41	-0.20	-0.13	1.19	0.08	2.42	0.12	-0.08	0.24	0.09	-0.09	-0.85	0.00
21	8.38	0.416	0.000	0.052	9.58	2.90	6.41	-1.50	-0.07	0.12	0.66	-0.03	2.02	0.25	-0.03	0.13	0.01	-0.02	-0.92	0.08
22	10.16	0.446	-0.002	0.060	9.30	3.16	6.27	-1.79	-0.11	0.12	0.56	-0.06	2.04	0.31	-0.04	0.16	0.21	-0.03	-0.18	0.10
23	12.70	0.467	-0.004	0.057	9.51	3.19	5.89	-1.60	-0.01	0.00	-0.67	-0.24	1.04	0.60	0.10	0.25	0.03	-0.01	-0.84	0.14
24	15.24	0.490	-0.004	0.058	8.78	3.33	5.57	-1.60	0.23	-0.37	-1.72	-0.41	0.71	0.65	0.32	0.38	-0.11	0.04	-0.36	0.00
25	17.78	0.518	-0.004	0.057	8.52	3.22	5.11	-1.71	0.28	-0.60	-2.68	-0.67	0.69	1.11	0.50	0.42	-0.27	0.11	-0.85	0.12
26	20.32	0.540	-0.005	0.059	7.47	2.93	4.68	-1.41	0.44	-0.69	-2.83	-0.67	0.04	1.16	0.56	0.47	0.26	0.10	-0.04	0.06
27	22.86	0.559	-0.005	0.056	6.58	2.82	4.29	-1.09	0.49	-0.88	-2.44	-0.54	0.36	0.98	0.56	0.31	-0.12	0.21	0.11	-0.09
28	25.40	0.578	-0.006	0.050	5.64	2.58	3.92	-0.94	0.54	-0.74	-2.36	-0.59	-0.21	0.99	0.65	0.37	0.23	0.25	0.76	-0.14
29	27.94	0.596	-0.006	0.046	4.59	2.13	3.16	-0.66	0.47	-0.78	-2.18	-0.51	0.06	0.93	0.38	0.33	0.29	0.24	0.76	-0.20
30	30.48	0.604	-0.004	0.042	4.00	2.02	3.02	-0.57	0.47	-0.90	-1.76	-0.44	0.24	0.66	0.45	0.28	0.03	0.29	0.77	-0.14
31	33.02	0.619	-0.003	0.032	3.16	1.74	2.90	-0.33	0.40	-0.78	-1.17	-0.38	0.43	0.55	0.36	0.17	0.01	0.23	-0.14	-0.12
32	35.56	0.626	-0.002	0.028	2.62	1.62	2.39	-0.28	0.32	-1.09	-1.01	-0.31	1.22	0.51	0.39	0.24	-0.33	0.31	0.83	-0.12
33	38.10	0.635	-0.003	0.021	1.96	1.22	1.75	-0.13	0.22	-0.52	-0.86	-0.26	0.23	0.33	0.24	0.22	0.08	0.22	0.69	-0.15
34	40.64	0.638	0.001	0.018	1.59	1.25	1.56	-0.15	0.23	-0.56	-0.51	-0.23	0.34	0.27	0.32	0.19	-0.06	0.20	0.56	-0.06
35	45.72	0.651	0.001	0.006	0.83	0.73	0.90	0.04	-0.02	-0.45	-0.17	-0.09	0.67	0.11	0.11	0.05	-0.26	0.10	0.24	-0.02
36	50.80	0.657	0.004	0.000	0.66	0.57	0.81	0.09	-0.05	-0.41	-0.07	-0.05	0.58	0.06	0.06	0.01	-0.21	0.07	0.25	-0.02
37	55.88	0.661	0.018	-0.003	0.43	0.77	0.71	0.11	-0.10	-0.34	0.01	0.00	0.70	0.02	0.05	0.01	-0.32	0.02	0.24	0.02
38	60.96	0.658	0.018	-0.007	0.35	0.65	0.58	0.11	-0.15	-0.39	0.03	0.01	0.78	0.06	0.00	0.00	-0.38	0.00	0.12	-0.01
39	66.04	0.658	0.020	-0.008	0.38	0.69	0.66	0.12	-0.14	-0.33	0.05	0.00	0.57	0.01	0.00	-0.02	-0.26	0.02	0.14	0.01
41	73.66	0.660	0.000	-0.012	0.44	0.00	0.76	0.00	0.00	-0.35	0.07	0.00	0.61	0.00	0.00	0.00	-0.27	0.00	0.16	0.00

Table C.5 Continued.

Case C.S1 Station= 1
X=-457.2mm Tunnel Run#= 687 Ue/Uref= 1.000 Date= 510.88 Time=11.21
Bias Corrected data using 1/sqrt(U*U + V*V + W*W + (.01Ur)^2)

					<-- normalized by 0.001 Ur^2 -->					<---------- normalized by 0.0001 Ur^3 ---------->									
LR	Y(mm)	U/Ur	V/Ur	W/Ur	uu	vv	ww	uv	vw	uw	uuu	uvv	uww	vuu	vvv	vww	wuu	wvv	www	uvw
1	0.00	0.000	0.000	1.000	0.00	0.00	0.00	-2.48	2.70	0.00	0.00	0.00	0.00	0.00	0.00	0.00	0.00	0.00	0.00	0.00
1	0.25	0.608	-0.029	0.311	13.04	3.47	15.28	-1.83	1.42	-5.25	-1.68	-0.44	-3.26	1.02	0.32	1.55	2.23	0.38	3.73	-0.66
2	0.38	0.628	-0.026	0.294	12.71	3.78	14.48	-1.93	1.49	-4.74	-1.67	-0.50	-2.22	0.89	0.64	1.15	1.33	0.38	3.00	-0.28
3	0.51	0.641	-0.025	0.280	11.85	3.86	13.72	-2.00	1.58	-4.55	-0.77	-0.53	-2.13	0.86	0.54	1.16	1.39	0.38	2.81	-0.38
4	0.63	0.654	-0.023	0.264	11.88	3.75	13.90	-2.04	1.62	-4.60	-1.61	-0.44	-2.23	1.08	0.56	1.31	1.69	0.38	2.90	-0.43
5	0.76	0.665	-0.023	0.253	11.01	3.91	12.88	-1.96	1.69	-4.17	-1.11	-0.55	-1.85	1.00	0.66	1.35	1.35	0.50	2.37	-0.57
6	1.02	0.685	-0.023	0.236	10.57	3.99	12.13	-1.91	1.69	-3.92	-1.71	-0.50	-1.59	0.84	0.50	1.22	1.38	0.55	2.53	-0.51
7	1.27	0.699	-0.021	0.219	10.15	3.98	11.48	-1.96	1.69	-4.01	-1.17	-0.57	-1.47	0.92	0.61	1.11	0.92	0.60	2.27	-0.43
8	1.52	0.711	-0.019	0.208	9.93	4.00	11.55	-1.87	1.74	-4.15	-1.26	-0.51	-1.23	0.87	0.54	1.21	1.00	0.68	2.24	-0.58
9	1.78	0.725	-0.019	0.196	9.84	4.16	10.85	-2.17	1.91	-3.75	-1.28	-0.67	-1.36	1.02	0.76	1.30	1.12	0.56	2.04	-0.61
10	2.03	0.731	-0.017	0.189	9.32	4.12	10.45	-1.95	1.79	-3.80	-1.03	-0.37	-1.16	0.63	0.61	0.96	1.05	0.49	2.41	-0.48
11	2.29	0.737	-0.018	0.181	9.25	4.19	10.13	-2.05	1.83	-3.61	-1.15	-0.47	-1.35	0.62	0.53	1.14	1.09	0.64	1.85	-0.67
12	2.54	0.750	-0.017	0.173	8.97	4.13	9.99	-2.02	1.85	-3.50	-1.37	-0.41	-1.25	0.65	0.47	0.99	1.05	0.55	2.39	-0.51
13	2.79	0.757	-0.015	0.170	8.78	4.25	9.78	-2.13	2.03	-3.44	-0.71	-0.38	-1.14	0.66	0.69	1.04	0.70	0.56	2.58	-0.44
14	3.30	0.770	-0.015	0.157	8.70	4.27	9.46	-2.20	2.00	-3.47	-1.50	-0.39	-0.89	0.63	0.48	0.89	0.92	0.47	1.84	-0.50
15	3.81	0.785	-0.014	0.148	8.46	4.20	9.00	-2.14	1.83	-3.31	-1.53	-0.60	-0.99	0.71	0.78	0.73	0.98	0.68	2.04	-0.44
16	4.32	0.799	-0.012	0.138	7.87	4.15	8.59	-2.05	1.87	-2.92	-1.36	-0.49	-0.99	0.61	0.70	0.94	0.85	0.63	2.15	-0.35
17	4.83	0.810	-0.012	0.127	7.55	4.01	8.05	-2.07	1.71	-2.65	-1.64	-0.66	-0.88	0.70	0.70	0.67	0.86	0.58	1.77	-0.47
18	5.59	0.828	-0.010	0.115	7.38	3.86	7.57	-2.10	1.73	-2.56	-1.93	-0.63	-1.07	0.74	0.80	0.73	1.00	0.58	2.20	-0.52
19	6.35	0.849	-0.010	0.103	6.92	3.58	7.15	-1.92	1.52	-2.32	-2.43	-0.73	-1.22	0.81	0.87	0.75	1.07	0.59	1.97	-0.49
20	7.11	0.867	-0.010	0.090	6.44	3.27	6.62	-1.81	1.44	-2.19	-2.29	-0.66	-1.13	0.83	0.80	0.86	1.01	0.62	2.52	-0.49
21	8.38	0.897	-0.008	0.071	5.46	2.82	5.44	-1.54	1.25	-1.86	-2.54	-0.76	-1.33	0.89	0.80	0.90	1.09	0.66	2.39	-0.56
22	10.16	0.938	-0.007	0.045	3.93	2.06	3.71	-1.12	0.78	-1.34	-2.52	-0.69	-1.20	0.87	0.72	0.69	1.06	0.54	2.08	-0.41
23	12.70	0.977	-0.004	0.018	1.74	1.19	1.65	-0.52	0.40	-0.62	-1.39	-0.42	-0.66	0.53	0.46	0.45	0.68	0.31	1.13	-0.27
24	15.24	0.996	-0.003	0.005	0.38	0.51	0.44	-0.10	0.09	-0.09	-0.18	-0.09	-0.09	0.10	0.21	0.10	0.08	0.09	0.15	-0.05
25	17.78	0.998	-0.004	0.003	0.11	0.19	0.17	-0.01	0.01	-0.02	-0.01	-0.01	0.00	0.01	0.03	0.02	0.00	0.01	0.01	0.00
26	20.32	1.001	-0.005	0.003	0.07	0.11	0.14	0.00	0.00	-0.01	0.00	0.00	0.01	0.00	0.00	0.00	0.00	0.00	0.01	0.00
27	22.86	1.000	-0.004	0.002	0.06	0.10	0.13	0.00	0.00	0.00	0.00	0.00	0.01	0.00	0.00	0.00	0.00	0.00	0.01	0.00
28	25.40	1.000	-0.004	0.001	0.05	0.09	0.12	0.00	0.00	-0.01	0.00	0.00	0.00	0.00	0.01	0.00	0.00	0.00	0.00	0.00
29	27.94	0.998	-0.004	0.000	0.05	0.08	0.12	0.00	0.00	-0.01	0.00	0.00	0.00	0.00	0.00	0.00	0.00	0.00	0.01	0.00
30	30.48	1.001	-0.006	-0.001	0.05	0.08	0.13	0.00	0.00	0.00	0.00	0.00	0.01	0.00	0.00	0.00	0.00	0.00	0.01	0.00
31	33.02	1.000	-0.004	0.002	0.06	0.09	0.17	0.00	0.00	0.02	0.01	0.00	0.01	0.00	0.00	0.00	0.01	0.00	0.03	0.00
32	35.56	1.001	-0.004	0.000	0.05	0.09	0.12	0.00	0.00	-0.01	0.00	0.00	0.00	0.00	0.00	0.00	0.00	0.00	0.00	0.00
33	38.10	1.002	-0.004	-0.001	0.05	0.09	0.13	0.00	0.00	-0.01	0.00	0.00	0.00	0.00	0.00	0.00	0.00	0.00	0.00	0.00
34	40.64	1.001	-0.004	0.001	0.05	0.11	0.12	0.00	0.00	-0.01	0.00	0.00	0.00	0.00	0.10	0.00	0.00	0.00	0.00	0.00
35	45.72	1.002	-0.004	0.002	0.04	0.09	0.12	0.00	0.00	-0.01	0.00	0.00	0.00	0.00	0.00	0.00	0.00	0.00	0.00	0.00
36	50.80	1.003	0.003	0.003	0.05	0.49	0.15	0.00	0.00	-0.01	0.00	0.00	0.01	0.00	0.04	0.00	0.00	0.00	0.01	0.00
37	55.88	1.003	0.002	0.002	0.05	0.55	0.12	0.00	0.00	-0.01	0.00	0.00	0.00	0.00	0.74	0.00	0.00	-0.01	0.00	0.00
38	60.96	1.000	0.000	-0.001	0.05	0.00	0.12	0.00	0.00	-0.01	0.00	0.00	0.00	0.00	0.00	0.00	0.00	0.00	0.00	0.00
39	66.04	1.003	0.000	-0.003	0.05	0.00	0.13	0.00	0.00	0.00	0.00	0.00	0.00	0.00	0.00	0.00	0.00	0.00	0.01	0.00

Table C.5 Continued.

Case C.S1 Station= 2
X=-330.2mm Tunnel Run#= 685 Ue/Uref= 1.012 Date= 510.88 Time= 9.09
Bias Corrected data using 1/sqrt(U*U + V*V + W*W + (.01Ur)^2)

					<-- normalized by 0.001 Ur^2 -->						<---------- normalized by 0.0001 Ur^3 ---------->								
LR	Y(mm)	U/Ur	V/Ur	W/Ur	uu	vv	ww	uv	vw	uw	uuu	uvv	uww	vuu	vvv	vww	wuu	wvv	www	uvw
1	0.00	0.000	0.000	1.000	0.00	0.00	0.00	-2.46	2.74	0.00	0.00	0.00	0.00	0.00	0.00	0.00	0.00	0.00	0.00	0.00
1	0.25	0.613	-0.030	0.336	13.94	3.79	17.30	-1.92	1.42	-5.81	-1.76	-0.53	-3.00	1.02	0.47	1.33	2.10	0.63	4.11	-0.48
2	0.38	0.633	-0.027	0.310	13.06	4.00	15.93	-1.87	1.46	-4.94	-0.89	-0.57	-2.50	0.92	0.80	1.35	1.60	0.37	3.66	-0.38
3	0.51	0.648	-0.025	0.290	12.73	4.03	14.85	-1.97	1.41	-4.75	-1.18	-0.58	-2.13	1.04	0.74	1.09	1.13	0.49	3.85	-0.35
4	0.63	0.664	-0.025	0.274	12.04	4.11	14.33	-1.93	1.52	-4.36	-2.11	-0.61	-1.87	1.12	0.92	1.13	1.62	0.42	2.77	-0.34
5	0.76	0.674	-0.023	0.264	11.95	4.00	13.90	-1.79	1.55	-4.56	-0.43	-0.51	-1.69	0.79	0.64	1.09	1.07	0.45	2.48	-0.32
6	1.02	0.692	-0.020	0.245	11.41	4.05	13.62	-2.06	1.86	-4.81	-1.05	-0.39	-2.01	0.96	0.66	1.54	1.26	0.53	3.25	-0.46
7	1.27	0.707	-0.019	0.231	10.87	4.23	13.37	-1.99	2.01	-4.61	-1.42	-0.58	-2.03	0.99	0.85	1.40	1.63	0.71	3.86	-0.53
8	1.52	0.722	-0.017	0.216	10.40	4.07	12.69	-1.99	1.96	-4.51	-0.82	-0.61	-2.01	0.83	0.73	1.45	1.19	0.66	3.93	-0.52
9	1.78	0.732	-0.016	0.208	10.31	4.11	12.29	-2.01	1.91	-4.55	-1.30	-0.54	-1.51	0.87	0.52	1.00	1.14	0.60	2.84	-0.51
10	2.03	0.739	-0.014	0.198	10.21	4.28	11.67	-2.18	1.99	-4.36	-1.72	-0.61	-1.52	1.05	0.68	1.46	1.34	0.64	3.44	-0.75
11	2.29	0.746	-0.013	0.191	9.85	4.29	11.27	-2.13	1.90	-4.23	-1.06	-0.59	-1.61	1.01	0.80	1.29	1.23	0.67	2.95	-0.54
12	2.54	0.755	-0.013	0.186	9.54	4.32	11.18	-2.20	1.99	-3.98	-1.66	-0.71	-1.49	1.09	0.93	1.19	1.18	0.90	3.28	-0.63
13	2.79	0.762	-0.013	0.178	9.42	4.29	10.59	-2.24	2.03	-4.00	-1.57	-0.53	-1.88	0.88	0.54	1.12	1.62	0.65	3.69	-0.68
14	3.30	0.772	-0.012	0.168	8.75	4.28	10.07	-2.21	2.05	-3.52	-1.28	-0.69	-1.23	0.78	0.59	1.21	1.02	0.74	2.92	-0.62
15	3.81	0.784	-0.010	0.163	8.40	4.49	9.94	-2.17	2.03	-3.49	-1.30	-0.52	-1.10	0.65	0.69	1.19	1.04	0.75	2.66	-0.52
16	4.32	0.792	-0.008	0.153	8.11	4.39	9.47	-2.17	1.96	-3.22	-1.15	-0.62	-1.16	0.77	0.75	1.22	0.95	0.79	2.54	-0.50
17	4.83	0.803	-0.007	0.147	8.18	4.39	9.01	-2.34	2.06	-3.21	-1.68	-0.52	-0.97	0.63	0.66	1.11	0.91	0.70	2.42	-0.51
18	5.59	0.817	-0.006	0.138	7.81	4.40	8.86	-2.25	2.09	-3.05	-1.58	-0.48	-1.00	0.73	0.82	0.97	1.07	0.69	2.05	-0.44
19	6.35	0.828	-0.004	0.128	7.47	4.23	8.41	-2.21	1.87	-2.69	-1.87	-0.50	-0.84	0.71	0.73	0.77	0.87	0.54	2.27	-0.31
20	7.11	0.845	-0.005	0.119	7.18	3.92	7.86	-2.12	1.86	-2.54	-1.76	-0.69	-0.95	0.73	0.80	0.86	0.77	0.68	2.13	-0.46
21	8.38	0.869	-0.003	0.104	6.45	3.62	7.08	-1.87	1.61	-2.08	-1.83	-0.63	-0.93	0.66	0.82	0.88	0.86	0.63	2.25	-0.41
22	10.16	0.899	0.000	0.081	5.78	3.33	6.04	-1.80	1.46	-1.99	-2.41	-0.84	-1.07	1.00	0.97	0.92	1.06	0.79	2.30	-0.52
23	12.70	0.942	0.001	0.053	4.16	2.51	4.27	-1.24	1.06	-1.51	-2.38	-0.80	-1.23	0.94	0.94	0.87	1.12	0.79	2.32	-0.51
24	15.24	0.975	0.003	0.027	2.43	1.78	2.45	-0.78	0.61	-0.83	-1.72	-0.63	-0.91	0.71	0.76	0.63	0.79	0.51	1.55	-0.36
25	17.78	0.997	0.003	0.012	1.04	1.12	1.13	-0.36	0.32	-0.31	-0.71	-0.34	-0.37	0.37	0.59	0.37	0.33	0.30	0.76	-0.17
26	20.32	1.005	0.000	0.005	0.33	0.47	0.36	-0.08	0.09	-0.05	-0.12	-0.07	-0.05	0.09	0.24	0.09	0.05	0.09	0.13	-0.03
27	22.86	1.005	-0.001	0.003	0.09	0.17	0.16	-0.01	0.01	-0.01	0.00	0.00	0.00	0.01	0.03	0.01	0.00	0.01	0.01	0.00
28	25.40	1.006	-0.002	0.003	0.06	0.12	0.13	0.00	0.00	-0.01	0.00	0.00	0.00	0.00	0.01	0.00	0.00	0.00	0.00	0.00
29	27.94	1.008	-0.002	0.001	0.06	0.11	0.14	0.00	0.00	0.00	0.00	0.00	0.01	0.00	0.00	0.00	0.00	0.00	0.01	0.00
30	30.48	1.010	-0.002	0.001	0.05	0.10	0.13	0.00	0.00	-0.01	0.00	0.00	0.00	0.00	0.00	0.00	0.00	0.00	0.01	0.00
31	33.02	1.009	-0.002	0.001	0.05	0.11	0.13	0.00	0.00	-0.01	0.00	0.00	0.01	0.00	0.00	0.08	0.00	0.00	0.00	0.00
32	35.56	1.008	-0.001	0.001	0.05	0.09	0.13	0.00	0.00	0.00	0.00	0.00	0.01	0.00	0.00	0.00	0.00	0.00	0.01	0.00
33	38.10	1.008	0.000	0.001	0.05	0.09	0.14	0.00	0.00	0.00	0.00	0.00	0.01	0.00	0.00	0.00	0.00	0.00	0.01	0.00
34	40.64	1.011	0.000	0.000	0.05	0.09	0.14	0.00	0.00	-0.01	0.00	0.00	0.01	0.00	0.00	0.00	0.00	0.00	0.00	0.00
35	45.72	1.013	0.000	0.000	0.05	0.09	0.15	0.00	0.00	0.00	0.00	0.00	0.01	0.00	0.00	0.00	0.01	0.00	0.02	0.00
36	50.80	1.019	0.003	-0.003	0.06	0.58	0.15	0.00	0.00	0.01	0.01	0.00	0.02	0.00	0.80	0.00	0.01	0.00	0.04	0.00
37	55.88	1.020	0.004	-0.004	0.05	0.47	0.12	0.00	0.00	0.00	0.00	0.00	0.00	0.00	-0.01	0.00	0.00	0.00	0.00	0.00
38	60.96	1.021	0.000	-0.005	0.05	0.00	0.13	0.00	0.00	0.01	0.00	0.00	0.01	0.00	0.00	0.00	0.01	0.00	0.02	0.00
39	66.04	1.018	0.000	-0.005	0.05	0.00	0.14	0.00	0.00	-0.01	0.00	0.00	0.00	0.00	0.00	0.00	0.00	0.00	0.00	0.00

Table C.5 Continued.

Case C.S1 Station= 3
X=-228.6mm Tunnel Run#= 683 Ue/Uref= 0.991 Date= 509.88 Time=19.42
Bias Corrected data using 1/sqrt(U*U + V*V + W*W + (.01Ur)^2)

					<-- normalized by 0.001 Ur^2 -->						<---------- normalized by 0.0001 Ur^3 ---------->									
LR	Y(mm)	U/Ur	V/Ur	W/Ur	uu	vv	ww	uv	vw	uw	uuu	uvv	uww	vuu	vvv	vww	wuu	wvv	www	uvw
1	0.00	0.000	0.000	1.000	0.00	0.00	0.00	-2.02	2.64	0.00	0.00	0.00	0.00	0.00	0.00	0.00	0.00	0.00	0.00	0.00
2	0.25	0.541	-0.024	0.354	15.21	3.14	19.20	-1.83	1.36	-7.17	-1.14	-0.32	-5.35	0.73	0.05	1.61	3.26	0.31	7.75	-0.74
3	0.38	0.572	-0.023	0.324	13.66	3.72	16.35	-1.61	1.27	-5.15	-1.15	-0.61	-2.70	0.91	0.50	1.25	2.05	0.44	3.54	-0.38
4	0.51	0.590	-0.021	0.304	13.51	3.89	15.94	-1.78	1.46	-4.77	-1.73	-0.56	-2.59	0.96	0.54	1.37	2.01	0.55	4.32	-0.44
5	0.63	0.611	-0.019	0.283	12.95	4.10	15.00	-1.95	1.58	-4.64	-0.34	-0.56	-2.19	0.87	0.69	0.88	1.43	0.48	3.57	-0.35
6	0.76	0.625	-0.019	0.271	12.86	4.06	14.67	-2.08	1.75	-4.52	-1.13	-0.52	-2.36	0.88	0.71	1.26	1.66	0.57	3.03	-0.41
7	1.02	0.645	-0.018	0.249	12.21	4.14	14.17	-2.01	1.92	-4.50	-0.97	-0.84	-1.90	1.17	0.94	1.51	1.24	0.93	3.04	-0.67
8	1.27	0.666	-0.017	0.230	11.71	4.18	13.36	-2.12	1.96	-4.57	-1.38	-0.57	-1.89	1.11	0.82	1.40	1.87	0.79	3.10	-0.57
9	1.52	0.678	-0.014	0.219	11.90	4.36	12.91	-2.31	2.04	-4.54	-1.87	-0.80	-2.15	1.29	0.77	1.52	1.90	0.80	4.10	-0.67
10	1.78	0.692	-0.013	0.204	11.61	4.28	12.24	-2.32	2.08	-4.71	-2.05	-0.99	-2.18	1.34	0.88	1.59	1.85	0.90	3.82	-0.78
11	2.03	0.698	-0.011	0.194	11.22	4.25	12.27	-2.34	2.02	-4.75	-1.56	-0.91	-2.23	1.05	1.00	1.49	1.68	0.88	3.71	-0.58
12	2.29	0.708	-0.011	0.184	10.49	4.31	11.51	-2.28	2.11	-4.31	-2.00	-0.73	-1.59	0.99	0.90	1.37	1.64	0.90	2.93	-0.69
13	2.54	0.715	-0.009	0.176	10.65	4.16	11.42	-2.41	2.16	-4.59	-2.54	-0.77	-2.08	1.37	0.84	1.71	2.01	0.85	3.74	-0.84
14	2.79	0.724	-0.009	0.169	10.24	4.18	10.97	-2.31	2.14	-4.29	-1.97	-0.90	-1.80	1.20	0.71	1.52	1.77	1.15	2.77	-0.96
15	3.30	0.736	-0.008	0.159	9.52	4.28	10.59	-2.16	2.12	-3.99	-2.01	-0.70	-1.53	0.95	0.78	1.54	1.54	0.87	3.30	-0.71
16	3.81	0.744	-0.006	0.153	9.49	4.29	10.39	-2.28	2.08	-3.94	-2.18	-0.88	-1.83	1.17	0.96	1.54	1.54	1.00	3.28	-0.90
17	4.32	0.750	-0.003	0.148	9.28	4.39	10.26	-2.41	2.21	-3.98	-2.31	-0.68	-1.08	0.99	0.85	1.16	1.25	0.87	2.42	-0.62
18	4.83	0.760	-0.003	0.141	8.85	4.52	9.97	-2.42	2.24	-3.61	-1.71	-0.73	-1.34	0.91	0.74	1.33	1.12	0.89	2.87	-0.69
19	5.59	0.772	0.000	0.134	8.44	4.37	9.67	-2.28	2.10	-3.34	-1.87	-0.61	-0.80	0.96	0.77	1.04	0.84	0.77	2.21	-0.59
20	6.35	0.782	0.002	0.128	8.27	4.37	9.13	-2.33	2.17	-3.11	-1.75	-0.57	-0.99	0.79	0.81	1.10	1.13	0.83	2.59	-0.59
21	7.11	0.794	0.004	0.120	7.68	4.08	8.62	-2.14	2.03	-2.82	-1.72	-0.63	-0.96	0.77	0.76	0.95	0.80	0.69	2.24	-0.50
22	8.38	0.812	0.007	0.108	7.28	4.14	7.93	-2.26	1.90	-2.51	-1.96	-0.72	-1.15	0.87	0.94	1.02	1.03	0.77	1.88	-0.52
23	10.16	0.842	0.011	0.092	6.83	3.67	7.25	-1.96	1.75	-2.33	-2.29	-0.72	-1.07	0.83	1.07	0.96	1.00	0.80	2.44	-0.48
24	12.70	0.878	0.016	0.068	5.60	3.09	5.93	-1.63	1.35	-1.96	-2.31	-0.75	-1.17	0.82	0.86	0.85	1.07	0.70	2.38	-0.45
25	15.24	0.912	0.020	0.043	4.40	2.37	4.49	-1.29	1.08	-1.62	-2.53	-0.78	-1.33	0.93	0.81	0.96	1.18	0.70	2.43	-0.58
26	17.78	0.944	0.024	0.022	2.80	1.69	2.70	-0.79	0.70	-0.96	-2.04	-0.61	-0.90	0.76	0.66	0.64	0.91	0.53	1.72	-0.38
27	20.32	0.965	0.027	0.007	1.37	1.04	1.42	-0.44	0.34	-0.46	-1.03	-0.37	-0.45	0.44	0.49	0.39	0.46	0.30	0.96	-0.19
28	22.86	0.975	0.029	-0.001	0.55	0.60	0.63	-0.17	0.13	-0.12	-0.34	-0.16	-0.16	0.19	0.36	0.18	0.13	0.17	0.35	-0.07
28	25.40	0.979	0.031	-0.007	0.24	0.30	0.29	-0.05	0.03	-0.03	-0.06	-0.04	-0.02	0.05	0.10	0.04	0.03	0.02	0.05	-0.01
30	27.94	0.983	0.033	-0.005	0.11	0.16	0.18	-0.01	0.00	0.00	0.00	-0.01	0.00	0.01	0.04	0.01	0.00	0.00	0.01	0.00
31	30.48	0.985	0.035	-0.006	0.07	0.11	0.15	0.00	0.00	0.00	0.00	0.00	0.01	0.00	0.01	0.00	0.00	0.00	0.01	0.00
32	33.02	0.986	0.037	-0.006	0.06	0.09	0.14	0.00	0.00	0.00	0.00	0.00	0.00	0.00	0.00	0.00	0.00	0.00	0.01	0.00
33	35.56	0.987	0.040	-0.006	0.06	0.08	0.14	0.00	0.00	0.00	0.00	0.00	0.01	0.00	0.00	0.00	0.00	0.00	0.02	0.00
34	38.10	0.989	0.042	-0.006	0.05	0.07	0.13	0.00	0.00	-0.01	0.00	0.00	0.00	0.00	0.00	0.00	0.00	0.00	0.00	0.00
35	40.64	0.990	0.045	-0.006	0.05	0.07	0.13	0.00	0.00	0.00	0.00	0.00	0.01	0.00	0.00	0.00	0.01	0.00	0.02	0.00
36	45.72	0.994	0.053	-0.005	0.06	0.08	0.15	0.00	0.00	0.00	0.00	0.00	0.01	0.00	0.00	0.00	0.00	0.00	0.01	0.00
37	50.80	0.999	0.063	-0.004	0.06	0.39	0.16	0.00	0.00	0.00	0.00	0.00	0.01	0.00	0.00	0.00	0.01	0.00	0.02	0.00
38	55.88	1.003	0.071	-0.005	0.06	0.38	0.15	0.00	0.00	0.00	0.00	0.00	0.01	0.00	0.00	0.00	0.01	0.00	0.02	0.00
39	60.96	1.011	0.081	-0.007	0.05	0.36	0.12	0.00	0.00	0.00	0.00	0.00	0.01	0.00	0.00	0.00	0.00	0.00	0.01	0.00
40	66.04	1.022	0.000	-0.010	0.05	0.00	0.13	0.00	0.00	0.00	0.00	0.00	0.00	0.00	0.00	0.00	0.00	0.00	0.01	0.00

Table C.5 Continued.

Case C.S1 Station= 4
X=-152.4mm Tunnel Run#= 679 Ue/Uref= 0.904 Date= 509.88 Time=15.51
Bias Corrected data using 1/sqrt(U*U + V*V + W*W + (.01Ur)^2)

					<-- normalized by 0.001 Ur^2 -->						<---------- normalized by 0.0001 Ur^3 ---------->									
LR	Y(mm)	U/Ur	V/Ur	W/Ur	uu	vv	ww	uv	vw	uw	uuu	uvv	uww	vuu	vvv	vww	wuu	wvv	www	uvw
1	0.00	0.000	0.000	1.000	0.00	0.00	0.00	-1.66	2.45	0.00	0.00	0.00	0.00	0.00	0.00	0.00	0.00	0.00	0.00	0.00
1	0.25	0.479	-0.025	0.326	12.37	2.93	15.70	-1.26	1.25	-4.41	0.79	-0.37	-3.20	0.76	0.24	1.20	1.64	0.50	3.91	-0.51
2	0.38	0.494	-0.024	0.302	11.70	3.36	14.56	-1.49	1.29	-4.02	0.59	-0.39	-2.29	0.70	0.53	1.07	1.34	0.50	3.27	-0.23
3	0.51	0.504	-0.020	0.283	11.76	3.46	14.07	-1.61	1.39	-3.60	0.45	-0.43	-1.72	0.37	0.51	1.21	1.08	0.65	2.41	-0.33
4	0.63	0.514	-0.020	0.272	11.43	3.63	13.39	-1.65	1.49	-3.73	-0.17	-0.47	-1.65	0.84	0.59	1.00	0.89	0.46	2.56	-0.33
5	0.76	0.525	-0.018	0.259	11.51	3.67	12.91	-1.75	1.59	-3.50	-0.31	-0.45	-1.34	0.64	0.69	1.05	0.55	0.50	2.47	-0.28
6	1.02	0.545	-0.017	0.240	11.02	3.80	12.76	-1.79	1.84	-3.97	0.23	-0.47	-1.59	0.61	0.64	1.37	0.96	0.77	3.51	-0.36
7	1.27	0.558	-0.015	0.224	11.18	3.86	12.48	-1.81	1.75	-3.91	-0.16	-0.41	-1.38	0.57	0.59	1.18	1.02	0.50	2.85	-0.26
8	1.52	0.570	-0.012	0.214	10.98	3.95	12.45	-1.96	1.93	-4.02	-0.54	-0.55	-1.49	0.89	0.72	1.43	1.40	0.63	3.15	-0.49
9	1.78	0.579	-0.012	0.202	10.71	3.85	11.64	-1.93	1.83	-4.07	-0.55	-0.42	-1.21	0.79	0.66	1.19	1.18	0.56	2.90	-0.37
10	2.03	0.590	-0.012	0.194	10.69	4.02	11.68	-2.05	1.96	-4.20	-0.71	-0.61	-1.59	0.78	0.91	1.48	1.49	0.81	2.96	-0.67
11	2.29	0.601	-0.012	0.186	10.31	4.04	11.21	-2.10	1.89	-3.77	-1.28	-0.57	-1.61	0.93	0.46	1.36	1.50	0.79	3.07	-0.55
12	2.54	0.605	-0.009	0.184	10.07	4.19	10.89	-2.12	2.07	-3.87	-1.18	-0.61	-1.44	1.03	0.69	1.51	1.59	0.91	3.12	-0.72
13	2.79	0.614	-0.010	0.176	9.79	4.11	10.53	-2.12	1.88	-3.75	-1.33	-0.63	-1.30	1.09	0.76	1.38	1.40	0.85	2.81	-0.60
14	3.30	0.626	-0.007	0.168	9.86	4.27	10.78	-2.27	2.05	-3.97	-1.51	-0.48	-1.44	0.80	0.66	1.47	1.32	0.81	2.98	-0.54
15	3.81	0.637	-0.006	0.161	9.30	4.41	10.19	-2.07	2.05	-3.58	-0.99	-0.61	-1.06	0.84	0.88	1.30	1.14	0.96	2.72	-0.73
16	4.32	0.643	-0.006	0.157	9.12	4.47	9.86	-2.18	1.99	-3.55	-1.29	-0.63	-0.93	0.84	0.48	1.16	1.21	0.72	2.23	-0.63
17	4.83	0.651	-0.003	0.151	9.07	4.58	9.59	-2.24	2.16	-3.25	-1.25	-0.61	-0.82	0.91	0.79	1.09	1.07	0.93	2.69	-0.54
18	5.59	0.666	-0.002	0.146	8.80	4.61	9.34	-2.16	2.20	-3.00	-1.23	-0.54	-0.81	0.76	0.79	1.15	1.08	0.80	2.39	-0.46
19	6.35	0.677	0.000	0.140	8.44	4.76	9.30	-2.17	2.18	-2.95	-1.19	-0.62	-0.74	0.55	1.18	1.16	0.88	0.97	2.17	-0.62
20	7.11	0.686	0.002	0.137	8.08	4.48	9.04	-2.16	2.16	-2.84	-0.81	-0.43	-0.72	0.48	0.88	1.00	0.70	0.80	1.94	-0.40
21	8.38	0.702	0.004	0.127	7.75	4.37	8.41	-2.18	1.98	-2.35	-1.43	-0.46	-0.40	0.71	0.75	0.78	0.63	0.66	1.43	-0.34
22	10.16	0.728	0.009	0.115	7.67	4.16	7.92	-2.15	2.09	-2.33	-1.14	-0.59	-0.47	0.55	0.94	0.90	0.45	0.73	1.94	-0.28
23	12.70	0.759	0.013	0.092	6.74	3.60	6.80	-1.83	1.47	-1.89	-1.50	-0.68	-0.74	0.72	0.96	0.69	0.70	0.75	1.88	-0.39
24	15.24	0.789	0.019	0.074	5.93	3.09	5.88	-1.64	1.37	-1.74	-2.26	-0.75	-0.98	0.88	0.86	0.90	1.04	0.72	2.27	-0.47
25	17.78	0.825	0.024	0.054	4.90	2.36	4.65	-1.19	0.93	-1.54	-2.56	-0.68	-1.13	0.84	0.75	0.73	1.09	0.66	2.21	-0.41
26	20.32	0.853	0.029	0.036	3.65	1.90	3.36	-0.91	0.71	-1.14	-2.23	-0.63	-1.07	0.74	0.67	0.67	0.97	0.58	1.95	-0.41
27	22.86	0.875	0.034	0.022	2.35	1.40	2.14	-0.63	0.45	-0.71	-1.71	-0.53	-0.71	0.60	0.61	0.45	0.77	0.42	1.37	-0.29
28	25.40	0.895	0.037	0.011	1.21	0.89	1.15	-0.34	0.19	-0.31	-0.90	-0.31	-0.35	0.36	0.34	0.22	0.38	0.21	0.65	-0.14
29	27.94	0.899	0.040	0.004	0.56	0.56	0.61	-0.12	0.11	-0.14	-0.27	-0.11	-0.17	0.13	0.28	0.13	0.17	0.11	0.32	-0.07
30	30.48	0.907	0.042	0.001	0.24	0.31	0.30	-0.05	0.04	-0.03	-0.07	-0.03	-0.02	0.05	0.10	0.05	0.05	0.03	0.10	-0.02
31	33.02	0.906	0.044	-0.001	0.13	0.18	0.17	-0.02	0.01	-0.01	-0.02	-0.02	0.01	0.02	0.04	0.01	0.01	0.01	0.03	0.00
32	35.56	0.909	0.046	-0.002	0.08	0.13	0.14	0.00	0.00	0.00	0.00	0.00	0.00	0.00	0.02	0.01	0.00	0.00	0.01	0.00
33	38.10	0.909	0.048	-0.003	0.07	0.11	0.13	0.00	0.00	0.00	0.00	0.00	0.01	0.00	0.03	0.00	0.00	0.00	0.01	0.00
34	40.64	0.912	0.051	-0.002	0.06	0.11	0.12	0.00	-0.01	0.00	0.00	0.00	0.00	0.00	0.09	0.00	0.00	0.00	0.01	0.00
35	45.72	0.911	0.058	-0.003	0.06	0.10	0.12	0.00	-0.01	0.01	0.00	0.00	0.01	0.00	0.00	0.00	0.00	0.00	0.01	0.00
36	50.80	0.910	0.065	-0.005	0.07	0.13	0.19	0.00	0.00	0.04	0.01	0.00	0.03	0.00	0.07	0.00	0.02	0.00	0.05	0.00
37	55.88	0.922	0.074	0.015	0.03	0.42	0.11	0.00	0.00	-0.02	0.00	0.00	0.00	0.00	0.00	0.00	0.00	0.00	0.00	0.00
38	60.96	0.923	0.080	0.008	0.10	0.45	0.25	0.01	0.00	0.07	0.02	0.00	0.05	0.00	0.24	0.00	0.03	0.00	0.09	0.00
39	66.04	0.935	0.000	0.009	0.06	0.00	0.18	0.00	0.00	0.02	0.00	0.00	0.00	0.00	0.00	0.00	0.00	0.00	0.00	0.00
40	68.58	0.932	0.000	0.004	0.08	0.00	0.24	0.00	0.00	0.06	0.01	0.00	0.02	0.00	0.00	0.00	0.01	0.00	0.02	0.00

Table C.5 Continued.

Case C.S1 Station= 5
X= -76.2mm Tunnel Run#= 677 Ue/Uref= 0.796 Date= 509.88 Time=14.03
Bias Corrected data using 1/sqrt(U*U + V*V + W*W + (.01Ur)^2)

					<-- normalized by 0.001 Ur^2 -->						<---------- normalized by 0.0001 Ur^3 ---------->									
LR	Y(mm)	U/Ur	V/Ur	W/Ur	uu	vv	ww	uv	vw	uw	uuu	uvv	uww	vuu	vvv	vww	wuu	wvv	www	uvw
1	0.00	0.000	0.000	1.000	0.00	0.00	0.00	-1.07	2.25	0.00	0.00	0.00	0.00	0.00	0.00	0.00	0.00	0.00	0.00	0.00
1	0.25	0.338	-0.020	0.329	11.26	2.72	17.04	-1.27	1.67	-4.77	0.12	-0.37	-4.88	0.69	0.33	1.94	2.03	0.48	7.29	-0.76
2	0.38	0.357	-0.019	0.300	10.68	3.09	15.01	-1.24	1.60	-3.54	0.13	-0.25	-3.66	0.92	0.34	1.69	2.12	0.63	5.50	-0.67
3	0.51	0.372	-0.018	0.283	10.28	3.20	13.97	-1.21	1.66	-3.20	0.29	-0.39	-2.18	0.72	0.51	1.44	1.15	0.67	3.60	-0.42
4	0.63	0.382	-0.014	0.267	10.05	3.45	12.95	-1.44	1.58	-2.93	-0.01	-0.48	-1.75	0.87	0.61	1.24	0.99	0.61	2.72	-0.36
5	0.76	0.393	-0.014	0.255	10.16	3.45	12.87	-1.40	1.76	-3.11	0.49	-0.42	-1.79	0.83	0.66	1.65	1.46	0.79	3.63	-0.55
6	1.02	0.406	-0.012	0.236	9.92	3.70	12.27	-1.57	1.76	-2.91	0.37	-0.32	-1.41	0.93	0.79	1.41	1.07	0.66	3.05	-0.33
7	1.27	0.418	-0.011	0.220	9.37	3.67	11.80	-1.46	1.83	-2.91	0.56	-0.29	-0.54	0.47	0.51	1.40	0.79	0.71	2.51	-0.32
8	1.52	0.428	-0.010	0.209	9.64	3.72	11.68	-1.77	1.87	-3.23	0.50	-0.23	-1.15	0.74	0.44	1.36	0.91	0.67	3.20	-0.45
9	1.78	0.435	-0.009	0.198	9.48	3.77	11.54	-1.65	1.83	-3.11	0.39	-0.24	-0.90	0.56	0.43	1.23	0.57	0.71	2.51	-0.25
10	2.03	0.444	-0.006	0.192	9.49	3.97	11.46	-1.88	2.05	-3.44	0.22	-0.35	-0.88	0.55	0.64	1.50	0.72	0.81	2.29	-0.34
11	2.29	0.450	-0.006	0.181	9.11	3.84	10.88	-1.76	1.97	-3.38	0.21	-0.35	-0.73	0.49	0.48	1.24	0.72	0.74	2.54	-0.43
12	2.54	0.456	-0.005	0.177	9.08	4.14	10.82	-1.95	2.06	-3.42	-0.39	-0.51	-0.88	0.69	0.63	1.33	0.79	0.86	2.38	-0.48
13	2.79	0.463	-0.003	0.173	9.38	4.12	11.11	-1.92	2.20	-3.52	-0.31	-0.31	-0.97	0.52	0.68	1.51	1.06	1.02	2.82	-0.43
14	3.30	0.471	-0.002	0.166	8.83	4.33	10.66	-1.99	2.17	-3.40	0.37	-0.39	-0.72	0.72	0.51	1.38	1.10	0.90	2.34	-0.62
15	3.81	0.483	0.000	0.159	9.08	4.29	9.84	-2.13	2.10	-3.21	-0.49	-0.42	-0.41	0.70	0.60	1.06	0.92	0.70	1.69	-0.42
16	4.32	0.491	0.003	0.154	8.62	4.58	9.55	-2.04	2.12	-3.81	-0.74	0.46	-0.33	0.64	0.66	1.18	0.77	0.79	1.45	-0.57
17	4.83	0.498	0.004	0.151	8.47	4.54	9.38	-2.10	2.11	-2.79	-0.16	-0.31	-0.35	0.30	0.66	0.92	0.61	0.75	1.67	-0.32
18	5.59	0.506	0.008	0.147	8.43	4.78	9.11	-2.22	2.19	-2.68	-0.57	-0.42	-0.46	0.51	0.69	1.06	0.78	0.85	1.32	-0.45
19	6.35	0.518	0.008	0.143	8.11	4.58	8.58	-2.02	2.10	-2.51	-0.58	-0.33	-0.16	0.32	0.65	0.78	0.54	0.59	1.27	-0.23
20	7.11	0.532	0.010	0.140	8.22	4.60	8.26	-2.24	2.03	-2.32	-0.70	-0.31	-0.25	0.42	0.48	0.77	0.46	0.62	0.82	-0.31
21	8.38	0.546	0.015	0.134	7.87	4.75	8.39	-2.09	2.04	-2.23	-0.36	-0.27	-0.28	0.32	0.66	0.76	0.47	0.53	0.99	-0.32
22	10.16	0.570	0.017	0.124	7.53	4.46	7.97	-1.91	1.86	-1.85	-0.81	-0.26	-0.17	0.42	0.57	0.45	0.40	0.44	0.51	-0.22
23	12.70	0.601	0.023	0.110	7.36	4.24	7.58	-2.01	1.79	-1.80	-0.81	-0.47	-0.31	0.40	0.60	0.48	0.28	0.47	0.79	-0.17
24	15.24	0.634	0.028	0.096	7.18	4.01	7.06	-1.92	1.72	-1.74	-1.25	-0.47	-0.40	0.43	0.70	0.55	0.47	0.50	1.05	-0.28
25	17.78	0.662	0.035	0.081	6.69	3.61	6.31	-1.70	1.58	-1.65	-1.67	-0.44	-0.56	0.41	0.69	0.67	0.55	0.62	1.32	-0.27
26	20.32	0.688	0.040	0.063	5.95	3.14	5.51	-1.66	1.28	-1.48	-1.93	-0.64	-0.75	0.84	0.72	0.67	0.62	0.58	1.65	-0.37
27	22.86	0.710	0.046	0.050	5.64	2.76	4.79	-1.36	1.05	-1.38	-2.10	-0.65	-0.83	0.68	0.76	0.72	0.71	0.62	1.87	-0.30
28	25.40	0.738	0.048	0.031	4.15	2.20	3.60	-1.02	0.80	-1.18	-2.01	-0.66	-0.81	0.74	0.71	0.55	0.78	0.51	1.68	-0.32
29	27.94	0.763	0.049	0.015	2.97	1.61	2.45	-0.69	0.47	-0.91	-1.94	-0.53	-0.74	0.57	0.60	0.44	0.77	0.42	1.35	-0.27
30	30.48	0.783	0.052	0.003	1.83	1.12	1.60	-0.39	0.28	-0.56	-1.41	-0.34	-0.58	0.36	0.38	0.30	0.58	0.29	0.93	-0.16
31	33.02	0.792	0.055	-0.004	0.97	0.78	0.93	-0.27	0.18	-0.28	-0.65	-0.24	-0.28	0.26	0.32	0.20	0.28	0.19	0.57	-0.12
32	35.56	0.799	0.057	-0.009	0.42	0.46	0.46	-0.09	0.08	-0.08	-0.17	-0.08	0.08	0.08	0.18	0.09	0.09	0.08	0.19	-0.03
33	38.10	0.802	0.059	-0.012	0.23	0.30	0.27	-0.03	0.02	-0.03	-0.05	-0.03	-0.02	0.03	0.08	0.03	0.03	0.02	0.07	-0.01
34	40.64	0.802	0.061	-0.014	0.12	0.19	0.17	-0.02	0.00	-0.01	0.00	-0.01	0.01	0.01	0.04	0.01	0.00	0.00	-0.02	0.00
35	45.72	0.802	0.066	-0.014	0.06	0.10	0.13	0.00	0.00	0.00	0.00	0.00	0.00	0.00	0.00	0.00	0.00	0.00	0.00	0.00
36	50.80	0.801	0.070	-0.013	0.07	0.10	0.15	0.00	-0.01	-0.01	0.01	0.00	0.02	0.00	0.08	0.00	-0.01	0.00	-0.03	0.00
37	55.88	0.797	0.081	-0.012	0.06	0.37	0.14	0.00	-0.01	0.00	0.00	0.00	0.01	0.00	0.00	0.00	0.00	0.00	0.01	0.00
38	60.96	0.796	0.086	-0.013	0.08	0.41	0.21	0.00	-0.01	0.02	0.02	0.00	0.07	0.00	-0.01	0.00	0.01	0.00	0.03	0.00
39	66.04	0.794	0.000	-0.017	0.08	0.00	0.21	0.00	0.00	0.02	0.02	0.00	0.06	0.00	0.00	0.00	0.01	0.00	0.02	0.00
40	68.58	0.792	0.000	-0.015	0.08	0.00	0.22	0.00	0.00	0.02	0.02	0.00	0.07	0.00	0.00	0.00	0.01	0.00	0.04	0.00

Table C.5 Continued.

Case C.S1 Station= 6
X= -12.7mm Tunnel Run#= 675 Ue/Uref= 0.723 Date= 509.88 Time=12.24
Bias Corrected data using 1/sqrt(U*U + V*V + W*W + (.01Ur)^2)

					<-- normalized by 0.001 Ur^2 -->						<---------- normalized by 0.0001 Ur^3 ---------->								
LR	Y(mm)	U/Ur	V/Ur	W/Ur	uu	vv	ww	uv	vw	uw	uuu	uvv	uww	vuu	vvv	vww	wuu	wvv	www	uvw
1	0.00	0.000	0.000	1.000	0.00	0.00	0.00	-0.75	2.15	0.00	0.00	0.00	0.00	0.00	0.00	0.00	0.00	0.00	0.00	0.00
10	0.25	0.260	-0.023	0.335	9.91	2.21	16.15	-0.85	1.41	-3.44	0.21	-0.13	-3.80	0.37	0.06	1.49	0.71	0.35	5.37	-0.48
11	0.38	0.275	-0.022	0.306	9.62	2.69	14.44	-0.90	1.61	-3.05	0.46	-0.32	-2.72	0.48	0.18	1.41	0.98	0.49	4.60	-0.45
12	0.51	0.288	-0.019	0.284	9.70	2.97	13.48	-0.98	1.48	-2.55	0.27	-0.23	-1.98	0.48	0.40	1.45	1.00	0.53	3.65	-0.26
13	0.63	0.296	-0.018	0.270	9.08	2.97	12.59	-0.91	1.56	-2.34	0.70	-0.29	-1.64	0.37	0.47	1.45	1.08	0.67	3.42	-0.33
14	0.76	0.306	-0.019	0.253	8.78	2.97	11.86	-0.95	1.58	-1.91	0.14	-0.20	-1.43	0.51	0.36	1.20	0.81	0.58	3.09	-0.31
15	1.02	0.318	-0.016	0.238	8.92	3.20	11.58	-1.16	1.58	-2.03	-0.18	-0.28	-1.43	0.68	0.52	1.29	0.83	0.55	2.88	-0.25
16	1.27	0.323	-0.015	0.224	8.35	3.20	11.25	-1.09	1.67	-2.01	0.50	-0.27	-1.24	0.39	0.47	1.49	0.54	0.60	2.47	-0.20
17	1.52	0.329	-0.015	0.209	7.99	3.17	10.69	-1.13	1.61	-2.03	0.12	-0.28	-0.92	0.44	0.43	1.17	0.63	0.62	2.22	-0.27
18	1.78	0.336	-0.012	0.200	8.13	3.38	10.32	-1.26	1.61	-2.30	0.57	-0.31	-0.89	0.49	0.45	1.34	0.68	0.62	2.47	-0.31
19	2.03	0.343	-0.011	0.191	7.82	3.35	10.02	-1.24	1.59	-2.10	0.60	-0.08	-0.61	0.32	0.36	1.22	0.50	0.49	2.37	-0.10
20	2.29	0.348	-0.010	0.187	7.86	3.51	9.68	-1.37	1.60	-2.22	0.39	-0.13	-0.72	0.30	0.33	1.27	0.62	0.58	2.71	-0.24
21	2.54	0.351	-0.009	0.181	7.68	3.49	9.57	-1.27	1.52	-2.09	0.49	-0.16	-0.61	0.32	0.42	1.29	0.51	0.63	1.91	-0.29
22	2.79	0.357	-0.008	0.175	7.62	3.64	9.34	-1.41	1.66	-2.22	0.40	-0.23	-0.39	0.38	0.32	1.12	0.56	0.57	2.18	-0.29
23	3.30	0.366	-0.007	0.170	7.89	3.80	9.12	-1.56	1.76	-2.26	0.34	-0.14	-0.51	0.36	0.48	1.32	0.62	0.71	1.92	-0.28
24	3.81	0.372	-0.005	0.164	7.69	3.94	8.85	-1.66	1.70	-2.12	0.51	-0.17	-0.23	0.10	0.33	1.17	0.28	0.61	1.47	-0.32
25	4.32	0.381	-0.004	0.162	7.78	4.05	8.80	-1.77	1.86	-2.19	0.28	-0.23	-0.30	0.28	0.41	1.04	0.46	0.50	2.07	-0.28
26	4.83	0.389	-0.003	0.156	7.57	4.05	8.11	-1.75	1.69	-2.03	-0.01	-0.31	-0.01	0.38	0.48	0.88	0.40	0.59	1.07	-0.24
27	5.59	0.398	-0.001	0.153	7.44	4.31	7.81	-1.84	1.70	-1.89	0.10	-0.37	-0.20	0.39	0.47	0.82	0.43	0.62	0.74	-0.34
28	6.35	0.410	0.000	0.150	7.59	4.29	7.84	-1.85	1.76	-1.82	0.20	-0.04	-0.02	0.12	0.36	0.62	0.29	0.53	0.94	-0.21
29	7.11	0.420	0.000	0.146	7.47	4.31	7.59	-1.83	1.70	-1.74	-0.16	-0.12	0.04	0.12	0.46	0.66	0.31	0.48	0.76	-0.18
30	8.38	0.437	0.004	0.142	7.68	4.39	7.60	-2.01	1.83	-1.78	-0.16	-0.12	0.01	0.14	0.48	0.59	0.31	0.49	0.68	-0.24
31	10.16	0.463	0.007	0.138	7.25	4.34	7.28	-1.89	1.74	-1.47	-0.12	-0.22	-0.13	0.15	0.52	0.50	0.13	0.48	0.50	-0.17
32	12.70	0.494	0.014	0.129	7.22	4.34	7.21	-1.90	1.62	-1.43	-0.49	-0.23	-0.08	0.14	0.37	0.30	0.22	0.30	0.48	-0.16
33	15.24	0.522	0.018	0.117	7.09	4.18	6.82	-1.94	1.65	-1.31	-0.83	-0.41	-0.09	0.49	0.76	0.51	0.19	0.40	0.47	-0.19
34	17.78	0.553	0.020	0.104	6.48	3.73	6.48	-1.72	1.57	-1.25	-0.86	-0.31	-0.35	0.32	0.64	0.45	0.30	0.39	0.93	-0.21
35	20.32	0.580	0.024	0.090	6.26	3.51	5.90	-1.62	1.38	-1.11	-1.09	-0.38	-0.38	0.48	0.53	0.55	0.36	0.41	0.83	-0.18
36	22.86	0.604	0.029	0.076	5.70	3.15	5.25	-1.48	1.15	-1.14	-1.28	-0.42	-0.43	0.44	0.65	0.52	0.39	0.49	0.85	-0.23
37	25.40	0.629	0.031	0.065	5.29	2.78	4.60	-1.33	0.96	-1.02	-1.60	-0.51	-0.48	0.63	0.65	0.45	0.46	0.39	1.09	-0.23
38	27.94	0.655	0.035	0.051	4.54	2.39	4.09	-1.14	0.92	-1.06	-1.76	-0.55	-0.64	0.66	0.65	0.59	0.47	0.47	1.49	-0.25
39	30.48	0.672	0.038	0.038	3.89	2.05	3.26	-0.96	0.66	-0.95	-1.79	-0.56	-0.64	0.67	0.62	0.53	0.61	0.43	1.24	-0.26
40	33.02	0.692	0.042	0.027	3.03	1.70	2.54	-0.76	0.54	-0.82	-1.78	-0.56	-0.71	0.63	0.62	0.49	0.65	0.38	1.23	-0.26
41	35.56	0.708	0.044	0.018	2.17	1.38	1.84	-0.54	0.38	-0.62	-1.46	-0.46	-0.53	0.49	0.57	0.38	0.54	0.33	1.02	-0.21
42	38.10	0.720	0.042	0.010	1.35	0.99	1.23	-0.34	0.23	-0.38	-1.00	-0.32	-0.37	0.33	0.42	0.25	0.39	0.25	0.69	-0.13
43	40.64	0.728	0.047	0.004	0.82	0.74	0.76	-0.22	0.18	-0.18	-0.50	-0.19	-0.20	0.23	0.32	0.18	0.19	0.14	0.35	-0.08
44	45.72	0.737	0.048	-0.002	0.23	0.29	0.27	-0.05	0.02	-0.03	-0.05	-0.03	0.00	0.05	0.10	0.03	0.02	0.03	0.01	-0.02
45	50.80	0.735	0.048	-0.003	0.10	0.16	0.16	-0.01	0.00	0.01	0.01	-0.01	0.02	0.01	0.04	0.01	0.01	0.00	0.03	0.00
46	55.88	0.734	0.057	-0.001	0.07	0.40	0.15	-0.01	0.00	0.00	0.01	0.00	0.03	0.00	0.00	0.00	-0.01	0.00	-0.02	0.00
47	60.96	0.733	0.060	0.000	0.08	0.45	0.18	0.00	0.00	-0.01	0.02	0.00	0.06	0.00	0.62	0.00	-0.02	0.00	-0.05	0.00
48	66.04	0.729	0.000	0.001	0.08	0.00	0.19	0.00	0.00	0.02	0.02	0.00	0.07	0.00	0.00	0.00	0.01	0.00	0.04	0.00
49	71.12	0.730	0.000	0.007	0.03	0.00	0.10	0.00	0.00	-0.05	0.02	0.00	0.06	0.00	0.00	0.00	-0.01	0.00	-0.03	0.00

Table C.5 Continued.

Case C.S1 Station= 7
X= 12.7mm Tunnel Run#= 673 Ue/Uref= 0.717 Date= 509.88 Time=10.04
Bias Corrected data using 1/sqrt(U*U + V*V + W*W + (.01Ur)^2)

					<-- normalized by 0.001 Ur^2 -->						<---------- normalized by 0.0001 Ur^3 ---------->									
LR	Y(mm)	U/Ur	V/Ur	W/Ur	uu	vv	ww	uv	vw	uw	uuu	uvv	uww	vuu	vvv	vww	wuu	wvv	www	uvw
1	0.00	0.000	0.000	0.000	0.00	0.00	0.00	-0.55	-0.45	0.00	0.00	0.00	0.00	0.00	0.00	0.00	0.00	0.00	0.00	0.00
1	0.25	0.216	-0.010	0.171	5.40	0.96	6.28	-0.66	-0.55	0.84	1.35	0.08	0.49	-0.03	-0.01	0.00	-0.01	-0.02	0.21	0.03
2	0.38	0.236	-0.010	0.182	5.59	1.23	6.69	-0.67	-0.39	0.40	1.11	0.06	0.55	-0.01	0.09	0.17	-0.14	-0.03	-0.41	0.13
3	0.51	0.253	-0.011	0.190	5.57	1.49	6.62	-0.70	-0.28	0.21	1.08	0.04	0.23	0.03	-0.02	0.12	-0.03	-0.06	-0.30	0.17
4	0.63	0.265	-0.011	0.192	5.65	1.58	6.93	-0.60	-0.11	0.03	0.87	0.07	0.22	0.03	-0.05	-0.09	-0.03	-0.09	-0.40	0.07
5	0.76	0.275	-0.011	0.194	5.56	1.73	7.22	-0.51	-0.01	-0.14	0.90	0.07	0.23	0.02	0.01	0.01	-0.17	-0.13	-0.30	0.15
6	1.02	0.291	-0.009	0.193	5.76	2.04	7.43	-0.58	0.30	-0.17	1.11	0.10	0.16	0.13	-0.16	0.00	-0.09	-0.08	0.10	0.25
7	1.27	0.300	-0.010	0.191	6.08	2.33	7.81	-0.53	0.61	-0.45	1.18	0.11	0.38	0.11	-0.10	0.16	0.02	-0.06	-0.10	0.11
8	1.52	0.307	-0.008	0.188	6.07	2.52	7.71	-0.63	0.77	-0.53	1.21	0.11	0.43	0.12	-0.05	0.16	-0.06	-0.08	0.16	0.21
9	1.78	0.312	-0.007	0.186	5.89	2.59	8.24	-0.66	0.95	-0.81	1.34	0.18	0.46	0.06	-0.13	0.23	-0.16	-0.03	0.08	0.13
10	2.03	0.316	-0.008	0.180	6.24	2.88	8.34	-0.72	1.03	-0.64	1.09	0.10	0.19	0.06	0.01	0.44	-0.12	0.02	0.60	0.14
11	2.29	0.321	-0.008	0.178	6.33	3.02	8.20	-0.87	1.25	-0.90	1.20	0.13	0.37	0.05	0.02	0.47	-0.09	0.26	0.65	0.12
12	2.54	0.326	-0.008	0.175	6.10	3.25	8.36	-1.01	1.34	-0.89	1.06	0.15	0.27	0.08	0.01	0.52	-0.21	0.26	0.76	0.16
13	2.79	0.330	-0.007	0.173	6.28	3.33	8.59	-1.07	1.44	-1.30	1.13	0.11	0.14	0.09	0.09	0.66	0.03	0.29	0.97	0.06
14	3.30	0.339	-0.007	0.164	6.47	3.63	8.16	-1.22	1.51	-1.33	0.79	0.03	0.11	0.04	0.27	0.82	0.04	0.42	1.00	-0.02
15	3.81	0.342	-0.004	0.166	6.75	3.76	8.38	-1.36	1.56	-1.40	0.80	0.04	0.01	0.12	0.16	0.79	0.14	0.43	1.16	-0.07
16	4.32	0.348	-0.004	0.161	6.69	3.89	8.15	-1.43	1.66	-1.48	0.67	-0.11	-0.03	0.15	0.27	1.10	0.18	0.61	1.40	-0.12
17	4.83	0.355	-0.003	0.156	6.73	4.06	7.82	-1.52	1.63	-1.55	0.48	-0.06	-0.05	0.17	0.25	0.83	0.21	0.46	1.44	-0.10
18	5.59	0.366	-0.001	0.152	7.11	4.14	7.84	-1.65	1.70	-1.68	0.19	-0.15	0.12	0.22	0.33	0.88	0.33	0.54	0.97	-0.22
19	6.35	0.375	0.001	0.151	6.92	4.24	7.72	-1.72	1.74	-1.61	0.32	-0.06	0.05	-0.02	0.47	0.77	0.35	0.57	0.86	-0.09
20	7.11	0.383	0.001	0.147	7.12	4.35	7.23	-1.84	1.71	-1.46	0.30	-0.04	-0.03	0.03	0.41	0.69	0.16	0.59	0.73	-0.18
21	8.38	0.400	0.004	0.146	7.16	4.58	7.61	-1.94	1.76	-1.73	0.60	-0.17	0.07	0.08	0.54	0.49	0.12	0.53	0.14	-0.12
22	10.16	0.421	0.008	0.140	7.06	4.30	7.13	-1.96	1.59	-1.46	0.06	-0.17	0.07	0.13	0.34	0.37	0.26	0.38	0.33	-0.16
23	12.70	0.452	0.015	0.135	7.28	4.41	6.97	-1.97	1.67	-1.44	-0.19	-0.19	0.07	0.15	0.44	0.28	0.14	0.34	0.46	-0.12
24	15.24	0.479	0.018	0.125	7.00	4.12	6.77	-1.86	1.52	-1.09	-0.53	-0.19	-0.13	0.22	0.53	0.41	0.12	0.37	0.51	-0.08
25	17.78	0.505	0.024	0.116	6.73	4.02	6.29	-1.84	1.53	-1.13	-0.71	-0.30	-0.23	0.30	0.51	0.33	0.22	0.33	0.38	-0.21
26	20.32	0.533	0.028	0.105	6.55	3.66	6.17	-1.70	1.43	-1.33	-0.86	-0.29	-0.41	0.26	0.54	0.44	0.25	0.36	0.62	-0.20
27	22.86	0.567	0.027	0.086	6.01	3.44	5.70	-1.66	1.22	-1.03	-1.02	-0.44	-0.36	0.50	0.67	0.52	0.39	0.40	1.05	-0.16
28	25.40	0.594	0.027	0.072	5.23	2.98	4.98	-1.32	1.12	-0.96	-1.24	-0.43	-0.51	0.54	0.73	0.49	0.42	0.46	1.19	-0.19
29	27.94	0.613	0.031	0.059	5.20	2.69	4.55	-1.33	1.06	-1.08	-1.65	-0.57	-0.62	0.67	0.79	0.65	0.57	0.53	1.50	-0.30
30	30.48	0.637	0.035	0.048	4.23	2.39	3.74	-1.05	0.84	-0.90	-1.55	-0.56	-0.56	0.64	0.76	0.49	0.43	0.44	1.32	-0.23
31	33.02	0.657	0.038	0.037	3.77	2.03	3.07	-0.97	0.69	-0.97	-1.92	-0.60	-0.65	0.66	0.70	0.51	0.69	0.46	1.21	-0.30
32	35.56	0.672	0.041	0.029	3.03	1.78	2.59	-0.77	0.62	-0.85	-1.68	-0.52	-0.59	0.60	0.62	0.50	0.65	0.45	1.29	-0.26
33	38.10	0.694	0.038	0.014	1.74	1.12	1.48	-0.37	0.32	-0.48	-1.10	-0.32	-0.34	0.35	0.40	0.29	0.42	0.26	0.69	-0.16
34	40.64	0.705	0.039	0.007	1.00	0.79	0.91	-0.23	0.16	-0.24	-0.65	-0.22	-0.17	0.24	0.34	0.19	0.23	0.15	0.36	-0.07
35	45.72	0.713	0.041	0.000	0.32	0.35	0.38	-0.07	0.03	-0.07	-0.08	-0.06	0.06	0.06	0.10	0.03	0.01	0.04	-0.04	-0.02
36	50.80	0.715	0.043	-0.003	0.15	0.18	0.27	-0.01	0.00	-0.03	0.02	-0.01	0.10	0.01	0.02	0.01	-0.03	0.00	-0.07	0.00
37	55.88	0.715	0.049	-0.002	0.10	0.41	0.22	0.00	-0.01	-0.02	0.03	0.00	0.08	0.00	0.00	0.00	-0.03	0.00	-0.08	0.00
38	60.96	0.713	0.053	0.000	0.08	0.39	0.19	0.00	0.00	-0.03	0.02	0.00	0.06	0.00	0.00	0.01	-0.03	0.00	-0.10	0.00
39	66.04	0.711	0.000	0.001	0.08	0.00	0.20	0.00	0.00	-0.02	0.03	0.00	0.08	0.00	0.00	0.00	-0.04	0.00	-0.11	0.00
40	71.12	0.710	0.000	0.003	0.07	0.00	0.20	0.00	0.00	0.02	0.03	0.00	0.08	0.00	0.00	0.00	0.02	0.00	0.06	0.00

Table C.5 Continued.

Case C.S1 Station= 8
X= 25.4mm Tunnel Run#= 671 Ue/Uref= 0.709 Date= 509.88 Time= 8.19
Bias Corrected data using 1/sqrt(U*U + V*V + W*W + (.01Ur)^2)

					<-- normalized by 0.001 Ur^2 -->						<---------- normalized by 0.0001 Ur^3 ---------->									
LR	Y(mm)	U/Ur	V/Ur	W/Ur	uu	vv	ww	uv	vw	uw	uuu	uvv	uww	vuu	vvv	vww	wuu	wvv	www	uvw
1	0.00	0.000	0.000	0.000	0.00	0.00	0.00	-0.55	-0.40	0.00	0.00	0.00	0.00	0.00	0.00	0.00	0.00	0.00	0.00	0.00
1	0.25	0.203	-0.009	0.129	4.89	0.80	5.30	-0.59	-0.51	0.77	0.88	0.03	0.76	0.03	0.08	0.07	0.03	0.03	0.53	-0.04
2	0.38	0.224	-0.010	0.142	5.00	1.04	5.57	-0.65	-0.44	0.51	0.78	0.06	0.61	0.03	-0.01	0.08	-0.11	-0.01	0.33	0.02
3	0.51	0.233	-0.010	0.145	4.99	1.18	5.75	-0.65	-0.39	0.35	0.93	0.08	0.66	-0.01	0.02	0.07	0.00	0.01	0.26	0.04
4	0.63	0.245	-0.010	0.150	4.90	1.38	5.85	-0.65	-0.30	0.14	0.89	0.10	0.72	-0.01	0.00	0.09	-0.01	-0.03	0.00	0.02
5	0.76	0.252	-0.009	0.153	4.86	1.47	5.84	-0.69	-0.24	0.01	0.88	0.12	0.49	-0.03	-0.05	0.06	-0.02	-0.07	-0.10	0.04
6	1.02	0.266	-0.009	0.157	5.10	1.75	6.04	-0.72	-0.19	0.05	0.92	0.10	0.50	0.00	0.01	0.14	-0.16	-0.02	-0.26	0.11
7	1.27	0.276	-0.009	0.156	5.21	1.87	6.23	-0.76	0.02	-0.30	1.11	0.10	0.51	0.06	-0.15	0.10	-0.04	-0.10	-0.14	0.08
8	1.52	0.286	-0.008	0.154	5.26	2.03	6.30	-0.78	0.16	-0.36	0.94	0.18	0.60	-0.09	-0.11	0.04	-0.13	-0.12	-0.36	0.08
9	1.78	0.296	-0.009	0.157	5.43	2.22	6.62	-0.75	0.29	-0.31	1.23	0.10	0.29	0.01	-0.10	0.06	0.00	-0.13	-0.29	0.11
10	2.03	0.303	-0.008	0.158	5.48	2.39	6.77	-0.82	0.42	-0.46	1.22	0.13	0.36	0.02	-0.11	0.10	-0.20	-0.14	0.01	0.16
11	2.29	0.310	-0.007	0.157	5.71	2.53	6.93	-0.83	0.49	-0.56	1.08	0.08	0.33	0.04	-0.07	0.10	-0.05	-0.07	-0.17	0.13
12	2.54	0.314	-0.006	0.158	5.73	2.69	7.11	-0.83	0.71	-0.60	1.21	0.19	0.58	0.02	-0.18	0.13	-0.08	0.01	0.25	0.12
13	2.79	0.319	-0.007	0.156	5.57	2.84	7.13	-0.88	0.77	-0.52	0.86	0.20	0.56	0.03	-0.18	0.18	-0.27	-0.03	0.09	0.17
14	3.30	0.329	-0.006	0.155	5.71	3.05	7.19	-0.96	0.99	-0.86	1.00	0.21	0.48	0.10	-0.20	0.27	-0.26	0.04	0.19	0.10
15	3.81	0.339	-0.006	0.156	5.82	3.38	7.31	-1.07	1.16	-0.88	0.82	0.16	0.66	-0.02	-0.11	0.41	-0.20	0.13	0.05	0.06
16	4.32	0.343	-0.004	0.157	5.65	3.51	7.46	-1.06	1.32	-1.04	0.87	0.21	0.54	-0.03	0.07	0.49	0.04	0.29	0.16	0.04
17	4.83	0.347	-0.004	0.153	6.06	3.72	7.41	-1.31	1.52	-1.14	1.03	0.23	0.44	-0.07	0.00	0.35	-0.17	0.26	0.32	0.02
18	5.59	0.355	-0.003	0.152	6.30	3.89	7.40	-1.46	1.45	-1.11	0.97	0.17	0.46	-0.10	0.17	0.41	-0.08	0.24	0.31	0.11
19	6.35	0.364	-0.003	0.146	6.27	4.09	7.31	-1.58	1.60	-1.26	0.87	0.18	0.38	-0.12	0.21	0.36	-0.02	0.32	0.60	0.02
20	7.11	0.371	-0.002	0.145	6.69	4.25	7.14	-1.69	1.55	-1.36	0.58	0.03	0.46	-0.03	0.24	0.48	0.13	0.33	0.27	-0.08
21	8.38	0.386	0.001	0.143	6.76	4.38	7.42	-1.97	1.72	-1.48	0.56	-0.12	0.31	0.03	0.44	0.53	0.13	0.53	0.54	-0.08
22	10.16	0.408	0.002	0.137	6.87	4.32	7.13	-1.99	1.58	-1.35	0.41	-0.07	0.23	0.02	0.41	0.40	0.07	0.42	0.29	-0.13
23	12.70	0.440	0.006	0.131	7.04	4.31	6.98	-1.85	1.69	-1.38	0.03	-0.23	0.04	0.07	0.61	0.45	0.11	0.46	0.61	-0.15
24	15.24	0.470	0.009	0.123	7.07	4.17	6.98	-2.05	1.59	-1.53	-0.51	-0.36	-0.25	0.33	0.50	0.24	0.30	0.35	0.21	-0.18
25	17.78	0.496	0.011	0.110	6.74	3.91	6.59	-1.77	1.52	-1.22	-0.70	-0.41	-0.19	0.43	0.51	0.55	0.17	0.41	0.63	-0.16
26	20.32	0.524	0.015	0.098	6.41	3.64	5.97	-1.68	1.42	-1.23	-0.97	-0.47	-0.25	0.44	0.68	0.48	0.35	0.40	0.59	-0.25
27	22.86	0.549	0.019	0.087	5.87	3.36	5.46	-1.50	1.11	-0.91	-0.94	-0.41	-0.30	0.51	0.68	0.49	0.35	0.44	0.80	-0.15
28	25.40	0.574	0.021	0.075	5.34	3.00	4.97	-1.33	1.05	-0.88	-1.17	0.44	-0.47	0.47	0.55	0.54	0.31	0.41	1.00	-0.20
29	27.94	0.595	0.026	0.063	5.02	2.80	4.46	-1.31	0.93	-0.83	-1.41	-0.47	-0.42	0.58	0.69	0.53	0.46	0.39	0.92	-0.26
30	30.48	0.619	0.028	0.051	4.43	2.41	3.93	-1.05	0.84	-0.89	-1.48	-0.49	-0.46	0.51	0.67	0.54	0.40	0.44	0.94	-0.21
31	33.02	0.641	0.031	0.039	3.68	2.10	3.19	-0.90	0.65	-0.82	-1.61	-0.52	-0.64	0.62	0.64	0.48	0.61	0.38	1.14	-0.25
32	35.56	0.661	0.034	0.028	3.00	1.68	2.47	-0.69	0.55	-0.75	-1.70	-0.41	-0.51	0.57	0.58	0.42	0.51	0.38	0.98	-0.21
33	38.10	0.676	0.035	0.019	2.08	1.29	1.76	-0.53	0.36	-0.50	-1.26	-0.36	-0.42	0.43	0.48	0.33	0.46	0.24	0.80	-0.18
34	40.64	0.689	0.037	0.012	1.43	1.05	1.30	-0.34	0.27	-0.34	-0.92	-0.30	-0.28	0.30	0.50	0.28	0.34	0.25	0.65	-0.12
35	45.72	0.701	0.039	0.002	0.48	0.49	0.55	-0.10	0.08	-0.10	-0.21	-0.07	-0.04	0.09	0.14	0.08	0.08	0.08	0.16	-0.03
36	50.80	0.704	0.041	-0.002	0.18	0.26	0.26	-0.02	0.02	0.00	-0.02	-0.02	0.04	0.02	0.09	0.02	0.01	0.01	0.02	0.00
37	55.88	0.704	0.046	-0.004	0.10	0.43	0.23	0.00	0.00	-0.01	0.03	0.00	0.08	0.00	0.01	0.00	-0.01	0.00	-0.04	0.00
38	60.96	0.704	0.048	-0.003	0.09	0.41	0.23	0.00	0.00	0.01	0.03	0.00	0.10	0.00	0.01	0.00	0.00	0.00	0.00	0.00
39	66.04	0.703	0.000	-0.001	0.08	0.00	0.22	0.00	0.00	0.01	0.03	0.00	0.09	0.00	0.00	0.00	0.00	0.00	0.00	0.00
40	71.12	0.702	0.000	0.000	0.06	0.00	0.17	0.00	0.00	0.01	0.01	0.00	0.03	0.00	0.00	0.00	0.00	0.00	0.01	0.00

Table C.5 Continued.

Case C.S1 Station= 9
X= 50.8mm Tunnel Run#= 669 Ue/Uref= 0.697 Date= 508.88 Time=17.33
Bias Corrected data using 1/sqrt(U*U + V*V + W*W + (.01Ur)^2)

					<-- normalized by 0.001 Ur^2 -->						<---------- normalized by 0.0001 Ur^3 ---------->									
LR	Y(mm)	U/Ur	V/Ur	W/Ur	uu	vv	ww	uv	vw	uw	uuu	uvv	uww	vuu	vvv	vww	wuu	wvv	www	uvw
1	0.00	0.000	0.000	0.000	0.00	0.00	0.00	-0.40	-0.24	0.00	0.00	0.00	0.00	0.00	0.00	0.00	0.00	0.00	0.00	0.00
1	0.25	0.164	-0.004	0.087	4.34	0.45	3.76	-0.41	-0.36	0.71	1.12	0.06	0.75	-0.05	-0.03	-0.02	0.08	0.03	0.75	-0.05
2	0.38	0.185	-0.004	0.095	4.41	0.64	3.96	-0.49	-0.35	0.54	0.82	0.06	0.64	0.01	-0.02	0.01	0.03	0.02	0.57	-0.02
3	0.51	0.203	-0.005	0.102	4.50	0.83	4.30	-0.54	-0.41	0.39	0.89	0.06	0.56	0.00	-0.02	0.04	0.00	0.00	0.37	-0.01
4	0.63	0.214	-0.005	0.109	4.45	0.99	4.41	-0.53	-0.37	0.35	0.89	0.06	0.52	-0.01	0.02	0.07	0.09	-0.01	0.61	0.01
5	0.76	0.222	-0.006	0.111	4.37	1.17	4.55	-0.62	-0.35	0.16	0.71	0.06	0.47	-0.03	-0.04	0.09	0.00	-0.02	0.23	0.02
6	1.02	0.235	-0.005	0.115	4.45	1.39	4.66	-0.66	-0.28	0.05	0.77	0.11	0.50	-0.01	0.06	0.03	0.00	-0.04	0.16	0.04
7	1.27	0.247	-0.006	0.116	4.57	1.56	4.68	-0.74	-0.17	-0.09	0.87	0.13	0.51	-0.06	-0.08	0.07	0.04	-0.06	0.05	0.02
8	1.52	0.253	-0.004	0.120	4.63	1.68	4.93	-0.72	-0.22	-0.17	0.83	0.13	0.60	-0.13	-0.01	0.15	-0.06	-0.11	-0.21	0.03
9	1.78	0.260	-0.004	0.120	4.55	1.79	4.99	-0.75	-0.16	-0.16	0.92	0.12	0.46	-0.08	-0.07	0.04	-0.04	-0.08	0.00	0.08
10	2.03	0.266	-0.004	0.124	4.68	1.93	5.07	-0.76	-0.08	-0.23	0.97	0.12	0.37	-0.08	-0.14	0.13	0.03	-0.09	-0.07	0.03
11	2.29	0.273	-0.003	0.123	4.76	2.05	5.01	-0.84	-0.02	-0.30	0.85	0.15	0.44	-0.07	-0.09	0.05	-0.02	-0.07	0.04	0.05
12	2.54	0.278	-0.003	0.123	5.01	2.15	5.27	-0.91	0.11	-0.18	0.85	0.17	0.53	-0.02	-0.05	0.00	0.00	-0.08	0.11	0.08
13	2.79	0.284	-0.002	0.125	4.96	2.19	5.06	-0.94	0.09	-0.32	0.92	0.14	0.53	-0.09	-0.15	0.05	-0.07	-0.09	-0.08	0.07
14	3.30	0.295	-0.002	0.124	5.20	2.38	5.28	-0.98	0.25	-0.33	0.94	0.16	0.45	-0.08	-0.15	0.05	-0.01	-0.14	-0.03	0.10
15	3.81	0.305	-0.002	0.125	5.17	2.64	5.42	-1.03	0.30	-0.48	1.05	0.19	0.43	-0.18	-0.21	0.03	-0.07	-0.10	-0.12	0.13
16	4.32	0.311	-0.001	0.127	5.42	2.72	5.52	-1.18	0.47	-0.52	0.88	0.13	0.50	-0.06	-0.25	0.03	-0.12	-0.07	-0.01	0.13
17	4.83	0.319	-0.001	0.128	5.38	2.89	5.42	-1.14	0.58	-0.60	0.77	0.28	0.46	-0.06	-0.18	0.02	-0.05	-0.10	0.18	0.10
18	5.59	0.329	0.002	0.131	5.44	3.09	5.67	-1.20	0.76	-0.72	0.89	0.24	0.35	-0.09	-0.24	0.21	0.02	-0.07	0.04	0.09
19	6.35	0.338	0.001	0.130	5.55	3.32	5.80	-1.31	0.81	-0.65	0.92	0.35	0.41	-0.18	-0.31	0.04	-0.01	0.00	0.07	0.15
20	7.11	0.345	0.003	0.130	5.77	3.48	5.88	-1.46	0.92	-0.83	0.75	0.21	0.37	-0.14	-0.10	0.03	0.01	0.03	-0.05	0.07
21	8.38	0.359	0.003	0.133	6.06	3.78	6.16	-1.55	1.26	-1.08	0.90	0.25	0.46	-0.20	-0.29	-0.06	-0.18	0.04	-0.02	0.10
22	10.16	0.379	0.006	0.131	6.30	4.06	6.34	-1.78	1.37	-1.00	0.78	0.12	0.46	-0.23	0.12	0.09	-0.15	0.17	0.19	0.06
23	12.70	0.412	0.008	0.129	6.60	3.99	6.56	-1.87	1.41	-1.16	0.43	0.05	0.18	-0.06	0.19	0.11	-0.02	0.32	0.25	-0.01
24	15.24	0.436	0.008	0.123	6.99	3.99	6.44	-1.95	1.38	-1.14	-0.30	-0.01	-0.12	0.14	0.16	0.27	0.09	0.23	0.36	-0.09
25	17.78	0.470	0.012	0.115	6.81	3.94	6.49	-1.97	1.44	-1.09	-0.34	-0.27	-0.23	0.31	0.45	0.35	-0.08	0.42	0.50	-0.16
26	20.32	0.496	0.015	0.103	6.63	3.76	6.21	-1.87	1.43	-1.21	-0.86	-0.38	-0.42	0.40	0.64	0.46	0.36	0.40	0.87	-0.19
27	22.86	0.523	0.019	0.093	6.17	3.54	5.74	-1.68	1.31	-0.97	-0.92	-0.40	-0.39	0.38	0.61	0.49	0.34	0.42	0.76	-0.24
28	25.40	0.544	0.024	0.081	5.86	3.21	5.43	-1.49	1.22	-0.93	-0.92	-0.32	-0.32	0.29	0.52	0.56	0.24	0.44	1.03	-0.16
29	27.94	0.571	0.026	0.069	5.40	3.03	4.76	-1.43	1.04	-0.87	-1.51	-0.44	-0.43	0.61	0.62	0.44	0.37	0.34	0.76	-0.16
30	30.48	0.593	0.028	0.059	4.76	2.75	4.23	-1.29	0.88	-0.92	-1.24	-0.47	-0.47	0.53	0.76	0.47	0.34	0.42	0.86	-0.19
31	33.02	0.612	0.030	0.048	4.48	2.37	3.72	-1.15	0.76	-0.84	-1.62	-0.47	-0.51	0.60	0.56	0.49	0.41	0.41	1.14	-0.19
32	35.56	0.633	0.031	0.037	3.63	2.07	3.07	-0.91	0.67	-0.75	-1.64	-0.51	-0.46	0.60	0.58	0.43	0.43	0.33	1.07	-0.18
33	38.10	0.651	0.032	0.028	2.89	1.77	2.48	-0.73	0.55	-0.77	-1.42	-0.47	-0.56	0.48	0.57	0.43	0.53	0.36	1.14	-0.22
34	40.64	0.668	0.033	0.017	2.18	1.42	1.87	-0.54	0.39	-0.55	-1.24	-0.41	-0.43	0.42	0.51	0.32	0.46	0.28	0.85	-0.18
35	45.72	0.688	0.034	0.005	0.85	0.75	0.84	-0.20	0.16	-0.17	-0.42	-0.15	-0.11	0.18	0.25	0.15	0.20	0.14	0.42	-0.05
36	50.80	0.697	0.033	-0.003	0.22	0.32	0.30	-0.04	0.04	-0.03	-0.03	-0.03	0.02	0.04	0.09	0.04	0.02	0.03	0.04	-0.01
37	55.88	0.695	0.038	-0.004	0.10	0.42	0.16	-0.01	0.01	0.00	0.00	0.00	0.01	0.01	0.02	0.00	0.01	0.00	0.02	0.00
38	60.96	0.695	0.039	-0.003	0.08	0.37	0.15	0.00	0.00	0.01	0.01	0.00	0.03	0.00	0.00	0.00	0.00	0.00	0.00	0.00
39	66.04	0.696	0.000	-0.003	0.07	0.00	0.15	0.00	0.00	0.00	0.01	0.00	0.03	0.00	0.00	0.00	-0.01	0.00	-0.02	0.00
40	71.12	0.695	0.000	-0.002	0.08	0.00	0.21	0.00	0.00	0.03	0.02	0.00	0.07	0.00	0.00	0.00	0.01	0.00	0.02	0.00

Table C.5 Continued.

Case C.S1 Station= 10
X= 101.6mm Tunnel Run#= 667 Ue/Uref= 0.678 Date= 508.88 Time=15.15
Bias Corrected data using 1/sqrt(U*U + V*V + W*W + (.01Ur)^2)

					<-- normalized by 0.001 Ur^2 -->						<---------- normalized by 0.0001 Ur^3 ---------->									
LR	Y(mm)	U/Ur	V/Ur	W/Ur	uu	vv	ww	uv	vw	uw	uuu	uvv	uww	vuu	vvv	vww	wuu	wvv	www	uvw
1	0.00	0.000	0.000	0.000	0.00	0.00	0.00	-0.28	-0.14	0.00	0.00	0.00	0.00	0.00	0.00	0.00	0.00	0.00	0.00	0.00
1	0.25	0.143	-0.003	0.059	3.69	0.36	2.97	-0.30	-0.26	0.44	0.94	0.04	0.60	-0.05	-0.02	-0.01	0.06	0.01	0.54	-0.05
2	0.38	0.165	-0.003	0.068	3.94	0.53	3.26	-0.38	-0.29	0.32	0.86	0.05	0.57	-0.04	-0.02	0.01	-0.02	0.01	0.53	-0.03
3	0.51	0.178	-0.004	0.076	3.81	0.71	3.49	-0.39	-0.29	0.22	0.77	0.04	0.46	0.00	0.07	0.03	0.02	-0.01	0.48	-0.03
4	0.63	0.187	-0.003	0.079	4.08	0.80	3.49	-0.48	-0.29	0.24	0.65	0.06	0.49	0.00	-0.02	0.02	-0.02	0.03	0.30	-0.02
5	0.76	0.195	-0.003	0.081	4.03	0.92	3.80	-0.47	-0.28	0.12	0.84	0.06	0.62	-0.01	-0.04	0.03	0.02	0.02	0.15	-0.04
6	1.02	0.207	-0.003	0.084	4.07	1.14	3.93	-0.54	-0.28	-0.05	0.85	0.09	0.70	-0.07	-0.02	0.09	0.05	0.03	0.16	-0.05
7	1.27	0.215	-0.002	0.088	4.04	1.28	4.03	-0.58	-0.22	-0.05	0.74	0.10	0.52	-0.07	-0.05	0.07	0.00	-0.01	0.30	-0.02
8	1.52	0.224	-0.002	0.091	4.16	1.37	3.98	-0.60	-0.22	0.00	0.83	0.12	0.57	-0.08	-0.09	0.06	0.02	-0.03	0.17	0.00
9	1.78	0.231	-0.003	0.089	4.41	1.60	4.00	-0.72	-0.20	0.02	0.79	0.11	0.48	-0.05	-0.09	0.05	0.00	-0.03	0.22	0.06
10	2.03	0.237	-0.003	0.093	4.31	1.63	3.97	-0.73	-0.20	-0.08	0.82	0.15	0.55	-0.10	-0.17	0.07	0.01	-0.02	0.22	-0.02
11	2.29	0.240	-0.003	0.093	4.49	1.72	4.13	-0.78	-0.14	-0.14	0.80	0.15	0.55	-0.10	-0.13	0.08	-0.04	-0.03	-0.14	0.02
12	2.54	0.244	-0.003	0.094	4.46	1.84	4.19	-0.82	-0.08	-0.19	0.87	0.15	0.51	-0.13	-0.06	0.03	0.03	-0.04	0.16	0.04
13	2.79	0.252	-0.002	0.095	4.53	1.81	4.23	-0.82	-0.08	-0.15	0.49	0.14	0.47	-0.07	-0.13	0.08	-0.02	-0.08	0.08	0.03
14	3.30	0.260	-0.002	0.097	4.85	2.15	4.24	-0.99	-0.03	-0.34	0.78	0.16	0.53	-0.10	-0.16	0.00	-0.04	-0.06	0.02	0.08
15	3.81	0.266	-0.002	0.097	4.78	2.20	4.43	-1.04	-0.02	-0.24	0.76	0.23	0.43	-0.17	-0.23	0.10	-0.01	-0.10	0.09	0.07
16	4.32	0.275	-0.002	0.097	4.84	2.35	4.50	-1.03	0.04	-0.30	0.76	0.19	0.40	-0.21	-0.23	0.06	-0.01	-0.09	0.16	0.04
17	4.83	0.283	-0.003	0.098	5.23	2.45	4.58	-1.17	0.09	-0.29	0.64	0.19	0.47	-0.18	-0.24	-0.03	-0.12	-0.05	0.22	0.07
18	5.59	0.295	-0.003	0.099	5.15	2.56	4.76	-1.21	0.18	-0.28	0.80	0.22	0.46	-0.14	-0.26	0.06	0.06	-0.05	-0.03	0.02
19	6.35	0.304	-0.002	0.102	5.46	2.89	4.80	-1.43	0.30	-0.45	0.84	0.25	0.42	-0.27	-0.30	-0.09	-0.04	-0.08	-0.02	0.09
20	7.11	0.315	-0.001	0.105	5.52	2.91	5.01	-1.39	0.39	-0.47	0.83	0.29	0.51	-0.21	-0.24	-0.02	0.21	-0.07	0.14	0.06
21	8.38	0.330	-0.001	0.108	5.84	3.15	5.07	-1.55	0.45	-0.57	0.77	0.25	0.41	-0.26	-0.22	-0.03	-0.08	-0.03	-0.20	0.08
22	10.16	0.352	-0.001	0.108	6.02	3.39	5.32	-1.66	0.67	-0.62	0.70	0.23	0.34	-0.30	-0.18	0.03	-0.01	0.00	0.09	0.08
23	12.70	0.382	0.000	0.110	6.23	3.67	5.86	-1.85	0.90	-0.88	0.39	0.08	0.41	-0.03	0.00	0.04	-0.01	0.02	-0.05	0.06
24	15.24	0.408	0.004	0.112	6.28	3.79	6.05	-1.92	1.13	-0.87	0.16	-0.04	0.09	0.03	0.15	0.13	-0.05	0.19	0.12	-0.02
25	17.78	0.433	0.004	0.107	6.33	3.76	6.09	-1.88	1.15	-0.94	0.02	-0.11	0.14	0.05	0.18	0.16	0.14	0.26	0.40	0.02
26	20.32	0.461	0.007	0.103	6.39	3.65	5.99	-1.87	1.19	-0.95	-0.53	-0.26	-0.11	0.27	0.48	0.21	0.20	0.26	0.49	-0.11
27	22.86	0.488	0.010	0.098	6.28	3.59	5.75	-1.73	1.29	-0.98	-0.70	-0.36	-0.20	0.40	0.61	0.44	0.30	0.46	0.66	-0.24
28	25.40	0.511	0.012	0.087	5.85	3.23	5.36	-1.53	1.05	-0.89	-1.07	-0.40	-0.35	0.44	0.69	0.44	0.40	0.37	0.78	-0.20
29	27.94	0.532	0.015	0.079	5.47	3.14	5.11	-1.47	1.10	-0.83	-1.25	-0.44	-0.34	0.53	0.61	0.50	0.46	0.42	1.03	-0.19
30	30.48	0.563	0.016	0.067	4.94	2.80	4.52	-1.36	1.09	-0.89	-1.45	-0.51	-0.43	0.61	0.74	0.58	0.55	0.50	0.98	-0.32
31	33.02	0.577	0.018	0.059	4.32	2.42	3.90	-1.12	0.80	-0.65	-1.39	-0.41	-0.44	0.56	0.56	0.40	0.42	0.42	1.15	-0.20
32	35.56	0.595	0.021	0.047	3.80	2.23	3.44	-1.00	0.75	-0.66	-1.38	-0.45	-0.46	0.57	0.61	0.44	0.43	0.41	1.07	-0.19
33	38.10	0.612	0.022	0.039	3.27	1.95	2.89	-0.83	0.61	-0.63	-1.28	-0.48	-0.48	0.49	0.60	0.42	0.32	0.34	1.02	-0.19
34	40.64	0.630	0.024	0.029	2.70	1.68	2.36	-0.64	0.48	-0.57	-1.24	-0.39	-0.45	0.40	0.65	0.37	0.39	0.32	0.98	-0.16
35	45.72	0.659	0.026	0.015	1.33	1.00	1.30	-0.29	0.23	-0.25	-0.65	-0.25	-0.20	0.23	0.30	0.22	0.31	0.20	0.64	-0.10
36	50.80	0.673	0.026	0.004	0.52	0.51	0.56	-0.11	0.07	-0.07	-0.23	-0.08	-0.06	0.10	0.12	0.09	0.08	0.07	0.21	-0.02
37	55.88	0.677	0.032	0.001	0.18	0.53	0.26	-0.02	0.02	0.00	-0.01	-0.01	0.04	0.02	0.04	0.02	0.01	0.01	0.02	0.00
38	60.96	0.678	0.033	0.001	0.12	0.41	0.24	0.00	0.01	0.02	0.02	0.00	0.07	0.01	0.00	0.01	0.01	0.00	0.06	0.00
39	66.04	0.676	0.000	0.001	0.10	0.00	0.19	0.00	0.00	0.02	0.02	0.00	0.06	0.00	0.00	0.00	0.02	0.00	0.06	0.00
40	71.12	0.675	0.000	0.002	0.09	0.00	0.20	0.00	0.00	0.02	0.02	0.00	0.05	0.00	0.00	0.00	0.01	0.00	0.03	0.00

Table C.5 Continued.

Case C.S1 Station= 11
X= 152.4mm Tunnel Run#= 665 Ue/Uref= 0.664 Date= 507.88 Time=12.34
Bias Corrected data using 1/sqrt(U*U + V*V + W*W + (.01Ur)^2)

					<-- normalized by 0.001 Ur^2 -->						<---------- normalized by 0.0001 Ur^3 ---------->									
LR	Y(mm)	U/Ur	V/Ur	W/Ur	uu	vv	ww	uv	vw	uw	uuu	uvv	uww	vuu	vvv	vww	wuu	wvv	www	uvw
1	0.00	0.000	0.000	0.000	0.00	0.00	0.00	-0.28	-0.12	0.00	0.00	0.00	0.00	0.00	0.00	0.00	0.00	0.00	0.00	0.00
1	0.25	0.126	-0.001	0.047	3.56	0.29	2.61	-0.25	-0.20	0.40	1.28	0.05	0.70	-0.05	0.04	-0.02	-0.01	0.01	0.57	-0.04
2	0.38	0.151	-0.001	0.054	3.83	0.44	2.97	-0.32	-0.24	0.36	1.07	0.04	0.59	-0.06	-0.01	-0.01	0.09	0.03	0.69	-0.04
3	0.51	0.166	-0.002	0.058	3.97	0.57	3.24	-0.40	-0.29	0.30	0.84	0.05	0.54	-0.05	-0.04	0.02	0.08	0.01	0.61	-0.01
4	0.63	0.178	-0.002	0.062	4.02	0.68	3.21	-0.39	-0.26	0.21	0.87	0.07	0.47	-0.04	-0.06	0.01	0.05	0.01	0.55	-0.03
5	0.76	0.183	-0.002	0.065	4.02	0.80	3.47	-0.42	-0.26	0.20	0.86	0.03	0.55	-0.01	0.00	0.04	0.02	0.03	0.55	-0.01
6	1.02	0.193	-0.001	0.069	4.29	0.95	3.54	-0.54	-0.26	0.13	0.74	0.06	0.52	0.01	-0.02	0.02	0.13	0.00	0.54	-0.01
7	1.27	0.201	-0.002	0.072	4.15	1.08	3.45	-0.50	-0.23	0.10	0.75	0.08	0.60	-0.03	-0.04	0.05	0.00	0.02	0.44	-0.03
8	1.52	0.208	-0.002	0.073	4.23	1.26	3.50	-0.62	-0.20	0.02	0.70	0.11	0.44	-0.04	-0.09	0.00	0.03	0.00	0.32	0.02
9	1.78	0.216	-0.002	0.075	4.35	1.33	3.68	-0.66	-0.17	0.04	0.71	0.13	0.56	-0.05	-0.11	0.05	0.04	-0.02	0.54	-0.01
10	2.03	0.219	-0.002	0.077	4.25	1.47	3.70	-0.66	-0.21	-0.03	0.68	0.14	0.49	-0.06	-0.16	0.02	-0.04	0.00	0.43	0.00
11	2.29	0.224	-0.002	0.078	4.28	1.53	3.73	-0.69	-0.21	-0.03	0.67	0.17	0.46	-0.05	-0.17	0.08	0.05	-0.02	0.30	-0.01
12	2.54	0.227	-0.002	0.076	4.32	1.60	3.80	-0.73	-0.11	-0.05	0.73	0.15	0.53	-0.13	-0.15	0.06	-0.04	-0.05	0.26	0.03
13	2.79	0.232	-0.003	0.079	4.61	1.67	3.88	-0.77	-0.12	-0.13	0.65	0.15	0.46	-0.08	-0.16	0.06	0.01	-0.02	0.45	0.00
14	3.30	0.240	-0.003	0.079	4.49	1.85	3.89	-0.81	-0.13	-0.13	0.72	0.18	0.43	-0.11	-0.13	0.03	-0.03	0.01	0.17	0.00
15	3.81	0.247	-0.002	0.080	4.84	2.00	4.00	-0.94	-0.07	-0.19	0.85	0.25	0.56	-0.22	-0.25	-0.02	0.11	-0.05	0.26	0.03
16	4.32	0.253	-0.003	0.082	4.89	2.11	4.03	-1.01	-0.05	-0.13	0.71	0.29	0.54	-0.19	-0.17	-0.01	-0.03	-0.04	0.33	0.06
17	4.83	0.259	-0.003	0.084	4.84	2.30	4.23	-1.01	0.02	-0.30	0.85	0.27	0.45	-0.20	-0.24	0.04	-0.03	-0.01	0.04	-0.01
18	5.59	0.268	-0.002	0.084	5.10	2.44	4.26	-1.12	0.05	-0.24	0.75	0.24	0.52	-0.25	-0.20	-0.03	-0.01	-0.03	0.08	0.04
19	6.35	0.278	-0.003	0.086	5.26	2.52	4.36	-1.18	0.13	-0.33	0.76	0.27	0.55	-0.22	-0.32	-0.08	-0.07	-0.05	0.10	0.08
20	7.11	0.287	-0.002	0.088	5.44	2.60	4.44	-1.29	0.14	-0.26	0.82	0.28	0.52	-0.26	-0.25	0.00	-0.05	-0.07	0.20	0.10
21	8.38	0.299	-0.001	0.091	5.58	2.90	4.74	-1.52	0.22	-0.44	0.79	0.29	0.44	-0.32	-0.35	-0.01	0.01	-0.12	-0.03	0.10
22	10.16	0.318	0.000	0.095	5.66	3.16	4.78	-1.55	0.38	-0.44	0.55	0.16	0.46	-0.20	-0.14	-0.10	0.04	-0.01	0.09	0.01
23	12.70	0.342	0.001	0.099	6.27	3.27	5.04	-1.73	0.50	-0.60	0.58	0.19	0.39	-0.15	-0.15	-0.02	0.00	-0.05	-0.01	0.06
24	15.24	0.370	0.003	0.100	6.33	3.56	5.40	-1.90	0.64	-0.71	0.40	0.20	0.30	-0.13	-0.15	-0.05	-0.03	-0.05	-0.09	0.02
25	17.78	0.401	0.002	0.101	6.56	3.63	5.59	-1.98	0.85	-0.73	0.09	0.05	0.28	0.03	0.10	0.08	0.11	0.11	0.37	0.05
26	20.32	0.426	0.003	0.099	6.42	3.64	5.91	-1.95	0.89	-0.80	0.00	-0.05	0.29	0.04	0.09	0.21	0.06	0.06	0.64	0.12
27	22.86	0.451	0.004	0.095	6.41	3.63	5.69	-1.94	1.10	-0.93	-0.74	-0.25	0.03	0.33	0.40	0.10	0.20	0.17	0.60	-0.05
28	25.40	0.473	0.007	0.091	6.33	3.52	5.55	-1.84	1.14	-0.92	-0.85	-0.38	-0.15	0.43	0.52	0.32	0.35	0.33	0.76	-0.13
29	27.94	0.498	0.008	0.083	5.98	3.40	5.26	-1.84	1.10	-0.86	-1.34	-0.47	-0.18	0.67	0.58	0.32	0.44	0.36	0.89	-0.22
30	30.48	0.519	0.011	0.075	5.40	3.17	4.99	-1.58	1.14	-1.01	-1.18	-0.54	-0.40	0.56	0.73	0.47	0.46	0.41	1.04	-0.27
31	33.02	0.541	0.013	0.065	4.81	2.84	4.48	-1.42	0.99	-0.82	-1.50	-0.52	-0.47	0.61	0.74	0.48	0.55	0.42	1.25	-0.21
32	35.56	0.562	0.013	0.055	4.36	2.49	3.95	-1.17	0.80	-0.75	-1.44	-0.46	-0.47	0.52	0.65	0.47	0.50	0.44	1.07	-0.20
33	38.10	0.578	0.015	0.044	3.84	2.28	3.47	-1.10	0.75	-0.72	-1.41	-0.53	-0.46	0.66	0.70	0.55	0.44	0.43	1.23	-0.22
34	40.64	0.595	0.016	0.035	3.21	1.97	2.72	-0.85	0.58	-0.61	-1.37	-0.49	-0.44	0.54	0.70	0.40	0.42	0.43	1.03	-0.17
35	45.72	0.625	0.019	0.020	2.09	1.43	1.81	-0.52	0.37	-0.47	-1.10	-0.33	-0.33	0.38	0.53	0.29	0.39	0.27	0.69	-0.14
36	50.80	0.645	0.020	0.006	1.03	0.86	0.94	-0.28	0.19	-0.20	-0.60	-0.23	-0.15	0.27	0.32	0.16	0.26	0.17	0.39	-0.10
37	55.88	0.657	0.024	-0.002	0.32	0.72	0.35	-0.08	0.04	-0.01	-0.09	-0.05	-0.02	0.06	0.10	0.05	0.03	0.04	0.09	-0.01
38	60.96	0.659	0.025	-0.004	0.16	0.53	0.26	-0.03	0.01	0.00	0.01	-0.01	0.09	0.02	0.02	0.01	0.01	0.01	0.01	-0.01
39	66.04	0.660	0.000	-0.003	0.11	0.00	0.23	0.00	0.00	0.01	0.03	0.00	0.08	0.00	0.00	0.00	0.00	0.00	0.00	0.00
41	71.12	0.660	0.000	-0.002	0.10	0.00	0.23	0.00	0.00	0.03	0.03	0.00	0.09	0.00	0.00	0.00	0.01	0.00	0.02	0.00

Table C.5 Continued.

Case C.S1 Station= 12
X= 228.6mm Tunnel Run#= 663 Ue/Uref= 0.645 Date= 507.88 Time=10.37
Bias Corrected data using 1/sqrt(U*U + V*V + W*W + (.01Ur)^2)

					<-- normalized by 0.001 Ur^2 -->						<---------- normalized by 0.0001 Ur^3 ---------->									
LR	Y(mm)	U/Ur	V/Ur	W/Ur	uu	vv	ww	uv	vw	uw	uuu	uvv	uww	vuu	vvv	vww	wuu	wvv	www	uvw
1	0.00	0.000	0.000	0.000	0.00	0.00	0.00	-0.28	-0.10	0.00	0.00	0.00	0.00	0.00	0.00	0.00	0.00	0.00	0.00	0.00
1	0.25	0.129	-0.002	0.037	3.51	0.26	2.51	-0.22	-0.17	0.28	1.28	0.03	0.67	-0.05	-0.01	-0.01	0.07	0.01	0.36	-0.03
2	0.38	0.151	-0.002	0.044	3.76	0.38	2.88	-0.31	-0.19	0.22	1.07	0.04	0.76	-0.05	-0.01	-0.02	0.01	0.01	0.29	-0.03
3	0.51	0.163	-0.001	0.047	3.91	0.48	3.05	-0.34	-0.20	0.12	1.07	0.05	0.61	-0.03	-0.01	0.02	-0.08	0.01	0.24	-0.03
4	0.63	0.170	-0.002	0.049	3.91	0.60	3.27	-0.38	-0.25	0.16	0.88	0.03	0.63	-0.01	-0.04	0.01	-0.02	0.02	0.31	-0.02
5	0.76	0.177	-0.002	0.053	3.98	0.69	3.30	-0.38	-0.22	0.15	0.97	0.04	0.58	-0.04	-0.04	0.03	-0.04	0.00	0.22	-0.02
6	1.02	0.189	-0.002	0.055	4.05	0.84	3.58	-0.42	-0.22	0.07	1.04	0.08	0.84	-0.02	-0.05	0.03	-0.03	0.00	0.34	-0.04
7	1.27	0.198	-0.002	0.059	4.27	1.03	3.50	-0.52	-0.22	0.13	0.93	0.10	0.75	-0.05	-0.02	0.05	0.04	0.01	0.42	-0.01
8	1.52	0.207	-0.003	0.061	4.15	1.16	3.56	-0.53	-0.20	-0.02	0.92	0.11	0.65	-0.11	-0.10	0.05	0.09	0.00	0.26	-0.01
9	1.78	0.210	-0.002	0.062	4.22	1.23	3.65	-0.61	-0.18	-0.02	0.89	0.13	0.73	-0.07	-0.07	0.07	-0.08	0.01	0.18	-0.02
10	2.03	0.215	-0.002	0.063	4.32	1.35	3.65	-0.66	-0.18	-0.10	0.78	0.15	0.75	-0.08	-0.07	0.07	-0.06	0.00	0.03	-0.03
11	2.29	0.214	0.000	0.063	4.13	1.45	3.47	-0.64	-0.18	-0.09	0.93	0.14	0.54	-0.10	-0.02	0.05	-0.03	-0.01	0.27	0.00
12	2.54	0.220	0.000	0.061	4.31	1.48	3.58	-0.65	-0.15	-0.13	0.85	0.16	0.60	-0.08	-0.09	0.07	-0.08	0.01	0.18	-0.01
13	2.79	0.224	0.000	0.064	4.34	1.52	3.65	-0.70	-0.11	-0.07	0.81	0.15	0.67	-0.11	-0.14	0.07	-0.12	-0.02	0.08	0.01
14	3.30	0.229	0.001	0.065	4.56	1.67	3.67	-0.75	-0.11	-0.06	0.90	0.20	0.49	-0.13	-0.18	0.03	0.05	0.00	0.25	-0.04
15	3.81	0.235	0.001	0.068	4.63	1.80	3.70	-0.88	-0.10	-0.12	0.79	0.23	0.48	-0.14	-0.21	0.05	0.00	-0.01	0.10	0.04
16	4.32	0.242	0.000	0.068	4.73	1.98	3.65	-0.99	-0.09	-0.20	0.72	0.25	0.44	-0.17	-0.24	0.07	-0.02	-0.02	-0.01	0.01
17	4.83	0.248	-0.001	0.071	4.97	2.04	3.88	-1.05	-0.01	-0.13	0.84	0.29	0.53	-0.20	-0.29	-0.01	-0.09	-0.03	0.24	0.05
18	5.59	0.254	-0.001	0.071	5.11	2.22	3.94	-1.08	-0.01	-0.20	0.94	0.29	0.50	-0.30	-0.16	-0.02	-0.11	-0.05	0.12	0.03
19	6.35	0.262	0.001	0.073	5.37	2.40	4.06	-1.29	0.05	-0.28	0.87	0.33	0.44	-0.28	-0.29	0.01	-0.02	-0.01	0.06	0.04
20	7.11	0.272	0.000	0.073	5.40	2.55	4.08	-1.34	0.07	-0.27	0.84	0.35	0.45	-0.23	-0.31	-0.03	-0.04	-0.02	-0.08	-0.03
21	8.38	0.281	-0.001	0.074	5.66	2.73	4.32	-1.37	0.11	-0.35	0.74	0.33	0.55	-0.26	-0.40	-0.04	-0.07	0.01	-0.04	0.02
22	10.16	0.299	0.000	0.076	6.09	3.07	4.58	-1.73	0.15	-0.38	0.73	0.37	0.45	-0.27	-0.34	-0.02	-0.15	-0.06	0.00	0.05
23	12.70	0.324	-0.001	0.078	6.28	3.35	4.87	-1.89	0.19	-0.43	0.81	0.33	0.50	-0.29	-0.18	-0.09	-0.05	-0.07	0.09	0.06
24	15.24	0.345	0.000	0.083	6.87	3.60	5.01	-2.10	0.41	-0.60	0.26	0.23	0.38	-0.11	-0.21	0.03	-0.04	-0.08	-0.04	0.08
25	17.78	0.370	0.000	0.085	6.85	3.73	5.41	-2.11	0.58	-0.72	0.30	0.11	0.33	-0.11	-0.08	0.06	-0.11	-0.07	-0.19	0.10
26	20.32	0.419	-0.009	0.087	6.53	3.78	5.32	-2.09	0.68	-0.83	-0.65	-0.20	-0.02	0.37	0.16	0.12	0.18	0.06	0.52	-0.01
27	22.86	0.423	-0.002	0.084	7.07	3.55	5.42	-2.19	0.81	-0.83	-0.97	-0.12	-0.07	0.27	0.16	0.13	0.23	0.10	0.30	-0.04
28	25.40	0.447	-0.003	0.081	6.75	3.52	5.27	-2.06	0.90	-0.91	-1.18	-0.35	-0.21	0.45	0.35	0.22	0.39	0.20	0.48	-0.08
29	27.94	0.473	-0.002	0.078	6.14	3.22	5.17	-1.73	0.84	-0.84	-1.06	-0.39	-0.24	0.49	0.42	0.26	0.42	0.25	0.62	-0.17
30	30.48	0.493	0.001	0.075	5.99	3.14	5.00	-1.86	0.93	-1.06	-1.44	-0.48	-0.44	0.64	0.51	0.37	0.55	0.31	0.77	-0.18
31	33.02	0.515	0.001	0.069	5.47	3.05	4.64	-1.62	0.95	-1.02	-1.99	-0.66	-0.54	0.75	0.80	0.39	0.61	0.49	1.11	-0.29
32	35.56	0.535	0.002	0.060	5.04	2.63	4.21	-1.48	0.78	-0.85	-1.91	-0.56	-0.52	0.69	0.59	0.52	0.59	0.36	1.22	-0.22
33	38.10	0.554	0.002	0.052	4.32	2.39	3.63	-1.19	0.73	-0.72	-1.67	-0.57	-0.62	0.65	0.67	0.55	0.53	0.40	1.24	-0.25
34	40.64	0.571	0.003	0.044	3.63	2.09	3.15	-1.00	0.62	-0.68	-1.67	-0.51	-0.42	0.61	0.65	0.41	0.55	0.36	1.08	-0.25
35	45.72	0.601	0.006	0.028	2.56	1.56	2.23	-0.66	0.45	-0.61	-1.33	-0.45	-0.51	0.50	0.51	0.37	0.49	0.34	0.81	-0.22
36	50.80	0.624	0.008	0.014	1.37	1.07	1.25	-0.35	0.22	-0.28	-0.66	-0.30	-0.15	0.28	0.40	0.20	0.22	0.20	0.47	-0.09
37	55.88	0.638	0.013	0.006	0.57	1.01	0.65	-0.12	0.09	-0.05	-0.18	-0.12	-0.01	0.10	0.27	0.10	0.09	0.12	0.23	-0.03
38	60.96	0.643	0.015	0.000	0.25	0.64	0.36	-0.03	0.03	-0.02	-0.01	-0.01	0.06	0.02	0.05	0.02	0.01	0.03	0.04	0.00
39	66.04	0.644	0.000	-0.001	0.15	0.00	0.28	0.00	0.00	0.02	0.03	0.00	0.09	0.00	0.00	0.00	0.02	0.00	0.06	0.00
40	71.12	0.644	0.000	-0.001	0.13	0.00	0.30	0.00	0.00	0.03	0.05	0.00	0.17	0.00	0.00	0.00	0.02	0.00	0.06	0.00

Table C.5 Continued.

Case C.S1 Station= 13
X= 304.8mm Tunnel Run#= 661 Ue/Uref= 0.628 Date= 506.88 Time=17.18
Bias Corrected data using 1/sqrt(U*U + V*V + W*W + (.01Ur)^2)

					<-- normalized by 0.001 Ur^2 -->						<---------- normalized by 0.0001 Ur^3 ---------->								
LR	Y(mm)	U/Ur	V/Ur	W/Ur	uu	vv	ww	uv	vw	uw	uuu	uvv	uww	vuu	vvv	vww	wuu	wvv	www	uvw
1	0.00	0.000	0.000	0.000	0.00	0.00	0.00	-0.28	-0.09	0.00	0.00	0.00	0.00	0.00	0.00	0.00	0.00	0.00	0.00	0.00
1	0.25	0.130	-0.001	0.032	3.32	0.22	2.26	-0.22	-0.14	0.34	1.24	0.03	0.55	-0.09	-0.01	-0.02	0.15	0.01	0.52	-0.04
2	0.38	0.152	-0.001	0.038	3.67	0.33	2.50	-0.27	-0.15	0.27	1.14	0.04	0.52	-0.06	0.02	0.00	0.10	0.02	0.36	-0.02
3	0.51	0.168	-0.001	0.042	3.90	0.45	2.89	-0.32	-0.20	0.22	1.07	0.05	0.62	-0.04	0.03	0.01	0.05	0.01	0.20	-0.04
4	0.63	0.177	-0.001	0.044	3.89	0.56	3.08	-0.32	-0.17	0.15	1.03	0.04	0.68	-0.05	0.05	0.02	-0.02	0.01	0.11	-0.02
5	0.76	0.185	-0.001	0.046	3.94	0.64	3.19	-0.35	-0.19	0.10	0.94	0.04	0.67	-0.04	-0.02	-0.01	-0.05	0.02	0.29	-0.03
6	1.02	0.196	-0.001	0.049	4.08	0.78	3.26	-0.38	-0.19	0.06	1.05	0.09	0.59	-0.06	0.04	0.04	0.00	0.02	0.47	-0.06
7	1.27	0.208	-0.002	0.052	4.11	0.96	3.50	-0.46	-0.19	0.06	0.76	0.06	0.56	-0.01	-0.02	0.07	0.02	0.01	0.18	-0.03
8	1.52	0.211	-0.002	0.053	4.15	1.03	3.30	-0.53	-0.15	-0.04	0.93	0.10	0.55	-0.06	-0.07	0.06	-0.16	0.01	0.07	-0.01
9	1.78	0.215	-0.003	0.054	3.97	1.17	3.31	-0.56	-0.15	0.00	0.88	0.11	0.52	-0.05	-0.12	0.03	0.03	0.00	0.24	-0.01
10	2.03	0.217	-0.002	0.054	4.15	1.30	3.43	-0.55	-0.14	-0.07	0.87	0.12	0.50	-0.12	0.04	0.05	-0.07	-0.01	0.14	-0.01
11	2.29	0.220	-0.002	0.054	4.23	1.32	3.36	-0.59	-0.16	0.07	0.93	0.15	0.65	-0.11	-0.05	0.04	0.12	-0.01	0.36	0.00
12	2.54	0.225	-0.003	0.056	4.36	1.41	3.45	-0.65	-0.14	-0.01	0.78	0.13	0.56	-0.11	-0.12	0.02	-0.05	0.02	0.24	0.00
13	2.79	0.228	-0.003	0.057	4.38	1.47	3.44	-0.65	-0.11	-0.02	0.89	0.16	0.61	-0.12	-0.17	0.01	-0.01	-0.01	0.07	-0.01
14	3.30	0.234	-0.003	0.058	4.40	1.66	3.52	-0.76	-0.09	-0.05	0.90	0.22	0.51	-0.17	-0.15	0.04	-0.04	0.03	0.10	-0.03
15	3.81	0.238	-0.003	0.060	4.64	1.73	3.44	-0.82	-0.07	-0.04	0.88	0.20	0.47	-0.15	-0.22	0.04	-0.04	0.03	0.09	-0.04
16	4.32	0.245	-0.004	0.061	4.62	1.86	3.59	-0.87	-0.07	-0.08	0.68	0.21	0.54	-0.13	-0.21	0.03	-0.08	0.01	0.10	0.02
17	4.83	0.251	-0.005	0.060	4.78	2.03	3.59	-1.01	-0.06	-0.15	0.85	0.26	0.52	-0.19	-0.27	0.02	-0.16	-0.04	-0.01	0.05
18	5.59	0.258	-0.005	0.062	4.90	2.26	3.66	-1.16	-0.05	-0.24	0.72	0.25	0.41	-0.24	-0.28	0.02	-0.18	0.00	-0.05	0.04
19	6.35	0.267	-0.005	0.062	5.06	2.31	3.79	-1.18	-0.02	-0.24	0.87	0.30	0.46	-0.32	-0.29	-0.01	-0.16	-0.04	-0.02	0.05
20	7.11	0.273	-0.005	0.064	5.03	2.50	3.77	-1.27	0.04	-0.26	0.77	0.29	0.41	-0.24	-0.34	-0.03	-0.08	-0.05	-0.10	0.02
21	8.38	0.284	-0.007	0.067	5.43	2.73	3.86	-1.41	0.05	-0.23	0.57	0.28	0.41	-0.16	-0.41	0.03	-0.07	-0.02	0.20	0.04
22	10.16	0.298	-0.006	0.070	5.76	3.04	4.24	-1.66	0.05	-0.24	0.57	0.26	0.40	-0.27	-0.30	-0.04	-0.18	-0.04	0.03	0.11
23	12.70	0.322	-0.007	0.072	5.83	3.17	4.40	-1.73	0.10	-0.36	0.38	0.21	0.38	-0.11	-0.24	-0.05	-0.14	0.02	-0.07	0.07
24	15.24	0.342	-0.007	0.074	6.37	3.34	4.76	-1.94	0.25	-0.53	0.37	0.19	0.38	-0.10	-0.22	-0.07	0.00	0.02	-0.03	0.03
25	17.78	0.357	-0.003	0.079	6.39	3.42	4.75	-2.08	0.40	-0.61	0.11	0.16	0.38	-0.02	-0.10	-0.14	0.06	-0.03	-0.12	0.02
26	20.32	0.385	-0.009	0.080	6.40	3.56	4.96	-2.03	0.46	-0.62	-0.35	-0.09	0.23	0.17	0.12	-0.02	-0.16	0.07	0.05	0.06
27	22.86	0.405	-0.008	0.080	6.38	3.58	4.90	-2.03	0.49	-0.65	-0.51	-0.27	0.07	0.29	0.33	0.04	-0.06	0.06	0.09	0.03
28	25.40	0.427	-0.009	0.079	6.20	3.39	4.97	-1.98	0.66	-0.83	-0.92	-0.25	-0.02	0.36	0.27	0.07	0.12	0.15	-0.07	-0.04
29	27.94	0.446	-0.008	0.078	5.95	3.34	4.98	-1.91	0.69	-0.90	-1.04	-0.30	-0.19	0.38	0.33	0.14	0.27	0.11	0.35	-0.08
30	30.48	0.466	-0.009	0.075	5.87	3.18	4.79	-1.77	0.75	-0.93	-1.26	-0.38	-0.25	0.51	0.53	0.37	0.36	0.24	0.44	-0.11
31	33.02	0.484	-0.007	0.070	5.56	3.13	4.46	-1.74	0.82	-0.89	-1.29	-0.43	-0.39	0.57	0.54	0.28	0.49	0.25	0.69	-0.21
32	35.56	0.504	-0.006	0.065	4.96	2.81	4.21	-1.53	0.76	-0.89	-1.43	-0.49	-0.41	0.53	0.64	0.36	0.42	0.32	1.05	-0.15
33	38.10	0.519	-0.007	0.058	4.50	2.57	3.95	-1.32	0.72	-0.83	-1.37	-0.50	-0.40	0.53	0.59	0.47	0.45	0.37	0.81	-0.22
34	40.64	0.534	-0.005	0.052	4.14	2.47	3.61	-1.29	0.67	-0.69	-1.62	-0.63	-0.49	0.69	0.82	0.43	0.49	0.38	0.98	-0.22
35	45.72	0.566	-0.004	0.038	3.31	2.00	2.76	-1.02	0.57	-0.63	-1.63	-0.59	-0.45	0.72	0.66	0.44	0.52	0.36	0.89	-0.26
36	50.80	0.591	-0.003	0.023	2.11	1.41	1.89	-0.64	0.37	-0.49	-1.19	-0.42	-0.34	0.49	0.53	0.33	0.44	0.29	0.86	-0.18
37	55.88	0.609	-0.001	0.013	1.14	1.69	1.13	-0.41	0.26	-0.20	-0.70	-0.41	-0.17	0.38	1.34	0.25	0.30	0.25	0.55	-0.11
38	60.96	0.620	-0.002	0.004	0.45	0.92	0.55	-0.10	0.08	-0.02	-0.12	-0.06	0.01	0.08	0.73	0.08	0.09	0.07	0.23	-0.03
39	66.04	0.624	-0.002	0.002	0.22	0.62	0.36	-0.04	0.04	0.03	0.01	-0.02	0.07	0.03	0.07	0.04	0.05	0.02	0.14	-0.01
40	71.12	0.624	0.000	-0.001	0.12	0.00	0.23	0.00	0.00	-0.01	0.02	0.00	0.06	0.00	0.00	0.00	-0.01	0.00	-0.02	0.00

Table C.5 Continued.

Case D.S1 Station= 1
X=-457.2mm Tunnel Run#= 796 Ue/Uref= 1.000 Date= 718.88 Time=16.21
Bias Corrected data using 1/sqrt(U*U + V*V + W*W + (.01Ur)^2)

					<-- normalized by 0.001 Ur^2 -->						<---------- normalized by 0.0001 Ur^3 ---------->							
LR	Y(mm)	U/Ur	V/Ur	W/Ur	uu	vv	ww	uv	vw	uw	uuu	uvv	uww	vuu	vvv	vww	wuu	wvv	www	uvw
1	0.00	0.000	0.000	1.000	0.00	0.00	0.00	-2.50	2.72	0.00	0.00	0.00	0.00	0.00	0.00	0.00	0.00	0.00	0.00	0.00
1	0.25	0.545	0.006	0.375	15.93	3.96	19.86	-2.18	2.40	-8.29	-2.41	-0.57	-4.83	1.68	3.96	2.18	4.43	0.58	3.90	-1.59
2	0.38	0.580	0.005	0.336	14.37	4.01	17.45	-2.34	2.35	-6.08	-0.94	-0.65	-2.47	1.43	1.29	1.98	1.93	0.67	1.48	-1.13
3	0.51	0.599	0.007	0.312	13.53	4.51	16.69	-2.41	2.55	-5.54	-1.05	-0.55	-1.35	1.32	1.64	2.12	1.26	0.67	0.50	-1.07
4	0.63	0.617	0.007	0.288	12.94	4.42	16.68	-2.23	1.86	-5.24	-0.18	-0.62	0.57	1.04	1.66	1.41	-0.21	0.46	-2.01	-0.53
5	0.76	0.626	0.007	0.276	12.28	4.53	15.55	-2.17	2.05	-4.87	-0.35	-0.54	0.97	1.19	1.57	1.75	-0.12	0.46	-2.52	-0.47
6	1.02	0.646	0.008	0.257	11.26	4.68	13.85	-2.12	2.26	-4.26	-0.03	-0.43	0.20	0.89	1.65	1.13	0.47	0.55	-0.54	-0.62
8	1.27	0.664	0.008	0.243	11.00	4.49	13.21	-2.23	2.30	-4.12	-0.20	-0.58	0.04	0.78	1.18	1.00	0.30	0.67	1.04	-0.26
9	1.52	0.674	0.010	0.230	10.02	4.63	12.83	-2.18	2.43	-4.03	-0.41	-0.48	-0.11	0.79	1.13	1.05	0.54	0.53	0.00	-0.50
10	1.78	0.689	0.010	0.218	10.03	4.57	12.60	-2.12	2.27	-4.11	0.13	-0.33	0.11	0.56	1.23	1.10	-0.09	0.51	0.29	-0.32
11	2.03	0.697	0.010	0.208	9.58	4.78	12.02	-2.25	2.35	-3.77	0.71	-0.39	-0.03	0.51	0.92	1.23	-0.01	0.51	0.93	-0.29
12	2.29	0.708	0.011	0.200	9.60	4.79	11.78	-2.21	2.24	-3.64	-0.48	-0.33	0.21	0.53	1.12	0.95	-0.10	0.43	0.03	-0.31
15	2.54	0.716	0.010	0.191	9.54	4.82	11.06	-2.34	2.27	-3.72	-0.98	-0.34	-0.37	0.73	1.00	0.75	0.52	0.39	0.68	-0.31
16	2.79	0.724	0.010	0.185	8.89	4.76	10.66	-2.26	2.37	-3.50	-0.43	-0.21	0.03	0.41	0.74	0.77	0.26	0.37	0.26	-0.34
17	3.30	0.737	0.012	0.174	8.69	4.72	10.22	-2.28	2.27	-3.30	-0.25	-0.19	0.09	0.18	0.82	0.69	0.04	0.20	0.62	-0.18
18	3.81	0.751	0.012	0.160	8.58	4.76	9.95	-2.32	2.28	-3.21	-0.34	-0.39	-0.05	0.39	0.76	0.78	-0.02	0.35	0.40	-0.34
16	4.32	0.771	0.010	0.147	8.21	4.59	9.08	-2.27	2.19	-2.72	-1.06	-0.37	-0.35	0.55	0.67	0.77	0.57	0.40	1.04	-0.37
17	4.83	0.782	0.013	0.139	8.14	4.59	8.52	-2.37	2.04	-2.66	-1.05	-0.34	-0.34	0.36	0.63	0.65	0.48	0.35	0.97	-0.30
18	5.59	0.802	0.013	0.126	7.47	4.48	8.30	-2.17	1.96	-2.23	-1.20	-0.39	-0.56	0.47	0.97	0.82	0.27	0.49	1.46	-0.27
19	6.35	0.822	0.012	0.114	7.42	4.29	7.81	-2.18	1.96	-2.15	-1.69	-0.46	-0.78	0.53	0.89	0.67	0.69	0.51	1.51	-0.30
20	7.11	0.840	0.014	0.101	7.06	4.22	7.13	-2.23	1.83	-2.02	-1.73	-0.67	-0.94	0.74	1.28	0.82	0.66	0.74	1.73	-0.49
21	8.38	0.877	0.009	0.078	6.22	3.65	6.12	-1.99	1.44	-1.87	-2.43	-0.78	-1.06	0.96	1.39	0.96	1.02	0.70	1.98	-0.47
22	10.16	0.922	0.008	0.052	4.81	2.76	4.35	-1.56	1.12	-1.46	-2.75	-0.89	-1.09	1.04	1.19	0.84	1.00	0.71	2.27	-0.46
23	12.70	0.971	0.004	0.023	2.14	1.56	2.02	-0.75	0.56	-0.61	-1.73	-0.60	-0.72	0.75	0.79	0.63	0.70	0.48	1.39	-0.33
24	15.24	0.993	0.001	0.010	0.51	0.58	0.67	-0.14	0.11	-0.04	-0.22	-0.14	-0.05	0.15	0.23	0.15	0.15	0.09	0.39	-0.06
25	17.78	0.999	0.000	0.006	0.15	0.27	0.28	-0.01	0.01	0.02	0.02	-0.01	0.05	0.01	0.21	0.01	0.03	0.00	0.09	0.00
26	20.32	0.997	0.000	0.004	0.09	0.19	0.19	0.00	0.00	0.01	0.01	0.00	0.03	0.00	0.21	0.00	0.02	0.00	0.05	0.00
27	22.86	0.999	-0.001	0.003	0.09	0.13	0.21	0.00	0.00	0.01	0.02	0.00	0.04	0.00	0.09	0.00	0.02	0.00	0.07	0.00
28	25.40	1.000	-0.001	0.003	0.10	0.13	0.25	0.00	0.00	0.03	0.02	0.01	0.07	0.00	0.05	0.00	0.04	0.01	0.11	0.00
29	27.94	0.998	-0.001	0.004	0.09	0.11	0.22	0.00	0.00	0.02	0.02	0.00	0.05	0.00	0.03	0.00	0.03	0.00	0.09	0.00
30	30.48	0.999	-0.003	0.005	0.10	0.14	0.28	0.00	-0.01	0.04	0.03	0.00	0.08	0.00	0.19	0.00	0.04	-0.01	0.13	0.00
31	33.02	0.998	-0.004	0.006	0.10	0.10	0.28	0.00	0.00	0.05	0.03	0.00	0.08	0.00	0.00	0.00	0.05	0.00	0.15	0.00
32	35.56	1.000	-0.005	0.007	0.11	0.10	0.32	0.00	0.00	0.06	0.03	0.00	0.10	0.00	0.01	0.00	0.05	0.00	0.16	0.00
33	38.10	1.001	-0.005	0.005	0.10	0.10	0.26	0.00	0.00	0.02	0.02	0.00	0.06	0.00	0.01	0.00	0.03	0.00	0.10	0.00
34	40.64	1.001	-0.005	0.002	0.10	0.10	0.27	0.00	0.00	-0.01	0.02	0.00	0.07	0.00	0.00	0.00	0.02	0.00	0.05	0.00
35	45.72	0.998	-0.003	0.003	0.08	0.12	0.23	0.00	0.00	0.00	0.02	0.00	0.05	0.00	0.08	0.00	0.02	0.00	0.07	0.00
36	50.80	1.000	0.001	0.002	0.09	0.09	0.25	0.00	0.00	0.01	0.02	0.00	0.06	0.00	0.00	0.00	0.03	0.00	0.08	0.00
37	55.88	0.996	0.001	0.000	0.09	0.10	0.24	0.00	0.00	0.00	0.02	0.00	0.05	0.00	0.00	0.00	0.02	0.00	0.07	0.00
38	60.96	0.996	0.018	-0.001	0.11	0.00	0.28	0.00	0.00	0.01	0.02	0.00	0.06	0.00	0.00	0.00	0.02	0.00	0.07	0.00
39	66.04	0.999	0.018	-0.001	0.11	0.00	0.35	0.00	0.00	0.04	0.03	0.00	0.09	0.00	0.00	0.00	0.04	0.00	0.12	0.00

Table C.5 Continued.

Case D.S1 Station= 2
X=-152.4mm Tunnel Run#= 790 Ue/Uref= 1.006 Date= 621.88 Time=12.54
Bias Corrected data using 1/sqrt(U*U + V*V + W*W + (.01Ur)^2)

					<-- normalized by 0.001 Ur^2 -->						<---------- normalized by 0.0001 Ur^3 ---------->									
LR	Y(mm)	U/Ur	V/Ur	W/Ur	uu	vv	ww	uv	vw	uw	uuu	uvv	uww	vuu	vvv	vww	wuu	wvv	www	uvw
1	0.00	0.000	0.000	1.000	0.00	0.00	0.00	-2.56	2.79	0.00	0.00	0.00	0.00	0.00	0.00	0.00	0.00	0.00	0.00	0.00
1	0.25	0.568	-0.002	0.373	16.56	3.05	19.77	-2.17	2.15	-7.86	-3.10	-0.62	-6.57	1.87	0.23	2.50	5.90	0.36	3.80	-1.73
2	0.38	0.607	-0.003	0.337	14.68	3.59	17.12	-2.12	2.18	-5.56	-2.11	-0.51	-3.87	1.21	0.42	2.31	3.12	0.65	3.59	-0.98
3	0.51	0.628	-0.003	0.313	14.05	4.07	15.54	-2.25	2.21	-4.65	-2.24	-0.68	-2.62	1.37	0.74	1.84	2.29	0.64	2.38	-0.98
4	0.63	0.644	-0.002	0.300	13.34	4.09	15.18	-2.19	2.38	-4.54	-1.36	-0.71	-2.24	1.16	0.67	1.65	1.59	0.65	2.05	-0.67
5	0.76	0.664	-0.004	0.280	12.91	3.98	14.30	-2.10	2.16	-4.03	-1.22	-0.52	-1.58	1.05	0.73	1.28	1.54	0.70	1.43	-0.56
6	1.02	0.687	-0.001	0.259	12.07	4.19	12.99	-2.37	2.32	-3.99	-1.93	-0.83	-1.76	1.44	0.92	1.56	1.49	0.71	2.54	-0.62
7	1.27	0.703	-0.002	0.238	11.79	4.15	12.69	-2.24	2.47	-4.16	-2.25	-0.71	-1.69	1.33	1.08	1.86	1.85	1.00	2.42	-0.82
8	1.52	0.721	-0.003	0.219	11.51	4.19	12.27	-2.32	2.37	-4.05	-2.53	-0.92	-2.39	1.35	1.05	1.71	1.90	1.04	3.28	-0.92
9	1.78	0.732	-0.003	0.205	10.86	4.10	11.90	-2.22	2.34	-4.02	-2.74	-0.94	-2.02	1.42	1.00	1.54	2.12	1.00	2.61	-0.86
10	2.03	0.742	-0.002	0.196	10.56	4.24	11.48	-2.39	2.24	-3.74	-2.20	-0.91	-1.97	1.51	0.81	1.75	1.62	0.85	3.20	-0.72
11	2.29	0.751	-0.002	0.188	10.42	4.29	11.06	-2.29	2.46	-3.68	-2.70	-0.91	-1.97	1.29	0.92	1.68	1.79	1.02	3.01	-0.88
12	2.54	0.766	-0.003	0.179	10.46	4.36	10.97	-2.40	2.42	-3.91	-3.05	-0.96	-2.14	1.49	0.95	1.96	1.97	1.10	3.66	-0.88
13	2.79	0.770	-0.003	0.172	9.81	4.40	10.64	-2.25	2.29	-3.50	-2.26	-0.87	-1.75	1.26	0.87	1.79	1.69	1.14	3.16	-0.85
14	3.30	0.778	-0.001	0.164	9.35	4.38	9.81	-2.31	2.27	-3.38	-1.91	-0.93	-1.59	1.23	1.03	1.78	1.66	1.23	2.87	-0.94
15	3.81	0.791	-0.005	0.153	8.88	4.38	9.34	-2.23	2.33	-3.10	-2.02	-0.80	-1.59	1.05	0.96	1.58	1.37	1.13	2.83	-0.84
16	4.32	0.796	-0.002	0.145	8.51	4.53	9.05	-2.36	2.32	-3.00	-1.78	-0.88	-1.49	1.04	1.11	1.60	1.37	1.11	3.36	-0.90
17	4.83	0.807	-0.002	0.140	8.46	4.55	8.98	-2.34	2.30	-3.05	-2.16	-0.77	-1.31	1.03	0.98	1.48	1.54	1.06	2.57	-0.79
18	5.59	0.815	-0.003	0.133	8.02	4.51	8.44	-2.30	2.24	-2.82	-2.11	-0.88	-1.04	1.18	1.23	1.30	1.32	1.02	2.25	-0.71
19	6.35	0.826	-0.003	0.125	7.62	4.34	7.80	-2.19	2.13	-2.45	-1.75	-0.76	-1.11	0.87	1.07	1.07	1.02	0.88	2.18	-0.61
20	7.11	0.830	0.002	0.123	7.47	4.39	7.86	-2.21	2.17	-2.39	-1.65	-0.64	-0.61	0.69	1.03	1.03	0.76	0.80	1.72	-0.51
21	8.38	0.846	0.003	0.114	7.03	4.30	7.64	-2.22	2.18	-2.13	-1.55	-0.78	-0.86	0.72	1.08	0.94	0.84	0.81	1.71	-0.60
22	10.16	0.868	0.003	0.099	6.39	3.91	6.69	-1.98	1.92	-1.75	-2.01	-0.77	-0.74	0.94	1.08	0.96	0.81	0.87	1.66	-0.53
23	12.70	0.896	0.005	0.078	5.83	3.39	5.50	-1.91	1.49	-1.64	-2.38	-0.89	-0.81	1.05	1.10	0.85	0.75	0.69	1.90	-0.44
24	15.24	0.931	0.007	0.058	4.53	2.71	4.33	-1.40	1.21	-1.33	-2.54	-0.78	-1.01	0.91	1.09	0.94	0.96	0.77	1.88	-0.49
25	17.78	0.959	0.008	0.039	3.31	2.13	3.08	-1.14	0.82	-1.02	-2.25	-0.83	-0.93	0.98	1.01	0.71	0.87	0.62	1.75	-0.44
26	20.32	0.987	0.007	0.021	1.75	1.33	1.72	-0.54	0.42	-0.46	-1.29	-0.47	-0.53	0.52	0.64	0.47	0.46	0.39	1.10	-0.23
27	22.86	0.997	0.007	0.012	0.80	0.76	0.85	-0.24	0.19	-0.17	-0.52	-0.22	-0.19	0.25	0.33	0.20	0.24	0.18	0.51	-0.10
28	25.40	1.004	0.007	0.007	0.35	0.51	0.43	-0.11	0.08	-0.03	-0.14	-0.12	-0.02	0.12	0.27	0.08	0.07	0.07	0.15	-0.03
29	27.94	1.008	0.007	0.005	0.17	0.25	0.26	-0.03	0.02	0.00	-0.03	-0.02	0.01	0.03	0.08	0.03	0.02	0.01	0.07	0.00
30	30.48	1.012	0.008	0.006	0.10	0.18	0.18	0.00	0.01	-0.01	0.01	0.00	0.01	0.01	0.11	0.01	0.01	0.01	0.03	0.00
31	33.02	1.010	0.007	0.007	0.09	0.11	0.18	0.00	0.00	0.01	0.01	0.00	0.03	0.00	0.00	0.00	0.02	0.00	0.05	0.00
32	35.56	1.007	0.007	0.008	0.08	0.10	0.16	0.00	0.00	0.01	0.01	0.00	0.02	0.00	0.03	0.00	0.01	0.00	0.04	0.00
33	38.10	1.008	0.006	0.008	0.09	0.09	0.18	0.00	0.00	0.02	0.01	0.00	0.03	0.00	0.00	0.00	0.02	0.00	0.05	0.00
34	40.64	1.010	0.006	0.006	0.09	0.09	0.19	0.00	0.00	0.03	0.01	0.00	0.04	0.00	0.00	0.00	0.02	0.00	0.07	0.00
35	45.72	1.013	0.004	0.005	0.08	0.09	0.20	0.00	0.00	0.02	0.01	0.00	0.04	0.00	0.00	0.00	0.02	0.00	0.07	0.00
36	50.80	1.015	0.012	0.004	0.09	0.45	0.19	0.00	0.00	0.01	0.01	0.00	0.03	0.00	0.06	0.00	0.02	0.00	0.05	0.00
37	55.88	1.016	0.011	-0.002	0.09	0.46	0.23	0.00	0.00	0.00	0.02	0.00	0.05	0.00	-0.01	0.00	0.01	0.00	0.02	0.00
38	60.96	1.022	0.000	-0.005	0.09	0.00	0.25	0.00	0.00	0.03	0.01	0.00	0.04	0.00	0.00	0.00	0.02	0.00	0.07	0.00
39	66.04	1.015	0.000	-0.008	0.17	0.00	0.47	0.00	0.00	0.11	0.00	0.00	0.00	0.00	0.00	0.00	0.00	0.00	0.00	0.00

Table C.5 Continued.

Case D.S1 Station= 3
X= -76.2mm Tunnel Run#= 788 Ue/Uref= 0.995 Date= 621.88 Time=11.22
Bias Corrected data using 1/sqrt(U*U + V*V + W*W + (.01Ur)^2)

					<-- normalized by 0.001 Ur^2 -->						<---------- normalized by 0.0001 Ur^3 ---------->									
LR	Y(mm)	U/Ur	V/Ur	W/Ur	uu	vv	ww	uv	vw	uw	uuu	uvv	uww	vuu	vvv	vww	wuu	wvv	www	uvw
1	0.00	0.000	0.000	1.000	0.00	0.00	0.00	-2.57	2.80	0.00	0.00	0.00	0.00	0.00	0.00	0.00	0.00	0.00	0.00	0.00
1	0.25	0.534	0.002	0.383	16.87	2.85	22.46	-1.99	1.95	-9.20	-2.44	-0.50	-6.04	1.43	0.52	2.38	5.11	0.54	3.05	-1.33
2	0.38	0.572	-0.001	0.346	15.58	3.49	18.60	-2.18	2.12	-6.19	-1.64	-0.57	-4.09	1.16	0.45	1.98	3.32	0.60	2.41	-1.07
3	0.51	0.598	0.000	0.320	14.58	3.90	17.03	-2.30	2.28	-5.20	-1.48	-0.55	-2.33	1.16	0.68	1.80	2.27	0.67	0.93	-1.07
4	0.63	0.622	-0.001	0.300	13.55	4.12	15.56	-2.19	2.22	-4.78	-1.11	-0.67	-1.87	1.38	0.68	1.63	2.03	0.63	0.59	-0.84
5	0.76	0.636	0.000	0.281	13.17	4.06	15.46	-2.16	2.23	-4.51	-1.19	-0.70	-1.17	1.18	0.74	1.78	1.22	0.58	1.59	-0.61
6	1.02	0.663	0.000	0.257	12.77	4.25	14.59	-2.19	2.35	-3.99	-2.18	-0.69	-1.59	1.06	0.98	1.74	1.35	0.76	1.14	-0.61
7	1.27	0.678	0.001	0.238	12.15	4.21	13.70	-2.33	2.28	-4.05	-2.08	-0.77	-1.35	1.36	0.93	1.60	1.36	0.71	1.37	-0.65
8	1.52	0.697	0.002	0.221	11.64	4.29	12.88	-2.24	2.50	-4.10	-1.72	-0.83	-2.14	1.30	0.89	2.06	2.00	0.97	3.01	-0.86
9	1.78	0.710	-0.001	0.208	11.32	4.21	12.34	-2.26	2.31	-3.96	-2.43	-0.78	-2.01	1.31	1.02	1.84	1.90	0.91	2.68	-0.67
10	2.03	0.720	0.001	0.198	11.10	4.14	11.79	-2.26	2.28	-4.02	-1.62	-0.68	-1.61	0.93	0.86	1.72	1.55	0.89	2.36	-0.68
11	2.29	0.730	0.001	0.187	10.84	4.05	11.62	-2.29	2.43	-3.89	-2.75	-0.76	-2.15	1.50	0.88	1.75	2.18	1.06	2.84	-0.92
12	2.54	0.737	0.002	0.179	10.73	4.19	11.08	-2.42	2.37	-3.99	-3.04	-0.90	-1.81	1.39	1.04	1.75	2.06	0.93	2.86	-0.83
13	2.79	0.746	0.001	0.174	10.12	4.20	10.70	-2.28	2.32	-3.75	-2.27	-0.96	-1.47	1.23	0.83	1.66	1.61	1.00	2.63	-0.90
14	3.30	0.757	0.003	0.161	9.80	4.40	10.40	-2.45	2.24	-3.63	-2.56	-1.08	-1.77	1.37	1.12	1.88	1.84	1.12	2.55	-1.06
15	3.81	0.765	0.004	0.156	9.34	4.37	10.22	-2.29	2.37	-3.49	-2.29	-0.86	-1.44	1.27	0.99	1.78	1.62	1.19	2.52	-0.91
16	4.32	0.772	0.004	0.149	9.32	4.59	9.78	-2.41	2.28	-3.26	-2.16	-0.92	-1.37	1.29	0.98	1.68	1.69	1.15	2.03	-0.88
17	4.83	0.776	0.005	0.144	8.88	4.52	9.53	-2.46	2.33	-3.35	-1.86	-0.86	-1.30	1.03	1.01	1.60	1.47	0.97	2.19	-0.82
18	5.59	0.790	0.004	0.135	8.39	4.54	9.06	-2.29	2.28	-2.92	-1.36	-0.70	-0.99	0.85	0.93	1.48	0.91	0.99	1.99	-0.69
19	6.35	0.799	0.006	0.131	7.92	4.58	8.66	-2.29	2.25	-2.69	-1.74	-0.84	-0.75	0.91	1.10	1.32	0.89	0.97	1.93	-0.61
20	7.11	0.807	0.006	0.125	7.94	4.65	8.29	-2.33	2.23	-2.50	-1.99	-0.75	-0.81	0.88	1.07	1.30	1.19	1.02	2.30	-0.61
21	8.38	0.816	0.011	0.119	7.29	4.50	7.93	-2.32	2.17	-2.37	-1.63	-0.79	-0.64	0.82	1.20	1.10	0.90	0.89	2.04	-0.47
22	10.16	0.840	0.012	0.106	6.94	4.24	7.31	-2.16	2.07	-2.00	-1.61	-0.53	-0.76	0.68	0.96	0.97	0.76	0.82	1.70	-0.45
23	12.70	0.865	0.016	0.091	6.51	3.93	6.65	-2.09	1.93	-1.84	-2.09	-0.82	-0.80	0.95	1.02	1.01	0.72	0.81	1.64	-0.51
24	15.24	0.898	0.018	0.069	5.50	3.18	5.31	-1.72	1.50	-1.58	-2.48	-0.86	-0.95	1.03	1.13	1.07	0.98	0.90	1.80	-0.58
25	17.78	0.923	0.021	0.052	4.46	2.69	4.30	-1.43	1.17	-1.33	-2.59	-0.91	-0.95	1.11	1.13	0.98	1.04	0.75	2.05	-0.53
26	20.32	0.947	0.024	0.036	3.36	2.11	3.13	-1.02	0.83	-1.04	-2.23	-0.78	-0.93	0.90	1.06	0.69	0.91	0.63	1.70	-0.44
27	22.86	0.971	0.026	0.022	1.99	1.47	2.05	-0.63	0.58	-0.61	-1.46	-0.56	-0.68	0.62	0.75	0.60	0.64	0.51	1.32	-0.30
28	25.40	0.988	0.027	0.011	0.95	0.92	1.10	-0.31	0.29	-0.25	-0.62	-0.27	-0.28	0.31	0.45	0.32	0.30	0.27	0.68	-0.15
29	27.94	0.993	0.029	0.005	0.53	0.60	0.59	-0.17	0.14	-0.12	-0.31	-0.15	-0.14	0.17	0.34	0.18	0.15	0.16	0.28	-0.09
30	30.48	0.998	0.030	0.003	0.23	0.33	0.31	-0.06	0.03	-0.03	-0.06	-0.07	0.00	0.07	0.16	0.05	0.02	0.03	0.07	-0.02
31	33.02	1.000	0.031	0.003	0.13	0.19	0.24	-0.01	0.01	0.01	0.00	0.00	0.04	0.02	0.06	0.02	0.03	0.02	0.08	0.00
32	35.56	1.002	0.032	0.003	0.09	0.12	0.19	0.00	0.00	0.00	0.01	0.00	0.03	0.00	0.01	0.00	0.01	0.00	0.04	0.00
33	38.10	1.004	0.033	0.004	0.08	0.11	0.18	0.00	0.00	0.00	0.01	0.00	0.03	0.00	0.01	0.00	0.02	0.00	0.05	0.00
34	40.64	1.005	0.033	0.004	0.06	0.08	0.16	0.00	0.00	0.01	0.01	0.00	0.02	0.00	0.00	0.00	0.01	0.00	0.04	0.00
35	45.72	1.012	0.035	0.001	0.07	0.08	0.18	0.00	0.00	0.01	0.01	0.00	0.03	0.00	0.00	0.00	0.02	0.00	0.05	0.00
36	50.80	1.018	0.045	0.003	0.07	0.37	0.19	0.00	0.00	0.01	0.01	0.00	0.03	0.00	0.00	0.00	0.02	0.00	0.06	0.00
37	55.88	1.016	0.049	0.007	0.09	0.43	0.25	0.00	0.00	0.02	0.02	0.00	0.06	0.00	0.00	0.00	0.03	0.00	0.08	0.00
38	60.96	1.028	0.064	0.005	0.07	0.23	0.19	0.02	-0.02	0.07	0.01	-0.01	0.04	0.00	-0.07	-0.01	0.03	0.01	0.08	0.00
39	66.04	1.037	0.000	0.012	0.19	0.00	0.56	0.00	0.00	-0.32	-0.03	0.00	-0.10	0.00	0.00	0.00	0.06	0.00	0.17	0.00

Table C.5 Continued.

Case D.S1 Station= 4
X= -12.7mm Tunnel Run#= 786 Ue/Uref= 0.936 Date= 621.88 Time= 9.42
Bias Corrected data using 1/sqrt(U*U + V*V + W*W + (.01Ur)^2)

					<-- normalized by 0.001 Ur^2 -->						<---------- normalized by 0.0001 Ur^3 ---------->								
LR	Y(mm)	U/Ur	V/Ur	W/Ur	uu	vv	ww	uv	vw	uw	uuu	uvv	uww	vuu	vvv	vww	wuu	wvv	www	uvw
1	0.00	0.000	0.000	1.000	0.00	0.00	0.00	-2.39	2.73	0.00	0.00	0.00	0.00	0.00	0.00	0.00	0.00	0.00	0.00	0.00
1	0.25	0.473	-0.004	0.378	15.51	2.52	22.13	-1.81	1.87	-8.85	-0.11	-0.22	-4.50	1.00	-0.07	2.38	3.18	0.22	2.64	-1.09
2	0.38	0.512	-0.005	0.340	14.13	3.33	19.18	-1.82	2.12	-5.90	0.48	-0.35	-2.64	0.95	0.24	1.69	2.20	0.56	0.87	-0.98
3	0.51	0.533	-0.004	0.310	13.36	3.67	16.74	-1.86	2.03	-4.97	0.40	-0.42	-1.53	0.72	0.60	1.86	1.59	0.66	0.76	-0.68
4	0.63	0.549	-0.004	0.295	13.07	3.78	15.96	-1.93	1.95	-4.49	-0.37	-0.27	-0.48	0.71	0.42	1.48	1.10	0.35	0.48	-0.28
5	0.76	0.561	-0.003	0.284	13.08	4.10	15.03	-2.16	2.38	-4.59	-0.58	-0.46	-1.26	0.83	0.72	1.62	1.64	0.81	0.79	-0.62
6	1.02	0.586	-0.003	0.255	12.58	4.14	14.55	-2.28	2.18	-4.42	-0.94	-0.64	-0.96	1.03	1.04	1.46	1.50	0.79	0.82	-0.47
7	1.27	0.608	-0.003	0.236	12.14	4.05	14.00	-2.02	2.06	-4.21	-0.69	-0.45	-1.11	0.87	0.83	1.44	1.31	0.73	1.32	-0.49
8	1.52	0.618	-0.001	0.223	12.06	4.14	13.65	-2.12	2.33	-4.41	-1.65	-0.48	-1.24	0.90	0.72	1.84	1.43	0.78	1.28	-0.71
9	1.78	0.631	0.000	0.211	11.91	4.32	13.32	-2.36	2.40	-4.49	-1.12	-0.73	-1.03	1.24	0.92	1.84	1.50	0.93	1.48	-0.89
10	2.03	0.644	-0.001	0.197	11.35	4.06	12.82	-2.11	2.21	-4.30	-1.72	-0.71	-1.09	1.25	0.83	1.67	1.35	0.81	0.61	-0.69
11	2.29	0.653	0.000	0.187	11.15	4.10	12.30	-2.14	2.30	-4.24	-1.33	-0.75	-1.39	1.18	0.90	1.81	1.73	1.07	1.98	-0.97
12	2.54	0.663	0.002	0.181	10.36	4.30	12.24	-2.20	2.36	-4.09	-1.34	-0.68	-1.20	0.86	1.18	1.86	1.32	0.94	2.03	-0.77
13	2.79	0.670	0.002	0.173	10.68	4.29	11.53	-2.33	2.30	-3.95	-2.13	-0.80	-1.34	1.21	1.06	1.67	1.74	1.08	2.01	-0.81
14	3.30	0.678	0.004	0.164	9.94	4.34	11.23	-2.24	2.56	-4.02	-1.49	-0.72	-1.02	1.11	0.75	1.98	1.24	1.13	2.24	-0.88
15	3.81	0.684	0.006	0.160	9.57	4.46	10.71	-2.28	2.58	-3.65	-1.61	-0.74	-1.22	1.12	0.81	1.62	1.25	1.04	2.69	-0.76
16	4.32	0.694	0.006	0.153	9.40	4.59	10.36	-2.31	2.44	-3.55	-1.91	-0.83	-1.18	1.27	1.00	1.46	1.42	1.09	2.50	-0.73
17	4.83	0.700	0.008	0.147	8.96	4.61	10.10	-2.18	2.32	-3.43	-1.42	-0.61	-0.82	0.93	0.84	1.45	1.16	1.00	1.88	-0.69
18	5.59	0.709	0.009	0.143	8.72	4.75	9.49	-2.15	2.46	-3.18	-1.27	-0.63	-0.77	0.70	1.04	1.33	0.69	0.98	1.33	-0.63
19	6.35	0.716	0.012	0.139	8.41	4.87	9.46	-2.29	2.48	-3.02	-1.20	-0.71	-0.43	0.84	1.20	1.23	0.90	1.08	1.80	-0.60
20	7.11	0.723	0.013	0.133	8.26	4.70	9.04	-2.22	2.35	-2.75	-1.30	-0.66	-0.46	0.86	0.87	1.14	0.96	0.84	1.68	-0.50
21	8.38	0.735	0.015	0.127	7.83	4.87	8.73	-2.21	2.38	-2.68	-0.85	-0.57	-0.22	0.42	0.95	1.11	0.43	0.83	1.17	-0.55
22	10.16	0.754	0.018	0.114	7.55	4.64	8.21	-2.07	2.18	-2.17	-1.09	-0.52	-0.01	0.51	0.93	0.82	0.32	0.67	1.12	-0.27
23	12.70	0.778	0.025	0.102	7.22	4.29	7.49	-2.08	1.99	-1.80	-1.10	-0.64	-0.20	0.49	1.05	0.63	0.32	0.61	0.95	-0.29
24	15.24	0.801	0.031	0.091	6.71	3.97	6.98	-1.95	1.84	-1.72	-1.25	-0.50	-0.52	0.52	1.05	0.72	0.55	0.67	1.07	-0.37
25	17.78	0.826	0.036	0.075	6.06	3.57	6.14	-1.73	1.66	-1.67	-2.01	-0.71	-0.70	0.67	1.10	0.90	0.77	0.72	1.44	-0.44
26	20.32	0.849	0.040	0.061	5.49	3.18	5.27	-1.56	1.36	-1.47	-2.12	-0.69	-0.77	0.80	0.93	0.79	0.81	0.69	1.52	-0.44
27	22.86	0.871	0.044	0.044	4.62	2.71	4.16	-1.30	1.14	-1.28	-2.35	-0.73	-0.85	0.83	0.91	0.79	0.81	0.64	1.65	-0.35
28	25.40	0.892	0.049	0.032	3.59	2.37	3.57	-1.10	0.99	-1.02	-1.98	-0.72	-0.78	0.81	0.97	0.85	0.83	0.65	1.82	-0.35
29	27.94	0.908	0.050	0.018	2.64	1.91	2.56	-0.76	0.65	-0.75	-1.79	-0.59	-0.66	0.69	0.84	0.66	0.71	0.53	1.41	-0.31
30	30.48	0.923	0.047	0.006	1.25	1.10	1.34	-0.41	0.34	-0.31	-0.91	-0.38	-0.34	0.39	0.63	0.39	0.40	0.30	0.85	-0.15
31	33.02	0.929	0.048	0.000	0.66	0.77	0.74	-0.21	0.15	-0.09	-0.31	-0.18	-0.08	0.21	0.43	0.19	0.16	0.16	0.39	-0.05
32	35.56	0.935	0.049	-0.002	0.34	0.46	0.45	-0.10	0.06	0.00	-0.12	-0.09	0.02	0.11	0.28	0.10	0.06	0.05	0.21	-0.01
33	38.10	0.937	0.050	-0.002	0.15	0.19	0.28	-0.02	0.00	0.00	0.01	-0.02	0.06	0.02	0.05	0.01	0.02	0.00	0.07	0.00
34	40.64	0.937	0.051	-0.001	0.11	0.14	0.25	-0.01	0.00	0.02	0.02	0.00	0.06	0.00	0.03	0.00	0.03	0.00	0.08	0.00
35	45.72	0.936	0.055	-0.001	0.09	0.12	0.24	0.00	0.00	0.03	0.02	0.00	0.07	0.00	0.08	0.00	0.04	0.00	0.11	0.00
36	50.80	0.935	0.057	-0.003	0.09	0.09	0.24	0.00	0.00	0.03	0.02	0.00	0.07	0.00	0.00	0.00	0.03	0.00	0.10	0.00
37	55.88	0.937	0.065	-0.003	0.10	0.38	0.29	0.00	0.00	0.05	0.03	0.00	0.09	0.00	0.00	0.00	0.04	0.00	0.14	0.00
38	60.96	0.937	0.066	-0.005	0.11	0.42	0.31	0.00	0.00	0.05	0.03	0.00	0.10	0.00	-0.01	0.00	0.04	0.00	0.13	0.00
39	66.04	0.935	0.000	-0.005	0.14	0.00	0.40	0.00	0.00	0.11	0.05	0.00	0.16	0.00	0.00	0.00	0.08	0.00	0.24	0.00
40	71.12	0.929	0.000	0.003	0.35	0.00	1.03	0.00	0.00	0.37	0.13	0.00	0.37	0.00	0.00	0.00	0.24	0.00	0.69	0.00

Table C.5 Continued.

Case D.S1 Station= 5
X= 0.0mm Tunnel Run#= 784 Ue/Uref= 0.922 Date= 621.88 Time= 8.19
Bias Corrected data using 1/sqrt(U*U + V*V + W*W + (.01Ur)^2)

					<-- normalized by 0.001 Ur^2 -->						<---------- normalized by 0.0001 Ur^3 ---------->									
LR	Y(mm)	U/Ur	V/Ur	W/Ur	uu	vv	ww	uv	vw	uw	uuu	uvv	uww	vuu	vvv	vww	wuu	wvv	www	uvw
1	0.00	0.000	0.000	1.000	0.00	0.00	0.00	-2.18	2.76	0.00	0.00	0.00	0.00	0.00	0.00	0.00	0.00	0.00	0.00	0.00
1	0.25	0.483	-0.033	0.338	13.93	3.35	18.55	-2.00	2.22	-6.49	0.85	-0.45	-1.28	0.84	0.48	2.18	1.26	0.59	-0.59	-1.22
2	0.38	0.509	-0.025	0.315	13.61	3.63	18.20	-1.92	2.20	-5.48	0.72	-0.43	-0.16	0.77	0.62	1.84	0.73	0.72	-1.20	-0.67
3	0.51	0.523	-0.019	0.301	12.89	4.06	16.00	-2.11	2.51	-4.59	0.71	-0.39	-0.72	0.64	0.64	1.77	0.75	0.69	0.55	-0.44
4	0.63	0.538	-0.016	0.281	12.77	4.19	15.89	-2.13	2.42	-4.41	0.27	-0.44	-0.13	1.05	1.11	1.78	0.81	0.67	0.51	-0.47
5	0.76	0.550	-0.014	0.268	12.32	4.05	14.97	-2.11	2.50	-4.31	0.40	-0.49	-0.62	0.81	0.75	1.30	0.99	0.54	0.35	-0.49
6	1.02	0.575	-0.012	0.249	12.37	4.06	14.68	-2.04	2.30	-4.24	-0.45	-0.41	-0.42	0.99	0.71	1.60	0.83	0.76	0.46	-0.49
7	1.27	0.589	-0.010	0.230	11.73	4.05	14.20	-2.03	2.28	-4.16	-1.18	-0.69	-0.53	1.30	0.88	1.68	1.20	0.61	0.53	-0.67
8	1.52	0.602	-0.008	0.218	11.56	4.18	13.55	-2.17	2.45	-4.40	-1.30	-0.58	-1.33	0.93	0.92	1.76	1.59	0.90	1.17	-0.72
9	1.78	0.616	-0.006	0.209	11.54	4.36	13.35	-2.26	2.35	-4.34	-1.84	-0.68	-1.68	1.28	1.55	1.81	1.64	0.84	2.55	-0.84
10	2.03	0.629	-0.005	0.196	10.93	4.16	12.77	-2.13	2.28	-3.92	-1.02	-0.51	-1.49	0.96	0.91	1.74	1.43	0.93	2.27	-0.67
11	2.29	0.637	-0.005	0.189	10.98	4.44	12.17	-2.41	2.36	-4.14	-1.89	-0.82	-1.48	1.39	1.32	2.08	1.95	1.13	2.38	-0.93
12	2.54	0.642	-0.004	0.183	10.96	4.32	12.04	-2.40	2.49	-4.13	-2.46	-0.74	-1.80	1.21	0.82	1.98	2.07	1.04	2.40	-0.96
13	2.79	0.650	-0.003	0.175	10.71	4.32	12.49	-2.32	2.46	-4.23	-1.75	-0.85	-1.34	1.33	1.06	1.89	1.83	0.97	2.35	-1.04
14	3.30	0.660	-0.001	0.166	10.08	4.51	11.49	-2.18	2.47	-3.79	-2.23	-0.79	-1.63	1.30	1.19	1.81	1.81	1.25	2.68	-0.90
15	3.81	0.674	0.000	0.158	10.16	4.53	11.39	-2.29	2.44	-3.93	-2.05	-0.86	-0.93	1.32	1.11	1.80	1.64	1.15	1.75	-0.90
16	4.32	0.679	0.001	0.153	9.56	4.64	11.05	-2.34	2.66	-3.58	-1.73	-0.83	-1.14	1.20	1.08	1.91	1.38	1.15	2.75	-0.91
17	4.83	0.685	0.003	0.148	9.55	4.90	10.61	-2.36	2.70	-3.60	-2.17	-0.85	-1.08	1.27	1.25	1.95	1.33	1.31	2.73	-0.87
18	5.59	0.696	0.005	0.144	8.88	4.79	10.16	-2.28	2.48	-3.20	-2.03	-0.81	-0.56	1.02	1.12	1.61	0.95	1.13	1.31	-0.66
19	6.35	0.701	0.007	0.139	8.95	4.95	9.86	-2.43	2.49	-3.12	-1.92	-0.73	-0.41	0.95	1.11	1.45	1.00	1.13	1.23	-0.77
20	7.11	0.711	0.009	0.135	8.46	5.05	9.66	-2.33	2.58	-2.98	-1.53	-0.82	-0.40	0.97	1.19	1.46	1.00	1.10	1.79	-0.62
21	8.38	0.723	0.010	0.127	8.04	4.85	8.82	-2.19	2.41	-2.42	-1.17	-0.59	-0.11	0.72	1.02	1.25	0.57	0.86	1.46	-0.46
22	10.16	0.737	0.014	0.119	7.75	4.72	8.69	-2.16	2.28	-2.27	-1.07	-0.63	0.09	0.57	1.13	1.01	0.24	0.75	0.79	-0.34
23	12.70	0.765	0.018	0.104	7.30	4.40	8.04	-2.08	2.14	-2.22	-1.23	-0.65	-0.11	0.52	1.06	0.88	0.19	0.93	0.49	-0.35
24	15.24	0.789	0.021	0.088	6.86	3.83	6.93	-1.98	1.89	-1.82	-1.97	-0.68	-0.23	0.74	1.12	0.75	0.48	0.74	0.80	-0.36
25	17.78	0.815	0.026	0.071	5.90	3.50	6.22	-1.73	1.60	-1.63	-2.01	-0.87	-0.57	0.87	1.33	1.03	0.78	0.87	1.25	-0.47
26	20.32	0.837	0.031	0.055	5.10	2.89	5.27	-1.51	1.36	-1.55	-2.30	-0.86	-0.79	0.94	1.09	1.01	0.86	0.83	1.86	-0.49
27	22.86	0.860	0.034	0.040	4.23	2.32	4.09	-1.14	0.98	-1.11	-2.46	-0.75	-0.73	0.91	0.93	0.88	0.80	0.66	1.58	-0.36
28	25.40	0.881	0.037	0.026	2.96	1.78	3.06	-0.78	0.74	-0.89	-1.88	-0.57	-0.67	0.70	0.77	0.72	0.75	0.60	1.54	-0.35
29	27.94	0.896	0.040	0.015	2.07	1.41	2.08	-0.61	0.50	-0.61	-1.47	-0.53	-0.48	0.60	0.69	0.53	0.56	0.47	0.99	-0.29
30	30.48	0.908	0.043	0.006	1.12	0.94	1.19	-0.32	0.25	-0.32	-0.76	-0.30	-0.21	0.34	0.46	0.30	0.33	0.25	0.50	-0.15
31	33.02	0.913	0.045	0.002	0.66	0.63	0.74	-0.21	0.14	-0.12	-0.35	-0.18	-0.04	0.21	0.29	0.17	0.14	0.13	0.31	-0.07
32	35.56	0.919	0.047	0.000	0.32	0.41	0.41	-0.07	0.05	-0.05	-0.09	-0.04	0.02	0.07	0.19	0.07	0.05	0.06	0.08	-0.02
33	38.10	0.920	0.048	-0.001	0.18	0.26	0.30	-0.04	0.03	-0.02	-0.01	-0.04	0.03	0.03	0.11	0.05	0.02	0.04	0.04	-0.02
34	40.64	0.920	0.050	0.000	0.13	0.16	0.26	0.00	0.00	-0.01	0.02	0.00	0.06	0.01	0.02	0.00	0.00	0.00	0.01	0.00
35	45.72	0.921	0.053	0.000	0.10	0.10	0.24	0.00	0.00	0.01	0.02	0.00	0.06	0.00	0.00	0.00	0.02	0.00	0.05	0.00
36	50.80	0.923	0.055	0.000	0.09	0.09	0.24	0.00	0.00	0.03	0.02	0.00	0.07	0.00	0.00	0.00	0.03	0.00	0.08	0.00
37	55.88	0.924	0.061	0.000	0.10	0.50	0.26	0.00	0.00	0.04	0.03	-0.01	0.08	0.00	0.78	0.00	0.04	0.01	0.11	0.00
38	60.96	0.923	0.062	0.000	0.11	0.41	0.28	0.00	0.00	0.04	0.03	0.00	0.09	0.00	0.00	0.00	0.03	0.00	0.10	0.00
39	66.04	0.929	0.000	-0.002	0.07	0.00	0.20	0.00	0.00	0.01	0.01	0.00	0.02	0.00	0.00	0.00	0.01	0.00	0.04	0.00

Table C.5 Continued.

Case D.S1 Station= 6
X= 12.7mm Tunnel Run#= 782 Ue/Uref= 0.908 Date= 617.88 Time= 7.50
Bias Corrected data using 1/sqrt(U*U + V*V + W*W + (.01Ur)^2)

					<-- normalized by 0.001 Ur^2 -->						<---------- normalized by 0.0001 Ur^3 ---------->								
LR	Y(mm)	U/Ur	V/Ur	W/Ur	uu	vv	ww	uv	vw	uw	uuu	uvv	uww	vuu	vvv	vww	wuu	wvv	www	uvw
1	0.00	0.000	0.000	0.000	0.00	0.00	0.00	-1.51	-0.69	0.00	0.00	0.00	0.00	0.00	0.00	0.00	0.00	0.00	0.00	0.00
1	0.25	0.389	-0.001	0.207	11.01	1.33	11.07	-1.34	-0.61	1.11	1.88	0.03	3.00	0.14	0.05	0.35	-2.04	-0.06	-3.50	0.30
2	0.38	0.466	-0.003	0.237	10.21	2.06	11.81	-1.54	-0.43	-0.49	0.95	-0.08	1.65	0.38	0.08	0.44	-1.21	-0.21	-3.49	0.43
3	0.51	0.504	-0.003	0.242	9.99	2.40	11.41	-1.54	-0.08	-1.17	0.73	-0.13	1.25	0.48	0.17	0.30	-0.60	-0.32	-2.09	0.54
4	0.63	0.532	-0.002	0.243	9.91	2.76	11.56	-1.54	0.37	-1.67	0.89	-0.16	0.69	0.43	0.25	0.18	-0.20	-0.19	-1.54	0.34
5	0.76	0.551	0.000	0.235	9.41	2.82	11.24	-1.33	0.66	-1.84	1.42	-0.07	0.69	0.28	0.12	0.16	-0.03	-0.28	-1.75	0.27
6	1.02	0.570	-0.001	0.224	9.12	2.99	12.01	-1.15	1.14	-2.34	1.48	0.08	0.34	0.33	0.14	0.37	0.01	-0.13	-1.02	0.18
7	1.27	0.585	-0.001	0.217	9.52	3.25	12.05	-1.29	1.58	-2.73	0.75	0.01	0.12	0.47	0.23	0.70	0.15	0.12	-1.12	0.01
8	1.52	0.599	0.000	0.209	9.75	3.58	12.00	-1.57	1.96	-2.91	0.83	-0.22	-0.20	0.57	0.41	0.70	0.35	0.35	0.74	-0.12
9	1.78	0.610	-0.002	0.199	9.63	3.74	12.21	-1.57	2.07	-3.22	0.29	-0.34	-0.27	0.52	0.47	0.98	0.68	0.51	0.84	-0.23
10	2.03	0.616	0.001	0.193	9.88	3.98	12.04	-1.86	2.26	-3.61	-0.47	-0.39	-1.04	0.87	0.67	1.06	0.98	0.60	2.07	-0.33
11	2.29	0.624	0.001	0.189	9.94	3.98	12.18	-1.91	2.26	-3.78	-0.72	-0.44	-1.12	0.82	0.52	1.42	1.26	0.75	2.41	-0.58
12	2.54	0.632	0.002	0.183	10.18	4.12	12.05	-1.98	2.44	-3.72	-0.53	-0.61	-1.09	1.10	0.93	1.76	1.17	1.07	2.85	-0.78
13	2.79	0.637	0.000	0.174	9.93	4.23	11.54	-2.04	2.30	-3.65	-1.41	-0.78	-1.55	1.16	0.79	1.73	1.69	0.90	2.64	-0.79
14	3.30	0.651	0.002	0.163	9.54	4.20	11.33	-2.15	2.26	-3.68	-1.36	-0.65	-1.16	1.10	1.15	1.60	1.43	0.88	2.56	-0.75
15	3.81	0.656	0.003	0.158	9.20	4.32	11.04	-2.12	2.41	-3.60	-1.07	-0.68	-1.25	1.16	0.99	1.82	1.62	1.06	2.31	-0.93
16	4.32	0.665	0.004	0.153	9.18	4.57	10.74	-2.21	2.51	-3.56	-1.60	-0.75	-1.25	1.29	1.23	1.68	1.71	1.15	2.45	-0.97
17	4.83	0.675	0.004	0.145	8.98	4.64	10.29	-2.12	2.35	-3.22	-1.66	-0.71	-0.60	1.11	1.26	1.67	1.00	1.07	2.27	-0.66
18	5.59	0.683	0.003	0.140	8.49	4.64	9.64	-2.19	2.38	-2.88	-1.58	-0.65	-0.74	1.10	1.10	1.56	1.13	1.11	2.22	-0.66
19	6.35	0.692	0.006	0.138	8.24	4.87	9.81	-2.19	2.48	-2.93	-1.23	-0.77	-0.64	0.82	1.09	1.53	0.74	1.11	2.40	-0.61
20	7.11	0.699	0.006	0.131	8.01	4.62	9.06	-2.01	2.33	-2.50	-1.52	-0.70	-0.31	0.85	1.06	1.25	0.78	0.97	1.77	-0.50
21	8.38	0.709	0.009	0.125	8.00	4.88	8.68	-2.20	2.34	-2.40	-1.10	-0.57	-0.13	0.61	1.42	1.05	0.47	0.95	0.54	-0.42
22	10.16	0.727	0.012	0.116	7.68	4.70	8.36	-2.19	2.24	-2.29	-1.30	-0.63	-0.28	0.69	1.29	1.00	0.74	0.86	1.05	-0.45
23	12.70	0.752	0.014	0.103	7.12	4.25	7.64	-2.00	2.11	-2.05	-1.38	-0.64	-0.32	0.75	1.19	0.93	0.46	0.83	0.74	-0.40
24	15.24	0.773	0.020	0.086	6.70	3.93	6.95	-1.92	1.80	-1.67	-1.47	-0.70	-0.36	0.61	1.20	0.98	0.46	0.86	0.86	-0.38
25	17.78	0.796	0.024	0.073	5.92	3.41	6.31	-1.70	1.57	-1.64	-1.78	-0.78	-0.31	0.85	1.11	0.87	0.54	0.84	1.40	-0.43
26	20.32	0.822	0.027	0.058	5.12	2.86	5.29	-1.35	1.29	-1.54	-2.03	-0.84	-0.63	0.86	1.06	0.92	0.69	0.84	1.61	-0.41
27	22.86	0.842	0.033	0.044	4.42	2.45	4.44	-1.21	1.06	-1.36	-2.24	-0.76	-0.62	0.94	1.00	0.85	0.65	0.76	1.61	-0.41
28	25.40	0.865	0.036	0.028	3.40	1.92	3.30	-0.89	0.76	-0.99	-2.19	-0.70	-0.70	0.85	0.86	0.71	0.77	0.65	1.62	-0.37
29	27.94	0.881	0.040	0.019	2.32	1.51	2.52	-0.62	0.58	-0.80	-1.51	-0.51	-0.56	0.59	0.63	0.61	0.70	0.51	1.24	-0.33
30	30.48	0.893	0.042	0.009	1.46	1.06	1.49	-0.38	0.33	-0.46	-1.05	-0.33	-0.39	0.42	0.44	0.40	0.47	0.28	0.74	-0.19
31	33.02	0.900	0.045	0.004	0.79	0.73	0.99	-0.23	0.18	-0.20	-0.43	-0.22	-0.06	0.23	0.34	0.21	0.18	0.17	0.36	-0.11
32	35.56	0.905	0.047	0.000	0.43	0.52	0.58	-0.09	0.11	-0.12	-0.14	-0.11	0.04	0.11	0.31	0.13	0.06	0.11	0.03	-0.06
33	38.10	0.908	0.048	-0.001	0.24	0.30	0.37	-0.04	0.02	-0.05	-0.03	-0.03	0.08	0.05	0.08	0.04	-0.01	0.02	-0.04	-0.02
34	40.64	0.909	0.050	-0.001	0.16	0.20	0.31	-0.01	0.02	-0.05	0.03	0.00	0.13	0.01	0.04	0.02	-0.03	0.01	-0.13	0.00
35	45.72	0.911	0.054	-0.002	0.10	0.13	0.25	-0.01	0.00	-0.03	0.03	0.00	0.10	0.00	0.00	0.00	-0.03	0.00	-0.09	0.00
36	50.80	0.914	0.060	-0.004	0.10	0.12	0.26	-0.01	0.00	-0.02	0.03	0.00	0.11	0.00	0.00	0.00	-0.02	0.00	-0.08	0.00
37	55.88	0.917	0.066	-0.003	0.08	0.68	0.21	0.00	0.00	-0.02	0.02	-0.01	0.07	0.00	1.58	0.00	-0.02	-0.02	-0.06	0.00
38	60.96	0.916	0.072	-0.004	0.08	0.52	0.23	0.00	0.00	0.00	0.02	0.00	0.07	0.00	0.18	0.00	-0.01	0.00	-0.02	0.00
39	66.04	0.918	0.000	-0.004	0.06	0.00	0.19	0.00	0.00	-0.01	0.00	0.00	0.01	0.00	0.00	0.00	0.00	0.00	-0.01	0.00

Table C.5 Continued.

Case D.S1 Station= 7
X= 25.4mm Tunnel Run#= 780 Ue/Uref= 0.896 Date= 616.88 Time=18.56
Bias Corrected data using 1/sqrt(U*U + V*V + W*W + (.01Ur)^2)

					<-- normalized by 0.001 Ur^2 -->						<---------- normalized by 0.0001 Ur^3 ---------->									
LR	Y(mm)	U/Ur	V/Ur	W/Ur	uu	vv	ww	uv	vw	uw	uuu	uvv	uww	vuu	vvv	vww	wuu	wvv	www	uvw
1	0.00	0.000	0.000	0.000	0.00	0.00	0.00	-1.29	-0.55	0.00	0.00	0.00	0.00	0.00	0.00	0.00	0.00	0.00	0.00	0.00
1	0.25	0.360	0.003	0.161	11.14	1.05	7.87	-1.25	-0.47	2.06	1.18	0.05	1.94	0.18	0.02	0.07	-1.13	0.08	0.85	0.04
2	0.38	0.414	0.001	0.180	10.04	1.52	8.99	-1.59	-0.48	0.99	0.15	0.00	1.27	0.41	-0.01	0.31	-1.20	-0.06	-1.08	0.31
3	0.51	0.451	0.001	0.189	9.38	2.03	9.06	-1.66	-0.38	0.14	0.41	-0.03	1.23	0.36	0.00	0.27	-1.11	-0.11	-1.21	0.30
4	0.63	0.474	0.002	0.197	8.45	2.29	9.18	-1.57	-0.21	-0.26	0.63	-0.12	0.80	0.40	0.08	0.24	-0.51	-0.18	-1.07	0.34
5	0.76	0.494	0.001	0.198	8.35	2.44	8.89	-1.56	-0.14	-0.73	1.12	-0.06	0.75	0.17	0.07	0.27	-0.48	-0.22	-1.25	0.33
6	1.02	0.529	0.002	0.197	8.28	2.69	9.63	-1.57	0.16	-1.21	1.18	-0.08	0.34	0.24	0.13	0.11	-0.20	-0.11	-0.51	0.32
7	1.27	0.554	0.002	0.194	8.13	2.89	9.23	-1.51	0.59	-1.58	0.98	-0.06	0.35	0.22	0.19	0.19	0.23	-0.17	-0.36	0.14
8	1.52	0.572	0.004	0.190	8.38	3.01	9.42	-1.50	0.80	-1.88	1.03	-0.03	0.06	0.23	0.09	0.20	0.21	-0.03	0.30	0.03
9	1.78	0.588	0.002	0.186	8.35	3.18	9.82	-1.44	1.02	-1.79	0.68	-0.18	0.05	0.52	0.02	0.34	0.38	0.06	0.36	0.10
10	2.03	0.599	0.003	0.181	8.32	3.27	10.00	-1.41	1.28	-2.08	0.59	-0.27	-0.29	0.43	0.24	0.42	0.34	0.19	0.30	-0.02
11	2.29	0.610	0.003	0.179	8.58	3.43	10.15	-1.49	1.51	-2.41	0.24	-0.24	-0.51	0.56	0.19	0.70	0.51	0.23	1.28	-0.13
12	2.54	0.617	0.005	0.177	8.67	3.62	10.23	-1.49	1.74	-2.65	0.15	-0.18	-0.29	0.54	0.21	0.69	0.64	0.38	0.70	-0.22
13	2.79	0.627	0.004	0.168	8.41	3.71	10.16	-1.55	1.82	-2.35	-0.08	-0.30	-0.69	0.61	0.34	0.94	0.78	0.47	1.35	-0.33
14	3.30	0.636	0.005	0.164	8.69	4.04	10.02	-1.71	2.04	-2.72	-0.19	-0.35	-0.59	0.65	0.50	1.00	0.79	0.54	1.27	-0.35
15	3.81	0.641	0.005	0.158	8.53	4.05	10.03	-1.77	2.11	-2.87	-0.52	-0.57	-0.75	0.69	0.66	1.27	0.96	0.83	1.98	-0.56
16	4.32	0.647	0.006	0.152	8.34	4.32	10.02	-1.85	2.27	-2.84	-0.66	-0.61	-0.75	0.78	0.80	1.41	0.98	0.97	1.69	-0.61
17	4.83	0.656	0.008	0.148	8.52	4.45	9.95	-2.09	2.26	-2.96	-0.74	-0.55	-0.69	0.76	1.02	1.59	0.68	1.00	2.12	-0.58
18	5.59	0.665	0.008	0.145	8.44	4.53	9.62	-2.11	2.37	-2.88	-1.25	-0.57	-0.95	0.79	1.05	1.26	1.06	1.13	1.93	-0.58
19	6.35	0.673	0.010	0.141	8.14	4.69	9.38	-2.13	2.35	-2.84	-0.93	-0.51	-0.80	0.82	0.93	1.27	0.93	0.92	2.14	-0.58
20	7.11	0.677	0.012	0.138	8.12	4.73	8.99	-2.15	2.34	-2.65	-0.96	-0.60	-0.34	0.89	0.84	1.15	0.67	0.88	1.59	-0.46
21	8.38	0.689	0.015	0.131	7.82	4.79	8.61	-2.19	2.43	-2.21	-0.99	-0.64	-0.43	0.73	1.04	1.13	0.48	0.94	1.80	-0.48
22	10.16	0.709	0.017	0.122	7.39	4.66	8.07	-2.08	2.16	-1.96	-0.89	-0.38	-0.38	0.42	0.82	0.80	0.48	0.72	1.27	-0.25
23	12.70	0.728	0.021	0.110	7.09	4.37	7.46	-1.99	1.95	-1.65	-1.34	-0.49	-0.28	0.56	1.03	0.65	0.55	0.71	1.12	-0.26
24	15.24	0.750	0.027	0.099	6.87	4.10	6.70	-2.03	1.84	-1.48	-1.40	-0.57	-0.38	0.60	0.96	0.64	0.54	0.68	1.11	-0.30
25	17.78	0.772	0.031	0.085	6.25	3.67	6.44	-1.77	1.63	-1.47	-1.64	-0.57	-0.64	0.65	0.99	0.86	0.75	0.70	1.61	-0.33
26	20.32	0.797	0.036	0.071	5.69	3.25	5.72	-1.63	1.55	-1.41	-1.89	-0.70	-0.77	0.75	1.05	0.94	0.76	0.74	1.86	-0.45
27	22.86	0.816	0.041	0.057	5.16	2.88	4.88	-1.47	1.36	-1.39	-2.25	-0.70	-0.67	0.87	0.97	0.86	0.78	0.73	1.72	-0.36
28	25.40	0.839	0.044	0.044	4.24	2.38	4.13	-1.15	1.00	-1.13	-2.14	-0.69	-0.85	0.77	0.86	0.79	0.82	0.59	2.04	-0.39
29	27.94	0.855	0.047	0.031	3.46	2.03	3.11	-0.94	0.80	-1.02	-2.24	-0.72	-0.80	0.86	0.89	0.70	0.91	0.58	1.72	-0.38
30	30.48	0.874	0.049	0.019	2.32	1.73	2.30	-0.68	0.63	-0.63	-1.64	-0.58	-0.67	0.70	0.83	0.66	0.67	0.60	1.43	-0.32
31	33.02	0.888	0.050	0.009	1.33	1.15	1.39	-0.39	0.37	-0.32	-0.92	-0.33	-0.33	0.38	0.60	0.42	0.41	0.33	0.88	-0.18
32	35.56	0.896	0.050	0.001	0.61	0.63	0.66	-0.19	0.16	-0.15	-0.37	-0.18	-0.14	0.20	0.34	0.20	0.18	0.18	0.34	-0.10
33	38.10	0.900	0.052	-0.001	0.32	0.40	0.39	-0.10	0.06	-0.05	-0.13	-0.10	-0.02	0.09	0.19	0.08	0.05	0.05	0.14	-0.03
34	40.64	0.902	0.053	-0.001	0.20	0.27	0.26	-0.03	0.02	-0.02	-0.02	-0.03	0.03	0.04	0.10	0.03	0.02	0.02	0.02	-0.01
35	45.72	0.903	0.058	0.001	0.12	0.16	0.24	-0.01	0.00	-0.01	0.03	0.00	0.08	0.00	0.09	0.00	-0.01	0.00	-0.02	0.00
36	50.80	0.902	0.059	0.003	0.09	0.22	0.24	0.00	-0.01	0.01	0.03	0.00	0.09	0.00	0.43	0.00	0.00	0.00	-0.01	0.00
37	55.88	0.904	0.072	0.002	0.09	0.43	0.26	0.00	0.00	0.03	0.03	0.00	0.10	0.00	-0.01	0.00	0.01	0.00	0.01	0.00
38	60.96	0.902	0.075	0.001	0.08	4.46	0.19	-0.01	0.00	0.00	0.02	0.08	0.05	0.00	38.61	-0.01	-0.02	0.13	-0.05	0.00
39	66.04	0.904	0.000	-0.006	0.08	0.00	0.24	0.00	0.00	0.04	0.02	0.00	0.06	0.00	0.00	0.00	0.03	0.00	0.08	0.00

Table C.5 Continued.

Case D.S1 Station= 8
X= 48.3mm Tunnel Run#= 778 Ue/Uref= 0.871 Date= 616.88 Time=16.42
Bias Corrected data using 1/sqrt(U*U + V*V + W*W + (.01Ur)^2)

					<-- normalized by 0.001 Ur^2 -->						<---------- normalized by 0.0001 Ur^3 ---------->								
LR	Y(mm)	U/Ur	V/Ur	W/Ur	uu	vv	ww	uv	vw	uw	uuu	uvv	uww	vuu	vvv	vww	wuu	wvv	www	uvw
1	0.00	0.000	0.000	0.000	0.00	0.00	0.00	-1.04	-0.44	0.00	0.00	0.00	0.00	0.00	0.00	0.00	0.00	0.00	0.00	0.00
1	0.25	0.347	0.002	0.119	10.09	0.87	7.30	-1.00	-0.37	1.32	0.97	0.09	2.02	0.08	0.02	0.12	-1.37	0.05	-0.57	0.01
2	0.38	0.391	0.002	0.132	9.07	1.30	7.09	-1.25	-0.42	0.59	-0.39	-0.01	1.27	0.37	0.02	0.14	-0.95	-0.01	-0.55	0.16
3	0.51	0.419	0.002	0.140	8.30	1.63	7.67	-1.28	-0.43	0.27	0.39	-0.04	1.11	0.22	0.04	0.36	-0.51	-0.01	-0.75	0.17
4	0.63	0.441	0.002	0.145	8.11	1.98	7.53	-1.42	-0.29	0.12	0.22	-0.04	0.80	0.29	0.12	0.20	-0.40	-0.11	-0.55	0.19
5	0.76	0.459	0.002	0.147	7.58	2.20	7.45	-1.33	-0.27	-0.25	0.61	-0.03	0.99	0.26	0.11	0.31	-0.34	-0.13	-0.42	0.19
6	1.02	0.484	0.003	0.151	7.27	2.52	7.64	-1.52	-0.11	-0.66	0.55	-0.04	0.63	0.11	0.13	0.12	-0.19	-0.18	-0.69	0.25
7	1.27	0.505	0.003	0.150	7.28	2.65	8.02	-1.65	0.19	-1.07	0.65	-0.15	0.60	0.27	0.15	0.22	0.04	-0.05	-0.33	0.09
8	1.52	0.524	0.004	0.151	7.20	2.70	7.88	-1.52	0.28	-1.03	0.58	-0.01	0.56	0.19	0.13	0.11	-0.03	-0.16	-0.42	0.20
9	1.78	0.538	0.005	0.149	7.50	2.86	7.95	-1.61	0.44	-1.16	0.93	0.00	0.41	0.16	0.05	0.14	0.13	-0.10	-0.27	0.21
10	2.03	0.554	0.006	0.146	7.25	3.00	8.15	-1.46	0.51	-1.43	0.30	-0.06	0.14	0.28	0.17	0.23	0.26	-0.05	0.23	0.06
11	2.29	0.564	0.005	0.145	7.20	2.97	8.04	-1.39	0.69	-1.54	0.53	-0.08	0.25	0.29	0.14	0.18	0.29	-0.01	0.02	0.03
12	2.54	0.579	0.005	0.141	7.25	2.97	8.20	-1.42	0.92	-1.59	0.35	-0.08	0.31	0.30	0.02	0.36	0.16	0.15	-0.24	0.05
13	2.79	0.582	0.007	0.141	7.40	3.15	8.23	-1.50	0.89	-1.72	0.42	-0.19	-0.02	0.39	0.15	0.43	0.25	0.09	0.58	-0.05
14	3.30	0.598	0.006	0.137	7.15	3.34	8.18	-1.46	1.14	-1.58	0.34	-0.24	0.01	0.59	0.16	0.46	0.46	0.19	0.39	-0.05
15	3.81	0.611	0.008	0.137	7.23	3.45	8.11	-1.41	1.35	-1.69	0.08	-0.11	-0.28	0.44	0.14	0.51	0.42	0.24	0.99	-0.08
16	4.32	0.614	0.010	0.139	7.29	3.74	8.33	-1.54	1.71	-2.03	0.25	-0.16	0.18	0.45	0.28	0.35	0.33	0.31	0.83	-0.09
17	4.83	0.622	0.012	0.138	7.03	3.92	8.49	-1.38	1.74	-2.11	0.28	-0.09	0.00	0.43	0.20	0.67	0.25	0.44	0.69	-0.09
18	5.59	0.631	0.013	0.136	6.99	4.15	8.27	-1.49	1.77	-2.02	-0.07	-0.17	-0.05	0.37	0.42	0.55	0.24	0.44	0.78	-0.09
19	6.35	0.644	0.014	0.135	7.22	4.31	8.45	-1.66	1.95	-2.08	0.23	-0.18	-0.06	0.29	0.47	0.74	0.23	0.54	0.89	-0.19
20	7.11	0.649	0.013	0.131	7.21	4.65	8.17	-1.86	1.93	-2.03	-0.38	-0.37	-0.12	0.57	0.70	0.75	0.33	0.60	0.74	-0.29
21	8.38	0.653	0.017	0.127	7.16	4.70	8.19	-2.04	2.19	-1.99	-0.38	-0.29	-0.18	0.34	0.47	0.83	0.46	0.69	1.28	-0.27
22	10.16	0.670	0.021	0.121	7.14	4.69	8.07	-1.99	2.16	-1.83	-0.58	-0.39	0.18	0.37	0.68	0.54	0.48	0.47	1.03	-0.31
23	12.70	0.697	0.024	0.110	7.31	4.57	7.46	-2.08	2.10	-1.81	-1.22	-0.43	-0.20	0.50	0.92	0.61	0.55	0.61	1.16	-0.27
24	15.24	0.711	0.031	0.101	6.94	4.33	7.07	-1.97	1.98	-1.57	-1.25	-0.56	-0.42	0.52	0.94	0.72	0.55	0.61	0.98	-0.36
25	17.78	0.732	0.036	0.087	6.60	3.84	6.70	-1.83	1.81	-1.56	-1.39	-0.56	-0.48	0.60	0.89	0.67	0.45	0.69	1.17	-0.33
26	20.32	0.750	0.042	0.075	6.24	3.65	6.02	-1.73	1.68	-1.44	-1.70	-0.65	-0.50	0.73	0.98	0.76	0.47	0.62	1.41	-0.30
27	22.86	0.775	0.046	0.062	5.71	3.31	5.48	-1.61	1.45	-1.44	-1.84	-0.76	-0.75	0.78	1.03	0.81	0.70	0.74	1.95	-0.39
28	25.40	0.799	0.049	0.047	5.09	2.76	4.60	-1.27	1.17	-1.10	-2.25	-0.68	-0.76	0.82	0.81	0.76	0.72	0.63	1.75	-0.32
29	27.94	0.814	0.055	0.037	4.25	2.36	3.77	-1.09	0.90	-1.16	-2.21	-0.60	-0.81	0.77	0.71	0.63	0.81	0.62	1.63	-0.37
30	30.48	0.834	0.060	0.025	3.44	2.11	3.18	-0.92	0.79	-0.95	-2.08	-0.59	-0.79	0.72	0.77	0.63	0.79	0.53	1.63	-0.28
31	33.02	0.857	0.057	0.009	2.02	1.37	1.83	-0.50	0.41	-0.54	-1.47	-0.45	-0.51	0.48	0.56	0.41	0.52	0.35	1.02	-0.18
32	35.56	0.866	0.058	0.000	1.02	0.78	1.00	-0.25	0.20	-0.24	-0.76	-0.22	-0.20	0.27	0.32	0.24	0.37	0.18	0.51	-0.13
33	38.10	0.875	0.061	-0.004	0.56	0.55	0.63	-0.15	0.11	-0.10	-0.25	-0.13	-0.03	0.15	0.23	0.12	0.10	0.12	0.24	-0.06
34	40.64	0.873	0.063	-0.005	0.34	0.37	0.43	-0.09	0.06	-0.03	-0.12	-0.08	0.04	0.09	0.15	0.07	0.06	0.06	0.12	-0.03
35	45.72	0.878	0.069	-0.004	0.17	0.18	0.31	-0.01	0.01	0.04	0.03	-0.01	0.11	0.01	0.04	0.02	0.04	0.01	0.12	-0.01
36	50.80	0.876	0.085	0.000	0.16	0.40	0.33	0.00	-0.01	0.01	0.06	0.00	0.19	0.00	0.00	-0.01	-0.03	0.00	-0.08	0.00
37	55.88	0.885	0.092	0.004	0.14	0.40	0.35	0.00	0.00	0.06	0.06	0.00	0.18	0.00	0.00	-0.01	0.02	0.00	0.07	0.00
38	60.96	0.892	0.098	0.012	0.15	0.61	0.36	0.01	0.00	0.11	0.04	0.01	0.13	0.00	1.38	0.00	0.05	0.01	0.19	0.00
39	66.04	0.895	0.000	0.015	0.13	0.00	0.31	0.00	0.00	0.05	0.03	0.00	0.10	0.00	0.00	0.00	0.00	0.00	-0.04	0.00

Table C.5 Continued.

Case D.S1 Station= 9
X= 101.6mm Tunnel Run#= 776 Ue/Uref= 0.800 Date= 616.88 Time=13.42
Bias Corrected data using 1/sqrt(U*U + V*V + W*W + (.01Ur)^2)

					<-- normalized by 0.001 Ur^2 -->						<---------- normalized by 0.0001 Ur^3 ---------->									
LR	Y(mm)	U/Ur	V/Ur	W/Ur	uu	vv	ww	uv	vw	uw	uuu	uvv	uww	vuu	vvv	vww	wuu	wvv	www	uvw
1	0.00	0.000	0.000	0.000	0.00	0.00	0.00	-0.70	-0.27	0.00	0.00	0.00	0.00	0.00	0.00	0.00	0.00	0.00	0.00	0.00
1	0.25	0.262	0.002	0.078	7.77	0.64	4.65	-0.76	-0.32	1.13	1.54	0.04	0.88	-0.04	0.05	0.05	-0.24	0.04	0.68	-0.06
2	0.38	0.300	0.002	0.087	7.79	0.91	4.89	-0.93	-0.28	0.73	1.29	0.04	0.78	0.09	-0.02	0.06	-0.42	0.01	0.55	0.08
3	0.51	0.324	0.003	0.093	7.54	1.23	4.99	-1.08	-0.28	0.35	1.00	-0.03	0.65	0.16	0.04	0.14	-0.54	0.00	0.27	0.10
4	0.63	0.346	0.003	0.100	7.08	1.47	5.16	-1.07	-0.25	0.17	0.95	-0.01	0.55	0.15	0.05	0.16	-0.12	-0.02	0.20	0.07
5	0.76	0.357	0.003	0.100	6.74	1.60	5.17	-1.07	-0.22	0.06	0.63	0.01	0.70	0.17	0.05	0.11	-0.18	-0.02	-0.04	0.11
6	1.02	0.378	0.003	0.102	6.65	1.90	5.32	-1.14	-0.24	-0.13	0.73	0.02	0.50	0.19	0.06	0.20	-0.18	-0.10	-0.14	0.14
7	1.27	0.394	0.004	0.106	6.52	2.13	5.29	-1.18	-0.10	-0.33	0.72	0.05	0.54	0.02	0.05	0.18	-0.10	-0.03	-0.18	0.07
8	1.52	0.403	0.004	0.106	6.39	2.21	5.35	-1.29	-0.08	-0.46	0.78	0.06	0.48	0.01	0.09	0.16	0.14	-0.09	-0.10	0.05
9	1.78	0.418	0.005	0.104	6.74	2.39	5.45	-1.45	0.00	-0.45	0.47	0.04	0.47	0.09	0.05	0.16	0.06	-0.01	0.13	0.09
10	2.03	0.432	0.005	0.104	6.41	2.51	5.53	-1.43	-0.01	-0.38	0.70	0.09	0.56	0.06	0.01	0.15	-0.02	-0.04	-0.08	0.13
11	2.29	0.440	0.005	0.106	6.62	2.63	5.70	-1.42	0.11	-0.60	0.53	0.06	0.47	0.02	0.07	0.12	0.13	-0.05	0.12	0.10
12	2.54	0.449	0.006	0.105	6.57	2.56	5.80	-1.44	0.06	-0.72	0.57	0.05	0.58	0.04	0.12	0.12	-0.03	-0.10	0.01	0.13
13	2.79	0.458	0.007	0.105	6.71	2.68	5.75	-1.45	0.13	-0.64	0.37	0.06	0.30	0.07	0.05	0.18	0.01	0.01	-0.06	0.12
14	3.30	0.474	0.007	0.104	6.48	2.75	5.82	-1.50	0.27	-0.76	0.23	0.01	0.45	0.13	0.00	0.20	0.04	-0.08	0.00	0.11
15	3.81	0.488	0.008	0.106	6.62	2.91	5.99	-1.52	0.37	-0.88	0.18	0.06	0.33	0.05	0.20	0.11	0.07	-0.16	-0.17	0.17
16	4.32	0.502	0.010	0.105	6.43	2.93	5.91	-1.43	0.42	-1.04	0.30	0.05	0.40	0.18	-0.01	0.19	0.00	-0.05	-0.12	0.12
17	4.83	0.513	0.010	0.104	6.30	2.96	6.19	-1.37	0.51	-1.06	0.27	-0.03	0.23	0.26	-0.05	0.12	0.22	-0.02	-0.07	0.09
18	5.59	0.527	0.013	0.107	6.37	3.10	6.08	-1.40	0.63	-1.00	-0.01	-0.10	0.12	0.45	0.24	0.09	-0.01	-0.12	0.02	0.13
19	6.35	0.539	0.013	0.106	6.13	3.20	6.16	-1.39	0.74	-0.93	0.11	0.04	0.18	0.30	0.03	0.16	0.19	0.02	0.12	-0.01
20	7.11	0.554	0.015	0.107	5.92	3.28	6.12	-1.28	0.96	-1.07	0.16	0.01	0.28	0.15	0.01	0.16	0.07	0.00	-0.12	0.01
21	8.38	0.568	0.018	0.107	5.95	3.49	6.21	-1.30	1.16	-1.10	0.38	0.05	0.15	0.23	0.00	0.18	0.03	0.02	0.06	0.06
22	10.16	0.587	0.020	0.107	5.88	3.81	6.17	-1.43	1.24	-0.98	0.27	0.09	0.20	0.08	0.03	0.08	0.13	0.04	0.17	0.04
23	12.70	0.610	0.023	0.101	5.85	3.98	6.13	-1.42	1.51	-0.93	0.02	0.07	0.14	0.08	0.21	0.08	0.08	0.09	0.00	0.01
24	15.24	0.621	0.028	0.097	6.20	4.04	6.29	-1.51	1.67	-1.10	-0.14	-0.12	0.07	0.16	0.44	0.18	0.01	0.23	0.24	-0.10
25	17.78	0.645	0.032	0.088	6.13	3.80	6.18	-1.45	1.54	-1.03	-0.38	-0.26	-0.10	0.32	0.62	0.33	0.14	0.35	0.41	-0.04
26	20.32	0.665	0.038	0.079	5.99	3.60	5.75	-1.54	1.49	-1.16	-0.70	-0.22	-0.08	0.28	0.67	0.39	0.31	0.35	0.72	-0.11
27	22.86	0.689	0.037	0.062	5.72	3.35	5.39	-1.50	1.43	-1.16	-1.15	-0.50	-0.44	0.47	0.82	0.64	0.35	0.56	1.26	-0.29
28	25.40	0.708	0.041	0.050	5.42	2.98	5.01	-1.39	1.24	-1.23	-1.60	-0.58	-0.55	0.61	0.86	0.68	0.50	0.59	1.47	-0.24
29	27.94	0.725	0.044	0.039	4.73	2.58	4.39	-1.06	1.02	-1.06	-1.79	-0.61	-0.64	0.60	0.78	0.65	0.64	0.58	1.46	-0.29
30	30.48	0.743	0.049	0.030	4.25	2.23	3.81	-1.00	0.86	-1.11	-2.11	-0.60	-0.77	0.67	0.75	0.62	0.66	0.56	1.62	-0.31
31	33.02	0.757	0.055	0.019	3.41	1.99	3.13	-0.79	0.70	-0.84	-1.74	-0.57	-0.62	0.57	0.73	0.59	0.76	0.52	1.61	-0.28
32	35.56	0.774	0.058	0.009	2.81	1.59	2.50	-0.64	0.56	-0.83	-1.76	-0.46	-0.73	0.58	0.55	0.51	0.72	0.41	1.39	-0.30
33	38.10	0.789	0.059	0.001	1.89	1.25	1.65	-0.43	0.36	-0.46	-1.31	-0.40	-0.43	0.44	0.48	0.37	0.46	0.29	0.88	-0.18
34	40.64	0.797	0.063	-0.005	1.22	1.01	1.13	-0.30	0.25	-0.25	-0.81	-0.29	-0.22	0.31	0.42	0.25	0.28	0.22	0.62	-0.13
35	45.72	0.805	0.067	-0.010	0.43	0.51	0.47	-0.11	0.10	-0.07	-0.17	-0.08	-0.05	0.11	0.27	0.11	0.10	0.10	0.23	-0.04
36	50.80	0.807	0.070	-0.011	0.18	0.23	0.23	-0.02	0.01	-0.01	0.00	-0.01	0.02	0.02	0.07	0.03	0.02	0.02	0.06	-0.01
37	55.88	0.805	0.081	-0.011	0.11	0.39	0.16	0.00	0.00	0.00	0.01	0.00	0.03	0.00	0.01	0.00	0.00	0.00	0.01	0.00
38	60.96	0.801	0.083	-0.012	0.08	0.37	0.16	0.00	-0.01	0.01	0.01	0.00	0.02	0.00	0.00	0.00	0.01	0.00	0.04	0.00
39	66.04	0.811	0.000	-0.013	0.13	0.00	0.27	0.00	0.00	0.05	0.04	0.00	0.12	0.00	0.00	0.00	0.03	0.00	0.09	0.00
40	69.85	0.813	0.000	-0.016	0.12	0.00	0.23	0.00	0.00	0.03	0.03	0.00	0.08	0.00	0.00	0.00	0.01	0.00	0.03	0.00

Table C.5 Continued.

Case D.S1 Station= 10
X= 152.4mm Tunnel Run#= 774 Ue/Uref= 0.752 Date= 616.88 Time=11.40
Bias Corrected data using 1/sqrt(U*U + V*V + W*W + (.01Ur)^2)

					<-- normalized by 0.001 Ur^2 -->						<---------- normalized by 0.0001 Ur^3 ---------->									
LR	Y(mm)	U/Ur	V/Ur	W/Ur	uu	vv	ww	uv	vw	uw	uuu	uvv	uww	vuu	vvv	vww	wuu	wvv	www	uvw
1	0.00	0.000	0.000	0.000	0.00	0.00	0.00	-0.55	-0.18	0.00	0.00	0.00	0.00	0.00	0.00	0.00	0.00	0.00	0.00	0.00
13	0.25	0.202	0.003	0.055	6.09	0.57	4.06	-0.51	-0.20	0.59	1.72	0.10	1.75	-0.06	0.38	0.00	-0.42	0.04	-0.89	-0.03
2	0.38	0.235	0.002	0.064	6.30	0.66	4.66	-0.61	-0.16	0.02	1.91	0.08	2.24	0.00	0.05	0.04	-1.00	-0.01	-2.06	0.00
3	0.51	0.257	0.003	0.072	6.22	0.92	4.67	-0.71	-0.26	0.20	1.37	0.07	1.55	0.01	0.07	0.12	-0.65	-0.01	-1.16	0.06
4	0.63	0.272	0.003	0.075	5.98	1.15	4.66	-0.80	-0.25	0.21	1.10	0.05	1.31	0.00	0.20	0.09	-0.33	-0.02	-0.84	0.01
5	0.76	0.282	0.003	0.078	5.84	1.30	4.36	-0.82	-0.21	0.09	0.96	0.07	0.85	0.02	0.09	0.13	-0.30	-0.01	-0.18	0.02
6	1.02	0.301	0.003	0.082	5.66	1.47	4.24	-0.89	-0.17	0.00	1.01	0.06	0.83	-0.01	0.06	0.04	-0.24	-0.06	-0.35	0.05
7	1.27	0.314	0.004	0.085	5.83	1.67	4.50	-1.00	-0.12	0.01	0.90	0.12	0.87	-0.04	0.16	0.17	-0.26	-0.01	-0.18	0.06
8	1.52	0.325	0.004	0.087	5.88	1.80	4.54	-1.03	-0.12	-0.11	0.75	0.06	0.85	-0.03	0.14	0.09	-0.23	0.00	-0.24	0.04
9	1.78	0.334	0.005	0.088	5.92	1.96	4.67	-1.13	-0.14	-0.12	0.99	0.17	0.89	-0.12	0.15	0.04	-0.17	-0.06	-0.37	0.03
10	2.03	0.341	0.006	0.090	6.11	1.98	4.49	-1.12	-0.05	-0.18	1.00	0.15	0.67	-0.12	-0.02	0.09	-0.09	-0.04	-0.23	0.06
11	2.29	0.352	0.006	0.091	5.94	2.10	4.62	-1.13	-0.04	-0.36	0.84	0.11	0.60	-0.03	-0.01	0.11	-0.11	-0.02	-0.43	0.09
14	2.54	0.361	0.005	0.093	6.10	2.19	4.65	-1.23	0.03	-0.27	0.66	0.07	0.61	-0.02	0.02	0.12	-0.13	-0.07	-0.37	0.07
15	2.79	0.369	0.006	0.094	6.18	2.27	4.61	-1.28	0.02	-0.32	0.70	0.06	0.51	0.00	0.19	0.10	-0.04	-0.07	-0.24	0.08
16	3.30	0.381	0.007	0.095	6.30	2.36	4.72	-1.39	0.06	-0.34	0.57	0.15	0.69	-0.07	0.17	0.06	-0.09	-0.08	-0.07	0.12
17	3.81	0.391	0.007	0.094	6.36	2.42	4.65	-1.36	0.13	-0.30	0.59	0.12	0.53	-0.04	-0.05	0.05	-0.06	-0.04	-0.02	0.09
18	4.32	0.401	0.009	0.095	6.15	2.55	4.82	-1.41	0.20	-0.45	0.60	0.18	0.38	-0.10	-0.09	0.11	-0.06	-0.01	-0.02	0.07
19	4.83	0.411	0.010	0.095	6.24	2.61	4.80	-1.39	0.20	-0.37	0.19	0.09	0.33	0.06	0.06	0.00	-0.05	0.00	-0.11	0.04
20	5.59	0.428	0.011	0.096	6.23	2.63	4.86	-1.44	0.24	-0.40	0.32	0.14	0.33	0.06	-0.01	0.04	0.00	-0.06	-0.07	0.09
21	6.35	0.442	0.013	0.097	6.13	2.72	5.00	-1.44	0.28	-0.49	0.10	0.04	0.50	0.02	0.04	0.02	0.02	-0.05	-0.28	0.10
22	7.11	0.455	0.014	0.097	6.11	2.72	5.05	-1.38	0.42	-0.58	0.08	0.02	0.38	0.16	0.03	0.08	-0.08	-0.10	-0.20	0.07
23	8.38	0.473	0.016	0.098	5.85	2.91	5.05	-1.42	0.51	-0.57	-0.13	0.04	0.40	0.18	0.01	0.04	0.09	-0.09	-0.29	0.06
24	10.16	0.498	0.020	0.100	5.96	3.07	5.24	-1.32	0.56	-0.49	0.00	0.02	0.29	0.23	-0.02	0.06	0.06	-0.10	-0.20	0.09
25	12.70	0.525	0.023	0.101	5.34	3.27	5.38	-1.26	0.86	-0.60	0.24	0.04	0.20	0.14	-0.05	0.12	-0.05	-0.02	0.02	0.09
26	15.24	0.546	0.028	0.099	5.22	3.34	5.33	-1.19	0.97	-0.48	0.26	0.16	0.16	0.01	0.03	0.12	0.01	0.10	0.00	0.01
27	17.78	0.565	0.032	0.095	5.37	3.45	5.27	-1.26	1.11	-0.57	0.19	0.09	0.20	-0.08	0.11	0.03	-0.01	0.00	-0.18	0.03
28	20.32	0.584	0.036	0.091	5.27	3.52	5.30	-1.23	1.20	-0.63	0.08	0.08	0.30	0.03	0.24	0.01	-0.02	0.09	-0.10	0.03
29	22.86	0.597	0.039	0.083	5.40	3.37	5.08	-1.31	1.18	-0.61	-0.20	-0.03	0.11	0.05	0.29	0.12	-0.07	0.16	0.03	0.03
30	25.40	0.618	0.042	0.076	5.36	3.40	5.04	-1.36	1.35	-0.74	-0.26	-0.13	-0.10	0.17	0.44	0.20	0.00	0.24	0.24	-0.06
31	27.94	0.631	0.047	0.070	5.34	3.19	4.91	-1.28	1.16	-0.75	-0.61	-0.27	-0.14	0.25	0.45	0.22	0.09	0.25	0.48	-0.13
32	30.48	0.649	0.050	0.061	5.07	3.06	4.71	-1.20	1.07	-0.77	-0.74	-0.33	-0.22	0.33	0.60	0.39	0.17	0.34	0.66	-0.16
33	33.02	0.666	0.052	0.050	4.78	2.81	4.26	-1.09	0.93	-0.71	-1.25	-0.39	-0.35	0.43	0.59	0.45	0.31	0.36	0.98	-0.13
43	35.56	0.693	0.045	0.030	3.89	2.03	3.22	-0.87	0.70	-0.87	-1.89	-0.49	-0.36	0.62	0.60	0.48	0.43	0.41	0.90	-0.21
44	38.10	0.710	0.048	0.022	3.14	1.73	2.67	-0.68	0.51	-0.74	-1.64	-0.53	-0.48	0.52	0.54	0.42	0.51	0.38	1.03	-0.21
45	40.64	0.722	0.050	0.013	2.44	1.44	2.03	-0.51	0.43	-0.56	-1.56	-0.39	-0.47	0.44	0.55	0.37	0.47	0.35	0.93	-0.15
37	45.72	0.748	0.053	0.000	0.95	0.81	0.90	-0.21	0.18	-0.22	-0.58	-0.18	-0.14	0.19	0.36	0.21	0.23	0.17	0.34	-0.09
38	50.80	0.751	0.056	-0.004	0.38	0.48	0.47	-0.08	0.07	-0.05	-0.08	-0.08	0.04	0.08	0.21	0.07	0.07	0.08	0.16	-0.02
39	55.88	0.752	0.063	-0.004	0.17	0.50	0.27	0.00	0.01	0.00	0.01	0.00	0.05	0.01	0.04	0.01	0.02	0.01	0.06	0.00
40	60.96	0.753	0.064	-0.005	0.11	0.41	0.23	0.00	0.00	0.01	0.03	0.00	0.09	0.00	0.01	0.00	0.00	0.00	0.01	0.00
41	66.04	0.751	0.000	-0.005	0.09	0.00	0.23	0.00	0.00	0.02	0.03	0.00	0.09	0.00	0.00	0.00	0.01	0.00	0.02	0.00
42	71.12	0.753	0.000	-0.004	0.11	0.00	0.31	0.00	0.00	0.01	0.05	0.00	0.16	0.00	0.00	0.00	-0.02	0.00	-0.06	0.00

Table C.5 Continued.

Case D.S1 Station= 11
X= 228.6mm Tunnel Run#= 772 Ue/Uref= 0.705 Date= 616.88 Time= 8.50
Bias Corrected data using 1/sqrt(U*U + V*V + W*W + (.01Ur)^2)

					<-- normalized by 0.001 Ur^2 -->						<---------- normalized by 0.0001 Ur^3 ---------->									
LR	Y(mm)	U/Ur	V/Ur	W/Ur	uu	vv	ww	uv	vw	uw	uuu	uvv	uww	vuu	vvv	vww	wuu	wvv	www	uvw
1	0.00	0.000	0.000	0.000	0.00	0.00	0.00	-0.39	-0.13	0.00	0.00	0.00	0.00	0.00	0.00	0.00	0.00	0.00	0.00	0.00
1	0.25	0.144	0.000	0.039	4.54	0.30	2.70	-0.28	-0.12	0.42	1.77	0.04	1.19	-0.11	0.06	-0.01	-0.17	0.02	-0.30	-0.02
2	0.38	0.173	0.000	0.047	4.72	0.41	3.17	-0.37	-0.12	0.21	1.47	0.05	1.31	-0.07	0.07	0.04	-0.37	0.02	-0.60	-0.02
3	0.51	0.191	0.001	0.052	5.03	0.56	3.38	-0.47	-0.18	0.24	1.56	0.05	1.22	-0.05	-0.03	0.02	-0.33	0.02	-0.34	-0.03
4	0.63	0.207	0.002	0.056	4.68	0.72	3.42	-0.48	-0.20	0.25	1.07	0.08	0.91	-0.04	0.05	0.03	-0.18	0.03	-0.23	-0.01
5	0.76	0.216	0.002	0.061	4.98	0.86	3.32	-0.55	-0.16	0.23	0.83	0.06	0.79	0.02	-0.01	0.05	-0.18	0.01	-0.04	-0.02
6	1.02	0.233	0.001	0.065	4.74	1.06	3.40	-0.56	-0.13	0.08	0.94	0.07	0.69	-0.04	0.07	0.08	-0.15	0.03	-0.02	0.00
7	1.27	0.240	0.002	0.066	4.86	1.19	3.49	-0.60	-0.12	0.07	0.88	0.08	0.78	-0.02	0.01	0.05	-0.17	0.02	-0.08	0.01
8	1.52	0.251	0.003	0.069	4.86	1.32	3.66	-0.67	-0.15	0.05	0.98	0.05	0.72	-0.03	0.04	0.15	-0.18	-0.01	-0.27	0.04
9	1.78	0.260	0.002	0.070	4.94	1.47	3.68	-0.78	-0.08	-0.14	1.02	0.08	0.72	-0.04	0.04	0.09	-0.21	0.03	-0.15	0.01
10	2.03	0.267	0.003	0.071	4.93	1.55	3.56	-0.77	-0.08	-0.05	1.10	0.15	0.58	-0.14	-0.03	0.05	-0.05	0.03	-0.11	-0.02
11	2.29	0.272	0.004	0.073	5.29	1.60	3.59	-0.93	-0.11	-0.02	1.08	0.14	0.61	-0.11	-0.08	0.01	-0.14	0.01	0.17	0.03
12	2.54	0.279	0.005	0.074	5.57	1.77	3.67	-1.01	-0.06	-0.05	1.07	0.12	0.74	-0.13	0.05	0.07	-0.08	0.01	-0.05	0.01
13	2.79	0.285	0.005	0.076	5.39	1.75	3.68	-0.90	0.03	-0.13	0.87	0.14	0.66	-0.08	-0.05	0.05	-0.19	0.00	-0.25	0.02
14	3.30	0.296	0.005	0.077	5.68	1.94	3.77	-1.00	0.04	-0.08	0.99	0.18	0.67	-0.16	0.07	0.02	-0.08	0.00	-0.05	-0.01
15	3.81	0.302	0.005	0.078	5.92	2.03	3.77	-1.13	-0.01	-0.09	1.13	0.22	0.70	-0.23	0.04	0.02	-0.22	0.00	-0.17	0.02
16	4.32	0.315	0.006	0.080	5.74	2.12	3.84	-1.18	0.07	-0.21	0.84	0.15	0.52	-0.17	0.06	0.04	-0.16	-0.02	0.04	0.07
17	4.83	0.323	0.006	0.080	5.81	2.15	4.02	-1.23	0.05	-0.13	0.83	0.21	0.50	-0.23	0.01	0.06	-0.13	-0.03	0.02	0.05
18	5.59	0.334	0.007	0.082	6.11	2.31	4.22	-1.39	0.09	-0.30	0.53	0.19	0.59	-0.04	-0.08	0.10	-0.19	0.01	-0.16	0.06
19	6.35	0.345	0.009	0.083	6.09	2.40	4.24	-1.36	0.15	-0.22	0.40	0.14	0.50	-0.09	-0.04	0.06	-0.21	-0.01	-0.22	0.05
20	7.11	0.359	0.008	0.082	6.35	2.50	4.40	-1.41	0.15	-0.26	0.53	0.09	0.60	0.05	-0.02	-0.01	-0.20	-0.06	-0.19	0.09
21	8.38	0.376	0.009	0.084	6.07	2.56	4.41	-1.43	0.31	-0.42	0.31	0.13	0.50	-0.02	-0.03	-0.01	-0.13	-0.04	-0.13	0.08
22	10.16	0.401	0.012	0.086	6.09	2.57	4.34	-1.43	0.29	-0.34	-0.07	0.02	0.29	0.11	-0.03	0.08	-0.18	-0.03	-0.16	0.08
23	12.70	0.433	0.014	0.086	5.67	2.68	4.56	-1.35	0.16	-0.53	-0.38	0.03	0.37	0.19	0.11	0.03	0.01	-0.01	-0.30	0.01
24	15.24	0.460	0.018	0.087	5.65	2.69	4.37	-1.36	0.55	-0.48	0.17	0.01	0.20	0.09	0.06	0.07	-0.01	0.02	-0.20	0.04
25	17.78	0.488	0.019	0.085	5.19	2.82	4.53	-1.29	0.63	-0.52	-0.30	-0.05	0.19	0.18	0.12	0.08	0.12	0.01	-0.24	0.03
26	20.32	0.509	0.023	0.082	4.97	2.79	4.37	-1.27	0.70	-0.44	-0.52	-0.09	0.11	0.24	0.13	0.08	0.12	0.04	-0.20	0.01
27	22.86	0.530	0.024	0.078	4.79	2.75	4.40	-1.18	0.70	-0.45	-0.18	0.01	0.00	0.10	0.10	0.11	0.05	0.03	-0.29	-0.02
28	25.40	0.547	0.027	0.074	4.60	2.78	4.41	-1.13	0.85	-0.48	-0.18	-0.03	0.10	0.04	0.12	0.10	0.04	-0.01	-0.04	0.01
29	27.94	0.562	0.029	0.069	4.61	2.70	4.29	-1.12	0.85	-0.42	-0.11	-0.06	0.13	0.09	0.26	0.17	0.07	0.08	0.20	0.05
30	30.48	0.579	0.032	0.064	4.48	2.72	4.14	-1.13	0.90	-0.48	-0.27	-0.12	-0.05	0.16	0.31	0.21	0.09	0.12	0.21	-0.02
31	33.02	0.596	0.033	0.057	4.31	2.56	3.85	-1.02	0.85	-0.53	-0.48	-0.19	-0.10	0.24	0.38	0.23	0.11	0.19	0.30	-0.06
32	35.56	0.609	0.038	0.052	4.24	2.55	3.80	-1.04	0.85	-0.62	-0.61	0.27	-0.13	0.30	0.40	0.26	0.12	0.20	0.41	-0.13
33	38.10	0.622	0.040	0.045	3.99	2.40	3.62	-0.96	0.76	-0.64	-0.76	-0.31	-0.15	0.29	0.50	0.34	0.12	0.22	0.39	-0.10
34	40.64	0.638	0.042	0.039	3.65	2.22	3.35	-0.85	0.71	-0.69	-0.91	-0.37	-0.19	0.37	0.51	0.39	0.17	0.29	0.67	-0.12
35	45.72	0.665	0.045	0.024	3.02	1.83	2.50	-0.66	0.52	-0.54	-1.25	-0.37	-0.25	0.43	0.53	0.34	0.34	0.31	0.82	-0.10
36	50.80	0.688	0.046	0.012	1.91	1.38	1.73	-0.49	0.29	-0.32	-1.05	-0.37	-0.21	0.40	0.48	0.29	0.34	0.22	0.76	-0.11
37	55.88	0.705	0.049	0.000	0.64	0.94	0.77	-0.12	0.07	-0.13	-0.20	-0.11	0.15	0.12	0.45	0.07	0.05	0.08	0.05	-0.03
38	60.96	0.708	0.050	-0.002	0.29	0.63	0.57	-0.02	0.02	-0.05	0.11	-0.02	0.37	0.03	0.57	0.00	-0.07	0.01	-0.19	0.00
39	66.04	0.709	0.000	-0.001	0.18	0.00	0.43	0.00	0.00	-0.01	0.09	0.00	0.28	0.00	0.00	0.00	-0.04	0.00	-0.13	0.00
40	71.12	0.709	0.000	0.002	0.15	0.00	0.34	0.00	0.00	0.02	0.08	0.00	0.19	0.00	0.00	0.00	0.00	0.00	-0.02	0.00

Table C.5 Continued.

Case D.S1 Station= 12
X= 304.8mm Tunnel Run#= 770 Ue/Uref= 0.676 Date= 615.88 Time=13.07
Bias Corrected data using 1/sqrt(U*U + V*V + W*W + (.01Ur)^2)

					<-- normalized by 0.001 Ur^2 -->						<---------- normalized by 0.0001 Ur^3 ---------->								
LR	Y(mm)	U/Ur	V/Ur	W/Ur	uu	vv	ww	uv	vw	uw	uuu	uvv	uww	vuu	vvv	vww	wuu	wvv	www	uvw
1	0.00	0.000	0.000	0.000	0.00	0.00	0.00	-0.32	-0.13	0.00	0.00	0.00	0.00	0.00	0.00	0.00	0.00	0.00	0.00	0.00
1	0.25	0.184	-0.002	0.047	4.06	0.62	2.75	-0.40	-0.30	0.12	0.97	0.05	0.71	-0.03	0.01	0.00	-0.14	0.02	-0.12	-0.03
2	0.38	0.194	-0.002	0.049	4.16	0.73	2.92	-0.45	-0.28	0.07	0.80	0.03	0.77	0.02	0.05	-0.02	-0.17	0.03	-0.07	-0.01
3	0.51	0.200	-0.002	0.050	4.31	0.79	3.08	-0.46	-0.26	-0.02	1.04	0.06	0.95	-0.03	-0.03	0.00	-0.27	0.01	-0.54	-0.04
4	0.63	0.207	-0.002	0.052	4.18	0.93	3.27	-0.47	-0.32	-0.04	1.05	0.08	0.94	-0.07	0.06	0.03	-0.26	0.00	-0.78	-0.01
5	0.76	0.212	-0.002	0.053	4.13	0.99	3.13	-0.49	-0.27	-0.08	0.94	0.05	0.75	-0.04	0.10	0.08	-0.25	-0.02	-0.47	0.01
6	1.02	0.221	-0.003	0.055	4.19	1.13	3.24	-0.59	-0.27	-0.04	0.90	0.07	0.84	-0.03	0.09	0.03	-0.32	0.02	-0.42	-0.04
7	1.27	0.227	-0.002	0.058	4.32	1.22	3.25	-0.59	-0.25	-0.08	1.03	0.11	0.95	-0.05	0.09	0.01	-0.30	-0.01	-0.54	-0.01
8	1.52	0.233	-0.002	0.060	4.27	1.33	3.30	-0.67	-0.26	-0.14	1.07	0.13	0.88	-0.07	0.03	0.07	-0.27	-0.01	-0.50	-0.03
9	1.78	0.237	-0.002	0.060	4.36	1.35	3.23	-0.70	-0.16	-0.20	0.92	0.13	0.70	-0.13	-0.07	0.04	-0.18	-0.01	-0.32	-0.02
10	2.03	0.242	-0.002	0.061	4.54	1.48	3.26	-0.75	-0.16	-0.15	1.09	0.08	0.83	-0.11	0.04	-0.02	-0.33	0.00	-0.47	0.03
11	2.29	0.247	-0.002	0.061	4.53	1.47	3.36	-0.73	-0.18	-0.24	1.02	0.12	0.75	-0.09	-0.04	0.06	-0.24	0.01	-0.48	-0.02
12	2.54	0.250	-0.002	0.063	4.75	1.55	3.32	-0.76	-0.21	-0.07	0.94	0.14	0.59	-0.13	-0.07	0.04	-0.16	-0.02	-0.32	0.03
13	2.79	0.256	-0.002	0.063	4.68	1.64	3.35	-0.88	-0.18	-0.14	0.97	0.16	0.62	-0.21	0.02	0.01	-0.15	0.00	-0.45	-0.01
14	3.30	0.263	-0.002	0.066	4.81	1.73	3.46	-0.90	-0.11	-0.25	1.06	0.16	0.77	-0.12	-0.10	-0.01	-0.31	-0.01	-0.52	0.01
15	3.81	0.269	-0.002	0.066	5.15	1.84	3.66	-0.99	-0.13	-0.42	1.12	0.18	0.98	-0.15	-0.11	0.00	-0.45	0.00	-0.82	-0.01
16	4.32	0.277	-0.002	0.067	5.09	1.97	3.68	-1.00	-0.12	-0.28	1.01	0.19	0.88	-0.13	0.04	0.04	-0.31	0.01	-0.64	0.03
17	4.83	0.284	-0.002	0.069	5.32	2.06	3.74	-1.08	-0.08	-0.32	0.87	0.19	0.78	-0.11	-0.16	0.00	-0.32	-0.03	-0.51	0.03
18	5.59	0.294	-0.001	0.069	5.36	2.11	3.82	-1.16	-0.04	-0.34	0.54	0.17	0.66	-0.06	-0.10	0.04	-0.30	-0.03	-0.54	-0.01
19	6.35	0.303	-0.001	0.071	5.66	2.23	3.83	-1.18	0.05	-0.32	0.82	0.20	0.87	-0.20	0.07	-0.05	-0.34	-0.01	-0.65	0.01
20	7.11	0.313	-0.001	0.071	5.63	2.29	4.06	-1.22	0.09	-0.48	0.63	0.14	0.86	-0.13	0.02	-0.01	-0.35	0.02	-0.62	0.02
21	8.38	0.329	0.000	0.073	5.79	2.40	4.11	-1.27	0.03	-0.44	0.52	0.18	0.73	-0.14	0.11	-0.05	-0.19	-0.04	-0.64	0.02
22	10.16	0.345	0.001	0.075	6.03	2.42	4.32	-1.41	0.14	-0.53	0.56	0.07	0.87	-0.09	0.00	0.03	-0.38	0.01	-1.19	0.04
23	12.70	0.375	0.003	0.076	6.01	2.46	4.28	-1.49	0.22	-0.49	-0.06	0.06	0.49	0.01	0.02	0.00	-0.20	0.03	-0.50	0.00
24	15.24	0.405	0.003	0.078	5.98	2.63	4.34	-1.43	0.26	-0.50	-0.42	-0.02	0.50	0.16	0.05	0.08	-0.03	0.02	-0.53	-0.02
25	17.78	0.429	0.006	0.079	5.69	2.52	4.26	-1.38	0.37	-0.44	-0.33	-0.02	0.26	0.11	0.14	0.08	-0.10	0.01	-0.23	-0.02
26	20.32	0.456	0.007	0.077	5.49	2.55	4.26	-1.45	0.43	-0.60	-0.27	-0.12	0.28	0.19	0.15	0.16	0.02	0.05	-0.34	-0.03
27	22.86	0.477	0.009	0.077	5.27	2.45	4.23	-1.26	0.48	-0.58	-0.54	-0.05	0.30	0.18	0.24	0.07	-0.06	0.08	-0.31	0.00
28	25.40	0.497	0.010	0.074	4.76	2.49	4.18	-1.09	0.56	-0.52	-0.43	-0.03	0.36	0.13	0.09	0.13	-0.06	0.04	-0.20	0.04
29	27.94	0.517	0.013	0.070	4.42	2.48	3.90	-1.17	0.53	-0.39	-0.41	-0.13	0.10	0.23	0.23	0.12	0.09	0.09	-0.17	-0.03
30	30.48	0.535	0.014	0.065	4.40	2.45	3.81	-1.10	0.59	-0.49	-0.54	-0.13	0.02	0.26	0.12	0.22	0.04	0.02	0.02	-0.04
31	33.02	0.551	0.016	0.061	4.03	2.25	3.66	-0.96	0.56	-0.39	-0.36	-0.11	0.09	0.22	0.17	0.17	0.07	0.11	0.01	-0.03
32	35.56	0.564	0.019	0.056	4.00	2.19	3.51	-0.97	0.50	-0.53	-0.47	-0.17	0.12	0.18	0.21	0.19	-0.06	0.13	-0.08	-0.03
33	38.10	0.581	0.022	0.051	3.83	2.13	3.31	-0.93	0.55	-0.45	-0.43	-0.17	0.04	0.19	0.26	0.21	-0.01	0.15	0.25	-0.05
34	40.64	0.595	0.023	0.046	3.62	2.05	3.13	-0.90	0.51	-0.54	-0.77	-0.19	-0.02	0.24	0.25	0.16	0.02	0.14	0.11	-0.03
35	45.72	0.619	0.025	0.035	3.05	1.76	2.57	-0.72	0.42	-0.51	-0.91	-0.27	-0.08	0.33	0.34	0.22	0.13	0.20	0.36	-0.09
36	50.80	0.645	0.027	0.023	2.24	1.46	1.92	-0.48	0.33	-0.51	-0.98	-0.29	-0.21	0.31	0.41	0.25	0.27	0.22	0.41	-0.11
37	55.88	0.668	0.031	0.010	0.99	1.13	1.05	-0.20	0.16	-0.24	-0.41	-0.15	0.00	0.15	0.20	0.13	0.10	0.11	0.13	-0.06
38	60.96	0.676	0.034	0.006	0.44	0.82	0.56	-0.10	0.07	-0.13	-0.09	-0.08	0.05	0.08	0.13	0.07	0.02	0.07	0.05	-0.03
39	66.04	0.680	0.000	0.003	0.25	0.00	0.37	0.00	0.00	-0.05	0.01	0.00	0.12	0.00	0.00	0.00	-0.02	0.00	-0.07	0.00
40	71.12	0.680	0.000	0.002	0.21	0.00	0.51	0.00	0.00	-0.16	0.14	0.00	0.41	0.00	0.00	0.00	-0.20	0.00	-0.58	0.00

Table C.5 Continued.

Case B.S0 Station= 1
X=-457.2mm Tunnel Run#= 688 Ue/Uref= 0.999 Date= 510.88 Time=11.45
Bias Corrected data using 1/sqrt(U*U + V*V + W*W + (.01Ur)^2)
The Y-position has been corrected by adding 0.254 to each measured Y-position in this profile.

					<-- normalized by 0.001 Ur^2 -->						<---------- normalized by 0.0001 Ur^3 ---------->									
LR	Y(mm)	U/Ur	V/Ur	W/Ur	uu	vv	ww	uv	vw	uw	uuu	uvv	uww	vuu	vvv	vww	wuu	wvv	www	uvw
1	0.00	0.000	0.000	0.000	0.00	0.00	0.00	-1.60	0.00	0.00	0.00	0.00	0.00	0.00	0.00	0.00	0.00	0.00	0.00	0.00
1	0.51	0.583	-0.001	0.008	8.78	1.62	5.98	-1.40	-0.35	-0.52	-1.49	-0.16	-0.15	0.60	0.02	0.15	0.13	-0.04	0.33	0.04
2	0.63	0.608	0.000	0.006	8.03	1.92	5.62	-1.49	-0.33	-0.44	-1.32	-0.18	-0.15	0.58	0.14	0.14	0.16	-0.03	0.08	0.02
3	0.76	0.627	-0.001	0.002	7.19	1.93	5.33	-1.34	-0.32	-0.43	-0.44	-0.11	-0.08	0.27	0.07	0.11	0.06	-0.03	-0.21	0.04
4	0.89	0.644	0.000	0.006	6.79	2.06	5.09	-1.39	-0.32	-0.35	-0.41	-0.17	-0.11	0.31	0.26	0.20	-0.08	-0.07	-0.24	0.07
5	1.02	0.651	0.000	0.003	7.03	2.14	4.95	-1.55	-0.32	-0.29	-0.56	-0.24	0.03	0.47	0.22	0.13	-0.04	-0.01	-0.32	0.00
6	1.27	0.674	-0.001	0.003	6.32	2.24	4.65	-1.50	-0.26	-0.36	-0.13	-0.11	0.02	0.24	0.19	0.15	-0.02	-0.02	-0.24	0.01
7	1.52	0.692	-0.001	0.002	5.97	2.24	4.26	-1.48	-0.22	-0.23	-0.15	-0.17	-0.11	0.19	0.28	0.17	-0.05	-0.07	-0.09	0.01
8	1.78	0.707	-0.001	0.003	5.82	2.23	4.11	-1.48	-0.25	-0.12	-0.32	-0.15	-0.05	0.28	0.19	0.13	-0.20	-0.05	-0.12	0.06
9	2.03	0.724	-0.001	0.002	5.58	2.27	3.78	-1.52	-0.17	-0.11	-0.41	-0.18	-0.02	0.31	0.20	0.14	0.03	0.01	-0.17	0.00
10	2.29	0.738	-0.002	0.003	5.54	2.17	3.64	-1.42	-0.08	-0.15	-0.57	-0.15	-0.11	0.30	0.17	0.14	0.02	-0.02	-0.11	-0.01
11	2.54	0.748	-0.001	0.004	5.37	2.18	3.59	-1.44	-0.19	-0.11	-0.38	-0.16	-0.06	0.23	0.17	0.10	-0.06	-0.04	-0.25	0.03
12	2.79	0.762	-0.003	0.001	5.02	2.08	3.41	-1.35	-0.10	-0.02	-0.69	-0.09	-0.15	0.20	0.14	0.09	-0.09	-0.01	-0.01	0.03
13	3.05	0.771	-0.002	0.002	4.84	2.04	3.42	-1.31	-0.07	-0.19	-0.49	-0.12	-0.14	0.18	0.13	0.16	-0.01	-0.01	0.00	0.02
14	3.56	0.788	-0.002	0.001	4.53	1.98	3.17	-1.26	-0.09	-0.07	-0.64	-0.16	-0.11	0.24	0.23	0.13	0.03	0.02	-0.10	0.01
15	4.06	0.815	-0.003	0.001	4.30	1.94	3.21	-1.24	-0.09	-0.11	-0.68	-0.17	-0.07	0.26	0.18	0.07	-0.02	-0.02	-0.24	0.00
16	4.57	0.831	-0.002	0.002	3.89	1.87	2.93	-1.13	-0.14	0.03	-0.62	-0.17	-0.16	0.22	0.25	0.10	-0.03	0.01	-0.12	0.03
17	5.08	0.847	-0.003	0.001	3.61	1.76	2.83	-1.06	-0.12	0.02	-0.60	-0.17	-0.21	0.21	0.19	0.15	-0.01	-0.02	-0.12	0.01
18	5.84	0.872	-0.003	0.003	3.33	1.59	2.53	-1.01	-0.12	-0.06	-0.84	-0.23	-0.21	0.29	0.27	0.08	0.03	-0.01	0.02	0.02
19	6.60	0.892	-0.003	0.001	2.88	1.46	2.16	-0.84	-0.04	-0.03	-0.78	-0.24	-0.26	0.27	0.34	0.14	0.02	-0.01	-0.08	0.00
20	7.37	0.913	-0.003	0.002	2.45	1.29	1.83	-0.76	-0.04	-0.04	-0.75	-0.24	-0.21	0.29	0.24	0.11	0.03	-0.01	-0.05	-0.01
21	8.64	0.944	-0.003	0.001	1.76	0.93	1.32	-0.52	-0.05	0.02	-0.61	-0.18	-0.21	0.23	0.19	0.13	0.01	0.01	-0.03	0.00
22	10.41	0.975	-0.002	0.003	0.87	0.57	0.67	-0.25	-0.01	-0.02	-0.39	-0.12	-0.11	0.14	0.11	0.07	0.01	0.00	0.02	0.00
23	12.95	0.996	-0.003	0.002	0.15	0.21	0.22	-0.02	0.01	-0.02	-0.03	-0.01	0.00	0.01	0.03	0.01	0.01	0.00	0.02	0.00
24	15.49	0.998	-0.003	0.002	0.07	0.11	0.15	0.00	0.00	-0.01	0.00	0.00	0.00	0.00	0.00	0.00	0.00	0.00	0.01	0.00
25	18.03	0.998	-0.004	0.002	0.05	0.11	0.13	0.00	0.00	-0.01	0.00	0.00	0.00	0.00	0.10	0.00	0.00	0.01	0.00	0.00
26	20.57	0.997	-0.004	0.001	0.05	0.08	0.14	0.00	0.00	-0.01	0.00	0.00	0.01	0.00	0.00	0.00	0.00	0.00	0.01	0.00
27	23.11	0.999	-0.004	0.000	0.05	0.09	0.14	0.00	0.00	-0.01	0.00	0.00	0.01	0.00	0.00	0.00	0.00	0.00	0.00	0.00
28	25.65	0.999	-0.004	-0.001	0.05	0.08	0.14	0.00	0.00	-0.01	0.00	0.00	0.00	0.00	0.00	0.00	0.00	0.00	0.01	0.00
29	28.19	1.001	-0.004	-0.001	0.05	0.09	0.14	0.00	0.00	-0.01	0.00	0.00	0.00	0.00	0.00	0.00	0.00	0.00	0.01	0.00
30	30.73	1.001	-0.005	-0.003	0.05	0.12	0.13	0.00	0.00	-0.01	0.00	0.00	0.00	0.00	0.17	0.00	0.00	0.00	0.01	0.00
31	33.27	1.002	-0.004	-0.002	0.06	0.08	0.16	0.00	0.00	0.01	0.00	0.00	0.01	0.00	0.00	0.00	0.00	0.00	0.01	0.00
32	35.81	0.997	-0.004	-0.003	0.05	0.08	0.12	0.00	0.00	-0.01	0.00	0.00	0.00	0.00	0.00	0.00	0.00	0.00	0.00	0.00
33	38.35	0.998	-0.003	-0.003	0.05	0.09	0.12	0.00	0.00	-0.01	0.00	0.00	0.00	0.00	0.00	0.00	0.00	0.00	0.00	0.00
34	40.89	0.999	-0.003	-0.002	0.04	0.09	0.12	0.00	0.00	-0.01	0.00	0.00	0.00	0.00	0.00	0.00	0.00	0.00	0.00	0.00
35	45.97	1.000	-0.003	0.000	0.04	0.09	0.11	0.00	0.00	-0.01	0.00	0.00	0.00	0.00	0.00	0.00	0.00	0.00	0.00	0.00
36	51.05	1.001	0.004	0.001	0.05	0.48	0.14	0.00	0.00	-0.01	0.00	0.00	0.00	0.00	0.04	0.00	0.00	0.00	0.01	0.00
37	56.13	1.001	0.004	0.000	0.05	0.48	0.12	0.00	0.00	-0.01	0.00	0.00	0.00	0.00	0.00	0.00	0.00	0.00	0.00	0.00
38	61.21	1.002	0.000	-0.004	0.05	0.00	0.12	0.00	0.00	-0.01	0.00	0.00	0.00	0.00	0.00	0.00	0.00	0.00	0.00	0.00
39	66.29	1.001	0.000	-0.004	0.05	0.00	0.12	0.00	0.00	0.00	0.00	0.00	0.00	0.00	0.00	0.00	0.00	0.00	0.00	0.00

Table C.5 Continued.

Case B.S0 Station= 2
X=-330.2mm Tunnel Run#= 600 Ue/Uref= 0.994 Date= 314.88 Time=14.43
Bias Corrected data using 1/sqrt(U*U + V*V + W*W + (.01Ur)^2)
The Y-position has been corrected by adding 0.203 to each measured Y-position in this profile.

					<-- normalized by 0.001 Ur^2 -->						<---------- normalized by 0.0001 Ur^3 ---------->									
LR	Y(mm)	U/Ur	V/Ur	W/Ur	uu	vv	ww	uv	vw	uw	uuu	uvv	uww	vuu	vvv	vww	wuu	wvv	www	uvw
1	0.00	0.000	0.000	0.000	0.00	0.00	0.00	-1.58	0.00	0.00	0.00	0.00	0.00	0.00	0.00	0.00	0.00	0.00	0.00	0.00
1	0.46	0.563	0.023	-0.005	9.93	3.17	7.55	-1.10	-0.48	0.21	-2.19	-0.12	-0.74	0.59	-0.11	0.51	0.29	-0.06	-0.80	0.04
2	0.58	0.593	0.024	-0.004	8.70	3.37	6.55	-1.13	-0.30	-0.51	-1.05	-0.13	1.67	0.55	-0.04	0.56	-0.82	0.43	-0.40	0.05
3	0.71	0.617	0.008	-0.003	8.20	2.24	5.97	-1.41	-0.33	-0.46	-0.91	-0.05	1.37	0.44	0.00	0.39	-0.44	-0.19	-0.66	-0.10
4	0.84	0.634	0.009	-0.004	7.94	2.40	5.93	-1.46	-0.32	-0.45	-0.68	-0.03	1.25	0.55	0.19	0.45	-0.33	-0.04	-1.82	-0.10
5	0.97	0.650	0.008	0.000	7.16	2.42	5.39	-1.48	-0.26	-0.32	-0.36	-0.45	1.01	0.36	0.18	0.24	-0.46	0.09	0.40	-0.01
6	1.22	0.675	0.007	-0.003	6.88	2.43	4.96	-1.42	-0.26	-0.28	-0.15	-0.20	0.52	0.27	0.11	0.32	-0.11	-0.12	-0.03	0.00
7	1.47	0.693	0.009	-0.001	6.51	2.48	4.64	-1.44	-0.23	-0.20	-0.25	-0.28	0.54	0.41	0.16	0.22	-0.05	-0.01	-0.11	-0.01
8	1.73	0.710	0.008	-0.001	6.40	2.44	4.48	-1.44	-0.22	-0.13	-0.65	-0.36	0.27	0.33	0.16	0.41	-0.10	-0.13	-0.13	0.04
9	1.98	0.727	0.008	-0.001	6.21	2.35	4.23	-1.41	-0.23	-0.08	-0.69	-0.18	0.10	0.34	0.15	0.22	0.03	-0.15	-0.08	-0.01
10	2.24	0.739	0.009	0.000	5.86	2.39	4.31	-1.38	-0.08	-0.09	-0.83	-0.27	0.06	0.33	0.13	0.25	0.11	0.12	0.03	-0.04
11	2.49	0.751	0.007	0.000	5.70	2.39	4.16	-1.36	-0.08	-0.20	-0.69	-0.25	-0.09	0.25	0.16	0.16	0.18	-0.07	0.06	0.00
12	2.74	0.764	0.010	0.000	5.50	2.35	4.05	-1.30	-0.15	-0.06	-0.74	-0.11	-0.09	0.30	0.13	0.15	0.20	-0.12	0.15	0.03
13	3.00	0.775	0.010	-0.001	5.25	2.29	3.93	-1.29	-0.11	-0.05	-0.77	-0.22	0.00	0.31	0.16	0.12	0.03	0.14	0.10	0.03
14	3.51	0.796	0.009	0.000	4.84	2.22	3.64	-1.24	-0.17	-0.06	-0.86	-0.23	-0.14	0.25	0.18	0.15	0.14	0.01	0.05	0.01
15	4.01	0.811	0.009	0.000	4.56	2.08	3.48	-1.15	-0.06	-0.04	-0.80	-0.18	-0.22	0.28	0.21	0.20	0.09	-0.02	-0.07	0.01
16	4.52	0.830	0.010	-0.001	4.32	2.09	3.24	-1.05	-0.11	-0.05	-0.97	-0.08	-0.09	0.28	0.15	0.12	0.09	0.01	0.09	0.02
17	5.03	0.847	0.009	0.001	3.97	2.01	3.03	-1.02	-0.07	-0.08	-0.93	-0.24	-0.27	0.29	0.22	0.18	-0.04	-0.01	-0.07	0.04
18	5.79	0.867	0.009	0.001	3.60	1.80	2.77	-0.96	0.01	-0.10	-0.74	-0.23	-0.22	0.26	0.17	0.18	0.00	0.05	0.05	0.05
19	6.55	0.889	0.012	0.000	3.14	1.71	2.65	-0.82	-0.08	-0.14	-0.64	-0.22	-0.25	0.24	0.20	0.12	0.03	-0.07	0.03	0.03
20	7.32	0.906	0.013	0.000	2.90	1.53	2.30	-0.74	-0.06	-0.14	-0.74	-0.20	-0.24	0.24	0.18	0.16	0.01	-0.07	0.05	0.01
21	8.59	0.935	0.011	-0.001	2.14	1.26	1.74	-0.57	0.02	-0.13	-0.70	-0.26	-0.21	0.25	0.15	0.09	0.00	0.00	0.01	0.01
22	10.36	0.968	0.011	-0.003	1.18	0.92	1.14	-0.34	0.01	-0.11	-0.49	-0.21	-0.16	0.20	0.14	0.09	0.00	0.03	-0.03	0.00
23	12.90	0.988	0.007	-0.003	0.30	0.48	0.70	-0.03	0.01	-0.13	-0.01	-0.01	0.00	0.01	0.00	0.01	0.00	-0.02	-0.01	0.00
24	15.44	0.992	0.007	-0.003	0.23	0.39	0.66	0.00	0.01	-0.12	0.00	0.00	0.00	0.00	0.00	0.00	0.00	0.02	-0.01	0.00
25	17.98	0.993	0.006	-0.007	0.23	0.40	0.65	0.01	0.00	-0.14	0.00	0.01	-0.02	0.00	-0.01	0.00	0.01	0.00	0.01	0.00
26	20.52	0.992	0.005	-0.006	0.22	0.38	0.68	0.00	-0.01	-0.14	0.00	0.00	-0.01	0.00	0.00	0.00	0.00	-0.03	0.01	0.00
27	23.06	0.992	0.004	-0.006	0.23	0.37	0.66	0.00	0.00	-0.13	0.00	-0.01	0.00	0.00	0.00	0.00	0.00	-0.01	0.00	0.00
28	25.60	0.994	0.003	-0.007	0.23	0.38	0.65	0.01	0.01	-0.14	0.00	0.00	-0.02	0.00	-0.01	-0.01	0.01	0.01	0.00	0.00
29	35.76	0.998	0.005	-0.004	0.22	0.38	0.62	0.00	0.00	-0.12	0.00	0.00	-0.01	0.00	0.00	0.01	0.00	0.00	0.00	0.00
30	45.92	1.000	0.007	-0.004	0.21	0.37	0.60	0.00	0.01	-0.11	0.00	-0.02	0.00	0.00	0.00	0.00	0.00	0.03	-0.01	0.00

Table C.5 Continued.

Case B.S0 Station= 3
X=-228.6mm Tunnel Run#= 622 Ue/Uref= 0.987 Date= 329.88 Time=12.52
Bias Corrected data using 1/sqrt(U*U + V*V + W*W + (.01Ur)^2)
The Y-position has been corrected by adding 0.127 to each measured Y-position in this profile.

					<-- normalized by 0.001 Ur^2 -->						<---------- normalized by 0.0001 Ur^3 ---------->									
LR	Y(mm)	U/Ur	V/Ur	W/Ur	uu	vv	ww	uv	vw	uw	uuu	uvv	uww	vuu	vvv	vww	wuu	wvv	www	uvw
39	2.67	0.725	0.008	0.004	6.68	2.22	3.70	-1.60	-0.05	-0.25	-0.62	-0.20	-0.03	0.30	0.15	0.11	-0.06	0.04	-0.03	-0.01
40	6.48	0.861	0.010	0.003	3.80	1.57	2.35	-1.04	0.03	-0.11	-1.17	-0.36	-0.28	0.45	0.24	0.13	0.05	0.02	-0.01	-0.02
41	12.83	0.973	0.018	0.000	0.29	0.28	0.30	-0.07	0.01	-0.01	-0.06	-0.04	-0.02	0.05	0.02	0.01	0.01	0.00	-0.01	0.00
42	19.18	0.982	0.021	-0.001	0.07	0.09	0.14	0.00	0.00	-0.01	0.00	0.00	0.01	0.00	0.00	0.00	0.01	0.00	0.00	0.00
43	25.53	0.985	0.027	0.002	0.06	0.08	0.14	0.00	0.00	-0.01	0.00	0.00	0.01	0.00	0.00	0.00	0.01	0.00	0.00	0.00
44	38.23	0.984	0.043	0.006	0.08	0.08	0.14	0.00	0.00	-0.01	0.00	0.00	0.01	0.00	0.00	0.00	0.01	0.00	0.00	0.00
45	50.93	0.997	0.033	0.003	0.06	0.08	0.14	0.00	0.00	-0.02	0.00	0.00	0.01	0.00	0.00	0.00	0.00	0.00	0.00	0.00

Table C.5 Continued.

Case B.S0 Station= 4
X=-152.4mm Tunnel Run#= 621 Ue/Uref= 0.911 Date= 329.88 Time=11.35
Bias Corrected data using 1/sqrt(U*U + V*V + W*W + (.01Ur)^2)
The Y-position has been corrected by adding 0.127 to each measured Y-position in this profile.

					<-- normalized by 0.001 Ur^2 -->						<---------- normalized by 0.0001 Ur^3 ---------->								
LR	Y(mm)	U/Ur	V/Ur	W/Ur	uu	vv	ww	uv	vw	uw	uuu	uvv	uww	vuu	vvv	vww	wuu	wvv	www	uvw
37	2.67	0.591	0.010	-0.020	6.48	2.39	3.89	-1.51	-0.06	-0.01	0.33	-0.07	0.04	0.06	0.05	0.14	0.03	-0.02	-0.15	0.02
38	6.48	0.722	0.019	-0.018	5.14	2.01	3.22	-1.24	-0.08	0.02	-0.70	-0.21	-0.26	0.29	0.22	0.15	0.05	-0.01	-0.13	0.00
39	12.83	0.868	0.028	-0.016	1.73	0.81	1.04	-0.46	-0.01	0.03	-0.80	-0.24	-0.20	0.31	0.18	0.09	-0.02	0.00	0.00	0.00
40	19.18	0.911	0.029	-0.016	0.09	0.13	0.16	0.00	0.00	0.00	0.00	0.00	0.01	0.00	0.00	0.00	0.00	0.00	0.00	0.00
41	25.53	0.909	0.029	-0.016	0.06	0.09	0.16	0.00	0.00	-0.01	0.00	0.00	0.01	0.00	0.00	0.00	0.01	0.00	0.00	0.00
42	38.23	0.912	0.046	-0.012	0.06	0.09	0.17	0.00	0.01	-0.01	0.00	0.00	0.01	0.00	0.00	0.00	0.01	0.00	0.00	0.00

Table C.5 Continued.

Case B.S0 Station= 5
X= -76.2mm Tunnel Run#= 620 Ue/Uref= 0.831 Date= 328.88 Time=18.00
Bias Corrected data using 1/sqrt(U*U + V*V + W*W + (.01Ur)^2)
The Y-position has been corrected by adding 0.127 to each measured Y-position in this profile.

				<-- normalized by 0.001 Ur^2 -->						<---------- normalized by 0.0001 Ur^3 ---------->								
LR	Y(mm)	U/Ur	V/Ur	W/Ur	uu	vv	ww	uv	vw	uw	uuu	uvv	uww	vuu	vvv	vww	wuu	wvv	www	uvw
41	2.67	0.449	0.009	-0.025	6.76	2.37	3.61	-1.50	-0.03	-0.02	0.46	0.00	0.25	0.10	-0.01	0.01	0.05	0.03	0.15	-0.01
42	6.48	0.569	0.015	-0.025	6.64	2.33	3.61	-1.59	-0.03	-0.01	-0.60	-0.10	-0.09	0.15	0.17	0.04	0.14	-0.02	0.11	-0.02
43	12.83	0.727	0.029	-0.028	3.99	1.47	2.20	-0.97	0.02	0.07	-1.57	-0.39	-0.35	0.47	0.33	0.16	-0.08	-0.01	-0.07	0.02
44	19.18	0.823	0.036	-0.030	0.52	0.38	0.40	-0.12	0.00	0.00	-0.21	-0.08	-0.01	0.08	0.06	0.03	0.00	0.00	0.00	0.00
45	25.53	0.834	0.040	-0.031	0.08	0.11	0.15	0.00	0.00	0.01	0.00	0.00	0.03	0.00	0.00	0.00	0.00	0.00	0.00	0.00
46	38.23	0.832	0.049	-0.030	0.06	0.09	0.16	0.00	0.01	0.00	0.00	0.00	0.01	0.00	0.00	0.00	0.01	0.00	0.00	0.00
47	50.93	0.828	0.067	-0.026	0.07	0.10	0.18	0.00	0.01	-0.01	0.00	0.00	0.04	0.00	0.00	0.00	-0.01	0.00	0.00	0.00

Table C.5 Continued.

Case B.S0 Station= 6
X= -12.7mm Tunnel Run#= 619 Ue/Uref= 0.780 Date= 328.88 Time=16.05
Bias Corrected data using 1/sqrt(U*U + V*V + W*W + (.01Ur)^2)
The Y-position has been corrected by adding 0.127 to each measured Y-position in this profile.

					<-- normalized by 0.001 Ur^2 -->						<---------- normalized by 0.0001 Ur^3 ---------->									
LR	Y(mm)	U/Ur	V/Ur	W/Ur	uu	vv	ww	uv	vw	uw	uuu	uvv	uww	vuu	vvv	vww	wuu	wvv	www	uvw
41	2.67	0.332	0.004	0.003	6.21	2.01	3.60	-1.10	-0.17	-0.46	1.26	0.21	0.35	-0.17	-0.16	0.06	-0.14	-0.04	-0.04	-0.01
42	6.48	0.430	0.009	0.012	7.19	2.67	3.92	-1.50	-0.12	-0.66	0.46	0.03	0.16	-0.01	0.00	0.02	-0.04	0.03	-0.06	-0.08
43	12.83	0.584	0.020	0.014	6.25	2.19	3.30	-1.27	-0.15	-0.71	-1.76	-0.29	-0.28	0.42	0.19	0.10	0.29	0.07	0.19	-0.02
44	19.18	0.714	0.030	0.013	2.96	1.10	1.55	-0.58	-0.04	-0.34	-1.48	-0.32	-0.32	0.41	0.19	0.10	0.19	0.03	0.14	0.00
45	25.53	0.776	0.038	0.011	0.35	0.32	0.36	-0.07	0.03	-0.02	-0.11	-0.05	-0.03	0.06	0.04	0.02	0.04	0.01	0.03	-0.01
46	38.23	0.782	0.044	0.021	0.10	0.10	0.18	0.00	-0.03	0.04	0.00	0.00	0.03	0.00	0.00	0.00	0.01	0.00	0.00	0.00
47	50.93	0.779	0.050	0.022	0.11	0.10	0.20	0.01	-0.03	0.02	0.00	0.00	0.01	0.00	0.00	0.00	0.00	0.00	0.01	0.00

Table C.5 Continued.

Case B.S0 Station= 7
X= 12.7mm Tunnel Run#= 618 Ue/Uref= 0.770 Date= 328.88 Time=13.09
Bias Corrected data using 1/sqrt(U*U + V*V + W*W + (.01Ur)^2)
The Y-position has been corrected by adding 0.127 to each measured Y-position in this profile.

					<-- normalized by 0.001 Ur^2 -->						<---------- normalized by 0.0001 Ur^3 ---------->									
LR	Y(mm)	U/Ur	V/Ur	W/Ur	uu	vv	ww	uv	vw	uw	uuu	uvv	uww	vuu	vvv	vww	wuu	wvv	www	uvw
43	2.67	0.303	0.007	-0.007	5.97	2.02	3.42	-1.01	-0.13	-0.45	1.01	0.26	0.57	-0.20	-0.16	0.05	-0.29	-0.06	-0.13	0.05
44	6.48	0.393	0.009	0.000	6.94	2.65	3.98	-1.55	-0.14	-0.65	1.00	0.16	0.21	-0.13	-0.08	0.03	-0.22	-0.02	-0.06	0.03
45	12.83	0.543	0.016	0.007	6.87	2.39	3.75	-1.47	-0.16	-0.68	-1.21	-0.24	-0.31	0.40	0.19	0.14	0.21	0.02	0.03	-0.11
46	25.53	0.751	0.035	0.007	0.78	0.50	0.57	-0.16	0.02	-0.10	-0.35	-0.12	-0.08	0.14	0.09	0.04	0.12	0.02	0.05	-0.01
47	38.23	0.769	0.041	0.015	0.14	0.11	0.21	0.01	-0.03	0.00	0.00	0.00	0.08	0.00	0.00	0.00	-0.02	0.00	0.00	0.00
48	50.93	0.771	0.043	0.016	0.14	0.10	0.24	0.02	-0.03	0.02	0.00	0.00	0.04	0.00	0.00	0.00	0.00	0.00	0.01	0.00

Table C.5 Continued.

Case B.S0 Station= 8
X= 152.4mm Tunnel Run#= 608 Ue/Uref= 0.710 Date= 323.88 Time=14.22
Bias Corrected data using 1/sqrt(U*U + V*V + W*W + (.01Ur)^2)
The Y-position has been corrected by adding 0.102 to each measured Y-position in this profile.

				<-- normalized by 0.001 Ur^2 -->						<---------- normalized by 0.0001 Ur^3 ---------->									
LR	Y(mm)	U/Ur	V/Ur	W/Ur	uu	vv	ww	uv	vw	uw	uuu	uvv	uww	vuu	vvv	vww	wuu	wvv	www	uvw
1	0.00	0.000	0.000	0.000	0.00	0.00	0.00	-0.17	0.00	0.00	0.00	0.00	0.00	0.00	0.00	0.00	0.00	0.00	0.00	0.00
1	0.36	0.095	0.008	-0.016	3.82	0.50	2.90	-0.03	-0.02	-0.30	2.00	0.03	2.32	-0.05	-0.02	0.01	-0.69	-0.01	-1.85	0.00
2	0.48	0.115	0.008	-0.018	4.25	0.62	2.72	-0.08	-0.02	0.20	1.48	0.06	1.00	-0.07	-0.02	-0.01	0.00	0.00	-0.26	-0.01
3	0.61	0.131	0.004	-0.022	4.95	0.45	3.00	-0.22	-0.05	0.29	1.49	0.06	1.14	-0.11	-0.04	0.02	0.00	-0.02	-0.28	-0.01
4	0.74	0.139	0.005	-0.022	5.02	0.56	3.18	-0.29	-0.05	0.37	1.41	0.08	1.09	-0.12	-0.05	0.02	0.05	-0.02	-0.25	-0.02
5	0.86	0.146	0.005	-0.023	5.16	0.68	3.40	-0.29	-0.06	0.35	1.09	0.08	1.12	-0.10	-0.06	0.01	-0.01	-0.01	-0.12	-0.03
6	1.12	0.160	0.005	-0.023	5.28	0.90	3.56	-0.38	-0.06	0.45	1.17	0.07	1.07	-0.09	-0.07	0.01	0.15	0.00	-0.29	-0.03
7	1.37	0.170	0.004	-0.025	5.60	1.04	3.58	-0.46	-0.09	0.54	1.33	0.10	1.05	-0.11	-0.13	-0.01	0.08	-0.01	-0.05	0.01
8	1.63	0.179	0.004	-0.024	5.76	1.17	3.86	-0.46	-0.07	0.66	1.13	0.10	1.12	-0.10	-0.12	0.02	0.00	-0.05	-0.26	0.01
9	1.88	0.186	0.006	-0.025	5.81	1.28	3.92	-0.54	-0.08	0.63	1.09	0.12	1.06	-0.15	-0.12	-0.01	-0.16	-0.04	-0.18	0.00
10	2.13	0.184	0.007	-0.026	6.05	1.41	3.85	-0.56	-0.06	0.60	1.30	0.16	1.17	-0.13	-0.15	0.00	-0.11	-0.08	-0.15	0.02
11	2.39	0.192	0.006	-0.026	5.93	1.54	3.92	-0.62	-0.09	0.52	0.94	0.16	0.93	-0.14	-0.20	-0.05	-0.27	-0.07	-0.31	0.01
12	2.64	0.197	0.006	-0.026	6.36	1.59	3.97	-0.74	-0.09	0.80	0.88	0.12	1.02	-0.12	-0.14	0.04	-0.08	-0.05	-0.05	0.07
13	2.90	0.204	0.006	-0.026	6.51	1.69	4.21	-0.76	-0.10	0.70	0.93	0.18	1.18	-0.17	-0.19	0.00	0.07	-0.05	-0.47	0.06
14	3.40	0.210	0.007	-0.026	6.81	1.82	4.17	-0.77	-0.04	0.72	0.89	0.14	0.96	-0.14	-0.16	-0.02	-0.12	-0.07	-0.19	0.06
15	3.91	0.218	0.007	-0.024	6.89	2.02	4.13	-0.95	-0.11	0.63	1.09	0.18	0.85	-0.21	-0.18	0.00	-0.18	-0.07	-0.45	-0.01
16	4.42	0.226	0.006	-0.023	6.76	2.01	4.16	-0.91	-0.08	0.53	1.09	0.14	0.84	-0.10	-0.14	-0.03	-0.11	-0.08	-0.20	0.00
17	4.93	0.233	0.008	-0.024	7.10	2.18	4.39	-1.07	-0.08	0.68	1.17	0.21	0.99	-0.20	-0.22	-0.05	-0.26	-0.03	-0.43	0.02
18	5.69	0.244	0.008	-0.022	7.39	2.29	4.35	-1.20	-0.08	0.60	1.05	0.18	0.95	-0.10	-0.32	-0.03	-0.21	-0.08	-0.73	0.07
19	6.45	0.262	0.008	-0.019	7.52	2.37	4.67	-1.24	-0.07	0.52	1.08	0.08	1.08	-0.14	-0.16	-0.10	-0.29	-0.08	-0.43	0.07
20	7.21	0.273	0.010	-0.020	8.14	2.54	4.93	-1.38	-0.04	0.48	0.11	0.23	0.68	-0.01	-0.21	-0.10	-0.50	-0.08	-0.83	0.11
21	8.48	0.292	0.011	-0.016	7.89	2.73	5.01	-1.50	-0.11	0.31	0.32	0.05	0.80	-0.03	-0.13	-0.05	-0.59	-0.11	-0.57	0.15
22	10.26	0.316	0.013	-0.014	7.97	2.81	4.97	-1.60	-0.16	0.22	0.58	0.03	0.58	0.03	-0.09	0.00	-0.43	-0.13	-0.62	0.17
23	12.80	0.358	0.013	-0.011	8.28	3.07	4.91	-1.65	-0.14	0.01	-0.26	0.06	0.43	0.11	-0.04	0.01	-0.29	-0.07	-0.53	0.16
24	15.34	0.409	0.017	-0.007	7.84	2.93	4.75	-1.58	-0.07	-0.25	-0.37	-0.23	0.25	0.31	0.03	0.04	-0.03	-0.14	-0.44	0.09
25	17.88	0.456	0.020	-0.004	7.81	2.87	4.56	-1.72	-0.06	-0.31	-1.02	-0.20	0.04	0.46	0.09	0.21	-0.19	-0.01	-0.37	0.09
26	20.42	0.499	0.019	-0.001	6.76	2.66	4.06	-1.51	0.03	-0.51	-1.19	-0.44	0.03	0.55	0.31	0.17	0.20	-0.05	-0.28	0.03
27	22.96	0.545	0.023	-0.001	6.25	2.39	3.68	-1.38	-0.03	-0.45	-1.94	-0.52	-0.21	0.82	0.24	0.24	0.10	0.05	-0.14	0.08
28	25.50	0.586	0.025	0.000	5.34	2.08	3.01	-1.18	-0.05	-0.36	-1.74	-0.47	-0.32	0.72	0.31	0.25	0.25	-0.01	-0.02	0.03
29	28.04	0.614	0.027	0.002	4.39	1.84	2.48	-0.95	0.05	-0.53	-2.06	-0.47	-0.33	0.60	0.34	0.18	0.28	0.06	0.17	-0.02
30	30.58	0.653	0.031	0.000	3.10	1.46	1.71	-0.66	0.05	-0.32	-1.61	-0.40	-0.28	0.53	0.33	0.17	0.14	0.03	0.20	-0.01
31	33.12	0.684	0.031	-0.002	1.72	1.10	1.13	-0.39	0.03	-0.14	-0.82	-0.29	-0.08	0.39	0.27	0.14	0.02	0.00	0.09	-0.01
32	35.66	0.698	0.033	-0.003	1.00	0.76	0.73	-0.14	0.03	-0.12	-0.44	-0.16	0.03	0.21	0.17	0.05	0.01	0.00	0.03	0.01
33	38.20	0.706	0.034	-0.003	0.52	0.54	0.48	0.04	0.00	-0.09	-0.08	-0.06	0.14	0.09	0.10	0.03	-0.05	0.01	0.01	0.00
34	40.74	0.711	0.034	-0.003	0.33	0.39	0.37	0.14	-0.03	-0.10	0.00	0.00	0.13	0.01	0.04	0.00	-0.05	0.00	0.02	0.00
35	45.82	0.709	0.032	-0.001	0.30	0.26	0.32	0.15	-0.04	-0.10	0.01	0.01	0.12	0.01	0.01	0.00	-0.04	0.00	0.02	0.00
36	50.90	0.711	0.032	-0.003	0.30	0.23	0.35	0.15	-0.04	-0.13	0.02	0.01	0.19	0.01	0.01	0.00	-0.07	0.00	0.03	0.00
37	55.98	0.708	0.042	-0.003	0.29	0.47	0.36	0.13	-0.05	-0.13	0.02	0.01	0.19	0.01	0.01	0.01	-0.07	0.00	0.03	0.00
38	61.06	0.708	0.043	-0.004	0.38	0.44	0.40	0.12	-0.04	-0.17	0.03	0.01	0.26	0.01	0.00	0.00	-0.10	0.00	0.05	0.00
39	66.14	0.711	0.000	-0.004	0.31	0.00	0.40	0.00	0.00	-0.11	0.02	0.00	0.23	0.00	0.00	0.00	-0.05	0.00	0.05	0.00
40	71.22	0.710	0.000	-0.002	0.35	0.00	0.45	0.00	0.00	-0.11	0.03	0.00	0.20	0.00	0.00	0.00	-0.06	0.00	0.09	0.00

Table C.5 Continued.

Case B.S0 Station= 9
X= 228.6mm Tunnel Run#= 626 Ue/Uref= 0.687 Date= 418.88 Time= 8.38
Bias Corrected data using 1/sqrt(U*U + V*V + W*W + (.01Ur)^2)
The Y-position has been corrected by adding 0.127 to each measured Y-position in this profile.

					<-- normalized by 0.001 Ur^2 -->							<---------- normalized by 0.0001 Ur^3 ----------->									
LR	Y(mm)	U/Ur	V/Ur	W/Ur	uu	vv	ww	uv	vw	uw	uuu	uvv	uww	vuu	vvv	vww	wuu	wvv	www	uvw
25	2.67	0.196	0.001	-0.015	6.17	1.71	3.99	-0.80	0.01	0.51	1.15	0.23	0.78	-0.26	-0.25	-0.05	-0.09	-0.04	-0.24	-0.03
26	6.48	0.263	-0.002	-0.015	8.19	2.98	4.83	-1.67	-0.09	0.47	0.34	0.15	0.51	-0.04	-0.29	-0.02	-0.45	-0.10	-0.08	0.11
27	12.83	0.358	-0.001	-0.015	9.15	3.44	5.39	-2.17	0.04	-0.18	-0.96	-0.27	0.14	0.58	0.08	0.13	-0.01	-0.12	-0.49	0.05
28	19.18	0.466	0.002	-0.016	7.93	3.14	4.74	-2.11	-0.16	-0.35	-2.51	-0.76	-0.53	1.05	0.56	0.39	-0.36	-0.07	-0.27	0.13
29	25.53	0.560	0.007	-0.009	5.53	2.25	3.21	-1.49	0.00	-0.60	-2.75	-0.71	-0.69	1.07	0.54	0.31	0.36	0.06	0.31	-0.01
30	38.23	0.674	0.017	-0.004	0.75	0.80	0.71	-0.12	0.17	-0.26	-0.15	-0.18	0.17	0.29	0.20	0.12	-0.06	0.08	0.11	-0.05
31	50.93	0.687	0.021	-0.005	0.42	0.44	0.37	0.24	0.04	-0.10	0.03	0.03	0.11	0.03	0.06	0.00	-0.02	0.01	0.03	0.01

Table C.5 Continued.

Case B.S0 Station= 10
X= 304.8mm Tunnel Run#= 605 Ue/Uref= 0.663 Date= 322.88 Time=18.41
Bias Corrected data using 1/sqrt(U*U + V*V + W*W + (.01Ur)^2)
The Y-position has been corrected by adding 0.178 to each measured Y-position in this profile.

						<-- normalized by 0.001 Ur^2 -->							<---------- normalized by 0.0001 Ur^3 ----------->				
LR	Y(mm)	U/Ur	V/Ur	W/Ur	uu	vv	ww	uv	vw	uw	uuu	uvv	uww	vuu	vvv	vww	wuu	wvv	www	uvw
1	0.00	0.000	0.000	0.000	0.00	0.00	0.00	-0.16	0.00	0.00	0.00	0.00	0.00	0.00	0.00	0.00	0.00	0.00	0.00	0.00
1	0.43	0.106	0.008	-0.006	4.40	0.50	3.37	0.02	-0.03	-0.14	1.99	0.05	3.43	-0.05	-0.01	0.04	-1.17	-0.02	-1.49	-0.01
2	0.56	0.123	0.008	-0.007	5.46	0.59	4.12	-0.05	-0.03	0.01	2.73	0.04	3.39	-0.08	-0.03	0.03	-1.09	-0.04	-1.71	-0.04
3	0.69	0.131	0.004	-0.007	5.30	0.42	4.25	-0.24	-0.06	0.03	2.25	0.06	2.91	-0.10	-0.03	0.00	-0.81	-0.01	-1.93	0.00
4	0.81	0.139	0.003	-0.009	5.94	0.54	4.33	-0.25	-0.06	0.15	2.31	0.07	2.97	-0.12	-0.04	0.01	-0.70	-0.01	-1.15	-0.01
5	0.94	0.147	0.004	-0.010	5.76	0.64	4.49	-0.29	-0.06	0.34	2.33	0.09	2.34	-0.13	-0.06	0.01	-0.40	-0.01	-1.20	-0.03
6	1.19	0.154	0.004	-0.010	6.20	0.76	4.57	-0.33	-0.02	0.52	2.36	0.13	2.40	-0.08	-0.07	0.02	-0.46	-0.03	-1.14	0.01
7	1.45	0.166	0.003	-0.010	5.86	0.95	4.62	-0.34	-0.03	0.66	2.25	0.08	2.32	-0.12	-0.09	0.03	-0.35	-0.04	-1.11	0.00
8	1.70	0.167	0.004	-0.010	5.94	1.04	4.51	-0.45	-0.06	0.52	1.58	0.13	2.19	-0.11	-0.13	0.03	-0.29	-0.04	-0.94	0.03
9	1.96	0.177	0.004	-0.008	6.15	1.21	4.73	-0.48	-0.01	0.66	2.13	0.13	2.36	-0.17	-0.11	0.00	-0.22	-0.05	-0.81	-0.03
10	2.21	0.179	0.004	-0.008	6.54	1.27	4.57	-0.54	-0.03	0.79	1.89	0.17	2.06	-0.15	-0.15	0.04	-0.09	-0.05	-0.48	0.03
11	2.46	0.180	0.005	-0.010	6.38	1.41	4.59	-0.56	-0.03	0.94	1.74	0.21	1.65	-0.20	-0.15	0.05	-0.11	-0.03	-0.44	0.02
12	2.72	0.187	0.004	-0.010	6.39	1.47	4.64	-0.60	-0.03	1.00	2.00	0.18	1.54	-0.15	-0.17	0.05	0.20	-0.02	-0.34	0.01
13	2.97	0.186	0.004	-0.012	6.25	1.61	4.58	-0.73	-0.06	0.97	2.24	0.22	1.77	-0.22	-0.24	-0.02	0.06	-0.04	-0.07	-0.01
14	3.48	0.194	0.004	-0.015	7.31	1.76	5.61	-0.88	-0.05	0.47	2.75	0.30	3.29	-0.28	-0.27	-0.05	-0.71	-0.04	-2.19	0.07
15	3.99	0.201	0.003	-0.015	7.70	1.97	5.67	-0.89	-0.02	0.40	3.03	0.24	3.48	-0.29	-0.32	0.04	-0.80	-0.04	-2.25	0.00
16	4.50	0.207	0.002	-0.013	7.53	2.09	5.04	-1.07	-0.01	0.87	2.29	0.36	1.89	-0.42	-0.35	-0.07	-0.07	-0.09	-0.85	0.05
17	5.00	0.217	0.003	-0.017	7.64	2.30	5.13	-1.07	-0.03	0.89	2.11	0.31	1.58	-0.30	-0.36	0.00	-0.10	-0.03	-0.90	0.07
18	5.77	0.221	0.002	-0.016	8.40	2.50	5.18	-1.31	0.02	0.79	1.97	0.31	1.63	-0.23	-0.38	-0.10	-0.06	-0.09	-0.94	0.03
19	6.53	0.236	0.002	-0.015	8.50	2.68	5.28	-1.53	0.15	0.85	2.25	0.38	1.27	-0.34	-0.37	0.01	0.15	-0.15	-0.63	0.05
20	7.29	0.242	0.003	-0.015	8.86	2.88	5.49	-1.67	-0.02	0.95	1.97	0.34	1.30	-0.26	-0.34	-0.17	0.03	-0.07	-0.60	0.12
21	8.56	0.254	0.002	-0.017	9.05	3.10	5.80	-1.78	0.06	0.78	1.68	0.31	1.13	-0.21	-0.33	0.05	-0.17	-0.11	-0.93	0.18
22	10.34	0.293	0.001	-0.008	10.02	3.36	6.19	-2.12	0.00	1.06	0.37	0.13	1.01	0.27	-0.33	0.04	-0.48	-0.21	-1.05	0.33
23	12.88	0.306	0.003	-0.017	10.76	3.61	5.99	-2.45	0.09	0.39	0.35	0.20	0.83	0.09	-0.22	0.02	-0.51	-0.15	-1.01	0.25
24	15.42	0.338	0.005	-0.019	11.51	3.80	6.53	-2.77	0.00	0.45	-1.50	-0.16	0.13	0.49	0.08	0.27	-0.60	-0.09	-0.69	0.39
25	17.96	0.381	0.001	-0.017	10.33	3.81	6.29	-2.63	0.15	0.18	-1.33	-0.55	-0.20	0.75	0.23	0.26	-0.58	-0.11	-1.04	0.33
26	20.50	0.410	0.003	-0.015	11.11	3.90	6.35	-2.79	0.25	-0.27	-4.11	-0.48	-0.28	1.11	0.52	0.46	-0.41	-0.14	-1.09	0.25
27	23.04	0.439	0.005	-0.010	10.33	3.94	6.02	-2.74	0.22	-0.36	-4.61	-1.10	-0.77	1.70	1.01	0.57	-0.18	-0.07	-0.76	0.25
28	25.58	0.472	0.004	-0.011	10.24	3.64	5.56	-2.64	0.22	-0.43	-6.56	-1.17	-1.08	2.13	0.94	0.76	-0.15	-0.03	-0.70	0.13
29	28.12	0.509	0.005	-0.007	8.61	3.24	4.78	-2.44	0.37	-0.61	-5.00	-1.35	-0.91	2.12	0.86	0.78	0.01	0.06	-0.26	0.02
30	30.66	0.532	0.007	-0.007	8.25	3.31	4.32	-2.37	0.33	-0.68	-5.91	-1.47	-1.22	2.23	1.15	0.77	0.44	0.20	0.00	0.03
31	33.20	0.565	0.006	-0.004	6.80	2.77	3.56	-1.99	0.41	-0.72	-5.84	-1.48	-1.04	2.52	1.04	0.78	0.63	0.28	0.44	-0.21
33	35.74	0.593	0.006	-0.004	4.58	2.31	2.77	-1.57	0.30	-0.68	-3.55	-1.07	-0.83	1.83	0.93	0.56	0.47	0.11	0.31	-0.08
34	38.28	0.616	0.007	-0.004	3.72	1.97	2.25	-1.19	0.52	-0.74	-3.15	-1.01	-0.78	1.77	0.78	0.64	0.73	0.31	0.53	-0.18
35	40.82	0.630	0.010	-0.003	2.94	1.86	1.85	-0.82	0.45	-0.46	-2.36	-0.72	-0.55	0.97	0.75	0.50	0.33	0.25	0.53	-0.13
36	45.90	0.654	0.009	-0.006	1.34	1.18	0.98	-0.31	0.32	-0.24	-0.80	-0.40	-0.06	0.62	0.43	0.28	0.15	0.19	0.23	-0.06
37	50.98	0.662	0.003	-0.009	0.60	0.60	0.48	0.13	0.18	-0.15	0.06	-0.04	0.09	0.13	0.14	0.08	0.04	0.07	0.06	-0.02
38	56.06	0.663	0.015	-0.008	0.53	0.80	0.44	0.22	0.08	-0.12	0.05	0.03	0.18	0.05	0.08	0.02	-0.02	0.01	0.07	0.01
39	61.14	0.664	0.015	-0.010	0.45	0.71	0.39	0.19	0.07	-0.15	0.03	0.03	0.19	0.03	0.03	0.01	-0.08	0.01	0.04	0.00
40	66.22	0.662	0.018	-0.010	0.48	0.72	0.45	0.20	0.03	-0.24	0.03	0.04	0.45	0.05	0.02	0.06	-0.15	0.00	0.06	-0.02
42	73.84	0.663	0.000	-0.013	0.47	0.00	0.49	0.00	0.00	-0.17	0.04	0.00	0.34	0.00	0.00	0.00	-0.03	0.00	0.10	0.00

Table C.5 Continued.

Case C.S0 Station= 1
X=-457.2mm Tunnel Run#= 688 Ue/Uref= 1.000 Date= 510.88 Time=11.45
Bias Corrected data using 1/sqrt(U*U + V*V + W*W + (.01Ur)^2)
The Y-position has been corrected by adding 0.254 to each measured Y-position in this profile.

					<-- normalized by 0.001 Ur^2 -->						<---------- normalized by 0.0001 Ur^3 ---------->									
LR	Y(mm)	U/Ur	V/Ur	W/Ur	uu	vv	ww	uv	vw	uw	uuu	uvv	uww	vuu	vvv	vww	wuu	wvv	www	uvw
1	0.00	0.000	0.000	0.000	0.00	0.00	0.00	-1.61	0.00	0.00	0.00	0.00	0.00	0.00	0.00	0.00	0.00	0.00	0.00	0.00
1	0.51	0.583	-0.001	0.008	8.80	1.63	5.99	-1.40	-0.35	-0.52	-1.49	-0.16	-0.15	0.60	0.02	0.15	0.13	-0.04	0.33	0.04
2	0.63	0.608	0.000	0.006	8.04	1.93	5.63	-1.50	-0.33	-0.44	-1.32	-0.18	-0.16	0.58	0.14	0.14	0.16	-0.03	0.08	0.02
3	0.76	0.628	-0.001	0.002	7.20	1.94	5.34	-1.34	-0.32	-0.43	-0.44	-0.11	-0.08	0.27	0.07	0.11	0.06	-0.03	-0.21	0.04
4	0.89	0.644	0.000	0.006	6.81	2.07	5.10	-1.39	-0.32	-0.35	-0.41	-0.17	-0.11	0.31	0.26	0.20	-0.08	-0.07	-0.24	0.07
5	1.02	0.651	0.000	0.003	7.04	2.15	4.96	-1.55	-0.32	-0.29	-0.56	-0.24	0.03	0.47	0.22	0.13	-0.04	-0.01	-0.32	0.00
6	1.27	0.675	-0.001	0.003	6.34	2.24	4.66	-1.50	-0.26	-0.36	-0.13	-0.11	0.02	0.24	0.19	0.15	-0.02	-0.02	-0.24	0.01
7	1.52	0.692	-0.001	0.002	5.98	2.24	4.26	-1.49	-0.22	-0.23	-0.15	-0.17	-0.11	0.19	0.28	0.17	-0.05	-0.07	-0.10	0.01
8	1.78	0.708	-0.001	0.003	5.83	2.23	4.11	-1.49	-0.25	-0.12	-0.32	-0.15	-0.05	0.28	0.19	0.13	-0.20	-0.05	-0.12	0.06
9	2.03	0.725	-0.001	0.002	5.59	2.28	3.79	-1.52	-0.17	-0.11	-0.41	-0.18	-0.02	0.31	0.20	0.14	0.03	0.01	-0.17	0.00
10	2.29	0.739	-0.002	0.003	5.55	2.18	3.64	-1.42	-0.08	-0.15	-0.57	-0.15	-0.11	0.30	0.17	0.14	0.02	-0.02	-0.11	-0.01
11	2.54	0.748	-0.001	0.004	5.38	2.18	3.59	-1.44	-0.19	-0.11	-0.39	-0.16	-0.06	0.23	0.17	0.10	-0.06	-0.04	-0.25	0.03
12	2.79	0.763	-0.003	0.001	5.03	2.09	3.42	-1.35	-0.10	-0.02	-0.70	-0.09	-0.15	0.21	0.14	0.09	-0.09	-0.01	-0.01	0.03
13	3.05	0.772	-0.002	0.002	4.85	2.05	3.43	-1.31	-0.07	-0.19	-0.49	-0.13	-0.14	0.18	0.13	0.16	-0.01	-0.01	0.00	0.02
14	3.56	0.789	-0.002	0.001	4.54	1.99	3.18	-1.26	-0.09	-0.07	-0.65	-0.16	-0.11	0.24	0.23	0.13	0.03	0.02	-0.10	0.01
15	4.06	0.816	-0.003	0.001	4.30	1.94	3.21	-1.24	-0.09	-0.11	-0.68	-0.17	-0.07	0.26	0.18	0.07	-0.02	-0.02	-0.24	0.00
16	4.57	0.832	-0.002	0.002	3.90	1.88	2.93	-1.14	-0.14	0.03	-0.62	-0.17	-0.16	0.22	0.25	0.10	-0.03	0.01	-0.12	0.03
17	5.08	0.848	-0.003	0.001	3.62	1.76	2.83	-1.06	-0.12	0.02	-0.60	-0.17	-0.21	0.21	0.19	0.15	-0.01	-0.02	-0.12	0.01
18	5.84	0.873	-0.003	0.003	3.34	1.59	2.54	-1.01	-0.12	-0.06	-0.84	-0.23	-0.21	0.29	0.27	0.08	0.03	-0.01	0.02	0.02
19	6.60	0.893	-0.003	0.001	2.88	1.46	2.16	-0.84	-0.04	-0.03	-0.79	-0.25	-0.26	0.27	0.34	0.15	0.02	-0.01	-0.08	0.00
20	7.37	0.914	-0.003	0.002	2.46	1.29	1.83	-0.76	-0.04	-0.04	-0.75	-0.25	-0.21	0.29	0.24	0.11	0.03	-0.01	-0.05	-0.01
21	8.64	0.945	-0.003	0.001	1.77	0.93	1.33	-0.52	-0.05	0.02	-0.61	-0.18	-0.21	0.23	0.19	0.13	0.01	0.01	-0.03	0.00
22	10.41	0.976	-0.002	0.003	0.87	0.57	0.67	-0.25	-0.01	-0.02	-0.39	-0.12	-0.12	0.14	0.11	0.07	0.01	0.00	0.02	0.00
23	12.95	0.997	-0.003	0.002	0.15	0.21	0.22	-0.02	0.01	-0.02	-0.03	-0.01	0.00	0.01	0.03	0.01	0.01	0.00	0.02	0.00
24	15.49	0.999	-0.003	0.002	0.07	0.11	0.15	0.00	0.00	-0.01	0.00	0.00	0.00	0.00	0.00	0.00	0.00	0.00	0.01	0.00
25	18.03	0.999	-0.004	0.002	0.05	0.11	0.13	0.00	0.00	-0.01	0.00	0.00	0.00	0.00	0.10	0.00	0.00	0.01	0.00	0.00
26	20.57	0.998	-0.004	0.001	0.05	0.08	0.14	0.00	0.00	-0.01	0.00	0.00	0.01	0.00	0.00	0.00	0.00	0.00	0.01	0.00
27	23.11	1.000	-0.004	0.000	0.05	0.09	0.14	0.00	0.00	-0.01	0.00	0.00	0.01	0.00	0.00	0.00	0.00	0.00	0.00	0.00
28	25.65	1.000	-0.004	-0.001	0.05	0.08	0.14	0.00	0.00	-0.01	0.00	0.00	0.00	0.00	0.00	0.00	0.00	0.00	0.01	0.00
29	28.19	1.001	-0.004	-0.001	0.05	0.09	0.14	0.00	0.00	-0.01	0.00	0.00	0.00	0.00	0.00	0.00	0.00	0.00	0.01	0.00
30	30.73	1.002	-0.005	-0.003	0.05	0.12	0.13	0.00	0.00	-0.01	0.00	0.00	0.00	0.00	0.17	0.00	0.00	0.00	0.01	0.00
31	33.27	1.003	-0.004	-0.002	0.06	0.08	0.16	0.00	0.00	0.01	0.00	0.00	0.01	0.00	0.00	0.00	0.00	0.00	0.01	0.00
32	35.81	0.998	-0.004	-0.003	0.05	0.09	0.12	0.00	0.00	-0.01	0.00	0.00	0.00	0.00	0.00	0.00	0.00	0.00	0.00	0.00
33	38.35	0.999	-0.003	-0.003	0.05	0.09	0.12	0.00	0.00	-0.01	0.00	0.00	0.00	0.00	0.00	0.00	0.00	0.00	0.00	0.00
34	40.89	1.000	-0.003	-0.002	0.04	0.09	0.12	0.00	0.00	-0.01	0.00	0.00	0.00	0.00	0.00	0.00	0.00	0.00	0.00	0.00
35	45.97	1.001	-0.003	0.000	0.04	0.09	0.11	0.00	0.00	-0.01	0.00	0.00	0.00	0.00	0.00	0.00	0.00	0.00	0.00	0.00
36	51.05	1.002	0.004	0.001	0.05	0.48	0.14	0.00	0.00	-0.01	0.00	0.00	0.00	0.00	0.04	0.00	0.00	-0.01	0.01	0.00
37	56.13	1.002	0.004	0.000	0.05	0.48	0.12	0.00	0.00	-0.01	0.00	0.00	0.00	0.00	0.00	0.00	0.00	0.00	0.00	0.00
38	61.21	1.003	0.000	-0.004	0.05	0.00	0.12	0.00	0.00	-0.01	0.00	0.00	0.00	0.00	0.00	0.00	0.00	0.00	0.00	0.00
39	66.29	1.002	0.000	-0.004	0.05	0.00	0.12	0.00	0.00	0.00	0.00	0.00	0.00	0.00	0.00	0.00	0.00	0.00	0.00	0.00

Table C.5 Continued.

Case C.S0 Station= 2
X=-330.2mm Tunnel Run#= 686 Ue/Uref= 1.011 Date= 510.88 Time= 9.49
Bias Corrected data using 1/sqrt(U*U + V*V + W*W + (.01Ur)^2)
The Y-position has been corrected by adding 0.254 to each measured Y-position in this profile.

						<-- normalized by 0.001 Ur^2 -->						<---------- normalized by 0.0001 Ur^3 ----------->					
LR	Y(mm)	U/Ur	V/Ur	W/Ur	uu	vv	ww	uv	vw	uw	uuu	uvv	uww	vuu	vvv	vww	wuu	wvv	www	uvw
1	0.00	0.000	0.000	0.000	0.00	0.00	0.00	-1.60	0.00	0.00	0.00	0.00	0.00	0.00	0.00	0.00	0.00	0.00	0.00	0.00
1	0.51	0.586	-0.002	0.005	8.83	1.67	5.59	-1.42	-0.35	-0.46	-1.59	-0.21	-0.47	0.67	0.03	0.16	-0.05	-0.02	0.90	0.06
2	0.63	0.609	-0.002	0.004	7.93	1.95	5.18	-1.49	-0.38	-0.17	-0.90	-0.19	-0.21	0.45	0.17	0.11	-0.10	-0.06	0.30	0.13
3	0.76	0.625	-0.001	0.003	7.34	2.03	5.12	-1.50	-0.28	-0.32	-0.54	-0.24	-0.22	0.42	0.24	0.14	-0.11	0.02	0.13	0.06
4	0.89	0.639	-0.001	0.002	7.04	2.12	4.70	-1.48	-0.34	-0.16	-0.54	-0.21	-0.29	0.37	0.21	0.22	0.04	-0.07	0.17	0.05
5	1.02	0.652	-0.001	0.002	6.81	2.12	4.62	-1.47	-0.32	-0.09	-0.26	-0.16	-0.02	0.34	0.17	0.21	-0.05	-0.05	0.12	0.06
6	1.27	0.673	0.000	0.003	6.47	2.20	4.31	-1.51	-0.27	-0.21	-0.33	-0.18	-0.12	0.23	0.16	0.22	-0.09	0.00	0.03	0.06
7	1.52	0.691	-0.001	0.002	6.00	2.18	4.27	-1.42	-0.20	-0.20	-0.14	-0.06	0.05	0.19	0.16	0.18	-0.02	-0.03	-0.31	-0.02
8	1.78	0.707	-0.002	0.001	5.90	2.21	3.86	-1.43	-0.24	-0.13	-0.15	-0.19	-0.07	0.21	0.18	0.16	-0.06	-0.03	0.01	-0.01
9	2.03	0.724	-0.002	0.001	5.70	2.17	3.72	-1.45	-0.17	-0.20	-0.61	-0.19	-0.13	0.29	0.24	0.15	-0.06	-0.03	0.03	0.02
10	2.29	0.736	-0.001	0.000	5.61	2.13	3.69	-1.43	-0.18	-0.16	-0.50	-0.18	-0.11	0.32	0.18	0.10	0.01	-0.01	-0.06	-0.01
11	2.54	0.743	-0.001	0.001	5.55	2.09	3.63	-1.42	-0.19	-0.18	-0.58	-0.14	-0.01	0.28	0.19	0.12	0.01	0.00	-0.18	-0.01
12	2.79	0.755	-0.002	0.002	5.31	2.11	3.42	-1.39	-0.16	-0.16	-0.63	-0.15	-0.19	0.28	0.14	0.12	0.14	0.01	0.00	0.02
13	3.05	0.769	-0.002	0.002	5.18	2.10	3.47	-1.39	-0.13	-0.12	-0.67	-0.15	-0.12	0.29	0.14	0.09	0.00	0.00	-0.03	-0.02
14	3.56	0.787	-0.002	0.003	4.84	2.04	3.16	-1.38	-0.11	-0.14	-0.80	-0.20	-0.11	0.30	0.24	0.07	0.09	0.00	0.04	-0.01
15	4.06	0.803	-0.002	0.002	4.68	1.98	3.17	-1.33	-0.08	-0.11	-0.86	-0.23	-0.13	0.35	0.23	0.11	-0.01	-0.01	-0.07	-0.02
16	4.57	0.820	-0.002	0.002	4.29	1.88	3.10	-1.23	-0.12	-0.08	-0.76	-0.22	-0.17	0.36	0.24	0.12	-0.04	0.01	0.03	-0.01
17	5.08	0.835	-0.002	0.002	3.98	1.86	2.81	-1.16	-0.11	-0.08	-0.79	-0.19	-0.13	0.29	0.17	0.08	0.01	0.01	-0.06	0.00
18	5.84	0.855	-0.002	0.002	3.74	1.74	2.65	-1.12	-0.12	-0.10	-0.91	-0.20	-0.21	0.31	0.30	0.10	0.05	0.01	-0.01	-0.01
19	6.60	0.876	0.000	0.002	3.26	1.61	2.46	-0.99	-0.09	-0.03	-0.77	-0.18	-0.23	0.24	0.30	0.10	0.05	-0.02	-0.03	-0.01
20	7.37	0.896	-0.001	0.002	2.87	1.40	2.18	-0.84	-0.09	-0.02	-0.85	-0.19	-0.20	0.29	0.19	0.09	-0.01	-0.03	0.05	0.03
21	8.64	0.925	-0.001	0.002	2.27	1.19	1.70	-0.70	-0.07	-0.02	-0.68	-0.23	-0.23	0.25	0.30	0.10	0.03	-0.01	0.06	0.01
22	10.41	0.959	-0.001	0.003	1.46	0.80	1.06	-0.43	-0.04	-0.02	-0.53	-0.16	-0.15	0.20	0.14	0.08	0.01	-0.01	-0.02	0.01
23	12.95	0.991	0.000	0.003	0.47	0.39	0.42	-0.13	0.01	-0.01	-0.20	-0.06	-0.04	0.08	0.07	0.04	0.00	0.00	0.05	0.01
24	15.49	1.003	-0.001	0.003	0.11	0.17	0.18	-0.01	0.00	-0.01	0.00	-0.01	0.01	0.01	0.02	0.00	0.01	0.00	0.02	0.00
25	18.03	1.005	-0.001	0.003	0.07	0.12	0.15	0.00	0.00	-0.01	0.00	0.00	0.01	0.00	0.03	0.00	0.00	0.00	0.01	0.00
26	20.57	1.005	-0.001	0.003	0.06	0.10	0.15	0.00	0.00	0.00	0.00	0.00	0.01	0.00	0.00	0.00	0.01	0.00	0.02	0.00
27	23.11	1.005	0.000	0.002	0.06	0.10	0.15	0.00	0.00	-0.01	0.00	0.00	0.01	0.00	0.00	0.00	0.00	0.00	0.02	0.00
28	25.65	1.004	0.000	0.002	0.06	0.10	0.16	0.00	0.00	0.00	0.00	0.00	0.01	0.00	0.00	0.00	0.01	0.00	0.02	0.00
29	28.19	1.003	0.000	0.001	0.06	0.10	0.15	0.00	0.00	-0.01	0.00	0.00	0.01	0.00	0.01	0.00	0.00	0.00	0.01	0.00
30	30.73	1.004	0.000	0.000	0.06	0.12	0.15	0.00	0.00	-0.01	0.00	0.00	0.01	0.00	0.09	0.00	0.00	0.00	0.01	0.00
31	33.27	1.005	0.000	0.000	0.06	0.09	0.16	0.00	0.00	-0.01	0.01	0.00	0.01	0.00	0.00	0.00	0.01	0.00	0.02	0.00
32	35.81	1.008	0.001	0.000	0.06	0.09	0.15	0.00	0.00	-0.01	0.00	0.00	0.00	0.00	0.00	0.00	0.00	0.00	0.01	0.00
33	38.35	1.007	0.002	0.000	0.06	0.09	0.16	0.00	0.00	-0.01	0.00	0.00	0.01	0.00	0.00	0.00	0.00	0.00	0.01	0.00
34	40.89	1.009	0.003	-0.001	0.06	0.09	0.15	0.00	0.00	-0.01	0.00	0.00	0.01	0.00	0.00	0.00	0.00	0.00	0.00	0.00
35	45.97	1.013	0.003	0.000	0.05	0.10	0.15	0.00	0.00	0.00	0.00	0.00	0.01	0.00	0.00	0.00	0.00	0.00	0.01	0.00
36	51.05	1.013	0.005	-0.003	0.06	0.52	0.14	0.00	0.00	0.00	0.00	0.00	0.01	0.00	0.12	0.00	0.01	0.00	0.01	0.00
37	56.13	1.015	0.003	-0.004	0.05	0.46	0.13	0.00	0.00	-0.01	0.00	0.00	0.01	0.00	-0.01	0.00	0.00	0.00	0.00	0.00
38	61.21	1.019	0.000	-0.008	0.06	0.00	0.14	0.00	0.00	0.01	0.00	0.00	0.01	0.00	0.00	0.00	0.01	0.00	0.02	0.00
39	66.29	1.017	0.000	-0.005	0.06	0.00	0.14	0.00	0.00	0.00	0.00	0.00	0.01	0.00	0.00	0.00	0.00	0.00	0.01	0.00

Table C.5 Continued.

Case C.S0 Station= 3
X=-228.6mm Tunnel Run#= 682 Ue/Uref= 0.988 Date= 509.88 Time=19.20
Bias Corrected data using 1/sqrt(U*U + V*V + W*W + (.01Ur)^2)
The Y-position has been corrected by adding 0.152 to each measured Y-position in this profile.

					<-- normalized by 0.001 Ur^2 -->						<---------- normalized by 0.0001 Ur^3 ---------->									
LR	Y(mm)	U/Ur	V/Ur	W/Ur	uu	vv	ww	uv	vw	uw	uuu	uvv	uww	vuu	vvv	vww	wuu	wvv	www	uvw
1	0.00	0.000	0.000	0.000	0.00	0.00	0.00	-1.30	0.00	0.00	0.00	0.00	0.00	0.00	0.00	0.00	0.00	0.00	0.00	0.00
1	0.41	0.483	-0.001	-0.003	9.57	1.44	5.98	-1.29	-0.36	-0.64	-1.08	-0.07	0.12	0.44	0.00	0.16	-0.15	0.00	0.07	0.06
2	0.53	0.513	0.000	-0.004	8.47	1.68	5.96	-1.25	-0.36	-0.67	-0.41	-0.13	0.19	0.32	0.06	0.05	-0.01	-0.03	-0.01	0.00
3	0.66	0.533	-0.001	-0.006	7.68	1.82	5.37	-1.30	-0.33	-0.47	0.19	-0.06	-0.07	0.24	0.01	0.15	0.03	-0.04	-0.46	-0.01
4	0.79	0.547	0.001	-0.004	7.59	1.95	5.20	-1.40	-0.27	-0.48	0.04	-0.12	0.18	0.24	0.09	0.16	0.01	-0.02	-0.31	0.03
5	0.91	0.562	0.000	-0.006	7.09	2.04	5.06	-1.33	-0.29	-0.43	0.25	-0.13	0.13	0.17	0.14	0.10	-0.06	-0.03	-0.42	0.04
6	1.17	0.585	0.002	-0.007	7.04	2.21	4.80	-1.53	-0.20	-0.29	0.11	-0.18	0.05	0.27	0.19	0.16	0.02	0.01	-0.47	-0.07
7	1.42	0.605	0.002	-0.006	6.79	2.25	4.54	-1.47	-0.25	-0.32	-0.05	-0.10	0.15	0.18	0.16	0.01	-0.12	0.04	-0.02	-0.01
8	1.68	0.624	0.003	-0.006	6.68	2.27	4.39	-1.53	-0.21	-0.30	0.15	-0.04	0.10	0.13	0.17	0.15	-0.11	-0.09	-0.15	0.02
9	1.93	0.641	0.003	-0.007	6.73	2.20	4.25	-1.52	-0.18	-0.35	-0.09	-0.12	0.11	0.14	0.28	0.07	-0.18	-0.02	-0.30	0.04
10	2.18	0.653	0.003	-0.006	6.52	2.18	4.26	-1.46	-0.18	-0.33	0.00	-0.04	0.02	0.04	0.10	0.05	-0.10	-0.03	-0.19	0.04
11	2.44	0.670	0.004	-0.007	6.49	2.18	4.04	-1.55	-0.15	-0.27	-0.35	-0.14	-0.06	0.25	0.12	0.09	0.01	0.00	-0.14	0.03
12	2.69	0.678	0.004	-0.009	6.34	2.14	3.83	-1.53	-0.10	-0.25	-0.54	-0.14	0.04	0.31	0.13	0.09	-0.06	0.02	-0.20	0.00
13	2.95	0.690	0.004	-0.008	6.14	2.16	3.84	-1.47	-0.08	-0.30	-0.34	-0.15	0.04	0.28	0.11	0.05	0.01	0.04	-0.33	-0.03
14	3.45	0.711	0.003	-0.008	5.79	2.07	3.84	-1.42	-0.10	-0.39	-0.53	-0.12	-0.03	0.29	0.12	0.11	0.04	0.00	-0.25	-0.03
15	3.96	0.727	0.004	-0.007	5.42	2.06	3.59	-1.31	-0.09	-0.29	-0.48	-0.14	-0.07	0.23	0.09	0.08	0.01	0.01	-0.13	0.00
16	4.47	0.744	0.006	-0.009	5.28	2.02	3.48	-1.27	-0.18	-0.23	-0.66	-0.18	-0.07	0.25	0.22	0.06	0.09	-0.02	-0.10	0.01
17	4.98	0.759	0.007	-0.008	4.85	1.93	3.40	-1.19	-0.13	-0.20	-0.70	-0.14	-0.23	0.21	0.16	0.10	0.03	-0.04	-0.10	-0.01
18	5.74	0.781	0.007	-0.009	4.47	1.85	3.25	-1.17	-0.10	-0.11	-0.80	-0.20	-0.15	0.26	0.19	0.10	0.04	0.00	-0.03	0.01
19	6.50	0.799	0.008	-0.007	4.20	1.69	3.02	-1.12	-0.08	-0.19	-0.83	-0.21	-0.20	0.28	0.19	0.12	-0.01	0.01	-0.13	-0.02
20	7.26	0.820	0.010	-0.007	3.77	1.62	2.69	-1.00	-0.06	-0.12	-0.92	-0.20	-0.19	0.32	0.25	0.14	0.06	-0.02	-0.05	-0.02
21	8.53	0.847	0.013	-0.007	3.23	1.37	2.34	-0.87	-0.06	-0.11	-0.91	-0.17	-0.21	0.26	0.25	0.11	0.05	-0.01	-0.08	-0.01
22	10.31	0.886	0.015	-0.007	2.45	1.09	1.80	-0.65	-0.03	-0.06	-0.81	-0.19	-0.26	0.24	0.16	0.09	0.02	0.00	0.07	0.00
23	12.85	0.927	0.020	-0.008	1.43	0.69	0.99	-0.37	-0.06	-0.02	-0.57	-0.15	-0.17	0.19	0.13	0.08	0.01	-0.02	-0.02	0.01
24	15.39	0.961	0.023	-0.006	0.45	0.34	0.42	-0.12	0.00	-0.01	-0.18	-0.05	-0.05	0.07	0.06	0.04	0.00	0.00	0.02	0.00
25	17.93	0.968	0.025	-0.005	0.14	0.16	0.21	-0.02	0.00	-0.01	-0.02	-0.01	0.00	0.01	0.02	0.01	0.00	0.00	0.00	0.00
26	20.47	0.971	0.027	-0.004	0.08	0.09	0.16	0.00	0.00	-0.01	0.00	0.00	0.01	0.00	0.00	0.00	0.00	0.00	0.01	0.00
27	23.01	0.969	0.029	-0.005	0.07	0.08	0.16	0.00	0.00	0.00	0.00	0.00	0.01	0.00	0.00	0.00	0.01	0.00	0.02	0.00
28	25.55	0.971	0.031	-0.005	0.06	0.07	0.16	0.00	0.00	-0.01	0.00	0.00	0.01	0.00	0.00	0.00	0.00	0.00	0.02	0.00
29	28.09	0.971	0.034	-0.006	0.07	0.07	0.17	0.00	0.00	0.00	0.00	0.00	0.01	0.00	0.00	0.00	0.01	0.00	0.02	0.00
30	30.63	0.974	0.036	-0.007	0.07	0.09	0.16	0.00	0.00	0.00	0.00	0.00	0.01	0.00	0.07	0.00	0.01	0.00	0.02	0.00
31	33.17	0.979	0.038	-0.007	0.06	0.08	0.16	0.00	0.00	0.00	0.00	0.00	0.01	0.00	0.03	0.00	0.01	0.00	0.02	0.00
32	35.71	0.978	0.040	-0.007	0.06	0.07	0.16	0.00	0.00	0.00	0.00	0.00	0.01	0.00	0.00	0.00	0.01	0.00	0.02	0.00
33	38.25	0.978	0.044	-0.007	0.06	0.07	0.15	0.00	0.00	0.00	0.00	0.00	0.01	0.00	0.00	0.00	0.00	0.00	0.02	0.00
34	40.79	0.981	0.047	-0.007	0.06	0.09	0.14	0.00	0.00	0.00	0.00	0.00	0.01	0.00	0.08	0.00	0.01	0.00	0.01	0.00
35	45.87	0.985	0.053	-0.006	0.06	0.08	0.15	0.00	0.00	0.00	0.01	0.00	0.02	0.00	0.00	0.00	0.01	0.00	0.02	0.00
36	50.95	0.990	0.064	-0.005	0.06	0.37	0.15	0.00	0.00	0.01	0.00	0.00	0.01	0.00	0.00	0.00	0.01	0.00	0.02	0.00
37	56.03	0.995	0.073	-0.006	0.06	0.37	0.14	0.00	0.00	0.00	0.00	0.00	0.01	0.00	0.00	0.00	0.00	0.00	0.01	0.00
38	61.11	1.001	0.000	-0.008	0.07	0.00	0.16	0.00	0.00	-0.02	0.00	0.00	0.01	0.00	0.00	0.00	0.00	0.00	0.01	0.00
39	66.19	1.014	0.000	-0.011	0.05	0.00	0.15	0.00	0.00	0.00	0.00	0.00	0.01	0.00	0.00	0.00	0.00	0.00	0.01	0.00

Table C.5 Continued.

Case C.S0 Station= 4
X=-152.4mm Tunnel Run#= 680 Ue/Uref= 0.898 Date= 509.88 Time=16.27
Bias Corrected data using 1/sqrt(U*U + V*V + W*W + (.01Ur)^2)
The Y-position has been corrected by adding 0.305 to each measured Y-position in this profile.

					<-- normalized by 0.001 Ur^2 -->						<---------- normalized by 0.0001 Ur^3 ---------->									
LR	Y(mm)	U/Ur	V/Ur	W/Ur	uu	vv	ww	uv	vw	uw	uuu	uvv	uww	vuu	vvv	vww	wuu	wvv	www	uvw
1	0.00	0.000	0.000	0.000	0.00	0.00	0.00	-0.76	0.00	0.00	0.00	0.00	0.00	0.00	0.00	0.00	0.00	0.00	0.00	0.00
1	0.56	0.367	0.000	0.005	8.03	1.19	4.61	-0.96	-0.23	-0.17	0.22	-0.01	0.37	0.21	-0.01	0.11	-0.04	0.01	0.21	0.02
2	0.69	0.380	0.002	0.003	7.63	1.49	4.51	-1.13	-0.26	-0.21	0.44	0.00	0.41	0.12	0.07	0.02	-0.16	0.02	0.24	0.03
3	0.81	0.388	0.001	0.003	7.20	1.59	4.37	-1.03	-0.19	-0.06	0.12	0.01	0.30	0.16	0.13	0.15	0.05	0.00	-0.08	-0.01
4	0.94	0.401	0.001	0.001	7.18	1.70	4.29	-1.18	-0.23	-0.12	0.36	0.01	0.45	0.14	0.01	0.11	0.02	-0.01	0.13	-0.01
5	1.07	0.406	0.002	0.001	6.99	1.85	4.17	-1.21	-0.14	-0.15	0.23	-0.04	0.27	0.18	0.06	0.10	-0.01	0.00	0.20	0.00
6	1.32	0.424	0.002	-0.002	7.02	2.03	4.11	-1.36	-0.14	-0.03	0.34	-0.06	0.45	0.16	0.10	0.11	-0.11	-0.02	-0.17	0.03
7	1.57	0.441	0.003	-0.001	6.89	2.08	4.03	-1.24	-0.13	-0.21	0.73	0.00	0.25	0.01	0.14	0.05	0.00	0.02	-0.03	0.04
8	1.83	0.450	0.004	-0.001	7.12	2.16	4.15	-1.47	-0.09	-0.27	0.52	0.03	0.28	0.11	0.04	0.07	-0.16	0.00	-0.03	0.03
9	2.08	0.468	0.004	0.000	7.19	2.23	3.84	-1.47	-0.06	-0.09	0.50	0.00	0.18	0.02	0.07	0.07	-0.16	0.03	0.01	0.01
10	2.34	0.481	0.004	-0.001	7.12	2.26	3.98	-1.49	-0.08	0.01	0.07	-0.02	0.15	0.13	0.10	0.08	-0.04	-0.07	0.06	0.02
11	2.59	0.492	0.005	0.000	7.14	2.29	3.92	-1.53	-0.10	-0.18	0.43	0.01	0.16	0.08	0.03	0.09	0.05	0.00	-0.14	-0.03
12	2.84	0.503	0.005	-0.001	7.10	2.34	3.83	-1.57	-0.04	-0.07	0.04	-0.04	0.25	0.11	0.05	0.04	0.22	0.00	0.07	-0.01
13	3.10	0.513	0.007	-0.002	6.99	2.27	3.82	-1.51	-0.06	0.03	0.08	0.02	0.11	0.09	0.06	0.07	0.20	-0.01	0.06	-0.04
14	3.61	0.533	0.007	-0.002	6.79	2.32	3.69	-1.51	-0.06	0.03	-0.05	-0.08	0.00	0.17	0.12	0.06	-0.02	0.01	0.21	0.03
15	4.11	0.552	0.008	-0.002	6.75	2.35	3.75	-1.56	-0.13	-0.01	-0.01	-0.04	-0.03	0.13	0.07	0.02	0.02	-0.01	0.04	0.03
16	4.62	0.572	0.008	-0.002	6.78	2.26	3.69	-1.48	-0.07	-0.01	-0.56	-0.12	-0.03	0.18	0.18	0.05	0.00	0.01	0.09	0.04
17	5.13	0.586	0.010	-0.002	6.34	2.22	3.79	-1.46	-0.14	-0.08	-0.44	-0.13	0.06	0.19	0.11	-0.01	-0.06	-0.03	-0.07	0.05
18	5.89	0.610	0.012	-0.002	6.11	2.14	3.73	-1.39	-0.05	-0.05	-0.48	-0.18	-0.06	0.24	0.22	0.13	-0.11	-0.03	0.03	0.04
19	6.65	0.634	0.013	-0.002	5.81	2.12	3.52	-1.35	-0.07	-0.01	-0.79	-0.19	-0.04	0.24	0.19	0.07	-0.12	0.00	-0.15	-0.02
20	7.42	0.655	0.015	-0.002	5.59	2.03	3.39	-1.33	-0.10	-0.05	-0.95	-0.21	-0.08	0.32	0.18	0.08	0.01	-0.01	-0.19	0.00
21	8.69	0.684	0.019	-0.002	4.92	1.84	3.08	-1.16	-0.06	-0.04	-0.78	-0.20	-0.12	0.23	0.31	0.11	-0.05	-0.01	-0.22	0.00
22	10.46	0.728	0.022	-0.001	4.25	1.56	2.67	-1.00	-0.07	0.04	-1.15	-0.22	-0.13	0.34	0.18	0.11	0.00	0.01	-0.24	-0.03
23	13.00	0.777	0.028	-0.002	3.07	1.20	2.07	-0.74	-0.05	-0.01	-0.95	-0.23	-0.08	0.28	0.20	0.10	-0.10	0.00	-0.28	0.02
24	15.54	0.827	0.033	-0.001	1.95	0.82	1.29	-0.45	-0.05	0.05	-0.70	-0.17	-0.09	0.21	0.14	0.07	-0.08	-0.01	-0.13	0.01
25	18.08	0.855	0.036	0.000	0.91	0.47	0.67	-0.19	-0.01	0.01	-0.38	-0.09	-0.05	0.11	0.08	0.05	-0.04	-0.01	-0.09	0.01
26	20.62	0.873	0.039	0.001	0.30	0.25	0.35	-0.06	0.00	-0.02	-0.06	-0.03	0.06	0.03	0.03	0.02	-0.04	0.00	-0.11	0.00
27	23.16	0.877	0.040	0.002	0.13	0.14	0.22	-0.01	0.00	-0.03	0.01	0.00	0.07	0.00	0.01	0.00	-0.03	0.00	-0.09	0.00
28	25.70	0.881	0.042	0.002	0.08	0.09	0.18	0.00	0.00	-0.02	0.01	0.00	0.04	0.00	0.00	0.00	-0.01	0.00	-0.03	0.00
29	28.24	0.881	0.044	0.002	0.07	0.08	0.14	0.00	0.00	-0.01	0.01	0.00	0.02	0.00	0.00	0.00	0.00	0.00	-0.01	0.00
30	30.78	0.881	0.047	0.001	0.07	0.08	0.15	0.00	0.00	-0.02	0.01	0.00	0.04	0.00	0.00	0.00	-0.02	0.00	-0.04	0.00
31	33.32	0.888	0.049	0.000	0.07	0.08	0.15	0.00	0.00	-0.02	0.01	0.00	0.04	0.00	0.00	0.00	-0.01	0.00	-0.05	0.00
32	35.86	0.887	0.051	-0.002	0.05	0.08	0.13	0.00	0.00	0.00	0.00	0.00	0.01	0.00	0.00	0.00	0.00	0.00	0.00	0.00
33	38.40	0.889	0.052	-0.004	0.05	0.08	0.12	0.00	0.00	-0.01	0.01	0.00	0.02	0.00	0.00	0.00	-0.01	0.00	-0.03	0.00
34	40.94	0.891	0.055	-0.003	0.05	0.08	0.11	0.00	0.00	-0.01	0.00	0.00	0.01	0.00	0.00	0.00	0.00	0.00	-0.01	0.00
35	46.02	0.894	0.062	-0.002	0.05	0.12	0.12	0.00	0.00	0.00	0.00	0.00	0.01	0.00	0.08	0.00	0.00	0.00	0.00	0.00
36	51.10	0.895	0.069	-0.005	0.07	0.11	0.18	0.00	0.00	0.04	0.01	0.00	0.03	0.00	0.08	0.00	0.02	0.00	0.05	0.00
37	56.18	0.892	0.077	-0.005	0.03	0.40	0.12	0.00	0.00	-0.01	0.00	0.00	0.01	0.00	0.00	0.00	0.00	0.00	0.02	0.00
38	61.26	0.908	0.082	0.005	0.04	0.42	0.11	0.00	0.00	-0.01	0.00	0.00	0.00	0.00	0.26	0.00	0.00	0.01	0.00	0.00
39	66.34	0.912	0.000	0.002	0.05	0.00	0.12	0.00	0.00	0.01	0.00	0.00	-0.01	0.00	0.00	0.00	0.00	0.00	-0.01	0.00
40	68.88	0.911	0.000	-0.004	0.02	0.00	0.07	0.00	0.00	-0.03	0.00	0.00	0.00	0.00	0.00	0.00	0.00	0.00	0.00	0.00

Table C.5 Continued.

Case C.S0 Station= 5
X= -76.2mm Tunnel Run#= 678 Ue/Uref= 0.790 Date= 509.88 Time=14.52
Bias Corrected data using 1/sqrt(U*U + V*V + W*W + (.01Ur)^2)
The Y-position has been corrected by adding 0.254 to each measured Y-position in this profile.

					<-- normalized by 0.001 Ur^2 -->							<---------- normalized by 0.0001 Ur^3 ----------->									
LR	Y(mm)	U/Ur	V/Ur	W/Ur	uu	vv	ww	uv	vw	uw	uuu	uvv	uww	vuu	vvv	vww	wuu	wvv	www	uvw
1	0.00	0.000	0.000	0.000	0.00	0.00	0.00	-0.31	0.00	0.00	0.00	0.00	0.00	0.00	0.00	0.00	0.00	0.00	0.00	0.00
2	1.52	0.246	0.006	0.002	6.73	1.85	3.45	-1.07	-0.12	0.16	1.38	0.21	0.59	-0.18	-0.09	-0.02	-0.06	-0.01	0.15	0.01
3	2.79	0.292	0.010	-0.002	7.63	2.34	3.85	-1.41	-0.08	-0.02	1.37	0.26	0.51	-0.30	-0.10	0.03	-0.34	-0.04	-0.21	-0.03
4	6.60	0.417	0.019	-0.005	7.99	2.77	4.20	-1.64	-0.11	-0.13	-0.57	-0.07	0.13	0.17	0.12	0.04	0.10	-0.01	-0.12	-0.04
5	10.41	0.518	0.030	-0.005	6.64	2.43	4.07	-1.40	-0.04	-0.12	-1.00	-0.25	-0.19	0.35	0.36	0.10	0.05	-0.04	0.10	0.04
6	15.49	0.649	0.043	-0.009	4.62	1.67	2.82	-1.02	-0.02	-0.11	-1.56	-0.28	-0.27	0.42	0.24	0.14	-0.03	0.01	-0.07	0.00
7	20.57	0.733	0.055	-0.010	2.13	0.87	1.41	-0.42	-0.06	0.00	-0.76	-0.17	-0.14	0.20	0.13	0.08	0.00	-0.02	-0.07	0.03
8	25.65	0.786	0.065	-0.010	0.46	0.34	0.41	-0.10	-0.01	-0.01	-0.16	-0.05	0.02	0.05	0.05	0.02	-0.01	0.00	-0.03	0.00
9	30.73	0.794	0.067	-0.009	0.10	0.11	0.21	0.00	0.00	-0.02	0.02	0.00	0.07	0.00	0.00	0.00	-0.03	0.00	-0.08	0.00
10	35.81	0.794	0.071	-0.010	0.08	0.08	0.21	0.00	0.00	-0.03	0.03	0.00	0.09	0.00	0.00	0.00	-0.03	0.00	-0.09	0.00
11	40.89	0.794	0.076	-0.012	0.07	0.08	0.18	0.00	0.00	-0.03	0.02	0.00	0.06	0.00	0.00	0.00	-0.02	0.00	-0.07	0.00
12	45.97	0.794	0.078	-0.014	0.06	0.07	0.15	0.00	0.00	-0.01	0.01	0.00	0.03	0.00	0.00	0.00	-0.01	0.00	-0.03	0.00
13	51.05	0.795	0.082	-0.013	0.06	0.09	0.16	0.00	0.00	-0.02	0.02	0.00	0.05	0.00	0.08	0.00	-0.02	0.00	-0.06	0.00
14	56.13	0.792	0.091	-0.012	0.08	0.36	0.15	0.00	0.00	0.00	0.01	0.00	0.03	0.00	0.00	0.00	0.00	0.00	0.01	0.00
15	61.21	0.790	0.097	-0.014	0.10	0.43	0.25	0.00	-0.01	-0.02	0.04	0.00	0.12	0.00	0.00	0.00	-0.04	0.00	-0.10	0.00
16	66.29	0.790	0.000	-0.017	0.10	0.00	0.29	0.00	0.00	0.03	0.05	0.00	0.14	0.00	0.00	0.00	0.01	0.00	0.03	0.00
17	68.83	0.790	0.000	-0.015	0.09	0.00	0.25	0.00	0.00	0.02	0.03	0.00	0.10	0.00	0.00	0.00	0.00	0.00	0.00	0.00

Table C.5 Continued.

Case C.S0 Station= 6
X= -12.7mm Tunnel Run#= 676 Ue/Uref= 0.730 Date= 509.88 Time=13.08
Bias Corrected data using 1/sqrt(U*U + V*V + W*W + (.01Ur)^2)
The Y-position has been corrected by adding 0.254 to each measured Y-position in this profile.

					<-- normalized by 0.001 Ur^2 -->						<---------- normalized by 0.0001 Ur^3 ---------->								
LR	Y(mm)	U/Ur	V/Ur	W/Ur	uu	vv	ww	uv	vw	uw	uuu	uvv	uww	vuu	vvv	vww	wuu	wvv	www	uvw
1	0.00	0.000	0.000	0.000	0.00	0.00	0.00	-0.10	0.00	0.00	0.00	0.00	0.00	0.00	0.00	0.00	0.00	0.00	0.00	0.00
1	1.52	0.074	0.003	0.007	5.00	1.23	2.54	-0.46	-0.07	0.20	1.54	0.21	0.48	-0.25	-0.18	-0.06	0.13	0.01	0.12	-0.01
2	2.79	0.102	0.005	0.006	6.24	1.79	3.03	-0.71	-0.09	0.18	1.64	0.35	0.62	-0.37	-0.23	-0.05	0.09	0.01	-0.06	-0.03
3	6.60	0.188	0.010	0.008	8.81	2.74	4.13	-1.46	-0.03	0.19	1.49	0.38	0.62	-0.59	-0.25	-0.09	0.05	0.00	-0.03	-0.05
4	10.41	0.281	0.019	0.005	9.96	3.23	4.91	-1.86	-0.02	0.19	0.11	0.06	0.29	-0.02	-0.06	-0.01	-0.20	0.01	-0.16	-0.02
5	15.49	0.414	0.033	0.005	8.84	3.04	4.98	-1.64	0.02	-0.04	-2.04	-0.27	-0.34	0.33	0.26	0.05	-0.25	-0.01	-0.10	-0.03
6	20.57	0.539	0.047	0.001	6.18	2.24	3.70	-1.27	-0.04	-0.03	-1.76	-0.40	-0.45	0.52	0.35	0.19	-0.01	0.02	-0.10	-0.04
7	25.65	0.628	0.059	0.001	3.85	1.35	2.33	-0.76	-0.01	-0.01	-1.55	-0.30	-0.39	0.38	0.23	0.12	-0.12	0.02	-0.07	0.02
8	30.73	0.711	0.067	0.003	1.13	0.61	0.73	-0.24	-0.02	0.01	-0.54	-0.13	-0.10	0.13	0.13	0.06	-0.01	-0.01	-0.04	0.01
9	35.81	0.734	0.068	0.004	0.16	0.21	0.20	-0.03	0.00	0.00	-0.01	-0.01	0.02	0.01	0.03	0.00	0.00	0.00	-0.01	0.00
10	40.89	0.734	0.069	0.004	0.08	0.09	0.13	-0.01	0.00	0.01	0.01	0.00	0.02	0.00	0.00	0.00	0.01	0.00	0.03	0.00
11	45.97	0.733	0.070	0.002	0.07	0.08	0.16	0.00	0.00	-0.01	0.02	0.00	0.05	0.00	0.00	0.00	-0.02	0.00	-0.07	0.00
12	51.05	0.735	0.068	0.001	0.06	0.08	0.12	0.00	0.00	0.01	0.00	0.00	0.01	0.00	0.00	0.00	0.00	0.00	0.01	0.00
13	56.13	0.733	0.074	0.001	0.06	0.34	0.14	0.00	0.00	0.00	0.01	0.00	0.03	0.00	0.00	0.00	0.00	0.00	-0.01	0.00
14	61.21	0.731	0.075	0.001	0.06	0.41	0.14	0.00	0.00	0.01	0.01	0.00	0.02	0.00	0.58	0.00	0.00	0.00	0.02	0.00
15	66.29	0.730	0.000	0.002	0.07	0.00	0.17	0.00	0.00	0.02	0.01	0.00	0.04	0.00	0.00	0.00	0.00	0.00	0.01	0.00
16	71.37	0.734	0.000	0.010	0.02	0.00	0.07	0.00	0.00	-0.04	0.00	0.00	0.01	0.00	0.00	0.00	-0.01	0.00	-0.02	0.00

Table C.5 Continued.

Case C.S0 Station= 7
X= 12.7mm Tunnel Run#= 674 Ue/Uref= 0.724 Date= 509.88 Time=11.00
Bias Corrected data using 1/sqrt(U*U + V*V + W*W + (.01Ur)^2)
The Y-position has been corrected by adding 0.254 to each measured Y-position in this profile.

					<-- normalized by 0.001 Ur^2 -->						<---------- normalized by 0.0001 Ur^3 ---------->								
LR	Y(mm)	U/Ur	V/Ur	W/Ur	uu	vv	ww	uv	vw	uw	uuu	uvv	uww	vuu	vvv	vww	wuu	wvv	www	uvw
1	0.00	0.000	0.000	0.000	0.00	0.00	0.00	-0.05	0.00	0.00	0.00	0.00	0.00	0.00	0.00	0.00	0.00	0.00	0.00	0.00
1	1.52	0.038	0.004	0.005	4.40	1.05	2.38	-0.26	-0.06	0.16	1.33	0.15	0.42	-0.15	-0.15	-0.01	0.12	0.01	0.24	-0.02
2	2.79	0.057	0.005	0.009	5.30	1.61	2.72	-0.55	-0.09	0.14	1.67	0.31	0.56	-0.33	-0.27	-0.08	0.09	0.03	0.32	-0.02
3	6.60	0.123	0.011	0.009	8.04	2.65	3.81	-1.37	-0.06	0.12	2.69	0.57	0.71	-0.65	-0.32	-0.15	0.07	0.07	0.08	0.02
4	10.41	0.211	0.017	0.010	10.35	3.20	4.97	-1.77	-0.09	0.21	1.30	0.35	0.46	-0.43	-0.27	-0.10	0.02	0.01	0.11	-0.02
5	15.49	0.332	0.027	0.008	10.98	3.40	5.54	-2.06	-0.01	-0.07	-1.61	-0.19	0.23	0.27	0.05	0.00	0.02	0.02	0.05	-0.09
6	20.57	0.463	0.041	0.005	8.51	2.90	5.05	-1.61	0.03	-0.24	-3.15	-0.48	-0.57	0.64	0.40	0.17	0.21	-0.03	-0.02	0.00
7	25.65	0.571	0.054	0.003	5.74	2.14	3.38	-1.25	-0.03	-0.03	-2.72	-0.50	-0.50	0.60	0.51	0.21	0.12	0.00	-0.09	-0.02
8	30.73	0.659	0.062	0.002	2.72	1.13	1.70	-0.57	-0.06	0.00	-1.28	-0.29	-0.32	0.36	0.23	0.15	-0.07	-0.05	-0.05	0.03
9	35.81	0.713	0.066	0.001	0.66	0.49	0.48	-0.17	0.02	-0.03	-0.30	-0.09	-0.02	0.11	0.11	0.05	0.00	0.01	-0.04	-0.02
10	40.89	0.724	0.065	0.002	0.10	0.15	0.16	0.00	0.01	0.00	0.00	0.00	0.02	0.00	0.01	0.00	0.00	0.00	-0.01	0.00
11	45.97	0.723	0.066	0.001	0.07	0.10	0.14	0.00	0.00	0.00	0.01	0.00	0.02	0.00	0.00	0.00	0.00	0.00	-0.01	0.00
12	51.05	0.722	0.066	0.001	0.07	0.09	0.18	0.00	0.00	0.00	0.02	0.00	0.06	0.00	0.00	0.00	-0.01	0.00	-0.01	0.00
13	56.13	0.721	0.069	-0.001	0.07	0.36	0.17	0.00	0.00	-0.01	0.02	0.00	0.06	0.00	0.00	0.00	-0.01	0.00	-0.03	0.00
14	61.21	0.719	0.070	0.000	0.07	0.37	0.20	0.00	0.00	-0.02	0.03	0.00	0.08	0.00	0.00	0.00	-0.03	0.00	-0.09	0.00
15	66.29	0.719	0.000	0.001	0.09	0.00	0.26	0.00	0.00	-0.02	0.05	0.00	0.14	0.00	0.00	0.00	-0.03	0.00	-0.09	0.00
16	71.37	0.716	0.000	0.003	0.10	0.00	0.27	0.00	0.00	0.00	0.04	0.00	0.12	0.00	0.00	0.00	-0.02	0.00	-0.07	0.00

Table C.5 Continued.

Case C.S0 Station= 8
X= 25.4mm Tunnel Run#= 672 Ue/Uref= 0.722 Date= 509.88 Time= 8.58
Bias Corrected data using 1/sqrt(U*U + V*V + W*W + (.01Ur)^2)
The Y-position has been corrected by adding 0.254 to each measured Y-position in this profile.

						<-- normalized by 0.001 Ur^2 -->						<---------- normalized by 0.0001 Ur^3 ----------->					
LR	Y(mm)	U/Ur	V/Ur	W/Ur	uu	vv	ww	uv	vw	uw	uuu	uvv	uww	vuu	vvv	vww	wuu	wvv	www	uvw
1	0.00	0.000	0.000	0.000	0.00	0.00	0.00	-0.03	0.00	0.00	0.00	0.00	0.00	0.00	0.00	0.00	0.00	0.00	0.00	0.00
1	1.52	0.013	0.002	0.008	3.97	1.02	2.55	-0.28	-0.09	0.07	1.00	0.12	0.55	-0.11	-0.14	-0.04	0.13	0.03	0.33	-0.04
2	2.79	0.029	0.004	0.009	4.69	1.47	2.74	-0.49	-0.12	0.02	1.67	0.30	0.60	-0.27	-0.25	-0.10	0.09	0.04	0.21	-0.04
3	6.60	0.086	0.007	0.012	7.36	2.57	3.97	-1.11	-0.14	0.22	2.80	0.53	0.89	-0.75	-0.45	-0.18	0.02	0.10	0.32	-0.03
4	10.41	0.161	0.012	0.017	10.38	3.33	5.39	-1.77	-0.11	0.05	2.26	0.51	0.86	-0.51	-0.37	-0.12	-0.28	0.06	0.21	-0.03
5	15.49	0.289	0.022	0.020	11.30	3.81	6.54	-2.13	-0.16	-0.10	-1.61	0.04	0.41	-0.04	0.04	-0.12	-0.22	0.07	0.25	0.03
6	20.57	0.419	0.034	0.013	10.05	3.34	5.87	-1.87	-0.03	-0.39	-4.02	-0.48	-0.54	0.52	0.42	0.09	-0.20	0.08	0.00	0.01
7	25.65	0.536	0.047	0.007	6.53	2.49	4.46	-1.36	-0.10	-0.32	-2.97	-0.56	-0.70	0.80	0.52	0.23	0.20	0.06	0.06	0.00
8	30.73	0.635	0.056	0.004	3.50	1.41	2.36	-0.72	-0.04	-0.05	-1.69	-0.41	-0.36	0.46	0.34	0.15	-0.09	0.00	-0.04	0.02
9	35.81	0.697	0.062	0.003	1.08	0.67	0.87	-0.22	0.00	-0.10	-0.51	-0.13	0.03	0.14	0.23	0.08	-0.03	-0.01	-0.16	0.00
10	40.89	0.718	0.063	0.003	0.23	0.25	0.42	-0.03	0.01	-0.10	0.06	-0.01	0.25	0.01	0.10	0.01	-0.09	0.00	-0.31	-0.01
11	45.97	0.718	0.063	0.002	0.13	0.13	0.31	0.00	0.00	-0.07	0.07	0.00	0.19	0.00	0.00	0.00	-0.09	0.00	-0.26	0.00
12	51.05	0.716	0.063	0.001	0.11	0.11	0.28	0.00	0.00	-0.04	0.05	0.00	0.15	0.00	0.02	0.00	-0.05	0.00	-0.16	0.00
13	56.13	0.716	0.065	-0.001	0.08	0.37	0.21	0.00	0.00	0.01	0.02	0.00	0.07	0.00	0.00	0.00	0.00	0.00	-0.01	0.00
14	61.21	0.716	0.066	-0.002	0.07	0.39	0.18	0.00	0.00	0.00	0.02	0.00	0.05	0.00	0.00	0.00	-0.01	0.00	-0.03	0.00
15	66.29	0.715	0.000	0.000	0.08	0.00	0.21	0.00	0.00	0.03	0.03	0.00	0.08	0.00	0.00	0.00	0.02	0.00	0.06	0.00
16	71.37	0.712	0.000	0.002	0.06	0.00	0.16	0.00	0.00	-0.01	0.01	0.00	0.03	0.00	0.00	0.00	-0.02	0.00	-0.04	0.00

Table C.5 Continued.

Case C.S0 Station= 9
X= 50.8mm Tunnel Run#= 670 Ue/Uref= 0.711 Date= 508.88 Time=18.24
Bias Corrected data using 1/sqrt(U*U + V*V + W*W + (.01Ur)^2)
The Y-position has been corrected by adding 0.254 to each measured Y-position in this profile.

					<-- normalized by 0.001 Ur^2 -->						<---------- normalized by 0.0001 Ur^3 ---------->								
LR	Y(mm)	U/Ur	V/Ur	W/Ur	uu	vv	ww	uv	vw	uw	uuu	uvv	uww	vuu	vvv	vww	wuu	wvv	www	uvw
1	0.00	0.000	0.000	0.000	0.00	0.00	0.00	0.00	0.00	0.00	0.00	0.00	0.00	0.00	0.00	0.00	0.00	0.00	0.00	0.00
1	1.52	-0.012	0.003	0.003	3.48	0.86	2.21	-0.12	-0.10	-0.05	0.63	0.10	0.29	-0.04	-0.12	-0.01	0.04	0.01	0.27	-0.02
2	2.79	-0.003	0.003	0.003	4.14	1.38	2.48	-0.33	-0.06	0.00	1.03	0.21	0.50	-0.18	-0.23	-0.08	0.08	0.01	0.26	-0.03
3	6.60	0.041	0.007	0.004	6.35	2.44	3.38	-1.01	-0.10	0.05	2.32	0.51	0.73	-0.66	-0.39	-0.16	0.21	0.04	0.35	-0.07
4	10.41	0.101	0.011	0.007	8.90	3.34	4.61	-1.62	-0.19	0.00	2.84	0.53	0.82	-0.73	-0.47	-0.19	-0.12	0.04	0.20	-0.01
5	15.49	0.203	0.017	0.011	12.39	4.03	5.91	-2.44	-0.16	0.10	0.29	0.33	0.57	-0.33	-0.27	-0.11	-0.24	0.08	0.48	-0.01
6	20.57	0.328	0.026	0.010	12.17	4.16	6.60	-2.40	-0.12	-0.41	-2.75	-0.50	-0.17	0.64	0.30	0.04	-0.03	0.20	0.19	0.04
7	25.65	0.445	0.036	0.006	10.14	3.51	5.44	-2.06	-0.01	-0.32	-4.41	-0.79	-0.77	1.00	0.67	0.18	0.05	0.07	0.40	0.01
8	30.73	0.566	0.046	0.002	6.05	2.30	3.40	-1.31	0.02	-0.13	-3.48	-0.70	-0.63	0.95	0.57	0.29	0.15	0.07	-0.13	-0.06
9	35.81	0.650	0.054	0.002	2.97	1.28	1.73	-0.67	0.04	-0.05	-2.13	-0.40	-0.41	0.50	0.38	0.19	0.01	0.04	0.12	0.00
10	40.89	0.704	0.057	0.001	0.58	0.50	0.51	-0.16	0.02	-0.02	-0.23	-0.07	0.00	0.10	0.11	0.05	0.00	0.01	0.00	-0.01
11	45.97	0.710	0.056	0.002	0.16	0.19	0.28	-0.01	0.00	0.01	0.04	0.00	0.11	0.01	0.01	0.01	0.00	0.00	-0.01	0.00
12	51.05	0.710	0.055	0.002	0.11	0.14	0.23	0.00	0.01	0.00	0.03	0.00	0.08	0.00	0.07	0.00	-0.01	0.00	-0.02	0.00
13	56.13	0.705	0.058	0.000	0.09	0.37	0.22	0.00	0.01	0.00	0.03	0.00	0.09	0.00	0.00	0.00	-0.01	0.00	-0.02	0.00
14	61.21	0.708	0.058	-0.001	0.07	0.45	0.17	0.00	0.00	0.00	0.01	0.00	0.04	0.00	0.68	0.00	0.00	-0.01	-0.02	0.00
15	66.29	0.706	0.000	-0.001	0.07	0.00	0.19	0.00	0.00	0.01	0.02	0.00	0.06	0.00	0.00	0.00	0.00	0.00	0.00	0.00
16	71.37	0.703	0.000	-0.002	0.08	0.00	0.22	0.00	0.00	0.06	0.04	0.00	0.12	0.00	0.00	0.00	0.06	0.00	0.17	0.00

Table C.5 Continued.

Case C.S0 Station= 10
X= 101.6mm Tunnel Run#= 668 Ue/Uref= 0.699 Date= 508.88 Time=16.31
Bias Corrected data using 1/sqrt(U*U + V*V + W*W + (.01Ur)^2)
The Y-position has been corrected by adding 0.254 to each measured Y-position in this profile.

					<-- normalized by 0.001 Ur^2 -->						<---------- normalized by 0.0001 Ur^3 ---------->								
LR	Y(mm)	U/Ur	V/Ur	W/Ur	uu	vv	ww	uv	vw	uw	uuu	uvv	uww	vuu	vvv	vww	wuu	wvv	www	uvw
1	0.00	0.000	0.000	0.000	0.00	0.00	0.00	0.04	0.00	0.00	0.00	0.00	0.00	0.00	0.00	0.00	0.00	0.00	0.00	0.00
1	1.52	-0.021	0.001	0.002	3.31	0.85	2.32	-0.14	-0.07	0.15	0.56	0.10	0.36	-0.03	-0.12	-0.01	0.13	0.00	0.42	-0.02
2	2.79	-0.014	0.002	0.002	3.69	1.29	2.42	-0.29	-0.04	0.06	0.89	0.22	0.42	-0.17	-0.18	-0.06	0.08	0.00	0.45	-0.01
3	6.60	0.017	0.004	0.001	5.48	2.25	3.14	-0.92	-0.05	0.06	2.03	0.52	0.62	-0.54	-0.52	-0.22	0.05	0.05	0.29	-0.01
4	10.41	0.061	0.005	0.004	7.62	3.13	4.06	-1.50	-0.10	0.18	2.73	0.72	0.89	-0.87	-0.61	-0.29	0.14	0.06	0.50	-0.04
5	15.49	0.144	0.007	0.006	10.86	4.08	5.56	-2.38	-0.22	0.30	2.80	0.66	0.96	-1.00	-0.63	-0.25	-0.11	0.14	0.23	0.00
6	20.57	0.241	0.013	0.006	13.40	4.66	6.69	-2.98	-0.14	0.30	-0.72	-0.05	0.30	0.11	-0.13	-0.08	-0.14	-0.05	0.43	0.12
7	25.65	0.351	0.020	0.007	12.54	4.42	6.55	-2.83	0.00	-0.06	-4.81	-0.67	-0.33	1.25	0.42	0.26	-0.20	0.06	0.29	0.05
8	30.73	0.461	0.025	0.006	10.17	3.69	5.66	-2.18	0.11	-0.31	-5.98	-1.06	-1.16	1.31	0.80	0.33	0.42	0.14	0.17	-0.10
9	35.81	0.564	0.033	0.003	6.95	2.49	3.67	-1.61	-0.02	-0.02	-5.55	-1.00	-1.11	1.51	0.76	0.36	0.13	0.04	0.27	-0.03
10	40.89	0.648	0.041	0.003	3.13	1.34	1.73	-0.77	-0.03	0.05	-2.69	-0.47	-0.54	0.73	0.40	0.25	-0.05	-0.02	0.10	0.02
11	45.97	0.692	0.043	0.003	0.58	0.58	0.50	-0.17	0.00	0.04	-0.30	-0.13	0.02	0.16	0.19	0.07	0.03	-0.01	0.12	0.00
12	51.05	0.698	0.042	0.004	0.19	0.23	0.27	-0.01	0.01	0.01	0.04	0.00	0.12	0.01	0.02	0.00	0.00	0.00	0.03	0.00
13	56.13	0.695	0.048	0.003	0.14	0.42	0.25	0.00	0.00	0.02	0.04	0.00	0.11	0.00	0.01	0.00	0.01	0.00	0.04	0.00
14	61.21	0.694	0.047	0.002	0.11	0.39	0.23	0.00	0.01	0.04	0.03	0.00	0.09	0.00	0.00	0.00	0.02	0.00	0.05	0.00
15	66.29	0.693	0.000	0.002	0.11	0.00	0.25	0.00	0.00	0.03	0.04	0.00	0.12	0.00	0.00	0.00	0.02	0.00	0.07	0.00
16	71.37	0.694	0.000	0.003	0.14	0.00	0.34	0.00	0.00	0.12	0.06	0.00	0.20	0.00	0.00	0.00	0.09	0.00	0.30	0.00

Table C.5 Continued.

Case C.S0 Station= 11
X= 152.4mm Tunnel Run#= 666 Ue/Uref= 0.685 Date= 507.88 Time=13.38
Bias Corrected data using 1/sqrt(U*U + V*V + W*W + (.01Ur)^2)
The Y-position has been corrected by adding 0.254 to each measured Y-position in this profile.

					<-- normalized by 0.001 Ur^2 -->						<---------- normalized by 0.0001 Ur^3 ---------->									
LR	Y(mm)	U/Ur	V/Ur	W/Ur	uu	vv	ww	uv	vw	uw	uuu	uvv	uww	vuu	vvv	vww	wuu	wvv	www	uvw
1	0.00	0.000	0.000	0.000	0.00	0.00	0.00	0.10	0.00	0.00	0.00	0.00	0.00	0.00	0.00	0.00	0.00	0.00	0.00	0.00
1	1.52	-0.022	0.000	0.002	3.45	0.89	2.52	-0.17	-0.07	0.04	0.74	0.13	0.40	-0.05	-0.15	0.00	0.05	0.01	0.34	0.00
2	2.79	-0.013	-0.002	0.002	3.87	1.37	2.64	-0.36	-0.08	0.08	0.94	0.24	0.50	-0.17	-0.26	-0.04	0.08	0.02	0.33	-0.02
3	6.60	0.014	-0.002	0.001	5.12	2.32	3.10	-0.90	-0.11	0.24	1.99	0.48	0.78	-0.51	-0.53	-0.21	0.23	0.06	0.54	-0.04
4	10.41	0.052	-0.003	0.003	6.99	3.27	4.12	-1.40	-0.13	0.22	2.71	0.67	1.04	-0.84	-0.68	-0.32	0.14	0.04	0.52	0.06
5	15.49	0.115	-0.003	0.002	9.89	4.36	5.42	-2.25	-0.05	0.15	3.27	0.78	1.22	-0.93	-0.67	-0.43	0.17	0.02	0.23	-0.02
6	20.57	0.201	-0.001	0.004	11.56	5.00	6.75	-2.86	-0.05	0.11	1.25	0.35	0.75	-0.33	-0.27	-0.18	0.15	0.06	0.42	-0.05
7	25.65	0.287	0.005	0.005	12.61	5.24	7.24	-3.06	-0.03	-0.03	-1.71	-0.39	0.29	0.39	0.27	-0.09	-0.17	0.02	0.37	0.04
8	30.73	0.373	0.014	0.000	12.46	4.85	6.97	-3.13	-0.06	0.06	-3.56	-0.80	-0.72	0.75	0.64	0.28	-0.26	0.05	0.29	0.09
9	35.81	0.480	0.018	0.001	10.47	3.93	5.61	-2.59	0.14	-0.34	-7.68	-1.63	-1.05	2.17	1.08	0.42	0.60	0.14	0.55	-0.21
10	40.89	0.560	0.023	0.000	7.89	2.94	3.97	-1.99	-0.01	-0.15	-7.12	-1.41	-1.64	1.88	0.96	0.57	0.20	0.05	0.41	0.02
11	45.97	0.643	0.028	-0.001	3.41	1.70	1.78	-0.98	0.02	-0.02	-4.06	-0.84	-0.72	1.24	0.80	0.40	0.22	0.01	0.11	-0.03
12	51.05	0.679	0.028	0.000	0.83	0.76	0.52	-0.27	0.03	-0.01	-0.93	-0.31	-0.14	0.42	0.29	0.13	0.04	0.03	0.04	-0.03
13	56.13	0.685	0.031	-0.001	0.21	0.58	0.21	-0.02	0.01	0.01	0.01	0.00	0.03	0.01	0.04	0.01	0.01	0.00	0.00	0.00
14	61.21	0.684	0.032	-0.002	0.12	0.45	0.17	0.00	0.01	0.01	0.01	0.00	0.02	0.00	0.01	0.00	0.01	0.00	0.02	0.00
15	66.29	0.682	0.000	-0.002	0.11	0.00	0.19	0.00	0.00	0.02	0.02	0.00	0.05	0.00	0.00	0.00	0.01	0.00	0.04	0.00
16	71.37	0.682	0.000	-0.001	0.10	0.00	0.19	0.00	0.00	0.03	0.02	0.00	0.05	0.00	0.00	0.00	0.02	0.00	0.06	0.00

Table C.5 Continued.

Case C.S0 Station= 12
X= 228.6mm Tunnel Run#= 664 Ue/Uref= 0.664 Date= 507.88 Time=11.49
Bias Corrected data using 1/sqrt(U*U + V*V + W*W + (.01Ur)^2)
The Y-position has been corrected by adding 0.254 to each measured Y-position in this profile.

					<-- normalized by 0.001 Ur^2 -->						<---------- normalized by 0.0001 Ur^3 ---------->								
LR	Y(mm)	U/Ur	V/Ur	W/Ur	uu	vv	ww	uv	vw	uw	uuu	uvv	uww	vuu	vvv	vww	wuu	wvv	www	uvw
1	0.00	0.000	0.000	0.000	0.00	0.00	0.00	0.00	0.00	0.00	0.00	0.00	0.00	0.00	0.00	0.00	0.00	0.00	0.00	0.00
1	1.52	0.003	0.001	0.004	3.54	0.95	2.98	-0.18	-0.11	0.07	1.02	0.12	0.55	-0.07	-0.13	-0.02	0.09	0.01	0.40	0.00
2	2.79	0.010	0.002	0.003	3.76	1.40	2.96	-0.35	-0.07	0.08	1.26	0.24	0.62	-0.18	-0.26	-0.03	0.10	0.03	0.46	-0.02
3	6.60	0.034	0.002	0.003	5.01	2.56	3.33	-0.96	-0.05	0.03	2.17	0.58	0.70	-0.58	-0.63	-0.14	0.15	0.00	0.25	-0.01
4	10.41	0.062	0.003	0.001	6.77	3.38	4.03	-1.65	-0.11	0.18	3.05	0.88	0.96	-1.04	-0.80	-0.29	0.21	0.10	0.34	-0.10
5	15.49	0.110	0.002	0.003	9.40	4.50	5.36	-2.69	-0.05	0.25	3.91	1.25	1.27	-1.52	-1.09	-0.52	0.24	0.10	0.27	0.00
6	20.57	0.187	-0.005	0.008	11.81	5.51	7.01	-3.36	-0.19	0.30	2.38	0.80	1.09	-0.92	-0.72	-0.37	-0.28	0.09	0.30	-0.05
7	25.65	0.245	-0.005	0.006	13.08	5.72	7.95	-3.69	-0.19	0.16	-0.34	0.29	0.86	-0.18	-0.31	-0.16	-0.24	-0.10	-0.30	0.07
8	30.73	0.326	-0.003	0.007	12.85	5.86	8.15	-3.88	0.01	-0.19	-2.70	-0.96	-0.06	1.11	0.63	0.31	-0.30	0.06	0.10	0.05
9	35.81	0.409	0.001	0.001	12.19	5.23	7.50	-3.68	0.08	-0.12	-5.31	-1.46	-1.15	2.16	0.88	0.62	-0.11	0.13	0.26	-0.06
10	40.89	0.492	0.003	0.002	10.42	4.36	5.78	-2.90	0.05	-0.24	-7.35	-1.86	-1.70	2.45	1.43	0.63	0.30	0.02	0.31	0.01
11	45.97	0.566	0.006	0.002	7.68	3.35	3.99	-2.31	0.06	-0.19	-8.25	-2.17	-1.75	2.91	1.63	0.77	0.50	0.10	0.12	-0.23
12	51.05	0.627	0.009	0.001	3.85	2.12	2.11	-1.08	0.00	-0.08	-4.63	-1.10	-1.10	1.37	0.88	0.47	0.23	0.02	0.07	0.00
13	56.13	0.660	0.012	0.001	1.30	1.45	0.78	-0.45	0.03	0.01	-1.71	-0.61	-0.27	0.76	0.70	0.22	-0.02	0.00	0.03	-0.01
14	61.21	0.664	0.014	0.001	0.42	0.84	0.37	-0.09	0.02	0.02	-0.16	-0.09	0.01	0.14	0.19	0.08	0.05	0.03	0.08	-0.01
15	66.29	0.664	0.000	0.000	0.23	0.00	0.24	0.00	0.00	0.02	0.01	0.00	0.04	0.00	0.00	0.00	0.02	0.00	0.04	0.00
16	71.37	0.661	0.000	-0.001	0.16	0.00	0.23	0.00	0.00	0.03	0.03	0.00	0.07	0.00	0.00	0.00	0.01	0.00	0.02	0.00

Table C.5 Continued.

Case C.S0 Station= 13
X= 304.8mm Tunnel Run#= 662 Ue/Uref= 0.645 Date= 506.88 Time=18.39
Bias Corrected data using 1/sqrt(U*U + V*V + W*W + (.01Ur)^2)
The Y-position has been corrected by adding 0.254 to each measured Y-position in this profile.

					<-- normalized by 0.001 Ur^2 -->						<---------- normalized by 0.0001 Ur^3 ---------->									
LR	Y(mm)	U/Ur	V/Ur	W/Ur	uu	vv	ww	uv	vw	uw	uuu	uvv	uww	vuu	vvv	vww	wuu	wvv	www	uvw
1	0.00	0.000	0.000	0.000	0.00	0.00	0.00	-0.09	0.00	0.00	0.00	0.00	0.00	0.00	0.00	0.00	0.00	0.00	0.00	0.00
1	1.52	0.040	0.001	0.005	3.93	0.93	3.36	-0.23	-0.13	0.18	1.47	0.15	0.84	-0.13	-0.11	0.03	0.21	0.01	0.35	-0.05
2	2.79	0.052	0.001	0.004	4.33	1.55	3.46	-0.42	-0.10	0.26	1.72	0.27	0.79	-0.20	-0.30	0.04	0.23	0.03	0.30	-0.02
3	6.60	0.080	0.001	0.005	5.56	2.79	3.90	-1.12	-0.12	0.33	2.39	0.71	0.87	-0.69	-0.67	-0.11	0.23	0.03	0.13	-0.06
4	10.41	0.106	-0.001	0.003	7.30	3.82	4.75	-1.77	-0.14	0.40	3.20	1.15	1.30	-1.22	-1.06	-0.28	0.28	0.12	0.30	-0.15
5	15.49	0.151	-0.005	0.005	9.67	4.94	6.00	-2.80	-0.25	0.84	3.88	1.12	1.32	-1.48	-0.85	-0.48	0.03	0.28	0.41	-0.14
6	20.57	0.204	-0.008	0.009	11.91	5.81	7.35	-3.75	-0.21	0.53	2.97	1.09	1.40	-1.14	-0.95	-0.45	0.07	-0.03	0.31	-0.01
7	25.65	0.269	-0.013	0.011	12.94	6.37	7.82	-4.35	-0.14	0.23	-0.60	0.08	0.77	0.05	-0.16	-0.03	-0.50	0.09	0.05	0.01
8	30.73	0.332	-0.016	0.009	12.61	6.23	8.28	-4.18	-0.02	-0.02	-2.77	-0.59	-0.03	1.02	0.73	0.43	-0.64	-0.10	0.53	0.34
9	35.81	0.399	-0.017	0.007	12.01	5.86	7.52	-4.16	-0.06	-0.12	-4.50	-1.72	-0.83	2.23	1.50	0.51	-0.55	-0.21	-0.14	0.32
10	40.89	0.460	-0.017	0.002	10.81	5.14	6.90	-3.51	0.09	-0.26	-6.86	-1.86	-1.47	2.25	1.70	0.83	-0.11	0.08	0.27	-0.02
11	45.97	0.523	-0.016	0.003	8.80	4.27	4.93	-2.77	0.21	-0.50	-7.62	-2.46	-1.75	3.00	2.05	0.76	0.55	0.10	0.26	-0.26
12	51.05	0.578	-0.014	0.002	6.21	2.97	3.15	-1.84	0.01	-0.22	-7.77	-1.81	-1.61	2.35	1.49	0.77	0.37	0.01	0.47	-0.06
13	56.13	0.613	-0.010	0.002	3.80	2.55	1.78	-1.25	0.09	-0.12	-5.97	-1.57	-1.01	2.02	1.39	0.55	0.29	0.13	0.13	-0.05
14	61.21	0.632	-0.010	0.001	1.69	1.69	0.95	-0.56	0.01	-0.04	-2.32	-0.75	-0.32	0.91	0.81	0.30	0.02	0.02	0.03	0.02
15	66.29	0.638	-0.009	-0.001	0.70	1.23	0.52	-0.21	0.04	0.01	-0.55	-0.26	-0.04	0.29	1.07	0.13	-0.01	0.06	-0.05	-0.06
16	71.37	0.640	0.000	-0.002	0.28	0.00	0.31	0.00	0.00	0.00	0.02	0.00	0.10	0.00	0.00	0.00	-0.01	0.00	-0.06	0.00

Table C.5 Continued.

Case D.S0 Station= 1
X=-457.2mm Tunnel Run#= 797 Ue/Uref= 1.000 Date= 718.88 Time=16.48
Bias Corrected data using 1/sqrt(U*U + V*V + W*W + (.01Ur)^2)

						<-- normalized by 0.001 Ur^2 -->						<---------- normalized by 0.0001 Ur^3 ----------->									
LR	Y(mm)	U/Ur	V/Ur	W/Ur	uu	vv	ww	uv	vw	uw	uuu	uvv	uww	vuu	vvv	vww	wuu	wvv	www	uvw
1	0.00	0.000	0.000	0.000	0.00	0.00	0.00	-1.62	0.00	0.00	0.00	0.00	0.00	0.00	0.00	0.00	0.00	0.00	0.00	0.00
1	0.63	0.612	0.008	0.002	8.39	2.31	4.91	-1.75	-0.11	0.09	-1.28	-0.27	0.20	0.67	0.67	0.11	-0.22	-0.02	-0.34	0.02
2	1.27	0.678	0.007	0.002	6.63	2.44	4.32	-1.66	-0.03	0.04	-0.16	-0.16	0.38	0.24	0.42	0.11	0.02	0.02	-0.43	-0.05
3	2.54	0.750	0.007	0.002	5.63	2.33	3.74	-1.53	-0.05	0.01	-0.36	-0.12	0.14	0.22	0.28	0.16	0.05	-0.05	-0.22	-0.02
4	6.35	0.889	0.004	0.004	3.41	1.72	2.24	-1.04	0.00	0.04	-0.96	-0.32	-0.23	0.42	0.99	0.14	-0.01	0.04	0.09	0.02
5	10.16	0.981	0.000	0.004	0.78	0.69	0.66	-0.23	0.01	0.04	-0.35	-0.13	-0.02	0.16	0.70	0.05	0.04	0.00	0.15	0.00
6	15.24	0.996	-0.001	0.006	0.11	0.14	0.26	0.00	0.00	0.03	0.02	0.00	0.07	0.00	0.07	0.00	0.04	0.00	0.11	0.00
7	20.32	0.995	-0.003	0.003	0.09	0.13	0.25	0.00	0.00	0.03	0.02	0.00	0.07	0.00	0.09	0.00	0.04	0.00	0.12	0.00
8	25.40	1.000	-0.002	0.003	0.10	0.14	0.21	0.00	0.00	0.01	0.01	0.00	0.04	0.00	0.18	0.00	0.02	0.00	0.08	0.00
9	30.48	0.998	-0.005	0.004	0.10	0.14	0.26	0.00	0.00	0.02	0.02	0.00	0.07	0.00	0.18	0.00	0.03	0.00	0.09	0.00
10	35.56	0.999	-0.006	0.006	0.08	0.11	0.23	0.00	0.00	0.00	0.02	0.00	0.06	0.00	0.08	0.00	0.02	0.00	0.06	0.00
11	40.64	1.001	-0.006	0.003	0.09	0.12	0.25	0.00	0.00	-0.01	0.02	0.00	0.06	0.00	0.08	0.00	0.02	0.00	0.06	0.00
12	45.72	0.996	-0.001	0.001	0.12	0.11	0.26	0.00	0.00	0.00	0.02	0.00	0.06	0.00	0.01	0.00	0.02	0.00	0.06	0.00
13	50.80	0.999	0.001	0.002	0.11	0.12	0.32	0.00	0.00	0.01	0.03	0.00	0.10	0.00	0.08	0.00	0.03	0.00	0.09	0.00
14	55.88	1.001	0.002	-0.001	0.13	0.10	0.32	0.00	0.00	-0.01	0.03	0.00	0.10	0.00	0.00	0.00	0.02	0.00	0.05	0.00
15	60.96	0.999	-0.006	-0.002	0.20	0.00	0.33	0.00	0.00	0.03	0.03	0.00	0.09	0.00	0.00	0.00	0.03	0.00	0.11	0.00
16	66.04	0.999	-0.006	-0.001	0.11	0.00	0.35	0.00	0.00	0.02	0.03	0.00	0.08	0.00	0.00	0.00	0.03	0.00	0.08	0.00

Table C.5 Continued.

Case D.S0 Station= 2
X=-152.4mm Tunnel Run#= 791 Ue/Uref= 1.001 Date= 621.88 Time=13.22
Bias Corrected data using 1/sqrt(U*U + V*V + W*W + (.01Ur)^2)

					<-- normalized by 0.001 Ur^2 -->						<---------- normalized by 0.0001 Ur^3 ---------->									
LR	Y(mm)	U/Ur	V/Ur	W/Ur	uu	vv	ww	uv	vw	uw	uuu	uvv	uww	vuu	vvv	vww	wuu	wvv	www	uvw
1	0.00	0.000	0.000	0.000	0.00	0.00	0.00	-1.55	0.00	0.00	0.00	0.00	0.00	0.00	0.00	0.00	0.00	0.00	0.00	0.00
1	0.25	0.480	0.002	0.001	13.56	0.97	5.21	-1.45	-0.09	-0.42	-2.82	0.00	1.04	0.62	0.03	0.14	0.01	-0.01	-0.95	-0.01
2	0.63	0.598	0.001	0.001	8.43	1.97	4.77	-1.54	-0.05	0.07	-1.26	-0.18	0.11	0.59	0.21	0.16	-0.06	-0.06	-0.11	0.05
3	1.27	0.658	0.002	0.002	6.98	2.12	4.32	-1.47	-0.05	0.04	0.00	-0.16	0.25	0.29	0.17	0.20	-0.18	0.00	-0.62	0.03
4	2.54	0.731	0.002	0.001	5.96	2.16	3.67	-1.48	-0.05	0.06	-0.64	-0.12	0.04	0.25	0.18	0.17	0.02	-0.01	-0.28	-0.03
5	6.35	0.846	0.003	0.004	4.03	1.74	2.65	-1.11	0.01	0.03	-0.82	-0.20	-0.04	0.28	0.19	0.15	-0.04	0.00	-0.14	-0.01
6	10.16	0.929	0.004	0.005	2.35	1.10	1.49	-0.66	-0.04	0.08	-0.82	-0.24	-0.16	0.28	0.24	0.10	0.03	0.00	-0.02	0.00
7	15.24	0.990	0.004	0.007	0.32	0.28	0.34	-0.07	0.00	0.01	-0.09	-0.03	0.01	0.04	0.04	0.02	0.02	0.00	0.03	0.00
8	20.32	1.002	0.004	0.005	0.07	0.10	0.15	0.00	0.00	0.00	0.01	0.00	0.01	0.00	0.00	0.00	0.01	0.00	0.02	0.00
9	25.40	1.003	0.005	0.005	0.09	0.08	0.17	0.00	0.00	0.02	0.01	0.00	0.03	0.00	0.00	0.00	0.02	0.00	0.05	0.00
10	30.48	1.003	0.006	0.005	0.07	0.08	0.18	0.00	0.00	0.00	0.01	0.00	0.03	0.00	0.00	0.00	0.01	0.00	0.04	0.00
11	35.56	1.004	0.005	0.007	0.07	0.08	0.19	0.00	0.00	0.00	0.01	0.00	0.03	0.00	0.00	0.00	0.01	0.00	0.04	0.00
12	40.64	1.006	0.005	0.006	0.08	0.11	0.19	0.00	0.00	0.01	0.01	0.00	0.03	0.00	0.09	0.00	0.01	0.00	0.05	0.00
13	45.72	1.007	0.005	0.005	0.09	0.09	0.21	0.00	0.00	0.01	0.01	0.00	0.04	0.00	0.00	0.00	0.02	0.00	0.06	0.00
14	50.80	1.004	0.005	0.005	0.09	0.08	0.19	0.00	0.00	0.01	0.01	0.00	0.03	0.00	0.00	0.00	0.02	0.00	0.05	0.00
15	55.88	1.009	0.010	0.001	0.09	0.44	0.21	0.00	0.00	0.01	0.01	0.00	0.03	0.00	-0.02	0.00	0.02	0.00	0.06	0.00
16	60.96	1.017	0.000	-0.004	0.11	0.00	0.26	0.00	0.00	0.01	0.02	0.00	0.05	0.00	0.00	0.00	0.02	0.00	0.05	0.00
17	66.04	1.013	0.000	-0.009	0.19	0.00	0.50	0.00	0.00	0.07	0.01	0.00	0.01	0.00	0.00	0.00	0.01	0.00	0.01	0.00

Table C.5 Continued.

Case D.S0 Station= 3
X= -76.2mm Tunnel Run#= 789 Ue/Uref= 0.990 Date= 621.88 Time=11.55
Bias Corrected data using 1/sqrt(U*U + V*V + W*W + (.01Ur)^2)

					<-- normalized by 0.001 Ur^2 -->						<---------- normalized by 0.0001 Ur^3 ---------->									
LR	Y(mm)	U/Ur	V/Ur	W/Ur	uu	vv	ww	uv	vw	uw	uuu	uvv	uww	vuu	vvv	vww	wuu	wvv	www	uvw
1	0.00	0.000	0.000	0.000	0.00	0.00	0.00	-1.35	0.00	0.00	0.00	0.00	0.00	0.00	0.00	0.00	0.00	0.00	0.00	0.00
1	0.25	0.455	0.003	0.001	12.78	1.17	4.37	-1.37	-0.05	-0.28	-2.01	0.11	1.00	0.40	0.50	0.13	-0.26	-0.01	-0.96	-0.01
2	0.63	0.550	0.004	0.000	8.68	1.86	4.43	-1.57	-0.06	-0.17	-0.97	-0.15	0.34	0.50	0.13	0.21	-0.01	-0.01	-0.40	0.04
3	1.27	0.614	0.005	0.001	7.24	2.19	4.07	-1.59	0.02	-0.03	-0.04	-0.10	0.37	0.25	0.21	0.11	0.10	0.02	-0.09	-0.02
4	2.54	0.684	0.008	0.000	6.32	2.17	3.51	-1.55	0.00	-0.03	-0.31	-0.10	0.10	0.22	0.15	0.13	-0.03	-0.01	-0.10	0.00
5	6.35	0.802	0.010	0.001	4.69	1.87	2.81	-1.25	0.01	0.01	-0.90	-0.23	-0.13	0.30	0.22	0.13	-0.03	0.01	-0.04	-0.01
6	10.16	0.889	0.013	0.003	2.88	1.22	1.75	-0.83	-0.04	0.03	-0.93	-0.24	-0.21	0.33	0.20	0.11	-0.01	0.00	-0.03	0.00
7	15.24	0.967	0.019	0.004	0.77	0.48	0.51	-0.22	0.00	0.01	-0.41	-0.11	-0.07	0.15	0.13	0.04	0.00	-0.01	0.01	0.00
8	20.32	0.983	0.022	0.004	0.09	0.13	0.17	-0.01	0.00	0.00	0.00	0.00	0.01	0.01	0.09	0.00	0.01	0.00	0.03	0.00
9	25.40	0.992	0.026	0.001	0.06	0.07	0.15	0.00	0.00	0.00	0.01	0.00	0.02	0.00	0.00	0.00	0.01	0.00	0.03	0.00
10	30.48	0.995	0.029	0.003	0.05	0.07	0.14	0.00	0.00	0.00	0.00	0.00	0.01	0.00	0.00	0.00	0.01	0.00	0.03	0.00
11	35.56	0.997	0.031	0.005	0.06	0.07	0.15	0.00	0.00	0.01	0.01	0.00	0.02	0.00	0.00	0.00	0.01	0.00	0.03	0.00
12	40.64	0.999	0.033	0.006	0.07	0.07	0.15	0.00	0.00	0.00	0.00	0.00	0.02	0.00	0.00	0.00	0.01	0.00	0.03	0.00
13	45.72	1.003	0.032	0.003	0.08	0.07	0.20	0.00	0.00	0.02	0.01	0.00	0.04	0.00	0.00	0.00	0.02	0.00	0.07	0.00
14	50.80	1.006	0.042	0.005	0.07	0.40	0.18	0.00	0.01	0.02	0.01	0.00	0.04	0.00	0.00	0.00	0.02	0.00	0.06	0.00
15	55.88	1.013	0.046	0.004	0.08	0.47	0.21	0.00	0.00	0.01	0.01	0.00	0.04	0.00	-0.01	0.00	0.02	0.00	0.06	0.00
16	60.96	1.023	0.048	-0.005	0.06	0.46	0.14	0.00	-0.01	0.04	0.01	0.00	0.03	0.00	0.05	0.00	0.02	0.00	0.05	0.00
17	66.04	1.019	0.000	-0.008	0.09	0.00	0.28	0.00	0.00	-0.16	-0.01	0.00	-0.04	0.00	0.00	0.00	0.02	0.00	0.06	0.00

Table C.5 Continued.

Case D.S0 Station= 4
X= -12.7mm Tunnel Run#= 787 Ue/Uref= 0.931 Date= 621.88 Time=10.18
Bias Corrected data using 1/sqrt(U*U + V*V + W*W + (.01Ur)^2)

					<-- normalized by 0.001 Ur^2 -->						<---------- normalized by 0.0001 Ur^3 ---------->									
LR	Y(mm)	U/Ur	V/Ur	W/Ur	uu	vv	ww	uv	vw	uw	uuu	uvv	uww	vuu	vvv	vww	wuu	wvv	www	uvw
1	0.00	0.000	0.000	0.000	0.00	0.00	0.00	-1.00	0.00	0.00	0.00	0.00	0.00	0.00	0.00	0.00	0.00	0.00	0.00	0.00
1	0.25	0.377	0.003	-0.003	10.96	0.99	4.66	-1.19	-0.08	-0.39	0.75	0.13	1.46	0.08	0.15	0.08	-0.34	0.00	-0.98	-0.03
2	0.63	0.464	0.003	-0.004	8.23	1.73	4.91	-1.32	-0.08	-0.35	-0.04	-0.04	0.98	0.33	0.03	0.21	-0.33	0.03	-1.18	-0.02
3	1.27	0.516	0.005	-0.005	7.16	2.15	4.64	-1.44	-0.09	-0.30	0.77	-0.05	0.77	0.08	0.15	0.16	-0.26	0.03	-0.73	0.00
4	2.54	0.586	0.007	-0.005	6.94	2.28	4.08	-1.58	-0.06	-0.17	0.32	-0.13	0.45	0.12	0.14	0.08	-0.08	0.01	-0.44	-0.03
5	6.35	0.709	0.014	-0.004	5.53	1.98	3.48	-1.31	-0.02	-0.11	-0.68	-0.20	0.27	0.26	0.18	0.10	-0.10	0.01	-0.61	-0.01
6	10.16	0.796	0.020	-0.004	3.96	1.50	2.64	-0.96	-0.02	-0.12	-0.90	-0.22	0.03	0.31	0.23	0.14	-0.03	0.02	-0.43	-0.02
7	15.24	0.886	0.027	-0.001	1.77	0.72	1.20	-0.36	-0.04	0.02	-0.72	-0.15	-0.09	0.18	0.12	0.07	-0.02	-0.01	0.03	0.02
8	20.32	0.926	0.035	0.000	0.28	0.24	0.33	-0.06	0.00	0.00	-0.07	-0.04	0.03	0.03	0.06	0.02	0.01	0.00	0.04	0.00
9	25.40	0.928	0.040	-0.002	0.08	0.09	0.19	0.00	0.00	0.01	0.01	0.00	0.04	0.00	0.00	0.00	0.02	0.00	0.05	0.00
10	30.48	0.931	0.044	-0.002	0.09	0.09	0.24	0.00	0.00	0.02	0.02	0.00	0.07	0.00	0.03	0.00	0.03	0.00	0.09	0.00
11	35.56	0.929	0.049	0.000	0.07	0.08	0.20	0.00	0.00	0.01	0.02	0.00	0.05	0.00	0.00	0.00	0.02	0.00	0.05	0.00
12	40.64	0.930	0.052	0.002	0.08	0.08	0.21	0.00	0.00	0.01	0.02	0.00	0.05	0.00	0.00	0.00	0.02	0.00	0.07	0.00
13	45.72	0.931	0.055	0.001	0.08	0.08	0.21	0.00	0.00	0.02	0.02	0.00	0.05	0.00	0.00	0.00	0.02	0.00	0.07	0.00
14	50.80	0.931	0.058	-0.001	0.09	0.09	0.25	0.00	0.00	0.02	0.02	0.00	0.07	0.00	0.01	0.00	0.03	0.00	0.10	0.00
15	55.88	0.931	0.066	0.000	0.09	0.37	0.26	0.00	-0.01	0.02	0.02	0.00	0.07	0.00	0.00	0.00	0.03	0.00	0.10	0.00
16	60.96	0.930	0.067	-0.001	0.10	0.38	0.29	0.00	0.00	0.06	0.03	0.00	0.10	0.00	0.00	0.00	0.05	0.00	0.15	0.00
17	66.04	0.929	0.000	-0.004	0.11	0.00	0.31	0.00	0.00	0.08	0.04	0.00	0.11	0.00	0.00	0.00	0.06	0.00	0.18	0.00
18	71.12	0.921	0.000	-0.002	0.10	0.00	0.28	0.00	0.00	-0.02	0.00	0.00	-0.01	0.00	0.00	0.00	0.00	0.00	0.00	0.00

Table C.5 Continued.

Case D.S0 Station= 5
X= 0.0mm Tunnel Run#= 785 Ue/Uref= 0.917 Date= 621.88 Time= 8.45
Bias Corrected data using 1/sqrt(U*U + V*V + W*W + (.01Ur)^2)

					<-- normalized by 0.001 Ur^2 -->						<---------- normalized by 0.0001 Ur^3 ---------->								
LR	Y(mm)	U/Ur	V/Ur	W/Ur	uu	vv	ww	uv	vw	uw	uuu	uvv	uww	vuu	vvv	vww	wuu	wvv	www	uvw
1	0.00	0.000	0.000	0.000	0.00	0.00	0.00	-0.98	0.00	0.00	0.00	0.00	0.00	0.00	0.00	0.00	0.00	0.00	0.00	0.00
1	0.25	0.332	-0.018	-0.015	11.39	1.22	7.39	-1.18	-0.06	-2.39	2.09	0.15	5.95	0.08	1.28	0.18	-3.12	0.01	-9.23	-0.06
2	0.63	0.426	-0.010	-0.005	8.23	1.67	5.19	-1.35	-0.05	-0.56	0.18	-0.01	1.55	0.25	0.04	0.23	-0.33	0.02	-2.22	-0.04
3	1.27	0.490	-0.003	-0.003	7.56	2.05	4.41	-1.46	-0.09	-0.31	0.30	-0.01	0.95	0.18	0.02	0.12	-0.32	0.00	-1.02	-0.08
4	2.54	0.555	0.004	-0.003	7.22	2.24	4.22	-1.48	-0.13	0.00	0.25	0.05	0.63	0.06	0.24	0.14	-0.18	0.01	-0.78	0.01
5	6.35	0.682	0.013	-0.002	5.78	1.99	3.55	-1.32	-0.11	-0.04	-0.70	-0.17	0.15	0.29	0.17	0.18	-0.22	-0.02	-0.59	0.00
6	10.16	0.772	0.020	0.001	4.12	1.59	2.65	-0.97	-0.02	-0.08	-1.02	-0.19	-0.05	0.28	0.22	0.10	0.01	0.03	-0.08	-0.02
7	15.24	0.859	0.028	0.003	1.97	0.86	1.38	-0.46	0.01	-0.01	-0.75	-0.16	-0.11	0.22	0.14	0.09	-0.04	0.01	-0.11	0.00
8	20.32	0.904	0.035	0.004	0.49	0.35	0.45	-0.12	0.01	-0.01	-0.18	-0.06	0.00	0.07	0.07	0.03	0.00	0.00	-0.01	0.00
9	25.40	0.915	0.039	0.002	0.10	0.11	0.25	0.00	0.00	-0.03	0.03	0.00	0.08	0.00	0.01	0.00	-0.01	0.00	-0.04	0.00
10	30.48	0.916	0.043	0.001	0.08	0.08	0.21	0.00	0.00	-0.01	0.02	0.00	0.06	0.00	0.00	0.00	0.01	0.00	0.01	0.00
11	35.56	0.916	0.047	0.002	0.07	0.07	0.19	0.00	0.00	0.00	0.01	0.00	0.04	0.00	0.00	0.00	0.02	0.00	0.05	0.00
12	40.64	0.918	0.049	0.003	0.07	0.07	0.20	0.00	0.00	0.01	0.01	0.00	0.05	0.00	0.00	0.00	0.01	0.00	0.04	0.00
13	45.72	0.918	0.054	0.004	0.07	0.10	0.20	0.00	0.00	0.01	0.01	0.00	0.04	0.00	0.08	0.00	0.01	0.00	0.04	0.00
14	50.80	0.921	0.056	0.002	0.09	0.08	0.24	0.00	0.00	0.03	0.02	0.00	0.07	0.00	0.00	0.00	0.03	0.00	0.09	0.00
15	55.88	0.922	0.064	0.003	0.09	0.48	0.26	0.00	0.01	0.06	0.02	0.00	0.08	0.00	0.75	0.01	0.04	0.02	0.13	0.00
16	60.96	0.925	0.064	0.002	0.11	0.42	0.31	0.00	0.01	0.06	0.03	0.00	0.10	0.00	0.00	0.00	0.05	0.00	0.14	0.00
17	66.04	0.926	0.000	0.000	0.13	0.00	0.35	0.00	0.00	0.11	0.05	0.00	0.14	0.00	0.00	0.00	0.08	0.00	0.24	0.00

Table C.5 Continued.

Case D.S0 Station= 6
X= 12.7mm Tunnel Run#= 783 Ue/Uref= 0.905 Date= 617.88 Time= 8.38
Bias Corrected data using 1/sqrt(U*U + V*V + W*W + (.01Ur)^2)

					<-- normalized by 0.001 Ur^2 -->						<---------- normalized by 0.0001 Ur^3 ---------->									
LR	Y(mm)	U/Ur	V/Ur	W/Ur	uu	vv	ww	uv	vw	uw	uuu	uvv	uww	vuu	vvv	vww	wuu	wvv	www	uvw
1	0.00	0.000	0.000	0.000	0.00	0.00	0.00	-0.88	0.00	0.00	0.00	0.00	0.00	0.00	0.00	0.00	0.00	0.00	0.00	0.00
1	0.38	0.372	0.002	-0.001	9.45	0.95	4.27	-1.05	-0.06	-0.25	0.11	0.02	1.34	0.27	0.03	0.13	-0.28	0.03	-0.93	0.01
2	0.63	0.419	0.003	0.000	7.78	1.41	4.24	-1.17	0.00	-0.23	0.04	0.00	0.76	0.33	-0.02	0.13	-0.12	0.00	-0.30	-0.01
3	1.27	0.471	0.003	0.001	7.09	2.01	3.85	-1.38	-0.02	-0.11	0.65	-0.01	0.45	0.03	0.15	0.11	-0.09	-0.04	-0.24	0.03
4	2.54	0.534	0.007	-0.001	7.27	2.32	4.29	-1.46	-0.06	-0.13	0.37	0.00	0.65	0.14	0.17	0.10	-0.35	0.03	-0.67	-0.02
5	6.35	0.656	0.014	-0.001	5.96	2.08	3.61	-1.35	-0.05	-0.16	-0.54	-0.11	0.26	0.23	0.15	0.08	-0.16	-0.01	-0.38	-0.02
6	10.16	0.746	0.021	0.000	4.47	1.67	2.73	-1.05	-0.01	-0.02	-1.00	-0.23	0.05	0.28	0.30	0.08	0.00	0.03	-0.20	-0.01
7	15.24	0.836	0.030	0.001	2.38	0.95	1.56	-0.55	-0.02	0.00	-0.93	-0.20	-0.10	0.25	0.17	0.11	-0.02	-0.01	-0.10	0.00
8	20.32	0.891	0.036	0.003	0.53	0.37	0.51	-0.11	-0.01	-0.03	-0.17	-0.06	0.08	0.06	0.13	0.02	-0.05	0.00	-0.14	0.00
9	25.40	0.904	0.041	0.002	0.13	0.12	0.28	-0.01	0.00	-0.01	0.04	0.00	0.13	0.00	0.01	0.00	-0.02	0.00	-0.06	0.00
10	30.48	0.905	0.045	-0.001	0.08	0.08	0.22	0.00	0.00	0.00	0.02	0.00	0.08	0.00	0.00	0.00	-0.01	0.00	-0.03	0.00
11	35.56	0.907	0.048	0.001	0.09	0.08	0.24	0.00	0.00	0.00	0.03	0.00	0.10	0.00	0.00	0.00	0.00	0.00	-0.01	0.00
12	40.64	0.908	0.051	0.002	0.08	0.11	0.23	0.00	0.00	0.00	0.03	0.00	0.08	0.00	0.09	0.00	-0.01	0.00	-0.04	0.00
13	45.72	0.910	0.057	0.001	0.08	0.10	0.22	0.00	0.00	-0.01	0.02	0.00	0.07	0.00	0.00	0.00	-0.01	0.00	-0.02	0.00
14	50.80	0.910	0.062	0.000	0.07	0.10	0.20	0.00	0.00	0.00	0.02	0.00	0.05	0.00	0.00	0.00	0.00	0.00	0.01	0.00
15	55.88	0.912	0.067	0.000	0.08	0.48	0.22	-0.01	0.00	0.00	0.02	0.00	0.06	0.00	0.24	-0.01	0.00	-0.01	0.00	0.00
16	60.96	0.912	0.074	0.000	0.09	0.69	0.26	0.00	0.00	0.02	0.03	0.01	0.09	0.00	1.75	0.00	0.02	0.02	0.05	0.00
17	66.04	0.915	0.000	-0.003	0.08	0.00	0.23	0.00	0.00	0.02	0.01	0.00	0.02	0.00	0.00	0.00	0.01	0.00	0.04	0.00

Table C.5 Continued.

Case D.S0 Station= 7
X= 25.4mm Tunnel Run#= 781 Ue/Uref= 0.889 Date= 616.88 Time=19.33
Bias Corrected data using 1/sqrt(U*U + V*V + W*W + (.01Ur)^2)

					<-- normalized by 0.001 Ur^2 -->						<---------- normalized by 0.0001 Ur^3 ---------->									
LR	Y(mm)	U/Ur	V/Ur	W/Ur	uu	vv	ww	uv	vw	uw	uuu	uvv	uww	vuu	vvv	vww	wuu	wvv	www	uvw
1	0.00	0.000	0.000	0.000	0.00	0.00	0.00	-0.85	0.00	0.00	0.00	0.00	0.00	0.00	0.00	0.00	0.00	0.00	0.00	0.00
1	0.38	0.314	0.003	0.002	9.41	0.80	3.85	-0.95	-0.03	-0.07	0.93	0.08	0.98	0.06	-0.03	0.09	-0.09	-0.03	-0.21	0.06
2	0.63	0.372	0.003	0.001	8.36	1.32	4.05	-1.12	-0.05	-0.11	0.44	0.04	0.68	0.19	0.00	0.13	-0.04	-0.02	-0.10	0.05
3	1.27	0.435	0.005	0.001	7.13	1.92	3.93	-1.33	-0.05	-0.08	0.49	-0.03	0.39	0.15	0.08	0.10	0.00	-0.03	0.01	0.00
4	2.54	0.498	0.008	0.002	7.06	2.23	3.91	-1.45	-0.05	-0.13	0.44	0.02	0.20	0.01	0.12	0.10	-0.02	0.05	-0.22	-0.01
5	6.35	0.617	0.017	0.001	6.08	2.16	3.46	-1.40	-0.05	0.01	-0.33	-0.10	-0.01	0.15	0.18	0.13	-0.07	-0.02	-0.07	0.05
6	10.16	0.711	0.024	0.002	4.92	1.73	3.01	-1.20	-0.01	0.00	-1.21	-0.17	-0.22	0.34	0.17	0.15	-0.07	-0.01	-0.11	0.02
7	15.24	0.808	0.033	0.002	2.71	1.06	1.70	-0.65	0.00	0.00	-1.03	-0.22	-0.16	0.32	0.19	0.11	0.02	0.01	0.07	-0.01
8	20.32	0.867	0.040	0.004	0.82	0.47	0.59	-0.19	0.00	0.00	-0.36	-0.09	-0.04	0.11	0.09	0.04	0.00	0.00	-0.02	0.00
9	25.40	0.885	0.045	0.004	0.12	0.19	0.22	-0.01	0.00	-0.01	0.01	-0.01	0.07	0.01	0.28	0.00	-0.01	0.00	-0.04	0.00
10	30.48	0.889	0.049	0.002	0.08	0.08	0.19	0.00	0.00	-0.01	0.02	0.00	0.07	0.00	0.00	0.00	-0.01	0.00	-0.04	0.00
11	35.56	0.891	0.053	0.002	0.08	0.08	0.20	0.00	0.00	-0.02	0.03	0.00	0.08	0.00	0.00	0.00	-0.01	0.00	-0.04	0.00
12	40.64	0.892	0.056	0.004	0.08	0.08	0.22	0.00	0.00	-0.02	0.03	0.00	0.10	0.00	0.00	0.00	-0.02	0.00	-0.07	0.00
13	45.72	0.893	0.060	0.005	0.08	0.13	0.21	0.00	0.00	-0.02	0.03	0.00	0.08	0.00	0.17	0.00	-0.02	0.00	-0.07	0.00
14	50.80	0.896	0.061	0.005	0.10	0.14	0.26	0.00	0.00	0.00	0.04	0.00	0.12	0.00	0.17	0.00	-0.02	0.00	-0.04	0.00
15	55.88	0.898	0.074	0.005	0.09	0.51	0.25	0.00	0.00	0.04	0.03	0.00	0.09	0.00	0.47	0.00	0.02	0.00	0.06	0.00
16	60.96	0.899	0.077	0.000	0.05	0.52	0.16	0.02	0.03	-0.02	0.01	0.00	0.03	0.00	0.08	0.00	-0.01	0.01	-0.04	0.00
17	66.04	0.903	0.000	0.001	0.10	0.00	0.27	0.00	0.00	0.06	0.02	0.00	0.06	0.00	0.00	0.00	0.02	0.00	0.05	0.00

Table C.5 Continued.

Case D.S0 Station= 8
X= 48.3mm Tunnel Run#= 779 Ue/Uref= 0.868 Date= 616.88 Time=17.35
Bias Corrected data using 1/sqrt(U*U + V*V + W*W + (.01Ur)^2)

					<-- normalized by 0.001 Ur^2 -->						<---------- normalized by 0.0001 Ur^3 ---------->									
LR	Y(mm)	U/Ur	V/Ur	W/Ur	uu	vv	ww	uv	vw	uw	uuu	uvv	uww	vuu	vvv	vww	wuu	wvv	www	uvw
1	0.00	0.000	0.000	0.000	0.00	0.00	0.00	-0.60	0.00	0.00	0.00	0.00	0.00	0.00	0.00	0.00	0.00	0.00	0.00	0.00
1	0.25	0.230	0.004	0.000	8.32	0.53	4.00	-0.57	-0.03	-0.21	2.77	0.10	2.15	-0.21	-0.01	0.06	-0.43	0.01	-1.05	0.02
2	0.63	0.328	0.004	-0.003	7.52	1.18	4.83	-0.84	-0.13	-0.35	1.05	0.04	1.23	0.13	-0.03	0.12	-0.57	-0.02	-0.99	0.03
3	1.27	0.384	0.006	-0.001	7.25	1.81	4.22	-1.18	-0.05	-0.33	1.12	0.09	0.76	-0.07	-0.02	0.11	-0.08	-0.01	-0.46	0.01
4	2.54	0.442	0.009	-0.002	7.13	2.17	3.89	-1.38	-0.05	-0.33	0.65	0.12	0.40	-0.12	-0.01	0.02	-0.05	0.03	-0.22	-0.03
5	6.35	0.566	0.017	-0.003	6.71	2.23	3.85	-1.39	-0.02	-0.14	-0.56	-0.05	0.10	0.11	0.06	0.06	0.00	0.01	-0.10	-0.06
6	10.16	0.659	0.027	-0.003	5.45	1.88	3.26	-1.20	0.00	-0.10	-0.95	-0.22	-0.09	0.29	0.21	0.14	-0.03	0.03	-0.22	0.00
7	15.24	0.760	0.038	-0.004	3.20	1.18	2.12	-0.71	0.01	-0.11	-0.85	-0.22	-0.16	0.26	0.17	0.12	-0.03	0.00	-0.14	-0.03
8	20.32	0.827	0.048	-0.003	1.36	0.59	0.88	-0.29	-0.02	-0.03	-0.60	-0.14	-0.06	0.18	0.18	0.05	-0.04	-0.02	-0.10	0.00
9	25.40	0.860	0.054	-0.002	0.23	0.23	0.32	-0.03	0.00	-0.05	-0.01	-0.01	0.10	0.02	0.11	0.00	-0.05	0.00	-0.15	0.00
10	30.48	0.863	0.059	-0.003	0.11	0.10	0.26	0.00	0.00	-0.02	0.04	0.00	0.13	0.00	0.00	0.00	-0.03	0.00	-0.10	0.00
11	35.56	0.868	0.064	-0.003	0.11	0.08	0.28	0.00	0.00	-0.01	0.05	0.00	0.15	0.00	0.00	0.00	-0.03	0.00	-0.10	0.00
12	40.64	0.866	0.068	-0.002	0.10	0.08	0.26	0.00	0.00	0.00	0.04	0.00	0.13	0.00	0.00	0.00	-0.02	0.00	-0.05	0.00
13	45.72	0.873	0.073	0.001	0.15	0.10	0.40	0.00	0.00	-0.01	0.10	0.00	0.28	0.00	0.08	0.00	-0.05	0.00	-0.15	0.00
14	50.80	0.873	0.089	0.004	0.15	0.56	0.34	0.01	0.00	0.04	0.07	0.00	0.20	0.00	0.95	0.00	0.00	-0.01	-0.01	0.00
15	55.88	0.877	0.094	0.008	0.13	0.53	0.34	0.00	0.01	0.09	0.05	0.00	0.15	0.00	0.25	0.01	0.05	-0.01	0.15	0.00
16	60.96	0.889	0.103	0.023	0.12	0.72	0.31	0.00	0.01	0.09	0.03	0.01	0.08	0.00	1.27	0.01	0.03	0.03	0.09	0.00
17	66.04	0.899	0.000	0.037	0.13	0.00	0.42	0.00	0.00	0.12	0.01	0.00	0.03	0.00	0.00	0.00	0.00	0.00	-0.02	0.00

Table C.5 Continued.

Case D.S0 Station= 9
X= 101.6mm Tunnel Run#= 777 Ue/Uref= 0.802 Date= 616.88 Time=14.36
Bias Corrected data using 1/sqrt(U*U + V*V + W*W + (.01Ur)^2)

						<-- normalized by 0.001 Ur^2 -->								<---------- normalized by 0.0001 Ur^3 ----------->					
LR	Y(mm)	U/Ur	V/Ur	W/Ur	uu	vv	ww	uv	vw	uw	uuu	uvv	uww	vuu	vvv	vww	wuu	wvv	www	uvw
1	0.00	0.000	0.000	0.000	0.00	0.00	0.00	-0.37	0.00	0.00	0.00	0.00	0.00	0.00	0.00	0.00	0.00	0.00	0.00	0.00
1	0.25	0.136	0.005	0.002	5.35	0.46	2.93	-0.36	-0.06	0.21	2.51	0.11	1.39	-0.15	0.36	0.03	0.16	-0.01	0.25	-0.03
2	0.63	0.207	0.005	0.002	6.59	0.97	3.42	-0.73	-0.06	-0.01	1.79	0.14	0.78	-0.11	-0.06	0.05	-0.05	0.01	0.07	0.01
3	1.27	0.241	0.007	0.005	6.72	1.62	3.52	-0.96	0.01	-0.12	1.40	0.19	0.65	-0.11	-0.09	0.05	-0.05	0.02	-0.07	-0.03
4	2.54	0.290	0.010	0.003	7.67	2.17	3.78	-1.30	0.00	-0.27	1.49	0.22	0.39	-0.27	-0.11	0.00	-0.03	-0.02	0.00	-0.04
5	6.35	0.414	0.017	0.000	8.49	2.61	4.23	-1.68	0.01	-0.31	-0.20	0.03	0.08	0.07	0.02	0.04	0.08	-0.01	-0.07	-0.02
6	10.16	0.514	0.027	-0.006	7.12	2.33	3.98	-1.46	0.10	-0.15	-0.88	-0.15	-0.25	0.26	0.12	0.07	-0.06	-0.02	-0.13	0.00
7	15.24	0.626	0.041	-0.005	5.18	1.76	2.95	-1.08	0.01	-0.07	-1.53	-0.26	-0.22	0.37	0.23	0.09	-0.06	0.02	0.00	0.02
8	20.32	0.713	0.053	-0.006	3.00	1.11	1.82	-0.59	0.02	-0.10	-0.99	-0.22	-0.21	0.26	0.19	0.10	0.03	0.01	0.05	-0.02
9	25.40	0.776	0.062	-0.006	1.14	0.54	0.70	-0.24	0.00	-0.02	-0.54	-0.12	-0.09	0.15	0.10	0.05	0.02	0.00	0.05	-0.01
10	30.48	0.799	0.068	-0.006	0.20	0.18	0.25	-0.03	0.00	0.03	-0.01	-0.01	0.04	0.01	0.02	0.01	0.02	0.00	0.06	0.00
11	35.56	0.804	0.071	-0.010	0.08	0.09	0.16	0.00	0.00	0.01	0.01	0.00	0.03	0.00	0.00	0.00	0.01	0.00	0.02	0.00
12	40.64	0.803	0.074	-0.009	0.09	0.07	0.15	0.00	0.00	0.01	0.01	0.00	0.02	0.00	0.00	0.00	0.01	0.00	0.04	0.00
13	45.72	0.804	0.077	-0.008	0.10	0.07	0.16	0.00	0.00	0.02	0.01	0.00	0.03	0.00	0.00	0.00	0.01	0.00	0.03	0.00
14	50.80	0.803	0.080	-0.008	0.08	0.07	0.18	0.00	0.00	0.02	0.02	0.00	0.05	0.00	0.00	0.00	0.01	0.00	0.05	0.00
15	55.88	0.803	0.090	-0.007	0.07	0.36	0.17	0.00	0.00	0.02	0.01	0.00	0.04	0.00	0.02	0.00	0.02	0.00	0.05	0.00
16	60.96	0.798	0.092	-0.008	0.07	0.42	0.18	0.00	0.00	0.02	0.01	0.00	0.04	0.00	0.73	0.00	0.02	0.00	0.05	0.00
17	66.04	0.805	0.000	-0.010	0.12	0.00	0.21	0.00	0.00	0.03	0.02	0.00	0.06	0.00	0.00	0.00	0.02	0.00	0.05	0.00
18	69.85	0.801	0.000	-0.009	0.06	0.00	0.16	0.00	0.00	0.02	0.01	0.00	0.03	0.00	0.00	0.00	0.01	0.00	0.04	0.00

Table C.5 Continued.

Case D.S0 Station= 10
X= 152.4mm Tunnel Run#= 775 Ue/Uref= 0.755 Date= 616.88 Time=12.37
Bias Corrected data using 1/sqrt(U*U + V*V + W*W + (.01Ur)^2)

					<-- normalized by 0.001 Ur^2 -->						<---------- normalized by 0.0001 Ur^3 ---------->									
LR	Y(mm)	U/Ur	V/Ur	W/Ur	uu	vv	ww	uv	vw	uw	uuu	uvv	uww	vuu	vvv	vww	wuu	wvv	www	uvw
1	0.00	0.000	0.000	0.000	0.00	0.00	0.00	-0.20	0.00	0.00	0.00	0.00	0.00	0.00	0.00	0.00	0.00	0.00	0.00	0.00
1	0.63	0.107	0.005	0.010	4.98	0.69	2.93	-0.34	-0.04	0.00	1.71	0.11	0.95	-0.14	0.00	0.02	-0.07	0.00	-0.10	-0.02
2	1.27	0.135	0.006	0.015	5.74	1.23	3.22	-0.54	-0.05	-0.08	1.37	0.19	0.86	-0.18	-0.12	-0.02	-0.28	0.01	-0.13	0.02
3	2.54	0.169	0.009	0.013	6.91	1.81	3.65	-0.91	-0.03	-0.10	1.87	0.33	0.86	-0.36	-0.23	0.00	-0.04	0.03	-0.18	-0.03
4	6.35	0.257	0.016	0.011	8.59	2.63	4.44	-1.54	-0.05	-0.09	0.99	0.33	0.66	-0.20	-0.24	-0.08	-0.15	-0.04	-0.15	0.01
5	10.16	0.354	0.024	0.010	8.98	2.94	4.97	-1.64	-0.02	-0.30	-0.34	0.02	0.29	-0.03	0.19	0.01	-0.07	0.00	-0.17	0.03
6	15.24	0.477	0.036	0.005	7.70	2.52	4.51	-1.41	0.00	-0.09	-1.59	-0.25	-0.10	0.28	0.21	0.20	-0.05	0.03	-0.14	-0.06
10	20.32	0.580	0.049	0.003	5.34	1.89	3.29	-1.06	-0.02	-0.02	-1.57	-0.29	-0.33	0.34	0.23	0.17	0.09	-0.01	0.05	-0.06
11	25.40	0.666	0.060	0.003	3.24	1.26	1.98	-0.69	0.01	-0.11	-1.20	-0.32	-0.19	0.33	0.32	0.13	-0.06	0.02	-0.08	-0.02
12	30.48	0.722	0.066	0.003	1.27	0.68	0.84	-0.27	0.03	-0.02	-0.60	-0.15	-0.06	0.17	0.23	0.06	-0.02	0.02	0.02	0.00
13	35.56	0.749	0.069	0.001	0.22	0.24	0.28	-0.04	0.00	-0.01	-0.05	-0.02	0.05	0.03	0.10	0.01	-0.01	-0.01	-0.04	0.00
14	40.64	0.752	0.070	-0.001	0.10	0.11	0.22	0.00	0.00	-0.01	0.03	0.00	0.10	0.00	0.00	0.00	-0.03	0.00	-0.08	0.00
15	45.72	0.750	0.070	0.000	0.08	0.09	0.18	0.00	0.01	0.00	0.02	0.00	0.06	0.00	0.01	0.00	-0.01	0.00	-0.02	0.00
16	50.80	0.752	0.071	0.000	0.07	0.10	0.17	0.00	0.00	0.00	0.02	0.00	0.06	0.00	0.07	0.00	-0.01	0.00	-0.03	0.00
17	55.88	0.751	0.076	0.000	0.08	0.37	0.20	0.00	0.00	0.02	0.03	0.00	0.07	0.00	0.02	0.00	0.02	0.00	0.04	-0.01
18	60.96	0.752	0.077	0.000	0.10	0.36	0.25	0.00	0.00	-0.02	0.05	0.00	0.13	0.00	0.00	0.00	-0.03	0.00	-0.09	0.00
19	66.04	0.750	0.000	-0.001	0.09	0.00	0.21	0.00	0.00	0.00	0.03	0.00	0.09	0.00	0.00	0.00	-0.01	0.00	-0.04	0.00
20	71.12	0.753	0.000	0.000	0.07	0.00	0.20	0.00	0.00	0.02	0.02	0.00	0.06	0.00	0.00	0.00	0.01	0.00	0.05	0.00

Table C.5 Continued.

Case D.S0 Station= 11
X= 228.6mm Tunnel Run#= 773 Ue/Uref= 0.720 Date= 616.88 Time= 9.45
Bias Corrected data using 1/sqrt(U*U + V*V + W*W + (.01Ur)^2)

					<-- normalized by 0.001 Ur^2 -->						<---------- normalized by 0.0001 Ur^3 ---------->									
LR	Y(mm)	U/Ur	V/Ur	W/Ur	uu	vv	ww	uv	vw	uw	uuu	uvv	uww	vuu	vvv	vww	wuu	wvv	www	uvw
1	0.00	0.000	0.000	0.000	0.00	0.00	0.00	-0.05	0.00	0.00	0.00	0.00	0.00	0.00	0.00	0.00	0.00	0.00	0.00	0.00
1	1.27	0.038	0.004	0.001	4.15	0.85	2.62	-0.18	-0.03	-0.06	1.35	0.11	0.64	-0.12	-0.12	0.00	0.12	-0.01	0.31	0.01
2	2.54	0.055	0.007	0.001	4.77	1.37	2.92	-0.38	-0.08	-0.03	1.49	0.26	0.64	-0.22	-0.18	-0.04	0.07	0.03	0.13	-0.03
3	6.35	0.106	0.011	0.001	7.08	2.39	3.71	-1.12	-0.07	-0.10	2.42	0.47	0.89	-0.60	-0.42	-0.14	0.03	0.05	-0.10	-0.01
4	10.16	0.173	0.016	0.005	8.92	2.97	4.64	-1.62	-0.06	-0.12	2.26	0.45	0.66	-0.58	-0.34	-0.17	-0.06	0.07	-0.14	-0.01
5	15.24	0.279	0.022	0.006	10.47	3.41	5.57	-1.95	-0.02	-0.26	0.03	0.10	0.34	-0.05	-0.12	-0.09	-0.08	0.13	-0.02	0.01
6	20.32	0.388	0.030	0.004	10.37	3.40	5.61	-2.01	-0.06	-0.35	-2.60	-0.36	-0.20	0.35	0.24	0.14	0.09	0.09	-0.19	0.02
7	25.40	0.498	0.040	0.004	7.84	2.65	4.56	-1.54	0.02	-0.12	-3.23	-0.52	-0.69	0.77	0.43	0.30	0.22	0.04	0.08	-0.04
8	30.48	0.595	0.049	0.005	4.87	1.79	2.97	-0.99	-0.05	-0.06	-2.31	-0.46	-0.41	0.56	0.33	0.19	-0.02	-0.02	-0.02	0.05
9	35.56	0.669	0.055	0.004	2.48	1.04	1.52	-0.53	0.00	-0.06	-1.33	-0.27	-0.19	0.38	0.24	0.13	0.02	0.03	0.01	-0.03
10	40.64	0.711	0.059	0.003	0.65	0.48	0.53	-0.16	0.02	-0.01	-0.27	-0.09	0.00	0.10	0.10	0.05	0.02	0.00	0.03	-0.01
11	45.72	0.719	0.059	0.002	0.15	0.18	0.25	-0.01	0.01	-0.01	0.02	0.00	0.08	0.00	0.01	0.00	-0.02	0.00	-0.06	0.00
12	50.80	0.717	0.059	0.001	0.12	0.11	0.28	0.00	0.00	-0.01	0.05	0.00	0.15	0.00	0.00	0.00	-0.03	0.00	-0.09	0.00
13	55.88	0.719	0.063	0.002	0.10	0.47	0.26	0.00	0.00	0.02	0.04	0.00	0.12	0.00	0.10	0.00	0.01	0.00	0.02	0.00
14	60.96	0.719	0.064	0.003	0.10	0.38	0.27	0.00	0.00	0.05	0.04	0.00	0.11	0.00	0.00	0.00	0.03	0.00	0.09	0.00
15	66.04	0.715	0.000	0.005	0.14	0.00	0.37	0.00	0.00	0.01	0.08	0.00	0.24	0.00	0.00	0.00	-0.02	0.00	-0.06	0.00
16	71.12	0.717	0.000	0.007	0.11	0.00	0.33	0.00	0.00	0.02	0.05	0.00	0.17	0.00	0.00	0.00	-0.01	0.00	-0.04	0.00

Table C.5 Continued.

Case D.S0 Station= 12
X= 304.8mm Tunnel Run#= 771 Ue/Uref= 0.697 Date= 615.88 Time=14.05
Bias Corrected data using 1/sqrt(U*U + V*V + W*W + (.01Ur)^2)

					<-- normalized by 0.001 Ur^2 -->						<---------- normalized by 0.0001 Ur^3 ---------->								
LR	Y(mm)	U/Ur	V/Ur	W/Ur	uu	vv	ww	uv	vw	uw	uuu	uvv	uww	vuu	vvv	vww	wuu	wvv	www	uvw
1	0.00	0.000	0.000	0.000	0.00	0.00	0.00	-0.02	0.00	0.00	0.00	0.00	0.00	0.00	0.00	0.00	0.00	0.00	0.00	0.00
1	1.27	0.012	0.004	-0.001	3.45	0.94	2.79	-0.18	-0.15	-0.21	1.10	0.13	1.07	-0.10	-0.09	-0.02	-0.31	0.00	-0.91	-0.01
2	2.54	0.021	0.003	-0.001	4.02	1.32	2.79	-0.37	-0.10	-0.16	1.44	0.23	1.05	-0.24	-0.20	-0.05	-0.30	-0.01	-0.83	-0.01
3	6.35	0.058	0.006	-0.001	5.45	2.22	3.40	-0.89	-0.13	-0.06	2.10	0.52	1.02	-0.57	-0.45	-0.13	-0.21	0.01	-0.51	0.00
4	10.16	0.105	0.005	0.000	7.82	2.92	4.61	-1.47	-0.18	-0.14	2.77	0.63	1.42	-0.80	-0.46	-0.20	-0.30	0.08	-0.70	0.00
5	15.24	0.178	0.009	0.002	10.08	3.74	5.93	-2.34	-0.23	-0.34	2.91	0.55	1.55	-0.76	-0.50	-0.27	-0.54	0.13	-1.22	-0.07
6	20.32	0.271	0.010	0.003	11.13	4.05	6.72	-2.48	-0.15	-0.19	0.01	0.05	1.19	-0.14	-0.07	-0.03	-0.49	0.04	-1.74	-0.05
7	25.40	0.369	0.015	0.002	11.07	3.76	6.65	-2.43	-0.12	-0.40	-2.85	-0.40	0.33	0.66	0.30	0.16	-0.59	0.07	-1.45	-0.06
8	30.48	0.462	0.020	0.004	9.25	3.20	5.73	-2.06	-0.05	-0.36	-4.26	-0.68	-0.35	1.06	0.57	0.40	-0.19	0.07	-0.86	-0.10
9	35.56	0.556	0.029	0.004	6.54	2.45	4.07	-1.55	-0.05	-0.23	-3.69	-0.80	-0.07	1.14	0.64	0.41	-0.37	-0.04	-0.94	0.03
10	40.64	0.638	0.032	0.005	3.30	1.40	2.28	-0.77	-0.03	-0.18	-1.71	-0.45	0.19	0.61	0.38	0.23	-0.43	-0.02	-1.07	0.00
11	45.72	0.681	0.034	0.006	1.19	0.79	1.03	-0.31	0.02	-0.15	-0.56	-0.22	0.25	0.25	0.22	0.09	-0.21	-0.01	-0.54	-0.02
12	50.80	0.696	0.033	0.004	0.29	0.28	0.49	-0.03	0.00	-0.14	0.10	-0.01	0.32	0.02	0.04	0.02	-0.17	0.00	-0.47	0.00
13	55.88	0.696	0.038	0.003	0.14	0.47	0.27	0.00	0.01	-0.05	0.05	0.00	0.15	0.00	0.19	0.00	-0.06	0.00	-0.18	0.00
14	60.96	0.694	0.039	0.003	0.12	0.45	0.27	0.00	0.00	-0.05	0.05	0.00	0.16	0.00	0.06	0.00	-0.06	0.00	-0.19	0.00
15	66.04	0.693	0.000	0.004	0.13	0.00	0.33	0.00	0.00	-0.07	0.07	0.00	0.23	0.00	0.00	0.00	-0.09	0.00	-0.28	0.00
16	71.12	0.692	0.000	0.005	0.19	0.00	0.51	0.00	0.00	-0.16	0.15	0.00	0.46	0.00	0.00	0.00	-0.21	0.00	-0.65	0.00

Table C.5 Concluded.

NASA
National Aeronautics and Space Administration

Report Documentation Page

1. Report No.	2. Government Accession No.	3. Recipient's Catalog No.
NASA TM-102211		

4. Title and Subtitle
Experimental Study of a Three-Dimensional Shear-Driven Turbulent Boundary Layer with Streamwise Adverse Pressure Gradient

5. Report Date
May 1990

6. Performing Organization Code

7. Author(s)
David M. Driver and James P. Johnston

8. Performing Organization Report No.
A-89104

10. Work Unit No.
505-60-11

9. Performing Organization Name and Address
Ames Research Center
Moffett Field, CA 94035-1000

11. Contract or Grant No.

13. Type of Report and Period Covered
Technical Memorandum

12. Sponsoring Agency Name and Address
National Aeronautics and Space Administration
Washington, DC 20546-0001

14. Sponsoring Agency Code

15. Supplementary Notes
Point of Contact: David M. Driver, Ames Research Center, MS 229-1
Moffett Field, CA 94035-1000
(415) 604-6156 or FTS 464-6156

16. Abstract

The effects of a strong adverse pressure gradient ($\frac{\delta^*}{\tau}\frac{\partial P}{\partial x}$=12) on a three-dimensional turbulent boundary layer are studied in an axisymmetric spinning cylinder geometry. Velocity measurements made with a three-component laser Doppler velocimeter include all three mean flow components, all six Reynolds stress components, and all ten triple-product correlations. Reynolds stress, $\sqrt{\overline{uv}^2 + \overline{vw}^2}$, diminishes as the flow becomes three-dimensional. Lower levels of shear stress were seen to persist under adverse pressure gradient conditions. This low level of stress was seen to roughly correlate with the magnitude of cross-flow (relative to free stream flow) for this experiment as well as most of the other experiments in the literature. Variations in pressure gradient do not appear to alter this correlation. For this reason, it is hypothesized that a three-dimensional boundary layer is more prone to separate than a two-dimensional boundary layer, although it could not be directly shown here. None of the computations performed with either a Prandtl mixing length, $k - \varepsilon$, or a Launder-Reece-Rodi full Reynolds-stress model were able to predict the reduction in Reynolds stress.

17. Key Words (Suggested by Author(s))	18. Distribution Statement
Three-dimensional Boundary layer Turbulent Pressure gradient	Unclassified-Unlimited Subject Category - 34

19. Security Classif. (of this report)	20. Security Classif. (of this page)	21. No. of Pages	22. Price
Unclassified	Unclassified	258	A12

NASA FORM 1626 OCT 86

For sale by the National Technical Information Service, Springfield, Virginia 22161

GPO 787-548/39191